



PALYNOLOGY AND VEGETATION HISTORY

EDITED BY: Valentí Rull, Encarni Montoya, Thomas Giesecke and Jesse L. Morris
PUBLISHED IN: *Frontiers in Earth Science*, *Frontiers in Plant Science* and
Frontiers in Ecology and Evolution



frontiers

Frontiers Copyright Statement

© Copyright 2007-2019 Frontiers Media SA. All rights reserved.

All content included on this site, such as text, graphics, logos, button icons, images, video/audio clips, downloads, data compilations and software, is the property of or is licensed to Frontiers Media SA ("Frontiers") or its licensees and/or subcontractors. The copyright in the text of individual articles is the property of their respective authors, subject to a license granted to Frontiers.

The compilation of articles constituting this e-book, wherever published, as well as the compilation of all other content on this site, is the exclusive property of Frontiers. For the conditions for downloading and copying of e-books from Frontiers' website, please see the Terms for Website Use. If purchasing Frontiers e-books from other websites or sources, the conditions of the website concerned apply.

Images and graphics not forming part of user-contributed materials may not be downloaded or copied without permission.

Individual articles may be downloaded and reproduced in accordance with the principles of the CC-BY licence subject to any copyright or other notices. They may not be re-sold as an e-book.

As author or other contributor you grant a CC-BY licence to others to reproduce your articles, including any graphics and third-party materials supplied by you, in accordance with the Conditions for Website Use and subject to any copyright notices which you include in connection with your articles and materials.

All copyright, and all rights therein, are protected by national and international copyright laws.

The above represents a summary only. For the full conditions see the Conditions for Authors and the Conditions for Website Use.

ISSN 1664-8714

ISBN 978-2-88945-687-1

DOI 10.3389/978-2-88945-687-1

About Frontiers

Frontiers is more than just an open-access publisher of scholarly articles: it is a pioneering approach to the world of academia, radically improving the way scholarly research is managed. The grand vision of Frontiers is a world where all people have an equal opportunity to seek, share and generate knowledge. Frontiers provides immediate and permanent online open access to all its publications, but this alone is not enough to realize our grand goals.

Frontiers Journal Series

The Frontiers Journal Series is a multi-tier and interdisciplinary set of open-access, online journals, promising a paradigm shift from the current review, selection and dissemination processes in academic publishing. All Frontiers journals are driven by researchers for researchers; therefore, they constitute a service to the scholarly community. At the same time, the Frontiers Journal Series operates on a revolutionary invention, the tiered publishing system, initially addressing specific communities of scholars, and gradually climbing up to broader public understanding, thus serving the interests of the lay society, too.

Dedication to Quality

Each Frontiers article is a landmark of the highest quality, thanks to genuinely collaborative interactions between authors and review editors, who include some of the world's best academicians. Research must be certified by peers before entering a stream of knowledge that may eventually reach the public - and shape society; therefore, Frontiers only applies the most rigorous and unbiased reviews.

Frontiers revolutionizes research publishing by freely delivering the most outstanding research, evaluated with no bias from both the academic and social point of view. By applying the most advanced information technologies, Frontiers is catapulting scholarly publishing into a new generation.

What are Frontiers Research Topics?

Frontiers Research Topics are very popular trademarks of the Frontiers Journals Series: they are collections of at least ten articles, all centered on a particular subject. With their unique mix of varied contributions from Original Research to Review Articles, Frontiers Research Topics unify the most influential researchers, the latest key findings and historical advances in a hot research area! Find out more on how to host your own Frontiers Research Topic or contribute to one as an author by contacting the Frontiers Editorial Office: researchtopics@frontiersin.org

PALYNOLOGY AND VEGETATION HISTORY

Topic Editors:

Valentí Rull, Institute of Earth Sciences Jaume Almera (CSIC), Spain

Encarni Montoya, Institute of Earth Sciences Jaume Almera (CSIC), Spain

Thomas Giesecke, Georg-August University, Germany

Jesse L. Morris, University of Utah, United States



Aerial view of a meandering river surrounded by tropical rainforests and patches of savanna near Wonkén (Gran Sabana, southeast Venezuela). An example of a pollen diagram, the usual tool to reconstruct vegetation history, is shown at the right bottom corner.
Image: Valentí Rull.

This Research Topic commemorates the centenary of the first quantitative pollen diagram by Lennart von Post, the founder of paleoecological palynology. The main aim is to provide a thorough view of the use of palynology in aspects such as the reconstruction of Quaternary vegetation and environmental changes, the role of natural and anthropogenic drivers in the development of the Quaternary vegetation, the shaping of present-day ecological and biogeographical patterns, the potential application of this knowledge in biodiversity conservation and landscape restoration and the development of new methods of pollen analysis and data management. The

Research Topic is subdivided into four main conceptual parts, namely (1) modern analog studies; (2) land cover estimates from pollen data; (3) vegetation dynamics reconstructions from Europe, North and South America, Africa and Oceania; and (4) large-scale reviews and meta-analyses. Hopefully, this Research Topic will serve to appraise the state of the art of modern palynology and highlight the usefulness of this discipline in long-term ecological research.

Citation: Rull, V., Montoya, E., Giesecke, T., Morris, J. L., eds. (2019). *Palynology and Vegetation History*. Lausanne: Frontiers Media. doi: 10.3389/978-2-88945-687-1

Table of Contents

06 Editorial: Palynology and Vegetation History

Valentí Rull, Encarni Montoya, Thomas Giesecke and Jesse L. Morris

PART 1

MODERN ANALOG STUDIES

09 Poaceae Pollen From Southern Brazil: Distinguishing Grasslands (Campos) From Forests by Analyzing a Diverse Range of Poaceae Species

Jefferson N. Radaeski, Soraia G. Bauermann and Antonio B. Pereira

27 The Representativeness of Olea Pollen From Olive Groves and the Late Holocene Landscape Reconstruction in Central Mediterranean

Assunta Florenzano, Anna Maria Mercuri, Rossella Rinaldi, Eleonora Rattighieri, Rita Fornaciari, Rita Messori and Laura Arru

38 Changes in Modern Pollen Assemblages and Soil Geochemistry Along Coastal Environmental Gradients in the Everglades of South Florida

Qiang Yao and Kam-biu Liu

PART 2

LAND COVER ESTIMATES FROM POLLEN DATA

51 ROPES Reveals Past Land Cover and PPEs From Single Pollen Records

Martin Theuerkauf and John Couwenberg

64 Maps From Mud—Using the Multiple Scenario Approach to Reconstruct Land Cover Dynamics From Pollen Records: A Case Study of Two Neolithic Landscapes

M. Jane Bunting, Michelle Farrell, Alex Bayliss, Peter Marshall and Alasdair Whittle

84 Quantitative Palynology Informing Conservation Ecology in the Bohemian/Bavarian Forests of Central Europe

Vachel A. Carter, Richard C. Chiverrell, Jennifer L. Clear, Niina Kuosmanen, Alice Moravcová, Miroslav Svoboda, Helena Svobodová-Svitavská, Jacqueline F. N. van Leeuwen, Willem O. van der Knaap and Petr Kuneš

PART 3

VEGETATION DYNAMICS AND ENVIRONMENTAL DRIVERS

98 Temperature Range Shifts for Three European Tree Species Over the Last 10,000 Years

Rachid Cheddadi, Miguel B. Araújo, Luigi Maiorano, Mary Edwards, Antoine Guisan, Matthieu Carré, Manuel Chevalier and Peter B. Pearman

111 Filling a Geographical Gap: New Paleoecological Reconstructions From the Desert Southwest, USA

Andrea Brunelle, Thomas A. Minckley, Jacqueline J. Shinker and Josh Heyer

128 Long-Term Vegetation Dynamics in a Megadiverse Hotspot: The Ice-Age Record of a Pre-montane Forest of Central Ecuador

Encarni Montoya, Hayley F. Keen, Carmen X. Luzuriaga and William D. Gosling

- 142** *First Pollen Record in South America. Commentary: Die Zeichenschrift der Pollenstatistik*
Vera Markgraf
- 145** *Modulation of Fire Regimes by Vegetation and Site Type in Southwestern Patagonia Since 13 ka*
Patricio I. Moreno, Isabel Vilanova, Rodrigo P. Villa-Martínez and Jean P. Francois
- 155** *Holocene Dynamics of Temperate Rainforests in West-Central Patagonia*
Virginia Iglesias, Simon G. Haberle, Andrés Holz and Cathy Whitlock
- 167** *Environmental Drivers of Holocene Forest Development in the Middle Atlas, Morocco*
Jennifer F. E. Campbell, William J. Fletcher, Sebastien Joannin, Philip D. Hughes, Mustapha Rhanem and Christoph Zielhofer
- 189** *Pollen, People and Place: Multidisciplinary Perspectives on Ecosystem Change at Amboseli, Kenya*
Esther N. Githumbi, Rebecca Kariuki, Anna Shoemaker, Colin J. Courtney-Mustaphi, Maxmillian Chuhilla, Suzi Richer, Paul Lane and Rob Marchant
- 215** *Palynology and the Ecology of the New Zealand Conifers*
Matt S. McGlone, Sarah J. Richardson, Olivia R. Burge, George L. W. Perry and Janet M. Wilmshurst

PART 4

LARGE-SCALE REVIEWS AND META-ANALYSES

- 238** *European Forest Cover During the Past 12,000 Years: A Palynological Reconstruction Based on Modern Analogs and Remote Sensing*
Marco Zanon, Basil A. S. Davis, Laurent Marquer, Simon Brewer and Jed O. Kaplan
- 263** *Pollen From the Deep-Sea: A Breakthrough in the Mystery of the Ice Ages*
María F. Sánchez Goñi, Stéphanie Desprat, William J. Fletcher, César Morales-Molino, Filipa Naughton, Dulce Oliveira, Dunia H. Urrego and Coralie Zorzi



Editorial: Palynology and Vegetation History

Valentí Rull^{1*}, Encarni Montoya¹, Thomas Giesecke² and Jesse L. Morris³

¹ Institute of Earth Sciences Jaume Almera (ICTJA), CSIC, Barcelona, Spain, ² Department of Palynology and Climate Dynamics, Georg-August Universität Göttingen, Göttingen, Germany, ³ Department of Geography, University of Utah, Salt Lake City, UT, United States

Keywords: palynology, paleoecology, vegetation change, quaternary, environmental change

Editorial on the Research Topic

Palynology and Vegetation History

This Research Topic (RT) was conceived as an homage to the Swedish geologist Lennart von Post (1884–1951), the founder of paleoecological palynology, to commemorate the centenary of his presentation of the first modern, quantitative pollen diagram in 1916 at the 16th Convention of Scandinavian Naturalists, held in Kristiania (now Oslo), Norway (Nordlund, 2018). His diagram and its interpretation were published two years later in Swedish (Von Post, 1918) and 51 years later in English (Von Post, 1967). The centenary was celebrated during November 2016, at the Royal Swedish Academy of Sciences in Stockholm, Sweden (Gaillard et al., 2018). Birks and Berglund (2018) summarized the development of Quaternary pollen analysis since von Post's foundational work as occurring in three main phases: (i) the pioneer phase (1916–1950), the building phase (1951–1973) and the mature phase (1974–present). At the beginning, pollen analysis was mainly a stratigraphic tool used for dating and stratigraphic correlation but it later proved to be useful in botanical, biogeographical and ecological research. Since then, palynology has developed into a fundamental tool to unravel the ecological and environmental trends and changes through the Quaternary. In particular, palynology has been instrumental for disentangling natural and anthropogenic drivers of vegetation change, which is needed to understand past and present patterns and processes, and also to predict potential future trends of vegetation in the face of the ongoing climate change.

This RT aimed to provide a thorough view of the use of palynology in aspects such as the reconstruction of Quaternary vegetation and environmental changes, the role of natural and anthropogenic drivers in the development of the Quaternary vegetation, the shaping of present-day ecological and biogeographical patterns, the potential application of this knowledge in biodiversity conservation and landscape restoration and the development of new methods of pollen analysis and data management. The papers published herein cover most of these topics, among others, as the aims and scope were sufficiently broad to include any aspect of modern palynology and its significance for vegetation history. These papers are grouped under four themes. The first two are essentially methodological while the other two provide examples where pollen studies have been applied to investigate ecological dynamics at local, regional and global scales.

MODERN ANALOG STUDIES

This section deals with studies where modern pollen assemblages have been applied to aid in the interpretation of past records. In the first paper, Radaeski et al. used a set of standard pollen measurements on ~70 grass species from Southern Brazil, and found a statistically significant difference between grass pollen from forests vs. open habitat species. The authors conclude that the size of grass pollen grains can be used to discriminate between forest and grassland vegetation in

OPEN ACCESS

Edited and reviewed by:

Steven L. Forman,
Baylor University, United States

*Correspondence:

Valentí Rull
vrull@ictja.csic.es

Specialty section:

This article was submitted to
Quaternary Science, Geomorphology
and Paleoenvironment,
a section of the journal
Frontiers in Earth Science

Received: 05 September 2018

Accepted: 12 October 2018

Published: 02 November 2018

Citation:

Rull V, Montoya E, Giesecke T and
Morris JL (2018) Editorial: Palynology
and Vegetation History.
Front. Earth Sci. 6:186.
doi: 10.3389/feart.2018.00186

past pollen records. The other two studies focused on modern pollen deposition and applications to past records. Florenzano et al. studied the modern deposition of *Olea* pollen in two regions of Italy and found that most of this pollen type was deposited locally, within olive groves, with sharp declines outside of the cultivated area. These results are used to infer the spatial pattern of olive farming during the Hellenistic, Roman and Medieval periods, on the basis of the *Olea* pollen preserved in archaeological sites. Yao and Liu studied surface pollen assemblages and soil chemistry along vegetation, edaphic and salinity gradients in the Florida Everglades (USA). Modern pollen spectra correspond perfectly with the vegetation types where samples have been collected. Soil chemistry is consistent with salinity and chemical gradients at local and regional scales.

LAND COVER ESTIMATES FROM POLLEN DATA

In the last decades, efforts to convert pollen data into quantitative estimates of past vegetation cover have increased, which is reflected here by three contributions. An important prerequisite for inferring past vegetation cover is to estimate the relative pollen production of plants (rPPE), which require detailed modern studies. Theuerkauf and Couwenberg introduce a method, called ROPES, to estimate rPPE's and plant cover from single pollen records with reliable pollen accumulation rates (PAR, in grains $\text{cm}^{-2} \text{yr}^{-1}$). The principle is that changes in PAR and plant abundance are linearly related. The performance of this method is evaluated and the ROPES advantages and limitations are discussed. Using such or differently derived rPPE's it is then possibly to attempt full landscape reconstructions, which may be achieved using the Multiple Scenario Approach (MSA) presented by Bunting et al. which combines GIS techniques with physical models of pollen dispersion and deposition. They applied the MSA method to two Neolithic sites from Britain and showed that the impact of neolithization on land cover was continuous with no reductions during periods when archaeological evidence suggests lower human activity. In the third paper of this section, Carter et al. use the Landscape Reconstruction Algorithm (LRA) to convert pollen records from Central Europe to forest cover estimates, in order to reconstruct the history of "natural" Holocene forests, as a guide for conservation and restoration practices. These forests have been dominated by spruce for the last 9000 years, which contradicts the prevailing assumption of beech and fir dominance. These latter two species did not reach the region until ca. 6000 cal yr BP, which opens new perspectives for reforestation strategies.

VEGETATION DYNAMICS AND ENVIRONMENTAL DRIVERS

This section encompasses studies on vegetation dynamics and the associated environmental drivers, notably climate change and anthropogenic activities, from a wide range of biomes and geographical areas including Europe, North and South America, Africa and Oceania.

Europe

Cheddadi et al. analyzed the response of European forests to Holocene temperature changes and observed that fir showed niche patterns similar to present, whereas beech and spruce occurred at temperature values different from their current ranges. The authors concluded that predictive models of forest distribution should not be based only on modern thermal niches.

North America

Brunelle et al. provide a regional perspective of the Holocene palynological studies developed by analyzing wetland records from the Desert Southwest (USA). Pollen preservation was useful to infer permanent vs. intermittent flood conditions, which the authors interpret to be a proxy for winter precipitation and moisture persistence as controlled by ENSO (El Niño-Southern Oscillation) activity. Therefore, variations in pollen preservation through time can be used as a proxy for past ENSO activity.

Tropical South America

Montoya et al. present a pollen record from the Ecuadorian Amazonia that documents the composition of premontane Andean forests during the last glaciation, between ca. 50,000 and 20,000 cal yr BP. The decline of formerly dominant trees with a reciprocal increase of heat-intolerant trees from higher Andean environments (*Podocarpus*, *Alnus*, *Hedyosmum*) during the LGM suggests that glacial cooling changed the composition of these Amazon forests by downward migration of sensitive taxa.

Southern South America

Markgraf presents the very first pollen record of vegetation dynamics from South America (Tierra del Fuego, Argentina), published by Lennart von Post in 1929. The paper reproduces the original diagrams showing a shift from steppe communities to *Nothofagus* forests, which was interpreted in terms of a climatic shift from warmer/drier to cooler/wetter conditions. Using pollen and charcoal analysis, Moreno et al. evaluate the effect of vegetation and site type on fire regimes in the Chilean Patagonia during the last 13,000 years. Steppe fires were of high frequency and low magnitude, whereas fires occurring in *Nothofagus* forests were less frequent but more intense. Divergences between fire histories reconstructed from either lake or bog records were attributed to local burning of bog vegetation. Also in Patagonia, Iglesias et al. used independent evidence for environmental, anthropogenic and ecological change to assess the influence of climate and human activities on Holocene vegetation dynamics. *Nothofagus-Pilgerodendron* forests remained fairly stable between 9000 and 2000 cal yr BP, despite long-term changes in climate and fire. Local forest fluctuations during the last two millennia were attributed to greater climatic variability and human deforestation.

Africa

Campbell et al. present a high-resolution reconstruction of Holocene vegetation changes in a semi-arid region from the Moroccan Atlas to gain insights on the response of forests to environmental drivers. Climatic shifts seem to have been more clearly recorded until ca. 4300 cal yr BP,

when forests started to decline gradually due to increasing pastoralism, fire and aridity. Forests significantly declined by 1300 cal yr BP due to human pressure. Githumbi et al. used multidisciplinary paleoecological, archaeological and historical evidence to understand environmental change and socio-ecological interactions across the Amboseli National Park (Kenya) during the last 5000 years. The combination of climatic aridity and fire, together with cattle and wild animal activity, have led to changes in woody to grass cover ratio. Especially significant is the recent reduction of woody vegetation and the increase of wetlands due to increasing runoff and flooding.

Oceania

McGlone et al. review the ecological dynamics of the New Zealand conifers since the LGM, on the basis of the existing pollen records. Conifer forests attained their maximum development by 18,000 years ago and declined during the Holocene, especially after the Māori settlement. The ecological success of conifers is explained in terms of a bimodal ability to endure climatic stress in cool/arid climates and to successfully compete with angiosperms in warmer/wetter environments.

LARGE-SCALE REVIEWS AND META-ANALYSES

This section includes two studies that use pollen data stored in global databases to address large-scale issues such as continental

forest cover trends and the potential causes of worldwide glaciations. Regarding forests, Zanon et al. used the available pollen records to map the evolution of forest cover on Europe during the last 12,000 years. The general forest cover increased in the Late Glacial-Holocene transition attaining a maximum between 8500 and 6000 cal yr BP, followed by a general decline due to anthropogenic deforestation. The full continental coverage and the spatio-temporal resolution of this reconstruction make it suitable for climatic, hydrological and geochemical modeling. Sánchez-Goñi et al. review the paleoclimatic information contained in long continuous deep-sea pollen records from the European margin, particularly in relation to the interplay among North Atlantic SST, continental ice volume, millennial-scale variability and orbital forcing. The authors propose that the interaction between long-term (orbital) and short-term (millennial) climatic variability may have amplified insolation decreases and triggered ice ages.

We hope that this RT will serve to appraise the state of the art of modern palynology and highlight the usefulness of our discipline in long-term ecological research.

AUTHOR CONTRIBUTIONS

All authors listed have made a substantial, direct and intellectual contribution to the work, and approved it for publication.

REFERENCES

- Birks, H. J. B., and Berglund, B. E. (2018). One hundred years of Quaternary pollen analysis 1916–2016. *Veget. Hist. Archaeobot.* 27, 271–309. doi: 10.1007/s00334-017-0630-2
- Gaillard, M.-J., Berglund, B. E., Birks, H. J. B., Edwards, K. J., and Bittmann, F. (2018). “Think horizontally, act vertically”: the centenary (1916–2016) of pollen analysis and the legacy of Lennart von Post. *Veget. Hist. Archaeobot.* 27, 267–269. doi: 10.1007/s00334-017-0656-5
- Nordlund, C. (2018). Four points on Lennart von Post and the invention of “pollen statistics”. *Veget. Hist. Archaeobot.* 27, 311–317. doi: 10.1007/s00334-017-0628-9
- Von Post, L. (1918). “Skogsträdpollen i sydsvenska torvmosselagerföljder,” in *Forhandlingar ved de Skandinaviske Naturforskere* 16. Møte i Kristiania den 10–15. Juli 1916. *Skandinaviska Naturforskaremöten* (Oslo), 432–465.

- Von Post, L. (1967). Forest tree pollen in South Swedish peat bog deposits, translated by Margaret Bryan Davis and Knut Fægri. *Pollen Spores* 9, 378–401.

Conflict of Interest Statement: The authors declare that the research was conducted in the absence of any commercial or financial relationships that could be construed as a potential conflict of interest.

Copyright © 2018 Rull, Montoya, Giesecke and Morris. This is an open-access article distributed under the terms of the Creative Commons Attribution License (CC BY). The use, distribution or reproduction in other forums is permitted, provided the original author(s) and the copyright owner(s) are credited and that the original publication in this journal is cited, in accordance with accepted academic practice. No use, distribution or reproduction is permitted which does not comply with these terms.



Poaceae Pollen from Southern Brazil: Distinguishing Grasslands (Campos) from Forests by Analyzing a Diverse Range of Poaceae Species

Jefferson N. Radaeski^{1,2}, Soraia G. Bauermann^{2*} and Antonio B. Pereira¹

¹ Universidade Federal do Pampa, São Gabriel, Brazil, ² Laboratório de Palinologia da Universidade Luterana do Brasil–ULBRA, Universidade Luterana do Brasil, Canoas, Brazil

This aim of this study was to distinguish grasslands from forests in southern Brazil by analyzing Poaceae pollen grains. Through light microscopy analysis, we measured the size of the pollen grain, pore, and annulus from 68 species of Rio Grande do Sul. Measurements were recorded of 10 forest species and 58 grassland species, representing all tribes of the Poaceae in Rio Grande do Sul. We measured the polar, equatorial, pore, and annulus diameter. Results of statistical tests showed that arboreal forest species have larger pollen grain sizes than grassland and herbaceous forest species, and in particular there are strongly significant differences between arboreal and grassland species. Discriminant analysis identified three distinct groups representing each vegetation type. Through the pollen measurements we established three pollen types: larger grains ($>46\ \mu\text{m}$), from the Bambuseae pollen type, medium-sized grains ($46\text{--}22\ \mu\text{m}$), from herbaceous pollen type, and small grains ($<22\ \mu\text{m}$), from grassland pollen type. The results of our compiled Poaceae pollen dataset may be applied to the fossil pollen of Quaternary sediments.

Keywords: pollen morphology, grasses, pampa, South America, Atlantic forest, bamboo pollen

OPEN ACCESS

Edited by:

Encarni Montoya,
Institute of Earth Sciences Jaime
Almera (CSIC), Spain

Reviewed by:

José Tasso Felix Guimarães,
Vale Institute of Technology, Brazil
Lisa Schüler-Goldbach,
Göttingen University, Germany

*Correspondence:

Jefferson N. Radaeski
jefferson.radaeski@gmail.com

Specialty section:

This article was submitted to
Agroecology and Land Use Systems,
a section of the journal
Frontiers in Plant Science

Received: 18 August 2016

Accepted: 21 November 2016

Published: 06 December 2016

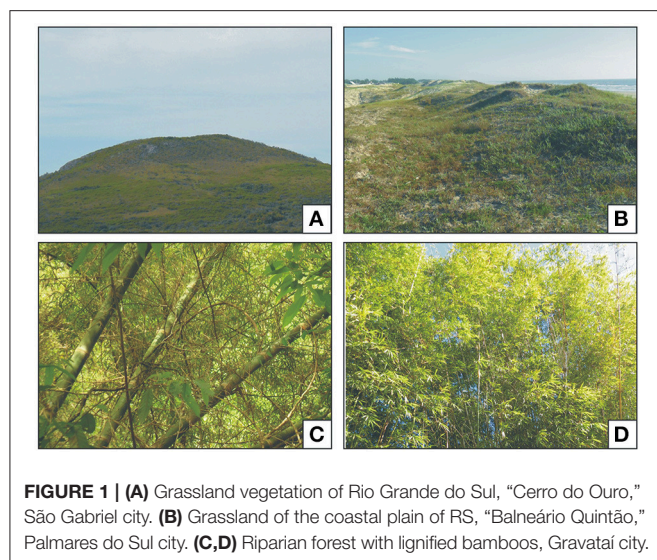
Citation:

Radaeski JN, Bauermann SG and
Pereira AB (2016) Poaceae Pollen
from Southern Brazil: Distinguishing
Grasslands (Campos) from Forests by
Analyzing a Diverse Range of Poaceae
Species. *Front. Plant Sci.* 7:1833.
doi: 10.3389/fpls.2016.01833

INTRODUCTION

Pollen grains of the family Poaceae are widely found in Quaternary sediments of southern Brazil (e.g., Behling et al., 2004; Macedo et al., 2007; Bauermann et al., 2008). However, the stenopalynous nature of the pollen from this family makes it difficult to determine subfamilies and genera using pollen data (Erdtman, 1952; Salgado-Labouriau, 1973). Consequently, low taxonomic resolution hampers paleoecological inferences. Being mainly associated with grassland vegetation (**Figure 1**), Poaceae pollen is usually interpreted as indicative of open formations. However in Rio Grande do Sul (RS), where more than 80% of Poaceae species occupy grasslands, a significant percentage (20%) of representatives of this family inhabit forest vegetation (Boldrini and Longhi-Wagner, 2011).

Although the Poaceae family is well represented and studied in RS, few studies have examined the pollen representatives of this family. The few descriptions or illustrations of pollen representatives presented in the study by Tedesco et al. (1999), which analyzed the diameter of the pollen grains of *Hemarthria altissima* under different ploidy levels, noted that the average diameters were variable, depending on the ploidy. However, the analyzed pollen grains were not acetolyzed. Medeanic et al. (2008) illustrated images of pollen grains from nine species, while Wilberger et al. (2004) presented images of pollen grains corresponding to three separate species. Nakamura et al. (2010), addressing the development of anther and pollen grains in *Axonopus aureus*, *Chloris elata*, *h*



Eragrostis solida, *Olyra humilis*, *Paspalum polyphyllum*, and *Sucrea monophylla*, found similar pollen morphology between taxa. This excludes those grains that have been observed to have patterns that are important for differentiation between species of the family. Radaeski et al. (2011) described the pollen morphology of *Paspalum notatum*, *Paspalum plicatulum*, and *Schizachyrium microstachyum*. Later, Bauermann et al. (2013) described the pollen grains of *Andropogon lateralis* and *Eragrostis bahiensis*. Radaeski et al. (2014a) described the pollen morphology of *Eragrostis neesii*, and Radaeski et al. (2014b) contributed to the pollen description of six taxa of Poaceae, which showed that, in general, the pollen grains are of average size, with a monoaperture and spherical forms, and noted the identified stenopalynous characteristic of the family.

In South America, studies have been conducted on Poaceae pollen grains from Venezuela, Chile, Brazil, and Argentina (Heusser, 1971; Markgraf and D'Antoni, 1978; Salgado-Labouriau and Rinaldi, 1990). In Chile, the overlap between dimensions of the pollen grains of some tribes made it difficult to differentiate between tribes or subfamilies (Heusser, 1971). Thus, further studies on the pollen grains from other taxa are needed. Likewise, the same is true of the pollen grains of Barro Colorado Island (Roubik and Moreno, 1991). However, analyses of many species that are based solely on one pollen grain cannot verify the variations in total pollen grain diameter of the species. Analyzing pollen grains from Argentina, Markgraf and D'Antoni (1978) observed—from other grassland species studied—the largest diameter of pollen grain of the bamboo *Chusquea culeou*. Thus, analysis of pollen grains from other forest species can provide patterns related to vegetation from this site.

The pollen grains of many species from other regions of the world (e.g., Europe, South America) have been analyzed by scanning electron microscopy (SEM). Some of these species also inhabit southern Brazil. Some studies (Table 1) have explored the surface of the Poaceae pollen grains through SEM, which has contributed to separation of taxonomic groups (Köhler and Lange, 1979; Linder and Ferguson, 1985; Chaturvedi et al., 1994,

TABLE 1 | Dataset of Poaceae analyzed species, type of microscopy used and vegetation type.

Vegetation type	Microscopy type	Number of species	Reference
Grassland	SEM	5	Ahmad et al., 2011
Grassland	LM	2	Bauermann et al., 2013
Grassland	LM/SEM	4	Chaturvedi and Datta, 2001
Grassland	SEM	2	Chaturvedi et al., 1994
Grassland	LM/SEM	19	Chaturvedi et al., 1998
Grassland/Forest	LM/SEM	30	Côrrea et al., 2005
Grassland	LM/SEM	6	Datta and Chaturvedi, 2004
Grassland/Forest	SEM	86	Dórea, 2011
Grassland/Forest	LM	16	Heusser, 1971
Grassland	LM	160	Jan et al., 2014
Grassland	LM	35	Joly et al., 2007
Grassland	LM/SEM	2	Kashikar and Kalkar, 2010
Grassland	LM	11	Katsiotis and Forsberg, 1995
Grassland	SEM	12	Köhler and Lange, 1979
Grassland	LM/SEM	1	Linder and Ferguson, 1985
Grassland	SEM	57	Liu et al., 2004
Grassland	LM/SEM	1	Liu et al., 2005
Grassland/Forest	SEM	19	Mander and Punyasena, 2016
Grassland	SEM	12	Mander et al., 2013
Grassland	SEM	12	Mander et al., 2014
Grassland/Forest	LM	17	Markgraf and D'Antoni, 1978
Grassland	LM	9	Medeanic et al., 2008
Grassland	LM	3	Melhem et al., 2003
Grassland	LM/SEM	45	Morgado et al., 2015
Grassland/Forest	LM	6	Nakamura et al., 2010
Grassland	LM/SEM	4	Nazir et al., 2013
Grassland	LM/SEM	31	Needham et al., 2015
Grassland	LM/SEM	54	Perveen and Qaiser, 2012
Grassland	LM/SEM	20	Perveen, 2006
Grassland	LM	3	Radaeski et al., 2011
Grassland	LM	1	Radaeski et al., 2014a
Grassland	LM	6	Radaeski et al., 2014b
Grassland/Forest	LM	64	Roubik and Moreno, 1991
Grassland/Forest	LM	49	Salgado-Labouriau and Rinaldi, 1990
Grassland	LM	—(fossil pollen)	Schüler and Behling, 2011a
Grassland	LM	—(fossil pollen)	Schüler and Behling, 2011b
Grassland/Forest	SEM	11	Skvarla et al., 2003
Grassland	LM	1	Tedesco et al., 1999
Grassland	LM	3	Wilberger et al., 2004

1998; Chaturvedi and Datta, 2001; Skvarla et al., 2003; Datta and Chaturvedi, 2004; Liu et al., 2004, 2005; Perveen, 2006; Kashikar and Kalkar, 2010; Ahmad et al., 2011; Dórea, 2011;

Perveen and Qaiser, 2012; Mander et al., 2013, 2014; Nazir et al., 2013; Morgado et al., 2015; Needham et al., 2015; Mander and Punyasena, 2016). However, other studies using light microscopy (LM) have shown morphometric differences in the size of the Poaceae pollen grain species (Salgado-Labouriau and Rinaldi, 1990; Katsiotis and Forsberg, 1995; Joly et al., 2007; Schüler and Behling, 2011a,b; Jan et al., 2014). In addition, when analyzing large sets of palynomorphs from quaternary sediments, the use of SEM is a difficult and time-consuming task. Thus, morphometric datasets may be valuable for use in studies of fossil Poaceae pollen analysis (Schüler and Behling, 2011a,b; Jan et al., 2014).

Recently, studying pollen grains of fossil Poaceae in the grassland ecosystems of South America, Schüler and Behling (2011a) discovered potential new ways to distinguish grassland types. In their later study, Schüler and Behling (2011b) were able to differentiate the ecosystems present in South America. Moreover, Jan et al. (2014) succeeded in identifying a pattern among changes in the size of Poaceae pollen grains according to the ploidy level and C₃ and C₄ metabolism, thereby demonstrating that polyploid species have a larger pollen grain size. C₄ species are tropical and inhabit warmer and drier regions, while temperate Poaceae species are C₃ and live in humid and cold conditions (Boldrini, 2006). C₃ and C₄ species are important for paleoclimate studies because they indicate past variation in temperature and precipitation (Schüler and Behling, 2011a).

The aim of the study was to distinguish Poaceae pollen grains from grassland and forest vegetation of southern Brazil. The pollen grains of 68 species were analyzed to answer the following questions: (1) Can Poaceae pollen grains be separated into those of grassland species and those of forest species? (2) Do the pollen grains of forest species differ in size according to their arboreal or herbaceous habit?

MATERIALS AND METHODS

Collection of Botanical Material

During the field expeditions, 98 specimens of Poaceae were obtained, anticipating the 21 taxa representatives of this family, and some pollen material, being fertile, was selected for extraction. To obtain hibernal and estival plants in the flowering seasons, the samples were gathered using the transversal method (Filgueiras et al., 1994) in winter, autumn, spring, and summer in May, August, September, October, November, and December of 2013, as well as in January of 2014.

After collection, the plants were pressed and dehydrated. The plants were identified by a skilled taxonomist (A. A. Schneider). The collection of herbarium specimens was deposited in the “Herbário do Museu de Ciências Naturais” from the Universidade Luterana do Brasil (MCNU/HERULBRA), and duplicates were deposited in the “Herbário Bruno Edgar Irgang” from Unipampa (HBEI/UNIPAMPA). The anthers were collected for chemical treatment of the herbarium materials from other Poaceae species. Since some species have state-restricted distribution, or sporadic bloom periods, samples were collected from pollen material in accordance with information provided by the ICN Herbarium (Figure 2, Table 2).

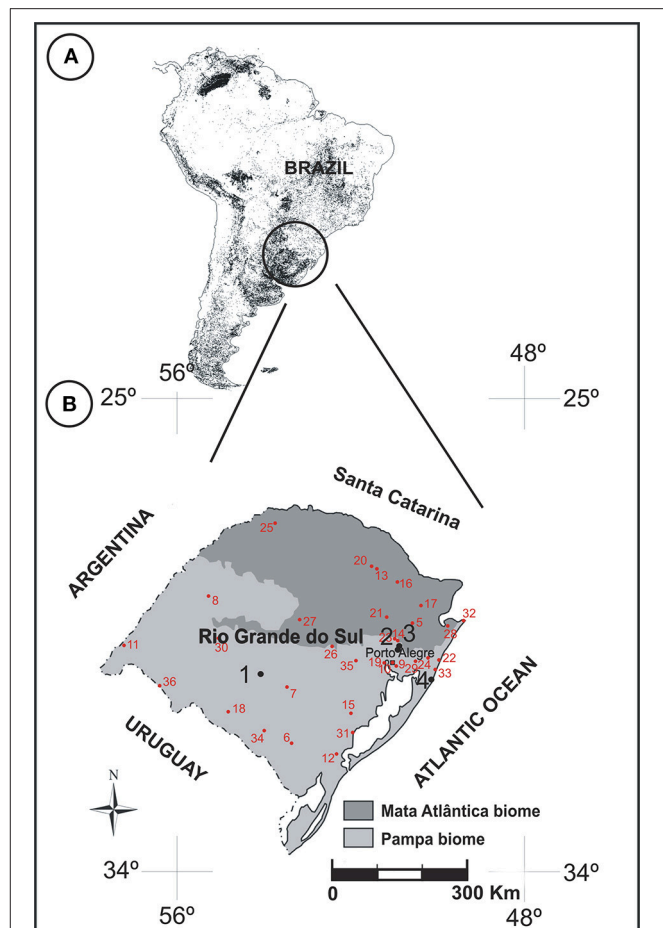


FIGURE 2 | (A) Distribution of grasslands in South America highlighting the southern region of Brazil (adapted from Eva et al., 2002). **(B)** Map of Rio Grande do Sul showing the sampling sites in RS (black circles): 1. “Cerro do Ouro,” São Gabriel city; 2. Cachoeirinha city; 3. “Sítio Laranjal,” Gravataí city; 4. “Balneário Quintão,” Palmares do Sul city. Red circles indicate regions of collection of herbarium species (see Table 2 for more details of the names of regions).

The collection of pollen materials from a herbarium (containing plants from different regions of the state) enabled the authors of this study to establish an overview of the modern grass pollen of RS. By combining the findings of this study with the work of Hasenack et al. (2010) on the vegetation physiognomy of the state, we were able to establish a relationship between the pollen and the regional flora. Only 50 Poaceae species of four subfamilies comprise forest vegetation. Thus, we considered the selection of 10 forest species from all tribes and subfamilies for pollen analysis to be adequate. More species of grassland (58 species) were analyzed because there are a greater number of Poaceae species (450 species) in southern Brazil (Boldrini and Longhi-Wagner, 2011) than forest species.

Treatment and Description of Pollen Grains

The anthers were chemically processed according to the acetolysis methodology proposed by Erdtman (1952). After acetolysis, using glycerinated jelly, five permanent slides were

TABLE 2 | Information of the examined material in the Rio Grande do Sul, Brazil.

Species	Collection site–Number*	Collector
<i>Agrostis</i> sp. L.	São Francisco de Paula–5	Z. Rúgolo, H. Longhi-Wagner, S. Boechat and A.M. Molina 1435
<i>Aira elegans</i> Willd. ex Gaudin	Pinheiro Machado–6	I. I. Boldrini 1143
<i>Amphibromus quadridentatus</i> (Döll) Swallen	São Francisco de Paula–5	Longhi-Wagner, Boldrini, and Miotto 2654
<i>Andropogon</i> cf. <i>lindmanii</i> Hack.	Palmares do Sul–4	J. N. Radaeski
<i>Andropogon lateralis</i> Nees	Caçapava do Sul–7	S. G. Bauermann
<i>Aristida</i> sp. L.	Itacurubi–8	S. G. Bauermann
<i>Arundinella hispida</i> (Humb. and Bonpl. ex Willd.) Kuntze	Viamão–9	R. Trevisan and Boldrini 830
<i>Axonopus</i> sp. P. Beauv	Itacurubi–8	S. G. Bauermann
<i>Bothriochloa laguroides</i> (DC.) Herter	Porto Alegre–10	M. Marchi 97
<i>Bouteloua megapotamica</i> (Spreng.) Kuntze	Uruguaiana–11	H. S. A. 74
<i>Bromus catharticus</i> Vahl	Cachoeirinha–2	J. N. Radaeski
<i>Calamagrostis viridiflavescens</i> (Poir.) Steud	Pelotas–12	I. Gabino 20
<i>Catapodium rigidum</i> (L.) C.E.Hubb	Porto Alegre–10	J. Valls
<i>Chascolytrum subaristatum</i> (Lam.) Desv	São Gabriel–1	J. N. Radaeski
<i>Chloris cantherae</i> Arechav	Uruguaiana–11	J. Valls and A. Barcellos 2477
<i>Chusquea juergensii</i> Hack.	Passo Fundo–13	J. Valls, H. Longhi-Wagner, and A. Barcellos 3081
<i>Colantheria cingulata</i> (McClure and L.B.Sm.) McClure	Araricá–14	R. Schmidt and Ene
<i>Cynodon dactylon</i> (L.) Pers	Gravataí–3	J. N. Radaeski
<i>Dactylis glomerata</i> L.	Porto Alegre–10	J. Valls
<i>Danthonia montana</i> Döll	Cristal–15	A. Guglieri, F. J. M. Caporal, S. Mochiutti, and M. Behling 533
<i>Digitaria ciliata</i> (Retz.) Koeler	Vacaria–16	B. Irgang and M. L. Porto
<i>Eleusine tristachya</i> (Lam.) Lam	Cachoeirinha–2	J. N. Radaeski
<i>Elionurus candidus</i> (Trin.) Hack.	Porto Alegre–10	R. Setubal 235
<i>Eragrostis bahiensis</i> Schrad. ex Schult	Gravataí–3	J. N. Radaeski
<i>Eragrostis neesii</i> Trin	São Gabriel–1	J. N. Radaeski
<i>Eustachys distichophylla</i> (Lag.) Nees	Porto Alegre–10	R. Setubal 683
<i>Festuca fimbriata</i> Nees	Jaquirana–17	I. Boldrini 1636
<i>Glyceria multiflora</i> Steud	Dom Pedrito–18	Valls, Gonçalves, Salles, and Moraes 6959
<i>Guadua trinii</i> (Nees) Nees ex Rupr	Guaíba–19	N. I. Matzembacher 2293
<i>Gymnopogon spicatus</i> (Spreng.) Kuntze	Lagoa Vermelha–20	Boldrini, Pillar, Kafpel, and Jacques 334
<i>Holcus lanatus</i> L.	Caxias do Sul–21	K. Hagelund 3797
<i>Hordeum stenostachys</i> Godr	Dom Pedrito–18	H. Longhi-Wagner 1560
<i>Ichnanthus pallens</i> (Sw.) Munro ex Benth	Guaíba–19	V. Citadini 59
<i>Imperata brasiliensis</i> Trin	Tramandaí–22	Waechter 1019
<i>Ischaemum minus</i> J.Presl	Gravataí–3	J. N. Radaeski
<i>Leersia</i> sp. Sol. ex Sw	Dois Irmãos–23	H. M. Longhi-Wagner
<i>Leptochloa fusca</i> (L.) Kunth	Osório–24	J. Valls et al. 4760
<i>Lithachne pauciflora</i> (Sw.) P.Beauv	Tenente Portela–25	Valls, Lindeman, Irgang, Oliveira, and Pott 1782
<i>Luziola peruviana</i> Juss. ex J.F.Gmel	Porto Alegre–10	Lacê
<i>Melica</i> sp. L.	São Gabriel–1	J. N. Radaeski
<i>Merostachys multiramea</i> Hack	Santa Cruz do Sul–26	V. Kinupp
<i>Microchloa indica</i> (L.f.) P. Beauv	Porto Alegre–10	H.M. Longhi-Wagner and C.A.D. Welker 9757a
<i>Muhlenbergia schreberi</i> J.F.Gmel	Estrela Velha–27	R. Trevisan
<i>Olyra latifolia</i> L.	Morrinhos do Sul–28	L. C. Mancino, T. B. Guimarães, L. R. M. Batista, and G. E. Ferreira
<i>Panicum aquaticum</i> Poir	Capivari do Sul–29	E. N. Garcia 892
<i>Pappophorum philippianum</i> Parodi	São Francisco de Assis–30	E. Freitas 359
<i>Parodiolyra micrantha</i> (Kunth) Davidse and Zuloaga	Gravataí–3	J. Valls, J. Jung, and A. M. Barcellos 2151
<i>Paspalum notatum</i> Flügge	Caçapava do Sul–7	S. G. Bauermann
<i>Paspalum pauciciliatum</i> (Parodi) Herter	Gravataí–3	J. N. Radaeski

(Continued)

TABLE 2 | Continued

Species	Collection site–Number*	Collector
<i>Paspalum unvillei</i> Steud	Palmares do Sul–4	J. N. Radaeski
<i>Phalaris angusta</i> Nees ex Trin	São Lourenço do Sul–31	C. Bonilha 486
<i>Pharus lappulaceus</i> Aubl	Gravataí–3	L. R. M. Baptista
<i>Piptochaetium montevidense</i> (Spreng.) Parodi	São Gabriel–1	J. N. Radaeski
<i>Poa bonariensis</i> (Lam.) Kunth	Vacaria–16	A. Kappel
<i>Polypogon elongatus</i> Kunth	Torres–32	A. Barcelos and B. Irgang 9
<i>Schizachyrium microstachyum</i> (Desv. ex Ham.) Roseng	Caçapava do Sul–7	S. G. Bauermann
<i>Setaria parviflora</i> (Poir.) Kerguelen	Gravataí–3	J. N. Radaeski
<i>Spartina ciliata</i> Brongn	Cidreira–33	H. M. Longhi-Wagner and S. Leite
<i>Sporobolus indicus</i> (L.) R.Br	Gravataí–3	J. N. Radaeski
<i>Stipa filifolia</i> Nees	Bagé–34	H. M. Longhi-Wagner 5042
<i>Stipa melanosperma</i> J. Presl	São Francisco de Paula–5	R. L. C. Bortoluzzi 816
<i>Stipa papposa</i> Nees	Bagé–34	I. Boldrini 1177
<i>Stipa setigera</i> J.Presl	Bagé–34	S. C. Boechat
<i>Streptochaeta spicata</i> Schrad. ex Nees	Torres–32	J. F. M. Valls 1055
<i>Tridens brasiliensis</i> (Nees ex Steud.) Parodi	Cachoeira do Sul–35	J. Valls
<i>Trachypogon filifolius</i> (Hack.) Hitchc	Quaraí–36	Boldrini and Pilz187
<i>Tripogon spicatus</i> (Nees) Ekman	Quaraí–36	Boldrini, Barreto, Boechat and Pillar 279

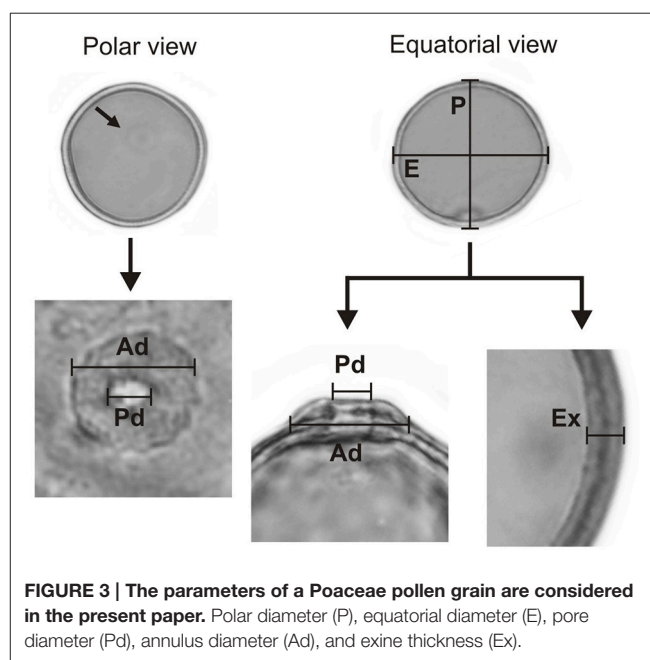
*Numbers corresponding to the Map of **Figure 2B**.

created for each sample and deposited in the Laboratório de Palinologia da ULBRA. The pollen grains were measured and the slides mounted on the same day to prevent any changes in pollen size (Salgado-Labouriau, 2007). Schüller and Behling (2011a) measured 60 pollen grains from fossil pollen samples, but in this paper we studied modern pollen grains, measuring 25 pollen grains according to the methodology used for the study of modern pollen grains (Erdtman, 1952; Barth and Melhem, 1988).

The morphological characteristics of the pollen grains were observed and described by LM. A Leica CME microscope was used for measurements and for recording images. Using a $\times 1000$ magnification, we recorded the polar diameter (P), equatorial diameter (E), or only the diameter (D) of spherical pollen grains, and the thickness of the exine (Ex) in 25 randomly selected pollen grains. In addition to the above, measurements of the pore and annulus width of the studied species were recorded (**Figure 3**). The pollen grains were then described in regard to their pollen unit, size, symmetry, polarity, amb, type of aperture, and ornamentation, using the terminology proposed by Barth and Melhem (1988) and Punt et al. (2007).

Statistical Analysis

BioEstat 5.0 and PAST 3.05 software was used for the statistical analysis. BioEstat 5.0 software was used to compile a frequency distribution histogram of pollen grain sizes. The histogram was then constructed from the size of the pollen grains of species inhabiting arboreous forest, grassland, and herbaceous forest. This program (BioEstat 5.0) was also used to determine size differences among pollen grains from arboreous forest, grassland, and herbaceous forest species using One-way ANOVA followed by Tukey's test. PAST 3.05 software was used for discriminant analysis (DA) of separate groups according to the size of the



pollen grains. In DA we use the minimum, maximum, and average size of pollen grains of all species to determine whether they can be grouped. We used this program (PAST 3.05) also to show the correlation between pollen grain, annulus, and pore sizes by Pearson correlation. The Pearson's correlation coefficient test was used to determine the average size of the pollen grains, the pore width, and the annulus width for all species (68 species studied). The PAST 3.05 software was also used to construct a box plot. The box plot shows overlapping measures and measures that

TABLE 3 | Pollen morphological measurements of 68 Poaceae species in the region of southern Brazil.

Subfamily	Tribe	Species	Vegetation	Size	Diameter pollen grain (μm)	Aperture	Pore diameter (μm)	Annulus diameter (μm)	Exine (μm)	Figs.
Anomochloideae	Streptochaeteae	<i>Streptochaeta spicata</i>	Forest	Medium	28 (23–32)	monoporate	3 (2–4)	9 (8–10)	1.32	3A-E
Bambusoideae	Bambuseae	<i>Chusquea juergensii</i>	Forest	Large	44 (40–52)	monoporate	5 (4–6)	12 (11–13)	1.08	3F-J
		<i>Colanthea cingulata</i>	Forest	Large	58 (47–74)	monoporate	5 (4–6)	14 (13–15)	1.32	
		<i>Guadua trinii</i>	Forest	Large	60 (50–77)	monoporate	5 (4–6)	14 (13–15)	1.52	
		<i>Merostachys multiramea</i>	Forest	Large	50 (44–55)	monoporate	5 (4–6)	14 (13–15)	1.52	
	Olyreae	<i>Lithachne pauciflora</i>	Forest	Medium	27 (25–28)	monoporate	2 (1–3)	7 (6–8)	1	
		<i>Olyra latifolia</i>	Forest	Medium	27 (23–30)	monoporate	2 (1–3)	6 (5–7)	1.08	3K-O
		<i>Paradiolysa micrantha</i>	Forest	Medium	30 (26–37)	monoporate	3 (2–4)	9 (8–10)	1	
Pharoideae	Phareae	<i>Pharus lappulaceus</i>	Forest	Medium	25 (23–27)	monoporate and diporate	3 (2–4)	8 (7–9)	1.08	3P-T
Ehrharthoideae	Onyzeae	<i>Leersia</i> sp.	Grassland	Medium	27 (23–34)	monoporate	2 (1–3)	7 (6–8)	1	4A-E
		<i>Luziola peruviana</i>	Grassland	Medium	26 (24–30)	monoporate	2 (1–3)	6 (5–7)	1.08	
Danthonioidae	Danthoniaceae	<i>Danthonia montana</i>	Grassland	Medium	28 (22–32)	monoporate	3 (2–4)	8 (7–9)	1	4F-J
Chloridoideae	Eragrostideae	<i>Eragrostis neesii</i>	Grassland	Small	22 (19–26)	monoporate	2,5 (2–3)	5 (4–6)	1	4K-O
		<i>Eleusine tristachya</i>	Grassland	Medium	28 (23–33)	monoporate	3 (2–4)	8 (7–9)	1	
		<i>Eragrostis bahiensis</i>	Grassland	Medium	29 (22–33)	monoporate	3 (2–4)	8 (7–9)	1	
		<i>Leptochloa fusca</i>	Grassland	Medium	25 (21–28)	monoporate	2 (1–3)	6 (5–7)	1	
		<i>Muhlenbergia schreberi</i>	Grassland	Medium	30 (26–35)	monoporate	2 (1–3)	6 (5–7)	1.04	
		<i>Sporobolus indicus</i>	Grassland	Small	22 (18–26)	monoporate	2 (1–3)	6 (5–7)	1	
		<i>Tridens brasiliensis</i>	Grassland	Medium	33 (30–36)	monoporate	3 (2–4)	8 (7–9)	1.1	
		<i>Tripogon spicatus</i>	Grassland	Medium	25 (20–27)	monoporate	2 (1–3)	6 (5–7)	1	
Cynodonteae		<i>Bouteloua megapotamica</i>	Grassland	Medium	34 (25–38)	monoporate	3 (2–4)	9 (8–10)	1	4P-T
		<i>Chloris carterae</i>	Grassland	Medium	33 (27–37)	monoporate	3 (2–4)	8 (7–9)	1.04	
		<i>Cynodon dactylon</i>	Grassland	Medium	28 (24–32)	monoporate	3 (2–4)	8 (7–9)	1.04	
		<i>Eustachys distichophylla</i>	Grassland	Medium	30 (25–35)	monoporate	2 (1–3)	7 (6–8)	1.08	
		<i>Gymnopogon spicatus</i>	Grassland	Medium	34 (29–39)	monoporate	3 (2–4)	9 (8–10)	1.12	
		<i>Microchloa indica</i>	Grassland	Medium	25 (22–30)	monoporate	2 (1–3)	6 (5–7)	1	
		<i>Spartina ciliata</i>	Grassland	Medium	34 (32–37)	monoporate	3 (2–4)	8 (7–9)	1	
Pappophoreae		<i>Pappophorum philippianum</i>	Grassland	Medium	30 (25–36)	monoporate	3 (2–4)	7 (6–8)	1	5A-E
Aristidoideae	Aristideae	<i>Aristida</i> sp.	Grassland	Medium	31 (26–33)	monoporate	3 (2–4)	8 (7–9)	1.08	5F-J; 8A,B
Pooideae	Poeae	<i>Agrostis</i> sp.	Grassland	Medium	29 (26–34)	monoporate	3 (2–4)	9 (8–10)	1	
		<i>Aira elegans</i>	Grassland	Small	22 (16–25)	monoporate	2 (1–3)	6 (5–7)	1.04	
		<i>Amphibromus quadridentatus</i>	Grassland	Medium	35 (32–38)	monoporate	3 (2–4)	9 (8–10)	1	
		<i>Calamagrostis viridiflavescens</i>	Grassland	Medium	28 (24–32)	monoporate	3 (2–4)	9 (8–10)	1.04	

(Continued)

TABLE 3 | Continued

Subfamily	Tribe	Species	Vegetation	Size	Diameter pollen grain (μm)	Aperture	Pore diameter (μm)	Annulus diameter (μm)	Exine (μm)	Figs.
Panicoideae		<i>Catapodium rigidum</i>	Grassland	Small	24 (22–27)	monoporate	2 (1–3)	6 (5–7)	1	5K-O
		<i>Chascolytrium subaristatum</i>	Grassland	Medium	29 (21–32)	monoporate	3 (2–4)	8 (7–9)	1.1	
		<i>Dactylis glomerata</i>	Grassland	Medium	33 (29–37)	monoporate	3 (2–4)	9 (8–10)	1.04	
		<i>Festuca fibrinata</i>	Grassland	Medium	35 (28–39)	monoporate	3 (2–4)	9 (8–10)	1	
		<i>Glyceria multiflora</i>	Grassland	Medium	36 (33–39)	monoporate	3 (2–4)	10 (9–11)	1	
		<i>Holcus lanatus</i>	Grassland	Medium	25 (23–28)	monoporate	2 (1–3)	6 (5–7)	1	5P-T 6A-E 6F-J 6K-O; 8C
		<i>Poa bonariensis</i>	Grassland	Medium	28 (25–32)	monoporate	3 (2–4)	9 (8–10)	1	
		<i>Phalaris angusta</i>	Grassland	Medium	35 (32–39)	monoporate	3 (2–4)	9 (8–10)	1	
		<i>Polypogon elongatus</i>	Grassland	Medium	32 (27–37)	monoporate	3 (2–4)	8 (7–9)	1	
		<i>Bromus catharticus</i>	Grassland	Medium	37 (32–43)	monoporate	3 (2–4)	9 (8–10)	1.2	
		<i>Melica</i> sp.	Grassland	Medium	30 (25–33)	monoporate	2 (1–3)	7 (6–8)	1	
		<i>Hordeum stenostachys</i>	Grassland	Medium	37 (33–40)	monoporate	3 (2–4)	9 (8–10)	1	
		<i>Piptochaetium montevidense</i>	Grassland	Medium	27 (23–29)	monoporate	3 (2–4)	9 (8–10)	1.04	
		<i>Stipa filifolia</i>	Grassland	Medium	30 (27–35)	monoporate	3 (2–4)	9 (8–10)	1.04	
		<i>Stipa melanosperma</i>	Grassland	Medium	38 (34–39)	monoporate	3 (2–4)	10 (9–11)	1	
		<i>Stipa papposa</i>	Grassland	Medium	28 (24–35)	monoporate	3 (2–4)	9 (8–10)	1.04	
		<i>Stipa setigera</i>	Grassland	Medium	31 (25–34)	monoporate	3 (2–4)	9 (8–10)	1.04	
		<i>Axonopus</i> sp.	Grassland	Medium	29 (22–37)	monoporate	3 (2–4)	7 (6–8)	1	
		<i>Digitaria ciliata</i>	Grassland	Medium	37 (34–40)	monoporate and diporate	3 (2–4)	9 (8–10)	1.04	
		<i>Ichnanthus pallens</i>	Forest	Small	23 (22–26)	monoporate	2 (1–3)	6 (5–7)	1	6P-T
		<i>Panicum aquaticum</i>	Grassland	Medium	35 (30–40)	monoporate	3 (2–4)	9 (8–10)	1.24	
		<i>Paspalum notatum</i>	Grassland	Medium	34 (32–39)	monoporate	2.5 (2–3)	6 (5–7)	1.2	
		<i>Paspalum pauciciliatum</i>	Grassland	Medium	42 (37–46)	monoporate and diporate	3 (2–4)	8 (7–9)	1.04	
		<i>Paspalum unvillei</i>	Grassland	Medium	33 (29–36)	monoporate	3 (2–4)	9 (8–10)	1	
Andropogoneae		<i>Setaria parviflora</i>	Grassland	Medium	34 (30–37)	monoporate	3 (2–4)	8 (7–9)	1.2	7A-E 7F-J
		<i>Steinchisma hians</i>	Grassland	Medium	24 (18–27)	monoporate	2 (1–3)	6 (5–7)	1	
		<i>Andropogon lateralis</i>	Grassland	Medium	32 (28–36)	monoporate	4 (3–5)	9 (8–10)	1.2	
		<i>Andropogon cf. lindmanii</i>	Grassland	Medium	38 (34–41)	monoporate	3 (2–4)	9 (8–10)	1	
		<i>Bothriochloa laguroides</i>	Grassland	Medium	36 (33–38)	monoporate	3 (2–4)	8 (7–9)	1.2	
		<i>Elionurus candidus</i>	Grassland	Medium	35 (28–39)	monoporate	3 (2–4)	9 (8–10)	1.04	
		<i>Imperata brasiliensis</i>	Grassland	Medium	36 (33–39)	monoporate	3 (2–4)	9 (8–10)	1.04	
		<i>Ischaemum minus</i>	Grassland	Medium	33 (30–37)	monoporate	3 (2–4)	8 (7–9)	1.04	
		<i>Schizachyrium microstachyum</i>	Grassland	Medium	30 (24–36)	monoporate	3 (2–4)	9 (8–10)	1.3	
		<i>Trachypogon filifolius</i>	Grassland	Medium	37 (31–42)	monoporate	3 (2–4)	9 (8–10)	1.24	
Arundinelleae		<i>Arundinella hispida</i>	Grassland	Medium	25 (21–30)	monoporate	2 (1–3)	7 (6–8)	1	

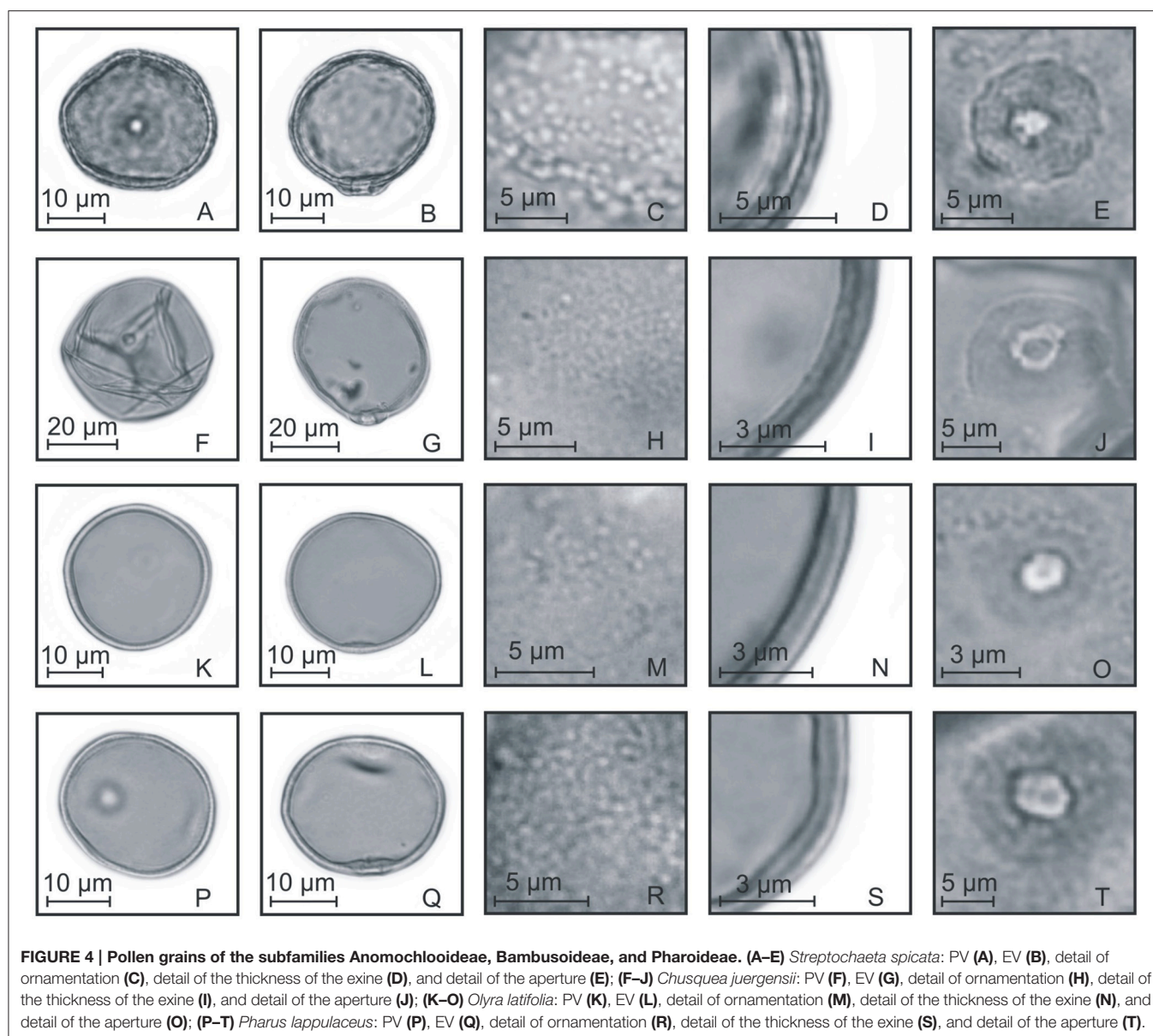


FIGURE 4 | Pollen grains of the subfamilies Anomochlooideae, Bambusoideae, and Pharoideae. (A–E) *Streptochaeta spicata*: PV (A), EV (B), detail of ornamentation (C), detail of the thickness of the exine (D), and detail of the aperture (E); (F–J) *Chusquea juergensii*: PV (F), EV (G), detail of ornamentation (H), detail of the thickness of the exine (I), and detail of the aperture (J); (K–O) *Olyra latifolia*: PV (K), EV (L), detail of ornamentation (M), detail of the thickness of the exine (N), and detail of the aperture (O); (P–T) *Pharus lappulaceus*: PV (P), EV (Q), detail of ornamentation (R), detail of the thickness of the exine (S), and detail of the aperture (T).

do not overlap. We used all the pollen grain size measurements for the box plot (i.e., 25 measures each of 68 species = total 1700 measures).

RESULTS

Measurement of Pollen Grains

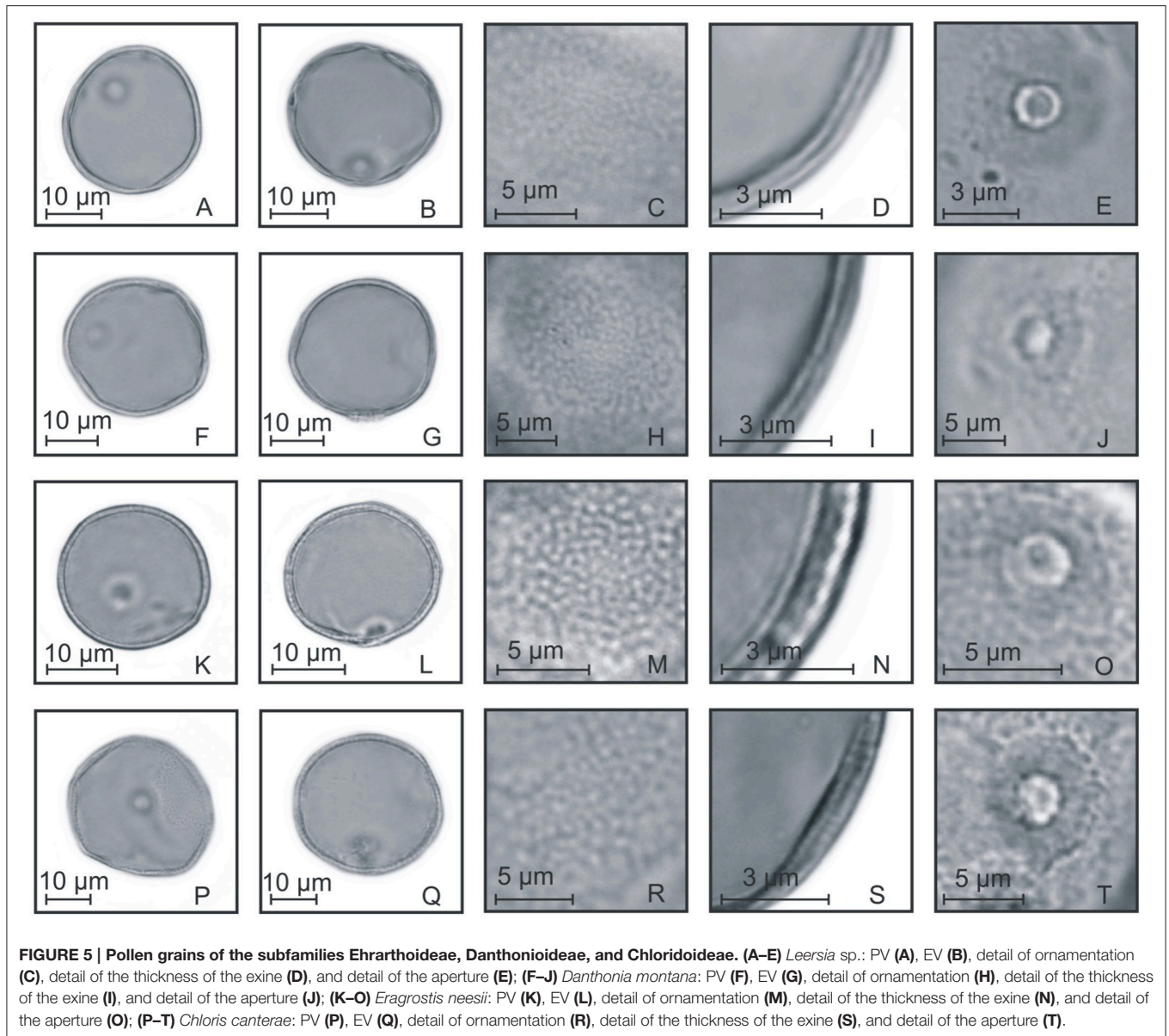
Table 3 presents the measurements of the pollen grains for the 68 species, in evolutionary order according to the GPWG (Grass Phylogeny Working Group) classification (2001). Yet, differences were observed in the measurements of pollen grains, pores, and annulus. Pollen grains of species of each tribe were selected to show the Poaceae morphological characteristics of all the tribes of southern Brazil (Figures 4–8).

A frequency distribution histogram of the measurements of pollen size is shown in Figure 9A. The average measurement

values were higher for arboreous forest (8% of the measurements of these species were 50 μm). Grassland and herbaceous forest species had lower average measurement values (16% of the forest herbaceous species measured 27 μm, and 8% of the grassland species measured 32 μm). Grain size distributions showed a Gaussian distribution for samples of arboreous forest, grassland, and herbaceous forest species (Figures 9B–E). The Gaussian distribution showed that ANOVA-Tukey can be applied to the data set.

Morphometric Variation in Diameters of the Pollen Grains, Pores, and Annulus

The ANOVA-Tukey test showed statistically significant differences between the size of pollen grains of arboreous forest, grassland, and herbaceous forest species (Table 4). This difference is clear in the comparison of samples that indicate



values (p) less than 0.01. The difference between the means of the arboreous forest and grassland samples was large (22.1719), while among the grassland and herbaceous forest samples the difference was small (4.3681).

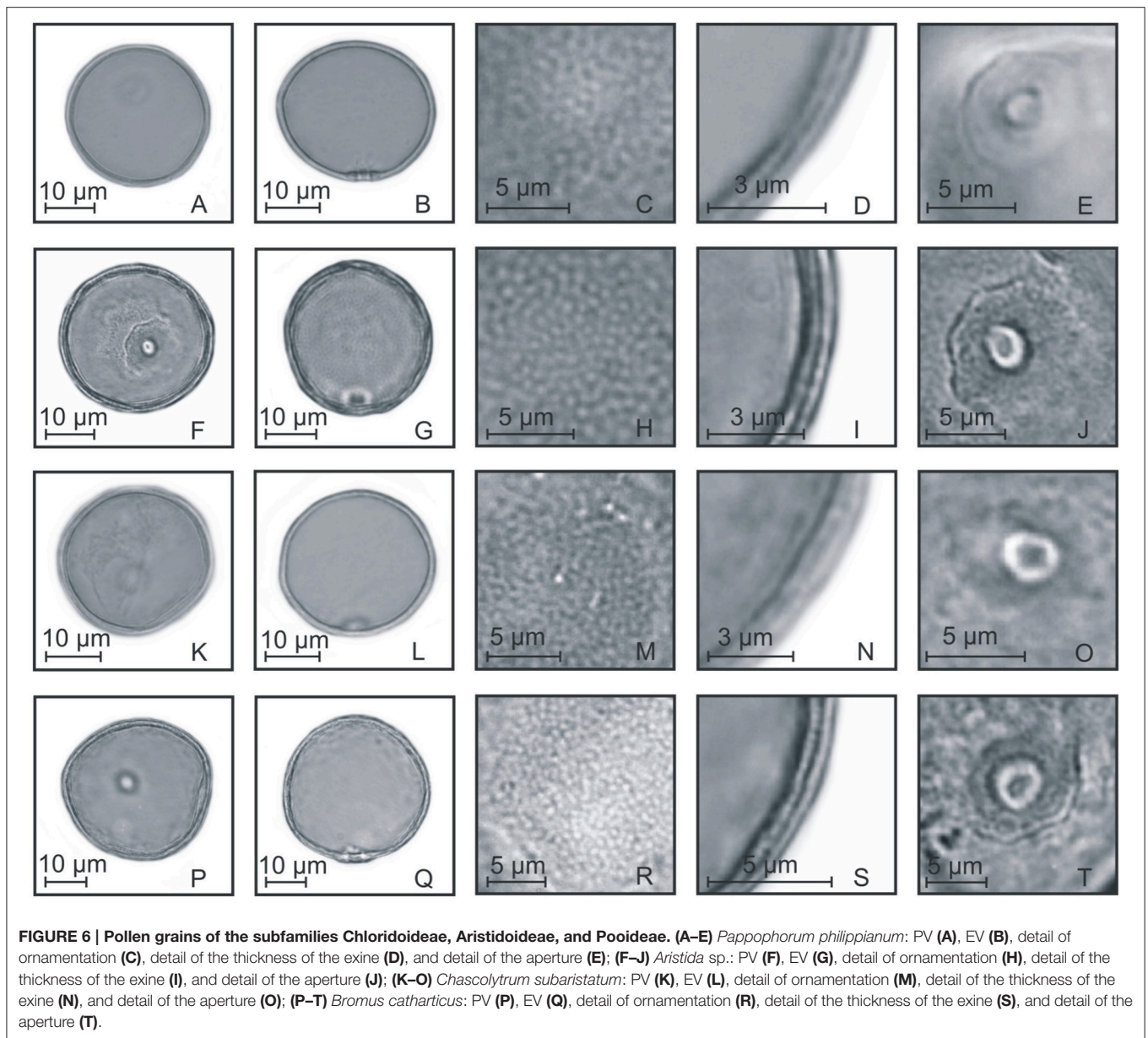
The DA test (Figure 10) determined the separation of three groups according to the values of the variables. The DA identified the separation of arboreous forest grassland and herbaceous forest groups. The arboreous forest group showed the greatest differences, and the grassland and herbaceous forest groups were mixed.

The Pearson correlation test (Table 5) showed values that indicate a strong relationship between the size of pollen grains and the width of the pore ($r = 0.8281$). It also showed a strong relationship between the size of pollen grains and the width of the annulus ($r = 0.8565$). The diagrams of the values obtained indicate a similarity between the size of pollen grains, the pore width, and the width of the annulus (Figure 11).

All taxa showed monoporate apertures with annulus around the pores, except for *Pharus lappulaceus*, *Digitaria ciliares*, and *Paspalum pauciciliatum*, which showed diporate as well as the monoporate pollen grains. However, these three species (*P. lappulaceus*, *D. ciliares*, and *P. pauciciliatum*) showed only a few diporate pollen grains; most of their pollen grains were found to be monoporate. Nevertheless, they were unique species in terms of having diporate pollen. In the herbaceous forest species with diporate pollen grains, the grains measured 23–27 μm in width, while in the grassland species with diporate pollen, the grains measured 34–46 μm in width.

Interpretation of, and Distinction between, the Grassland and Forest Pollen Grains

In southern Brazil, 80% of Poaceae species are grassland species, while 20% are forest species. In our data set (68 species), 85.29% were grassland species and 14.71% were forest species. Thus,



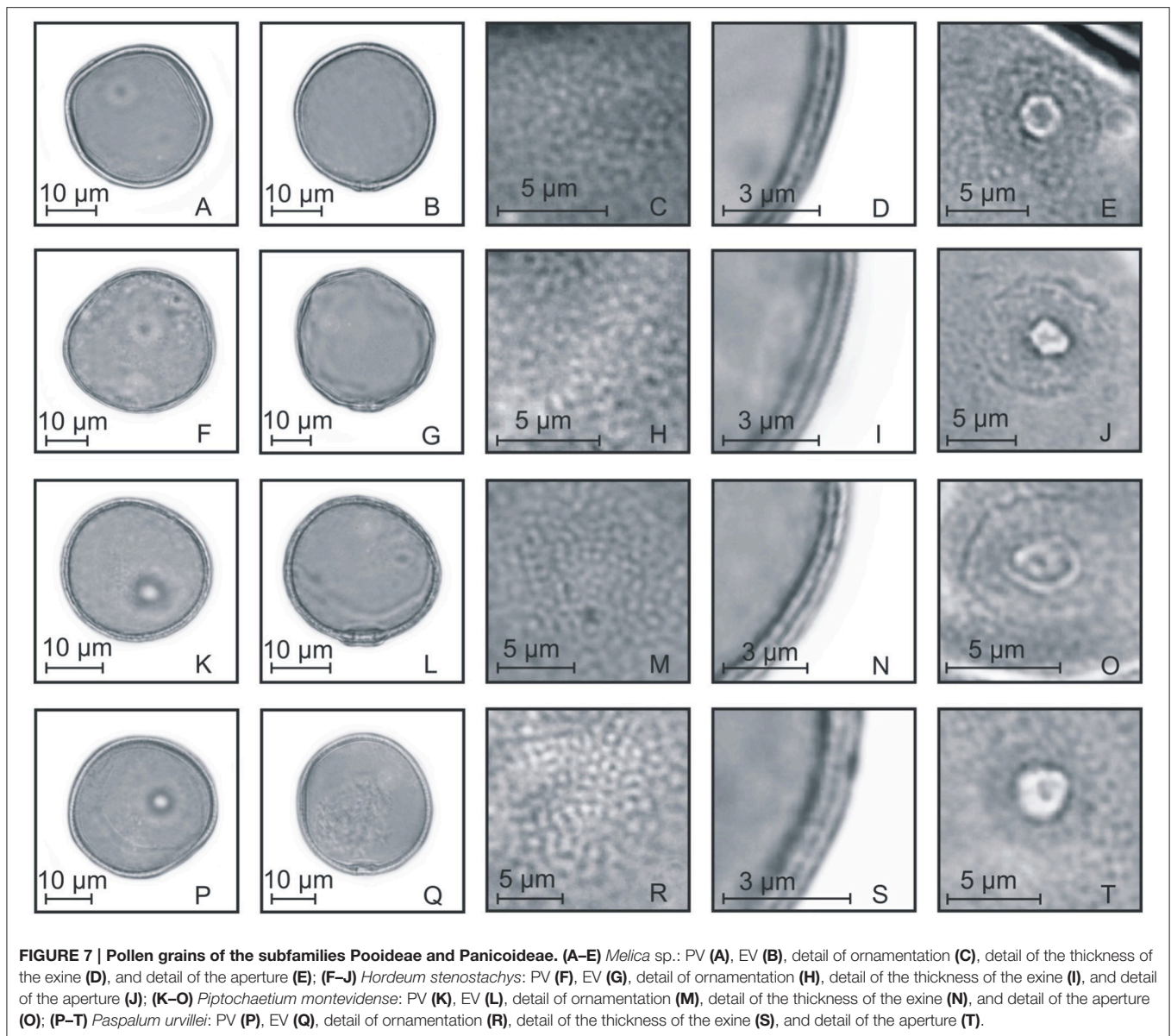
we analyzed the appropriate proportions of species relating to grassland and forest vegetation in the region.

The box plot of data sets relating to different Poaceae vegetation (arboreous forest, grassland, and herbaceous forest) showed pollen grains of different size ranges (Figure 12). The pollen grains of arboreous forest species were larger than those of grassland and herbaceous forest species. The pollen grains of grassland species and herbaceous forest species were found to be of similar size. However, the pollen of the grassland species had a lower minimum size than that of the forest herbaceous species. Three pollen types could be separated based on pollen grain size (Table 6). The Bambuseae pollen type was found to have pollen grains larger than 46 µm in width. Pollen grains that vary in size between 22 and 46 µm are of the herbaceous pollen

type; these pollen grains belong to either grassland or herbaceous forest species. The grassland pollen type has small pollen grains, measuring less than 22 µm.

DISCUSSION

Based on measurements of pollen grains, previous studies have allowed scholars to distinguish between Poaceae pollen grains of South American ecosystems, and also to show the trends in pollen grain size among C₃ and C₄ Poaceae species (Schüler and Behling, 2011a,b; Jan et al., 2014). In this work, it was possible to distinguish the Poaceae pollen grains relating to grassland and forest species of southern Brazil. Jan et al. (2014) analyzed a large data set with species from various locations around the



world. In our work we wanted to analyze the variability within one ecosystem; therefore, we chose to analyze a large set of data relating to only one region (southern Brazil).

Studies of Poaceae pollen grains have revealed a strong correlation between size of pollen grain, pore, and annulus (Skvarla et al., 2003; Joly et al., 2007; Schüler and Behling, 2011a,b; Jan et al., 2014). The results of our own study also showed a relationship between size of pollen, pore, and annulus, as determined through correlation analysis.

Analysis of the Poaceae pollen of the plants deposited in the herbarium provided a description of the variation in pollen grain size of species that occur in different regions of the state of RS. According to the results, relating pollen data to information on the current vegetation of RS, the main variations in size of Poaceae pollen grains in the state (Figure 13) could be mapped.

Taking into account the vegetation types that are based on more representative genera from different regions (Hasenack et al., 2010), we can assign to regions the probable main pollen types occurring in different locations. Thus, the northern half of RS seems to be composed of larger pollen grains. We also found a reduction in size toward the southern half of the state, where the concentration of smaller pollen grains can be associated with the western part of RS, especially in the region of grassland with shallow soils (where the range of diameters for pollen grains is 22–34 µm).

Forest Vegetation

Pollen grains of forest Poaceae species showed distinctions between species. Arboreous species showed larger pollen grains than herbaceous species. The pollen grain size of the arboreous

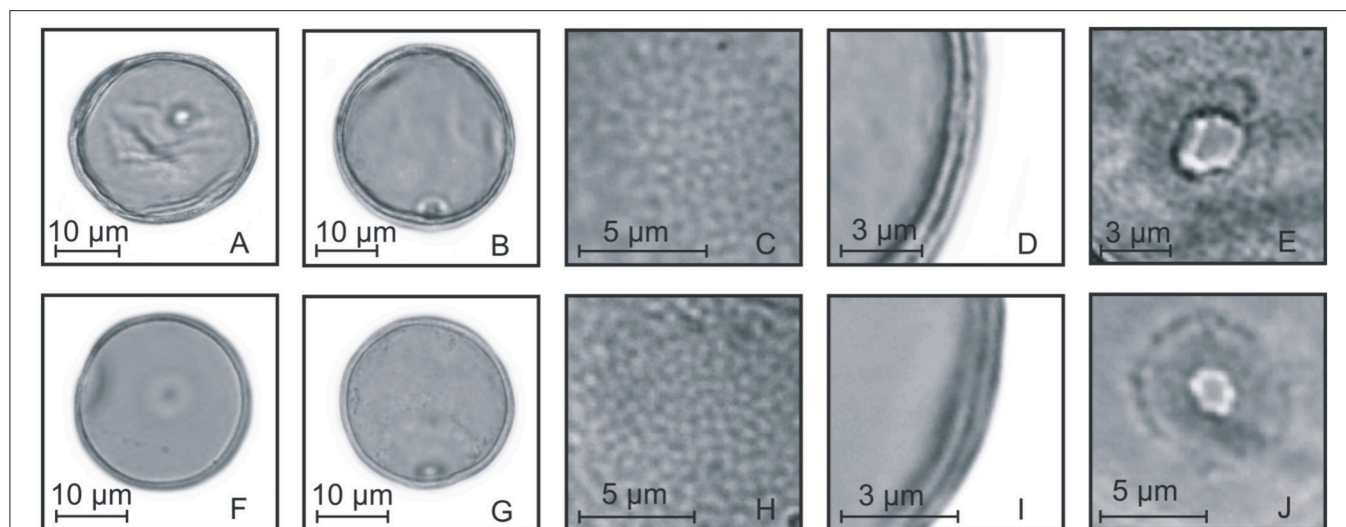


FIGURE 8 | Pollen grains of the subfamily Panicoideae. (A–E) *Schizachyrium microstachyum*: PV (A), EV (B), detail of ornamentation (C), detail of the thickness of the exine (D), and detail of the aperture (E); **(F–J) *Arundinella hispida*:** PV (F), EV (G), detail of ornamentation (H), detail of the thickness of the exine (I), and detail of the aperture (J).

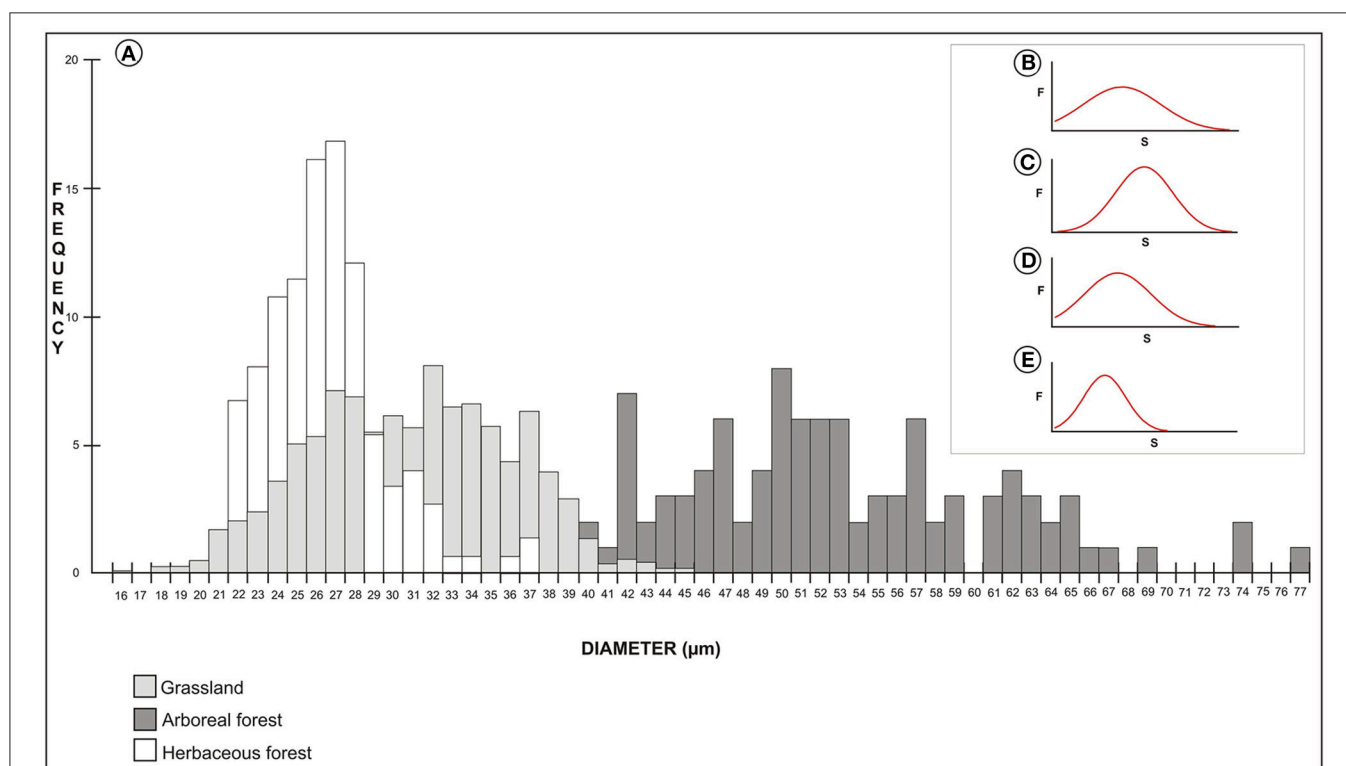


FIGURE 9 | Frequency distribution histogram of the pollen size measurements (A). Gaussian distribution of size measurements of pollen grains of arboreal species (B), grassland species (C), herbaceous forest species (D), and all species studied (E). F, frequency; S, pollen grain size.

species ranged from medium to large, while that of the herbaceous species ranged from small to medium. The pollen grains of arboreal Poaceae species showed a tendency toward larger sizes (Markgraf and D'Antoni, 1978; Salgado-Labouriau

and Rinaldi, 1990). The differently sized grains of pollen forest species may be related to the small wind flow inside the forests and may also be influenced by pollination (Dórea, 2011). Some variations in the size of the pollen grains of modern

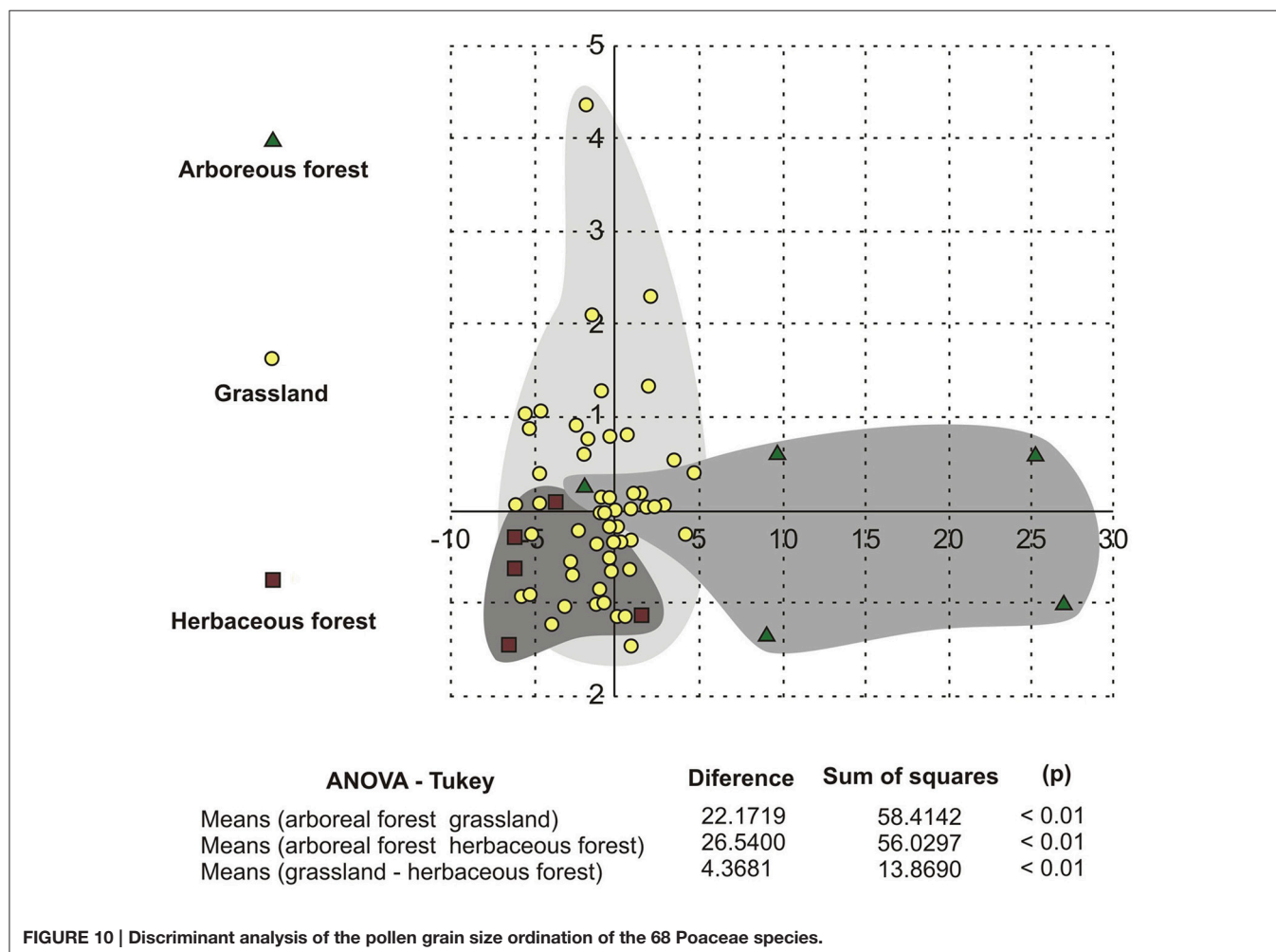
TABLE 4 | Significances between the size of pollen grains of forest arboreous, grassland, and forest herbaceous species obtained with ANOVA-Tukey.

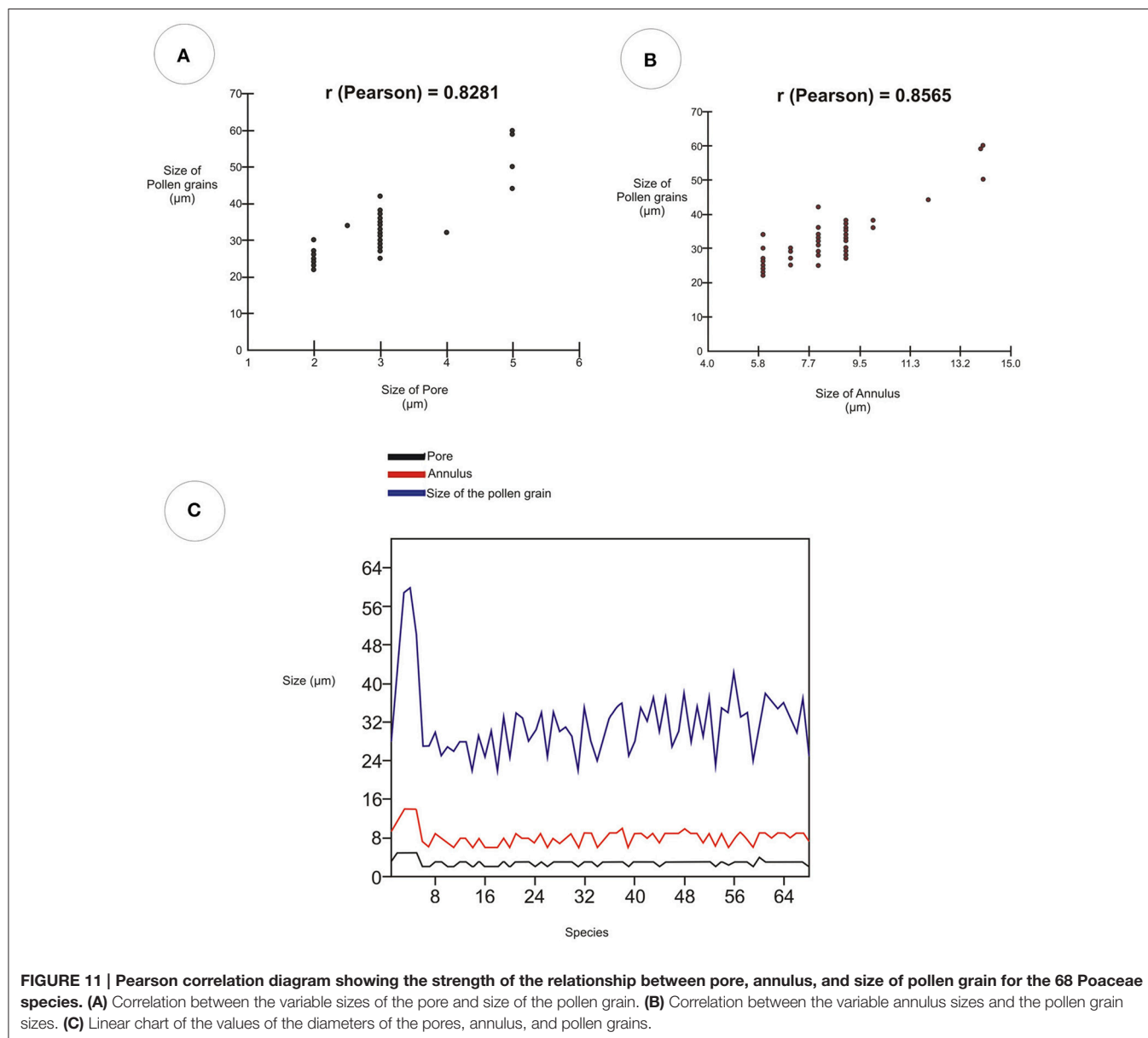
Sources of variation	DF	Sum of squares	Mean squares (variances)
Treatments	2	50.6 e + 03	25.3 e + 03
error	1672	45.0 e + 03	26.924
F =	939.0160		
(p) =	<0.0001		
Mean (arboreal forest pollen grains)	53.0800		
Mean (grassland pollen grains)	30.9081		
Mean (herbaceous forest pollen grains)	26.5400		
Tukey:	Diference	S	(p)
Means (arboreal forest–grassland)	22.1719	58.4142	<0.01
Means (arboreal forest–herbaceous forest)	26.5400	56.0297	<0.01
Means (grassland–herbaceous forest)	4.3681	13.8690	<0.01

Poaceae species has already been reported in South America. In Venezuela, larger pollen grains have already been reported to be related to the Bambusoideae and Pooideae subfamilies (Salgado-Labouriau and Rinaldi, 1990). However, in southern Brazil, we are able to differentiate at the level of tribes determining the Bambuseae pollen type. The Bambuseae pollen type is indicative of arboreal grasses and humid regions (Schmidt and Longhi-Wagner, 2009).

TABLE 5 | Pearson correlation coefficient values showing the strength of relationship among the pore, annulus and size of the pollen grain.

	Pore–annulus	Pore–pollen grain	Annulus–pollen grain
n =	68	68	68
r (Pearson) =	0.9257	0.8281	0.8565
IC 95% =	0.88–0.95	0.73–0.89	0.78–0.91
IC 99% =	0.86–0.96	0.70–0.91	0.74–0.92
R2 =	0.8569	0.6858	0.7336
t =	19.8779	12.0019	13.4797
(p) =	<0.0001	<0.0001	<0.0001





Grassland Vegetation

Pollen grains of grassland species are smaller than those of arboreal forest species and similar to those of herbaceous forest species. These results make it possible to identify the herbaceous pollen type. The smaller size of pollen grains in grassland species allows identification of the grassland pollen type. The small and medium sizes of pollen grains of grassland Poaceae species correspond to previous data relating to South American species (Heusser, 1971; Markgraf and D'Antoni, 1978; Salgado-Labouriau and Rinaldi, 1990; Melhem et al., 2003; Côrrea et al., 2005; Bauermann et al., 2013; Radaeski et al., 2014a,b) and species from other regions of the world (Joly et al., 2007; Jan et al., 2014; Morgado et al., 2015). The small size of pollen grains of grassland species can also be related to the type of dispersion involved, since grassland species produce

more pollen than forest species (Radaeski and Bauermann, 2016).

Exine

Many studies have revealed differences in the exine sculpture of Poaceae pollen grains. Such differences are evident through the use of SEM, which allows adequate analysis of the surface (Köhler and Lange, 1979; Linder and Ferguson, 1985; Chaturvedi et al., 1994, 1998; Chaturvedi and Datta, 2001; Skvarla et al., 2003; Datta and Chaturvedi, 2004; Liu et al., 2004, 2005; Perveen, 2006; Kashikar and Kalkar, 2010; Ahmad et al., 2011; Dórea, 2011; Perveen and Kaiser, 2012; Mander et al., 2013, 2014; Nazir et al., 2013; Morgado et al., 2015; Needham et al., 2015; Mander and Punyasena, 2016). Light microscopy is used to study the fossil pollen of Quaternary sediments at smaller magnifications

($\times 400$); SEM is not suitable for such study. Thus, data pollen measures seem to be more suitable to use in comparison with fossil pollen.

The thin exine of the Poaceae pollen grains is a remarkable characteristic, not exceeding $2\text{ }\mu\text{m}$ in thickness and having equivalent sexine and nexine values. Because of this thin layer, many pollen grains—especially the larger ones—may display small changes in their spherical shape owing to the flattening of the pollen grain. This often provides the impression of pollen grains with prolate or oblate forms. However, these shapes are easily observed in crushed pollen grains, for when the non-deformed (used as parameters) pollen grains are examined,

their spherical form—characteristic of the Poaceae family—is noted.

The surface of the exine of Poaceae pollen grains, when viewed by SEM, exhibits several variations among species (Dórea, 2011). However, when observed under light microscopy, the pollen surface exhibits a tectate exine with columellae and spinulose ornamentation. The variations in the surface of the exine observed by SEM cannot be observed by light microscopy. To identify the pollen grains (from pollen records) involving smaller increases, mainly occurring in Quaternary sediments, the ornamentation is often not observed. With a magnification of $\times 400$, much ornamentation of the studied taxa is not visible (Schüler and Behling, 2011a,b), for the ornamentation is often interpreted as psilate, scabrate, or microrreticulate surfaces. However, under higher (SEM) magnifications, the sculptured grain surfaces may be evident (Chaturvedi et al., 1998; Liu et al., 2004; Dórea, 2011; Mander et al., 2013).

CONCLUSIONS

Using a data set of 68 species, we found that types of vegetation can be distinguished according to Poaceae pollen grains. The size of pollen grains of arboreous forest Poaceae species differs from that of grassland and herbaceous forest species. The pollen grains of forest species of arboreal habit are larger than those of forest species of herbaceous habit. Through measurements and statistical analysis, we found that these Poaceae species exhibit variation in the size of pollen grains in species inhabiting arboreous forest, grassland, and herbaceous forest. Thus, three pollen types were identified: Bambuseae, herbaceous, and grassland pollen types.

Grassland and forest vegetation may be distinguished by examining Poaceae pollen grains from southern Brazil. Thus, the dynamics of the grassland and forest vegetation during the Pleistocene and Holocene periods can be demonstrated based on Poaceae pollen grains. Also, pollen characterization by vegetation

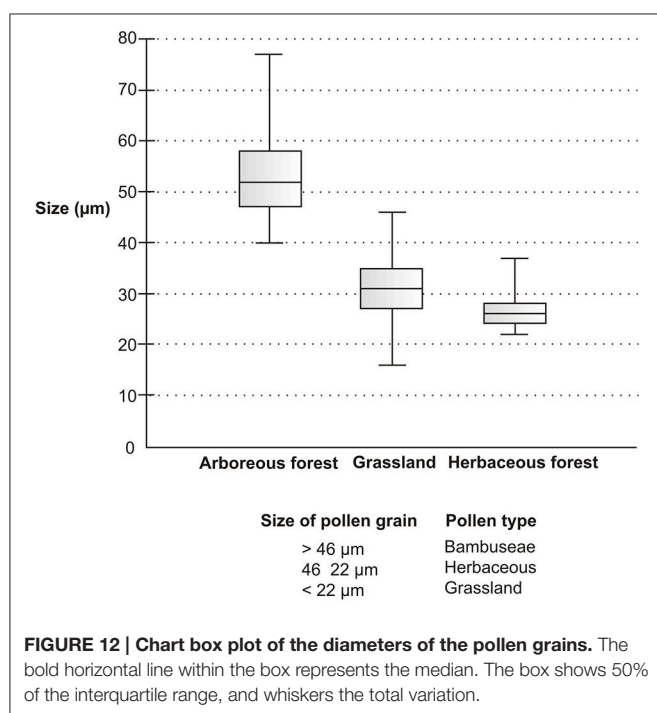
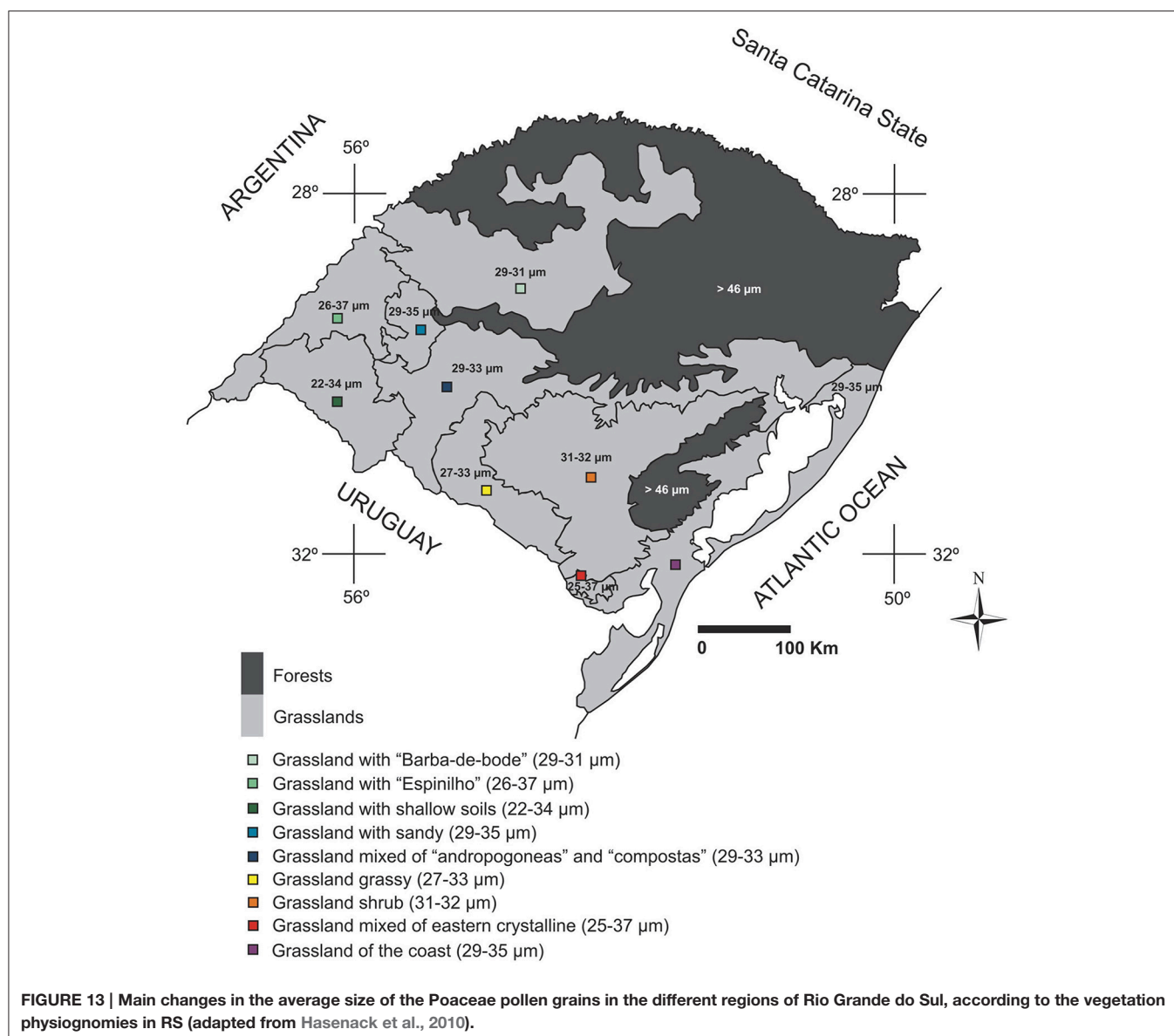


TABLE 6 | Pollen measures and establishment of pollen types.

Size of pollen grain	Pollen type	Species included
>46 μm	Bambuseae	<i>Chusquea juergensii</i> , <i>Colantheia cingulata</i> , <i>Guadua trinitii</i> , <i>Merostachys multiramea</i>
46–22 μm	Herbaceous	<i>Streptochaeta spicata</i> , <i>Lithachne pauciflora</i> , <i>Olyra latifolia</i> , <i>Parodiolyra micrantha</i> , <i>Pharus lappulaceus</i> , <i>Leersia</i> sp., <i>Luziola peruviana</i> , <i>Danthonia montana</i> , <i>Eleusine tristachya</i> , <i>Eragrostis bahiensis</i> , <i>Muhlenbergia schreberi</i> , <i>Tridens brasiliensis</i> , <i>Bouteloua megapotamica</i> , <i>Chloris cantherae</i> , <i>Cynodon dactylon</i> , <i>Eustachys distichophylla</i> , <i>Gymnopogon spicatus</i> , <i>Microchloa indica</i> , <i>Spartina ciliata</i> , <i>Pappophorum philippianum</i> , <i>Aristida</i> sp., <i>Agrostis</i> sp., <i>Amphibromus quadridentulus</i> , <i>Calamagrostis viridiflavescens</i> , <i>Catapodium rigidum</i> , <i>Dactylis glomerata</i> , <i>Festuca fimbriata</i> , <i>Glyceria multiflora</i> , <i>Holcus lanatus</i> , <i>Poa bonariensis</i> , <i>Phalaris angusta</i> , <i>Polypogon elongatus</i> , <i>Bromus catharticus</i> , <i>Melica</i> sp., <i>Hordeum stenostachys</i> , <i>Piptochaetium montevidense</i> , <i>Stipa filifolia</i> , <i>Stipa melanosperma</i> , <i>Stipa papposa</i> , <i>Stipa setigera</i> , <i>Axonopus</i> sp., <i>Digitaria ciliata</i> , <i>Ichnanthus pallens</i> , <i>Panicum aquaticum</i> , <i>Paspalum notatum</i> , <i>Paspalum pauciciliatum</i> , <i>Paspalum urvillei</i> , <i>Setaria parviflora</i> , <i>Andropogon lateralis</i> , <i>Andropogon</i> cf. <i>lindmanii</i> , <i>Bothriochloa laguroides</i> , <i>Elionurus candidus</i> , <i>Imperata brasiliensis</i> , <i>Ischaemum minus</i> , <i>Schizachyrium microstachyum</i> , <i>Trachypogon filifolius</i>
<22 μm	Grassland	<i>Eragrostis neesii</i> , <i>Leptochloa fusca</i> , <i>Sporobolus indicus</i> , <i>Tripogon spicatus</i> , <i>Aira elegans</i> , <i>Chascolytrum subaristatum</i> , <i>Steinchisma hians</i> , <i>Arundinella hispida</i>



is of great importance, since the pollen morphology of the grasslands and forests can be used as indicators of humid or dry environments, respectively.

By determining the size of pollen grains of 68 Poaceae species in RS, it was possible to indicate previously inaccessible information for ecological inferences concerning southern Brazil grasslands. Attaining better taxonomic resolution of both vegetation types allows new opportunities to expand the pollen records beyond the family level. Further research is needed on the pollen morphology of other native genera and species of the Poaceae family for RS. It is expected that further studies will allow greater differentiation between groups and improved knowledge of pollen morphology at a family level. The presented method is being applied to the development of pollen records for southern Brazil and may favor climatic reconstruction of past environments and an evaluation of the dynamics of Quaternary grassland Poaceae vegetation.

AUTHOR CONTRIBUTIONS

JR provided the images of the pollen grains and pollen measurements. JR, SB, AP structured and edited the manuscript during all phases. SB and AP supervised the project. JR and SB supported the paleoecological interpretations. JR and AP developed the botanical implications.

ACKNOWLEDGMENTS

This work is part of the M.Sc. dissertation of the first authors, sponsored by CAPES. Our appreciation goes to Dr. Angelo Alberto Schneider from UNIPAMPA, for the great help with the identification of botanical materials. Also, we want to thank the ICN herbarium. We thank Jim Kernaghan and Guy Barcellos for the linguistic revision.

REFERENCES

- Ahmad, F. A., Khan, M. A., Ahmad, M., Zafar, M., Khan, A., and Iqbal, Z. (2011). Palynological studies in tribe Chloridoideae (Poaceae) from salt range of Pakistan. *Afr. J. Biotechnol.* 10, 8909–8913. doi: 10.5897/AJB10.2512
- Barth, O. M., and Melhem, T. S. (1988). *Glossário Ilustrado de Palinologia*. Campinas: Editora da UNICAMP.
- Bauermann, S. G., Macedo, R. B., Behling, H., Pillar, V., and Neves, P. C. P. (2008). Dinâmicas vegetacionais, climáticas e do fogo com base em palinologia e análise multivariada no Quaternário Tardio no sul do Brasil. *Rev. Bras. Paleontol.* 11, 87–96. doi: 10.4072/rbp.2008.2.02
- Bauermann, S. G., Radaeski, J. N., Evaldt, A. C. P., Queiroz, E. P., Mourelle, D., Prieto, A. R., et al. (2013). *Pólen nas Angiospermas: Diversidade e Evolução*. Canoas: Editora da ULBRA.
- Behling, H., Pillar, V., and Bauermann, S. G. (2004). Late Quaternary Araucaria forest, grassland (Campos), fire and climate dynamics, inferred from a high-resolution pollen record of Cambará do Sul in southern Brazil. *Palaeogeogr. Palaeoclimatol. Palaeoecol.* 203, 277–297. doi:10.1016/S0031-0182(03)00687-4
- Boldrini, I. I. (2006). *Biodiversidade dos Campos Sulinos. i Simpósio de Forrageiras e Produção Animal – Ênfase: Importância e Potencial Produtivo da Pastagem Nativa*, Vol. 1. UFRGS, Departamento de Plantas Forrageiras e Agrometeorologia, 11–24.
- Boldrini, I. I., and Longhi-Wagner, H. M. (2011). Poaceae no rio grande do sul: diversidade, importância na fitofisionomia e conservação. *Ciência Ambiente* 42, 71–92.
- Chaturvedi, M., and Datta, K. (2001). Pollen morphology in *Saccharum* L. (Poaceae) - wild and cultivated sugar cane species. *Feddes Repertorium* 112, 387–390. doi: 10.1002/fedr.4921120509
- Chaturvedi, M., Datta, K., and Nair, P. K. K. (1998). Pollen morphology of *Oryza* (Poaceae). *Grana* 37, 79–86. doi: 10.1080/00173139809362647
- Chaturvedi, M., Yunus, D., and Datta, K. (1994). Pollen morphology of sorghum moench-sections eu-sorghum and para-sorghum. *Grana* 33, 117–123. doi: 10.1080/00173139409428987
- Côrrea, A. M. S., Guimarães, M. I. T. M., Cruz-Barros, M. A. V., and Begale, F. F. (2005). Flora polínica da reserva do parque estadual das fontes do ipiranga (São Paulo, Brasil). *Hoehnea* 32, 269–282. doi: 10.1590/S2236-89062011000100009
- Datta, K., and Chaturvedi, M. (2004). Pollen morphology of Basmati cultivars (*Oryza sativa* race Indica) - exine surface ultrastructure. *Grana* 43, 89–93. doi: 10.1080/00173130310017391
- Dórea, M. C. (2011). *Morfologia polínica, Fenologia Reprodutiva e Biologia Floral de Espécies Florestais de Poaceae*. Ph.D. thesis, Universidade Estadual de Feira de Santana.
- Eva, H. D., Miranda, E. E., Di Bella, C. M., Gond, V., Huber, O., Sgrenzaroli, S., et al. (2002). *A Vegetation Map of South America*. Luxembourg: Join Research Centre. Office for Official Publications of the European Communities.
- Erdtman, G. (1952). *Pollen Morphology and Plant Taxonomy*. Angiosperms. Stockholm: Almqvist & Wiksell.
- Filgueiras, T. S., Brochado, A. L., Nogueira, P. E., and Guala, I. I., G.F. (1994). Caminhamento - um método expedito para levantamentos florísticos quantitativos. *Cadernos Geociê* 12, 39–44.
- Grass Phylogeny Working Group (GPWG). (2001). Phylogeny and subfamilial classification of the grasses (Poaceae). *Ann. Missouri Bot. Garden* 88, 373–457. doi: 10.2307/3298585
- Hasenack, H., Weber, E., Boldrini, I. I., and Trevisan, R. (2010). *Mapa de Sistemas Ecológicos da Ecorregião das Savanas Uruguaias em escala 1:500.000 ou superior e Relatório Técnico descrevendo insumos e metodologia de elaboração do mapa de Sistemas Ecológicos*. Relatório Técnico, The Nature Conservancy.
- Heusser, C. J. (1971). *Pollen and Spores of Chile*. Tucson: The university of Arizona Press.
- Jan, F., Schüller, L., and Behling, H. (2014). Trends of pollen grain size variation in C3 and C4 Poaceae species using pollen morphology for future assessment of grassland ecosystem dynamics. *Grana* 53, 1–17. doi: 10.1080/00173134.2014.966754
- Joly, C., Barillé, L., Barreau, M., Mancheron, A., and Visset, L. (2007). Grain and annulus diameter as criteria for distinguishing pollen grains of cereals from wild grasses. *Rev. Palaeobot. Palynol.* 146, 221–233. doi: 10.1016/j.revpalbo.2007.04.003
- Kashikar, N., and Kalkar, S. A. (2010). Pollen morphology of millets-exine surface ultrastructure. *Asian J. Exp. Biol. Sci. Spl.* 85–90. Available online at: <http://www.ajebs.com/special/SP-17.pdf>
- Katsiotis, A., and Forsberg, R. A. (1995). Pollen grain size in four ploidy levels of genus *Avena*. *Euphytica* 83, 103–108. doi: 10.1007/BF01678036
- Köhler, E., and Lange, E. (1979). A contribution to distinguishing cereal from wild grass pollen grains by LM and SEM. *Grana* 18, 133–140. doi: 10.1080/00173137909424973
- Linder, H. P., and Ferguson, I. K. (1985). On the pollen morphology and phylogeny of the Restionales and Poales. *Grana* 24, 65–76. doi: 10.1080/00173138509429917
- Liu, Q., Zhao, N., and Hao, G. (2004). Pollen morphology of the Chloridoideae (Gramineae). *Grana* 43, 238–248. doi: 10.1080/00173130410000776
- Liu, Q., Zhao, N., and Hao, G. (2005). Pollen morphology of *Eustachys tenera* (Chloridoideae, Gramineae). *Pak. J. Bot.* 37, 503–506. Available online at: [http://www.pakbs.org/pjbot/PDFs/37\(3\)/PJB37\(3\)503.pdf](http://www.pakbs.org/pjbot/PDFs/37(3)/PJB37(3)503.pdf)
- Macedo, R. B., Cancelli, R. R., Bauermann, S. G., Neves, P. C. P., and Bordignon, S. A. L. (2007). Palinologia de níveis do Holoceno da Planície Costeira do Rio Grande do Sul (localidade de Passinhos), Brasil. *Rev. Gaea Unisinos* 3, 68–74. Available online at: <http://revistas.unisinos.br/index.php/gaea/article/view/5867/3053>
- Mander, L., Baker, S. J., Belcher, C. M., Haselhorst, D. S., Rodriguez, J., Thorn, J. L., et al. (2014). Accuracy and consistency of grass pollen identification by human analysts using electron micrographs of surface ornamentation. *Applications in Plant Sciences* 2, 1–11. doi: 10.3732/apps.1400031
- Mander, L., Li, M., Mio, W., Fowlkes, C. C., and Punyasena, S. W. (2013). Classification of grass pollen through the quantitative analysis of surface ornamentation and texture. *Proc. Biol. Sci.* 280, 1–7. doi: 10.1098/rspb.2013.1905
- Mander, L., and Punyasena, S. W. (2016). Grass pollen surface ornamentation: a review of morphotypes and taxonomic utility. *J. Micropalaeontol.* 35, 121–124. doi: 10.1144/jmpaleo2015-025
- Markgraf, V., and D'Antoni, H. (1978). *Pollen flora of Argentina*. Tucson: University of Arizona Press.
- Medeane, S., Cordazzo, C. V., and Lima, L. G. (2008). *Diversidade Polínica de Plantas em Dunas no Extremo Sul do Brasil*. Porto Alegre: Gravel.
- Melhem, T. S., Cruz-Barros, M. A. V., Corrêa, M. A. S., Makino-Watanabe, H., Silvestre-Capelato, M. S. F., and Esteves, V. G. L. (2003). Variabilidade polínica em plantas de Campos do Jordão (São Paulo, Brasil). *Bol. Inst. Bot.* 16, 16–104.
- Morgado, L. N., Gonçalves-Esteves, V., Resendes, R., and Ventura, M. A. M. (2015). Pollen morphology of Poaceae (Poales) in the Azores, Portugal. *Grana* 54, 282–293. doi: 10.1080/00173134.2015.1096301
- Nakamura, A. T., Longhi-Wagner, H. M., and Scatena, V. L. (2010). Anther and pollen development in some species of Poaceae (Poales). *Br. J. Biol.* 70, 351–360. doi: 10.1590/S1519-69842010005000005
- Nazir, A., Khan, M. A., Abbasi, A. M., Zahidullah. (2013). Palynological studies in Tribe Aveneae (Poaceae) from Potohar of Pakistan. *Int. J. Sci.* 10, 120–125.
- Needham, I., Vorontsova, M. S., Banks, H., and Rudall, P. J. (2015). Pollen of Malagasy grasses as a potential tool for interpreting grassland palaeohistory. *Grana* 54, 247–262. doi: 10.1080/00173134.2015.1057220
- Perveen, A. (2006). A contribution to the pollen morphology of family gramineae. *World Appl. Sci. J.* 1, 60–65.
- Perveen, A., and Kaiser, M. (2012). Pollen flora of Pakistan - LXIX. Poaceae. *Pak. J. Bot.* 44, 747–756. Available online at: [http://www.pakbs.org/pjbot/PDFs/44\(2\)/42.pdf](http://www.pakbs.org/pjbot/PDFs/44(2)/42.pdf)
- Punt, W., Hoen, P. P., Blackmore, S., Nilsson, S., and Le Thomas, A. (2007). Glossary of pollen and spore terminology. *Rev. Palaeobot. Palynol.* 143, 1–81. doi: 10.1016/j.revpalbo.2006.06.008
- Radaeski, J. N., and Bauermann, S. G. (2016). Avaliação da produção polínica de *Bromus catharticus* Vahl e *Guadua trinii* (Nees) Nees ex Rupr. (Poaceae) para a interpretação de dados fósseis. *Biotemas* 29, 9–18.
- Radaeski, J. N., Evaldt, A. C. P., and Bauermann, S. G. (2014a). Grãos de pólen de espécies ocorrentes na Unidade de Conservação Parque Estadual do Espinilho, Barra do Quaraí, Rio Grande do Sul, Brasil. *Pesqui. Bot.* 65, 305–331. Available online at: <http://www.anchietano.unisinos.br/publicacoes/botanica/botanica65/BOTANICA%2065.pdf>
- Radaeski, J. N., Evaldt, A. C. P., Bauermann, S. G., and Lima, G. L. (2014b). Diversidade de grãos de pólen e esporos dos Campos do sul do Brasil: descrições

- morfológicas e implicações paleoecológicas. *Iheringia Série Bot.* 69, 107–132. Available online at: http://www.fzb.rs.gov.br/upload/20140805153253ih69_1_p107_132.pdf
- Radaeski, J. N., Evaldt, A. C. P., Lima, G. L., and Bauermann, S. G. (2011). Grãos de pólen das formações campestres sul-brasileiras. *Rev. Iniciação Científica* 9, 59–67. Available online at: <http://sites.ulbra.br/palinologia/graos-de-polen-das-formacoes-campestres-sul-brasileiras.pdf>
- Roubik, D. W., and Moreno, J. E. (1991). *Pollen and Spores of Barro Colorado Island*. St. Louis, MO: Missouri Botanical Garden.
- Salgado-Labouriau, M. L. (1973). *Contribuição à Palinologia dos Cerrados*. Rio de Janeiro: Academia Brasileira de Ciências, 291.
- Salgado-Labouriau, M. L. (2007). *Crîtérios e Técnicas Para o Quaternário*. São Paulo: Editora Blücher.
- Salgado-Labouriau, M. L., and Rinaldi, M. (1990). Palynology of gramineae of the venezuelan mountains. *Grana* 29, 119–128. doi: 10.1080/00173139009427742
- Schmidt, R., and Longhi-Wagner, H. M. (2009). A tribo Bambuseae (Poaceae, Bambusoideae) no Rio Grande do Sul, Brasil. *Rev. Bras. Biociências* 7, 71–128. Available online at: <http://www.bamusc.org.br/wp-content/uploads/2009/05/a-tribo-bambuseae-no-rs.pdf>
- Schüler, L., and Behling, H. (2011a). Characteristics of Poaceae pollen grains as a tool to assess palaeoecological grassland dynamics in South America. *Veget. Hist. Archaeobot.* 20, 97–108. doi: 10.1007/s00334-010-0264-0
- Schüler, L., and Behling, H. (2011b). Poaceae pollen grain size as a tool to distinguish past grasslands in South America: a new methodological approach. *Veget. Hist. Archaeobot.* 20, 83–96. doi: 10.1007/s00334-010-0265-z
- Skvarla, J. J., Rowley, J. R., Hollowell, V. C., and Chissoe, W. F. (2003). Annulus-Pore relationship in Gramineae (Poaceae) pollen: the pore margin of *Pariana*. *Am. J. Bot.* 90, 924–930. doi: 10.3732/ajb.90.6.924
- Tedesco, S. B., Battistin, A., and Valls, J. F. M. (1999). Diâmetro dos grãos de pólen e tamanho dos estômatos em acessos diplóides e tetraplóides de *Hemarthria altissima* (Poir.) Stapf & Hubbard (Gramineae). *Santa Maria. Ciência Rural* 29, 273–276. doi: 10.1590/S0103-84781999000200014
- Wilberger, T. P., Stranz, A., Paz, C., Boeni, B., Cancelli, R. R., Bauermann, S. B., et al. (2004). *Flora do Setor Oriental do Planalto sul-rio-grandense. Guia de espécies vegetais*. 1ª Edn. São Leopoldo, ALPP.

Conflict of Interest Statement: The authors declare that the research was conducted in the absence of any commercial or financial relationships that could be construed as a potential conflict of interest.

Copyright © 2016 Radaeski, Bauermann and Pereira. This is an open-access article distributed under the terms of the Creative Commons Attribution License (CC BY). The use, distribution or reproduction in other forums is permitted, provided the original author(s) or licensor are credited and that the original publication in this journal is cited, in accordance with accepted academic practice. No use, distribution or reproduction is permitted which does not comply with these terms.



The Representativeness of *Olea* Pollen from Olive Groves and the Late Holocene Landscape Reconstruction in Central Mediterranean

Assunta Florenzano¹, Anna Maria Mercuri¹, Rossella Rinaldi¹, Eleonora Rattighieri¹, Rita Fornaciari^{1,2*}, Rita Messora^{1,2} and Laura Arru²

¹ Laboratorio di Palinologia e Paleobotanica, Dipartimento di Scienze della Vita, Università di Modena e Reggio Emilia, Modena, Italy, ² Plant Physiology Lab, Dipartimento di Scienze della Vita, Università di Modena e Reggio Emilia, Reggio Emilia, Italy

OPEN ACCESS

Edited by:

Encarni Montoya,
Instituto de Ciencias de la Tierra
Jaume Almera (CSIC), Spain

Reviewed by:

Josu Aranbarri,
University of the Basque Country
(UPV/EHU), Spain
Donatella Magri,
Sapienza Università di Roma, Italy

*Correspondence:

Rita Fornaciari
rita.fornaciari@unimore.it

Specialty section:

This article was submitted to
Quaternary Science, Geomorphology
and Paleoenvironment,
a section of the journal
Frontiers in Earth Science

Received: 30 July 2017

Accepted: 05 October 2017

Published: 20 October 2017

Citation:

Florenzano A, Mercuri AM, Rinaldi R, Rattighieri E, Fornaciari R, Messora R and Arru L (2017) The Representativeness of *Olea* Pollen from Olive Groves and the Late Holocene Landscape Reconstruction in Central Mediterranean. *Front. Earth Sci.* 5:85. doi: 10.3389/feart.2017.00085

Modern pollen spectra are an invaluable reference tool for paleoenvironmental and cultural landscape reconstructions, but the importance of knowing the pollen rain released from orchards remains underexplored. In particular, the role of cultivated trees is in past and current agrarian landscapes has not been fully investigated. Here, we present a pollen analysis of 70 surface soil samples taken from 12 olive groves in Basilicata and Tuscany, two regions of Italy that exemplify this cultivation in the Mediterranean basin. This study was carried out to assess the representativeness of *Olea* pollen in modern cultivations. Although many variables can influence the amount of pollen observed in soils, it was clear that most of the pollen was deposited below the trees in the olive groves. A rapid decline in the olive pollen percentages (c. 85% on average) was found when comparing samples taken from IN vs. OUT of each grove. The mean percentages of *Olea* pollen obtained from the archeological sites close to the studied orchards suggest that olive groves were established far from the Roman farmhouses of Tuscany. Further south, in the core of the Mediterranean basin, the cultivation of *Olea* trees was likely situated ~500–1,000 m from the rural sites in Basilicata, and dated from the Hellenistic to the Medieval period.

Keywords: *Olea europaea* L., pollen, surface soil, archeological site, Basilicata, Tuscany, Roman landscape

INTRODUCTION

The olive tree is an important marker of the Mediterranean cultural landscapes. Molecular, archaeobotanical, and paleoenvironmental data are acknowledged as essential for reconstructing the history of the domesticated olive tree (Zohary and Hopf, 2000; Newton et al., 2014). Together with the walnut and chestnut trees, the present geographical distribution of genetic diversity in *Olea europaea* L. was perhaps more influenced by human activities than by its natural migration and colonization (Bottema and Woldring, 1990; Baldoni et al., 2006), a view confirmed by the frequent recovery of this pollen in the deposits from archeological sites (Mercuri et al., 2013). Accordingly, *Olea* pollen may be regarded as an indicator of human presence and activity in a certain area. However, the species includes both wild and domesticated subspecies (*O. europaea* L. ssp. *sylvestris* and *O. europaea* L. ssp. *europaea*, respectively) that have quite similar pollen morphology

(Roselli, 1979; Ribeiro et al., 2012; Messori et al., 2017). Another problem arises from the fact that *O. europaea* is an evergreen xerophilous tree, whose growth is promoted by a warming climate (Moriondo et al., 2013). Recent studies have demonstrated that a seasonal analysis is required to establish robust relationships between the Mediterranean climate and olive development (Aguilera et al., 2015); therefore, an increasing trend in the pollen curves may have ambiguous significance in the diagrams from the Mediterranean Holocene records. Palynologists have concluded that *Olea* pollen may be considered both a proxy of warming and drought conditions, as well as the product of a fruit-bearing plant dispersed and cultivated by humans. High percentages of this pollen recovered in the spectra from archeological sites, or from human-influenced off-sites, can reasonably result from a process of cultivation. However, it is not clear how much “high” may be the percentage of *Olea* pollen in modern agrarian landscapes. Today, *Olea* pollen is common and among the most abundant airborne pollen in the Mediterranean countries (e.g., Galán et al., 2004; Ziello et al., 2012; Mercuri, 2015). In aerobiology, volumetric spore traps were placed in olive groves to study the phenology and the delayed pollination season of olive groves located at higher altitudes (in SE Spain: Aguilera and Valenzuela, 2012). Nevertheless, the amount of pollen that fell to the ground and was trapped in sediments below olive trees and near modern groves has not yet been systematically assessed.

In this paper, we discuss the representativeness of *Olea* pollen in surface soil samples taken from modern Italian olive groves, with the aim of contributing to the interpretation of past pollen spectra. To our best knowledge, this is the first study of surface soil sediments from this widespread type of crop cultivation. This is somewhat surprising, considering that knowledge of current pollen rain may be the best reference tool for understanding and reconstructing the environments and agrosystems of the past (e.g., Cañellas-Boltà et al., 2009; Fall, 2012; Davis et al., 2013). Since most pollen-based landscape reconstructions are based on sophisticated quantitative pollen analyses and modeling estimates, this paper instead proposes a basic observational test to provide much-needed reference data for the complex and fragmented Mediterranean landscapes during the late Holocene. This simpler approach can improve our understanding of the historical development of Mediterranean cultural landscapes. The same methodology, but applied in a different approach, was used by Vermoere et al. (2003) to compare the modern and subfossil pollen assemblages through “modern analogs” and multivariate statistics in their study of an “olive landscape” in SW Turkey (Sagalassos).

Today, most of the total area with olive groves is estimated to lie in the Mediterranean basin, with the highest olive production quantities occurring in Spain and Italy (FAOSTAT, 2017; Figure 1). The focus of our palynological research is centered on the olive plantations located in Italy, a country extraordinarily rich of agroforestry traditions and olive cultivars of the central Mediterranean basin (Rühl et al., 2011). Such cultivation is widespread in the central-southern regions and the islands where the local environmental conditions are most favorable to olive growth. For our study, we selected Tuscany and Basilicata, two of the most productive agrarian regions in Italy, with large olive

groves in their territories (Pisante et al., 2009; Figure 2). These regions couple modern plantations, characterized by different cultivars, with an impressive record of archeological sites preserving evidence of long-term agricultural activity carried out for millennia (Florenzano, 2013; Vaccaro et al., 2013; Bowes et al., 2015). Therefore, we have the opportunity to directly compare past (archeological) and present (olive grove) pollen spectra from the same areas. The results should be useful for assessing the significance of this pollen and tree in the late Holocene history of these two regions, which can serve as an exemplar for the entire peninsula.

MATERIALS AND METHODS

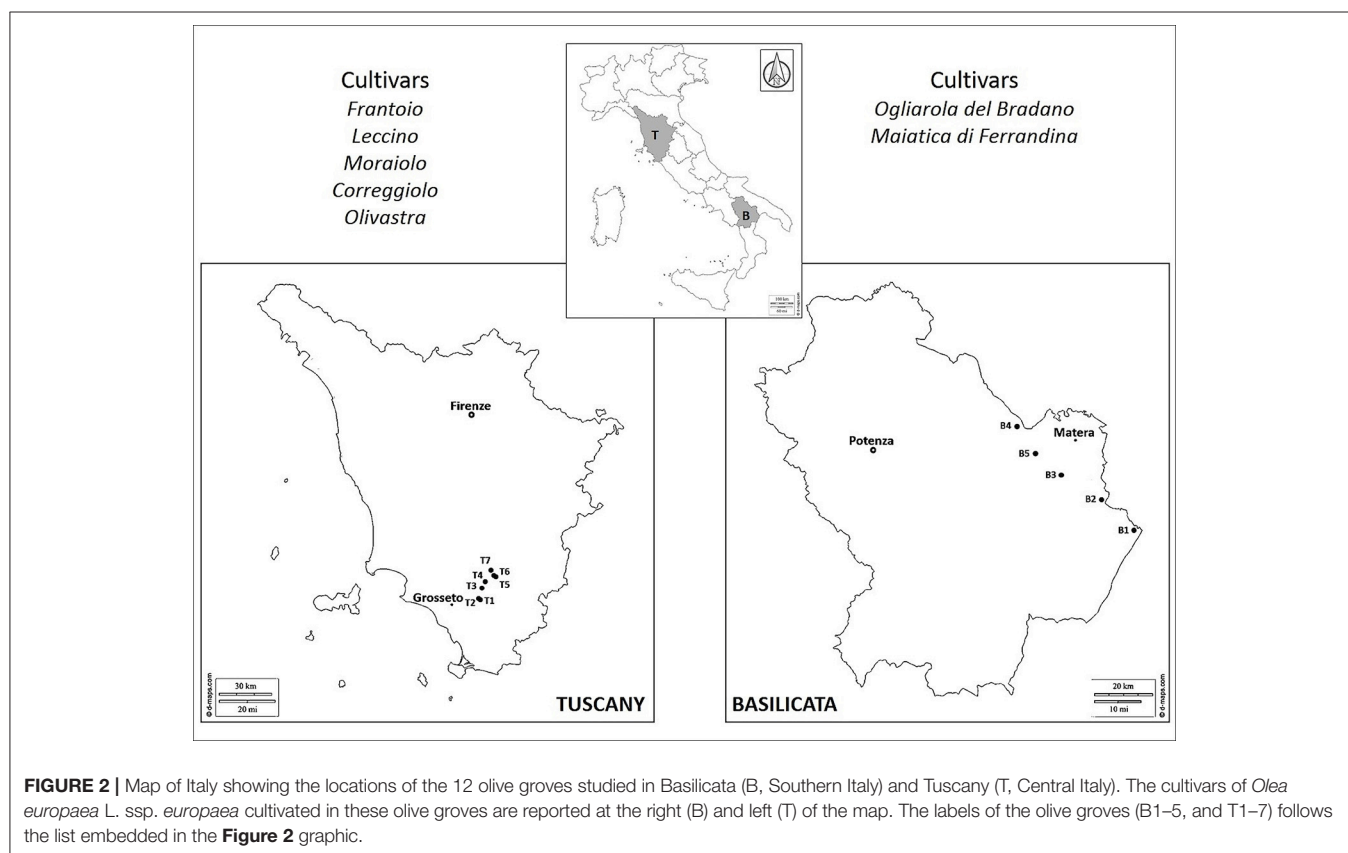
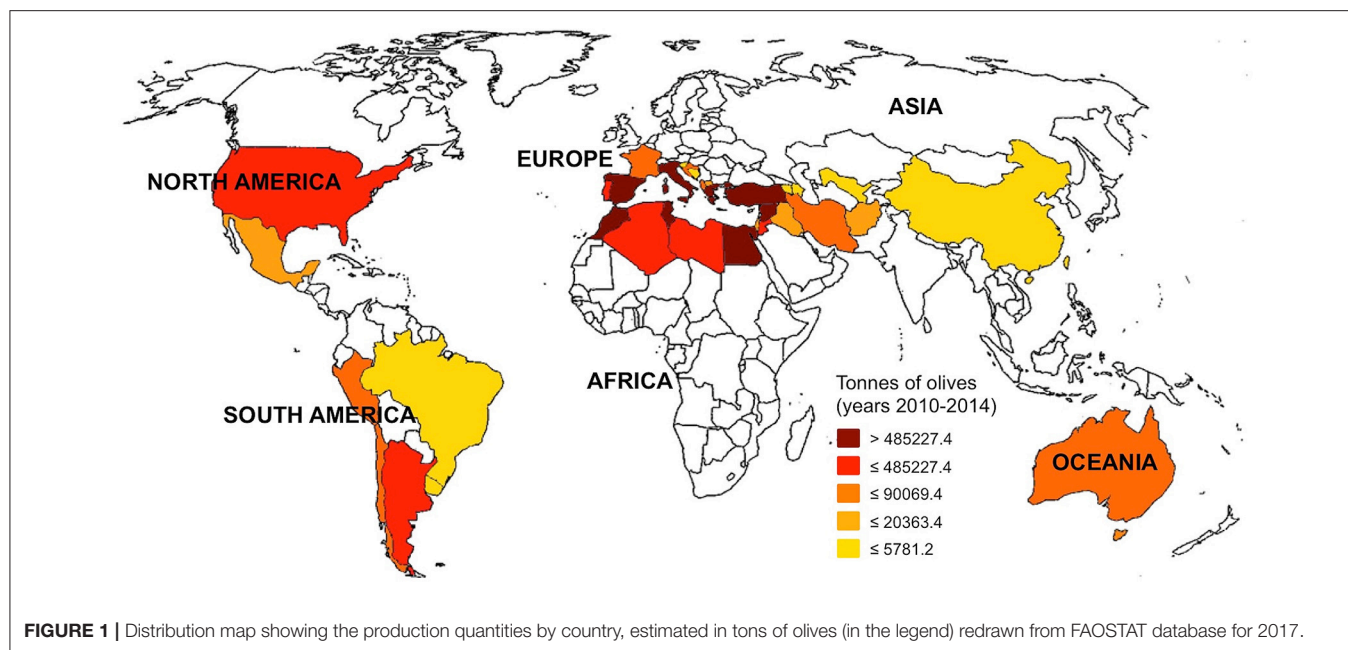
Pollen Sampling and Study Areas

Surface soils were collected from 12 olive groves: five were located in Basilicata (B1–5, cultivated along the Bradano River, in the province of Matera) and seven in Tuscany (T1–7, grown in the commune of Cinigiano, in the province of Grosseto; Figure 2). These two regions have quite heterogeneous soil structures, ranging from alluvial soils along the rivers to marine-origin sandy-gravel deposits in the hinterlands (Pieri et al., 1996; Costantini and Righini, 2002).

The climate of the two regions has a typical Mediterranean seasonality, with rainy winters and dry summers, but with regional differences depending on the latitude and elevation. In Basilicata, the climate is influenced by both the hydrographic basin of the Bradano River and the Ionian Sea, while in Tuscany it is by the warm current from the Tyrrhenian Sea (mean annual temperatures from both regions: from 13 to 16°C; mean annual rainfall: from 300 to 700 mm. Data from regional meteorological archives of Archivio Meteo Storico).

Mediterranean vegetation characterizes the two regions, although mesophilous plant associations are also distributed in the studied areas. In Basilicata, broadleaved deciduous forests are the dominant vegetation communities of the inner lands, whereas *Pinus halepensis* Mill. forest are spread along the coast (Blasi, 2010). A widespread occurrence of woodlands composed of evergreen sclerophylls and broadleaf deciduous trees and shrubs characterize the southern Tuscany vegetation (Selvi, 2010). Some pine tree stands (*Pinus nigra* J. F. Arnold, *P. pinaster* Aiton, *P. pinea* L., and *P. halepensis*) now cover this territory after being reforested over the last two centuries (Ciabatti et al., 2009). The olive groves include different cultivars, commonly organized in mixed plantations of variable size and expansion (Figure 3). In this study, each olive grove was selected to be the farthest away possible from other groves in the same area (Florenzano et al., 2011). However, in Basilicata and Tuscany olive groves account approximately for c. 11% of the Italian territory planted with olive trees, and the density of these tree cultivations is so high that they often color and characterize the landscape of these two regions (from ISTAT—National Institute of Statistics 2011: Basilicata: 31,350 ha, and Toscana: 97,241 ha of olive orchards).

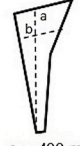
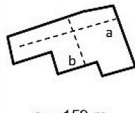

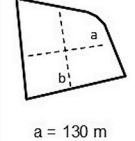

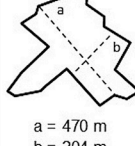
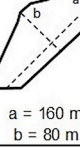
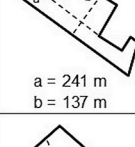
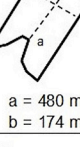
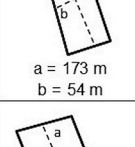
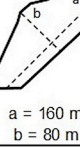
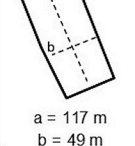

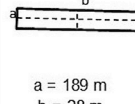
Two samples were taken from the center of each plantation (IN), and four samples from the peripheral positions (OUT), at a distance of c. 250–500 and 1,000 m depending on

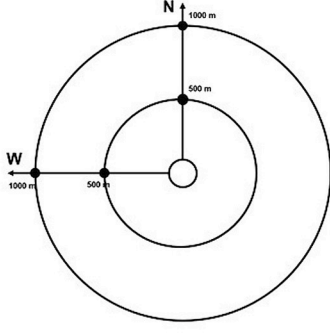


geomorphologic and anthropogenic limits, but always along the SE and the NW transects.

A total of 70 samples were collected from bare ground—not covered by grass—“by cutting” out an c. 2-cm thick portion

of the surface soils. One of the IN samples was picked up according to the method of sampling “by pinches” (e.g., used in forensic palynology; Horrocks et al., 1998; Bryant and Jones, 2006): soil sub-samples were taken from several points over

Basilicata				Tuscany					
Olive groves	Geographic coordinates	Stimate extent and shape	Sampling	Olive groves	Geographic coordinates	Stimate extent and shape	Sampling		
B1 Metaponto	40°24.681' N 16°48.196' E 28 m asl		IN	by cutting	T1 Podere Santucci	42°48'06.83" N 11°18'10.67" E 123 m asl		IN	by cutting
				by pinches					by pinches
			OUT	500 m N				OUT	500 m N
				1000 m N					1000 m N
				500 m W					500 m W
B2 Difesa San Biagio	40°30.203' N 16°41.076' E 58 m asl		IN	by cutting	T2 Podere Salami	42°48.341' N 11°18.049' E 123 m asl		IN	by cutting
				by pinches					by pinches
			OUT	500 m N				OUT	500 m N
				1000 m N					1000 m N
				500 m W					200 m W
B3 Miglionico	40°34.380' N 16°31.631' E 175 m asl		IN	by cutting	T3 Podere Montecucco	42°51'37.79" N 11°19'18.05" E 140 m asl		IN	by cutting
				by pinches					by pinches
			OUT	270 m N				OUT	500 m N
				500 m N					1000 m N
				270 m W					500 m W
B4 Grottole	40°38.213' N 16°25.845' E 114 m asl		IN	by cutting	T4 Colle Massari	42°53.580' N 11°20.777' E 270 m asl		IN	by cutting
				by pinches					by pinches
			OUT	500 m NE				OUT	500 m N
				1000 m NE					800 m N
				500 m W					300 m W
B5 Irsina	40°42.806' N 16°21.904' E 161 m asl		IN	by cutting	T5 Podere Cherzo	42°55.215' N 11°25.219' E 206 m asl		IN	by cutting
				by pinches					by pinches
			OUT	500 m N				OUT	330 m N
				1000 m N					500 m N
				500 m W					300 m W
B6 Grottole	40°38.213' N 16°25.845' E 114 m asl		IN	by cutting	T6 Poggio dell'Amore	42°55'36.21"N 11°24'31.59"E 348 m asl		IN	by cutting
				by pinches					by pinches
			OUT	500 m NW				OUT	500 m NW
				1000 m NW					500 m S
				500 m SW					500 m SW
B7 San Martino	42°57'21.39"N 11°23'9.11"E 374 m asl		IN	by cutting	T7 San Martino	42°57'21.39"N 11°23'9.11"E 374 m asl		IN	by cutting
				by pinches					by pinches
			OUT	500 m NW				OUT	500 m NW
				1000 m NW					1000 m NW
				500 m SW					1000 m SW



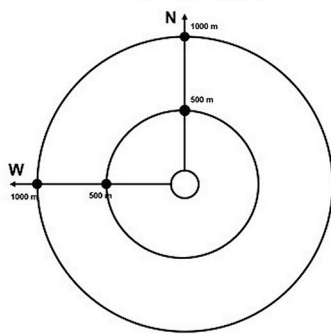


FIGURE 3 | Surface pollen samples taken from the olive groves located in Basilicata (B) and Tuscany (T), Italy; the geographical coordinates, size of the plantation, and type of sampling are shown. a, maximum length; b, maximum width; IN, samples taken from the center of the olive groves; OUT, peripheral samples. The olive grove extent is that for the sampling year (2010 for Basilicata, 2011–13 for Tuscany). Bottom left: the model of pollen sampling in the olive groves.

a c. 1 m² area, mixed, and put into a single small plastic bag per sample. Since the pollination of different cultivated crops occurs at different periods, normally between April and

June in the western and central Mediterranean (Fornaciari et al., 2000; Osborne et al., 2000), the samples were collected in the spring or summer seasons, i.e., immediately before

(early April) or after (July) the blooming periods of the olive trees.

Reference Data from Archeological Literature

Data from the archeological layers were obtained from the pollen analyses of 12 sites located in Basilicata (BI–VII) and in Tuscany (TI–V)—as part of multidisciplinary research carried out by independent projects (for list and references see **Table 1**)—and selected to compare the presence of *Olea* in modern and past pollen spectra. The archeological sites were mainly rural settlements and farmhouses belonging to different cultural periods, from Hellenistic to Medieval in Basilicata, and from the Augustean Roman age in Tuscany. The chronology of the sites was mainly determined by their archeological materials (e.g., pottery), and to a lesser extent by radiocarbon dates and layer correlations. Based on both the pollen data and archeological evidences, environmental reconstructions emphasize the importance of oliviculture in the past economies of these lands (Florenzano, 2013; Bowes et al., 2017). In Basilicata, the Greek and Roman settlements were characterized by well-developed economic activities, including agricultural and pastoral practices (Florenzano and Mercuri, 2012). An organized road network and an efficient irrigation and drainage system characterized this land (Carter and Prieto, 2011). After a period of crisis linked to the fall of the Roman Empire (ca. 4–11th century AD), agricultural practices resumed during the Medieval period, and included olive cultivations within the monastic communities (Sogliani and Marchetta, 2010). In Tuscany, the archaeobotanical and archeological data point to a phase of intensive land use in the late Republican/early Imperial date (ca. 1st century BC/1st century AD). Along

with the significant presence of cereals, the grape vines, and olives attest to the importance of Mediterranean crops in rural contexts, which were small and mainly occupied on a temporary/short-period basis (Rattighieri et al., 2013; Bowes et al., 2015).

Pollen Analysis

An amount of 2–5 g of wet weight per sample of surface soil sediment was treated for pollen extraction (Florenzano et al., 2012). *Lycopodium* spores were added for the calculation of pollen concentration (expressed in pollen grains per gram = p/g). The method involves deflocculation with Na-pyrophosphate 10%, sieving with nylon filter of 7 µm mesh, carbonate dissolution with HCl 10%, acetolysis (Erdtman, 1960) to remove part of the organic substance, enrichment with heavy liquid (Na-metatungstate hydrate) to concentrate the pollen with flotation, dissolution of silicates with HF 40%. The residues were mounted in slides, fixed in glycerol jelly and sealed with paraffin. Pollen counts (up to about 500 pollen grains per sample) were carried out under 400x with a light microscope. For the purpose of this research, we counted only *Olea*, *Pinus*, and the number of total pollen grains in the Pollen Sum. *Olea* was identified as trizonocolpate-colporate pollen with reticulate exine, and a polar axis of ~20 µm. *Pinus* is a high pollen producing tree, and has a saccatae pollen with a maximum diameter of c. 70 µm in many species (e.g., *P. nigra*—Accorsi et al., 1983; *Pinus pinea*—Accorsi et al., 1978; Desprat et al., 2015). As *Pinus* was an important component of some pollen spectra, obtaining the pine values helped us assess the underestimation of *Olea* pollen in several olive groves.

Pollen values reported in the Results section below are the mean pollen concentrations or percentages calculated from the

TABLE 1 | Percentage of *Olea* pollen from the archeological sites close to the modern olive groves studied in this paper, and relevant references.

Archeological site (label and name)	Archeological chronology	Number of pollen samples	Olea %		Main references
			Mean	Max	
BASILICATA					
B I - Pizzica	H	5	2.5	11.8	Florenzano and Mercuri, 2012
B II - Fattoria Fabrizio	H	10	2.6	4.6	Florenzano et al., 2013; Florenzano, 2014
B III - Pantanello	R	12	0.4	2.1	Florenzano and Mercuri, 2012, 2017
B IV - Sant'Angelo Vecchio	H-R	27	1.9	13.1	Florenzano, 2016
B V - Difesa San Biagio	H	9	0.7	1.8	Mercuri et al., 2010
B VI - Miglionico	M	10	0.8	2.4	Florenzano, 2013
B VII - Altojanni	M	7	1.6	6.5	Mercuri et al., 2010
TUSCANY					
T I - San Martino	R	8	<0.1	0.2	Rattighieri et al., 2013
T II - Colle Massari	R	4	0.2	0.4	Bowes et al., 2015, 2017
T III - Podere Terrato	R	11	<0.1	0.4	Bowes et al., 2015, 2017
T IV - Case Nuove	R	15	0.1	1.0	Vaccaro et al., 2013
T V - Poggio dell'Amore	R	5	0.1	0.3	Bowes et al., 2015, 2017

The detailed pollen analyses are reported in Florenzano (2013) (Basilicata) and Rattighieri (2016) (Tuscany). H, Hellenistic; R, Roman; M, Medieval.

average data of the two (IN) or four (OUT) pollen samples per olive grove.

Pollen Data Elaboration

Data were imported into Microsoft Excel 2013 and used to make the graphs. Data elaborations show the trends of olive pollen deposition at three distances from their source (IN, 500 and 1,000 m). Their linear trends were based on the coefficient of determination (R^2) by using linear analysis tools. Principal component analysis (PCA) was performed, by using the XLSTAT 2014 software, to display the distribution of the samples (variables) with respect to *Olea*, *Pinus*, and the total pollen from other taxa observed in the samples.

RESULTS

The pollen analysis from surface soils (Table 2) shows that the total pollen concentrations are always significant, ranging from min. c. 20,000 p/g (B5, higher IN than OUT) to max. c. 130,000 p/g (T2, higher OUT than IN). One half of the samples IN contains higher total concentrations than OUT. The total pollen concentrations are higher in Tuscany than in Basilicata (73,138 vs. 40,137 p/g on average), possibly reflecting the different soil composition and richness of organic matter.

The mean percentage of *Olea* pollen in the samples was similar between the two regions (T = 29.8% vs. B = 29.3%). The IN samples had significant percentages of *Olea*, from 8% in B4 to 58% in B1, but only three olive groves showed *Olea* at >50% for the IN spectra (B1, B5, and T4). In five IN samples, *Olea* occurred at <20% (B2, B3, B4; T2, T7); these values, however, reached to 30–40% when *Pinus* was excluded from the counts. The highest *Olea* percentages came from the sites B1 (IN: c. 58%) and T4 (IN: c. 53%). However, the more extensive olive groves (B5 and T3; Figure 3) had lower values (IN: c. 51% in B5, and c. 23% in T3). This indicated that an evident relationship was lacking between

the size and representativeness of *Olea* pollen taken from the center of an olive grove.

The presence of *Olea* strongly decreased for OUT, at 500 m (2–9%), whereas *Olea* values were more variable for OUT at 1,000 m (Table 2; Figure 4). In some cases (B2, B4), an increase in *Olea* percentage is observed reflecting the pollen rain from other olive trees/groves growing in the area.

The PCA (Figure 5) allowed for the comparison of pollen spectra and sites, and separated them along the distance and composition features. In the sectors III and II, the IN samples—taken from the center of olive groves—are concentrated with the highest *Olea* percentages; moreover, samples with a significant presence of *Pinus* are concentrated in sector II. By contrast, most of the OUT samples taken at 500 m and 1,000 m from the groves center, were plotted in the sectors I and IV; hence this revealed that other taxa influenced these spectra.

DISCUSSION

The Representativeness of *Olea* in the Olive Orchards

As expected, *Olea* pollen was consistently present in the pollen spectra from the olive groves. Generally, we know that pollen released from trees is transported, in part, by wind through the canopy, and partly is trapped by the foliage and eventually falls by gravity in the wood (McKibbin, 2006). The local signal and the anemophilous pollination are predictive of a good amount of *Olea* pollen grains in and around the groves. Although this pollen is one of the main components in the airborne pollen rain of Mediterranean countries, the yearly percentage of *Olea* pollen is not usually reported, and so direct comparison between such aerobiological data and soil pollen spectra is not possible (Ziello et al., 2012). Data from airborne pollen monitoring by the station of Matera (years 2005–2006, by ARPAB) suggested that *Olea* pollen is generally less represented in the air than in the surface soil layers (Florenzano et al., 2011), a pattern

TABLE 2 | Results of the pollen analyses: concentration (p/g = pollen per gram) of all the pollen grains found in the soil surface samples, and the percentages of *Olea* pollen counted in the IN and OUT samples of each plantation.

Olive grove		Total pollen concentration (p/g)			Olea pollen (%)			
Label	Number of pollen samples	Total	IN	OUT	IN	500 m	1,000 m	Mean
B1	6	31,620	25,337	34,761	58.4	7.6	4.4	23.5
B2	6	71,746	40,002	87,617	11.1	1.5	6.4	6.3
B3	6	22,338	20,746	23,134	18.7	2.8	/	9.1
B4	6	55,097	75,992	44,649	7.6	2.1	4.0	4.6
B5	6	19,884	27,200	16,226	50.9	4.0	3.1	19.3
T1	6	73,450	123,290	48,531	26.6	3.4	2.2	10.7
T2	6	127,836	72,232	164,905	13.2	1.6	/	4.6
T3	6	49,154	42,804	52,329	22.8	9.0	5.3	12.4
T4	6	79,093	99,066	65,777	52.8	2.3	/	23.2
T5	6	31,844	32,720	30,968	28.6	4.0	/	16.3
T6	4	45,146	43,968	46,323	48.6	2.1	/	25.3
T7	6	105,441	229,453	43,435	16.2	1.9	1.1	6.4

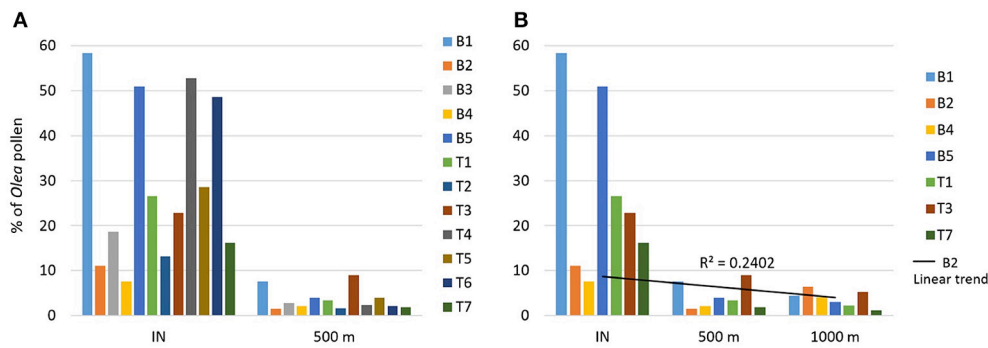


FIGURE 4 | Trends of *Olea* pollen deposition observed in the olive groves: **(A)** IN and 500 m (for all 12 sites), and **(B)** IN, 500 and 1,000 m (for seven sites: the sites without samples at 1,000 m were excluded). R^2 = coefficient of determination.

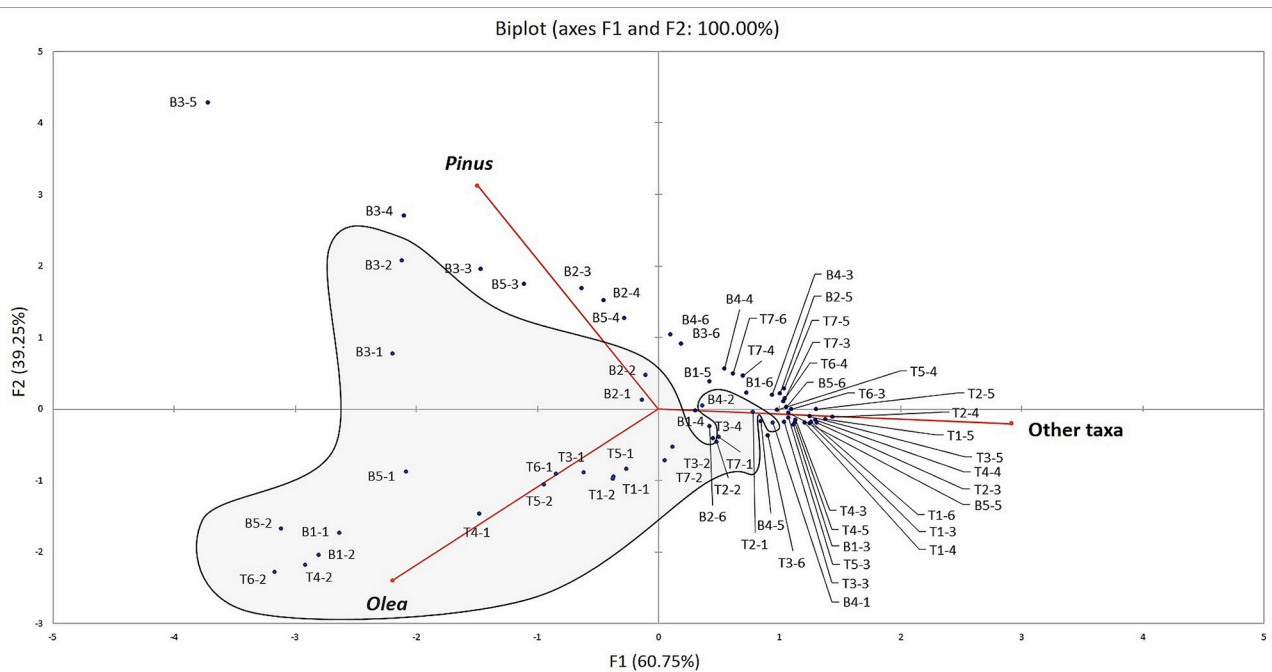


FIGURE 5 | Principal component analysis (PCA; elaboration: XLSTAT 2014) for the 70 samples from the 12 studied olive groves. The modern pollen spectra shows that the percentage of *Olea* depends on the distance from the olive groves (sector III), and on the presence of *Pinus* (II) or other taxa (IV, I).

also evident for *Prunus* orchards (Mercuri, 2015). The pollen of *Olea* was c. 7–11% of the yearly pollen rain, while, in our study, it was 13% on average in the IN and OUT surface soil samples of the B-groves (this value was calculated from the Table 2 data). Nevertheless, we found that *Olea* pollen had very variable percentages (2–58%) depending on the IN and OUT point locations of sampling. We found that, in general, the highest values of *Olea* pollen were recorded in those samples taken from the center of the plantation but no relationship between the size of the olive groves and the amount of olive pollen accumulated in these IN samples. We estimated that the highest values observed in the IN samples, from B1 and T4, sharply dropped from c. 58–53 to c. 5% at 500 m. Hence, *Olea* pollen

could be estimated to decrease by 61–96% in the first few hundred meters from its source. Accordingly, Adams-Groom et al. (2017) showed that most pollen from isolated trees [*Carpinus betulus* L., *Cedrus atlantica* (Endl.) Manetti ex Carrière, *Juglans nigra* L., and *Platanus acerifolia* (Aiton) Willd.] was deposited beneath the canopy (range 63–94%), following an exponentially decreasing curve. An exponential decline was also observed in *Vitis* pollen as function of its distance away from the vineyard edge: *Vitis* pollen can be detected within vineyard soils, but rapidly reaches very low concentrations (<0.1%) or disappears altogether in soils outside vineyards (Turner and Brown, 2004). In the surface soil pollen-deposition patterns of hornbeam, cedar, walnut, and plane pollen, the tailing-off began at the outer edge of the canopy; the amount

of pollen deposited at 50 m was <2.6% and at 100 m it was <0.2% of total deposition in the samples for any tree (Adams-Groom et al., 2017). Bunting (2002), who studied modern pollen deposition in and around woodlands, by using moss polsters and surface sediments from small lakes, also found that local woody pollen percentages generally reached background levels of <100 m from the woodland edge. The rapid decline of tree pollen grains with distance is reported from additional studies (e.g., Broström et al., 2005), which often remark on the 100-m threshold from the woodland edge for the dramatic decrease of tree pollen (Tinsley and Smith, 1974).

The slope of imaginary lines connecting each percentage value at the IN and 500 m sampling sites was negative for each olive grove we considered. This confirms a substantial decrease of pollen deposition at 500 m (Figure 4A). Farther, however, the percentages remain fairly constant, or even increase in the samples taken at 1,000 m sites, and thus inconsistent with the previous one (Figure 4B). A plausible explanation for this result is that the great density of olive groves in the studied areas (mentioned above) caused an abundant pollen emission of airborne pollen in the relevant sampled areas. Many factors likely contributed to the variability of *Olea* pollen percentages in our samples. For example, aerobiological data report that olive-growing areas act as good *Olea* pollen sources but give contribute differently to the airborne pollen rain depending on the prevalent wind direction and the size of groves (Hernandez-Ceballos et al., 2012). Besides the extent of olive groves, the tree size- and age-distributions, the gap between the sampling date and the start of the pollination period (April), the tree density and canopy closure, the abundance of overrepresented pollen from other taxa in the pollen spectra (*Pinus*), the occurrence of particular agricultural practices (e.g., plowing), and the spread of olive groves or the presence of wild olive specimens in the same area, are all variables capable of influencing our olive grove spectra.

The Pollen Evidence of Past Olive Groves near Archeological Sites

Our results obtained from the modern pollen spectra may help to interpret spectra from archeological sites (Table 3). The mean percentages of olive pollen from the archeological sites located in Basilicata suggest that the olive groves were c. 500 m in distance from BI, BII, BIV, and BVII, yet > 500 m from BIII, BV, and BVI. According to these data, oliviculture was one of the most relevant features of the past landscape and economy of Basilicata (Florenzano, 2013). Although Mediterranean vegetation was prevalent in southern Italy, the influence of wild olive does not seem to have had significant incidence in the past spectra from this region: according to the archeological and historical literature, olive cultivation was spread since the 7–6th century BC and favored by the Greek colonization. From that period onward, this crop has largely influenced the agrarian system of this territory (van der Mersch, 1994; De Siena, 2001).

The archeological sites located in Tuscany always had very low *Olea* pollen values ($\leq 0.2\%$), suggesting that the olive groves were not distributed within 1,000 m of the Roman farmhouses of the Cinigiano district. This is due, in part, to the fact that the sites

TABLE 3 | Percentage of *Olea* pollen from the archeological sites of Basilicata and Tuscany, in relation to the distance from the center of an olive grove.

Distance	<i>Olea</i> pollen (%)	
	Modern olive groves	Archeological sites
BASILICATA		
IN	7.6–58.7	No sites
500 m	1.5–7.6	2.5 (B I), 2.6 (B II), 1.9 (B IV), 1.6 (B VII)
>500 m	<1.5	0.4 (B III), 0.7 (B V), 0.8 (B VI)
TUSCANY		
IN	13.2–58.8	No sites
500 m	1.6 - 9	No sites
>500 m	<1.6	<0.1 (T I, T III), 0.2 (T II), 0.1 (T IV, T V)

The estimated distance was based on the results obtained from the soil samples of the modern olive groves. The labels of the archeological sites (B I–VII, and T I–V) follow the list in Table 1.

were small facilities, mainly used seasonally to process cereals, or for animal husbandry, so that herbaceous crops cultivated for food and fodder especially influenced the pollen spectra. However, the low values of *Olea* pollen are recurrent in these sites of Tuscany. Although the Roman agriculture was intensive and complex, we can conclude that oliviculture was not a landscape feature of this region at that time.

A net of off-sites helps to reconstruct the history of this plant in the Italian peninsula. In southern Italy, many off-site records contain *Olea* pollen dating back to the early Holocene (Pergusa lake and Gorgo Basso in Sicily: Sadori and Narcisi, 2001; Tinner et al., 2009; Lago di Trifoglietti in Calabria: Joannin et al., 2012). Afterwards, the fairly continuous curve of *Olea* begins at c. 6500 cal BP during the mid-Holocene (Lago Salso and Lago Alimini Piccolo in Apulia: Di Rita and Magri, 2009; Di Rita et al., 2011; Lago Battaglia: Caroli and Caldara, 2007). From c. 3,600 cal BP onward, *Olea* curves increase in Lago Alimini Piccolo and Lago di Pergusa (c. 20% in both sites), but also increasing in Lago Battaglia at c. 3,100 and 2,600 cal BP. Similarly, in central Italy, some off-site cores show the occurrence of *Olea* during the early Holocene (Lago dell'Accesa in Tuscany: Drescher-Schneider et al., 2007), with its continuous presence from c. 7,300 to 7,000 cal BP also at Lago del Greppo (Vescovi et al., 2010). In Tuscany, at Lago di Massaciuccoli (Mariotti Lippi et al., 2007), *Olea* pollen is present in traces amounts, and found only in the layers dating to the Roman Age; also elsewhere in the region, *Olea* was discontinuously recorded in low amount (Mariotti Lippi et al., 2015; Mariotti Lippi *in verbis*). Then, at c. 2,800–2,700 cal BP, *Olea* increased together with *Juglans* and *Castanea*, and with cereals and other anthropogenic indicators, thus clearly showing the development of cultural/agrarian systems (at Lago di Vico, Lago dell'Accesa and Lago Battaglia: Magri and Sadori, 1999; Caroli and Caldara, 2007; Drescher-Schneider et al., 2007). These data show the general chronological trend of olive pollen from traces to high percentages in the Holocene off-sites (e.g., Lago Alimini Piccolo), but the meaning of *Olea* presence in the off-site and on-site cores is different (Mercuri et al., 2013). We must remember that these records are from areas that lie within the distribution of wild olive trees. In lake records, where we

cannot expect the growth of olive trees at the sampling locations, the presence of pollen from these trees does not strictly mean that they were cultivated. The high amounts of *Olea* in these records (>2%) may be evidence of (mixed) wild stands that occurred besides the plantations in the area (as regional pollen rain is recorded in off-sites); hence, the significance of this pollen requires careful consideration of the chronology and proximity of archeological sites to the off-site.

CONCLUSIONS

Our data show that olive trees can depict a significant picture in pollen spectra, and that their highest percentages are evidence of the local presence of cultivations in a given area. Low percentages of *Olea* pollen may be interpreted as being the result of long-distance transport, while percentages of >2% may indicate the presence of plantations at least 1,000 m from the sampling point(s).

Olea pollen from modern olive groves provides a reference-tool that is useful for paleoenvironmental reconstructions (as generally attested: Davis et al., 2013), and it is important to know the role of olive cultivation in the development of cultural landscapes. As mentioned above, the significance of olive pollen in past spectra is sometimes controversial, since the presence of wild trees enlarge the signal of the species, and the warming phases have a role in spreading olive trees in the Mediterranean landscapes.

The transformation of natural to human-influenced environments (Zanchetta et al., 2013; Mercuri and Sadori, 2014), from the local to trans-regional spatial scales (Mercuri, 2014), may be tracked by observing the presence and trends of *Olea* both in and near the archeological sites. Our work suggests the cultivation of olive trees has been a long-time activity along

the Bradano River in Basilicata, whereas it is a relatively recent one for the agrarian landscape of the Cinigiano district in Tuscany. The research reported in this paper, carried out in two regions with a strong agriculture vocation, shows that the long tradition in olive cultivation marks the present and past pollen spectra, and that it clearly remains evident in the current Mediterranean landscapes.

AUTHOR CONTRIBUTIONS

AM and AF planned the research, and wrote the paper with the cooperation of RF; RR, ER, and AF made pollen sampling and analyses; RF made statistic and graphical elaborations; RM and LA studied olive grove distribution and pollen morphology. All authors read and approved the final manuscript.

FUNDING

This work was supported by the national-funded project SUCCESSO-TERRA (Human societies, climate, environment changes and resource exploitation/sustainability in the Po Plain at the Mid-Holocene times: the Terramara; Ministero dell'Istruzione, dell'Università e della Ricerca PRIN-20158KBLNB).

ACKNOWLEDGMENTS

Archaeological sites are listed in the BRAIN database (<http://brainplants.unimore.it/>). Meteorological data are available from Archivio Meteo Storico (https://www.ilmeteo.it/portale/archivio-meteo/Montescaglioso?refresh_cens; https://www.ilmeteo.it/portale/medie-climatiche/Cinigiano?refresh_ce).

REFERENCES

- Accorsi, C. A. A., Aiello, M., Bandini Mazzanti, M., Bertolani Marchetti, D., De Leonardis, W., Forlani, L., et al. (1983). *Flora Palinologica Italiana: Schede Elaborate Tramite Computer*. Forlì: Publisher Valbonesi.
- Accorsi, C. A. A., Bandini Mazzanti, M., and Forlani, L. (1978). *Modello di schede palinologiche di Pini Italiani: Pinus cembra L., Pinus pinea L., Pinus silvestris L. subsp. silvestris* (ecotipo emiliano). Forlì: Publisher Valbonesi.
- Adams-Groom, B., Skjoth, C. A., Baker, M., and Welch, T. E. (2017). Modelled and observed surface soil pollen deposition distance curves for isolated trees of *Carpinus betulus*, *Cedrus atlantica*, *Juglans nigra* and *Platanus acerifolia*. *Aerobiologia* 33, 407–416. doi: 10.1007/s10453-017-9479-1
- Aguilera, F., and Valenzuela, L. R. (2012). Altitudinal fluctuations in the olive pollen emission: an approximation from the olive groves of the south-east Iberian Peninsula. *Aerobiologia* 28, 403–411. doi: 10.1007/s10453-011-9244-9
- Aguilera, F., Fornaciari, M., Ruiz-Valenzuela, L., Galán, C., Msallem, M., Dhiab, A., et al. (2015). Phenological models to predict the main flowering phases of olive (*Olea europaea* L.) along a latitudinal and longitudinal gradient across the Mediterranean region. *Int. J. Biometeorol.* 59, 629–641. doi: 10.1007/s00484-014-0876-7
- Baldoni, L., Tosti, N., Ricciolini, C., Belaj, A., Arcioni, S., Pannelli, G., et al. (2006). Genetic structure of wild and cultivated olives in the Central Mediterranean Basin. *Ann. Bot.* 98, 935–942. doi: 10.1093/aob/mcl178
- Blasi, C. (ed.) (2010). *La Vegetazione d'Italia*. Rome: Palombi & Partner S.r.l.
- Bottema, S., and Woldring, H. (1990). "Anthropogenic indicators in the pollen record of the Eastern Mediterranean," in *Handbook of Man's Role in the Shaping of the Eastern Mediterranean Landscape*, eds S. Bottema, G. Entjes-Nieborg, and W. van Zeist (Rotterdam: Balkema), 231–264.
- Bowes, K., Mercuri, A. M., and Rattighieri, E. (2015). Palaeoenvironment and land-use of Roman peasant farmhouses in southern Tuscany. *Plant Biosyst.* 149, 174–184. doi: 10.1080/11263504.2014.992997
- Bowes, K., Mercuri, A. M., Rattighieri, E., Rinaldi, R., Arnoldus-Huyzendveld, A., Ghisleni, M., et al. (2017). "Peasant agricultural strategies in Southern Tuscany: convertible agriculture and the importance of pasture," in *Rural Communities in a Globalizing Economy*, eds T. de Haas and G. W. Tol (Leiden: Brill), 170–199.
- Broström, A., Sugita, S., Gaillard, M. J., and Pilesjö, P. (2005). Estimating the spatial scale of pollen dispersal in the cultural landscape of southern Sweden. *Holocene* 15, 252–262. doi: 10.1191/0959683605h1790rp
- Bryant, V. M., and Jones, G. D. (2006). Forensic palynology: current status of a rarely used technique in the United States of America. *Forens. Sci. Int.* 163, 183–197. doi: 10.1016/j.forsciint.2005.11.021
- Bunting, M. J. (2002). Detecting woodland remnants in cultural landscapes: modern pollen deposition around small woodlands in northwest Scotland. *Holocene* 12, 291–301. doi: 10.1191/0959683602h1545rp
- Cañellas-Boltà, N., Rull, V., Vigo, J., and Mercadé, A. (2009). Modern pollen—vegetation relationships along an altitudinal transect in the central Pyrenees (southwestern Europe). *Holocene* 19, 1185–1200. doi: 10.1177/0959683609345082

- Caroli, I., and Caldara, M. (2007). Vegetation history of Lago Battaglia (eastern Gargano coast, Apulia, Italy) during the middle-late Holocene. *Veg. Hist. Archaeobot.* 16, 317–327. doi: 10.1007/s00334-006-0045-y
- Carter, J. C., and Prieto, A. (2011). *The Chora of Metaponto 3. Archaeological survey - Bradano to Basento*. Austin, TX: University of Texas Press.
- Ciabatti, G., Gabellini, A., Ottaviani, C., and Perugi, A. (2009). *I rimboschimenti in Toscana e la loro gestione*. Firenze: Ersi Regione Toscana.
- Costantini, E. A. C., and Righini, G. (2002). “Processi degradativi dei suoli nelle regioni pedologiche italiane,” in *Problematiche del Parametro Suolo. Uno Sguardo Preoccupato alla Situazione Regionale*, ed P. P. Paolillo (Milano: Franco Angeli Urbanistica), 51–78.
- Davis, D. A. S., Zanon, M., Collins, P., Mauri, A., Bakker, J., Barboni, D., et al. (2013). The European modern pollen database (EMPD) project. *Veg. Hist. Archaeobot.* 22, 521–530. doi: 10.1007/s00334-012-0388-5
- De Siena, A. (2001). *Metaponto. Archeologia di una Colonia Greca*. Taranto: Scorpione Editrice.
- Desprat, S., Diaz-Fernández, P. M., Coulon, T., Ezzat, L., Pessarossi-Langlois, J., Gil, L., et al. (2015). *Pinus nigra* (European black pine) as the dominant species of the last glacial pinewoods in south-western to central Iberia: a morphological study of modern and fossil pollen. *J. Biogeogr.* 42, 1998–2009. doi: 10.1111/jbi.12566
- Di Rita, F., and Magri, D. (2009). Holocene drought, deforestation and evergreen vegetation development in the central Mediterranean: a 5500 year record from Lago Alimini Piccolo, Apulia, southeast Italy. *Holocene* 19, 295–306. doi: 10.1177/0959683608100574
- Di Rita, F., Simone, O., Caldara, M., Gehrels, W. R., and Magri, D. (2011). Holocene environmental changes in the coastal Tavoliere Plain (Apulia, southern Italy): a multiproxy approach. *Palaeogeogr. Palaeoecol.* 310, 139–151. doi: 10.1016/j.palaeo.2011.06.012
- Drescher-Schneider, R., de Beaulieu, J. L., Magny, M., Walter-Simonnet, A. V., Bossuet, G., Millet, L., et al. (2007). Vegetation history, climate and human impact over the last 15,000 years at Lago dell'Accesa (Tuscany, Central Italy). *Veg. Hist. Archaeobot.* 16, 279–299. doi: 10.1007/s00334-006-0089-z
- Erdtman, G. (1960). The acetolysis method—a revised description. *Sven. Bot. Tidskr.* 54, 516–564.
- Fall, P. L. (2012). Modern vegetation, pollen and climate relationships on the Mediterranean island of Cyprus. *Rev. Palaeobot. Palynol.* 185, 79–92. doi: 10.1016/j.revpalbo.2012.08.002
- FAOSTAT (2017). *Statistical Databases of the Food and Agriculture Organization of the United Nations*. Available online at: <http://www.fao.org/faostat/en/#data/QC> (retrieved September 16, 2017).
- Florenzano, A. (2013). *Evolution of a Mediterranean Landscape as Shown by the Archaeo-Environmental Reconstruction of Lucanian Sites*. PhD thesis, Università degli Studi di Modena e Reggio Emilia, Modena.
- Florenzano, A. (2014). “Archaeobotany at Fattoria Fabrizio,” in *The Chora of Metaponto 5: A Greek Farmhouse at Ponte Fabrizio*, eds E. Lanza Catti, K. Swift, and J. C. Carter (Austin, TX: University of Texas Press), 113–138.
- Florenzano, A. (2016). “Archaeobotanical analysis,” in *The Chora of Metaponto 6: A Greek Settlement at Sant'Angelo Vecchio*, eds F. Silvestrelli, I. E. M. Edlund-Berry, and J. C. Carter (Austin, TX: University of Texas Press), 159–171.
- Florenzano, A., and Mercuri, A. M. (2012). Palynology of archaeological sites: the example of economy and human impact of the Metaponto area (6th–1st century BC). *Rendiconti Online Soc. Geol. It.* 21, 750–752.
- Florenzano, A., and Mercuri, A. M. (2017). “Pollen evidence and the reconstruction of plant landscape of the Pantanello area (from the 7th to the 1st century BC),” in *The Chora of Metaponto 7: A Greek Sanctuary at Pantanello*, eds J. C. Carter and K. Swift (Austin, TX: University of Texas Press), 461–472.
- Florenzano, A., Benassi, S., and Mercuri, A. M. (2011). Pioggia pollinica e qualità dell'aria: polline di *Olea* negli uliveti dal caso studio della regione Basilicata (sud Italia). *Atti Soc. Nat. Mat. Modena* 142, 175–189.
- Florenzano, A., Mercuri, A. M., and Carter, J. C. (2013). Economy and environment of the Greek colonial system in southern Italy: pollen and NPPs evidence of grazing from the rural site of Fattoria Fabrizio (6th–4th cent. BC; Metaponto, Basilicata). *Ann. Bot.* 3, 173–181. doi: 10.4462/annbotrm-10248
- Florenzano, A., Mercuri, A. M., Pederzoli, A., Torri, P., Bosi, G., Olmi, L., et al. (2012). The significance of intestinal parasite remains in pollen samples from medieval pits in the Piazza Garibaldi di Parma, Emilia Romagna, Northern Italy. *Geoarchaeology* 27, 34–47. doi: 10.1002/gea.21390
- Fornaciari, M., Romano, B., Galan, C., Mediavilla, A., and Dominquez, E. (2000). Aeropalynological and phenological study in two different Mediterranean olive areas: Cordoba (Spain) and Perugia (Italy). *Plant Biosyst.* 134, 199–204. doi: 10.1080/11263500012331358474
- Galán, C., Vazquez, L., Garcia-Mozo, H., and Dominguez, E. (2004). Forecasting olive (*Olea europaea*) crop yield based on pollen emission. *Field Crops Res.* 86, 43–51. doi: 10.1016/S0378-4290(03)00170-9
- Hernandez-Ceballos, M. A., Garcia Mozo, H., Adame, J. A., and Galan, C. (2012). “Last advances in the study of olive airborne pollen dynamic,” in *Olive Consumption and Health*, eds C. A. Savalas and S. M. Nicolau (Hauppauge, NY: Nova Science Publisher).
- Horrocks, M., Coulson, S. A., and Walsh, K. A. (1998). Forensic palynology: variation in the pollen content of soil surface samples. *J. Forens. Sci.* 43, 320–323. doi: 10.1520/JFS16139J
- Joannin, S., Brugiapaglia, E., de Beaulieu, J. L., Bernardo, L., Magny, M., Peyron, O., et al. (2012). Pollen-based reconstruction of Holocene vegetation and climate in Southern Italy: the case of Lago di Trifoglietti. *Clim. Past.* 8, 2223–2279. doi: 10.5194/cpd-8-2223-2012
- Magri, D., and Sadori, L. (1999). Late Pleistocene and Holocene pollen stratigraphy at Lago di Vico (central Italy). *Veg. Hist. Archaeobot.* 8, 247–260.
- Mariotti Lippi, M., Bellini, C., Mori Secci, M., Gonnelli, T., and Pallecchi, P. (2015). Archaeobotany in Florence (Italy): landscape and urban development from the late Roman to the Middle Ages. *Plant Biosyst.* 149, 216–227. doi: 10.1080/11263504.2013.822433
- Mariotti Lippi, M., Guido, M., Menozzi, B. I., Bellini, C., and Montanari, C. (2007). The Massaciuccoli Holocene pollen sequence and the vegetation history of the coastal plains by the Mar Ligure (Tuscany and Liguria, Italy). *Veg. Hist. Archaeobot.* 16, 267–277. doi: 10.1007/s00334-006-0090-6
- McKibbin, R. (2006). Modelling pollen distribution by wind through a forest canopy. *JSME Int. J. B Fluid. T.* 49, 583–589. doi: 10.1299/jsmeb.49.583
- Mercuri, A. M. (2014). Genesis and evolution of the cultural landscape in central Mediterranean: the ‘where, when and how’ through the palynological approach. *Landsc. Ecol.* 29, 1799–1810. doi: 10.1007/s10980-014-0093-0
- Mercuri, A. M. (2015). Applied palynology as a trans-disciplinary science: the contribution of aerobiology data to forensic and palaeoenvironmental issues. *Aerobiologia* 31, 323–339. doi: 10.1007/s10453-015-9367-5
- Mercuri, A. M., and Sadori, L. (2014). “Mediterranean culture and climatic change: past patterns and future trends,” in *The Mediterranean Sea: Its History and Present Challenges*, eds S. Goffredo and Z. Dubinsky (Dordrecht: Springer), 507–527.
- Mercuri, A. M., Florenzano, A., Massamba N'siala, I., Olmi, L., Roubis, D., and Sogliani, F. (2010). Pollen from archaeological layers and cultural landscape reconstruction: case studies from the Bradano Valley (Basilicata, southern Italy). *Plant Biosyst.* 144, 888–901. doi: 10.1080/11263504.2010.491979
- Mercuri, A. M., Mazzanti, M. B., Florenzano, A., Montecchi, M. C., and Rattighieri, E. (2013). *Olea*, *Juglans* and *Castanea*: the OJC group as pollen evidence of the development of human-induced environments in the Italian peninsula. *Quatern. Int.* 303, 24–42. doi: 10.1016/j.quaint.2013.01.005
- Messora, R., Florenzano, A., Torri, P., Mercuri, A. M., Muzzalupo, I., and Arru, L. (2017). Morphology and discrimination features of pollen from Italian olive cultivars (*Olea europaea* L.). *Grana* 56, 204–214. doi: 10.1080/00173134.2016.1216594
- Moriondo, M., Trombi, G., Ferrise, R., Brandani, G., Dibari, C., Ammann, C. M., et al. (2013). Olive trees as bio-indicators of climate evolution in the Mediterranean Basin. *Global Ecol. Biogeogr.* 22, 818–833. doi: 10.1111/geb.12061
- Newton, C., Lorre, C., Sauvage, C., Ivorra, S., and Terral, J. F. (2014). On the origins and spread of *Olea europaea* L. (olive) domestication: evidence for shape variation of olive stones at Ugarit, Late Bronze Age, Syria - a window on the Mediterranean Basin and on the westward diffusion of olive varieties. *Veg. Hist. Archaeobot.* 23, 567–575. doi: 10.1007/s00334-013-0412-4
- Osborne, C. P., Chuine, I., Viner, D., and Woodward, F. I. (2000). Olive phenology as a sensitive indicator of future climatic warming in the Mediterranean. *Plant Cell Environ.* 23, 701–710. doi: 10.1046/j.1365-3040.2000.00584.x
- Pieri, P., Sabato, L., and Tropeano, M. (1996). Significato geodinamico dei caratteri deposizionali e strutturali della Fossa Bradanica nel Pleistocene. *Mem. Soc. Geol. It.* 51, 501–515.

- Pisante, M., Inglese, P., and Lercker, G. (eds.) (2009). *L'ulivo e l'olio. Collana Cultura & Cultura, ideata e coordinata da R. Angelini, Bayer CropScience*. Bologna: Ed. Script.
- Rattighieri, E. (2016). *The Cultural Landscape of Roman Rural Sites in Central Southern Italy: Case Studies from Tuscany and Sicily*. PhD thesis, Università degli Studi di Modena e Reggio Emilia, Modena.
- Rattighieri, E., Rinaldi, R., Bowes, K., and Mercuri, A. M. (2013). Land use from seasonal archaeological sites: the archaeobotanical evidence of small Roman farmhouses in Cinigiano, south-eastern Tuscany - central Italy. *Ann. Bot.* 3, 207–215. doi: 10.4462/annbotrm-10267
- Ribeiro, H., Cunha, M., Calado, L., and Abreu, I. (2012). Pollen morphology and quality of twenty olive (*Olea europaea* L.) cultivars grown in Portugal. *Acta Hort.* 949, 259–264. doi: 10.17660/ActaHortic.2012.949.37
- Roselli, G. (1979). Identificazione di cultivar di ulivo da alcuni caratteri del polline. *Riv. Ortoflorofrutt. It.* 63, 435–445.
- Rühl, J., Caruso, T., Giucastro, M., and La Mantia, T. (2011). Olive agroforestry systems in Sicily: cultivated typologies and secondary succession processes after abandonment. *Plant Biosyst.* 145, 120–130. doi: 10.1080/11263504.2010.540383
- Sadori, L., and Narcisi, B. (2001). The Postglacial record of environmental history from Lago di Pergusa, Sicily. *Holocene* 11, 655–671. doi: 10.1191/09596830195681
- Selvi, F. (2010). A critical checklist of the vascular flora of Tuscan Maremma (Grosseto province, Italy). *Flora Mediterr.* 20, 47–139.
- Sogliani, F., and Marchetta, I. (2010). “Il mondo rurale nella Basilicata nel Medioevo,” in *Archeologia Medievale XXXVII*, ed A. Molinari (Firenze: All'Insegna del Giglio), 171–195.
- Tinner, W., van Leeuwen, J. F. N., Colombaroli, D., Vescovi, E., van der Knaap, W. O., Henne, P. D., et al. (2009). Holocene environmental and climatic changes at Gorgo Basso, a coastal lake in southern Sicily, Italy. *Quatern. Sci. Rev.* 28, 1498–1510. doi: 10.1016/j.quascirev.2009.02.001
- Tinsley, H. M., and Smith, R. T. (1974). Surface pollen studies across a woodland/heath transition and their application to the interpretation of pollen diagrams. *New Phytol.* 73, 547–565. doi: 10.1111/j.1469-8137.1974.tb02132.x
- Turner, S. D., and Brown, A. G. (2004). *Vitis* pollen dispersal in and from organic vineyards: I. Pollen trap and soil pollen data. *Rev. Palaeobot. Palynol.* 129, 117–132. doi: 10.1016/j.revpalbo.2003.12.002
- Vaccaro, E., Bowes, K., Ghisleni, M., Grey, C., Arnoldus-Huyzendveld, A., Cau Ontiveros, M. A., et al. (2013). Excavating the roman peasant II: excavations at Case Nuove, Cinigiano (GR). *Pap. Br. Sch. Rome* 81, 129–179. doi: 10.1017/S006824621300007X
- van der Mersch, C. (1994). *Vins et Amphores de Grande Grèce et de Sicile, IVe-IIIe s. Avant J.-C.* Napoli: Centre Jean Bérard.
- Vermoere, M., Vanhecke, L., Waelkens, M., and Smets, E. (2003). Modern and ancient olive stands near Sagalassos (south-west Turkey) and reconstruction of the ancient agricultural landscape in two valleys. *Global Ecol. Biogeogr.* 12, 217–235. doi: 10.1046/j.1466-822X.2003.00014.x
- Vescovi, E., Ammann, B., Ravazzi, C., and Tinner, W. (2010). A new Late-glacial and Holocene record of vegetation and fire history from Lago del Greppo, northern Apennines, Italy. *Veg. Hist. Archaeobot.* 19, 219–233. doi: 10.1007/s00334-010-0243-5
- Zanchetta, G., Bini, M., Cremaschi, M., Magny, M., and Sadori, L. (2013). The transition from natural to anthropogenic-dominated environmental change in Italy and the surrounding regions since the Neolithic: an introduction. *Quat. Int.* 303, 1–9. doi: 10.1016/j.quaint.2013.05.009
- Ziello, C., Sparks, T. H., Estrella, N., Belmonte, J., Bergmann, K. C., et al. (2012). Changes to airborne pollen counts across Europe. *PLoS ONE* 7:e34076. doi: 10.1371/journal.pone.0034076
- Zohary, D., and Hopf, M. (2000). *Domestication of Plants in the Old World, 3rd Edn*. New York, NY: Oxford University Press.

Conflict of Interest Statement: The authors declare that the research was conducted in the absence of any commercial or financial relationships that could be construed as a potential conflict of interest.

Copyright © 2017 Florenzano, Mercuri, Rinaldi, Rattighieri, Fornaciari, Messori and Arru. This is an open-access article distributed under the terms of the Creative Commons Attribution License (CC BY). The use, distribution or reproduction in other forums is permitted, provided the original author(s) or licensor are credited and that the original publication in this journal is cited, in accordance with accepted academic practice. No use, distribution or reproduction is permitted which does not comply with these terms.



Changes in Modern Pollen Assemblages and Soil Geochemistry along Coastal Environmental Gradients in the Everglades of South Florida

Qiang Yao* and Kam-biu Liu

Department of Oceanography and Coastal Sciences, College of the Coast and Environment, Louisiana State University, Baton Rouge, LA, United States

OPEN ACCESS

Edited by:

Jesse L. Morris,
University of Utah, United States

Reviewed by:

Fabienne Marret,
University of Liverpool,
United Kingdom
Mark Bush,
Florida Institute of Technology,
United States

*Correspondence:

Qiang Yao
qyao4@lsu.edu

Specialty section:

This article was submitted to
Paleoecology,
a section of the journal
Frontiers in Ecology and Evolution

Received: 03 October 2017

Accepted: 28 December 2017

Published: 25 January 2018

Citation:

Yao Q and Liu K (2018) Changes in
Modern Pollen Assemblages and Soil
Geochemistry along Coastal
Environmental Gradients in the
Everglades of South Florida.
Front. Ecol. Evol. 5:178.
doi: 10.3389/fevo.2017.00178

This study aims to document the changes in modern pollen assemblages and soil elemental chemistry along broad edaphic, hydrological, and salinity gradients, including a previously undocumented secondary environmental gradient, in a vast mangrove-dominated wetland region in the Everglades, South Florida. Twenty-five soil surface samples were collected along an interior wetland transect and an estuarine mangrove transect across coastal zones in the Everglades National Park and subjected to palynological and XRF analyses. Modern pollen spectra from the sampling sites were classified into five *a priori* groups—wet prairie, pineland, inland mangroves, coastal mangroves, and fringe mangroves, based on the five vegetation types and sub-environments from which they were collected. Discriminant analysis shows that all (100%) of the samples are correctly classified into their *a priori* groups. On a broad scale, the modern pollen assemblages in surface samples collected from different vegetation types reflect the primary environmental gradient in the Florida Coastal Everglades. A distinct salinity and chemical gradient is also recorded in the XRF results, and the complexity of these gradients is captured at both regional and local scales. At the regional scale, concentrations of all the elements increase from terrestrial toward coastal sites. At the local scale, XRF results show a progressive decrease in most chemical concentrations and in the Cl/Br and Ca/Ti ratios away from the Shark River Slough at each individual site, suggesting that a secondary fluvial/tidal gradient also exists locally as a function of the distance from the river, the main carrier of these chemicals. This study provides new evidence to show that tidal flooding from the Shark River Estuary is directly related to the nutrient availability in the surrounding mangrove forests. These data will deepen our understanding of the environmental drivers behind the vegetation zonation in the region, especially in the mangrove ecosystems, and fill a gap in the pollen data network for the Everglades.

Keywords: surface pollen assemblages, coastal environmental gradients, shark river slough, Everglades National Park, x-ray fluorescence (XRF), mangroves

INTRODUCTION

Delineating the interface between the land and the sea, the coastal zone is marked by environmental gradients as defined by elevation, soil, hydrology, and salinity. Most of the coastal ecosystems are influenced by a primary environmental gradient as a function of distance away from the sea. In some cases, particularly along estuaries, a secondary environmental gradient may also occur as a function of distance away from the river. Superimposed on these environmental gradients are biotic gradients, as defined by a land-to-sea array of vegetation communities. Pollen analysis and X-ray fluorescence (XRF) analysis have been used in paleoecological studies to reconstruct the Holocene history of vegetation changes in the coastal wetlands of the southeastern U.S. (Willard et al., 2001; Donders et al., 2005; van Soelen et al., 2010, 2012; Yao et al., 2015; Yao and Liu, 2017). However, with few exceptions (e.g., Willard et al., 2001), these reconstructions are not supported by surface samples documenting the changes in modern pollen assemblages and soil chemistry along various environmental gradients in these coastal wetland sites, particularly along the secondary environmental gradient in estuarine wetlands.

The Everglades, situated at the southern tip of the Florida peninsula, contain the largest freshwater marshes and contiguous mangrove swamps in North America drained by sloughs and estuaries along hundreds of miles of shoreline (Lodge, 2010). Since the early twentieth century, anthropogenic activities (agriculture and urbanization) have dramatically reduced the seasonality of freshwater flow (Light and Dineen, 1994) and have affected the surface and groundwater flows throughout the Everglades (Saha et al., 2012). In order to provide essential baseline data for the restoration of the hydrological conditions of the Everglades, numerous studies are being conducted along the coastal zones in the Everglades National Park (ENP) to understand the long-term ecological processes and developmental history of these natural wetlands. Recent paleoecological studies from the region suggest that the vegetation shifts in wetland communities during the middle and late Holocene are closely associated with the regional and global-scale climatic phenomena such as position of the Intertropical Convergence Zone (ITCZ) (Donders et al., 2005), the state of the North Atlantic Oscillation (NAO) (Willard and Cronin, 2007; Bernhardt and Willard, 2009), and the Holocene sea-level rise (Yao et al., 2015; Yao and Liu, 2017). To produce accurate results using fossil pollen analysis, it is important to understand how the modern vegetation and environmental gradients are represented in the modern pollen rain of the study area. In the Everglades National Park, few such studies have been conducted. Willard et al. (2001) documented the modern pollen rain from wetland sub-environments in the Florida Everglades and the results show that they have distinctive surface pollen assemblages. Their study, which focuses on the freshwater wetlands and more inland communities, also suggests that pollen record is useful for reconstructing past hydrologic and edaphic changes in the Everglades. More importantly, although estuarine mangroves are the dominant mangrove types in the Everglades, most studies only focus on the primary environmental gradient

between coastal and inland sites (Chen and Twilley, 1999a,b; Willard et al., 2001; Castañeda-Moya et al., 2010, 2013). Modern pollen assemblages and soil chemistry along the secondary environmental gradient away from the river has been overlooked in the research literature from the Everglades.

Here we present the results of palynological and XRF analyses on 25 soil surface samples collected from two transects in the Everglades. Our study focuses on the mangrove-dominated, more clearly marine-influenced wetlands in the southern and southwestern tip of the Everglades, especially the primary and secondary environmental gradients along the Shark River Estuary, where the slow-flowing freshwater originated from Lake Okeechobee meets the saltwater being pushed up by tides from the Gulf of Mexico. The main research questions we seek to answer are: (1) how are coastal environmental gradients expressed in an estuarine environment that encompasses a variety of vegetation communities from pineland and wet prairie to different mangrove ecosystems? (2) As the Shark River is the main conduit in the transportation of chemical nutrients, does a secondary environmental gradient exist in mangrove dominated coastal wetlands, as a function of distance away from the river? Here we present data that relate soil salinity and geochemistry to modern pollen assemblages across that gradient. Data from this study can provide useful baselines for monitoring future environmental changes relating to ongoing disturbance from rising sea-level, hurricanes, and anthropogenic activities.

STUDY REGION AND STUDY SITES

The study region (~600,000 ha) lies between 25°24'06" and 25°21'10" N latitude, and between 80°36'02" and 81°06'53.6" W longitude (**Figure 1**). Tides are semi-diurnal with >0.5 m mean tidal amplitude (Wanless et al., 1994). During the wet season, water overflowing Lake Okeechobee from the rainfall results in a southward sheet flow along a gentle slope of ~3 cm/km into the Shark River Slough (SRS) (Lodge, 2010). The water entering SRS flows through long-hydroperiod prairie sloughs into mangrove swamps at the river estuary and then into Whitewater Bay or the Gulf of Mexico along the southwestern coast of the Everglades. However, these densely vegetated wetlands are phosphate-limited (Castañeda-Moya et al., 2010), where the limited nutrient is supplied by the Gulf of Mexico, rather than the upper watershed (Chen and Twilley, 1999a,b). The study region is also frequently impacted by hurricanes. The sedimentary record revealed that at least 6 paleo-hurricanes made direct landfall at the Shark River Estuary during the past 3000 years (Yao et al., 2015). Instrumental record documented 17 hurricanes near the study area since the nineteenth century (NOAA, 2016), the most recent one being Hurricane Wilma in 2005, a category 3 hurricane that caused massive mangrove mortality and deposited a 10-cm thick storm deposit at the mouth of the SRS (Castañeda-Moya et al., 2010; Yao et al., 2015).

At the regional scale, the coastal vegetation in the Everglades is arranged in well-defined floristic zones parallel to the coast, with mixed mangrove stands near the coast giving way to brackish marshes (graminoid-mangrove mixtures) and then

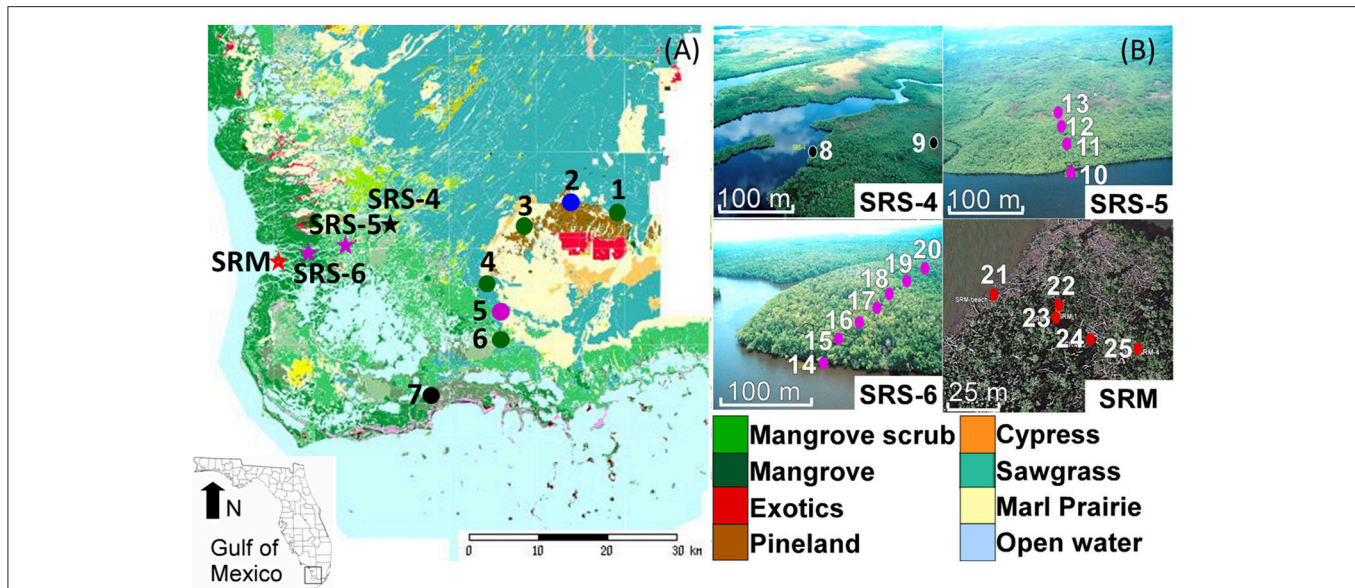


FIGURE 1 | (A) Location of surface sample sites in the Everglades National Park, South Florida, in relation to the vegetation map according to FCE LTER (2018). Colored circles indicate locations of the individual samples along the inland-to-coast transect. Stars indicate sites along the estuarine mangrove transect where multiple samples were taken at each site. Sample numbers correspond to Site IDs described in **Table 1**. **(B)** Aerial photos of sites SRS-4, SRS-5, and SRS-6, and SRM showing locations of individual samples (colored dots). Note the massive mortality of mangroves caused by Hurricane Wilma (2005) evident at site SRM. The vegetation map and aerial photos in this figure were retrieved from FCE LTER. Copyright permission has been acquired.

freshwater marshes further inland (Ross et al., 2000). This distinct vegetation gradient is the result of varying tolerances of mangroves (*Rhizophora mangle*, *Avicennia germinans*, *Laguncularia racemosa*, and *Conocarpus erectus*—a mangrove associate) and coastal wetland plants (e.g., *Cladium jamaicense* and *Spartina alterniflora*) to environmental parameters such as substrate, hydrology, and salinity (Ross et al., 2000; Lodge, 2010; Yao et al., 2015). Within our study region, we recognize five major vegetation types that are controlled by the primary (inland-to-coast) environmental gradient according to elevation, soil, hydrology, and salinity, as follows.

Pineland

Pinelands lie in the vicinity of the wet prairie mosaic, and their substrates typically consist of sand and rocks (Willard et al., 2001). They grow in the higher grounds, thereby having short hydroperiod and burned frequently (Platt, 1999). Pine savannas in the ENP are dominated by *Pinus*, *Quercus*, and containing Burseraceae, Poaceae, Asteraceae, and subtropical hammocks. Such areas are also present in the interior region of the Everglades (e.g., Lostman's Pines and Raccoon Point regions of Big Cypress National Preserve; Doren et al., 1993; Willard et al., 2001; Schmitz et al., 2002; Bernhardt and Willard, 2009; Hanan et al., 2010).

Wet Prairie

Wet prairies occupy most of the interior region in the Everglades and are the driest marsh type in the Everglades (Gleason and Stone, 1994; Lodge, 2010). Wet prairies typically have hydroperiods of less than 12 months and are thus dry seasonally, tending to burn more than once a decade, and even every 1–2

years if adjacent to pine savannas (Platt, 1999; Schmitz et al., 2002; Slocum et al., 2003).

Marl forming periphyton is a common component of wet prairies and is responsible for calcite marl deposits on the limestone terrain (Willard et al., 2001). Patches of well-developed cypress forests, pinelands, and inland mangroves are common sub-environments that lie within the wet prairie mosaics. Cypress forests can be found in deep depressions, thereby having a long hydroperiod resulting in thick peat accumulation (up to 2 m) (Duever et al., 1984). Such wetlands are found from the northern Everglades to the Shark River Slough, Whitewater Bay, Cape Sable, and Florida Bay (Gleason and Stone, 1994; Lodge, 2010).

Inland Mangrove Forests

The coastal area of the ENP, from Naples to Florida Bay, is covered by ~15,000 ha of dense mangrove forests consisting of *R. mangle*, *A. germinans*, *L. racemosa*, and *C. erectus* (Simard et al., 2006; Lodge, 2010). In our study area, all these mangrove species can be found and they form unique sub-mangrove habitats along the primary environmental gradient. Based on their composition and relative distance to the ocean, we categorize these mangrove forests into three groups, which are inland mangrove forests, coastal mangrove forests, and fringe mangrove forests. Inland mangrove forests occur in the innermost zone of the mangrove ecosystem and constitute a broad ecotone between the zones of marine and freshwater influences. This vegetation zone has very low salinity (<5 ppt) and is characterized by graminoid-mangrove mixtures consisting of sawgrass marsh and dwarf mixed mangrove stands (Castañeda-Moya, 2010). *Conocarpus*, a mangrove associate

growing in slightly fresher and inland environments (Hogarth, 2007; Urrego et al., 2010), dominates inland mangrove forests.

Coastal Mangrove Forests

Across the graminoid-mangrove ecotone, areas that receive more marine influences are characterized by coastal mangrove forests. A clear zonation pattern can be observed within this vegetation zone. *Rhizophora* trees are found in areas closer to the shoreline, because they have unique aerial roots which allow them to colonize sites with an unstable substrate and direct tidal influence (Hogarth, 2007). Moving further inland, *Avicennia* typically colonizes highly saline environments. They have pneumatophores that supply oxygen to the underground roots in anaerobic sediments. *Laguncularia*, often lacking special root adaptations, occurs in the interior of the coastal mangrove forest, followed by *Conocarpus* in the upland transitional areas adjunct to inland mangrove forests (Hogarth, 2007).

Fringe Mangrove Forests

Fringe mangrove forests in the Everglades grow as a relatively thin fringe along the coasts facing directly toward the Gulf of Mexico and the Atlantic Ocean. They are directly exposed to tides and waves, as well as storm surges and strong winds. Therefore, *Rhizophora* is usually the dominant species in fringe mangrove forests. Typically, because the mangroves growing in fringe mangrove forests are flushed daily by tides, they are not as tall and productive as coastal mangrove forests growing in more inland and upstream areas. However, because the limited nutrients in the coastal Everglades are supplied by the Gulf of Mexico through tides, waves, and storms (Castañeda-Moya et al., 2010), fringe mangrove forests contain the tallest mangrove trees, and the tree height decreases toward coastal and inland mangrove forests (Table 1) (Chen and Twilley, 1999a,b; Simard et al., 2006).

MATERIALS AND METHODS

Surface Samples and Sampled Coastal Sub-environments

In this study, we collected 25 surface samples along two primary transects in the Everglades—an inland-to-coast transect across major ecosystems from pinelands to wetlands along the main road in the Everglades National Park (ENP), and an estuarine transect through mangrove-dominated communities along the Shark River Slough (Table 1, Figure 1). The two transects parallel distinct primary coastal environmental gradients and cut across major vegetation communities. The surface samples were collected by pushing a small shovel into the ground to collect up to 5 cm of upper materials. After removing plant litter, roots, and algae on the surface of the samples, the very top layer of the sediments was used for pollen and geochemical analyses.

Interior Wetland Transect (Samples 1–7)

The inland transect follows a clear edaphic and hydrological gradient from inland to coast and encompasses a variety of vegetation types. It starts from a wet prairie close to the entrance of ENP, through patches of pineland and cypress forest, and then ends in a patch of inland mangrove forest. Patches of mixed

mangrove and inland mangrove forests can be found along the ecotone between wet prairies and coastal mangrove swamps.

Samples 1, 3, 4, and 6 were taken from prairies outside the woodland habitats but adjacent to the park entrance marsh (EM), Rock Reef Pass (RRP), Mohagony Hammock (MHE), and Nine Mile Pond (NMP), respectively, along the main park road (Figure 1, Table 1). Vegetation at these four sampling locations is typical of wet prairies consisting of mainly sawgrass marsh (*C. jamaicense*) and willow thickets (*Salix*), with *Sagittaria* and *Typha* in more open areas (Slocum et al., 2003). Vegetation at RRP (#3) is dominated by bald cypress (*Taxodium distichum*), with other bottomland hardwood species (e.g., *Acer*, *Fraxinus*, *Annona*) forming the subcanopy, and *Utricularia*, *Eleocharis*, ferns, and Asteraceae present in the understory.

Sample 2 was taken at Long Pine Key (LPK) within patches of pineland surrounded by wet prairies (Figure 1, Table 1). Distinctive from the herbaceous wetlands of the surrounding area, LPK sits directly on the limestone bedrock that is marginally higher than the surrounding landscape, allowing the area to drain properly and support more diverse, upland plants. Vegetation at LPK is dominated by *Pinus elliottii* var *densa*, *Quercus virginiana*, graminoids, and saw palmettos.

Samples 5 and 7 were taken at Paurotis Pond (PP) and Coot Bay (CB) amid patches of mixed mangrove and inland mangrove forests along the wet prairie-mangrove ecotone (Figure 1, Table 1). Vegetation at PP consists of a mixture of *Rhizophora*, *Laguncularia*, *Avicennia*, and some bottomland hardwood species. Vegetation at CB contains mainly *Conocarpus*, a mangrove associate species typically found in more inland and upland areas adjacent to coastal mangrove forests.

Estuarine Mangrove Transect (Samples 8–25)

The estuarine transect follows the channel of SRS, the largest freshwater outlet in the Everglades (Lodge, 2010), and parallels a unique hydrological and salinity gradient controlled by the interaction between tidal activities and river discharge (Castañeda-Moya, 2010). This transect consists of four main study sites (SRM, SRS-6, SRS-5, and SRS-4) extending from the mouth of the SRS to about 18 km upstream. Within each site, surface samples were taken along a secondary transect perpendicular to the river (Figure 1) to capture the secondary environmental gradients as a function of the distance away from the river, which transports not only water but also chemicals from the watershed to the sea (Chen and Twilley, 1999a,b; Castañeda-Moya et al., 2010). A total of 18 samples were collected from the four main study sites. Data for nutrient availability at all sites along the estuarine mangrove transect and salinity data for site SRS-4, SRS-5, and SRS-6 were retrieved from long-term monitoring studies conducted by our collaborators (Castañeda-Moya, 2010; Castañeda-Moya et al., 2010, 2013). Salinity data for site SRM were measured during our field expeditions. Canopy height data at all sites along this transect were retrieved from Simard et al. (2006).

Samples 8 and 9 were taken at SRS-4 (Table 1, Figure 1), located at ~18.2 km upstream from the mouth of the estuary. Due to its most inland location, site SRS-4 has the lowest salinity along the estuarine transect as it is mainly influenced by

TABLE 1 | Surface sample sites in the Everglades National Park, South Florida.

Map ID	Sample ID	GPS	Salinity (ppt)	N:P	Canopy height	Vegetation type	Site description
1	EM	25°24'06", –80°36'02"	\	\	\	Wet prairie	<i>Cladium/Eleocharis</i> marsh close to pine savanna, marl forming
2	LPK	25°25'02", –80°39'58"	\	\	\	Pine savannah	Tall, sparse pineland imbedded in marl prairies, frequent fire
3	RRP	25°24'35", –80°47'05"	\	\	\	Tall cypress	Tall cypress surrounded by dense <i>Cladium</i> marsh
4	MHE	25°20'27", –80°48'51"	\	\	\	Wet prairie	Scrub cypress surrounded by dense <i>Cladium</i> marsh, marl forming
5	PP	25°17'17", –80°47'53"	\	\	<3 m	Mixed mangroves	Scrub <i>Rhizophora</i> , <i>Laguncularia</i> , <i>Avicennia</i> , and hardwood forest
6	NMP	25°14'36", –80°48'19"	\	\	\	Wet prairie	<i>Eleocharis</i> marsh, associate with <i>Cladium</i> , marl forming
7	CB	25°10'51", –80°53'57"	\	\	<5 m	Inland mangroves	<i>Conocarpus</i> forest near brackish marsh
8	SRS4-1	25°24'35", –80°57'51"	4.6 ± 1.1	105	<5 m	Inland mangroves	Scrub <i>Rhizophora</i> >60%, <i>Laguncularia</i> > <i>Conocarpus</i> , no <i>Avicennia</i>
9	SRS4-2	25°24'32", –80°57'43"	4.6 ± 1.1	105	<5 m	Inland mangroves	<i>Cladium</i> marsh behind the mangrove forest, about 200 m from the river
10	SRS5-1	25°22'37", –81°01'57"	20.8 ± 3.1	46	8–10 m	Coastal mangroves	Tall <i>Rhizophora</i> >80%, few <i>Laguncularia</i> and <i>Avicennia</i> , No <i>Conocarpus</i>
11	SRS5-2	25°22'35", –81°01'53"	20.8 ± 3.1	46	8–10 m	Coastal mangroves	Tall <i>Rhizophora</i> >80%, few <i>Laguncularia</i> and <i>Avicennia</i> , No <i>Conocarpus</i>
12	SRS5-3	25°22'33", –81°01'52"	20.8 ± 3.1	46	8–10 m	Ecotone	Ecotone between tall <i>Rhizophora</i> forest and <i>Cladium</i> marsh
13	SRS5-4	25°22'33", –81°01'51"	20.8 ± 3.1	46	8–10 m	Brackish marsh	<i>Cladium</i> marsh behind the mangrove fringe, about 200 m from the river
14	SRS6-1	25°21'53", –81°04'40"	27 ± 2.6	28	>10 m	Coastal mangroves	<i>Laguncularia</i> >40%, <i>Rhizophora</i> >25%, <i>Avicennia</i> >25%, No <i>Conocarpus</i>
15	SRS6-2	25°21'52", –81°04'40"	27 ± 2.6	28	>10 m	Coastal mangroves	
16	SRS6-3	25°21'51", –81°04'40"	27 ± 2.6	28	>10 m	Coastal mangroves	
17	SRS6-4	25°21'50", –81°04'40"	27 ± 2.6	28	>10 m	Coastal mangroves	
18	SRS6-5	25°21'49", –81°04'40"	27 ± 2.6	28	>10 m	Coastal mangroves	
19	SRS6-6	25°21'48", –81°04'40"	27 ± 2.6	28	>10 m	Coastal mangroves	
20	SRS6-7	25°21'48", –81°04'39"	27 ± 2.6	28	>10 m	Coastal mangroves	
21	SRM-1	25°21'11", –81°06'54"	>30	~16	>15 m	Fringe mangroves	Hurricane damaged mangrove forest, <i>Avicennia</i> fringe, <i>Laguncularia</i> and <i>Rhizophora</i> co-dominant, no <i>Conocarpus</i>
22	SRM-2	25°21'11", –81°06'53"	>30	~16	>15 m	Fringe mangroves	
23	SRM-3	25°21'10", –81°06'52"	>30	~16	>15 m	Fringe mangroves	
24	SRM-4	25°21'10", –81°06'51"	>30	~16	>15 m	Fringe mangroves	
25	SRM-5	25°21'10", –81°06'50"	>30	~16	>15 m	Fringe mangroves	

Sample ID is keyed to site numbers in **Figure 1**. Latitudes and longitudes for sites are determined using global positioning systems. The salinity, nutrient, and canopy height gradients along the Shark River transect are retrieved from Castañeda-Moya (2010) and Simard et al. (2006).

groundwater and freshwater runoff. The soil has a pore-water salinity of 4.6 ± 1.1 ppt and is very nutrient-limited (Chen and Twilley, 1999b; Castañeda-Moya, 2010). Hydrologically this site

is flooded 165 days annually. The vegetation here, characterized as an inland mangrove forest, is dominated by *Rhizophora* (67% of total aboveground biomass) with *Laguncularia* and

Conocarpus as co-dominant species. This is the only site along this transect where *Conocarpus* is found and *Avicennia* is absent due to low salinity. In addition, the average mangrove canopy height (<5 m) at this site is the lowest along the transect.

Samples 10–13 and 14–20 were taken at sites SRS-5 and SRS-6, which are located 9.9 km and 4.6 km from the mouth of SRS, respectively (**Figure 1**). Tidal influence gradually increases downstream while fluvial influence decreases; thus nutrient availability, salinity, and canopy height progressively increase from site SRS-4 toward the mouth of the estuary (**Table 1**). Vegetation at these two sites is both characterized as a coastal mangrove forest, although local variations in floristic composition and species abundance exist. Site SRS-5 is flooded 197 days annually. *Rhizophora* is the dominant species (87% of total aboveground biomass) with very few other mangrove species (Castañeda-Moya, 2010). Site SRS-6 is flooded 233 days annually. *Laguncularia* is the dominant species (43% of total aboveground biomass) with *Rhizophora* and *Avicennia* as co-dominant species (43% of total aboveground biomass each). In addition, site SRS-6 has the highest complexity index along the estuarine transect (Castañeda-Moya, 2010).

Samples 21–25 were taken at site SRM (**Table 1**, **Figure 1**). This site is located on the edge of Ponce de Leon Bay, at the mouths of Whitewater Bay and Shark River Estuary (Yao et al., 2015). Flooded by tides 90% of the year, site SRM has the highest salinity and the longest tidal inundation along the estuarine transect. The vegetation is characterized as a fringing mangrove forest, where *Laguncularia* and *Rhizophora* are co-dominant species (Chen and Twilley, 1999a,b; Yao et al., 2015). The average mangrove canopy height at SRM is the highest (>15 m) among all four sites (Simard et al., 2006; Yao et al., 2015). Hurricane Wilma, the most recent major hurricane to cross SRS, made landfall as a category 3 storm near site SRM in 2005. Strong winds and storm surge from this hurricane caused damage to ~1,250 ha of mangrove forest along the west coast of the ENP, resulting in 90% mortality of trees with diameters at breast height greater than 2.5 cm (Smith et al., 2009; Whelan et al., 2009). The storm surge flooded site SRM with 3–4 m of water and deposited ~10 cm of marine sediment as far as 10 km inland (Castañeda-Moya et al., 2010; Yao et al., 2015).

Laboratory Analyses

In the laboratory, all surface samples were subjected to pollen and X-ray fluorescence (XRF) analyses. XRF analysis was conducted by using a handheld Olympus Innov-X DELTA Premium XRF analyzer, which measures the elemental concentrations (ppm) of 25+ elements with an atomic number >15. Fifteen elements were detected in our samples, but six of them were in traceable amount with no systematic changes. Therefore, nine major chemical elements and Cl/Br and Ca/Ti ratios were used in this study as a proxy to present the chemical nutrient availability (**Figure 3**).

For palynological analysis, one commercial *Lycopodium* (L_c) tablet (~18,583 grains) was added to each sample (0.9 mL) as an exotic marker to calculate pollen concentration (grains/cm³) (sum = L_c added * no. of grains counted/ L_c counted/volume

of sample). Laboratory procedures for pollen and XRF analyses followed those described in Yao et al. (2015). Except for samples taken from wet prairies, the hydrofluoric acid treatment was omitted because samples contain mostly peat and a limited amount of silicates. The main pollen taxa, non-pollen microfossils, and charcoal were counted and photographed with an objective of 400x magnification (see Supplement Figure for photos of selected microfossils). The identification of pollen was based on published pollen illustrations by McAndrews et al. (1973) and Willard et al. (2004). Approximately 300 grains of pollen and spores were counted in most of the samples, and this pollen sum was used for the calculation of pollen percentages. The palynological results are reported in percentage (%) diagrams (**Figure 2**), and the common pollen grains are photographed (Supplementary Material).

Statistical Analyses

Principal component analysis (PCA) was performed by using the C-2 version 1.7 on all surface samples to reveal the distribution of pollen taxa according to the environmental gradients (**Figure 4**). The PCA results provide a basis to classify different pollen taxa into statistically meaningful groups, which can be interpreted in terms of different wetland sub-environment. In addition, discriminant analysis (*sensu* Liu and Lam, 1985), an inferential statistical technique, was performed using the IBM SPSS version 22.0 to verify the pollen assemblages with reference to the inferred vegetation types. The stepwise method was used to derive the discriminant functions.

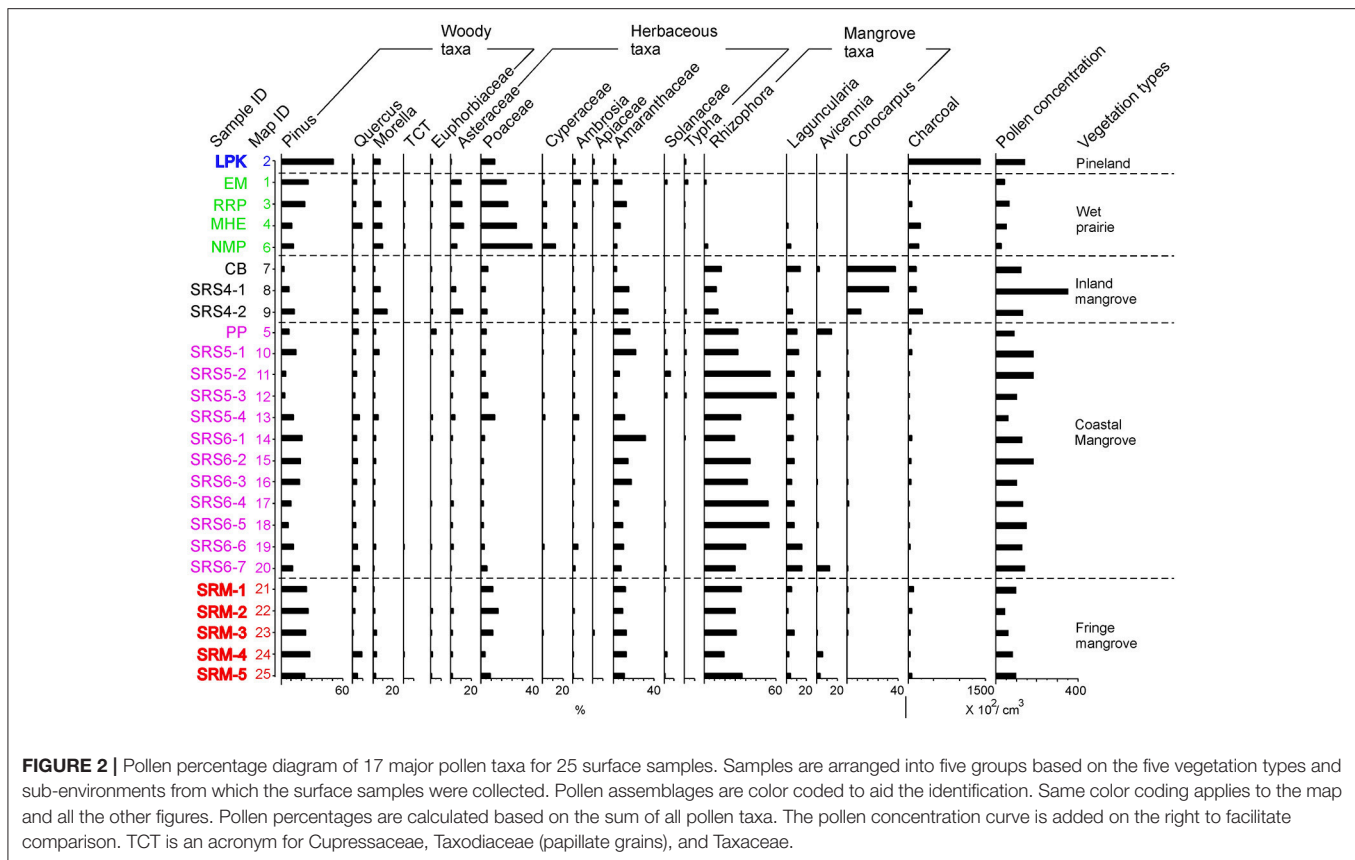
RESULTS

Pollen Assemblages in Vegetation Sub-environments

Seventeen pollen taxa were identified in the 25 surface samples (**Figure 2**). Samples are arranged into five *a priori* groups based on the five vegetation types and sub-environments from which the surface samples were collected, i.e., pineland, wet prairies, inland mangroves, coastal mangroves, and fringing mangroves. The resultant pollen diagram shows that each vegetation type contains a characteristic modern pollen assemblage that can be distinguished from the others (**Figure 2**).

Pineland

The pineland group includes only sample 2 (**Figure 2**). Pollen concentration of this sample is ~15,000 grains/cm³. The relatively high pollen concentration of this sample is due to the fact that *Pinus* (>50%), the dominant pollen taxon of this sample (**Figure 2**), is a very prolific pollen producer. The concentration of charcoal fragments in this sample is also very high (>150,000/cm³). This result is in agreement with the short hydroperiod and frequent wildfires in pine savannas in the Everglades (Platt, 1999). Overall, the pollen assemblage of pineland is closely associated with the local vegetation and environment previously described (Doren et al., 1993; Willard et al., 2001; Schmitz et al., 2002; Bernhardt and Willard, 2009; Hanan et al., 2010).



Wet Prairies

The wet prairie group includes samples 1, 3, 4, and 6 (Figure 2). Pollen concentrations are relatively low in wet prairie assemblages, with less than 6,000 grains/cm³ sediment, compared to 15,000 grains/cm³ in mangrove and pineland assemblages. The main reason may be that Poaceae, the dominant plant group in the wet prairies, tend to be a low pollen producer (Ma et al., 2008). It may also be due to greater oxidation of sediments associated with marl (Willard et al., 2001) and relatively dry substrates. Pollen assemblages in wet prairie group (Figure 2) are characterized by high percentages of herbaceous taxa (Poaceae >20%, Asteraceae >10%, Cyperaceae 5–10%) and *Pinus* (10–30%), and low percentages of all other pollen taxa. Although sample 3 is taken from cypress forest surrounded by wet prairies, *Taxodium* is poorly represented in the pollen record. *Taxodium* pollen is often not well-preserved in dry substrates due to their thin walls (exine). Therefore, the pollen assemblages of cypress forest patches cannot be differentiated from the surrounding wet prairies.

Inland Mangroves

The inland mangrove group includes samples 7, 8, and 9 (Figure 2). Pollen concentrations of this group are relatively high, ranging from 15,000 to 35,000 grains/cm³. The most abundant pollen type is *Conocarpus* (15–35%) (Figure 2). *Rhizophora* and *Amaranthaceae* are also common at these sites, ranging from 5 to 10 and 2 to 5%, respectively, of the total pollen sum.

The lower percentages of upland taxa (e.g., *Pinus* and *Quercus*) and higher pollen concentrations in these samples from Coot Bay and SRS-4 reflect the relatively longer hydroperiod at these sites than the wet prairie sites due to their closer proximity to the Gulf of Mexico and Florida Bay. The local vegetation at Coot Bay is dominated by *Conocarpus*, and SRS-4 is the only site along the Shark River transect where *Conocarpus* is found (Castañeda-Moya, 2010). Therefore, the surface pollen assemblages at these sites are a remarkably good representation of the local vegetation.

Coastal Mangroves

This group includes sample 5 taken at Paurotis Pond (PP), a mixed mangrove forest, and samples 10–20 taken from sites SRS-5 and SRS-6 (Figure 2). Pollen concentrations of these samples range from 10,000 to 20,000 grains/cm³. Pollen assemblages of this group are distinguishable by maximum percentages of *Rhizophora* pollen (20–55%); *Laguncularia*, *Amaranthaceae*, and *Pinus* are also common at these sites, ranging from 5 to 15, 5 to 30, and 10 to 30% of the total pollen sum, respectively (Figure 2). The concentration of charcoal fragments in this group is the lowest among all surface samples (<2,000/cm³). This probably reflects long hydroperiod and the absence of fires at these sites since SRS-5 and SRS-6 are 9.9 and 4.1 miles from the Gulf of Mexico and regularly receive tidal flooding (Castañeda-Moya et al., 2010; Yao and Liu, 2017).

Fringe Mangroves

The fringe mangrove fringe group includes all the samples from site SRM (samples 21–25), which is located at the mouth of the Shark River Estuary (**Figure 1**). Pollen concentrations of this group are all below 10,000/cm³, the lowest among mangrove sub-environments. Comparing with the coastal mangroves group, *Rhizophora* becomes less frequent while a distinct increase of *Pinus* and *Poaceae* is observed in the pollen diagram (**Figure 2**). *Pinus* might be wind transported or washed in from offshore by tides and waves, thereby representing a regional pollen signal. *Poaceae* may represent post-disturbance successional vegetation growing in gaps created by lightning or hurricanes (e.g., Hurricane Wilma).

Numerical Analysis of Modern Pollen Data

Percentage data of all 17 identified pollen taxa were used in PCA and discriminant analysis. On the PCA biplot of the 17 identified pollen taxa (**Figure 4**), the first two principal components (PC) account for 31.1% and 14.4% of the variance, respectively. Along PC1 axis, freshwater marsh species (*Morella*, *Poaceae*, *Asteraceae*, TCT, *Typha*, and *Cyperaceae*) have the highest positive loadings, whereas mangrove species (*Rhizophora*, *Laguncularia*, and *Avicennia*) have the highest negative loadings. It is likely that PC1 represents a salinity gradient whereby salinity increases from positive toward the negative end of the axis. On PC2, freshwater wetland species (*Cyperaceae*, TCT, *Morella*, and *Poaceae*) have the highest negative loadings, and *Apiaceae*, *Typha*, *Pinus*, and *Ambrosia* have the highest positive loadings. Although *Apiaceae* and *Typha* have the highest scores on PC2, they have very low percentages in the pollen assemblage, whereas *Pinus* is very abundant. *Pinus* is the dominant pollen and plant taxon in the pinelands and wet prairies, the vegetation type with the driest substrate and shortest hydroperiod in the Everglades. Thus it is reasonable to interpret that PC2 represents a hydrological gradient reflecting moisture in the substrate.

Discriminant analysis was used to validate the classification of the inferred pollen groups (Liu and Lam, 1985). All (100%) of the samples are correctly classified into their *a priori* groups, and 84% of cross-validated grouped cases were correctly classified (**Table 2**). **Figure 5** shows the five groups of surface samples plotted against discriminant functions 1 and 2, which account for 46.2 and 33.8% of the variance, respectively. The five groups and their centroids are clearly distinct from each other with little overlap between groups (**Figure 5**). The high degree of correct classification suggests that the identification of the inferred vegetation types is statistically robust.

X-Ray Fluorescence Data

The XRF results show that the pineland sample (#2) is characterized by high contents of Ca, Fe, and Ti (**Figure 3**). The high Ca value is probably derived from the limestone bedrock and calcareous sandy substrates that are characteristic of the pinelands in the Everglades (Duever et al., 1984; Willard et al., 2001). Fe and Ti are indicators of terrestrial sediment source, which is consistent with the inland locations of these samples.

The overall XRF signature for samples 1, 3, 4, and 6 from the wet prairies resembles that of the pinelands, although it

contains lower contents of terrestrial components (Ti, and Fe) because these samples are taken from wetland environments. High concentrations of Ca and Sr in samples 1 and 6 are likely derived from periphyton, which is a common feature in wet prairies (Willard et al., 2001). Generally, the chemical elemental assemblages still bear the overall imprint of the underlying marl substrate in the wet prairies and adjacent areas (Lodge, 2010).

Among the mangrove swamp groups, inland mangrove samples (#7–9) have the lowest concentrations of all measured elements (**Figure 3**), suggesting low chemical availability in these sampling locations. This is probably due to the diminished influence of the bedrock and marl substrate as the thickness of the mangrove peat increases downstream, so that the nutrient-poor freshwater carried by the Shark River Slough becomes the main source of chemicals for the soils at these inland mangrove sites.

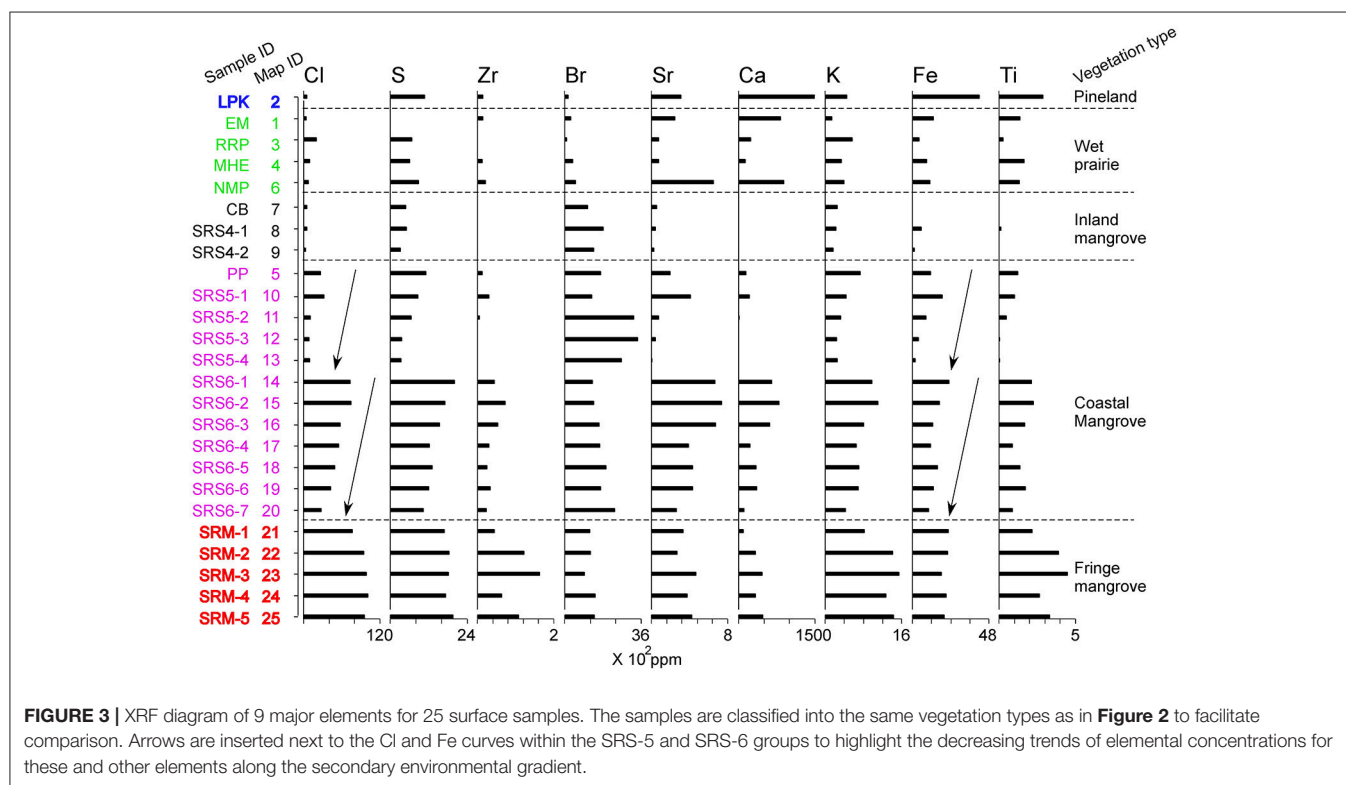
Chemical richness increases distinctly toward the coastal mangrove sites. Samples from site SRS-5 has higher contents of all measured elements than samples from the inland mangrove group, but elemental concentrations increase even more remarkably in samples (#14–20) from site SRS-6 (**Figure 3**). These stepwise jumps in chemical availability downstream from sites SRS-4 to SRS-5 and SRS-6 follow the primary environmental gradient of increasing salinity from land to sea, as the marine influences increase downstream. This implies that tidal waters become an increasingly important supplier of chemicals to the mangrove forests as the distance from the coast decreases. In addition, close examination of the XRF data within each group of samples along the secondary transect at sites SRS-5 and SRS-6 (**Figure 1**, **Table 1**) reveals a striking trend of decreasing elemental concentrations away from the river (depicted by arrows in **Figure 3**). This trend applies to Cl/Br and Ca/Ti ratios and nearly all chemical elements including Cl, S, Zr, Sr, Ca, K, Fe, and Ti. The only exception is Br, which seems to show an opposite or mixed trend. This spatial pattern suggests that the river itself is the primary supplier of chemical elements to the coastal mangrove forests along its course.

Samples from site SRM, representing fringing mangrove forests, generally contain higher concentrations of most measured elements than samples from other mangrove sites (**Figure 3**). Previous studies have shown that ~10 cm of storm sediments from Hurricane Wilma was deposited on the surface of site SRM in 2005 (Castañeda-Moya et al., 2010; Yao et al., 2015). We believe that while surface samples from site SRM capture the pollen signature of local vegetation, their chemical signature was strongly influenced by the Wilma storm deposit rather than the *in situ* accumulation. These sediments came from the nearshore shelf of southern Florida (i.e., Ponce de Leon Bay) and are richer in chemicals than those derived from the nutrient-deficient ecosystems in the Everglades (Chen and Twilley, 1999a,b; Lodge, 2010). It is also remarkable that the trend of decreasing elemental concentrations away from the river, which was observed along the secondary transect of samples within sites SRS-5 and SRS-6 (see the last paragraph), is not apparent along the secondary transect of samples (#21–26) within the SRM group. The absence of a secondary environmental gradient away from the river further supports our interpretation that in the fringing mangrove

TABLE 2 | Classification results of the discriminant analysis performed on 25 surface samples.

Actual group			Predicted Group Membership					Total cases
			1	2	3	4	5	
			Pineland	Wet prairie	Inland mangrove	Coastal mangrove	Fringe mangrove	
Original	1	Pineland	1 ^a (100%) ^b	0	0	0	0	1
	2	Wet prairie	0	4 (100%)	0	0	0	4
	3	Inland mangrove	0	0	3 (100%)	0	0	3
	4	Coastal mangrove	0	0	0	12 (100%)	0	12
	5	Fringe mangrove	0	0	0	0	5 (100%)	5
Cross-validated	1	Pineland	0	0	0	0	1 (100%)	1
	2	Wet prairie	0	3 (75%)	0	0	1 (25%)	4
	3	Inland mangrove	0	0	2 (66.7%)	1 (33.3%)	0	3
	4	Coastal mangrove	0	0	0	11 (91.7%)	1 (8.3%)	12
	5	Fringe mangrove	0	0	0	0	5 (100%)	5

^a100% of the original grouped cases are correctly classified.



forests chemical availability is largely controlled by geochemical release from the storm deposit on the substrate, and the river is no longer the primary source of chemical supply to sites located further away from the channel.

DISCUSSION AND CONCLUSION

On a broad scale, the modern pollen deposition in surface samples collected from different vegetation types reflects the

regional environmental gradients in the Florida Everglades (**Figures 2, 3**). The pollen surface sample from the pinelands is dominated by *Pinus* pollen with very a high abundance of microscopic charcoal, indicating frequent fires in this upland ecosystem. The pineland sample also has a distinctive chemical elemental signature, characterized by high concentrations of Ca, Fe, and Ti. Samples from the wet prairies are characterized by high percentages of herbaceous taxa, and the chemical elemental assemblages reflect the underlying marl substrate. The surface samples from the estuarine transect show clear

vegetation zonation with *Conocarpus* dominating the inland mangroves and *Rhizophora* increasing toward coastal mangrove forests. *Rhizophora* becomes less frequent in fringe mangrove forests while a distinct increase in regional and disturbance taxa (*Pinus* and *Poaceae*) is observed. The XRF data show very low concentrations of all elements in inland mangrove sites but concentrations increase progressively toward coastal and fringe mangrove sites.

Despite these broad-scale correspondences between regional vegetation pattern and modern pollen rain, local variations exist, partly as a result of differential pollen representation among different plant taxa. For example, along the inland transect, *Cladium/Eleocharis* (Cyperaceae) plants are common or dominant components in most of the wet prairie sites (Willard et al., 2001), yet Cyperaceae pollen only account for 5–10% of the total pollen sum and the predominant pollen taxa of the wet prairies group are *Pinus* and *Poaceae*. A likely explanation for this discrepancy is that Cyperaceae pollen has very thin walls (exine) and is remarkably under-represented in the pollen record due to their poor preservation. In the coastal mangrove group, although the most common plant at site SRS-6 is *Laguncularia* (>40% of aboveground biomass), the surface pollen assemblages from SRS-6 do not show a significant increase in *Laguncularia* pollen relative to those from SRS-5. This is because the pollen of *Laguncularia* is insect-pollinated and usually under-represented in the pollen record (Ellison, 2008). A percentage of 2–5% of *Laguncularia* in total pollen sum have been interpreted to represent mangrove forests dominated by white mangrove in previous studies (Behling et al., 2001; Urrego et al., 2009, 2010). Only in two (#19, 20) out of the seven samples in the SRS-6 group do *Laguncularia* pollen exceed 10% of the pollen sum. These low percentages, while seemingly unremarkable, are sufficient to support the inference of the predominance of *Laguncularia* at the study site. In addition, our pollen results also revealed an interesting point regarding the abundance of *Amaranthaceae*. Among the 25 surface samples retrieved from two transects, the average and maximum percentage for *Amaranthaceae* pollen is ~15% and ~30% of the total pollen sum, far less than the *Amaranthaceae* dominated environments (up to 90%) revealed by paleoecological records prior to 2,000 cal yr BP from the Shark River Slough (Willard and Bernhardt, 2011; Yao et al., 2015; Yao and Liu, 2017) and during the last two millennia from the north and central Everglades (Willard et al., 2001, 2006; Bernhardt and Willard, 2009). This discrepancy raises the possibility that the high *Amaranthaceae* zones in these pollen records represent no-analog vegetation communities.

As suggested by the PCA biplot, PC1 represents a salinity gradient whereby *Rhizophora* indicates higher salinity and freshwater wetland plants point to lower salinity (Figure 4). This salinity gradient is also clearly documented in the pollen diagram (Figure 2). At a regional scale, from wet prairies to inland mangroves and coastal mangroves, the overall percentages of herbaceous taxa gradually decrease while *Rhizophora* pollen becomes more abundant, indicating increasing salinity from inland toward coastal sites. This salinity gradient is even more prominent along the estuarine transect. From the inland mangrove group to the coastal mangrove group, the overall

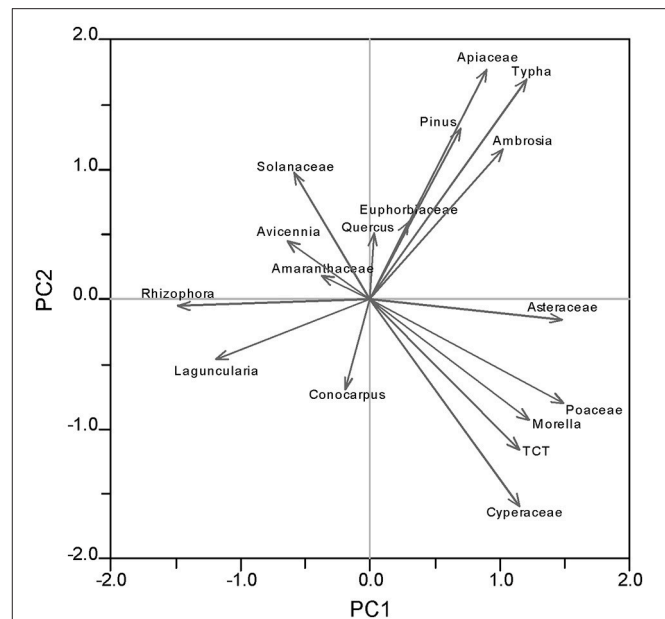


FIGURE 4 | PCA biplot showing coordinates of charcoal and 17 pollen taxa from pollen diagram of surface samples plotted along component 1 and 2.

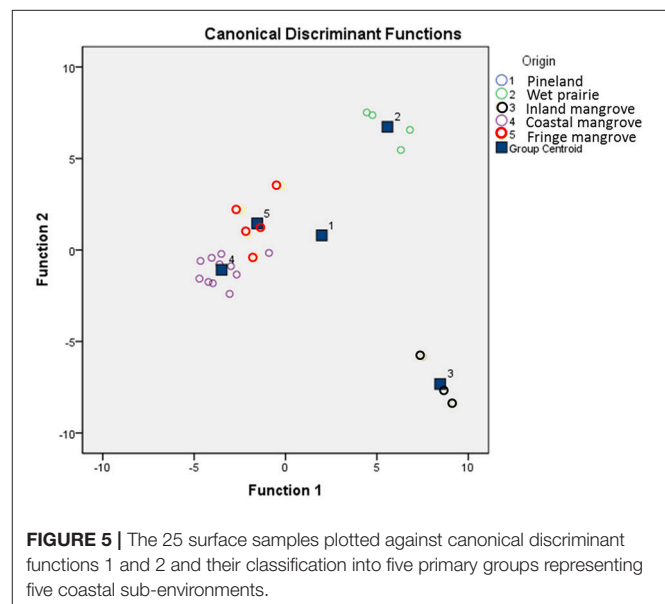


FIGURE 5 | The 25 surface samples plotted against canonical discriminant functions 1 and 2 and their classification into five primary groups representing five coastal sub-environments.

percentages of *Rhizophora* increase significantly. These results are consistent with previous studies indicating that tidal influences and salinity increase toward the mouth of the Shark River Estuary (Castañeda-Moya, 2010). One exception is site SRM located at the mouth of the estuary. One would expect that *Rhizophora* pollen would be more abundant at this site because it has the highest salinity among all sampling locations. However, surface pollen assemblages from site SRM have lower percentages of *Rhizophora* and lower total pollen concentrations in comparison with other mangrove sites along the estuarine transect (Figure 2). This irony is most likely related to severe disturbance from

Hurricane Wilma, which caused massive mortality of mangrove trees at site SRM (Smith et al., 2009). As documented by previous studies, killing of the tall *Rhizophora* trees in the canopy trees lowered the population and flowering rate of *Rhizophora* and provided opportunities for heliophytic herbaceous plants to colonize (Smith et al., 1994, 2009; Baldwin et al., 1995, 2001; Vegas-Vilarrúbia and Rull, 2002; Piou et al., 2006; Hogarth, 2007; Thaxton et al., 2007). A distinct increase in Poaceae in the pollen diagram may represent early successional vegetation communities due to gap creation (Zhang et al., 2012). The elevated pollen percentages of *Pinus* in the SRM group of samples can also be partly explained by a relative increase in the wind-transported regional pollen input (of which *Pinus* is a major component) into the more open mangrove forest after the hurricane disturbance. *Pinus* is also a major component of marine-transported pollen in coastal seawater (Chmura et al., 1999) and could have been deposited in this coastal/estuarine mouth site by tidal currents or storm surge currents.

Distinct salinity and nutrient gradients are also recorded in the XRF results, and their complexities are captured along both primary and secondary environmental gradients. At the regional scale, concentrations of all the elements increase from terrestrial toward coastal sites. Particularly along the estuarine transect, samples from site SRS-6 contain much higher contents of all measured elements than samples from site SRS-5 (Figure 3). These observations are consistent with results from previous studies, which revealed that the limited nutrients available to ecosystems along the Shark River Estuary are supplied from the Gulf of Mexico by tidal and storm activities, rather than from the upper watershed (Chen and Twilley, 1999a,b). From site SRS-4 toward site SRM, tidal influence gradually increases while river discharge asserts less control. Overall, our XRF results further elucidate the primary environmental gradient in the Everglades, which in this case, follows the tidal and chemical gradients along the Shark River Estuary. This primary environmental and biogeochemical gradient also explains the mangrove canopy height gradient along the Shark River Estuary (Table 1), with taller mangrove trees occurring at sites closer to the ocean (Castañeda-Moya et al., 2010).

At the local scale, a clear secondary environmental gradient is also demonstrated within each study site along the estuarine transect (Figure 3). Because samples were taken perpendicularly to the river at sites SRS-4, SRS-5, and SRS-6, each sample is located further away from the river than the previous sample at each individual site (Figure 1). XRF results show a progressive decrease in Ca/Ti and Cl/Br ratios and elemental concentrations toward samples farther away from the Shark River Slough at each individual site (SRS4-1 toward SRS4-2, SRS-5-1 toward SRS-5-4, and SRS-6-1 toward SRS-6-7) (Figure 3). High Ca/Ti and Cl/Br ratios have been described to indicate marine and tidal influences in previous studies (Ingram et al., 2010; Liu et al., 2014). This phenomenon of decreasing Ca/Ti and Cl/Br ratios and elemental concentrations along the secondary environmental gradient suggests that samples taken farther away from the river will receive less fluvial and tidal influence, hence less nutrients. An intriguing exception is offered by Br, which shows an opposite trend of increasing elemental concentrations away

from the Shark River Slough. One possible explanation is that due to the relatively higher electron density and smaller bond strength of the bromine atom, electrophilic substitution is more favorable for aqueous bromine (HOBr/OBr^-), thus making Br more preferential to react with natural organic matter and more concentrated in shallower water (Westerhoff et al., 2004). In our case, the increasing Br concentration away from the river may reflect a progressive decrease in water depth and increase in organic matter away from the Shark River Slough. However, much work is needed to better understand the behavior of Br in the environmental context of this coastal region.

Previous studies have only documented the primary environmental gradient as a function of tidal influence along the Shark River Estuary at a regional scale (i.e., upstream and downstream along the river) (Chen and Twilley, 1999a,b), but our results reveal that a secondary (fluvial/tidal and chemical) gradient exists also at the local scale, as a function of the distance from the river that is the main carrier of these chemicals. This secondary environmental gradient is perpendicular to the regional upstream-downstream gradient and is parallel to the distance from the river to the sampling site. Our results provide new and additional evidence to show that tidal flooding from the Shark River Estuary is directly related to the nutrient availability in the surrounding mangrove forests. In order to fully understand the environmental drivers along the coastal vegetation gradient, more studies are needed to document the vegetation dynamics along the environmental gradients, particularly the secondary environmental gradient, at both the regional and local scales.

AUTHOR CONTRIBUTIONS

QY conducted fieldwork, collected the samples, and undertook palynological and XRF analyses for this study. He also drafted the manuscript and revised it in response to reviewers' comments. KL contributed to the conception and design of the work and the interpretation of the data. He also critically revised the manuscript and gave final approval of the version to be published. Both QY and KL agree to be accountable for all aspects of the work in ensuring that questions related to the accuracy or integrity of any part of the work are appropriately investigated and resolved.

FUNDING

This research was supported by grants from the National Science Foundation (NSF DDRI Grant No. BCS-1303114) and the Inter-American Institute for Global Change Research (IAI #SGP-CRA-2050).

ACKNOWLEDGMENTS

We thank T. A. McCloskey, T. A. Bianchette, V. H. Rivera-Monroy, and E. Castañeda-Moya for their assistance in fieldwork, and to the two reviewers for their thoughtful reviews.

Special thanks go to the Florida Coastal Everglades, Long-term Ecological Research (FCE LTER) program and Florida International University for field and logistical support during this study.

SUPPLEMENTARY MATERIAL

The Supplementary Material for this article can be found online at: <https://www.frontiersin.org/articles/10.3389/fevo.2017.00178/full#supplementary-material>

Figure S1 | Common trees and shrubs: 1–2. *Pinus*, 3. Moraceae, 4. Burseraceae, 5. *Morella*, 6–7. *Quercus*, 8. TCT, 9–12. Euphorbiaceae, 13–15. Rubiaceae, 16–17. *Salix*.

Figure S2 | Common herbaceous taxa: 1–2. Cyperaceae, 3–4. Poaceae, 5–6. Amaranthaceae, 7–8. *Typha*, 9–10. *Sagittaria*, 11 *Ambrosia* (Asteraceae short-spine), 12–16. Asteraceae (long-spine), 17–18. Solanaceae, 19–20. *Batis maritima* (Bataceae), 21–23. Apiaceae.

Figure S3 | Mangrove taxa: 1–5. *Rhizophora mangle*, 6–10. *Laguncularia racemosa*, 11–14. *Avicennia germinans*, 15–20. *Conocarpus erecta*.

Figure S4 | Other pollen taxa: 1. *Alternanthera* (Amaranthaceae), 2. *Liquidambar*, 3. *Alnus*, 4. *Ulmus*, 5. *Corylus*, 6. Haloragaceae, 7–8. *Nyssa*, 9–10. Fabaceae, 11. *Hydrocotyle*, 12–13. Nymphaeaceae, 14–15. *Ilex*.

Figure S5 | Spores: 1. *Lycopodium*, 2–3. *Salvinia minima*, 4. *Pteridium*, 5–7. Polypodiaceae, 8. *Glomus*, 9–18. Unidentified fungal spores.

Figure S6 | Non-pollen/spore microfossil: 1–2. Test linings of foraminifera, 3. *Pediastrum* (green algae), 4 and 6. cysts of *Lingulodinium machaerophorum* (dinoflagellates), 5. cyst of *Polysphaeridium zoharyi* (dinoflagellate), 7. cyst of *Spiniferites* sp. (dinoflagellate), 8 and 9. possibly reworked dinoflagellate cysts.

REFERENCES

- Baldwin, A. H., Egnatovich, M. S., Ford, M. A., and Platt, W. J. (2001). Regeneration in fringe mangrove forests damaged by Hurricane Andrew. *Plant Ecol.* 57, 151–164. doi: 10.1023/A:1013941304875
- Baldwin, A. H., Platt, W. J., Gathen, K. L., Lessman, J. M., and Rauch, T. J. (1995). Hurricane damage and regeneration in fringe mangrove forests of southeast Florida USA. *J. Coast. Res.* 21, 169–183.
- Behling, H., Cohen, M. C. L., and Lara, R. J. (2001). Studies on Holocene mangrove ecosystem dynamics of the Bragança, a Peninsula in North-Eastern Pará, Brazil. *Palaeogeogr. Palaeoclimatol. Palaeoecol.* 167, 225–242. doi: 10.1016/S0031-0182(00)00239-X
- Bernhardt, C. E., and Willard, D. A. (2009). Response of the Everglades ridge and slough landscape to climate variability and 20th-century water management. *Ecol. Appl.* 19, 1723–1738. doi: 10.1890/08-0779.1
- Castañeda-Moya, E. (2010). *Landscape Patterns of Community Structure, Biomass and Net Primary Productivity of Mangrove Forests in the Florida Coastal Everglades as a Function of Resources, Regulators, Hydroperiod, and Hurricane Disturbance*. Dissertation, Louisiana State University.
- Castañeda-Moya, E., Twilley, R. R., and Rivera-Monroy, V. H. (2013). Allocation of biomass and net primary productivity of mangrove forests along environmental gradients in the Florida Coastal Everglades, USA. *For. Ecol. Manage.* 307, 226–241. doi: 10.1016/j.foreco.2013.07.011
- Castañeda-Moya, E., Twilley, R. R., Rivera-Monroy, V. H., Zhang, K. Q., Davis, S. E. III, and Ross, M. S. (2010). Sediment and nutrient deposition associated with Hurricane Wilma in mangroves of the Florida Coastal Everglades. *Estuar. Coasts* 33, 45–58. doi: 10.1007/s12237-009-9242-0
- Chen, R., and Twilley, R. R. (1999a). A simulation model of organic matter and nutrient accumulation in mangrove wetland soils. *Biogeochemistry* 44, 93–118. doi: 10.1007/BF00993000
- Chen, R., and Twilley, R. R. (1999b). Patterns of mangrove forest structure and soil nutrient dynamics along the Shark River Estuary, Florida. *Estuaries* 22, 955–970. doi: 10.2307/1353075
- Chmura, G. L., Smirnov, A. N., and Campbell, I. A. (1999). Pollen transport through distributaries and depositional patterns in coastal waters. *Palaeogeogr. Palaeoclimatol. Palaeoecol.* 149, 257–270. doi: 10.1016/S0031-0182(98)00205-3
- Donders, T. H., Wagner, F., Dilcher, D. L., and Visscher, H. (2005). Mid-to late-Holocene El Niño-Southern Oscillation dynamics reflected in the subtropical terrestrial realm. *Proc. Natl. Acad. Sci. U.S.A.* 102, 10904–10908. doi: 10.1073/pnas.0505015102
- Doren, R. F., Platt, W. J., and Whiteaker, L. D. (1993). Density and size structure of slash pine stands in the everglades region of south Florida. *For. Ecol. Manage.* 59, 295–311. doi: 10.1016/0378-1127(93)90009-C
- Duever, M. J., Meeder, J. F., and Duever, L. C. (1984). “Ecosystems of the big cypress swamp,” in *Cypress Swamps*, eds K. C. Ewel and H. J. Odum (Gainesville, FL: University of Florida Press), 294–303.
- Ellison, J. C. (2008). Long-term retrospection on mangrove development using sediment cores and pollen analysis: a review. *Aquat. Bot.* 89, 93–104. doi: 10.1016/j.aquabot.2008.02.007
- FCE LTER (2018). *Florida Coastal Everglades LTER Mapserver Project*. Available online at: <http://fcelter.fiu.edu/gis/everglades-map/> (Accessed October 2, 2017).
- Gleason, P. J., and Stone, P. A. (1994). “Age, origin and landscape evolution of the Everglades peatland,” in *Everglades, the Ecosystem and its Restoration*, eds S. M. Davis and J. C. Ogden (Delray Beach, FL: St. Lucie Press), 149–198.
- Hanan, E. J., Ross, M. S., Ruiz, P. L., and Saht, J. P. (2010). Multi-scaled grassland-woody plant dynamics in the heterogeneous marl prairies of the southern everglades. *Ecosystems* 13, 1256–1274. doi: 10.1007/s10021-010-9386-6
- Hogarth, P. J. (2007). *The Biology of Mangroves and Seagrasses, 2nd Edn*. New York, NY: Oxford University Press.
- Ingram, W. C., Meyers, S. R., Brunner, C. A., and Martens, C. S. (2010). Late Pleistocene–Holocene sedimentation surrounding an active seafloor gas hydrate and cold-seep field on the Northern Gulf of Mexico Slope. *Mar. Geol.* 278, 43–53. doi: 10.1016/j.margeo.2010.09.002
- Light, S. S., and Dineen, J. W. (1994). “Water control in the Everglades: a historical perspective,” in *Everglades: The Ecosystem and Its Restoration*, eds S. M. Davis and J. C. Ogden (Delray Beach, FL: St. Lucie Press), 47–84.
- Liu, K. B., and Lam, N. S. N. (1985). Paleovegetational reconstruction based on modern and fossil pollen data: an application of discriminant analysis. *Ann. Assoc. Am. Geograph.* 75, 115–130. doi: 10.1111/j.1467-8306.1985.tb00062.x
- Liu, K. B., McCloskey, T. A., Ortego, S., and Maiti, K. (2014). Sedimentary signature of Hurricane Isaac in a Taxodium swamp on the western margin of Lake Pontchartrain, Louisiana, USA. *Proc. Int. Assoc. Hydrol. Sci.* 367, 421–428. doi: 10.5194/pias-367-421-2015
- Lodge, T. E. (2010). *The Everglades Handbook: Understanding the Ecosystem, 2nd Edn*. Boca Raton, FL: CRC Press.
- Ma, Y., Liu, K. B., Feng, Z., Sang, Y., Wang, W., and Sun, A. (2008). A survey of modern pollen and vegetation along a south–north transect in Mongolia. *J. Biogeogr.* 35, 1512–1532. doi: 10.1111/j.1365-2699.2007.01871.x
- McAndrews, J. H., Berti, A. A., and Norris, G. (1973). *Key to the Quaternary Pollen and Spores of the Great Lakes Region*. Toronto, ON: Royal Ontario Museum.
- NOAA (2016). *National Oceanic and Atmospheric Administration, Hurricane Center, Historical Hurricane Tracks website*. Available online at: <https://coast.noaa.gov/hurricanes/> (Accessed October 5, 2015).
- Piou, C., Feller, I., Berger, U., and Chi, F. (2006). Zonation patterns of Belizean offshore mangrove forests 41 years after a catastrophic hurricane. *Biotropica* 38, 365–374. doi: 10.1111/j.1744-7429.2006.00156.x
- Platt, W. J. (1999). “Southeastern pine savannas,” in *The Savanna, Barren, and Rock Outcrop Communities of North America*, eds R. C. Anderson, J. S. Fralish, and J. Baskin (Cambridge: Cambridge University Press), 23–51.
- Ross, M. S., Meeder, J. F., Sah, J. P., Ruiz, P. L., and Telesnicki, G. J. (2000). The southeast saline Everglades revisited: 50 years of coastal vegetation change. *J. Veg. Sci.* 11, 101–112. doi: 10.2307/3236781

- Saha, A. K., Moses, C. S., Price, R. M., Engel, V., Smith, T. J., and Anderson, G. (2012). A hydrological budget (2002–2008) for a large subtropical wetland ecosystem indicates marine groundwater discharge accompanies diminished freshwater flow. *Estuar. Coasts* 35, 459–474. doi: 10.1007/s12237-011-9454-y
- Schmitz, M., Platt, W. J., and DeCoster, J. (2002). Substrate heterogeneity and numbers of plant species in Everglades savannas (Florida, USA). *Plant Ecol.* 160, 137–148. doi: 10.1023/A:1015848300802
- Simard, M., Zhang, K. Q., Rivera-Monroy, V. H., Ross, M. S., Ruiz, P. L., Castañeda-Moya, M., et al. (2006). Mapping height and biomass of mangrove forests in Everglades National Park with SRTM elevation data. *Photogramm. Eng. Remote Sensing* 72, 299–311. doi: 10.14358/PERS.72.3.299
- Slocum, M. G., Platt, W. J., and Cooley, H. C. (2003). Effects of differences in prescribed fire regimes on patchiness and intensity of fires in subtropical savannas of Everglades National Park, Florida. *Restor. Ecol.* 11, 91–102. doi: 10.1046/j.1526-100X.2003.00115.x
- Smith, T. J., Anderson, G. H., Balentine, K., Tiling, G., Ward, G. A., and Whelan, K. R. T. (2009). Cumulative impacts of hurricanes on Florida mangrove ecosystems: sediment deposition, storm surges and vegetation. *Wetlands* 29, 24–34. doi: 10.1672/08-40.1
- Smith, T. J., Robblee, M. B., Wanless, H. R., and Doyle, T. W. (1994). Mangroves, hurricanes, and lightning strikes. *Bioscience* 44, 256–263. doi: 10.2307/1312230
- Thaxton, J. M., DeWalt, S. J., and Platt, W. J. (2007). Spatial patterns of regeneration after Hurricane Andrew in two south Florida fringe mangrove forests. *Florida Sci.* 70, 148–156.
- Urrego, L. E., Bernal, G., and Polanía, J. (2009). Comparison of pollen distribution patterns in surface sediments of a Colombian Caribbean mangrove with geomorphology and vegetation. *Rev. Palaeobot. Palynol.* 156, 358–375. doi: 10.1016/j.revpalbo.2009.04.004
- Urrego, L. E., González, C., Urán, G., and Polanía, J. (2010). Modern pollen rain in mangroves from San Andres Island, Colombian Caribbean. *Rev. Palaeobot. Palynol.* 162, 168–182. doi: 10.1016/j.revpalbo.2010.06.006
- van Soelen, E. E., Brooks, G. R., Larson, R. A., Sinninghe Damsté, J. S., and Reichart, G. J. (2012). Mid-to late-Holocene coastal environmental changes in Southwest Florida, USA. *Holocene* 22, 929–938. doi: 10.1177/0959683611434226
- van Soelen, E. E., Lammertsma, E. I., Cremer, H., Donders, T. H., Sangiorgi, F., Brooks, G. R., et al. (2010). Late Holocene sea-level rise in Tampa Bay: integrated reconstruction using biomarkers, pollen, organic-walled dinoflagellate cysts, and diatoms. *Estuar. Coast. Shelf Sci.* 86, 216–224. doi: 10.1016/j.ecss.2009.11.010
- Vegas-Vilarrúbia, T., and Rull, V. (2002). Natural and human disturbance history of the Playa Medina mangrove community (Eastern Venezuela). *Caribb. J. Sci.* 38, 66–76.
- Wanless, H. R., Parkinson, R. W., and Tedesco, L. P. (1994). “Sea level control on stability of everglades wetlands,” in *Everglades: The Ecosystem and Its Restoration*, eds S. M. Davis and J. C. Ogden (Delray Beach, FL: St. Lucie Press), 199–223.
- Westerhoff, P., Chao, P., and Mash, H. (2004). Reactivity of natural organic matter with aqueous chlorine and bromine. *Water Res.* 38, 1502–1513. doi: 10.1016/j.watres.2003.12.014
- Whelan, K. R. T., Smith, T. J. I., Anderson, G. H., and Ouellette, M. L. (2009). Hurricane Wilma’s impact on overall soil elevation and zones within the soil profile in a mangrove forest. *Wetlands* 29, 16–23. doi: 10.1672/08-125.1
- Willard, D. A., and Bernhardt, C. E. (2011). Impacts of past climate and sea level change on Everglades wetlands: placing a century of anthropogenic change into a late-Holocene context. *Clim. Change* 107, 59–80. doi: 10.1007/s10584-011-0078-9
- Willard, D. A., and Cronin, T. M. (2007). Paleocology and ecosystem restoration: case studies from Chesapeake Bay and the Florida Everglades. *Front. Ecol. Environ.* 5, 491–498. doi: 10.1890/070015
- Willard, D. A., Bernhardt, C. E., Holmes, C. W., Landacre, B., and Marot, M. (2006). Response of Everglades tree islands to environmental change. *Ecol. Monogr.* 76, 565–583. doi: 10.1890/0012-9615(2006)076[0565:ROETT]2.0.CO;2
- Willard, D. A., Cooper, S. R., Gamez, D., and Jensen, J. (2004). Atlas of pollen and spores of the Florida Everglades. *Palynology* 28, 175–227. doi: 10.2113/28.1.175
- Willard, D. A., Weimera, L. M., and Riegel, W. L. (2001). Pollen assemblages as paleoenvironmental proxies in the Florida Everglades. *Rev. Palaeobot. Palynol.* 113, 213–235. doi: 10.1016/S0034-6667(00)00042-7
- Yao, Q., and Liu, K. B. (2017). Dynamics of marsh-mangrove ecotone since the mid-Holocene: a palynological study of mangrove encroachment and sea level rise in the Shark River Estuary, Florida. *PLoS ONE* 12:e0173670. doi: 10.1371/journal.pone.0173670
- Yao, Q., Liu, K. B., Platt, W. J., and Rivera-Monroy, V. H. (2015). Palynological reconstruction of environmental changes in coastal wetlands of the Florida Everglades since the mid-Holocene. *Q. Res.* 83, 449–458. doi: 10.1016/j.yqres.2015.03.005
- Zhang, K., Liu, H., Li, Y., Xu, H., Shen, J., Rhome, J., et al. (2012). The role of mangroves in attenuating storm surges. *Estuar. Coast. Shelf Sci.* 102, 11–23. doi: 10.1016/j.ecss.2012.02.021

Conflict of Interest Statement: The authors declare that the research was conducted in the absence of any commercial or financial relationships that could be construed as a potential conflict of interest.

Copyright © 2018 Yao and Liu. This is an open-access article distributed under the terms of the Creative Commons Attribution License (CC BY). The use, distribution or reproduction in other forums is permitted, provided the original author(s) or licensor are credited and that the original publication in this journal is cited, in accordance with accepted academic practice. No use, distribution or reproduction is permitted which does not comply with these terms.



ROPES Reveals Past Land Cover and PPEs From Single Pollen Records

Martin Theuerkauf^{1,2*} and John Couwenberg^{1,2}

¹ Working Group on Peatland Studies and Palaeoecology, Institute of Botany and Landscape Ecology, University of Greifswald, Greifswald, Germany, ² Partner in the Greifswald Mire Centre, Greifswald, Germany

OPEN ACCESS

Edited by:

Thomas Giesecke,
University of Göttingen, Germany

Reviewed by:

Per Sjögren,
UiT The Arctic University of Norway,
Norway
Andria Dawson,
University of California, Berkeley,
United States

*Correspondence:

Martin Theuerkauf
martin.theuerkauf@uni-greifswald.de

Specialty section:

This article was submitted to
Quaternary Science, Geomorphology
and Paleoenvironment,
a section of the journal
Frontiers in Earth Science

Received: 17 November 2017

Accepted: 09 February 2018

Published: 10 April 2018

Citation:

Theuerkauf M and Couwenberg J
(2018) ROPES Reveals Past Land
Cover and PPEs From Single Pollen
Records. *Front. Earth Sci.* 6:14.
doi: 10.3389/feart.2018.00014

Quantitative reconstructions of past vegetation cover commonly require pollen productivity estimates (PPEs). PPEs are calibrated in extensive and rather cumbersome surface-sample studies, and are so far only available for selected regions. Moreover, it may be questioned whether present-day pollen-landcover relationships are valid for palaeo-situations. We here introduce the ROPES approach that simultaneously derives PPEs and mean plant abundances from single pollen records. ROPES requires pollen counts and pollen accumulation rates (PARs, grains cm⁻² year⁻¹). Pollen counts are used to reconstruct plant abundances following the REVEALS approach. The principle of ROPES is that changes in plant abundance are linearly represented in observed PAR values. For example, if the PAR of pine doubles, so should the REVEALS reconstructed abundance of pine. Consequently, if a REVEALS reconstruction is “correct” (i.e., “correct” PPEs are used) the ratio “PAR over REVEALS” is constant for each taxon along all samples of a record. With incorrect PPEs, the ratio will instead vary. ROPES starts from random (likely incorrect) PPEs, but then adjusts them using an optimization algorithm with the aim to minimize variation in the “PAR over REVEALS” ratio across the record. ROPES thus simultaneously calculates mean plant abundances and PPEs. We illustrate the approach with test applications on nine synthetic pollen records. The results show that good performance of ROPES requires data sets with high underlying variation, many samples and low noise in the PAR data. ROPES can deliver first landcover reconstructions in regions for which PPEs are not yet available. The PPEs provided by ROPES may then allow for further REVEALS-based reconstructions. Similarly, ROPES can provide insight in pollen productivity during distinct periods of the past such as the Lateglacial. We see a potential to study spatial and temporal variation in pollen productivity for example in relation to site parameters, climate and land use. It may even be possible to detect expansion of non-pollen producing areas in a landscape. Overall, ROPES will help produce more accurate landcover reconstructions and expand reconstructions into new study regions and non-analog situations of the past. ROPES is available within the R package DISCOVER.

Keywords: DISCOVER, landcover reconstruction, palynology, pollen accumulation rates, pollen productivity estimates, vegetation history

OBJECTIVES

The field of pollen analysis was established 100 years ago, following the presentation of first pollen diagrams by Swedish geologist Lennart von Post (von Post, 1918). Initially used for stratigraphic purposes, the power of pollen analysis to reconstruct past landcover was soon recognized—and it has remained the most powerful tool in that field until today. Reconstructing past landcover from the pollen record is far from simple, however. The most obvious limitations arise from the production bias and the dispersal bias: pollen productivity as well as pollen dispersal differ among plant taxa. Moreover, pollen deposition at each site is composed of pollen arriving from the vicinity of the sample site as well as of pollen arriving from farther away. Because nearby pollen sources contribute more pollen than distant ones, the pollen record represents the surrounding vegetation in a distance weighted manner.

Despite the long history of the field, quantitative methods to correct for these biases only came into regular use over the past decade. The most widespread approach is the REVEALS model (Regional Estimates of VEgetation Abundance from Large Sites, Sugita, 2007), which aims to translate pollen deposition from large lakes into regional vegetation composition. REVEALS is a correction factor approach; it employs pollen productivity estimates (PPEs) to correct for the production bias and models of pollen dispersal to correct for the dispersal bias in pollen data. PPEs so far derive from calibration studies that relate present day vegetation to modern pollen deposition across a series of sites. Calibration of such surface sample PPEs is cumbersome: it requires pollen data from multiple sites, plant abundances in the pollen source area of each site and a profound understanding of pollen dispersal and deposition. The surface sample PPEs are then applied in palaeo-reconstructions under the assumption that pollen productivity of plant taxa in the past equals present day productivity. This assumption may often be violated, however, because pollen productivity is influenced by climate (Hicks, 1999), stand structure (Matthias et al., 2012; Feaser and Dörfler, 2014) or land management (Theuerkauf et al., 2015). Furthermore, for pollen morphotypes that include numerous taxa, natural or human induced changes in actual species composition may alter overall pollen productivity. This effect is most obvious for grasses, because pollen productivity differs significantly between the various species (Prieto-Baena et al., 2003). The use of PPEs based on (modern) surface sample studies therefore introduces a yet unknown error in REVEALS applications. In addition, because REVEALS produces proportional abundances, error in the PPE of just one taxon will introduce error in the reconstructed cover of all taxa in the record.

Already von Post (1918) recognized that absolute pollen data, i.e. pollen accumulation rates (PAR), potentially provide an independent record for each taxon, devoid of such mutual disturbances. Yet, calculating PARs requires exact chronologies and so only became feasible with radiocarbon dating in the 1960s. Early applications showed that PAR values can be very noisy, however; even across a single lake they may differ by orders of magnitude due to sediment redeposition and focusing

(Davis, 1967). These results raised much skepticism against the usability of PARs to quantify past abundances so that the field was largely abandoned, with the exception of treeline studies. Across treelines, changes in PAR values are large compared to the noise so that they have been proven a useful tool (Hicks, 2001; Seppä and Hicks, 2006; Theuerkauf and Joosten, 2012). Giesecke and Fontana (2008) have demonstrated that the noise in PAR data can be reduced with careful site selection. The question arises whether and how PAR values can be used in a sensible and robust way in quantitative vegetation reconstruction. We here suggest the ROPES approach (REVEALS withOut PpES), which combines PAR values with the REVEALS model in an optimization algorithm. The main underlying idea is that not the PAR values as such, but changes in the PAR values are meaningful and robust.

VALIDATION

The Principle of ROPES

ROPES derives from two main assumptions: (i) the REVEALS model allows to translate pollen counts from large lakes into past regional plant abundances and (ii) for each taxon, absolute pollen deposition at a site is a linear representation of its distance weighted abundance (Prentice and Webb, 1986). Hence, changes in abundance result in similar changes in pollen deposition. For example, if the abundance of pine around a site has doubled at some time in the past, then also deposition of pine pollen at that site has doubled. Because of the production and dispersal bias in pollen data, such a linear relationship does not exist for proportional (percentage) pollen data. If the abundance of pine doubles, the change in percentage values can be very different, depending on overall vegetation composition. Correction with REVEALS would reconstruct a doubling in pine abundance in accordance with a doubling in pollen deposition. However, correction will only be accurate with appropriate parameters, including PPEs. We suggest that this relationship can be used to test the performance of REVEALS applications with PAR data: each change in abundances reconstructed with REVEALS should correspond to similar changes in PAR values. Moreover, we can use this relationship to apply REVEALS without predefined PPEs. To that end we suggest the ROPES approach.

We illustrate the approach using just two samples and two taxa, A and B (**Table S1**). For both samples, PAR and percentage values are known: the PAR value of A increases from 1,000 to 2,000 grains $\text{cm}^{-2} \text{ year}^{-1}$ from sample 2 to sample 1, the PAR value of B decreases from 800 to 600 grains $\text{cm}^{-2} \text{ year}^{-1}$. The pollen percentages of A increase from 55.8 to 76.9% while those of B decrease from 44.4 to 23.1%.

We do not know pollen productivity (or PPEs) of A and B—so we apparently cannot apply REVEALS to reconstruct the actual abundances. Still, from the PAR values we can infer that the abundance of A has doubled from sample 2 to sample 1, while the abundance of B declined by 25%. We now argue that a REVEALS reconstruction should show the same trends in both taxa: a doubling in A and a 25% decline in B. With that premise, we can try and find PPEs that produce this pattern. Let us use B as the reference taxon, i.e., the PPE of B = 1. For taxon A we

apply REVEALS with different PPEs: 1, 2, 3, ..., 10. Only with a PPE of $A = 5$, REVEALS produces the expected changes: a doubling in A and a 25% decline in B . Correspondingly, the ratio of PAR values to reconstructed abundance (PAR over REVEALS, or PoR ratio) is constant for both taxa, 50 for A and 10 for B , because reconstructed abundance is linearly represented in the PAR values. We now know that the PPE of A is 5 (with that of B set to 1), and that the abundance of taxon A increased from 20% to 40% while that of B declined from 80 to 60%.

To summarize, ROPES assumes that a REVEALS reconstruction is correct only if changes in the reconstructed abundance of each taxon are proportional to changes in the respective PAR values. To find PPEs that produce such a reconstruction, ROPES applies an optimization algorithm that minimizes variation in the PoR ratio between samples by adjusting initially random PPEs. After optimization, the PoR ratio will (in absence of noise) be constant along the record. In the end, ROPES simultaneously calculates mean plant abundances and PPEs.

Assumptions of ROPES

As the REVEALS model is an integral part of the ROPES approach, ROPES inherently assumes that the assumptions underlying the REVEALS model (Sugita, 2007) are valid. ROPES finds suitable PPEs and plant abundances by minimizing variation in the PoR ratio. However, this ratio is expected to be constant only under certain conditions, as we outline below. For each taxon i , the PoR ratio along a pollen record is calculated as the PAR value divided by the cover reconstructed with the REVEALS model:

$$PoR_i = \frac{PAR_i}{\text{Reconstructed abundance of } i} \quad (1)$$

It is a general assumption in palynology that in a basin pollen deposition of taxon i , here expressed as PAR values, is a function of absolute pollen productivity of i [P_i], the abundance of i as a function of distance z [$X_i(z)$] and the pollen dispersal and deposition function [$g_i(z)$] integrated over distance Z_{\max} starting from the edge of the basin with radius R (cf. Sugita, 2007):

$$PAR_i = P_i \cdot \int_R^{Z_{\max}} X_i(z) \cdot g_i(z) \cdot dz \quad (2)$$

Sugita (2007) argues that for large lakes in a homogeneous landscape, $X_i(z)$ equals mean regional abundance \bar{X} of taxon i :

$$PAR_i = P_i \cdot \int_R^{Z_{\max}} \bar{X}_i \cdot g_i(z) \cdot dz \quad (3)$$

In the REVEALS model (Sugita, 2007) the integral over the dispersal and deposition function $g_i(z)$ is expressed as the K factor:

$$PAR_i = P_i \cdot \bar{X}_i \cdot K_i \quad (4)$$

REVEALS produces the reconstructed abundances as proportion of total regional abundances, or the total area A represented in the pollen record (i.e. the sum of all X_i):

$$\text{Reconstructed abundance of } i = \frac{\bar{X}_i}{A} \quad (5)$$

In result, the PoR ratio of taxon i is the absolute pollen productivity of taxon i multiplied with dispersal factor K_i and the total area A represented in the pollen record:

$$PoR_i = P_i \cdot K_i \cdot A \quad (6)$$

The final equation shows that the PoR ratio is constant along a record if three conditions are fulfilled: (i) pollen productivity is constant over time, (ii) pollen dispersal and deposition processes remained unchanged, and (iii) the area represented in the pollen record is stable. We illustrate and discuss how changes in pollen productivity and in the total area affect the PoR ratio using a simple model (Figure 1). The model is based on a vegetation scenario with 3 taxa and 20 time steps. Taxon A is dominant in the younger, taxon C in the middle and taxon B in the older section. To create a pollen record, taxon abundances in each time step are translated into pollen deposition (=PAR) by multiplying with pollen productivity, by default 5 for A , 1 for B and 0.2 for C . Then pollen proportions are calculated and translated into reconstructed plant abundances using the REVEALS model. For REVEALS modeling we use PPEs that equal the default pollen productivities ($A = 5$, $B = 1$, $C = 0.2$), except for example 1. Dispersal factor K is assumed to be 1 for all taxa. Finally, PoR ratios are calculated by dividing PAR values of A , B , and C by the reconstructed abundances.

A spreadsheet file containing raw data and calculations of all following examples is available as Supplementary Data.

The PoR Ratio With a Wrong PPE

The first experiment shows an error in one of the PPEs used in the reconstruction; this is the type of error ROPES is designed to remove. In the example, abundances are reconstructed with an incorrect PPE of 0.5 instead of the correct PPE of 0.2 for taxon C . With this one PPE set too high, REVEALS produces a too low cover for taxon C and consequently a too high cover for A and B . Because the PAR values remain unchanged, all PoR ratios are affected. For C , the ratio is higher than it should be because the REVEALS reconstructed cover is too low in all samples. The effect is high in the top and bottom sections—where C is rare—and lower in the middle section—where C is abundant. If C is rare, the wrong PPE introduces a small absolute but high relative error in the reconstruction: in the top and bottom section the true cover is 5%, whereas the REVEALS reconstructed cover is only 2%, i.e., 60% lower. If C is abundant, the wrong PPE introduces a large absolute but a smaller relative error: in the middle section, the true cover is 75% while the REVEALS reconstructed cover is 50%, i.e., only 33% lower. For A and B , the PoR ratios are too low because total REVEALS reconstructed abundance is 100% and if the reconstructed abundance of C is too low, that of the two other taxa is necessarily too high. The aberration in the PoR ratios of A and B is highest where C is abundant

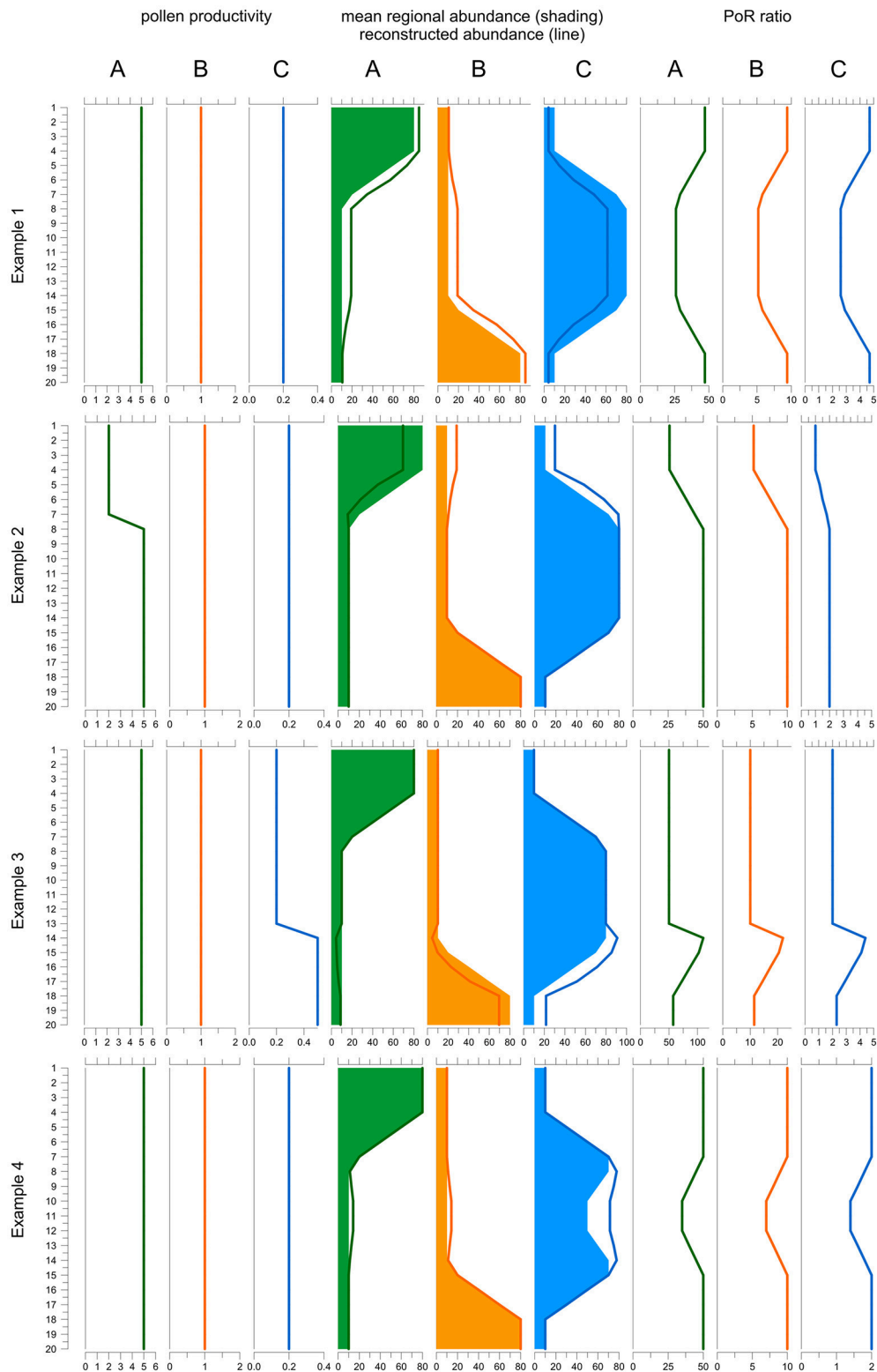


FIGURE 1 | Behavior of the PAR over REVEALS (PoR) ratio when one PPE is wrong (example 1), under changing pollen productivity (example 2 and 3) and under changing total regional plant abundances (example 4). The model includes three taxa A, B, and C over 20 time steps (y-axis): Taxon A (green) is dominant in the top part, B (orange) in the lower part and C (blue) in the middle part of the record. Default pollen productivity is 5 for A, 1 for B and 0.2 for C. Line graphs to the left depict (Continued)

FIGURE 1 | actual pollen productivity in each example. Graphs in the middle depict true abundances (shading) and abundances reconstructed with REVEALS (lines). Graphs to the right depict the PoR ratio. In example 1, the PPE of C used in the REVEALS reconstruction is set at 0.5 instead of 0.2. As a result, the cover of C is underestimated and consequently that of A and B overestimated. The PoR ratio is lower for all taxa where C is abundant. In example 2, pollen productivity of A is reduced from 5 to 2 in the upper 7 samples. REVEALS is still applied with a PPE of 5. Hence, the cover of A is underestimated and consequently that of B and C overestimated. The PoR ratio is reduced for all three taxa. In example 3, the pollen productivity of C is increased from 0.2 to 0.5 in the 7 lower samples, with opposite effects to example 2. In example 4, the sum of all abundances is reduced from 100 to 70% in samples 10–12. REVEALS does not reflect this change in total abundances. Hence the reconstructed cover of all three taxa is too high in the central part and PoR values are reduced correspondingly. Note that if the correct PPEs and total abundances are used, reconstructions fit true abundances and PoR ratios are always the same (samples 20–8 in example 2, 13–1 in example 3, and 20–15 plus 7–1 in example 3). As the K-factor is equal for all taxa the ratio between the PoR values equals the ratio between the PPEs.

because the absolute error in reconstructed cover is highest here. So, the use of *wrong PPEs* introduces variations in the PoR ratios of *all taxa* and these variations *always run parallel* for all taxa.

Variations in Pollen Productivity P

In example 2 (Figure 1), pollen productivity of taxon A is lowered from 5 to 2 in the upper 7 samples, so that its PAR values are 2.5 times lower than before. REVEALS is still applied with a PPE of 5. Hence, in the upper 7 samples the actual pollen productivity of A is lower than the applied PPE, so that the reconstructed cover of A is too low and consequently that of B and C too high. Now we observe that the PoR ratio of all three taxa is lower in the upper 7 samples. For B and C the explanation is simple; the reconstructed abundance is higher while PARs remain unchanged. For A the explanation is less obvious as both PAR values and reconstructed abundances are lower. However, the strong decline in PAR values is much suppressed in pollen proportions, which always add up to 100%, so that the decline is underestimated in the reconstructed abundances.

In example 3, pollen productivity of taxon C is elevated from 0.2 to 0.5 in the lower 7 samples (13–20); REVEALS is still applied with the default PPE of 0.2. Hence, in sample 13–20 actual pollen productivity is higher than the applied PPE, so that the reconstructed abundance of C is too high and consequently that of A and B too low. We observe that the PoR ratio of all three taxa is higher in sample 13–20. Again, for A and B the ratio is elevated simply because their reconstructed abundance is lower while PARs remain unchanged. For C, the strong increase in PARs is suppressed in the pollen proportions, so that the increase is also underestimated in the reconstructed abundances. So, a *temporarily lower pollen productivity* of one taxon causes lower PoR ratios for *all taxa* and vice versa. These variations *always run parallel* for all taxa.

Variations in the Total Area A

The PoR ratio is expected to be constant only if the sum of all mean regional abundances (A in Equation 6) is constant. This sum may change for example when sea level rise reduces the area of pollen producing land or when humans create bareland. Furthermore, the sum of regional abundances only reflects taxa that are represented in the pollen record, i.e., it may change when plants that are not or poorly represented in the pollen record expand or decline, e.g. immature trees or potato. In our example 4, the total cover of the three taxa is 100% in the top and bottom section but only 70% in sample 10–12. The REVEALS reconstructed abundance necessarily sums up to 100% in all

samples and does not reflect changes in total plant abundance in the middle section. PAR values do reflect the change and are lower, so that the PoR ratio of all taxa is lower as well. So, if the sum of regional abundances *declines*, the PoR ratio of *all taxa* will decline as well, and vice versa.

Variations in the Dispersal and Deposition Factor K

The PoR ratio will also be influenced by the processes of pollen dispersal and finally deposition in a lake as expressed by the K factor (cf. Equation 6). Whether and how atmospheric circulation has changed in the past, and how such changes may have altered pollen dispersal, is poorly understood. Pollen deposition in a large lake may change when lake size and morphometry change. ROPES is limitedly suited for records affected by such changes.

In addition to the above three modes of variation (in P, A, and K), error in the PAR values will introduce short-lived fluctuations in the PoR ratio around a mean value. Error in the PAR values is mainly related to dating uncertainties and error in exotic marker counts. In the following tests we will explore how error in the PAR values affects ROPES by adding noise to the PAR data in our tests.

EXAMPLE APPLICATIONS

Methods

Implementation of ROPES

We have implemented ROPES in the R environment for statistical computing (R Core Team, 2016). The core of ROPES is to minimize variation in the PoR ratio by adjusting initially random PPEs for each taxon. For optimization we use the “DEoptim” function (Ardia et al., 2011a,b, 2015; Mullen et al., 2011), an algorithm suited to find global optima. Before optimization, first the dispersal- and deposition factor K is calculated for each taxon. K is a distance-weighted representation of the amount of pollen arriving from beyond the basin radius. Mathematically, K is expressed as the pollen deposition of a taxon in a lake or peatland with a given diameter divided by deposition in a basin with zero diameter. K depends on the fall speed of a pollen taxon and on the dispersal model used for simulations. In ROPES, K is calculated with the “DispersalFaktorK” function from the DISCOVER package, which by default uses the state-of-the-art Lagrangian stochastic dispersal model (Theuerkauf et al., 2016).

Optimization starts with assigning a random PPE between 0.01 and 20 to each taxon. DEoptim then calls a target function,

which in three steps calculates the single target value that is to be optimized. It first calculates vegetation composition for each pollen sample using the “REVEALSinR” function from the DISCOVER package, with the respective K factors and the initially random PPEs. It then calculates the PoR ratio for each taxon and sample by dividing PAR values by the reconstructed abundances. For each taxon, the PoR ratio is normalized through division by the average PoR ratio over all samples. Finally, the target function calculates and returns overall variance in the PoR ratios. Overall variance is expressed as the sum of variance over all taxa, calculated as standard deviation of the PoR ratio divided by the mean PoR ratio over all samples. The optimization algorithm iteratively optimizes PPEs to arrive at the lowest possible overall variance.

Synthetic Data

To test and illustrate the potentials of ROPES, we use synthetic datasets based on virtual landcover and associated pollen. For these synthetic datasets the true relationship between pollen and vegetation is known so that the performance of the ROPES reconstruction tool can be evaluated. We wanted to create realistic datasets that show similar pollen composition and changes as real pollen records. For that reason, time series of virtual landcover were not created randomly but constructed on the basis of real pollen datasets from three lakes in NE-Germany (Gadowsee GAD, Stinhorst STI and Tiefer See TSK). To that end, we translated these empiric pollen data into vegetation composition using the REVEALSinR function from the R package DISCOVER with standard settings for pollen dispersal and PPEs from the PPE.MV 2015 data set (PPEs derived from sites in NE Germany, Theuerkauf et al., 2016). For REVEALS modeling, only the 19 most common taxa were selected (Table 1). We adopted these reconstructions as the time series of virtual landcover.

In step two, these time series were used to derive synthetic pollen records. Pollen accumulation rates (PAR) were calculated by multiplying virtual abundance of each taxon by its respective (synthetic) PPE (Table 1), K factor and an arbitrary scaling factor of 100 so that the resulting values are of similar magnitude as empiric PARs. Based on these synthetic PAR data, pollen counts were calculated assuming a pollen sum of 1,000. These synthetic pollen counts deviate from the empiric counts they are based on, but do show similar trends and complexity. Both synthetic PARs and pollen counts were then used in the ROPES tests.

We created 3 synthetic data sets: GAD, STI, and TSK (Tables 1, 2). Experiments with these data sets focus on data complexity and error in pollen data. To explore the influence of sample size on ROPES, we use three versions of each data set with 60, 130, and 250 pollen samples, respectively. The original number of samples for the GAD record was 60, for STI 130 and for TSK 250. Additional versions of the three records were created by either deleting or adding samples in the original data sets. PAR values for new samples were calculated as the mean of the two adjoining samples. ROPES was thus tested on a total of 9 data sets (Table 2). To underline the hypothetical nature of our reconstructions, pollen and plant taxa are written in normal font throughout the manuscript.

TABLE 1 | PPEs and fall speed of pollen used to prepare synthetic pollen data sets.

Taxon	Fallspeed m s ⁻¹	PPE
Alnus	0.021	15
Betula	0.024	10
Carpinus	0.042	4
Corylus	0.025	2
Fagus	0.057	3
Fraxinus	0.022	1.5
Picea	0.056	1
Pinus	0.031	6
Quercus	0.035	11
Tilia	0.032	3
Ulmus	0.032	3
Artemisia	0.025	4
Calluna	0.038	0.8
Cerealia excl. Secale	0.060	0.2
Cyperaceae	0.035	0.9
Gramineae	0.035	1
Plantago lanceolata	0.029	1.5
Rumex acetosella	0.018	3
Secale	0.060	1

TABLE 2 | Main parameters of the pollen data sets.

Data set	GAD	STI	TSK
Samples in original version	60	130	250
Samples in additional versions	130, 250	60, 250	60, 130

Error in Pollen Data

To mimic uncertainty in pollen data, noise was added in pollen counts and PARs. Noise in the counts is calculated by randomly drawing pollen samples with 1,000 pollen grains based on the composition of the synthetic pollen deposition. Samples were drawn with the R-function “rmultinom,” where probabilities “prob” equal pollen proportions in the synthetic data and sample “size” represents the pollen sum (=1000). Noise in PARs is in addition related to uncertainty in the exotic marker counts and error in sample accumulation rates—both affect all taxa in a sample in a similar way. We thus added a random component to the PAR value of all taxa in a sample. This component is calculated as the actual PAR value times a random value drawn from a normal distribution, centered around 0, and divided by a fixed factor. For each data set we tested two variants, one with division factor 10 to mimic intermediate error and one with division factor 5 to mimic large error in PAR data. In this way, the noise is similar to noise observed in real pollen data sets, as illustrated by a comparison with data from the partly laminated Lake Tiefer See (Dräger et al., 2017, Figure 2). For this quick comparison, we calculated sample to sample variation in the pollen data sets as the absolute difference in PAR between two consecutive samples divided by the PAR of the first of those samples. It should be noted that this calculation

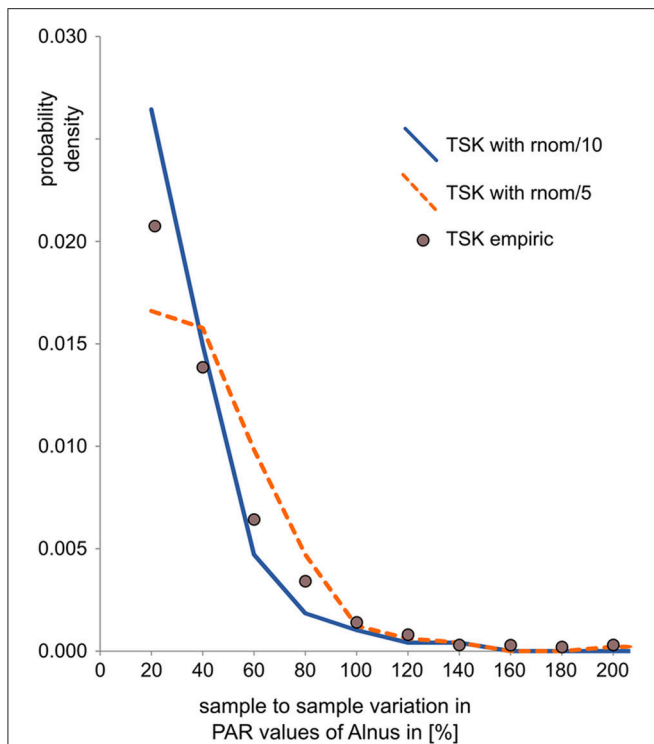


FIGURE 2 | Comparison of sample-to-sample variation (as an indicator of noise) in empiric and synthetic PAR records. Sample-to-sample variation is calculated as the relative difference between two consecutive PAR values, here for *Alnus*. The values, plotted as probability density, show that noise in the empiric PAR record from Lake Tiefer See is somewhat larger than in the derived synthetic PAR record with intermediate error added (TSK with $rnom/10$) and somewhat smaller than in the derived PAR record with large error added (TSK with $rnom/5$).

actually conflates signal and noise and thus overestimates true noise.

Model Runs and Evaluation

We applied ROPES on the 9 synthetic data sets with 4 types of error in the pollen data, making a total of 36 experiments (Figure 3). For each experiment, 100 model runs were conducted with newly drawn random error added in each run. To guarantee that global optima are found, convergence parameters of DEoptim are set to high sensitivity: $reltol$ to 0.00001 and $steptol$ to 500 (see Ardia et al., 2015). To evaluate model performance we assess accuracy of the reconstructed plant cover as well as of the ROPES-based PPEs. To assess accuracy of reconstructed plant cover, first the absolute difference is calculated for each pair of the original (synthetic) and the reconstructed plant cover (i.e., 3 records times 19 taxa times 60, 130, and 250 pairs). To represent the proportion of the landscape for which the reconstruction is wrong for a given pollen sample, the difference is summed up over all taxa and divided by two. Division by 2 corrects for the fact that values are expressed as percentages and any error in the cover of one taxon is mirrored by an equally large opposite error in other taxa, resulting in a maximum possible absolute error of 200% (cf. Theuerkauf and Couwenberg, 2017). Finally, the mean

error over all samples in a record is calculated to represent the inaccuracy of a given model run. To assess accuracy of the ROPES-based PPEs we compare the median PPE of the 100 model runs with the original PPEs of Table 1.

Real World Example

As a first real world example, we apply ROPES with original pollen data from Lake Tiefer See (cf. Dräger et al., 2017). Also here analysis is restricted to the 19 most common taxa. The range of potential PPEs is again set to 0.01–20. ROPES is applied with the same settings as before, no additional error was added to the pollen data.

Results and Interpretation

Reconstructed Landcover

With no error added in pollen data, ROPES produces near-perfect results in all 9 synthetic data sets. Error in the reconstructed landcover amounts to around 1%, i.e., the reconstruction is correct for 99% of the synthetic study area. With ideal data ROPES is evidently well able to reconstruct past landcover with short as well as long pollen records. With noise added to the pollen counts, error in the reconstructed landcover amounts to ~5% in the TSK data sets and to ~10% in the GAD and STI data sets. ROPES performs somewhat better with the longer records, but overall the number of samples has limited effect on the results if noise is added to the counts only.

Adding noise also in the PAR data further increases the error in the reconstruction. With intermediate noise, error in the reconstructed landcover increases to 9–19%. The error is smallest in the long STI and TSK records (STI130, STI250, TSK130, and TSK250), intermediate in STI60 and TSK60, and highest in GAD130 and GAD60. With large noise in the PAR data, error ranges from 12 to 29%. Again, performance is best with the long STI and TSK records whereas the largest error occurs with the short records GAD60 and GAD130. Still, also with large noise added, ROPES in most cases correctly reconstructs landcover for more than 75% of the landscape.

Pollen Productivities

Besides landcover, ROPES also reconstructs PPEs for the taxa involved. With no noise in the pollen data, the median PPE over 100 model runs is mostly close to the true PPE in the experiments with GAD and TSK records. Experiments with the STI record for some taxa produce too low (*Plantago lanceolata*, *Secale*) or too high PPEs (*Artemisia*, *Cerealia*, Figure 4). With noise in the pollen data, the median PPEs deviate more from true pollen productivity. The error remains lowest with the TSK records, where—with full noise added to the data—for most taxa (e.g., *Carpinus*, *Fagus*, *Calluna*, and *Secale*) the reconstructed PPEs deviate little (<20%) from true pollen productivity. The largest mismatch with TSK is for *Fraxinus*, for which PPEs with full noise are ~30% too low. Error tends to be higher with the GAD records, where with GAD60 and full noise the overall highest mismatch occurs for the PPE of *Tilia* (20 instead of 3). For *Artemisia*, *Rumex* and *Ulmus*, PPEs derived from noisy or short GAD records are less than half the original pollen productivity. In all other cases, PPEs are within 50–200% of the original

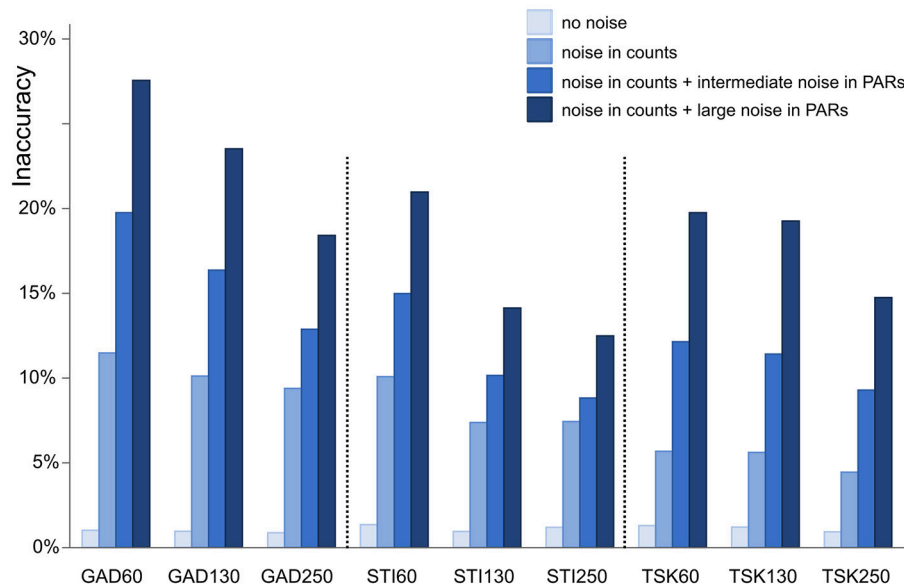


FIGURE 3 | Inaccuracy of ROPES reconstructed landcover expressed as mean proportion of the landscape for which the reconstruction is wrong. Accuracy is assessed for 9 synthetic data sets representing 3 sites (GAD, STI, and TSK) each with 3 sizes (60, 130, and 250 samples). Four different types of error are applied (no error, error in pollen counts, error in counts plus intermediate noise in PAR values, and error in counts plus large noise in PAR values).

value. With noise added to the data, STI produces PPEs that are outside this error range for *Carpinus*, *Fagus*, *Artemisia*, *Plantago lanceolata*, *Rumex*, and *Secale*.

With full noise in the data, a number of single ROPES runs for some taxa approximate PPEs at the pre-defined upper margin of 20 (see Supplementary Data). This mainly applies to *Alnus*, *Betula* and *Quercus*, i.e., the taxa with highest pollen productivity, and only rarely for other taxa.

We have outlined before that ROPES requires sufficient variation and number of samples in the pollen record. This raises the question whether taxa with little variation (including rare taxa) hamper the reconstruction of taxa with sufficient variation. To answer this question we explore how error in the PPE of a taxon relates to its range in pollen percentage values and number of samples (Figure 5). With no noise in the pollen data, error in the PPEs is mostly small (<10%), except for some taxa from the STI record which show very little variation along the record. With noise in pollen counts error in the PPEs is clearly higher, increasing slightly with intermediate and large noise added in the PAR data. As before, high errors (>40%) are restricted to taxa with little variation through the pollen record, i.e. taxa that are either always rare or occur with very stable values. Errors >40% rarely occur when total range in pollen values times number of samples in a record is larger than 2,000. We conclude that short, noisy data sets are still suited to produce suitable PPEs for taxa that cover a large range in pollen percentage data. As a tentative rule of thumb, PPEs tend to be reliable when the range in pollen values multiplied by the number of samples is larger than 2,000.

Application of ROPES with pollen data from Lake Tiefer See produced a set of palaeo-PPEs, i.e., PPEs based on a long Holocene pollen record, which we compare with PPEs based

on surface studies (Figure 6). Both data sets show high PPEs for most tree taxa, in particular *Alnus*, *Betula*, *Corylus*, and *Quercus*, and low PPEs for most herb taxa. Despite the overall similarities, we also observe some differences. For *Alnus*, *Betula*, *Corylus*, *Artemisia* and *Rumex acetosella*, PPEs produced with ROPES are clearly lower than those from the surface sample record, for *Cerealia* excl. *Secale* and *Gramineae*, PPEs produced with ROPES are clearly higher.

ADVANTAGES AND LIMITATIONS

Our tests have shown that ROPES is indeed able to reconstruct landcover and PPEs. The performance differs among the 36 experiments, mainly in response to sample size, variance along the record and noise in the pollen data. ROPES performs near perfect in the experiments with no noise in the pollen data, which demonstrates the validity of the approach. Particularly noise in the PAR data introduces error in the reconstructions of landcover and PPEs. Error is larger the shorter and less diverse the record. Increasing sample size in almost all cases reduces error in the reconstruction both in terms of landcover and PPEs. It is likely that performance will further improve with records longer than those tested here. Still, also short records are suited to estimate the pollen productivity at least for taxa with a wide range of percentage values along the record.

Variation along the pollen record is essential for the functioning of ROPES: with no variation in the pollen record there is no variation in the PoR ratio with any set of PPEs so that ROPES cannot approach an optimal solution. In turn, the larger the variation in the pollen record, the better ROPES performs.

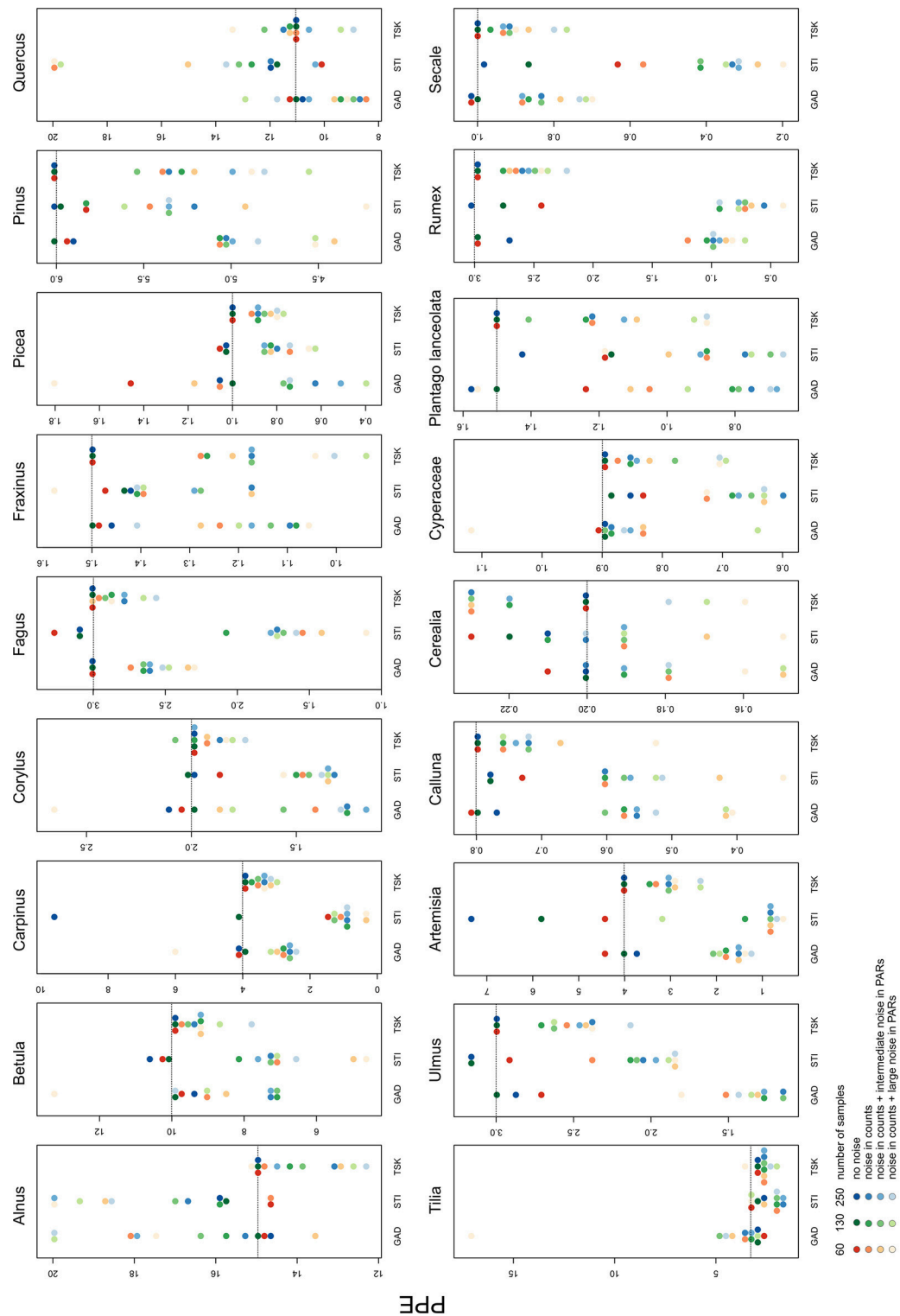


FIGURE 4 | Median of PPEs produced in each of the 36 experiments. The colors represent the sample size, shades represent the noise added in the pollen data. Dotted lines show original pollen productivity of each taxon. Note the scaling of the y-axes. For full results see Supplementary Material.

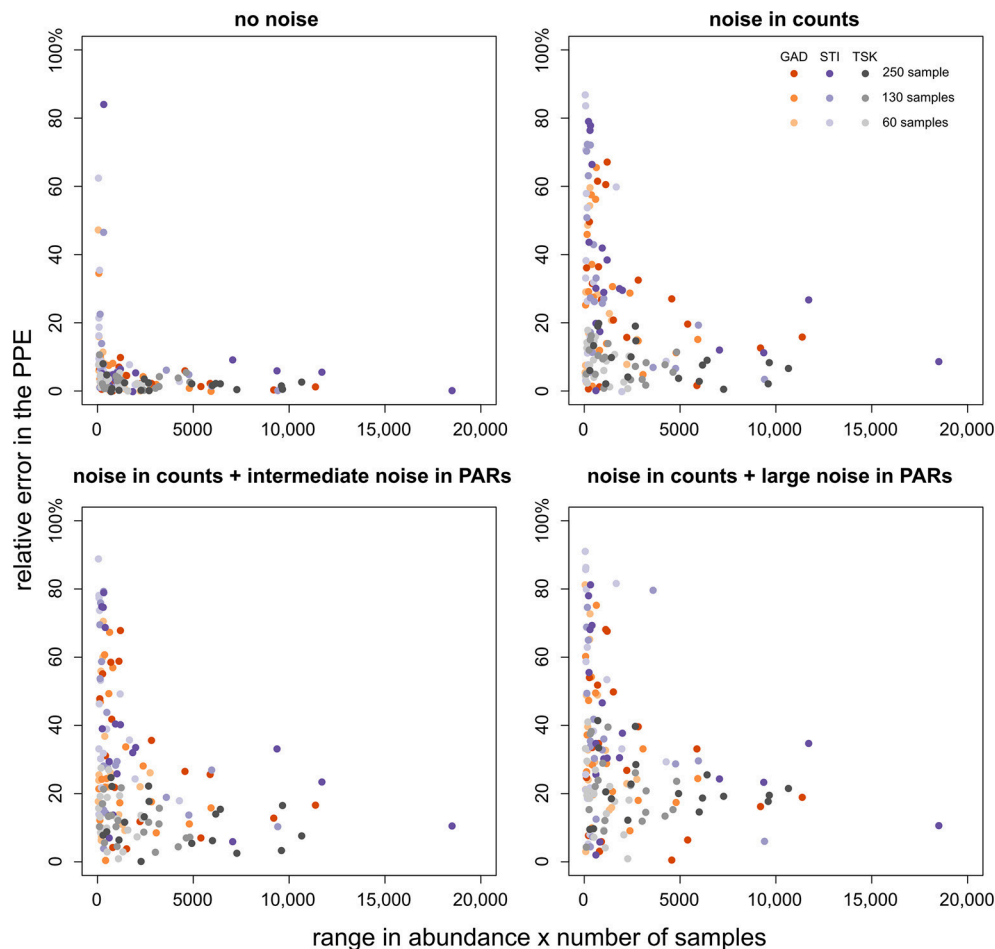


FIGURE 5 | Relative PPE error (y-axis) plotted over the range of values of the respective taxon multiplied by the number of samples (x-axis). PPE error is calculated as the absolute difference between the median from 100 model runs and true pollen productivity divided by true pollen productivity ($\times 100\%$). The colors denote the pollen record, shade its size.

We find that this relationship applies to each separate taxon in a record, i.e., ROPES performs better for the more variable taxa. The STI record is dominated by *Pinus* in all samples, leaving low proportional abundance and little variation for the other taxa. Correspondingly, ROPES performs well in reconstructing cover and pollen productivity of *Pinus* but not of the rare taxa. The TSK record is more diverse; most taxa are abundant at least in some sections of the record. ROPES therefore performs well in reconstructing PPEs and cover of most taxa. Still, the overall landcover reconstruction for STI is as good as or even better than that for TSK because of the good result for *Pinus* as the dominant taxon. So, if the aim is to produce pollen productivity of as many taxa as possible, diverse data sets with large variations in all taxa are needed. If the focus is on the landcover reconstructions itself, less diverse data sets dominated by one or few taxa are still suitable.

As a tentative rule of thumb we suggest that PPEs can be reconstructed for taxa for which the amplitude in the pollen percentage data multiplied by the number of samples is larger

than 2,000. For an in depth evaluation of a data set we suggest to apply sensitivity tests similar to those presented here. Such an evaluation, in which synthetic data are tested that are based on an actual pollen record, can show the specific capabilities and limits of a particular data set.

Future Applications-Potentials and Limits

ROPES does not depend on pre-defined PPEs—it thus has the potential to expand quantitative landcover reconstruction into areas for which such calibration is not yet available or not feasible. For these areas, ROPES would then not only provide initial landcover reconstructions but also PPEs. Each successful ROPES application may thus trigger follow-up reconstructions with existing approaches, such as REVEALS, that employ percentage pollen data and PPEs.

Although often disregarded, application of quantitative reconstructions is so far limited to areas and periods for which the available correction factors are suited. PPEs for example are derived and only applicable in a specific space-time.

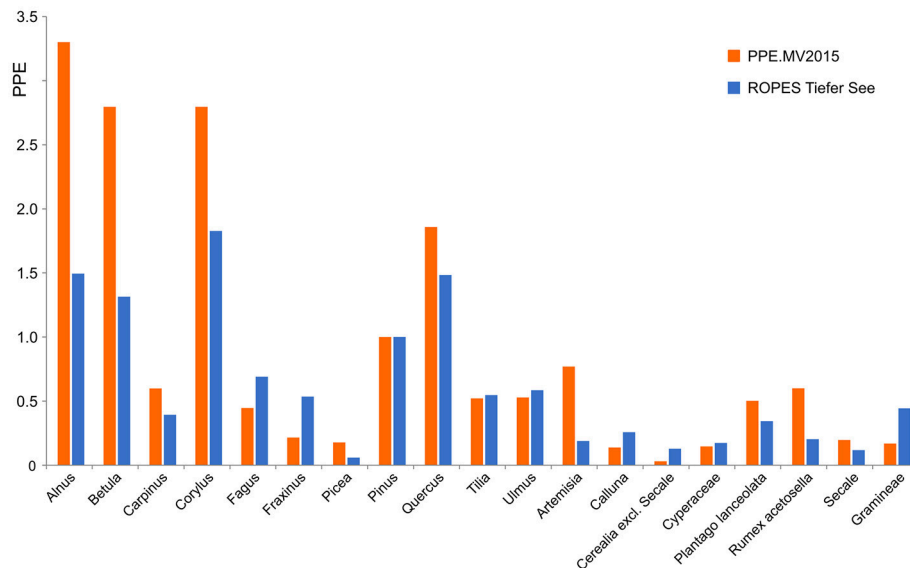


FIGURE 6 | PPEs produced with ROPES from the Lake Tiefer See record (TSK, 250 samples) compared with the PPE.MV 2015 set of PPEs from Theuerkauf et al. (2016).

Consequently, the common use of mean PPEs amalgamated across large areas that show considerable differences in land use, soil types, slope and climate (Broström et al., 2008; Mazier et al., 2012) implies additional error in the reconstruction. Moreover, PPEs derived from modern pollen-landcover relationships are applied to ancient situations, although pollen productivity has changed in the past (Waller et al., 2012; Feeser and Dörfler, 2014; Theuerkauf et al., 2015). ROPES may help reduce these limitations and provide targeted reconstructions for non-analog situations, e.g., of Lateglacial vegetation of Europe. In this way, ROPES may contribute to a better understanding of vegetation dynamics in times of climate change. It probably can help explore whether and how pollen productivity of plant taxa responds to changes in climate, species composition or land management. In ROPES, periods of changing pollen productivity are expressed as changes in the PoR ratio. To fully explore the actual changes in pollen productivity, ROPES has to be applied separately on those sections of the record that were identified as distinct in the first round. The limitation to this approach is that each section is required to retain sufficient variation, i.e., it has to have a minimum length. Approaches to optimize between section length and accuracy of the resulting PPEs still need to be developed. Changes in pollen productivity will likely be observable over millennial, rather than centennial time scales.

A problem so far neglected in quantitative vegetation reconstruction is the presence of non-pollen producing areas. Quantitative approaches such as REVEALS assume that the taxa involved cover a fixed proportion of the surrounding area (commonly assumed to be 100%). In reality, some proportion of this area may be barren, open water, or covered by taxa that are virtually not represented in the pollen record, e.g., crops such as potato or trees such as *Acer*. ROPES has the potential to

detect such effects and actually reconstruct non-pollen producing areas. The tests presented in this paper do not address the effect, but first attempts at reconstructing non-pollen producing areas have shown promising results. Approaches to proper weighing between correcting for errors in pollen productivity and total land cover are currently under development.

Our tests show that ROPES requires pollen records with limited noise in the PAR data. We already identified a number of suitable records, and are optimistic that many more exist. With the option to use PAR data in ROPES, we encourage analysts to estimate PARs as precisely as possible. To arrive at accurate pollen concentrations, sample volumes should be well defined and a sufficient number of exotic marker grains should be added to each sample. As the exotic marker grains serve as the basis for all further calculations, counts should amount to at least several hundred exotic grains to reduce statistical noise in PAR values. To guarantee that such an amount of exotic markers is counted it may be necessary to add multiple marker tablets to each sample. Care should be taken to still count at least as many “pollensum”-pollen, so as not to burden the REVEALS reconstructions with too much noise.

The next step, from pollen concentrations to PARs, requires sediment accumulation rates. Annually laminated sediments allow for exact dating and therefore such records appear most suited for ROPES. In non-laminated records accumulation rates can only be approximated from age-depth models. Giesecke and Fontana (2008) have shown that PARs with little noise can indeed be estimated in non-laminated lakes. We assume that also large peatlands may be suited to produce robust PAR values. In any case, the pollen dispersal model underlying ROPES assumes atmospheric pollen deposition exclusively. As implemented, ROPES is therefore thus far only applicable to closed lake basins and peat deposits.

The first application of ROPES on the empiric pollen record from Lake Tiefer See shows an overall good match between surface sample PPEs and PPEs produced with ROPES, which supports the general validity of the ROPES approach. There may be various reasons for the observed differences in the PPEs.

For example, the ROPES PPE of *Corylus* is lower than its surface sample PPE. The surface sample PPE is likely too high because *Corylus* is underrepresented in the forest inventories underlying surface sample PPEs (Theuerkauf et al., 2013). Similarly, the cover of herbs such as *Artemisia* and *Rumex* has likely been underestimated in surface sample studies, again resulting in too high PPEs. A higher palaeo-PPE for *Cerealia* excl. *Secale* could be explained by a focus on different species or cultivars within this group in the past, which were better reflected in the pollen record. The surface sample PPE of grasses is likely too low because pollen production in grasses is suppressed under present-day land management (Theuerkauf et al., 2015). A comprehensive discussion on PPEs produced with ROPES requires a more in depth analysis of further data sets.

CONCLUDING REMARKS

Existing methods of quantitative vegetation reconstruction correct for the productivity bias in pollen data with correction factors such as PPEs that are calibrated in the present day cultural landscape. This approach is not only laborious and far from simple, it also introduces unknown error in the reconstruction of past vegetation because PPEs calibrated in the modern cultural landscape may not be representative for the past. ROPES corrects for the productivity bias using pollen data only and without calibration. We see three major benefits for future landcover reconstructions.

First, ROPES may provide a shortcut to landcover reconstructions in new study regions if at least one site with suitable PAR and percentage pollen data is available. ROPES can deliver a landcover reconstruction for that site, and the PPEs needed to produce landcover reconstructions from further records in the region that are not suited for ROPES using other quantitative methods.

Secondly, ROPES can help improve and sharpen landcover reconstructions. The ability to estimate PPEs from single sites may allow exploring spatial patterns in pollen productivity within and between regions, e.g., in relation to variations in climate, soils and species composition. A better understanding of these interactions will enable more detailed reconstructions.

Thirdly, ROPES allows for landcover reconstructions for periods with non-analog climate and landcover, like the Lateglacial. Landcover reconstructions have been problematic for such periods because PPEs calibrated in the modern world are obviously unsuited.

REFERENCES

Ardia, D., Arango, J. O., and Gomez, N. G. (2011a). Jump-diffusion calibration using differential evolution. *Wilmott Magazine* 55, 76–79. doi: 10.1002/wilm.10034

Overall, our first tests suggest that ROPES will help shift away from PPEs as static parameters toward PPEs that are reconstructed from the (palaeo-)pollen record. ROPES thus adds past pollen productivity as an observable variable to palaeoecology. The approach has the potential to significantly improve landcover reconstructions and broaden their application, while adding additional insights.

AUTHOR CONTRIBUTIONS

MT und JC jointly developed the idea of ROPES and the theory behind it. Both created the tests and wrote the manuscript. MT analyzed pollen of the original GAD, STI, and TSK records and implemented ROPES in R for the DISCOVER package.

FUNDING

This study is a contribution to the Virtual Institute of Integrated Climate and Landscape Evolution Analysis—ICLEA—of the Helmholtz Association (VH-VI-415) and to BaltRap: the Baltic Sea and its southern Lowlands: proxy—environment interactions in times of Rapid change (SAW-2017-IOW2). The work of JC was funded by the European Social Fund (ESF) and the Ministry of Education, Science and Culture of Mecklenburg-Western Pomerania (project WETSCAPES, ESF/14-BM-A55-0030/16).

ACKNOWLEDGMENTS

We thank Almut Mrotzek and Marie-José Gaillard for valuable comments on the manuscript. We gratefully acknowledge the friendly and constructive remarks of two reviewers.

SUPPLEMENTARY MATERIAL

The Supplementary Material for this article can be found online at: <https://www.frontiersin.org/articles/10.3389/feart.2018.00014/full#supplementary-material>

Table S1 | Principle of the ROPES approach illustrated using a record with just two samples and two taxa A and B. For both samples, PAR values and pollen counts (shown as percentage values) are known (left part of the table). REVEALS is applied on the pollen counts with the PPE of taxon A set to 1, 2, 3, ..., 10. B is the reference taxon with a PPE of 1. The right part of the table shows relative abundance reconstructed in each of these 10 REVEALS applications and the PoR ratio, i.e., the ratio of PAR value over REVEALS reconstructed cover. Only if the PPE of A = 5, the change in the reconstructed abundance of A and B (expressed as the value of sample 1 divided by sample 2 × 100%) is the same as the change in PAR values. As a result the PoR ratio is the same for both samples.

The synthetic and empiric pollen data used in the ROPES example applications are available for download from <https://doi.pangaea.de/10.1594/PANGAEA.886900>.

The R-code for ROPES is available from <https://github.com/MartinTheuerkauf/ROPES>.

Ardia, D., Boudt, K., Carl, P., Mullen, K. M., and Peterson, B. G. (2011b). Differential evolution with DEoptim: an application to non-convex portfolio optimization. *R J.* 3, 27–34. Available online at: https://journal.r-project.org/archive/2011-1/RJournal_2011-1_Ardia_et_al.pdf

- Ardia, D., Mullen, K. M., Peterson, B., G., and Ulrich, J. (2015). DEoptim: differential evolution in R. Available online at: <https://cran.r-project.org/web/packages/DEoptim/index.html>
- Broström, A., Nielsen, A. B., Gaillard, M.-J., Hjelle, K. L., Mazier, F., Binney, H. A., et al. (2008). Pollen productivity estimates of key European plant taxa for quantitative reconstruction of past vegetation: a review. *Veg. Hist. Archaeobot.* 17, 461–478. doi: 10.1007/s00334-008-0148-8
- Davis, M. B. (1967). Pollen accumulation rates at Rogers Lake, Connecticut, during late- and postglacial time. *Rev. Palaeobot. Palynol.* 2, 219–230. doi: 10.1016/0034-6667(67)90150-9
- Dräger, N., Theuerkauf, M., Szeroczyńska, K., Wulf, S., Tjallingii, R., Plessen, B., et al. (2017). Varve microfacies and varve preservation record of climate change and human impact for the last 6000 years at Lake Tiefer See (NE Germany). *Holocene* 27, 1–15. doi: 10.1177/0959683616660173
- Feeser, I., and Dörfler, W. (2014). The glade effect: vegetation openness and structure and their influences on arboreal pollen production and the reconstruction of anthropogenic forest opening. *Anthropocene* 8, 92–100. doi: 10.1016/j.ancene.2015.02.002
- Giesecke, T., and Fontana, S. L. (2008). Revisiting pollen accumulation rates from Swedish lake sediments. *Holocene* 18, 293–305. doi: 10.1177/0959683607086767
- Hicks, S. (1999). The relationship between climate and annual pollen deposition at northern tree-lines. *Chemos. Glob. Change Sci.* 1, 403–416. doi: 10.1016/S1465-9972(99)00043-4
- Hicks, S. (2001). The use of annual arboreal pollen deposition values for delimiting tree-lines in the landscape and exploring models of pollen dispersal. *Rev. Palaeobot. Palynol.* 117, 1–29. doi: 10.1016/S0034-6667(01)00074-4
- Matthias, I., Nielsen, A. B., and Giesecke, T. (2012). Evaluating the effect of flowering age and forest structure on pollen productivity estimates. *Veg. Hist. Archaeobot.* 21, 471–484. doi: 10.1007/s00334-012-0373-z
- Mazier, F., Gaillard, M. J., Kuneš, P., Sugita, S., Trondman, A. K., and Broström, A. (2012). Testing the effect of site selection and parameter setting on REVEALS-model estimates of plant abundance using the Czech quaternary palynological database. *Rev. Palaeobot. Palynol.* 187, 38–49. doi: 10.1016/j.revpalbo.2012.07.017
- Mullen, K., Ardia, D., Gil, D., Windover, D., and Cline, J. (2011). DEoptim: an R package for global optimization by differential evolution. *J. Stat. Softw.* 40, 1–26. doi: 10.18637/jss.v040.i06
- Prentice, I. C., and Webb, T. (1986). Pollen percentages, tree abundances and the Fagerlinde effect. *J. quarter. Sci.* 1, 35–43. doi: 10.1002/jqs.3390010105
- Prieto-Baena, J. C., Hidalgo, P. J., Domínguez, E., and Galán, C. (2003). Pollen production in the Poaceae family. *Grana* 42, 153–159. doi: 10.1080/00173130310011810
- R Core Team. (2016). *R: A Language and Environment for Statistical Computing*. Vienna: R Foundation for Statistical Computing.
- Seppä, H., and Hicks, S. (2006). Integration of modern and past pollen accumulation rate (PAR) records across the arctic tree-line: a method for more precise vegetation reconstructions. *Quarter. Sci. Rev.* 25, 1501–1516. doi: 10.1016/j.quascirev.2005.12.002
- Sugita, S. (2007). Theory of quantitative reconstruction of vegetation I: pollen from large sites REVEALS regional vegetation composition. *Holocene* 17, 229–241. doi: 10.1177/0959683607075837
- Theuerkauf, M., and Couwenberg, J. (2017). The extended downscaling approach: a new R-tool for pollen-based reconstruction of vegetation patterns. *Holocene* 27, 1252–1258. doi: 10.1177/0959683616683256
- Theuerkauf, M., Couwenberg, J., Kuparinen, A., and Liebscher, V. (2016). A matter of dispersal: REVEALSinR introduces state-of-the-art dispersal models to quantitative vegetation reconstruction. *Veget. Hist. Archaeobot.* 25, 541–553. doi: 10.1007/s00334-016-0572-0
- Theuerkauf, M., Dräger, N., Kienel, U., Kuparinen, A., and Brauer, A. (2015). Effects of changes in land management practices on pollen productivity of open vegetation during the last century derived from varved lake sediments. *Holocene* 25, 733–744. doi: 10.1177/0959683614567881
- Theuerkauf, M., and Joosten, H. (2012). Younger Dryas cold stage vegetation patterns of central Europe - climate, soil and relief controls. *Boreas* 41, 391–407. doi: 10.1111/j.1502-3885.2011.00240.x
- Theuerkauf, M., Kuparinen, A., and Joosten, H. (2013). Pollen productivity estimates strongly depend on assumed pollen dispersal. *Holocene* 23, 14–24. doi: 10.1177/0959683612450194
- von Post, L. (1918). Skogsträdpollen i sydsvenska torvmosselagerföljder. *Forhandlingar ved de 16. Skandinaviske Naturforskeres møte* 1916, 433–465.
- Waller, M., Grant, M. J., and Bunting, M. J. (2012). Modern pollen studies from coppiced woodlands and their implications for the detection of woodland management in Holocene pollen records. *Rev. Palaeobot. Palynol.* 187, 11–28. doi: 10.1016/j.revpalbo.2012.08.008

Conflict of Interest Statement: The authors declare that the research was conducted in the absence of any commercial or financial relationships that could be construed as a potential conflict of interest.

Copyright © 2018 Theuerkauf and Couwenberg. This is an open-access article distributed under the terms of the Creative Commons Attribution License (CC BY). The use, distribution or reproduction in other forums is permitted, provided the original author(s) and the copyright owner are credited and that the original publication in this journal is cited, in accordance with accepted academic practice. No use, distribution or reproduction is permitted which does not comply with these terms.



Maps From Mud—Using the Multiple Scenario Approach to Reconstruct Land Cover Dynamics From Pollen Records: A Case Study of Two Neolithic Landscapes

M. Jane Bunting^{1*}, Michelle Farrell^{2,3}, Alex Bayliss^{4,5}, Peter Marshall⁴ and Alasdair Whittle⁶

¹ Geography, School of Environmental Sciences, University of Hull, Hull, United Kingdom, ² School of Energy, Construction and Environment, Coventry University, Coventry, United Kingdom, ³ Centre for Research in the Built and Natural Environment, Coventry University, Coventry, United Kingdom, ⁴ Historic England, London, United Kingdom, ⁵ Biological and Environmental Sciences, University of Stirling, Stirling, United Kingdom, ⁶ Department of Archaeology and Conservation, Cardiff University, University of Cardiff, Cardiff, United Kingdom

OPEN ACCESS

Edited by:

Valentí Rull,
Instituto de Ciencias de la Tierra
Jaume Almera (CSIC), Spain

Reviewed by:

Chris J. Caseldine,
University of Exeter, United Kingdom
Petr Kuneš,
Charles University, Czechia

*Correspondence:

M. Jane Bunting
m.j.bunting@hull.ac.uk

Specialty section:

This article was submitted to
Paleoecology,
a section of the journal
Frontiers in Ecology and Evolution

Received: 20 November 2017

Accepted: 20 March 2018

Published: 13 April 2018

Citation:

Bunting MJ, Farrell M, Bayliss A,
Marshall P and Whittle A (2018) Maps
From Mud—Using the Multiple
Scenario Approach to Reconstruct
Land Cover Dynamics From Pollen
Records: A Case Study of Two
Neolithic Landscapes.
Front. Ecol. Evol. 6:36.
doi: 10.3389/fevo.2018.00036

Pollen records contain a wide range of information about past land cover, but translation from the pollen diagram to other formats remains a challenge. In this paper, we present LandPolFlow, a software package enabling Multiple Scenario Approach (MSA) based land cover reconstruction from pollen records for specific landscapes. It has two components: a basic Geographic Information System which takes grids of landscape constraints (e.g., topography, geology) and generates possible “scenarios” of past land cover using a combination of probabilistic and deterministic placement rules to distribute defined plant communities within the landscape, and a pollen dispersal and deposition model which simulates pollen loading at specified points within each scenario and compares that statistically with actual pollen assemblages from the same location. Goodness of fit statistics from multiple pollen site locations are used to identify which scenarios are likely reconstructions of past land cover. We apply this approach to two case studies of Neolithisation in Britain, the first from the Somerset Levels and Moors and the second from Mainland, Orkney. Both landscapes contain significant evidence of Neolithic activity, but present contrasting contexts. In Somerset, wet-preserved Neolithic remains such as trackways are abundant, but little dry land settlement archaeology is known, and the pre-Neolithic landscape was extensively wooded. In Orkney, the Neolithic archaeology includes domestic and monumental stone-built structures forming a UNESCO World Heritage Site, and the pre-Neolithic landscape was largely treeless. Existing pollen records were collated from both landscapes and correlated within new chronological frameworks (presented elsewhere). This allowed pollen data to be grouped into 200 year periods, or “timeslices,” for reconstruction of land cover through time using the MSA. Reconstruction suggests that subtle but clear and persistent impacts of Neolithisation on land cover occurred in both landscapes, with no reduction in impact during periods when archaeological records suggest lower activity levels. By applying the methodology

to specific landscapes, we critically evaluate the strengths and weaknesses and identify potential remedies, which we then expand into consideration of how simulation can be incorporated into palynological research practice. We argue that the MSA deserves a place within the palynologist's standard tool kit.

Keywords: archaeology, Neolithic, paleoecology, palynology, pollen dispersal and deposition modelling, pollen analysis, vegetation reconstruction

INTRODUCTION

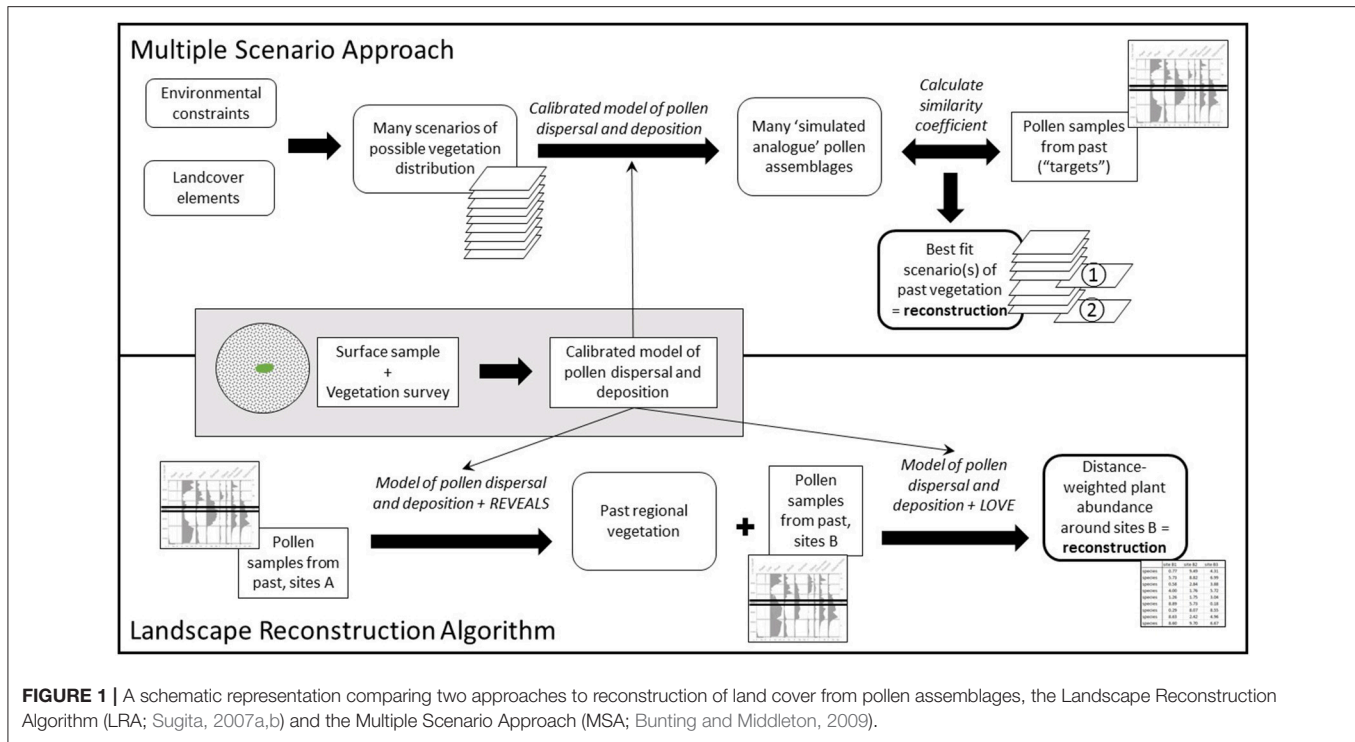
Land cover is an important component of the earth system, through the habitats it provides for living things and through its interactions with the other major components, for example with the hydrosphere via modification of water flow and water quality, and with the atmosphere and climate system through albedo and evapotranspiration. Land cover develops in response to a range of environmental drivers, including climate zone, substrate, topography, and feedback interactions between biota and between biotic elements and the physical environment. Human activity is a major shaper of these feedback interactions, both directly (e.g., through tree felling, ploughing, or construction of novel habitats) and indirectly (e.g., through changing distributions and intensities of grazing animals, which in turn can reduce ground cover or transform forest into scrub or grassland). Land cover is variable in both space and time, and reconstructing past land cover is therefore an important contribution to understanding the longer-term dynamics of the earth system (for example for testing regional climate models or framing the context of archaeological records of human activity), as well as for ecological studies of ecosystem processes and dynamics and archaeological investigation of the controls on and environmental impacts of past human activity.

Pollen analysis offers a means of indirectly observing past vegetation, and therefore pollen records (sequences of pollen assemblages recovered from sedimentary archives such as mires or lake sediments) are an important source of information about past land cover. Translation of standard pollen diagrams—information-packed, but often an active barrier to engagement by non-specialists within and beyond academic communities because they are very difficult to read without extensive experience—into measures of land cover is an ongoing research challenge. Von Post (1918) and Edwards et al. (2017) described the task of the pollen analyst as being to “think horizontally, work vertically,” showing that from the earliest days of the discipline reconstruction of spatial variations in land cover at different points in the past was seen as the main goal of the activity. Pollen assemblages form through a complex combination of taphonomic processes reflecting both the biology and ecology of the plants producing the pollen and the shape, size, type, and setting of the sedimentary system where the assemblage forms and will be preserved, and therefore translation into land cover is not a trivial exercise, especially if the land cover measure is to be quantitative and spatially referenced rather than qualitative. Various methodologies have been explored, such as biomisation (e.g., Prentice et al., 1996), modern analog comparison methods

(e.g., Overpeck et al., 1985), and the use of models of the relationship between pollen and vegetation or the process of pollen dispersal and deposition.

Algebraic models connecting pollen assemblages at a known location and the source vegetation in the wider landscape offer a means of reconstructing past land cover. The main approach currently in use is the Landscape Reconstruction Algorithm (LRA; Sugita, 2007a,b; Gaillard et al., 2008, 2010; Hellman S. et al., 2008; Trondman et al., 2015; PAGES, 2017). The LRA is not the only possible use of the algebraic models. Interpretation can also be informed by simulation studies or “thought experiments” (e.g., Bunting et al., 2004; Caseldine and Fyfe, 2006; Caseldine et al., 2007; Hellman et al., 2009a,b) using the HUMPOL suite (Middleton and Bunting, 2004; Bunting and Middleton, 2005). This approach was developed into the Multiple Scenario Approach (MSA; Bunting and Middleton, 2009); where the LRA takes an algebraic approach to reconstructing past land cover numerically, which can then be extrapolated into mapped forms (e.g., Pirzamanbein et al., 2014), the MSA uses computer simulations to produce many possible reconstructions, which are then tested using the model (see **Figure 1** for a comparison of the two approaches). This paper presents two examples of the use of the MSA to address landscape-scale questions about land cover and land use during the Neolithic in the British Isles, and considers lessons learned for future development of this relatively new and under-explored method.

The nature of Neolithic agriculture in the British Isles remains poorly understood. Evidence for the prior presence of Mesolithic people is widespread, but their population levels were probably very low, and direct environmental impacts would have been localized. Impacts may have included modification of woodland structure (e.g., Bishop et al., 2015). The repeated use of fire, and possible knock-on effects on the location of wild native herbivores, particularly deer, are argued to have modified woodland edge habitats in the uplands (Innes et al., 2010, 2013; Ryan and Blackford, 2010) and at wetland margins (Mellars and Dark, 1998), at least in some locations and at some times. The early Holocene woodland cannot be considered pristine and unsettled, but existing evidence suggests that Mesolithic people caused only minor disturbance, with effects comparable to other components of the natural disturbance regime. Neolithisation introduced two new potential disturbance factors into the landscape, livestock management, and crop cultivation. The introduction of non-native herbivores, especially sheep and goats which are particularly effective at suppressing regeneration of deciduous woodland, and increased management



of the numbers and locations of large animals in the landscape will have increased grazing and associated landscape effects such as creation of paths and trampling and erosion at watering points and gathering yards, which will both create small clearings and favour ruderal forb plant species over woodland understorey species.

Crop cultivation requires removal of pre-existing vegetation, especially in woodland, and management of soil fertility and weeds. Various models for achieving this have been suggested for Neolithic Europe, with strong evidence for long-term cultivation at specific locations ("gardens") supported by manuring practices alongside cyclic use of the wider landscape through coppicing and movement of animal herds for the Central European lake dwellings area (Jacomet et al., 2016), although some argue that shifting "slash and burn" type cultivation would have been more effective in wooded areas (e.g., Schier, 2009; Rösch et al., 2017). In lowland areas of the UK, Neolithic practices were introduced into landscapes dominated by mixed deciduous woodland, and the pollen signal of Neolithisation is largely seen through an increase in non-arboreal pollen types reflecting the crops themselves, ruderal species associated with the newly available areas of disturbed ground, and the species which replaced the dominant canopy trees both in areas kept open by grazing and as part of the successional sequence once garden-patches were abandoned. Whilst the crops and settlements of these Neolithic populations will have occupied a very small fraction of a landscape at any one point in time, the effects of these cultural practices will have been more widely seen, both through the impacts of grazing livestock and through the persistence of an ecological signal of disturbance for decades and sometimes centuries following abandonment and movement of the farming population. However, not all parts of

the UK were fully wooded at the start of the Neolithic, and some of the most exciting archaeological finds of recent years (e.g., Ness of Brodgar; Card et al., 2017) come from the far North, where woodland cover was probably never complete in the Holocene, and certainly by the mid-Holocene the landscape contained extensive areas of naturally treeless grassland. Here woodland did not have to be cleared to permit agricultural activity, and indeed may have been sufficiently limited that it required deliberate protection. The pollen signal of agricultural activity in such a landscape will probably lack the classic "decrease of tree pollen" signal of a "landnám" in a woodland area, but should still be seen through an increase in ruderal species and possibly crop plants.

In this paper, we use pollen records and the MSA to reconstruct the landscape level impact of Neolithisation on land cover in two contrasting British landscapes, the Somerset Levels and Moors and Mainland Orkney, both with a rich and well dated archaeological record of Neolithic activity which provides an indication of variations in the amount and intensity of activity over the period, for comparison with the reconstructed land cover record. The Somerset Levels are a complex of lowland wetlands within a densely wooded mid-Holocene landscape, with substantial tree removal only beginning to be recorded in the Iron Age. In Orkney, pollen records come from discrete basins scattered across Mainland, and the northerly, hyperoceanic setting of the islands meant that full forest cover probably never developed.

The aims of this paper are to:

- Use the pollen record for the Neolithic period (broadly defined) in two UK landscapes containing important Neolithic archaeology which have contrasting late-Mesolithic

- land cover, to reconstruct the extent and timing of land cover modification associated with Neolithisation and determine whether land cover changes occur in the same pattern as archaeologically-derived estimates of occupation levels.
- (b) Consider the strengths and weaknesses of the MSA for land cover reconstruction.
 - (c) Demonstrate how pollen dispersal and deposition models and the MSA can be used to strengthen the relationship between pollen data and archaeological research questions, and be incorporated into the palynologist's standard workflow.

MATERIALS AND METHODS

In this section we outline the MSA and introduce the case studies.

The Multiple Scenario Approach

The MSA is outlined in Bunting and Middleton (2009) and schematically presented in **Figure 1**. Reconstruction begins with a landscape of interest, from which one or more empirical pollen records covering the relevant time period are available.

First, the analyst identifies the main environmental constraints in that landscape which can be known for the relevant time period (e.g., topography, geology, paleogeography) and the palynological equivalent¹ (hereafter p.e.) vegetation components which might have formed part of past land cover. These components can be a single p.e. (e.g., *Quercus*) which can represent one or many plant species, or a community comprising a defined mixture of p.e. taxa (e.g., every pixel assigned to grassland is modelled as containing 80% Poaceae, 10% Cyperaceae, and 10% *Plantago lanceolata*).

This information is used as input into a Geographic Information System (GIS) to create many possible maps of distribution of those land cover components, combining gridded environmental data with both environmental constraints (e.g., *Quercus* can only occur below 600 m asl) and random placement rules (for example a pixel in the area below 600 m has a 20% chance of being occupied by *Quercus*, a 10% chance of being occupied by *Betula* and a 70% chance of being occupied by grazed grassland) to assign each pixel in the grid to one of the vegetation components. For each of these possible maps, pollen assemblages are simulated at the location of the actual pollen records using a pollen dispersal and deposition model. These simulated pollen assemblages are then compared with the empirical pollen assemblages using similarity coefficients; scenarios producing the most similar pollen assemblages or similarity scores meeting some pre-determined criterion are considered to be possible reconstructions of the past land cover at the time when the pollen assemblage was formed.

One strength of this method is its ability to identify multiple different possible reconstructions, including arrangements of past land cover which are ecologically distinct (e.g., birch

woodland and oak woodland or mixed birch-oak woodland, copses in open fields or wood-pasture; see Bunting and Farrell, 2017) but cannot be distinguished palynologically from the available pollen records. This both reduces analyst bias in favor of particular types of landscape and offers up clear alternative hypotheses for testing via either future pollen analysis or by seeking out other lines of evidence. Whereas LRA reconstructions are presented as percentage cover (for "regional" vegetation, e.g., an average for an area on the order of 50–100 km radius around the study sites) or distance weighted plant abundance (within the Relevant Source Area of Pollen for small sites, typically 500–2,000 m radius), which are then converted into spatial representations of land cover using GIS (see e.g., Pirzamanbein et al., 2014), MSA reconstructions are produced in a mapped form from which quantitative measures can be derived if required.

LandPolFlow Software Package

LandPolFlow is a specialist simplified GIS coded in Borland Delphi. The principal simplification made is the requirement that all gridded data are in raster format and for any given analysis run all grids have the same dimensions, resolution and geographic location, although there is some capacity to nest larger land cover grids or to otherwise incorporate a "background" pollen component sourced beyond the modelled landscape. LandPolFlow was written by Mr. R. Middleton, now retired from the University of Hull. The software is available on request from Dr. M. Jane Bunting (and via worktribe, the University of Hull repository).

Inputs: environmental data

Input grids define the physical environment on which land cover forms. The format used for all grid types is that used by the 16 bit (DOS) version of Idrisi and later by Openland (Eklöf et al., 2004) and HUMPOL (Bunting and Middleton, 2005). Three kinds of grids can be used, class grids (coded using numbers in the range 0–255) which can be linked to tables which assign numerical values to specific classes, Boolean grids and real data grids (containing quantitative information stored as IEEE single precision real values). Provision has been made within the package to derive slope and aspect grids from digital elevation models (DEMs), and to smooth the derived grids. In the examples presented here we use class grids for surficial geology and definition of known water bodies and coastline, and real grids for DEMs. A script file is then used to instruct the program to create one or more new grids with the same dimensions as the environmental grids, showing land cover classes. The available land cover classes are defined in a separate input file, the "PolSack" file (see section Simulated Pollen Assemblages below).

Scripts and scripting

All operations in LandPolFlow are performed under the control of a script file. The scripting language makes use of loops and system-defined variables (e.g., limiting altitudes, the probability of a particular land cover element being present) to allow many land cover grids to be made in a single run reflecting varying land cover placement "rules." These placement "rules" can be

¹Plant species organized into groups on the basis of identifiability of their pollen grains; some types can be identified to species level e.g., *Plantago lanceolata*, whilst others can only be identified to genus e.g., *Betula* or family e.g., Brassicaceae, and some pollen types do not map neatly onto plant taxonomic groups (see e.g., Bennett K. D., 2007).

prescriptive (e.g., *Betula* never occurs on limestone/above 600 m asl) or probabilistic (e.g., the likelihood of *Betula* occurring on steep slopes is 80%, on moderate slopes is 50% and on shallow slopes is 20%), and rule parameters can also be varied (e.g., maximum altitude can be 550, 600, 650 m asl etc., or the probability of occurrence on a moderate slope can vary between 10 and 50% in 4% steps). Land cover types can be placed into the grid as single pixels or as larger blocks within the landscape, allowing scenarios to explore the effects of different sizes of patches (e.g., the pollen signal of a farming landscape where human activity is centered around multiple scattered “farmsteads” vs. a single large “village”) as well as of different proportions of total cover. The number of grids defined by combinations of placement rules and taxa can be very large.

Simulated pollen assemblages

A second set of commands within the script simulate the pollen assemblage for a land cover grid at one or more specified locations, and calculate the similarity coefficient between the simulated assemblage and the actual target pollen assemblage. Two input files are required for these commands in addition to the environmental grids; the first defines the composition of the land cover classes, the properties of the pollen types produced by the p.e. taxa (e.g., Relative Pollen Productivity), and the specific locations for which pollen assemblages are to be simulated (the “PolSack” file), and the second is a lookup table containing taxon-specific distance weightings for each pollen type, based on the pollen dispersal and deposition model chosen. Using a lookup table increases the speed of calculation of simulated pollen loading, which is valuable when many possible land cover scenarios are being considered. Details of the calculations are presented in the Supplementary Material to this paper.

Handling output data

Software output is in two forms, as grids (which can be saved in IDRISI format, as jpegs or as bitmaps) and as a text file containing the simulated pollen assemblages, calculated fit statistics (a selection of similarity measures are available; in this study we used squared-chord distance) and other model parameters as defined by the user (e.g., the system variables used in the script loops to vary abundance or location of land cover classes). Within the script a saving threshold can be set to ensure that grids are only saved for scenarios with a good fit, reducing the memory demands of the program. Output files can then be processed in many ways. In this study, we used R scripts to help extract the output for best fit solutions for individual target locations and for the landscape as a whole from the text files (identified from the sum of fits for all target locations). Scripts are available from the authors on request.

Two approaches to identifying the “best” landscape reconstructions were used, a site-led approach and a whole-landscape approach. For the site-led approach, the best fit scenarios for each individual pollen core location were identified by the site fit score, and the overall landscape character determined as a mean of the model parameters for the scenarios providing those best fit scores with variation expressed as standard error around that mean. This site-led

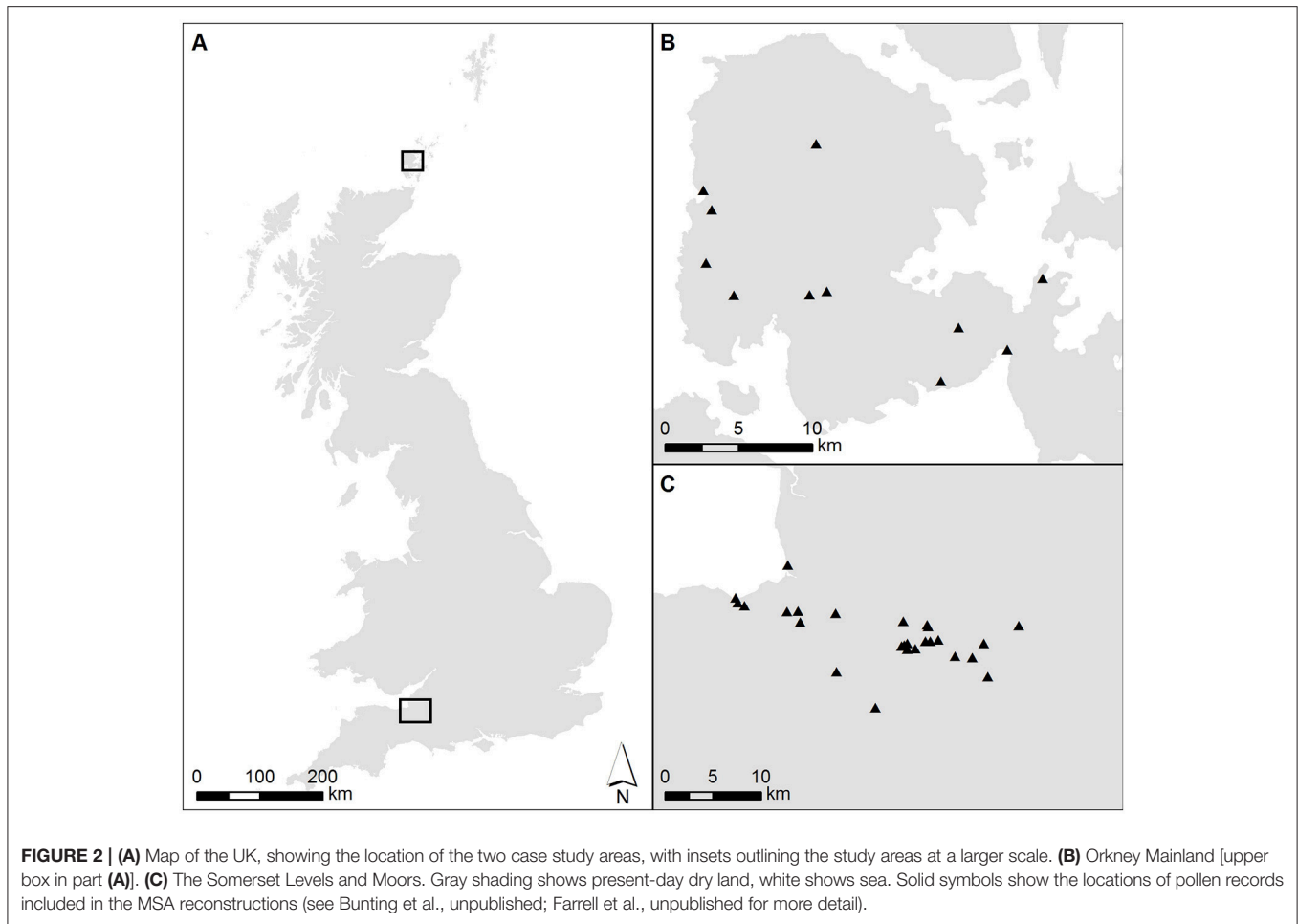
approach produces reconstructions of trends in land cover and changes between timeslices expressed in model parameters (e.g., probability that a pixel meeting specified criteria will be allocated “woodland”) rather than land cover parameters (e.g., hectares of woodland in the final grid). For the Somerset Levels and Moors dryland land cover reconstruction the average of parameters for the single best fit scenario for each pollen site was used. For the Orkney case study, where there were fewer pollen sites available, model parameter averages were taken from the best five fits for each site. This approach made more allowance for local variation in land cover both on and around each individual site than the whole-landscape approach, useful in this project where the number of repeat runs was limited (a high number of repeats of each scenario is ideally required since random placement of vegetation can lead to highly varied site pollen signals in sensitive locations).

For the whole landscape approach, the best-fit scenario was that which produced the lowest overall fit score based on the sum of scores for all sites, that is, it is effectively the reconstruction which offers the best compromise across the target pollen records. To extract land cover data in this approach, the best fit grid was saved and the coverage of each community within the grid determined using mosaic5 (updated from Middleton and Bunting, 2004) then converted into hectares.

Single grids for each timeslice were also selected to create a visual sequence of landscape development. These grids were chosen from the selection of grids saved by the software, i.e., those with fit scores below a pre-determined threshold. In most cases the grid with the lowest overall fit score was chosen, but in some cases a different grid was selected on grounds of being more “plausible” (*sensu* Caseldine et al., 2008)—that is, that it fitted logically into the sequence in such a way that known ecological processes could be evoked to explain the transition from and to the landscape scenarios on either side. There is considerable scope for improvement in determining the best and most efficient methods of extracting and presenting land cover data from MSA reconstruction output, but the methods chosen here are replicable and produce consistent and reasonable results.

Case Study Landscapes

The Somerset Levels and Moors (**Figure 2**) were chosen as a case study from the lowlands of England, within the deciduous forest potential vegetation zone. Significant paleoenvironmental and archaeological research has been undertaken in the region, which has a long history of collaboration between environmental and archaeological specialists, particularly during the Somerset Levels Project (Coles and Coles, 1986; Coles, 1989). Neolithic archaeological remains are characterized by wooden trackways of various types, with only hints of occupation sites in the form of lithic scatters discovered as yet. All evidence suggests that the wider landscape was wooded throughout the Neolithic, with human activity leading to small-scale, periodic clearance (Beckett and Hibbert, 1978). The earliest Neolithic activity identified from archaeological dates was around 3800 cal BC, and land-cover was reconstructed for a series of 200-year intervals (referred to as “timeslices”) over the period 4200–2000 cal BC.



In contrast to the Somerset Moors and Levels, the landscape of Orkney is generally understood to have been largely or entirely treeless during the Neolithic (e.g., Davidson and Jones, 1985), though paleoenvironmental work suggests that occasional stands of woodland were present into the Bronze Age (Farrell et al., 2014). The wealth of Neolithic archaeological remains in Orkney also contrasts with the Somerset case study, with well-preserved settlements, tombs and monuments still dominating the landscape in many places even today. Recently developed chronologies for Neolithic archaeology (Griffiths, 2016; Bayliss et al., 2017) can be compared with land-cover reconstructions which were made for 200-year “timeslices” over the period 4200–2200 cal BC.

The Physical Environment

For both case studies, a DEM of modern surface elevations derived from Ordnance Survey PANORAMA DTM NTF geospatial data supplied by EDINA Digimap at a scale of 1:50,000 was used as a starting point for land-cover modelling. The NTF data were clipped to the spatial extent of the study area and converted to IDRISI format using the GridIn application (Middleton, unpublished). Surficial geology grids were prepared based on British Geological Survey SHAPE geospatial data

provided by EDINA Digimap at a scale of 1:50,000 for Somerset and at a scale of 1:625,000 for Orkney. A simplified classification was created in ArcGIS 10.3.1 and converted to IDRISI format using the GridIn application (Middleton, unpublished). The basic grids had 50×50 m pixels, and covered 36×49 km for the Somerset Moors and Levels case study and 32×30 km for the Orkney case study (see Figure 2).

Both areas have been affected by sea-level change in the early and mid-Holocene, but paleogeographical reconstructions at suitable resolution are not available. In the Somerset Levels and Moors, published paleogeographic maps of Bridgwater Bay show profound changes during the early and mid-Holocene (Kidson and Heyworth, 1976; Long et al., 2002), but by the start of the Neolithic, most of the area of interest was free from marine influence, and current understanding suggests that the paleogeography was broadly the same as at present from around 4200 cal BC. We therefore used the present-day surficial geology maps (showing the distribution of peat, alluvium, and coastal sediments) as the main guide for the distribution of wetland communities. The position of the Orcadian coastline has changed significantly during the Holocene due to rising sea-levels, with its present position having been reached at c. 2000 cal BC (Wickham-Jones et al., 2016, 2017). Current understanding

of Holocene sea-level change in Orkney largely relies on general models produced for North-West Europe (e.g., Sturt et al., 2013). Local sea-level data for Orkney is currently being produced (Dawson and Wickham-Jones, 2007; Bates et al., 2013), but at present chronological resolution is too coarse to allow for estimation of sea-level in 200-year timeslices, therefore in this study modern coastline position was used for all timeslices.

The Vegetation Communities and Their Distribution

The main pollen types found in diagrams from each region were used as the basis for simplified plant community definition based on literature and understanding of the ecology of each case study area (summarized in **Table 1**).

In the Somerset Levels and Moors case study, placement of communities within the landscape assumed that vegetation could be divided into wetland and dryland areas, with saltmarsh, reed swamp and mudflats present in the western Levels where tidal influences dominated, floodplain and carr wet woodlands in the eastern Moors, and mixed deciduous woodland on the surrounding dryland and on raised burtle islands within the wetlands. Distribution of wetland communities is based on the modern surficial geology in all timeslices. Where peat is mapped as present, wet woodland was placed, and floodplain woodland was placed on areas of alluvium. In areas mapped as Holocene tidal sediment, beach deposits or sand, pixels were allocated to either bare mud, marsh or saltmarsh with a probability distribution of 0.2:0.4:0.4. All other land areas above 3 m asl were modelled as supporting mixed deciduous woodland. In the Orkney case study the landscape was modelled as a mosaic of birch-hazel woodland and grassland suitable for grazing animals. Areas of disturbed grassland, which could either occur naturally, for example in response to storm deposits of sand and/or salt, or due to anthropogenic activity, were placed below 30 m asl, and given a single community composition including low pollen production cereals, some bare ground and some high-pollen-producing weeds associated with disturbance (*Artemisia*-type, *P. lanceolata* and *Rumex*-type). Stands of pine and oak woodland were placed in sheltered, well-drained situations (slope >5°, altitude <100 m, aspect E, SE, or S). The amount of woodland present was varied independently between “upland” (defined following Lamb, 1989 as land above 60 m asl) and “lowland” areas, since it is possible that anthropogenic clearance might have been greater in the lowlands, and edaphic processes and exposure might contribute more to woodland loss in the uplands. Local wetland vegetation at each coring site was inferred from the published records. Where data were insufficient to allow this multiple possibilities were tested during the early “scoping runs” (see section Pollen Assemblage and Radiocarbon Age Estimate Data below).

Pollen Assemblages and Chronologies

All available radiocarbon dated pollen records were collected, and new age-depth models constructed to ensure a common chronological framework. The age of each sample was determined as the median of the Highest Probability Density Interval and pollen data for all samples falling within a particular timeslice were summed and averaged to produce a single pollen

assemblage at each location during each 200-year timeslice as the targets for reconstruction. Not all pollen sequences contained samples dating from every timeslice, so each timeslice uses a slightly different set of pollen records.

Scripts and Scripting/Workflow

For each landscape, initial scoping runs explored a wide range of possible levels of woodland cover and variations in local wetland structure, then more focused runs were carried out using a narrower range of vegetation options, which allowed for a larger number of repeats of each scenario and therefore better incorporation of random placement effects in outputs. For example, in the Somerset Levels and Moors, the scoping run assessed the fit for landscapes with clearings occurring in either just the dry land woodland or in all types of woodland, with the proportion of clearings in each woodland type ranging from 0 to 100% in 10% increments, and in addition at each coring point, local wetland vegetation was modelled as either marsh or raised bog within wet woodland, and marsh or raised bog with a surrounding ring of alder carr of varying width. The radius of the bog or marsh was varied in 50 m increments from 50 to 800 m, and the width of the surrounding alder carr was also varied from 50 to 750 m. In combination, this gave 512 different configurations for the local wetland vegetation and 22 woodland clearing configurations, generating 11,264 possible scenarios for each timeslice. For the Orkney case study, the first scoping run considered a very broad range of scenarios from a 100% open landscape to a 100% wooded landscape, along with different proportions of heathland, oak-pine woodland and disturbed ground. Later runs varied the structure of vegetation as well as the proportion of cover (e.g., whether woodland occurred as discrete patches or scattered pixels). The vegetation placement constraints used in the final scripts are described in section The Vegetation Communities and Their Distribution above, and multiple replicates of each scenario were run, since vegetation patches were placed randomly and pollen records are known to be sensitive to vegetation patterning as well as overall vegetation composition (Bunting et al., 2004).

Model Uncertainties

No model is a perfect reconstruction of a natural process, and the complexities of the pollen-vegetation relationship mean that the models used here are likely to be highly imperfect. Both the LRA and the MSA rely on the assumption that the dispersal and deposition model chosen is appropriate to the system being studied, and that the p.e. type properties of Relative Pollen Productivity and fall speed (see Supplementary Material) can be treated as constants for a given study location. Empirical measurements of these variables suggest that this is not a good assumption, and research is ongoing to improve understanding of the range of and controls on these variables (reviewed in detail elsewhere e.g., Mazier et al., 2012; Bunting et al., 2013) and the size of the errors introduced by variation.

Unlike the LRA, which treats all p.e. taxa individually, the MSA includes the option to group taxa into communities. Since the MSA produces a grid output rather than numerical, the pixel

TABLE 1 | Pollen dispersal and deposition model parameters and vegetation community compositions used in the pollen dispersal and deposition modelling.

Pollen taxon	Fall speed (m/s)	RPP ^g Poaceae	Community composition (%) Somerset										Community composition (%) Orkney					
			Mixed deciduous woodland	Floodplain woodland	Mixed carr woodland	Marsh	Saltmarsh	Raised bog	Clearings	Arable	Alder carr	Grassland suitable for grazing	Birch-hazel woodland	Oak-pine woodland	Lowland disturbed grassland	Dry heath	Wet heath	Glims Moss surface vegetation
<i>Alnus glutinosa</i> ^a	0.021	4.2			20						75							
<i>Betula</i> spp. ^a	0.024	8.9			20								75					
<i>Corylus avellana</i> ^a	0.025	1.4		30	20								25					
Dryland trees ^f	0.034	2.0	100	70														
<i>Fraxinus excelsior</i> ^a	0.022	0.7			20													
<i>Pinus sylvestris</i> ^a	0.031	5.7												50				
<i>Quercus</i> spp. ^a	0.035	7.6												50				
<i>Salix</i> spp. ^a	0.022	1.3			20													
<i>Artemisia</i> spp. ^d	0.025	3.5					5			1					3			
Cereal-type ^{a,b}	0.06	3.2 ^a /0.8 ^b								80					80			
Chenopodiaceae ^e	0.019	1					20			1								
Cyperaceae ^a	0.035	1						10	5			5					20	20
<i>Calluna vulgaris</i> ^{a,b}	0.038	4.7 ^a /1.1 ^b														50	50	20
Ericaceae ^c	0.038	4.7 ^a /1.1 ^b						10								20		
<i>Plantago lanceolata</i> ^{a,b}	0.029	12.8 ^a /0.9 ^b							5	1		2			5			
Poaceae ^a	0.035	1				95	20		85			90				20	10	10
<i>Rumex</i> -type ^b	0.018	1.6							5	1		3			2			

^a(Hellman S. V. et al., 2008). ^b(Hellman S. V. et al., 2008)—Danish value. ^cAs for *Calluna vulgaris*. ^d(Poska et al., 2011). ^eNo published estimates available—fall speed was calculated by applying Stokes Law (Gregory, 1973) to measurements of pollen grains photographed in Moore et al. (1991). RPP is an estimate. ^fRPP and fall speeds derived from a woodland consisting of lime:oak:elm in the ratios 20:40:40 using values from Hellman S. V. et al. (2008). ^gIn the Somerset case study RPP values for three taxa, Cereal-type, *Calluna vulgaris*, and *Plantago lanceolata* type followed Hellman S. V. et al. (2008) original values, whilst in the Orkney case study the Danish values were used instead.

size of the grid acts as a limitation on the variability possible in the landscape. The landscape is conceived as a mosaic of communities, although p.e. taxa can be components of multiple communities. This is partly driven by concern over pixel size. Assigning each pixel to a single taxon allows each taxon to have different specified environmental constraints, and communities should emerge from the co-occurrence of types with similar ecological requirements at particular locations. However, this is only reasonable if the pixel size is comparable to the size of a vegetation unit, e.g., an individual tree or heather bush, or a grass tussock. Pixel size is determined by three factors: the available resolution of input data (although resampling can change the resolution of a grid, finer sampling risks introducing rounding errors), computer processing capacity and time available for analysis (more pixels means more calculation steps for each simulated pollen sample therefore longer run times for software), and thirdly the overall size of the landscape grid, since the HUMPOL approach of calculating values for each pixel and summing them across the landscape requires at least some rounding of values for holding in the computer memory, and the larger the grid, the greater the risk of introducing errors.

Grid size in turn is determined by the spatial properties of pollen dispersal and deposition, since the MSA approach requires that the landscape considered includes most of the pollen source area of the sites sampled. There are many definitions of pollen source area, multiple factors that affect the value for different combinations of taxa, landscapes, site types, and pollen dispersal and deposition models chosen, and many estimates of its value, but there is general agreement that grids need to be large (at least 10 s of km) to capture some of the background component of the pollen rain. The 50 m pixel size chosen for these case studies was a compromise between these different factors, is larger than most individual trees, and can contain hundreds of thousands of individuals of herbaceous taxa.

For these case studies, we chose to assign each pixel to a community, which would allow us to explore the behavior of “indicator taxa” in the pollen record (distinctive p.e. taxa associated strongly with particular land uses or communities, but rarely present in great abundance). We defined community composition from field observation, evidence from regional pollen diagrams and ecological understanding; clearly the assumptions here are extensive and introduce

uncertainties which are difficult to quantify (e.g., dryland woodland composition in Somerset will have been far more varied at multiple scales than was modelled here). One possible future approach might be to use REVEALS to reconstruct the proportion of each p.e. type in the entire landscape, and use those values to define the community compositions. These choices can also be refined by drawing on multiple lines of evidence (e.g., woodland composition could be estimated from trackway construction materials in the Somerset Levels), although these bring their own uncertainties into the analysis.

Over-complex models are not better models, and a balance between multiplying assumptions and achieving outputs of use to the intended research community needs to be struck. Clearly specifying the choices made, so that the user of model outputs can critically evaluate the results, is essential. Limiting the number of taxa to a very small group, where each taxon is representative of and largely confined to a distinctive land cover element, may be a viable alternative strategy, as shown by Nielsen and Odgaard's (2005) study of historic land cover in Denmark using four taxa, *Poaceae* (pasture), *Calluna* (heath), tree pollen (a composite taxon; woodland), and *Cerealia* (arable cultivation). Definition and quantification of uncertainties associated with MSA reconstructions is a challenging task for the future; in this paper, we focus on outputs expressed as trends and estimates of the extent of change, and use of output grids as hypotheses to be tested by designed collection of palaeoecological or other data.

RESULTS

Results in the form of single best-fit land cover grids and summary landscape characters for each time slice were extracted as described above. Standardized overall fit scores (overall fit for the grid as a whole, divided by the number of sites included) for all these grids lie mainly between 20 and 30 (overall possible range of 0–200), mostly at the lower end, which modern sample comparison suggests is within the range of typical values when comparing modern pollen samples collected within the same broad vegetation communities (e.g., Lytle and Wahl, 2005). Standardized overall fit generally lies within the standard error of the mean of the individual site best fits, suggesting that the two different methods of summarizing land cover described in the methods (section Handling Output Data) are based on comparably good (or bad) reconstructions.

Reconstruction results are shown in **Figures 3–6**. Examples of good-fit land-cover maps for each timeslice from Orkney are given in **Figure 3** and landcover proportion trends are plotted in **Figure 4**. **Figures 5, 6** show the same data for Somerset.

DISCUSSION

Here we consider what MSA reconstructions offer in terms of understanding the Neolithisation of the contrasting case study landscapes, then briefly discuss issues arising from this first full application of the MSA as a reconstruction tool and explore possible remedies, before evaluating the potential place of the approach within main-stream palynological research.

Landscapes of Neolithisation Orkney: Neolithisation in a Largely Treeless Landscape

In the Orkney case study, pollen records came from discrete wetlands scattered across the landscape. Some sites consistently yielded lower fit scores than others, at least partly due to uncertainty about the nature of the local wetland vegetation at the pollen sites. The characteristics of some study sites (e.g., Hobbister—Farrell, 2015) were clearly changing during the study period, and full investigation and mapping of the stratigraphic units and hence former sedimentary environments to support better reconstruction is not always possible (e.g., due to active peat extraction at Hobbister).

“Plausible” (*sensu* Caseldine and Fyfe, 2006) mapped land-cover reconstructions for all 10 timeslices across the period 4200–2200 cal BC are shown in **Figure 3** and land-cover trends plotted in **Figure 4**, compared with the intensity of settlement activity in “core” and “peripheral” areas across Orkney derived from the number of dated structures in use on individual sites (**Figure 4A**; Bayliss et al., 2017). A baseline for disturbed grassland communities in the pre-Neolithic landscape (communities with higher proportions of anthropogenic indicator taxa than the “natural” grassland) can be taken from the timeslice 4200–4000 cal BC. At this point c. 12% of the landscape was wooded, mainly birch-hazel. Less than 1% of the study area was made up of the “disturbed grassland” community.

The first dated archaeological evidence of settlement in Mainland Orkney is recorded during the 3600–3400 cal BC timeslice (Bayliss et al., 2017). The increase in dated settlement activity, particularly in the “core” Brodgar-Stenness area, over the period 3200–2800 cal BC is associated with a significant increase in inferred landscape disturbance. The subsequent decline in dated structures in both “core” and “peripheral” areas of Mainland is not associated with a reduction in cover of the disturbed grassland community, which actually increases in the 2800–2600 cal BC timeslice, following abandonment of the “core” area of Neolithic activity, and the 2400–2200 cal BC timeslice, following abandonment of settlements in the “peripheral” area of Mainland.

Established Neolithic activity on Mainland Orkney probably began in the thirty-fifth century cal BC (Bayliss et al., 2017; Bunting et al., unpublished), about 300 years later than elsewhere in Britain and Ireland (Whittle et al., 2011), implying that Neolithic people were slow to establish themselves on Mainland. The MSA reconstructions support this relatively late start date. Prior to any dated Neolithic activity, the landscape was dominated by grassland suitable for pasture. This natural prevalence of grassland may help to explain the rapid expansion of Neolithic settlement on Mainland, since the Neolithic Orcadian economy probably relied heavily on cattle (see Mainland et al., 2014; Card et al., 2017) and extensive clearance would not have been necessary to provide land for grazing. Inferred variations in the amount of “disturbed ground” above the baseline from the 4000 to 3800 cal BC timeslice onwards may hint at earlier anthropogenic disturbance by either late hunter-gatherers or farming pioneers; Sharples (1992) has suggested that the comparatively heavy

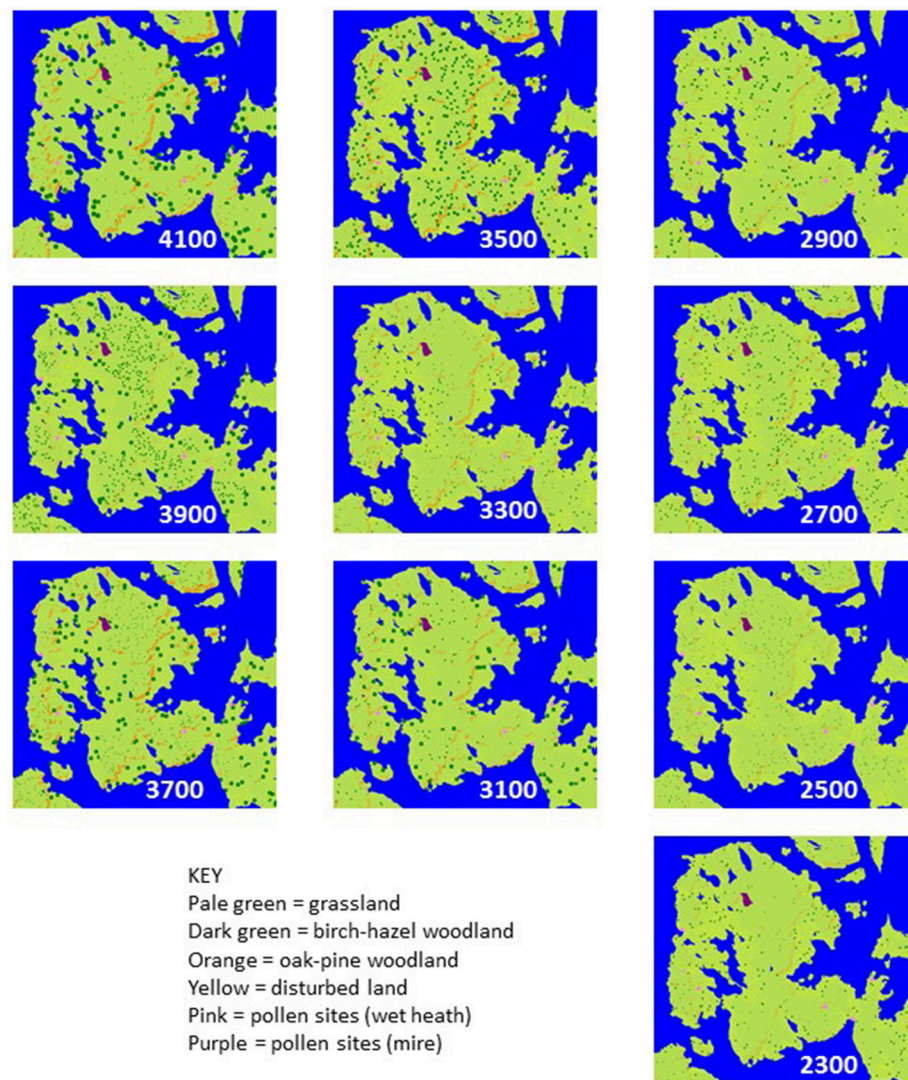


FIGURE 3 | Example best-fit grids of land cover for Orkney case study in 200 year timeslices between 4200–2200 cal BC (age shown is midpoint of timeslice).

soils on Mainland Orkney were exploited later than other islands.

A distinct shift in land-cover is reconstructed between 3400 and 3000 cal BC (see **Figure 4**), the period that covers the first sustained tomb building, the shift from timber to stone houses, and the concentration of settlement in the “core” Brodgar-Stenness area of Mainland (Bayliss et al., 2017; Bunting et al., unpublished). There is an increase in coverage of the “disturbed ground” community and a reduction in woodland cover, but woodland does not disappear from the landscape entirely. Woodland would have been a valuable resource for Neolithic Orcadians (Farrell et al., 2014), and was already scarce (**Figures 3, 4**) at the time of the first dated settlement activity (3600–3400 cal BC timeslice), and falls by around 50% between the 3400–3200 cal BC timeslice and the 3200–3000 cal BC one, suggesting that some loss of woodland occurred with the first dated

Neolithic activity in the area. The clear coincidence between changes in land cover and settlement occupation, dated using the same age model construction approach but independent sets of radiocarbon dates, suggests that land cover reconstruction using the MSA may provide a proxy for settlement activity even in landscapes where impacts are expected to have been small scale.

A decline in settlement activity in the Stenness-Brodgar “core” area in the 2800–2600 cal BC timeslice does not coincide with any reduction in potentially cultivated “disturbed ground” or with woodland regeneration in the MSA reconstructions; human population may have become dispersed into smaller settlement units, away from the socially unsustainable concentrations of people in the major Neolithic complexes of the Stenness-Brodgar peninsula, rather than actually reducing in size. A further decline in woodland coverage is seen in the last two time-slices, coinciding with the time activity was re-established

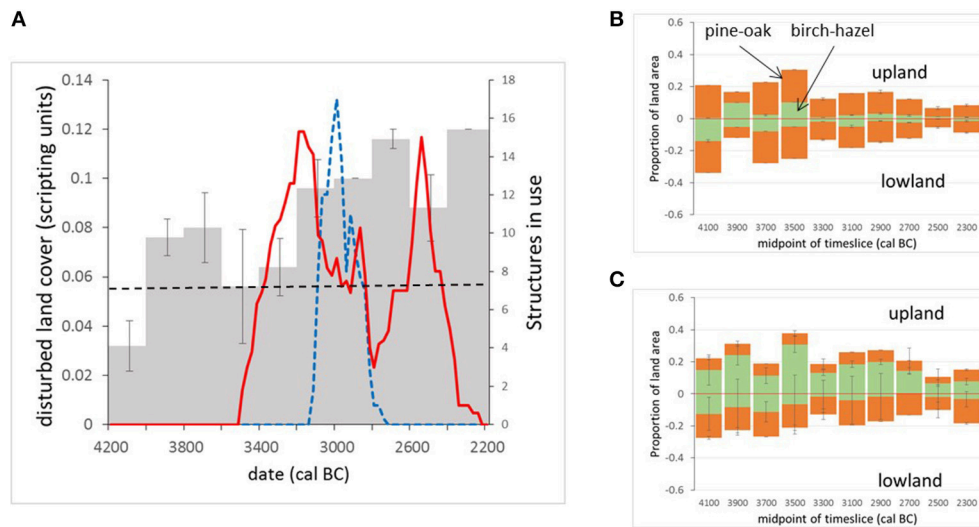


FIGURE 4 | Trends in land cover extracted from MSA reconstructions for Neolithic Mainland, Orkney (axis labels in modelling units—see text for details). **(A)** Variation in disturbed land community presence below 30 m a.s.l. (dashed line marks baseline from timeslice pre-dating first substantial archaeological dating evidence in the studied area). Solid red line shows radiocarbon-derived activity estimates in the “peripheral” area, blue dashed line shows radiocarbon-derived activity estimates in the “core” area (see Farrell et al., unpublished for more information). **(B)** Tree cover modelled as discrete woodland stands—trends in the upland and lowland areas of the modelled landscape (above and below 60 m asl). **(C)** Tree cover modelled as scattered trees or small copses—trends in the upland and lowland areas of the modelled landscape (above and below 60 m asl).

in the “core” area in the twenty-sixth century cal BC. These MSA reconstructions also contribute to understanding the end of the Neolithic in Orkney. Several possible reasons for the decline of the Grooved Ware culture have been proposed (see Clarke et al., 2018, for a review), including environmental stress and climatic deterioration (cf. Meller et al., 2015). The reconstructions presented here do not show the changes in land-cover which might be expected to accompany a climatic downturn (e.g., spread of acid heathland), nor do they provide evidence for abandonment. This suggests continuity of land-use, and it seems more likely that the cause of the Grooved Ware decline has its root in social factors rather than environmental deterioration (Farrell, 2009; Bunting et al., unpublished). This interpretation supports Downes (2005) suggestion that the apparent scarcity of Bronze Age settlements in Orkney is probably the result of failure to identify them rather than a true lack of occupation.

Even at the time of most intensive dated settlement activity in the 3200–3000 cal BC timeslice, the “disturbed” community accounts for only around 4% of available land (from the landscape-scale reconstruction: see section Handling Output Data above), although anthropogenic activity is also the most likely cause of the observed woodland cover decline. Many classic anthropogenic indicator plants were already present as part of the grassland community, and would also have existed in naturally disturbed habitats close to the coast; consequently increases in these indicator taxa and changes in composition of open vegetation communities have a much more subtle palynological signal compared with reductions in tree pollen. Figure 4 shows how the quantification of changes made possible by applying

the MSA allows us to draw out this relatively subtle signal and compare it with the archaeological record.

Differences in woodland coverage in Orkney above and below the 60 m asl limit of prehistoric cereal cultivation are illustrated in Figure 4B (tree cover modelled as woodland patches) and Figure 4C (tree cover modelled as scattered trees). The results clearly illustrate the equifinality associated with MSA reconstructions. Where trees are modelled as patches of woodland (Figure 4B), woodland cover is generally similar in both upland and lowland areas, and the more diverse woodland incorporating oak and pine tends to be more abundant than the pure birch-hazel “scrub” community. Where scattered trees are modelled (Figure 4C), the upland areas tend to contain more woodland than the lowlands, and the more diverse woodland is more abundant in the lowlands. This second option is perhaps more realistic from an ecological point, but the two sets of scenarios cannot be distinguished on the basis of the existing pollen records.

These outputs can be used to identify pollen sites for future studies designed to test these two contrasting hypotheses for former woodland distribution, by taking pollen records from small basins whose pollen source area lies above or below the 60 m asl limit and comparing pollen assemblages across the study period at an appropriate sampling interval (e.g., 100–200 years, comparable with the reconstruction) to determine whether there is a systematic difference in woodland coverage or not. The modelling approach used here assumes that all pollen at the target sites originates from within the modelled area of Mainland. Certainly for pine, a long-distance component from Hoy and Northern Scotland will also have formed part of the target pollen

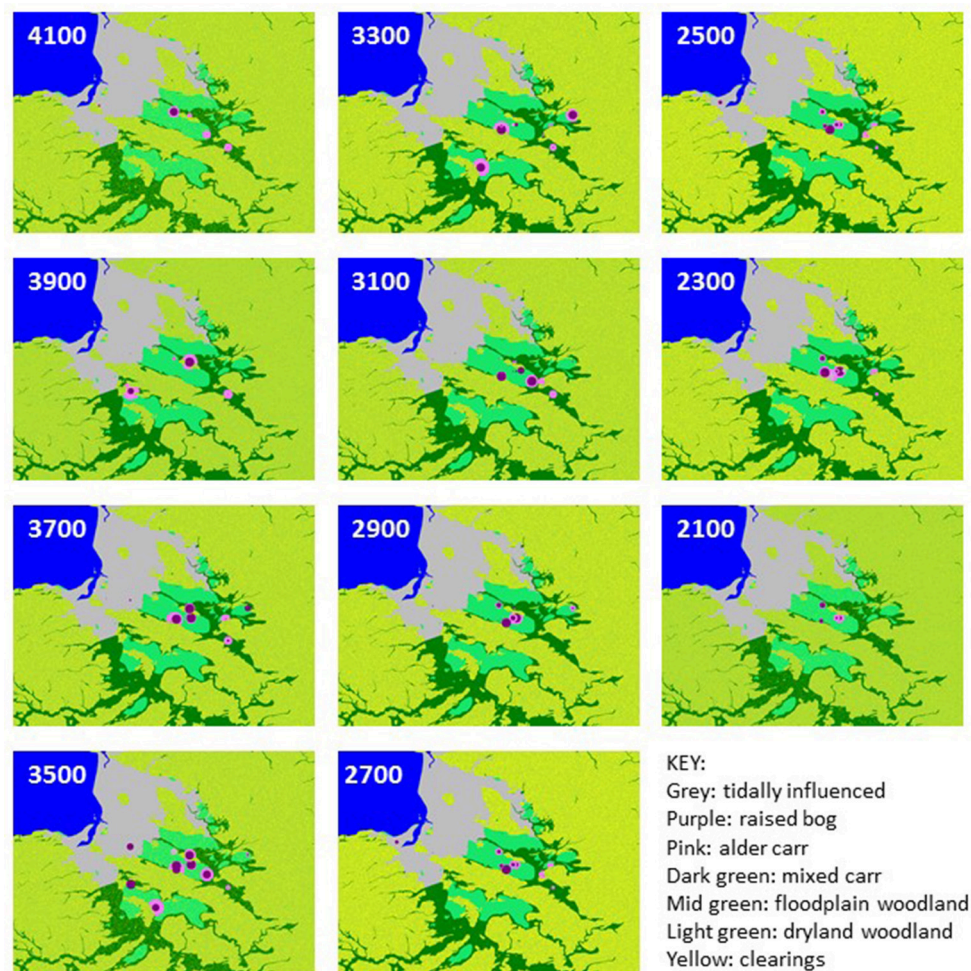


FIGURE 5 | Example best-fit grids of land cover for the Somerset case study in 200 year timeslices between 4200 and 2000 cal BC (age shown is midpoint of timeslice).

assemblages, although simple “thought experiment” modelling suggests that non-Orcadian sources contribute <20% of the total pine pollen recorded. This component may partly explain the apparent stability of oak-pine woodland coverage in comparison with the variation in coverage of the birch-hazel community. A relatively small number of target pollen sites are included in any single timeslice, and the differences in which sites are included in each timeslice are also likely to contribute to the variability seen in the reconstructed land-cover, but the overall patterns provide some more detail on the likely location of woodland in Neolithic Orkney.

Somerset: Neolithisation of a Densely Wooded Landscape

Examples of good-fit land-cover maps for each timeslice in the Somerset case study area are given in **Figure 5** and landcover proportion trends are plotted in **Figure 6**. The start of the Neolithic in this area occurs during the 3800–3600 cal BC timeslice (see Farrell et al., unpublished) and the 4000–3800 cal

BC timeslice is used to define the pre-Neolithic landscape. The initial openness level of c. 10% is presumably due to natural processes such as wind-throw, lightning strikes and grazing by wild herbivores (Brown, 1997). The higher level of clearings implied for the earlier 4200–4000 cal BC timeslice is assumed to reflect the response of land cover to the end of a phase of falling relative sea-level, as the lower-lying parts of the Levels and Moors become wooded. The proportion of woodland clearings within the timeslices 3800–3600 and 3600–3400 cal BC rises, which is interpreted as anthropogenic clearance of woodland in the wider landscape. Between 3400 and 2800 cal BC, the standard errors of estimated clearance overlap with the baseline clearance level, which is interpreted as a reduction in the extent of human-related woodland openings; in two of these three timeslices the mean is still above the 10% baseline. For 2800–2600 cal BC, clearings increase to c. 20% of the potential woodland area, interpreted as an increase in landscape modifying human activity. The proportion of cleared land then falls back to approximate baseline between 2600 and 2200 cal

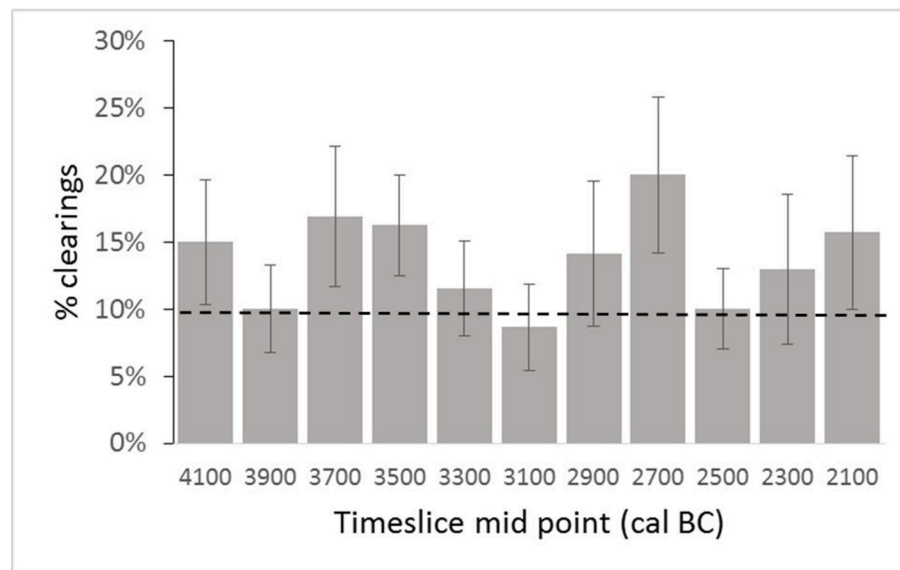


FIGURE 6 | Changing proportion of clearings in the Somerset case study landscape in 200 year timeslices between 4200 and 2000 cal BC based on mean of the five best fit reconstructions identified through the MSA. Dashed line represents pre-Neolithic base-line conditions (see text for details).

BC, and rises to around 16% in the final timeslice (2200–2000 cal BC).

MSA land-cover reconstruction shows that at times the proportion of cleared land increases to 50–100% above the pre-Neolithic baseline, which is interpreted as reflecting additional disturbance of the woodland due to anthropogenic clearance. Some of these clearances may result from woodland management, since coppiced wood was used in the construction of Neolithic trackways in the region (Coles and Coles, 1986, 1992), and others may be associated with agricultural activity on the dryland such as small-scale cultivation or management of grazing animals. These results may be taken as a kind of proxy settlement record in an archaeological landscape that currently lacks evidence for occupation sites, allowing some preliminary comparisons and contrasts to be drawn with neighboring regions. The suggestion of initial activity in the thirty-ninth century cal BC conforms with the wider picture for the beginning of the Neolithic proposed by Whittle et al. (2011), and increased woodland clearance between 3800 and 3400 cal BC corresponds with the scale of monument construction seen in southern Britain during this time. The reduction in clearance seen in the 3200–3000 cal BC timeslice is also of interest, given recent debate about possible discontinuity of cereal cultivation in the later fourth millennium cal BC (Stevens and Fuller, 2012). Decreased activity in the 2600–2400 cal BC timeslice serves as a valuable reminder of regional variation at a time when major constructions and cultural changes were taking place in the Stonehenge area.

Future modelling-supported research questions to be explored in the Somerset area include investigating the location of early human activity in this landscape complex. In this analysis, woodland disturbance could occur anywhere with equal probability, but prehistoric human populations are known to use different parts of landscapes differently. Modelling could be used

to determine whether it is possible to separate a pollen signal from human activity focused around the Levels and Moors on one or more wetland margin settings, river margins, or burtle islands and the Polden Hills from activity spread more widely in the landscape, using archaeological understandings of Neolithic landscape utilisation to inform the “rules” which control possible location of clearings, and to explore the effects of different models of landscape utilisation on the pollen signal (through different lengths of cropping, fallow/grazing, and woodland successional phases). In future archaeological research programmes, the reconstructions presented can be used as a starting point for identifying the coring locations most likely to produce pollen records which include archaeological sites of interest within their source areas, and thereby improve the integration of the two methodologies.

Evaluation of the Reconstruction Approach

The studies reported here are the first full implementation of the MSA for reconstruction of past land cover from pollen records, therefore it has brought both strengths and weaknesses into clear focus. Discussion is organized around the stages of reconstruction.

Input Data

The MSA incorporates landscape characteristics overtly in the reconstruction of past land cover, which improves the plausibility and usefulness of the output, but depends on being able to clearly define these characters. Topographical (DEMs) and geological data are readily available in mapped forms for the UK, and at the temporal and spatial scales used can be considered invariant. Palaeogeography proved more challenging, as sea level and the distribution of water bodies are known to have changed during the Holocene substantially enough to affect the reconstructions.

In both case studies, after consulting all available evidence, we decided to assume the coastline was in its modern position, and in Orkney it was also assumed that extant lochs were in the same size and position, and that no loss of water bodies through drainage or hydrosere succession had occurred. These assumptions are clearly wrong, but how to improve them without introducing additional sources of uncertainty was not obvious.

Reconstructing paleo sea level, paleo coastal geomorphology and paleo landscape hydrology is a non-trivial exercise. For the Somerset case study, we were able to access a reconstruction of paleogeography which used a basemap derived from Sturt et al. (2016; see SI3 in Farrell et al., unpublished for details). However, translating this into pre-Neolithic coastline position and identifying areas subject to marine influence would also require reconstruction of sediment infilling across this landscape from coastal, fluvial, and hydrosere processes, and whilst sediment stratigraphy and dating evidence do exist for much of the area which could form the basis for such an exercise, it was beyond the scope of the present study. By allowing for a wide range of local wetland conditions at the coring points (combinations of mire, marsh and alder carr in Somerset, and of mire and marsh in Orkney) in the scoping runs the MSA was able to incorporate some of the variation in wetland conditions that would have resulted from changing sea level and paleogeography in both case studies and therefore reduce the impact of incomplete knowledge of past coastline. Some sites used as targets in both case study areas are in locations where paleogeographical changes could have made a large difference to the landcover within a few hundred metres of the basin edge, and where such sites are identified they could be downweighted when identifying the quality of fit of the overall reconstruction. In both our case studies, reconstructed land cover from such sites was close to that from sites without such influences, showing that all sites were picking up a comparable regional pollen signal and such down weighting would not change the outcomes substantially.

An unanticipated problem was the difficulty of accessing data for published pollen records, and in some cases values had to be “read” from published diagrams rather than using original counts, showing the challenges of maintaining access to data over the longer term.

Specification of Land Cover Units

After identifying the main pollen taxa (palynological equivalent types, as discussed in section Model Uncertainties above), the next step is to decide what land cover units will be used in the reconstruction. For these case studies, 50 × 50 m pixels were used and land cover was specified as communities (see section Model Uncertainties above). Using communities as land cover classes does enable us to include the pollen signal from “indicator taxa” such as *P. lanceolata* in the analysis, but the problem of defining past community composition is particularly apparent in the Orkney case study. A single disturbed ground community was used, including low pollen production cereals, some bare ground and some high-pollen-producing weeds associated with disturbance (*Artemisia*-type, *P. lanceolata* and *Rumex*-type). Future work should clearly use at least two

disturbance communities, with and without cereals present, but the run time available in the project reported here did not allow us to start again once this became apparent—adding an extra community to the analysis increases the run time for analysis almost two-fold. All the taxa involved are present at low abundance in the target pollen signal, so the results of re-analysis are not expected to change the interpretations presented here.

Over-complex models are not better models, and a balance between multiplying assumptions and achieving outputs of use to the intended research community needs to be struck. One approach for future testing may be to reduce the number of taxa to a very small group, where each taxon is representative of and largely confined to a distinctive land cover element, as shown by Nielsen and Odgaard's (2005) study of historic land cover in Denmark using four taxa, Poaceae (pasture), *Calluna* (heath), tree pollen (a composite taxon; woodland), and Cerealia (arable cultivation).

A strength of the MSA over other reconstruction approaches is that it is possible to overtly include local wetland vegetation in the reconstructions. Identifying the pollen rain component sourced from “local” or “extra-local” vegetation (*sensu* Janssen, 1984) is a common concern in pollen record interpretation. One approach is to select sites where such vegetation can easily be identified and excluded (e.g., lakes—obligate aquatic plant pollen can be excluded—or ombrotrophic *Sphagnum* mires with minimal vascular plant vegetation). However, nature rarely obliges in the availability and distribution of such sites, and especially in lowland areas wetlands of many types are the main or only sources of pollen data. On-site vegetation contributes to the pollen signal in multiple ways (Bunting, 2008), which can obscure the signal of the upland landscape. Some scientists, especially for studies where data from multiple paleoecological proxies are available, take considerable pains to first reconstruct the wetland vegetation and then consider the surrounding dry land, whereas in other cases and in most multi-site synthesis studies local vegetation contributions are treated as “noise” or otherwise ignored. Interest in the variety and complexity of sedimentary systems which preserve pollen records was one of the incentives to develop the MSA. In the LRA, wetland vegetation must be removed or ignored (by either removing possible wetland taxa such as Cyperaceae, or assuming that the contribution of on-site taxa to the pollen record is negligible) which can restrict the selection of sites to those where the assumption of negligible input is most reasonable, e.g., lakes or pure *Sphagnum* mires. For the many landscapes where lake sites or ombrotrophic mires which are effectively pure *Sphagnum* lawns are not available to act as sources of pollen records, this ability to not just consider but address the potential concerns is a clear strength of the MSA over other reconstruction methods.

Both case studies demonstrate how the MSA can overtly address the issues of local site vegetation. Including variation in the size and type of on-site vegetation was an important part of the scoping stage for both case studies. In the Somerset case, pre-existing data about site stratigraphy which might inform interpretation was not easily available, so a strategy of very wide scoping of options was used. This allowed us to identify a single range of conditions which led to the lowest best fit

scores, which we assumed for efficiency represented a reasonable reconstruction of the local wetland conditions, and then used in further analysis. In the Orkney case, determining local vegetation was more straightforward since sites were discrete entities and a combination of geomorphological limits with published stratigraphic data and site reconstructions allowed us to assign broad community types to each wetland. In some cases multiple good-fit sets of conditions were identified during scoping. **Figure 7** shows an example from Somerset, where site WLT has two possible wetland configurations producing good fits, a moderate-sized mire with no alder carr fringe in a landscape with levels of clearing between 0 and 40% or a mire of variable size with an alder carr fringe 500–550 m wide in a landscape with about 20% clearings during the scoping process. For expediency, the set with the overall lowest fit score was used in further analysis, but a fuller study would either explore other data to test which was the more plausible alternative (*sensu* Caseldine et al., 2008) or run the further analyses with both options to avoid cutting off possible solutions. Hydroseres are spatially as well as temporally variable and the complexity of surface arrangement of palynologically distinct wetland communities in extensive peatlands can be considerable (Waller et al., 2005, 2017). Reconstructing this complexity in the past is challenging, requiring extensive coring work for robust results, but is increasingly included in new studies of hydroserally complex sedimentary sequences.

Future Developments

Four main strengths of the approach are identified. First, the MSA allows the analyst to overtly incorporate wetland vegetation (discussed in Specification of Land Cover Units above) and changing wetland conditions into the reconstruction, rather than avoiding or ignoring the potential complications. Secondly, the MSA is suitable for reconstruction of land cover where the assumption of uniform vegetation within the “region” (e.g., within 50–100 km radius of the studied sites), required by the LRA for reconstruction of vegetation detail at a 1–2 km level from small pollen sites, is clearly problematic. This opens up many more landscapes to possible reconstruction, including much of the UK. Thirdly, the MSA package makes landscape specific “thought experiment” type approaches which incorporate known landscape constraints relatively easy to carry out (e.g., Caseldine et al., 2007). Finally, the MSA also encourages the analyst, and potential end users of paleoecological data who may not have the detailed understanding of the complexities, limitations, and uncertainties of analysis outputs, to be more aware of equifinality. Paleoecological data offer a “muddy time machine,” an invaluable insight into past ecologies and landscapes, but the view out of the window is obscured and fragmentary. Identification of a range of possible reconstructions moderates the tendency to tell a good story as if it is the only possible reconstruction of a landscape, and creates natural hypotheses for future testing, thus contributing to the ongoing challenge of improving the level of scientific reasoning in paleoecological circles.

There remains considerable challenge in communicating uncertainty in a visual way. One option might be to add together

all the grids satisfying the fit threshold and create maps of the probability of a land cover type being present at a given pixel across all the grids. We expect that greater confidence in reconstruction would be found close to sites, within the zone which is sensitively recorded by the pollen assemblages, and lesser confidence with increasing distance from the sites. It is important that results are communicated to end users in ways which emphasise that these are hypotheses, and the use of the models to identify ranges of probable past land cover characters (e.g., Gillson and Duffin, 2007), rather than a single “correct” reconstruction.

Direct outputs from LandPolFlow are in the form of a.csv file of simulated pollen loadings, model parameters, and fit scores, and in the form of grids showing mapped land cover. In this paper we have presented sample grids and summaries based on model parameters which produced the best fit scores, but there are multiple other ways of presenting the output, and developing strategies for effective communication of results is an important area of model development for future attention.

Maps are visually appealing and striking, and the ease of choosing a single best-fit map as the reconstruction makes it a tempting solution, but one which doesn’t make full use of the information provided by the MSA. For these case studies we mostly worked with a small number of scenarios with the lowest scores, largely due to resource restrictions, but for future projects analysis should logically take into account all scenarios with fits below a pre-defined threshold. That will require the analyst to set a threshold (using e.g., consideration of the sampling effects within count data, or criteria derived from modern studies of samples from different communities such as Lytle and Wahl, 2005). In some runs a large number of scenarios may produce fits below the threshold, but this diversity could be reduced by using model parameters to identify which families (groups of scenarios with the same environmental constraints repeated so that probabilistic elements such as patch placement vary), and how many members of each family, are present. Each family may represent an equifinal reconstruction option.

A method of further choosing amongst possible reconstructions is to consider their plausibility. Caseldine et al. (2008) argued that to be considered a reconstruction, a scenario should not just be capable of producing a simulated pollen signal which is statistically similar to the actual data, but should also be capable of being linked temporally with landcover arrangements (maps) which pre-date and post-date it, through reasonable ecological processes and patterns of change. Within this study, an example of a reconstruction which was a good fit but not plausible was obtained for the Orkney 2800–2600 cal BC timeslice, when several of the best-fit grids were from scenario families with 10% of the area above 60 m asl supporting heathland. Reconstructions for timeslices both before and after did not include any options with heathland present, and development of heathlands in the uplands is usually a progressive process. Therefore we deemed the reconstruction implausible, and used the land cover grid with the best fit and no heathland for the reconstruction sequence. In this case, we believe that the implausible scenario was reflecting variation in the on-site vegetation in one or more of the sites included for that timeslice.

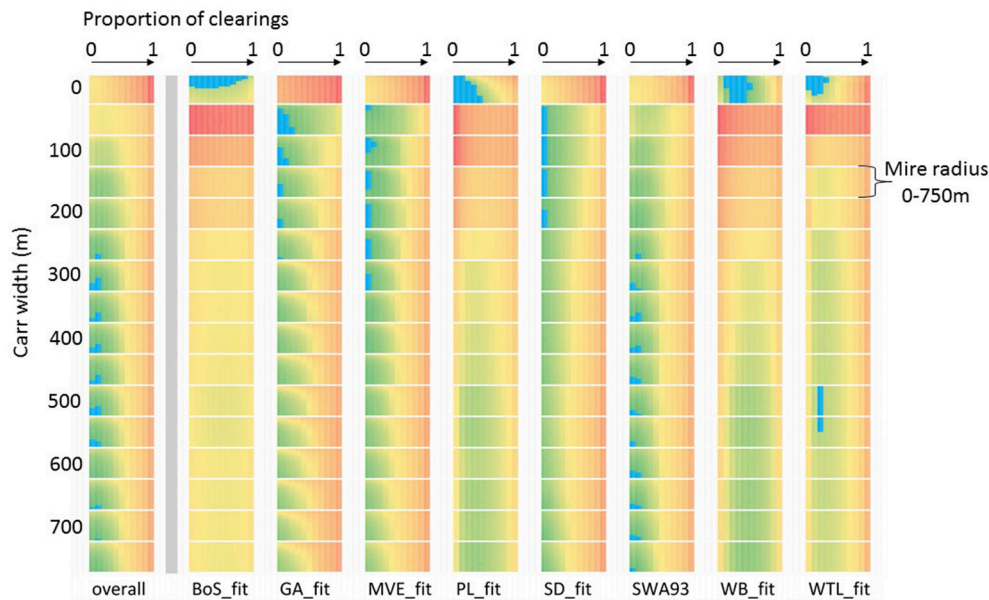


FIGURE 7 | Example of equifinality in Multiple Scenario Approach outputs: Somerset case study scoping run for the 4400–4200 cal BC timeslice (not presented in **Figure 5**). Comparison of fit scores summed across the landscape (overall) and for eight individual sites (see Farrell et al., unpublished for details) for scenarios where each coring point is modelled as an area of mire surrounded by an alder carr belt, and mire size, carr width and proportion of clearings in the wider landscape are all varied. Colour shows relative fit score value for each dataset (single column, 2,816 scores), where green is low and red is high. The lowest 2% of values (identifying the scenarios which produce simulated pollen assemblages most similar to the actual pollen recorded) are highlighted with blue overlay.

In the case studies presented here, each time slice was treated individually, in order that a problem in one time slice would not be propagated into others, and could more easily be detected as an anomaly. An alternative way to use the MSA is to work on timeslices sequentially, beginning each timeslice with one or more grids from the best-fit family for the previous timeslice, and modifying the vegetation until suitable reconstructions are identified. This would ensure a plausible sequence, but would need to be carefully planned and carried out to avoid missing out on equifinal solutions along the way.

As an alternative to maps, results can be presented quantitatively, as landscape metrics. Examples here showed metrics taken from the output file, based on the model parameters of the best fit scenarios (e.g., the mean and standard deviation of the probability that a pixel in a defined landscape setting could be occupied by oak-pine woodland), which are not the same as land cover metrics (due to the random nature of land cover map creation). The trends they show can be interpreted with confidence, but the absolute values will not be accurate. Values of area of landscape occupied by a given community can be extracted directly from the land cover grids, and are a more attractive metric for end users, but at present are also far more labor-intensive to obtain. Improving the extraction of information from grids is a development priority for the MSA.

The MSA and the Palynological Workflow

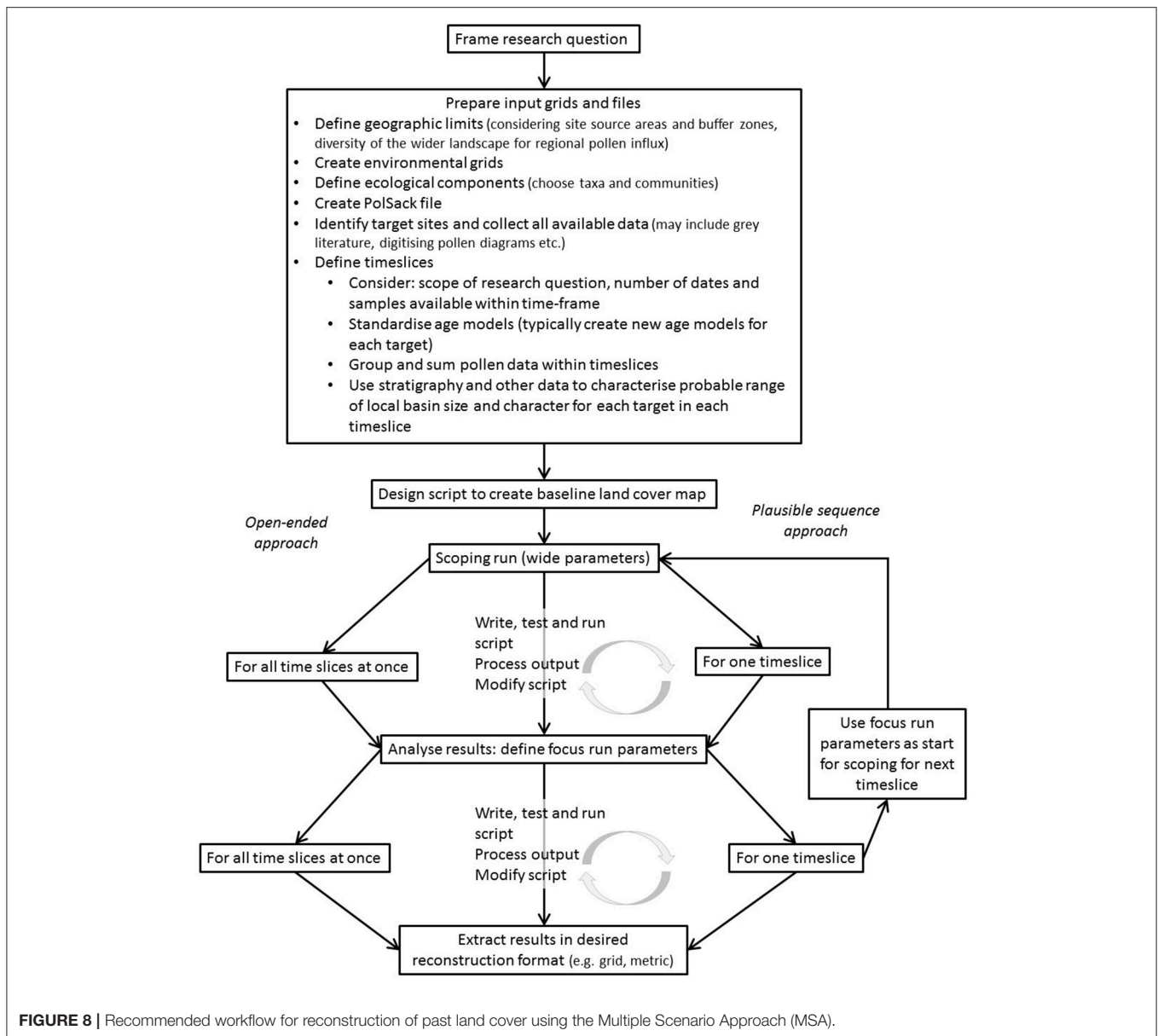
Whilst the LandPolFlow package is complete and documented, the use of the MSA is in its infancy and not all package features are considered here. A suggested workflow for future studies

is shown in **Figure 8** based on our experience with these case studies, and **Figure 9** shows how the methods could be built into palynological studies more generally. For these case studies we used R to speed up the manipulation of output files, and see considerable potential to use automation to increase the capacity of the method. More detailed validation of the MSA using modern pollen and vegetation datasets, currently under way, will also help understand its capacity and limitations better, and improve its deployment.

As more sets of pollen dispersal and deposition parameters are published for different taxa and geographic areas, and as increasing processor speed reduces the time and computational resource needed to run LandPolFlow, we believe that modelling approaches should become a routine part of the pollen analysts' tool kit, as zonation using a constrained clustering approach such as CONISS rather than merely visual inspection has become routine since its introduction (Grimm, 1987).

CONCLUSION

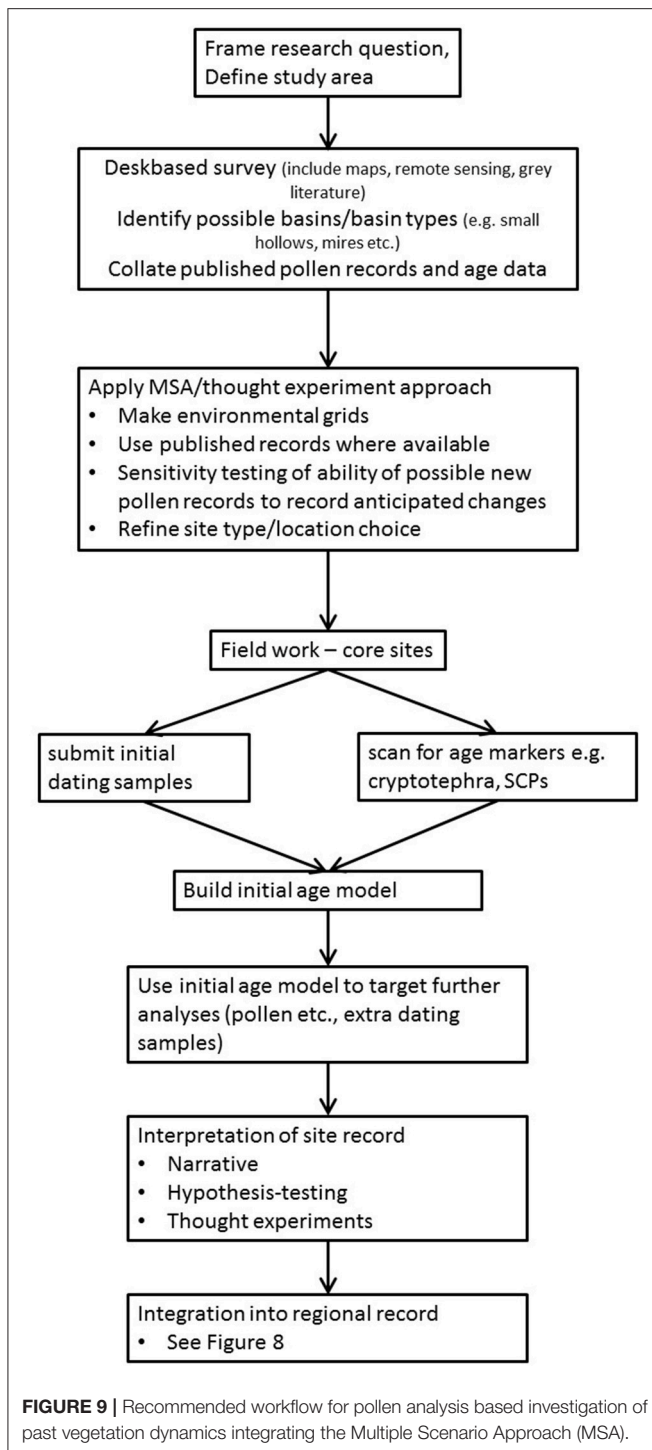
Modelling approaches such as the MSA offer a clear route to getting more information from existing published pollen records, which represent a huge investment of time and money. This paper presents two case studies of the MSA in use at a landscape level, filling the gap between the regional land cover reconstructions offered by REVEALS (Sugita, 2007a; 100 × 100 km squares in e.g., Trondman et al., 2015) and the single-site reconstruction of distance-weighted plant abundance made possible by LOVE (Sugita,



2007b; distance of c. 500 m–2.5 km depending on site-specific Relevant Source Area of Pollen), and generating reconstructions in forms which are both transparent and useful for a wide range of end users, whether paleoecologists, environmental archaeologists, conservation biologists, neoecologists, or science communicators. The land cover hypotheses produced by the MSA can serve as the starting point for more structured, hypothesis-testing uses of paleoecology and environmental archaeology methods, including not only pollen analysis but also other techniques recording different aspects of land cover.

Our reconstructions of Neolithisation in both a heavily wooded and a largely treeless landscape show that, although the extent of land cover modification was limited and did not alter the essential character of each landscape, it was persistent. In Orkney, the timing of land cover change occurred at the

same time as the start of settlement use as determined from an independent set of radiocarbon dates from archaeological sites, strongly supporting our interpretation of land cover change as a proxy for human activity in the wider landscape in the Somerset case study where archaeological evidence for Neolithic settlement is minimal. Increased levels of clearance or disturbance in both locations persisted even when archaeological evidence implied a reduction in intensity of landscape use and occupation, suggesting a significant transition in landscape character and ecology occurred with Neolithisation. Modelling, and its ability to support targeted selection of sites for pollen analysis in specific environmental contexts and to address specific archaeological questions, clearly has a useful role to play in improving our understanding of landscape impacts and development, and in fostering better collaboration between



paleoecologists and other disciplines concerned with past landscapes.

We argue that the MSA deserves a place within the pollen analyst's standard tool kit (**Figure 9**). There is still work to do in improving the use of the approach and the communication

of outputs, and as with all models, outputs are dependent on assumptions and calibration and therefore “wrong” in an absolute sense. The case studies presented here show how LandPolFlow makes environmentally informed reconstruction of land cover accessible to pollen analysts, and therefore has the capacity to improve research design, prompt more overt, and thoughtful exploration of assumptions and site taphonomy, and improve communication between subject specialists and with wider stake holders.

AUTHOR CONTRIBUTIONS

MB and MF: worked together on designing model strategy, iterative analysis of output of each run, interpretation of findings, and led the authoring of paper. MF: prepared input GIS grids, collated pollen targets, and carried out most model runs. PM: collated datasets and modelled radiocarbon chronologies for allocation of samples to timeslices with AB. PM, AB, and AW: selected sites in light of archaeological relevance and contributed to hypothesis development and output interpretation and representation.

FUNDING

This study was supported as part of *The Times of Their Lives* project (www.totl.eu), funded by the European Research Council (Advanced Investigator Grant 295412) and led by AW and AB.

ACKNOWLEDGMENTS

First and most significantly, we wish to acknowledge the work of Richard Middleton. Now retired and busy with other projects (e.g., as Vice County Recorder of Botany for VC 61), he did not choose to be a co-author of this manuscript, but without his talent, enthusiasm, and willingness to explore unfamiliar intellectual territory this paper, and the wider MSA project, would never have come to fruition. We next acknowledge the many researchers who contributed pollen count data to the Somerset case study. We also wish to acknowledge the many members of the PolLandCal and LandClim networks, and of the PAGES Landcover 6k Working Group, for fruitful discussion of land cover reconstruction. We consider this work to be in part a contribution to the work of the PAGES Landcover 6k Working Group (<http://www.pages-igbp.org/ini/wg/landcover6k/intro>), included as part of the Past Global Changes (PAGES) project, which in turn received support from the US National Science Foundation and the Swiss Academy of Sciences. We thank two reviewers for comments on an earlier version of the manuscript.

SUPPLEMENTARY MATERIAL

The Supplementary Material for this article can be found online at: <https://www.frontiersin.org/articles/10.3389/fevo.2018.00036/full#supplementary-material>

REFERENCES

- Bates, M. R., Nayling, N., Bates, R., Dawson, S., Huws, D., and Wickham-Jones, C. (2013). A multi-disciplinary approach to the archaeological investigation of a bedrock-dominated shallow marine landscape: an example from the Bay of Firth, Orkney, U. K. *Int. J. Nautical Archaeol.* 42, 24–43. doi: 10.1111/j.1095-9270.2012.00360.x
- Bayliss, A., Marshall, P., Richards, C., and Whittle, A. (2017). Islands of history: the late neolithic timescape of Orkney. *Antiquity* 91, 1171–1188. doi: 10.15184/aqy.2017.140
- Beckett, S. C., and Hibbert, F. A. (1978). The influence of man on the vegetation of the Somerset Levels - a summary. *Somerset Levels Pap.* 4, 86–89.
- Bennett K. D. (2007). *Catalogue of Pollen Types*. Available online at: <http://chronon.qub.ac.uk/pollen/pc-intro.html#introduction> (Accessed November 17, 2017).
- Bishop, R. R., Church, M. J., and Rowley-Conwy, P. A. (2015). Firewood, food and human niche construction: the potential role of Mesolithic hunter-gatherers in actively structuring Scotland's woodlands. *Quat. Sci. Rev.* 108, 51–75. doi: 10.1016/j.quascirev.2014.11.004
- Brown, A. (1997). Clearances and clearings: deforestation in mesolithic/neolithic Britain. *Oxf. J. Archaeol.* 16, 133–146. doi: 10.1111/1468-0092.00030
- Bunting, M. J. (2008). Pollen in wetlands: using simulations of pollen dispersal and deposition to better interpret the pollen signal. *Biodivers. Conserv.* 17, 2079–2096. doi: 10.1007/s10531-007-9219-x
- Bunting, M. J., and Farrell, M. (2017). Seeing the wood for the trees: recent advances in the reconstruction of woodland in archaeological landscapes using pollen data. *Environ. Archaeol.* doi: 10.1080/14614103.2017.1377405. [Epub ahead of print].
- Bunting, M. J., Farrell, M., Broström, A., Hjelle, K. L., Mazier, F., Middleton, R., et al. (2013). Palynological perspectives on vegetation survey: a critical step for model-based reconstruction of quaternary land cover. *Quat. Sci. Rev.* 82, 41–55. doi: 10.1016/j.quascirev.2013.10.006
- Bunting, M. J., Gaillard, M.-J., Sugita, S., Middleton, R., and Broström, A. (2004). Vegetation structure and pollen source area. *Holocene* 14, 651–660. doi: 10.1191/0959683604hl744rp
- Bunting, M. J., and Middleton, D. (2005). Modelling pollen dispersal and deposition using HUMPOL software, including simulating windroses and irregular lakes. *Rev. Palaeobot. Palynol.* 134, 185–196. doi: 10.1016/j.revpalbo.2004.12.009
- Bunting, M. J., and Middleton, R. (2009). Equifinality and uncertainty in the interpretation of pollen data: the multiple scenario approach to reconstruction of past vegetation mosaics. *Holocene* 19, 799–803. doi: 10.1177/0959683609105304
- Card, N., Mainland, I., Timpany, S., Towers, R., Batt, C., Bronk Ramsey, C., et al. (2017). To cut a long story short: formal chronological modelling for the Late Neolithic site of Ness of Brodgar, Orkney. *Eur. J. Archaeol.* doi: 10.1017/eea.2016.29. [Epub ahead of print].
- Caseldine, C., and Fyfe, R. (2006). A modelling approach to locating and characterising elm decline/landnam landscapes. *Quat. Sci. Rev.* 25, 632–644. doi: 10.1016/j.quascirev.2005.07.015
- Caseldine, C., Fyfe, R., and Hjelle, K. (2008). Pollen modelling, palaeoecology and archaeology: virtualisation and/or visualisation of the past? *Veg. Hist. Archaeobot.* 17, 543–549. doi: 10.1007/s00334-007-0093-y
- Caseldine, C., Fyfe, R., Langdon, C., and Thompson, G. (2007). Simulating the nature of vegetation communities at the opening of the Neolithic on Achill Island, Co. Mayo, Ireland — the potential role of models of pollen dispersal and deposition. *Rev. Palaeobot. Palynol.* 144, 135–144. doi: 10.1016/j.revpalbo.2006.07.002
- Clarke, D. V., Sheridan, A., Shepherd, A. N., Sharples, N. M., Armour-Chelu, M. J., Hamlet, L., et al. (2018). “The end of the world, or just ‘Goodbye to all that’? Contextualising the late 3rd-millennium cal BC deer heap at Links of Noltland, Westray, Orkney,” in *Proceedings of the Society of Antiquaries of Scotland*, Vol. 146, 57–89. doi: 10.9750/PSAS.146.1226
- Coles, B., and Coles, J. (1986). *Sweet Track to Glastonbury. The Somerset Levels in Prehistory*. New York, NY: Thames and Hudson.
- Coles, B., and Coles, J. (1992). Passages of time. *Arch. Mitteil. Nordwestdeutschland* 15, 29–44.
- Coles, J. M. (1989). The Somerset Levels Project 1973–1989. *Somerset Levels Papers* 15, 5–33.
- Davidson, D. A., and Jones, R. L. (1985). “The environment of Orkney,” in *The Prehistory of Orkney*, ed C. Renfrew (Edinburgh: Edinburgh University Press), 10–35.
- Dawson, S., and Wickham-Jones, C. R. (2007). Sea-level change and the prehistory of Orkney. *Antiquity* 81:312.
- Downes, J. (2005). *Cremation Practice in Bronze Age Orkney*. Unpublished Ph.D. thesis, University of Sheffield.
- Edwards, K. J., Fyfe, R. M., and Jackson, S. T. (2017). The first 100 years of pollen analysis. *Nature Plants* 3, 1–4. doi:10.1038/nplants.2017.1
- Eklöf, M., Broström, A., Gaillard, M.-J., and Pilesjö, P. (2004). Openland3: a computer program to estimate plant abundance around pollen sampling sites from vegetation maps: a necessary step for calculation of pollen productivity estimates. *Rev. Palaeobot. Palynol.* 132, 67–77. doi: 10.1016/j.revpalbo.2004.04.005
- Farrell, M. (2009). *The Environmental Context of Later Prehistoric Human Activity in Orkney, Scotland*. Unpublished Ph.D. thesis, University of Hull.
- Farrell, M. (2015). Later prehistoric vegetation dynamics and Bronze Age agriculture at Hobbister, Orkney, Scotland. *Veg. Hist. Archaeobot.* 24, 467–486. doi: 10.1007/s00334-014-0507-6
- Farrell, M., Bunting, M. J., Lee, D. H. J., and Thomas, A. (2014). Neolithic settlement at the woodland's edge: palynological data and timber architecture in Orkney, Scotland. *J. Archaeol. Sci.* 51, 225–236. doi: 10.1016/j.jas.2012.05.042
- Gaillard, M.-J., Sugita, S., Bunting, M. J., Middleton, R., Broström, A., Caseldine, C., et al. (2008). The use of modelling and simulation approach in reconstructing past landscapes from fossil pollen data: a review and results from the pollandcal network. *Veg. Hist. Archaeobot.* 17, 419–443. doi: 10.1007/s00334-008-0169-3
- Gaillard, M.-J., Sugita, S., Mazier, F., Trondman, A.-K., Broström, A., Hickler, T., et al. (2010). Holocene land-cover reconstructions for studies on land cover-climate feedbacks. *Clim. Past* 6, 483–499. doi: 10.5194/cp-6-483-2010
- Gillson, L., and Duffin, K. I. (2007). Thresholds of potential concern as benchmarks in the management of African savannahs. *Philos. Trans. R. Soc. B* 362, 309–319. doi: 10.1098/rstb.2006.1988
- Gregory, P. H. (1973). *Microbiology of the Atmosphere, 2nd Edn.* Aylesbury: Leonard Hill.
- Griffiths, S. (2016). “Beside the ocean of time: a chronology of neolithic burial monuments and houses in Orkney,” in *The Development of Neolithic house Societies in Orkney*, eds C. Richards and R. Jones (Oxford: Windgather Press), 254–302.
- Grimm, E. C. (1987). CONISS: a FORTRAN 77 program for stratigraphically constrained cluster analysis by the method of incremental sum of squares. *Comput. Geosci.* 13, 13–35. doi: 10.1016/0098-3004(87)90022-7
- Hellman, S., Bunting, M. J., and Gaillard, M.-J. (2009a). Relevant Source Area of Pollen in patchy cultural landscapes and signals of anthropogenic landscape disturbance in the pollen record: a simulation approach. *Rev. Palaeobot. Palynol.* 153, 245–258. doi: 10.1016/j.revpalbo.2008.08.006
- Hellman, S., Gaillard, M.-J., Broström, A., and Sugita, S. (2008). The REVEALS model, a new tool to estimate past regional plant abundance from pollen data in large lakes: validation in southern Sweden. *J. Quat. Sci.* 23, 21–42. doi: 10.1002/jqs.1126
- Hellman, S., Gaillard, M.-J., Bunting, J. M., and Mazier, F. (2009b). Estimating the relevant source area of pollen in the past cultural landscapes of southern Sweden — a forward modelling approach. *Rev. Palaeobot. Palynol.* 153, 259–271. doi: 10.1016/j.revpalbo.2008.08.008
- Hellman, S. V., Gaillard, M.-J., Broström, A., and Sugita, S. (2008). Effects of the sampling design and selection of parameter values on pollen-based quantitative reconstructions of regional vegetation: a case study in southern Sweden using the REVEALS model. *Veg. Hist. Archaeobot.* 17, 445–459. doi: 10.1007/s00334-008-0149-7
- Innes, J. B., Blackford, J. J., and Rowley-Conwy, P. A. (2013). Late Mesolithic and early Neolithic forest disturbance: a high resolution palaeoecological test of human impact hypotheses. *Quat. Sci. Rev.* 77, 80–100. doi: 10.1016/j.quascirev.2013.07.012
- Innes, J., Blackford, J., and Simmons, I. (2010). Woodland disturbance and possible land-use regimes during the Late Mesolithic in the English uplands: pollen, charcoal and non-pollen palynomorph evidence from Bluwath Beck, North York Moors, UK. *Veg. Hist. Archaeobot.* 19, 439–452. doi: 10.1007/s00334-010-0266-y

- Jacomet, S., Ebersbach, R., Akeret, Ö., Antolí, F., Baum, T., Bogaard, A., et al. (2016). On-site data casts doubt on the hypothesis of shifting cultivation in the late Neolithic (c. 4300–2400 cal. BC): landscape management as an alternative paradigm. *Holocene* 26, 1858–1874. doi: 10.1177/0959683616645941
- Janssen, C. R. (1984). Modern pollen assemblages and vegetation in the Myrtle Lake peatland. *Minn. Ecol. Monogr.* 54, 213–252. doi: 10.2307/1942662
- Kidson, C., and Heyworth, A. (1976). The Quaternary deposits of the Somerset levels. *Q. J. Eng. Geol.* 9, 217–235. doi: 10.1144/GSL.QJEG.1976.009.03.05
- Lamb, R. G. (1989). *The Archaeological Sites and Monuments of Scotland 29: Hoy and Waas*. Edinburgh: RCAHMS.
- Long, A. J., Dix, J. K., Kirby, R., Lloyd-Jones, D., Roberts, D. H., Croudace, I. W., et al. (2002). *The Holocene and Recent Evolution of Bridgwater Bay and the Somerset Levels*. Unpublished Report, University of Durham.
- Lytle, D. E., and Wahl, E. R. (2005). Palaeoenvironmental reconstructions using the modern analogue technique: the effects of sample size and decision rules. *Holocene* 15, 554–566. doi: 10.1191/0959683605hl830rp
- Mainland, I., Card, N., Saunders, M. K., Webster, C., Isaksen, L., Downes, J., et al. (2014). ‘Smartfauna’: a microscale GIS-based multi-dimensional approach to faunal deposition at the Ness of Brodgar, Orkney. *J. Archaeol. Sci.* 41, 868–878. doi: 10.1016/j.jas.2013.10.019
- Mazier, F., Gaillard, M.-J., Kuneš, P., Sugita, S., Trondman, A.-K., and Broström, A. (2012). Testing the effect of site selection and parameter setting on REVEALS-model estimates of plant abundance using the Czech quaternary palynological database. *Rev. Palaeobot. Palynol.* 187, 38–49. doi: 10.1016/j.revpalbo.2012.07.017
- Mellars, P., and Dark, P. (1998). *Star Carr in Context*. Cambridge: McDonald Institute for Archaeological Research.
- Meller, H., Arz, H. E., Jung, R., and Risch, R. (2015). *2200 BC – A Climatic Breakdown as a Cause for the Collapse of the Old World?* Halle: Landesamt für Denkmalpflege und Archäologie Sachsen-Anhalt, Landesmuseum für Vorgeschichte.
- Middleton, R., and Bunting, M. J. (2004). Mosaic v1.1: landscape scenario creation software for simulation of pollen dispersal and deposition. *Rev. Palaeobot. Palynol.* 132, 61–66. doi: 10.1016/j.revpalbo.2004.04.004
- Moore, P. D., Collinson, M., and Webb, J. A. (1991). *Pollen Analysis, 2nd Edn*. Oxford: Blackwell Scientific.
- Nielsen, A. B., and Odgaard, B. V. (2005). Reconstructing land cover from pollen assemblages from small lakes in Denmark. *Rev. Palaeobot. Palynol.* 133, 1–21. doi: 10.1016/j.revpalbo.2004.08.002
- Overpeck, J. T., Webb, T. III, and Prentice, I. C. (1985). Quantitative interpretation of fossil pollen spectra: dissimilarity coefficients and the method of modern analogs. *Q. Res.* 23, 87–108. doi: 10.1016/0033-5894(85)90074-2
- PAGES (2017). *LandCover6k*. Available online at: <http://www.pages-igbp.org/init/wg/landcover6k/intro> (Accessed November 17, 2017).
- Pirzamanbein, B., Lindström, J., Poska, A., Sugita, S., Trondman, A.-K., Fyfe, R., et al. (2014). Creating spatially continuous maps of past land cover from point estimates: a new statistical approach applied to pollen data. *Ecol. Complex.* 20, 127–141. doi: 10.1016/j.ecocom.2014.09.005
- Poska, A., Meltsov, V., Sugita, S., and Vassiljev, J. (2011). Relative pollen productivity estimates of major anemophilous taxa and relevant source area of pollen in a cultural landscape of the hemi-boreal forest zone (Estonia). *Rev. Palaeobot. Palynol.* 167, 30–39. doi: 10.1016/j.revpalbo.2011.07.001
- Prentice, C., Guiot, J., Huntley, B., Jolly, D., and Cheddadi, R. (1996). Reconstructing biomes from palaeoecological data: a general method and its application to European Pollen data at 0 and 6 ka. *Clim. Dyn.* 12, 185–194. doi: 10.1007/BF00211617
- Rösch, M., Biester, H., Bogenrieder, A., Eckmeier, E., Ehrmann, O., Gerlach, R., et al. (2017). Late neolithic agriculture in temperate Europe—a long-term experimental approach. *Land* 6, 11–28. doi: 10.3390/land6010011
- Ryan, P. A., and Blackford, J. J. (2010). Late Mesolithic environmental change at Black Heath, south Pennines, UK: a test of Mesolithic woodland management models using pollen, charcoal and non-pollen palynomorph data. *Veg. Hist. Archaeobot.* 19, 545–558. doi: 10.1007/s00334-010-0263-1
- Schier, W. (2009). Extensiver Brandfeldbau und die Ausbreitung der neolithischen Wirtschaftsweise in Mitteleuropa und Südkandinavien am Ende der 5. Jt. v. Chr. *Prähistor. Z.* 84, 15–43. doi: 10.1515/pz.2009.002
- Sharples, N. (1992). “Aspects of regionalisation in the Scottish Neolithic,” in *Vessels for the Ancestors: Essays on the Neolithic of Britain and Ireland in Honour of Audrey Henshall*, eds N. Sharples and J. A. Sheridan (Edinburgh: Edinburgh University Press), 322–331.
- Stevens, C. J., and Fuller, D. Q. (2012). Did neolithic farming fail? The case for a bronze age agricultural revolution in the British Isles. *Antiquity* 86, 707–722. doi: 10.1017/S0003598X00047864
- Sturt, F. D., Garrow, D., and Bardley, S. (2013). New models of North West European Holocene palaeogeography and inundation. *J. Archaeol. Sci.* 40, 3963–3976. doi: 10.1016/j.jas.2013.05.023
- Sturt, F., Standen, T., Grant, M., and Dix, J. (2016). *Determining Potential: Onshore/Offshore Prehistory Project 6918*. Unpublished Report, University of Southampton.
- Sugita, S. (2007a). Theory of quantitative reconstruction of vegetation I: pollen from large sites REVEALS regional vegetation composition. *Holocene* 17, 229–241. doi: 10.1177/0959683607075837
- Sugita, S. (2007b). Theory of quantitative reconstruction of vegetation II: all you need is LOVE. *Holocene* 17, 243–257. doi: 10.1177/0959683607075838
- Trondman, A. K., Gaillard, M. J., Mazier, F., Sugita, S., Fyfe, R., Nielsen, A. B., et al. (2015). Pollen-based quantitative reconstructions of Holocene regional vegetation cover (plant-functional types and land-cover types) in Europe suitable for climate modelling. *Glob. Chang. Biol.* 21, 676–697. doi: 10.1111/gcb.12737
- Von Post, L. (1918). “Skogsträdpollen i sydsvenska torvmosselagerföljder,” in *Forhandlingar ved de Skandinaviske Naturforskeres 16. Møte i Kristiania den 10–15. Juli 1916* (Kristiania: Skandinaviska Naturforskaremöten), 432–465.
- Waller, M., Carvalho, F., Grant, M. J., Bunting, M. J., and Brown, K. (2017). Disentangling the pollen signal from fen systems: modern and holocene studies from southern and eastern England. *Rev. Palaeobot. Palynol.* 238, 15–33. doi: 10.1016/j.revpalbo.2016.11.007
- Waller, M. P., Binney, H. A., Bunting, M. J., and Armitage, R. A. (2005). The interpretation of fen carr pollen diagrams: pollen-vegetation relationships within the fen carr. *Rev. Palaeobot. Palynol.* 133, 179–202. doi: 10.1016/j.revpalbo.2004.10.001
- Whittle, A., Healy, F., and Bayliss, A. (2011). *Gathering Time: Dating the Early Neolithic Enclosures of Southern Britain and Ireland*. Oxford: Oxbow.
- Wickham-Jones, C. R., Bates, C. R., Dawson, S., Dawson, A. G., and Bates, M. R. (2017). “The changing landscape of prehistoric Orkney,” in *Early Settlement in North-Western Europe: Climate, Human Ecology and Subsistence*, eds P. Persson, F. Riede, B. Skar, H. M. Breivik, and L. Jonsson (Sheffield: Equinox), 393–413.
- Wickham-Jones, C. R., Bates, M., Bates, C. R., Dawson, S., and Kavanagh, E. (2016). People and landscape at the heart of Neolithic Orkney. *Archaeol. Rev. Camb.* 31, 26–47.

Conflict of Interest Statement: The authors declare that the research was conducted in the absence of any commercial or financial relationships that could be construed as a potential conflict of interest.

Copyright © 2018 Bunting, Farrell, Bayliss, Marshall and Whittle. This is an open-access article distributed under the terms of the Creative Commons Attribution License (CC BY). The use, distribution or reproduction in other forums is permitted, provided the original author(s) and the copyright owner are credited and that the original publication in this journal is cited, in accordance with accepted academic practice. No use, distribution or reproduction is permitted which does not comply with these terms.



Quantitative Palynology Informing Conservation Ecology in the Bohemian/Bavarian Forests of Central Europe

Vachel A. Carter^{1*}, Richard C. Chiverrell², Jennifer L. Clear^{3,4}, Niina Kuosmanen⁴, Alice Moravcová¹, Miroslav Svoboda⁴, Helena Svobodová-Svitavská⁵, Jacqueline F. N. van Leeuwen⁶, Willem O. van der Knaap⁶ and Petr Kuneš¹

¹ Department of Botany, Faculty of Science, Charles University, Prague, Czechia, ² Department of Geography and Planning, University of Liverpool, Liverpool, United Kingdom, ³ Department of Geography and Environmental Science, Liverpool Hope University, Liverpool, United Kingdom, ⁴ Department of Forest Ecology, Faculty of Forestry and Wood Sciences, Czech University of Life Sciences, Prague, Czechia, ⁵ Institute of Botany, v.v.i., Czech Academy of Sciences, Průhonice, Czechia, ⁶ Institute of Plant Sciences and Oeschger Centre for Climate Change Research, University of Bern, Bern, Switzerland

OPEN ACCESS

Edited by:

Jesse L. Morris,
University of Utah, United States

Reviewed by:

Heikki Tapani Seppä,
University of Helsinki, Finland
Ranae Dietzel,
Iowa State University, United States

*Correspondence:

Vachel A. Carter
vachel.carter@gmail.com

Specialty section:

This article was submitted to
Agroecology and Land Use Systems,
a section of the journal
Frontiers in Plant Science

Received: 28 July 2017

Accepted: 27 December 2017

Published: 17 January 2018

Citation:

Carter VA, Chiverrell RC, Clear JL, Kuosmanen N, Moravcová A, Svoboda M, Svobodová-Svitavská H, van Leeuwen JFN, van der Knaap WO and Kuneš P (2018) Quantitative Palynology Informing Conservation Ecology in the Bohemian/Bavarian Forests of Central Europe. *Front. Plant Sci.* 8:2268. doi: 10.3389/fpls.2017.02268

In 1927, the first pollen diagram was published from the Bohemian/Bavarian Forest region of Central Europe, providing one of the first qualitative views of the long-term vegetation development in the region. Since then significant methodological advances in quantitative approaches such as pollen influx and pollen-based vegetation models (e.g., Landscape Reconstruction Algorithm, LRA) have contributed to enhance our understanding of temporal and spatial ecology. These types of quantitative reconstructions are fundamental for conservation and restoration ecology because they provide long-term perspectives on ecosystem functioning. In the Bohemian/Bavarian Forests, forest managers have a goal to restore the original forest composition at mid-elevation forests, yet they rely on natural potential vegetation maps that do not take into account long-term vegetation dynamics. Here we reconstruct the Holocene history of forest composition and discuss the implications the LRA has for regional forest management and conservation. Two newly analyzed pollen records from Prášilské jezero and Rachelsee were compared to 10 regional peat bogs/mires and two other regional lakes to reconstruct total land-cover abundance at both the regional- and local-scales. The results demonstrate that spruce has been the dominant canopy cover across the region for the past 9,000 years at both high- (>900 m) and mid-elevations (>700–900 m). At the regional-scale inferred from lake records, spruce has comprised an average of ~50% of the total forest canopy; whereas at the more local-scale at mid-elevations, spruce formed ~59%. Beech established ~6,000 cal. years BP while fir established later around 5,500 cal. years BP. Beech and fir growing at mid-elevations reached a maximum land-cover abundance of 24% and 13% roughly 1,000 years ago. Over the past 500 years spruce has comprised ~47% land-cover, while beech and fir comprised ~8% and <5% at mid-elevations. This approach argues for the “natural” development of spruce and fir locally in zones where the paleoecology indicates the

persistence of these species for millennia. Contrasting local and regional reconstructions of forest canopy cover points to a patchwork mosaic with local variability in the dominant taxa. Incorporation of paleoecological data in dialogues about biodiversity and ecosystem management is an approach that has wider utility.

Keywords: biodiversity, Holocene, land-cover, palynology, pollen, REVEALS

INTRODUCTION

Quantitative reconstructions are fundamental for providing long-term perspectives of ecosystem processes because they can be used to develop baselines for conservation and restoration ecology (National Research Council, 2005; Froyd and Willis, 2008). Paleoecological records have utility in conservation strategies related to biodiversity maintenance, ecosystem naturalness, conservation evaluation, habitat alteration, changing disturbance regimes, and species invasions (e.g., Birks, 1996; Jackson, 1997; Landres et al., 1999; Swetnam et al., 1999; Foster et al., 2003; Gillson and Willis, 2004). Unfortunately, paleoecological research is still largely ignored by conservation biologists and conservationists (Willis and Birks, 2006; Birks, 2012). In 1916, Lennart von Post published the first pollen diagram, providing one of the first qualitative reconstructions of vegetation change that extended over millennial timescales, as well as benchmarking the foundation of palynology (Manten, 1967). Müller (1927) published the first pollen diagram from the Bohemian Forest more than a decade later. Over the past 100 years, palynology has developed from a qualitative tool to a more quantitative analysis of vegetation dynamics that is increasingly well constrained in time (Davis, 2000).

Pollen diagrams produced from mires, peat bogs, and lake sediment profiles, with the data expressed as percentages against time or depth, have been the main way to present data (e.g., Stalling, 1987; Knipping, 1989; Svobodová et al., 2001, 2002; Jankovská, 2006). While percentage pollen diagrams identify changes in vegetation through time, changes in one taxon can affect the percentage proportions of all other taxa. This effect, termed data-closure (Birks and Birks, 1980), can produce disconnections between the trends of pollen and the actual vegetation land-cover. Several quantitative methodologies have been developed to address these issues. Data closure artifacts in pollen percentages can be identified by comparison with pollen influxes (i.e., pollen accumulation rates; grains $\text{cm}^{-2} \text{yr}^{-1}$), but this requires robust age-to-depth relationships for the sediments. Even then, both percentage and influx data fail to take account of differences in the ecological and environmental factors that influence pollen production and dispersal, nor do they define a spatial scale in reconstructions of vegetation cover (Loidi et al., 2010; Loidi and Fernández-González, 2012). Additionally, because pollen influxes are dependent upon age-to-depth relationships, changes in sedimentation rates can influence pollen concentrations and the subsequent accuracy of influx calculations. Therefore, Sugita (2007a,b) developed the Landscape Reconstruction Algorithm (LRA) which incorporates pollen productivity and pollen dispersal capacity, as well as factors that influence pollen dispersal, such as the size and type

of the sedimentation basin. Thus, the LRA provides a more quantitative approach of estimating past vegetation abundance in a defined space. The LRA has two steps: (1) the REgional Vegetation Estimates from Large Sites (REVEALS) model (Sugita, 2007a) estimates pollen-derived regional vegetation cover from large sites ($>100 \text{ ha}$) or alternatively many small sites across an area of 10^6 km^2 (e.g., Abraham et al., 2014, 2016); and (2) the LOcal Vegetation Estimates (LOVE) model (Sugita, 2007b) uses the regional estimates from REVEALS to estimate pollen-derived local vegetation composition in smaller areas (5–104 ha).

Long-term perspectives on forest dynamics are beneficial for conservation and restoration, and here we demonstrate the utility of quantitative palynological data in the management of Bohemian/Bavarian Forests, including the use of pollen influx data and pollen-landscape reconstruction models (e.g., REVEALS: Sugita, 2007a). Abraham et al. (2016) used the REVEALS model to estimate vegetation cover by integrating pollen sequences from the Šumava region and estimate that spruce has comprised over 50% of the regional forest canopy for the past 7,000 years. Here, we synthesize two newly analyzed, well-dated pollen records from Prášlské jezero (Šumava, Bohemian Forest; Czech Republic) and Rachelsee (Bavarian Forest; Germany) and several previously analyzed pollen records from peat bogs/mires and lakes using multiple quantitative methods to determine the ecological development and vegetation change during the Holocene. The objectives are: (1) to critically evaluate the multiple quantitative approaches used in palynology to reconstruct the history of forest composition; and (2) to explore the utility of quantitative land-cover reconstructions in regional conservation and restoration.

BACKGROUND: THE BOHEMIAN/BAVARIAN FOREST REGION OF CENTRAL EUROPE

The Bohemian/Bavarian Forest region of central Europe includes two national parks located along the border of the Czech Republic (Šumava National Park, Bohemian Forest), and Germany (Bavarian Forest National Park¹, Bavarian Forest; **Figure 1**). Together, these two parks with their surrounding area comprise one of the largest forested landscapes in central Europe, which is home to many endangered flora (see Křenová and Hruška, 2012) and fauna, and provides a close-to-nature ecosystem of ecological value (Meyer et al., 2009). The Bavarian Forest National Park

¹Bavarian Forest National Park Authority: <http://www.nationalpark-bayerischer-wald.de/english/nationalpark/management/index.htm>.

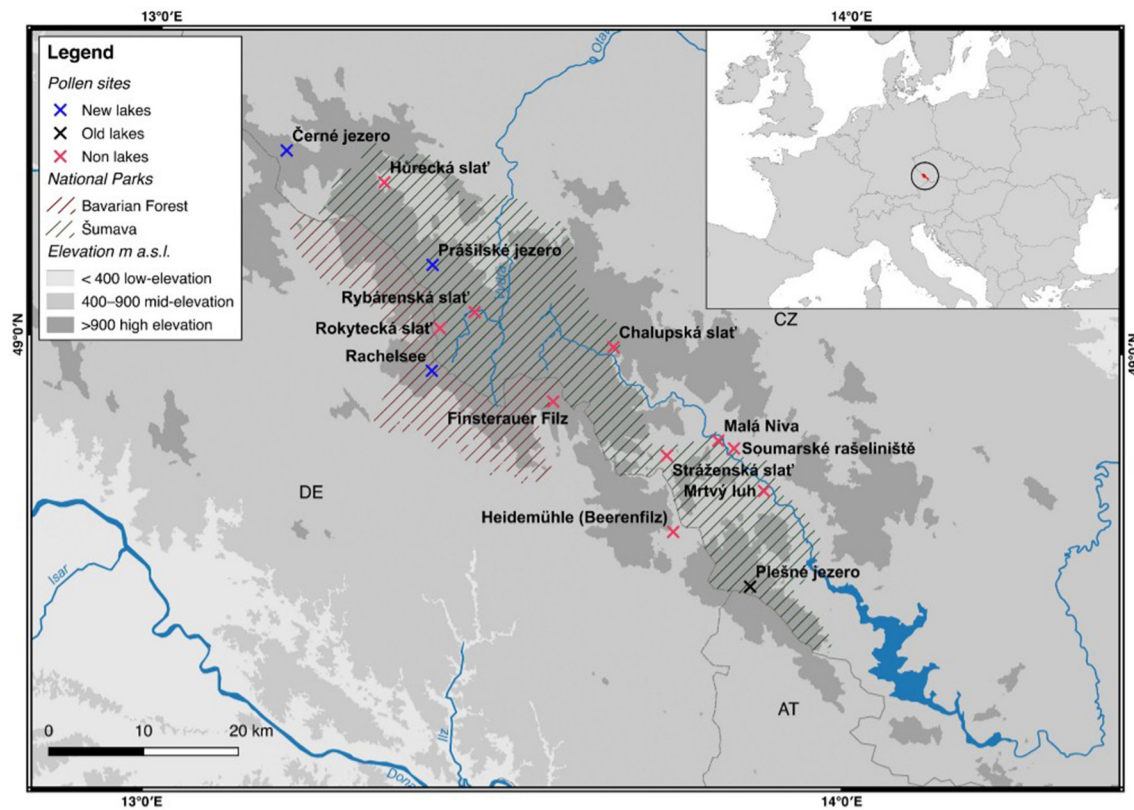


FIGURE 1 | Site map of the Bohemian/Bavarian Forest region of central Europe. Non-lakes (i.e., bogs and/or forest mires) are indicated by a red cross. Newly analyzed lakes presented in this study are indicated by a blue cross. Previously published lakes are indicated by a black cross. The National Park boundaries are indicated by green (Šumava) and red (Bavarian Forest) solid lines.

was established in 1970 with part of Šumava declared a UNESCO Biosphere Reserve in 1990, and Šumava National Park established in 1991.

Subject to long-term human influence, management practices in the Bohemian/Bavarian Forests have ranged from natural development to intensive forest management which has modified both the structure and composition of the forest. Currently, the two parks are divided into wilderness (i.e., not managed), and non-wilderness (i.e., managed). Within the non-wilderness areas, management focuses on sanitary logging of spruce trees killed by previous disturbance events, specifically bark beetle outbreaks. Within Šumava National Park, forest management restoration practices involve reducing spruce populations from the current 84% to a target “natural” representation of 30–40%, and increase beech (ca. 6%) and fir (ca. 1%) up to 35% (Šumava NP Authority). Forest management policies in the Czech Republic direct that the lands between 400 and 900 m altitude should be dominated by beech forests with spruce as a secondary component (Vacek and Mayová, 2000; Průša, 2001). This management plan is likely based on the Geobotanical Map (Mikyška et al., 1968–1972) and the Map of Potential Natural Vegetation (Neuhäuslová et al., 1998) with beech considered the natural dominant species at mid-elevations in central Europe (Ellenberg and Leuschner, 1996). Within the Bavarian Forest

National Park, land managers are concerned with the rapid decline of fir populations in valley bottoms and have focused their attention to factors that could facilitate the natural development of this species (Heurich and Englmaier, 2010), rather than focusing on the removal of spruce which has doubled its range in the Bavarian Forest since the nineteenth century. This strategy is in response to previous paleoecological work documenting that the Bavarian Forests consisted of ~32% fir ~3,000 years ago (Stalling, 1987).

Palynological research has a long history in the Bohemian/Bavarian region of central Europe with Müller (1927) publishing one of the first qualitative glimpses of long-term vegetation development in pollen diagrams from several moors in the region (Figure 2). Müller (1927) documented the long-term presence of spruce in the Bohemian/Bavarian Forests, but was unable to discuss these changes relative to time. With widespread application of radiocarbon dating, pollen data from peat sequences (i.e., small peaty wetlands within forests) in Šumava National Park confirm that spruce has dominated the forest canopy cover at elevations >700 m a.s.l. for the past 7,000–8,000 years (Svobodová et al., 2001, 2002). Notwithstanding the better chronological control, the reconstructions presented by Svobodová et al. (2001, 2002) are still limited in that; (1), pollen percentage diagrams offer

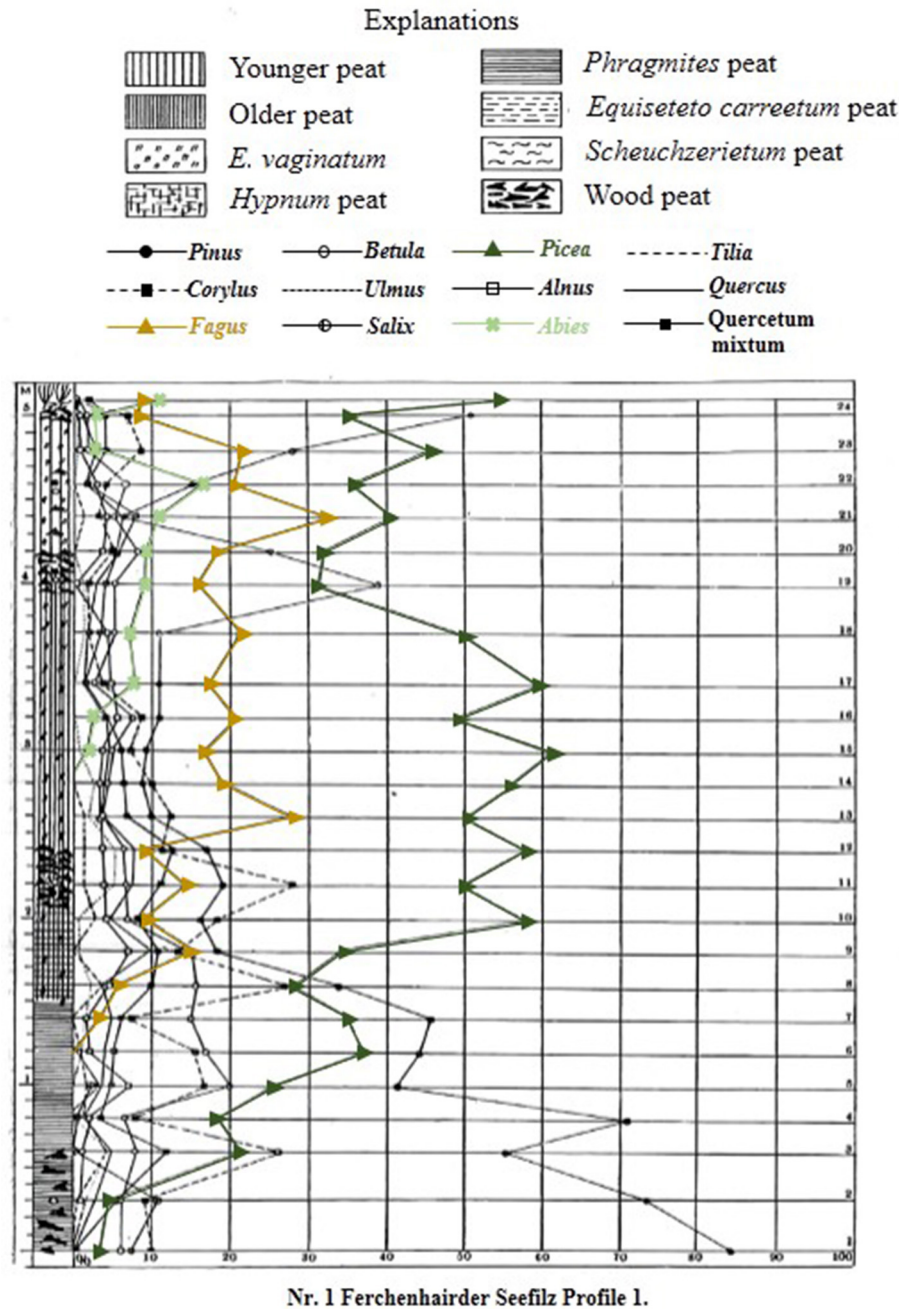


FIGURE 2 | Original pollen percentage diagram of Ferchenhaider Seefilz profile I from the Bohemian/Bavarian Forest region of central Europe. Digitized from Müller (1927), and translated from German into English. Dominant species found in the Bohemian/Bavarian Forests are shown in color; spruce (green line), beech (gold line), and fir (light green line).

a qualitative reconstruction of vegetation change through time; and (2) peat bogs/mires and wetlands capture changes in vegetation at various spatial scales [i.e., a forest-stand scale (forest mire) to the extra-local scale (open, wetland mire)]. Reconstructing extra-local to regional-scale vegetation changes is possible by analyzing sediments from lakes as well as open mires, which typically have a much larger pollen catchment area

than forest mires. However, pollen-based land-cover models (i.e., REVEALS) are the best approach for reconstructing vegetation abundances at the regional-scale. Currently, the only quantitative land-cover reconstruction of vegetation change in the region using the REVEALS model (Sugita, 2007a) and 14 sediment sequences suggests that spruce forests have comprised ~50% of the forest canopy throughout the past ~7,000 years (Abraham

et al., 2016). However, to develop more detailed descriptions of regional-scale vegetation dynamics, further quantitative data are needed. This study provides a more detailed description of land-cover change by analyzing lakes and peat bogs/mires that vary spatially across mid- (700–900 m a.s.l.) and high-elevations (>900 m a.s.l.) from the Bohemian/Bavarian Forests (**Table 1**), and addresses whether beech has been the dominant forest canopy type at mid-elevations over millennial time-scales.

METHODS

Core Retrieval, Sediment Limnology, and Radiocarbon Dating

A 2.18 m sediment profile was collected in August 2015 from the deepest (14.8 m) part of Prášílské jezero (49° 04' N, 13° 24' E, 1,079 m a.s.l.) and is comprised of two parallel and overlapping cores (PRA 15-2-1 and PRA 15-2-2). The sediment profile was sampled from a floating platform using a hand-percussion Russian-style corer (1.5 × 0.075 m). The sediment–water interface was collected using a 0.1 m diameter gravity corer (PRA15-2GC) (Boyle, 1995). At Rachelsee (48° 58' 29" N, 13° 24' 7" E, 1,071 m a.s.l.), 11.8 m of sediment was collected in August

2012 at 12.5 m water depth using a Livingstone piston corer (Wright, 1967) (RAA1-4). Sediment was not recovered between depths 0–57 cm, therefore, the mud–water interface depth begins at 57 cm. Sediment age–depth relationships were established using ¹⁴C radiocarbon dating at Prášílské jezero (*n* = 10) and Rachelsee (*n* = 7), with an additional ²¹⁰Pb series (Appleby, 1978) at Prášílské jezero (**Table 1**). For all sites, the geochronological data including the sediment surface were compiled within the Bayesian routine “BACON” (Blaauw and Christen, 2011). This analysis partitioned both cores into 0.05 m thick sections and estimated the accumulation rates for each segment using a Markov Chain Monte Carlo (MCMC) approach (Christen and Pérez, 2009). The analyses were constrained by a prior model of sediment accumulation rate (a gamma distribution with mean 50-year cm^{−1} and shape 1.5) and its variability (memory, a beta distribution with mean 0.5 and shape 16) for both sites. All ¹⁴C ages were calibrated and modeled in “BACON” using the IntCal13 curve (Reimer et al., 2013), with a Student-t distribution to account scatter in the ¹⁴C measurements and to allow for statistical outliers (Blaauw and Christen, 2011). The weighted mean modeled ages against depth were smoothed using a 21-point moving average (**Figure 3**).

TABLE 1 | Summary of age–depth relationships for Prášílské jezero (Core IDS, PRA-15GC2, PRA 15-2-1, and PRA 15-2-2), Czech Republic and Rachelsee (Core ID, RAA1-4), Germany.

Depth (cm)	Core ID	¹⁴ C Age ± 1σb	Assigned ²¹⁰ Pb (Year AD)	Assigned age (cal yr BP)	Material dated	Lab ID Number
1,480	PRA 15-2GC		2015 ± 1	−65		Surface
1,480.5	PRA 15-2GC		1995 ± 2	−55		Pb210-1
1,481.5	PRA 15-2GC		1986 ± 3	−36		Pb210-2
1,482.5	PRA 15-2GC		1976 ± 4	−26		Pb210-3
1,483.5	PRA 15-2GC		1963 ± 4	−13		Pb210-4
1,484.5	PRA 15-2GC		1943 ± 5	7		Pb210-5
1,485.5	PRA 15-2GC		1918 ± 7	32		Pb210-6
1,486.5	PRA 15-2GC		1889 ± 9	61		Pb210-7
1,487.5	PRA 15-2GC		1861 ± 12	89		Pb210-8
1,500.5	PRA 15-2-1	590 ± 30			Plant material	Poz-84783
1,539.2	PRA 15-2-1	2,545 ± 30			Plant material	Poz-81580
1,571.75	PRA 15-2-2	4,040 ± 35			Plant material	Poz-81582
1,599.75	PRA 15-2-2	5,700 ± 40			Plant material	Poz-81583
1,628.5	PRA 15-2-1	7,055 ± 40			Plant material	Poz-87722
1,628.5	PRA 15-2-2	7,550 ± 40			Plant material	Poz-80182
1,637	PRA 15-2-2	7,460 ± 40			Plant material	Poz-87724
1,651	PRA 15-2-2	8,210 ± 50			Plant material	Poz-84781
1,669.5	PRA 15-2-2	9,330 ± 60			Plant material	Poz-84780
1,690.25	PRA 15-2-2	9,620 ± 50			Plant material	Poz-80183
57	RAA-1	−62 ± 1				Surface
117	RAA-1	693 ± 30			Plant material	BE-3035
128	RAA-1	1,170 ± 29			Plant material	BE-3036
147	RAA-1	1,861 ± 22			Plant material	BE-3037
216	RAA-2	4,910 ± 35			Plant material	Poz-85119
276	RAA-3	9,120 ± 50			Plant material	Poz-85121
308	RAA-3	9,980 ± 60			Plant material	Poz-85122
371	RAA-4	11,310 ± 40			Organic sediment	Beta-420353

Pollen Analysis

At Prášilské jezero, pollen analysis was conducted at 1–2 cm resolution throughout the core by V. A. Carter. For each sample, 0.5 cm^{-3} was processed using standard pollen procedures (Faegri et al., 1989). At Rachelsee, pollen analysis was conducted at 1 cm resolution for 72–124 cm, 2 cm for 126–184 cm, and 4 cm for 188–540 cm by J. F. N. van Leeuwen. The sediment between depths 57–71 cm was too watery and could not be subsampled for pollen. Here, we present data from depths 72–368 cm. At Rachelsee, a minimum of 300 tree pollen grains, and at Prášilské jezero, a minimum of 500 pollen grains were counted in each sample. A *Lycopodium* tablet with a known amount of spores were added to each sample as an exotic tracer in order to calculate pollen concentration and influx rates (Stockmarr, 1972). Total pollen counts were converted into pollen percentages and plotted using Tilia software (Grimm, 1987) based on the abundance of each pollen type relative to the sum of all terrestrial identified pollen. The pollen profiles were divided into pollen assemblage zones based on optimal splitting using the broken-stick model (Bennett, 1996). Pollen counts were converted to concentrations (grains cm^{-3}) in Tilia using the counts of *Lycopodium* tracers and sample sediment volumes (Grimm, 1987). The smoothed Bayesian age-depth model for both sites was used to calculate and plot pollen influx rates from the concentration data using Tilia software.

REVEALS

The REVEALS model (Sugita, 2007a) was applied to estimate pollen-derived regional vegetation cover during the Holocene. Previous studies from the region (e.g., Abraham et al., 2014) mainly used records from peat bogs to calculate a REVEALS output, with the model showing the robustness of peat sequences in portraying present-day vegetation in a realistic manner.

Here, the REVEALS model was used to estimate land-cover abundance from both lakes and non-lakes (i.e., peat bogs and mires) using new (this paper) and previously published and unpublished pollen data obtained from the Czech Quaternary Pollen Database (Kuneš et al., 2009; **Table 2**). Pollen counts were aggregated into 500-year intervals for the entire Holocene, and then all available sites in each 500-year time window were used to estimate mean vegetation abundances within a 60 km radius. The following parameters were selected: 4 m s^{-1} wind speed, different dispersal-deposition models for bogs and mires (Prentice, 1985) and lakes (Sugita, 1994), and taxon-specific relative pollen productivities for 28 selected pollen-equivalent taxa (see Supplementary Table 1; Abraham and Kozáková, 2012; Mazier et al., 2012; Abraham et al., 2014). For model calculations, we adjusted the basin sizes of non-lakes to 4.5 ha. Larger basin sizes produce unrealistic estimates for some taxa as some trees may still grow within the basin, violating the model's assumptions (Abraham et al., 2014). Therefore, assuming smaller non-lake basins was more appropriate for our calculations. Openness was calculated by the summation of all herbs included in the model. All calculations were conducted in R (R Core Team, 2016) using functions to calculate mean vegetation abundances and their error estimates based on bootstrap methods (<https://github.com/petrkunes/LRA>).

RESULTS

Regional Vegetation Development

Müller (1927) originally presented data for 12 tree taxa (**Figure 2**), however, the discussion of this research will focus on the three dominant canopy species growing in the Bohemian/Bavarian Forests at modern times; spruce (*Picea abies*), beech (*Fagus sylvatica*), and fir (*Abies alba*). Based on

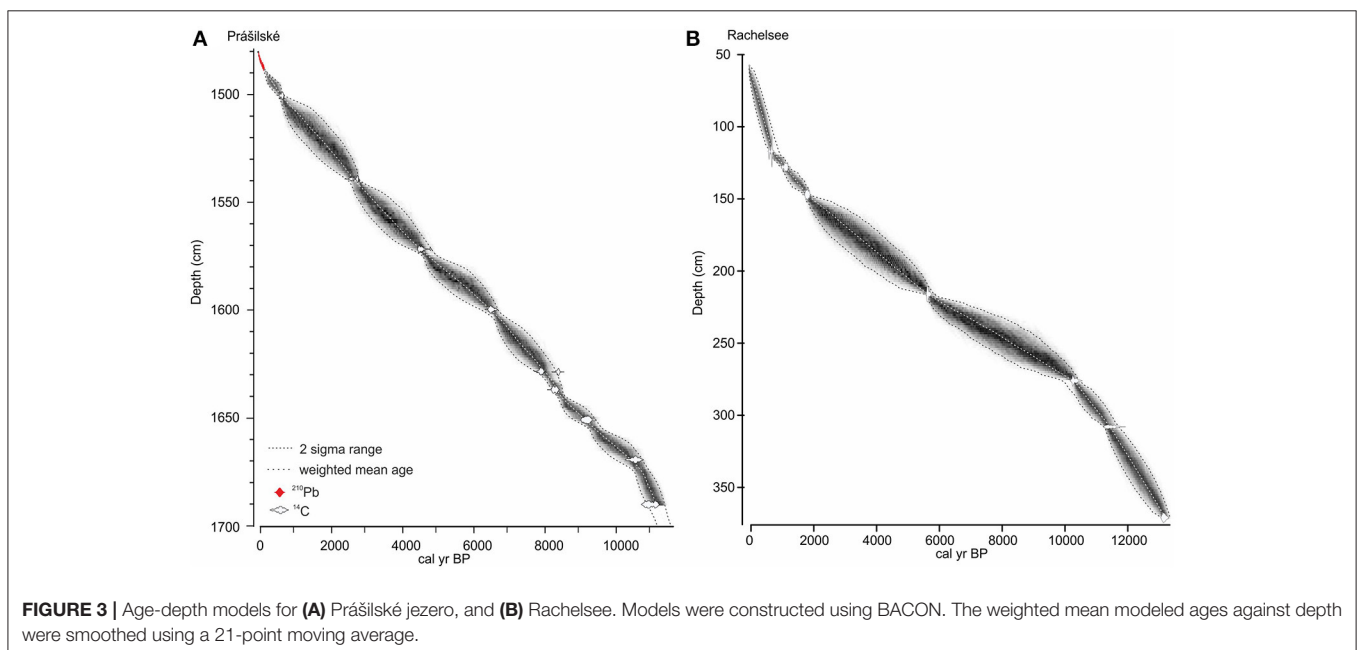


TABLE 2 | Regional sites used to create the REVEALS pollen-based vegetation model.

Site name	Lake or Mire	Latitude	Longitude	Area of site (ha)	Adjusted area of site for REVEALS	Elevation (m.a.s.l.)	Citation
Černé jezero*	Lake	49.18035	13.18538	18.5	18.5	1,008	Unpublished data*
Chalupská slat'	Mire	49.00061	13.66286	49	4.5	906	Unpublished data
Finsterauer Filz	Mire	48.948127	13.57751	7.6	4.5	1,055	Stalling, 1987
Heidemühle (Beerenfilz)	Mire	48.826771	13.753396	17	4.5	835	Stalling, 1987
Hůrecká slat'	Mire	49.15222	13.32755	62.2	4.5	870	Svobodová et al., 2002
Malá Niva	Mire	48.91376	13.81606	65	4.5	754	Svobodová et al., 2002
Mrtvý luh	Mire	48.8668	13.88292	250	4.5	737	Svobodová et al., 2001
Plešné jezero	Lake	48.77674	13.86571	7.5	7.5	1,105	Jankovská, 2006
Prášilské jezero	Lake	49.07519	13.39976	3.7	3.7	1,080	This study
Rachelsee	Lake	48.974945	13.4019381	5.7	5.7	1,071	This study
Rokytecká slat'	Mire	49.0153	13.4122	200	4.5	1,097	Svobodová et al., 2002
Rybářská slat'	Mire	49.03129	13.46181	32	4.5	1,014	Svobodová et al., 2002
Soumarské rašeliníště	Mire	48.9066019	13.8388078	30	4.5	750	Svobodová et al., 2001
Stráženská slat'	Mire	48.89887	13.74226	120	4.5	804	Svobodová et al., 2001

Sites with a "*" symbol indicate new, but unpublished data that was used to refine the REVEALS model (see Supplementary Material).

the broken-stick model (Bennett, 1996), the pollen percentages profiles from Prášilské jezero and Rachelsee were divided into seven and eight pollen assemblage zones, but for simplicity, the pollen reconstructions were grouped into three main periods; (1) Early- to Mid-Holocene, (2) Mid- to Late-Holocene, and (3) Last-Millennium.

Early- to Mid-Holocene (12,000–~6,800 cal. Years BP)

Spruce first arrived at the high-elevation lakes Prášilské jezero and Rachelsee between 10,500 and 10,000 years ago, but was present at mid-elevation peat bogs/mires by ~11,500 cal. years BP (Figure 4). Spruce rises to dominance between 10,000–8,500 cal. years BP across all elevations (Figure 4) replacing pine (*Pinus*) and hazel (*Corylus*) as the dominant canopy species (see Supplementary Figures 3–5). Thereafter, spruce percentages fluctuated between 35% and >20% pollen at both Prášilské jezero and Rachelsee, and around 30% at mid-elevation peat bogs/mires, respectively. Pollen influx data for spruce conversely differ between the two sites with a peak of 4,000 grains cm⁻² yr⁻¹ at Prášilské jezero, whereas the increases at Rachelsee are more subdued at <500 grains cm⁻² yr⁻¹ (Figure 5). Quantitative land-cover reconstructions of spruce percentages calculated using REVEALS (Sugita, 2007a) rise around 10,000 cal. years BP from ~5% to >60% calculated on a local (using peat bogs/mire records) basis (Figure 6). On a regional basis (using lake records), spruce comprised >50% total land-cover. The REVEALS land-cover reconstructions suggest that spruce forms close to double the land-cover percentages compared to pollen percentages. Beech begins to expand at both sites from 7,000 cal. years BP onwards, but is at low percentages in the Early- to Mid-Holocene. The dynamics of fir are restricted to after 5,000 cal. years BP. Total herb percentages decrease from ~20% and oscillate around 10% at both Prášilské jezero and Rachelsee. Pollen influx data for total herbs decrease ~10,500 cal. years BP from values >2,000 grains cm⁻² yr⁻¹. The REVEALS reconstruction also suggests

that the percent of landscape openness is close to double that of pollen percentage data at both the regional and local-scale (Figure 6).

Mid- to Late-Holocene (~6,800–1,000 cal. Years BP)

Between 6,800 and 6,000 cal. years BP beech increases gradually in pollen percentages at both Prášilské jezero and Rachelsee, and then oscillates around 25% (Figure 4). Beech percentages from mid-elevation peat bogs/mires begin to increase ~500 years earlier than in the high-elevation lakes. At the local-scale (peat bogs/mires), beech percentages gradually increase throughout the Mid- to Late-Holocene peaking at ~25% roughly 1,000 cal. years BP. Fir expansion commences 5,500–5,000 cal. years BP to around 20% at both Prášilské jezero and Rachelsee. These increases in pollen percentages are associated with no substantial reduction in spruce pollen percentages at Prášilské jezero and Rachelsee, but spruce percentages decrease from ~40% to ~20% <900 m a.s.l. (Figure 4). Viewed from a perspective of pollen influx, the down core pattern of increase and stability in species percentage data are reflected in the influx data (Figure 5). Though as with spruce, influx rates for beech and fir are much lower at Rachelsee. The REVEALS land-cover reconstructions for spruce and fir are lower at the regional scale (i.e., lake sites) relative to the more local-scale (i.e., peat bog/mire sequences), whereas beech is an equally abundant component in both reconstructions comprising ~25% land-cover (Figure 6). The land-cover contribution of spruce remains double (>40%) the values indicated by pollen percentage data (>15%), but these differences are not present for beech and fir. Land-cover percentages of spruce remained relatively stable at the lake sites however, spruce decreases from >60% to ~40% at mid-elevation peat bog/mire sequences during this period. The REVEALS reconstruction also suggests that the percent of openness is <5% at both the regional and local-scales (Figure 6).

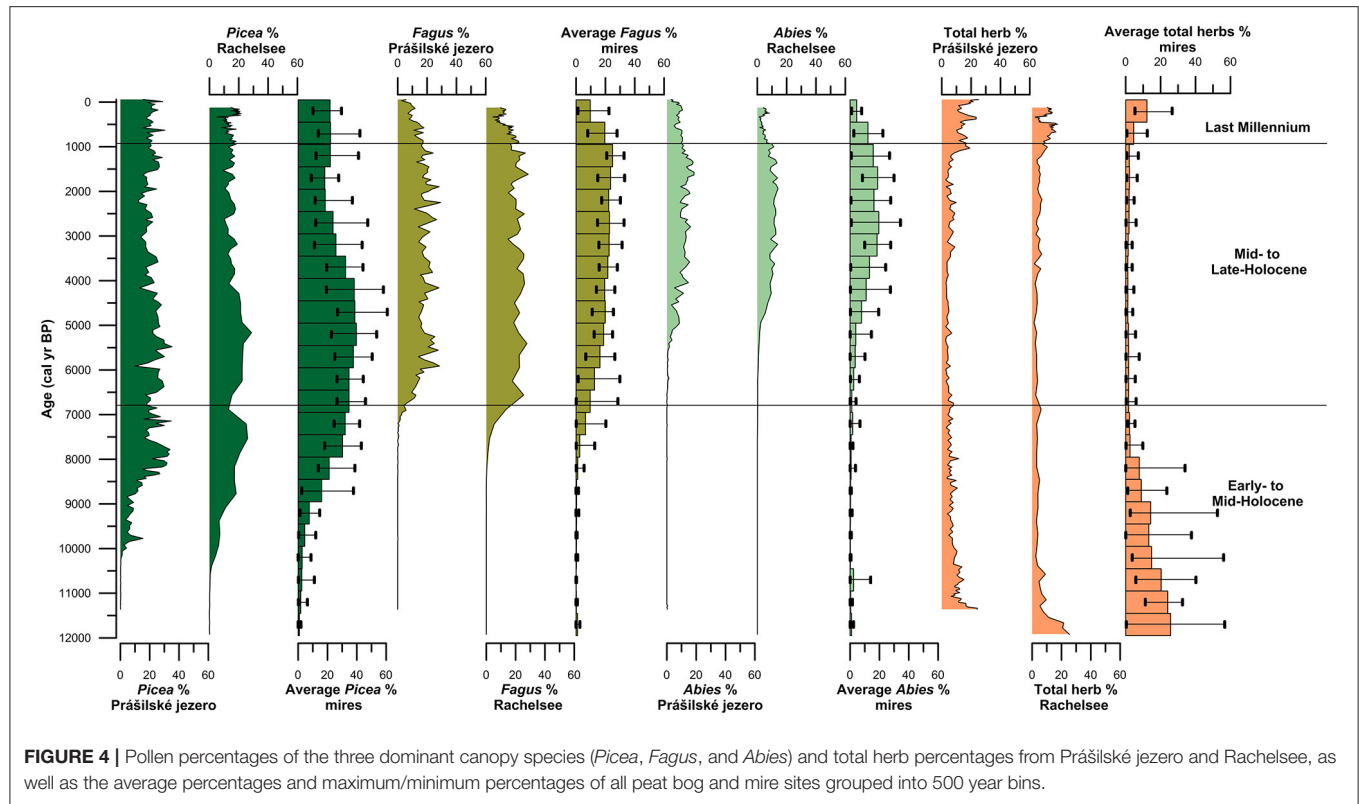


FIGURE 4 | Pollen percentages of the three dominant canopy species (*Picea*, *Fagus*, and *Abies*) and total herb percentages from Prášilské jezero and Rachelsee, as well as the average percentages and maximum/minimum percentages of all peat bog and mire sites grouped into 500 year bins.

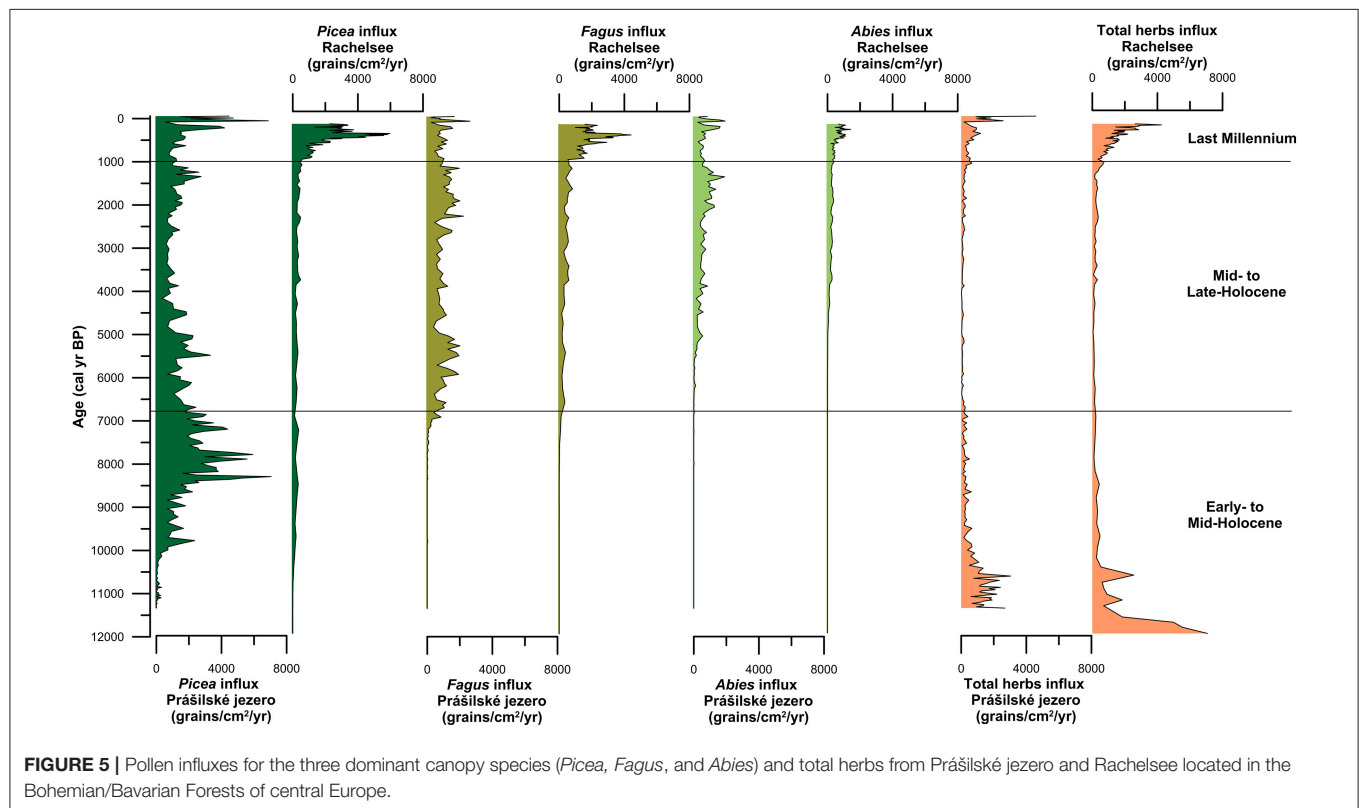
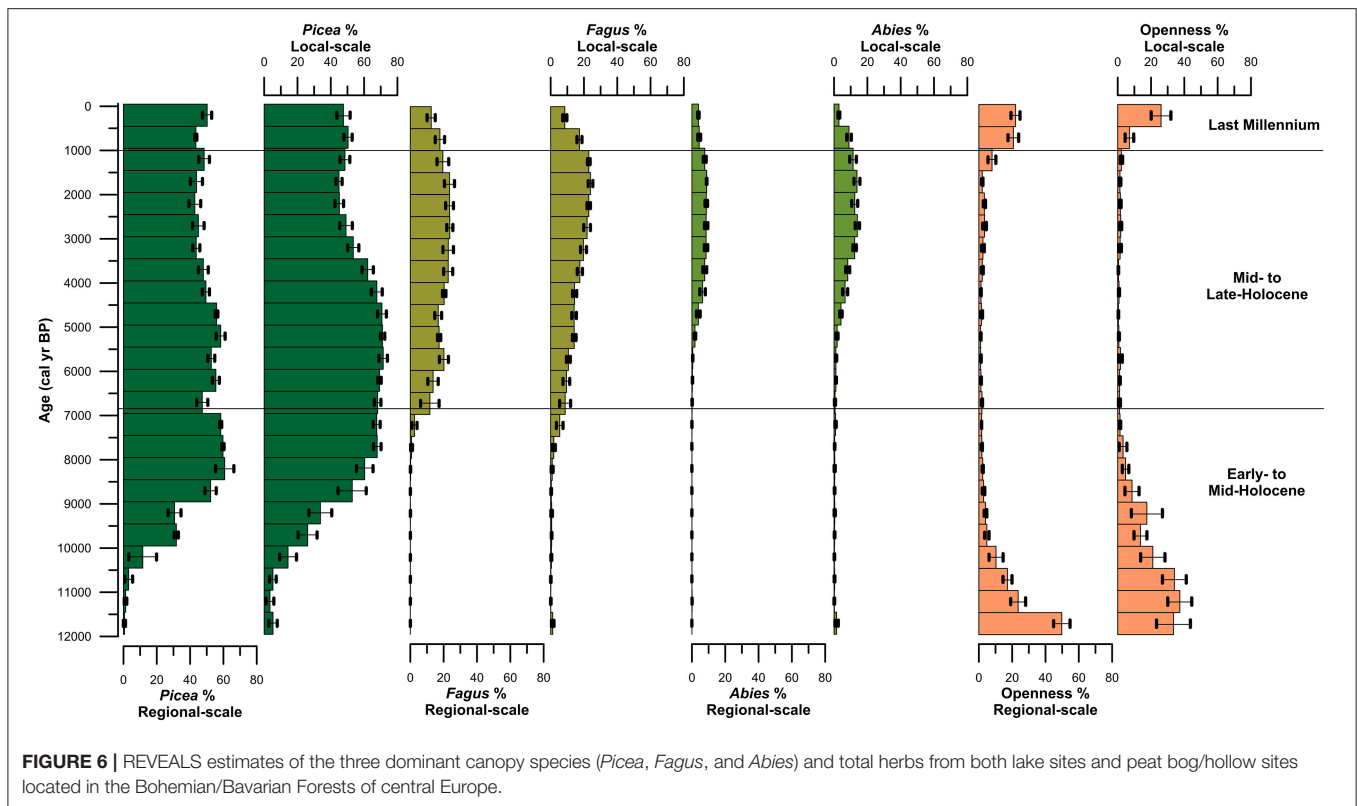


FIGURE 5 | Pollen influxes for the three dominant canopy species (*Picea*, *Fagus*, and *Abies*) and total herbs from Prášilské jezero and Rachelsee located in the Bohemian/Bavarian Forests of central Europe.



Last-Millennium (1,000 cal. Years BP-Present)

At both lakes, spruce percentages remain unchanged initially and then increase ~5% in the last 300 years (Figure 4). Spruce percentages remain unchanged at mid-elevation peat bogs/mires. Both beech and fir pollen percentages decline at both lakes and mires sequences through the last 1,000 years (Figure 4). Openness percentages increased dramatically over the past 1,000 years to ~12% (Figure 4). Pollen influx rates for all three taxa increase during the last 1,000 years at both lakes, and sharply in the last 300 years which likely reflects focusing of pollen toward the lake center (i.e., in-lake lateral redistribution of materials toward the deeper waters) rather than any change in species abundance (Figure 5). The REVEALS reconstructions broadly confirm the indications seen in the percentage pollen data, with declines in beech and fir occupied by open-ground indicators rather than any expansion in spruce. This is also shown in the pollen influx data, showing a dramatic rise in the influx of open-ground taxa (Figure 5).

DISCUSSION

Developments in Understanding Dominant Ecology of the Bohemian/Bavarian Forests

Over the past 100 years, methodological improvements in the field of paleoecology such as radiocarbon dating and pollen-based quantitative land-cover modeling (i.e., REVEALS; Sugita, 2007a) have led to more realistic reconstructions of past vegetation

change across temporal and spatial scales. Applying these approaches to the palaeoenvironmental records from Prášilské jezero and Rachelsee illustrates the long-term presence and dominance of spruce in the Bohemian/Bavarian Forests. First appearing in the pollen record ~10,000 cal. years BP, the local presence of spruce in the region is supported by *Picea* stomata at Prášilské jezero and Rachelsee, which agrees with previous paleoecological research in the region (Müller, 1927; Svobodová et al., 2001, 2002; Jankovská, 2006; Abraham et al., 2016). At the regional scale (i.e., lake sites), the REVEALS model suggests that spruce has comprised an average of ~50% of the total forest canopy, whereas at the more local scale (i.e., peat bogs/mires) spruce has comprised ~59%. Thus, spruce has been a dominant component of the forest canopy across a range of elevations >700 m a.s.l. in the Bohemian/Bavarian Forests.

Modern quantitative approaches also illustrate a unique history of forest composition throughout the region with beech and fir contributing as secondary canopy species relative to spruce at mid-elevations found between 700 and 900 m a.s.l. Beech established around 7,000 cal yr BP and became an abundant canopy species around 6,000 cal. years BP, with the REVEALS model indicating that it contributed ~20% of the total land-cover at the regional scale. However, at the more local-scale between 700 and 900 m a.s.l. beech comprised just 16% of the total land-cover during the Mid-Holocene. After the establishment of beech, Müller (1927) found an increase in fir percentages. Svobodová et al. (2001, 2002) suggested that fir

had spread to elevations >700 m a.s.l. across the entire region between 6,300 and 3,400 cal. years BP. However, these records were constrained by few radiocarbon dates. At Prášilské jezero and Rachelsee, fir first appeared between 7,000–6,300 cal. years BP but did not become an important component of the canopy until 5,000–4,500 cal. years BP. The REVEALS model output indicates that for the last 4,000 years, fir has comprised an average of ~7% of the total land-cover at the regional-scale, but slightly higher (10%) at the more local-scale between 700 and 900 m a.s.l. As beech and fir expanded around 4,000 cal. years BP, spruce percentages declined to some extent but still comprised ~40% of the regional total land-cover, and >60% of the local-scale (i.e., mid-elevation) forest composition in the Bohemian/Bavarian Forests (**Figure 6**). This further demonstrates that beech has been a secondary canopy species relative to spruce at mid-elevations, specifically between 700 and 900 m a.s.l. Total land-cover of beech and fir populations found at mid-elevations began to decrease from their maximum values of 24% and 13% total land-cover ~1,000 years ago at both the regional and more local-scale (**Figure 6**). The decrease in beech and fir forests are likely the result of increasing anthropogenic landscape modifications. However, climate could also explain the decline in beech and fir as temperatures were likely unfavorable for these species during the Little Ice Age (Grove, 2001; Brázdil et al., 2017).

Declines in beech and fir characterize the last millennium with an expansion in open ground taxa in both the percentage pollen data and the quantitative REVEALS land-cover reconstructions, though spruce is slightly more abundant in terms of total land-cover (**Figure 6**). Svobodová et al. (2002) also indicate that beech-spruce-fir forests have decreased over the past three centuries, and are being replaced by spruce and *Pinus rotundata* in forest bogs at lower elevations. The regional reconstructions presented here point to a change in forest composition toward more open ground within the forest, and slightly increased dominance by spruce. Over the past 500 years spruce has comprised ~47% land-cover, while beech and fir has comprised ~8% and <5% at mid-elevations. The pollen influx values show a radically different story with the records from Prášilské jezero and Rachelsee illustrating an increase in all pollen taxa through the last 500 years. This increase in pollen influx likely reflects increased in-lake focusing of pollen to the lake center assisted by wind currents from a more open landscape (see **Figure 5** for percent openness), rather than increased pollen rain from spruce plantations found at low-elevations. Openings within high-elevation forests are generally attributed to human clearance, fire, windthrow, or bark beetle outbreaks (*Ips typographus*) which are key disturbance drivers influencing Norway spruce forest dynamics (Holeksa and Cybulski, 2001; Fischer et al., 2002; Holeksa et al., 2007; Svoboda et al., 2012, 2014; Čada et al., 2016; Janda et al., 2017; Kulakowski, 2017). During the 1990s, an *I. typographus* bark beetle outbreak occurred in the region creating gaps (i.e., openings) in the canopy. Severe windstorms occurred in the region in 1986, 1999, 2007, and 2008, which also caused widespread forest damage (Svoboda et al., 2010). Yet, Zeppenfeld et al. (2015) found that spruce seedlings and young spruce trees already occur in areas affected by these large-scale disturbances, encouraging rapid recovery of spruce and not limiting flux of pollen to the lakes in the region. Therefore,

increase in pollen fluxes especially at Prášilské jezero is likely a result of natural processes and not a result of spruce plantations found at lower elevations.

While the REVEALS model demonstrates that spruce has been the dominant canopy cover at both high- and mid-elevations, the model only provides an average percentage of land-cover for the entire Bohemian/Bavarian Forest. Local site conditions such as slope and aspect affect forest composition at the more local-scale (i.e., stand-scale). For example, spruce generally dominates on north-facing mesic sites with poorly-drained soils, whereas beech typically dominates on south-facing xeric sites where soils drain well. These local conditions can lead to stands of monospecific spruce or beech at mid-elevations, specifically in the Bavarian Forest National Park. However, the REVEALS model used in this study was used to inform managers of the natural average forest composition for elevations >700 m a.s.l. for the area through time.

Applications to Conservation and Restoration in the Bohemian/Bavarian Forests

The overall management goal of the parks is to restore the original forest composition (IUCN, 1994). Within the Šumava National Park forest management has likely based their target “natural” forest composition from Geobotanical Maps (Mikyška et al., 1968–1972), and the Map of Potential Natural Vegetation (Neuhäuslová et al., 1998), which suggest that beech dominate over spruce at mid-elevations in central Europe (Ellenberg and Leuschner, 1996). More recently, Vacek and Mayová, 2000, suggest that beech is dominant over spruce at mid-elevations between 650 and 900 m. Together, these previous maps and research have influenced the management strategy of removing spruce from mid-elevation forests within Šumava National Park so that spruce will comprise 30–40% instead of its current representation of “84%” (Šumava National Park Authority²). However, these maps and previous research do not consider paleoecological studies which provide long-term dynamics of vegetation abundance through time. Paleoecological studies have utility in conservation and restoration in that they can provide baseline targets (i.e., more accurate representations of forest composition), as well as provide the natural range of variability within vegetation composition through time. While the REVEALS model shows that beech and fir forests reached a combined maximum of 37% at mid-elevations (between 700 and 900 m a.s.l.) ~2,000 years ago, spruce forests still comprised 45% of the total forest composition at these elevations (**Figure 6**). A regional paleoecological perspective of the past 500 years shows that the forest composition at mid-elevations has been a mixed-forest cover of spruce (~50%), beech (~22%), and fir (~10%), which counters the findings of Vacek and Mayová (2000). Our findings support previous investigations that highlight that mixed-forests consisting of spruce-beech-fir typically occur between 650 and 1,150 m in the Šumava National Park (Röder et al., 2010), as well as showing the long-term dominance of coniferous forests in the Bohemian-Moravian

²Šumava National Park Authority. <http://www.npsumava.cz/en/3291/sekce/the-species-composition-of-the-forests/>.

highlands over the past 9,000 years (Szabó et al., 2017). The long-term presence of spruce throughout the Holocene illustrates that forest management practices involving the formation of spruce plantations at mid-elevations have not suppressed beech (Szabó et al., 2017). During the late Holocene the results from the regional-scale sites show some suppression of beech (~15% land-cover) that is not related to spruce dominance, but rather to the extent of open ground. This supports previous research from Šumava National Park with beech rarely reaching >20% from mid-elevation sites (Hrubý et al., 2014).

Within the Bavarian Forest National Park, soil conditions and south-facing slopes create more favorable conditions for beech and fir forests. While spruce has doubled its range since the nineteenth century in the region, foresters have been more concerned with the recent decline of fir. At the time of establishment of the Bavarian Forest National Park, fir comprised only 3.2% of the total forest composition (Heurich and Englmaier, 2010). This is supported by the regional-scale REVEALS reconstruction which shows the decline of fir over the past 500 years to 3.8%. However, at the more local-scale (i.e., peat bogs/mires) at mid-elevations fir has declined to just 2.9% (**Figure 6**). Stalling (1987) found that fir pollen frequencies reached a peak of ~32% fir roughly 3,000 years ago on the basis of 15 sites with a mean elevation of 837 m a.s.l. in the Bavarian Forest. However, quantitative land-cover reconstructions presented here indicate that fir reached a maximum regional land-cover of just 13% between 3,500 and 1,000 cal. years BP, and a maximum of ~20% at the more local-scale at mid-elevations (**Figure 6**). Methodological improvements such as quantitative land-cover modeling offer a more robust reconstruction of vegetation abundance from the Bohemian/Bavarian Forests of central Europe. Thus, the results presented here provide a more accurate and updated description of fir abundances than the previous work by Stalling (1987). However, the REVEALS model is limited in that all of the mid-elevation sites used in the model are located within the park boundaries of Šumava National Park. Mid-elevation paleoecological reconstructions do exist from the Bavarian Forest National Park, yet, the sites were not incorporated into the model because they were either not available publicly or they lacked radiocarbon dating. Therefore, the results interpreted here may be more reflective of vegetation abundances from mid-elevation in Šumava National Park. Regardless, the REVEALS model reconstructed the regional decline of fir, and it is therefore a concern that should be addressed by foresters in the Bavarian Forests. Heurich and Englmaier (2010) suggest that the trend of declining fir populations relative to increasing spruce populations in the Bavarian Forests is likely not solely related to human activity but also to natural causes such as the Little Ice Age and bark beetle outbreaks. Because spruce is a cold adapted species, conditions during the Little Ice Age would have favored spruce over fir. Additionally, downed logs from windthrow and bark beetle outbreaks are the preferred natural substrate that gives spruce seedlings a competitive advantage over other tree species (Svoboda et al., 2010). While several studies suggest that fir is sensitive to human activities and anthropogenically caused air pollution (Tinner et al., 1999; van der Knaap et al., 2004;

Tinner and Lotter, 2005; Feurdean and Willis, 2008), human impacts in the form of pasturing, selective logging and litter raking have been shown to be beneficial for fir growth (Nožička, 1957; Málek, 1981; Kozáková et al., 2011). Tinner et al. (2013) suggest that the range of fir has the potential to increase with climate change as long as precipitation does not decrease below 700–800 mm/yr, or anthropogenic disturbances such as fire and grazing do not become excessive.

One of the benefits of the Šumava and Bavarian Forest National Parks is that it serves to protect montane spruce forests (Svoboda et al., 2010). Spruce is likely to be the species most impacted by climate change, and so is under threat in a warmer world (Bolte et al., 2009). Norway spruce is considered a cold-adapted species growing on mesic sites. Therefore, expected changes in temperature and precipitation in the future specifically the increased likelihood of more frequent and intense summer droughts across central and southern Europe (Gao and Giorgi, 2008; Feyen and Dankers, 2009), will likely result in the loss of available habitat for spruce (Hanewinkel et al., 2012). In the Bohemian/Bavarian Forests, Norway spruce has already occupied the highest possible altitudes and ostensibly the species has nowhere to go with climate change (Spathef et al., 2014). Conversely, beech and fir forests, the main competitors of spruce in the region, could continue to impinge on and expand in the lower altitude habitat of spruce. However, areas where beech predominates likely will also be threatened with increasing temperatures (Cheddadi et al., 2016). Migration of the optimum climate windows for these dominant forest taxa is a concern for forest managers, yet our paleoecological data show these plant communities have comprised a mixed-forest for >5,000 years in the region surviving previous climatic fluctuations during the Holocene. Mixed-forests with multiple tree species provide higher levels of ecosystem services (Gamfeldt et al., 2013) and should therefore be incorporated into forest management in the Bohemian Forests. We suggest that forest managers in the Šumava National Park consider utilizing information gained by paleoecological reconstructions that use pollen-based land-cover models that more accurately represent the natural vegetation abundances found at mid-elevations.

CONCLUSIONS

Methodological advances in the field of palynology and paleoecology, including quantitative land-cover models and robust chronologies have allowed for more accurate reconstructions of vegetation dynamics through time. Using these methodologies the results of this study demonstrate that spruce has been the dominant canopy cover in the Bohemian/Bavarian Forests for the past 9,000 years across a range of elevations including mid-elevations (between 700 and 900 m a.s.l.) where beech and fir forests were previously thought to dominant. When beech and fir forests peaked around 2,000 years ago, together they comprised a total land-cover of 37%. However, spruce contributed 40% of the total land-cover, further documenting the dominance of this species in mixed beech/fir forests. Over the past 500 years, spruce has comprised ~47%

land-cover, while beech and fir comprised $\sim 8\%$ and $<5\%$ at mid-elevations.

Paleoecological results have considerable utility in forest management and ecosystem conservation (e.g., Birks, 1996; Jackson, 1997; Landres et al., 1999; Swetnam et al., 1999; Foster et al., 2003; Gillson and Willis, 2004). For example, forest management in the Šumava National Park base current management strategies on outdated information that states that beech and fir forests are the natural, dominant vegetation at mid-elevations. However, the results presented here demonstrate that mid-elevations forests have been a mixed-forest with spruce dominating the forest canopy. The current management plan is to remove spruce to a natural representation of 30–40%, while increasing beech and fir up to a total of 35% (Šumava National Park Authority²). The longer perspective afforded by paleoecology suggests that the Šumava National Park should aim for 45% spruce as that is within the natural range of total land-cover for the species, but ecosystem managers should take into account the potential for climate change to significantly impact the range of spruce within the park and take steps toward preserving the species. As for the Bavarian Forest National Park, the REVEALS model was able to capture a decline of fir cover to levels previously recorded (see Heurich and Englmaier, 2010), yet the results may be more indicative of vegetation abundances within Šumava National Park. Additional paleoecological sites with robust chronologies are needed from the region, specifically from between 400 and 700 m a.s.l. in order to compare local-scale vegetation dynamics through time.

REFERENCES

- Abraham, V., and Kozáková, R. (2012). Relative pollen productivity estimates in the modern agricultural landscape of Central Bohemia (Czech Republic). *Rev. Palaeob. Palynol.* 179, 1–12. doi: 10.1016/j.revpalbo.2012.04.004
- Abraham, V., Oušková, V., and Kuneš, P. (2014). Present-day vegetation helps quantifying past land cover in selected regions of the Czech Republic. *PLoS ONE* 9:e100117. doi: 10.1371/journal.pone.0100117
- Abraham, V., Kuneš, P., Petr, L., Svitavská-Svobodová, H., Kozáková, R., Jamrichová, E., et al. (2016). A pollen-based quantitative reconstruction of the Holocene vegetation updates a perspective on the natural vegetation in the Czech Republic and Slovakia. *Preslia* 88, 409–434. Available online at: <http://www.preslia.cz/P164Abraham.pdf>
- Appleby, P. G. (1978). The calculation of lead-210 dates assuming a constant rate of supply of unsupported ^{210}Pb to the sediment. *Catena* 5, 1–8. doi: 10.1016/S0341-8162(78)80002-2
- Bennett, K. D. (1996). Determination of the number of zones in a biostratigraphical sequence. *New Phytol.* 132, 155–170. doi: 10.1111/j.1469-8137.1996.tb04521.x
- Birks, H. J. B., and Birks, H. H. (1980). *Quaternary Palaeoecology*. London: Edward Arnold.
- Birks, H. J. B. (1996). Contributions of quaternary palaeoecology to nature conservation. *J. Veg. Sci.* 7, 89–98. doi: 10.2307/3263420
- Birks, H. J. B. (2012). Ecological palaeoecology and conservation biology: controversies, challenges, and compromises. *Int. J. Biodivers. Sci. Ecosyst. Serv. Manage.* 8, 292–304. doi: 10.1080/21513732.2012.701667
- Blauw, M., and Christen, J. A. (2011). Flexible paleoclimate age-depth models using an autoregressive gamma process. *Bayesian Anal.* 6, 457–474. doi: 10.1214/11-BA618
- Bolte, A., Ammer, C., Löf, M., Madsen, P., Nabuurs, G.-J., Schall, P., et al. (2009). Adaptive forest management in central Europe: climate change impacts, strategies, and integrative concept. *Scand. J. For. Res.* 24, 473–482. doi: 10.1080/02827580903418224

AUTHOR CONTRIBUTIONS

PK and JC: obtained funding to support the project; PK, JC, RC, and AM: collected the data; PK, JvL, RC, and VC: analyzed the data; VC and PK: conceived ideas and led the manuscript writing; VC, RC, JC, NK, AM, MS, HS-S, JvL, and WvdK: edited the manuscript during all phases.

FUNDING

This research was supported by the Czech Science Foundation EUROPIA project no. 16-06915S, and PEDECO project no. 16-23183Y.

ACKNOWLEDGMENTS

We would like to thank Vojtěch Abraham for his suggestions on how to improve the REVEALS model, and Daniel Vondrák and Günther Kletetschka for their help with radiocarbon dating. We also thank Vlasta Jankovská and Maurice Reille for providing their published data through the Czech Quaternary Pollen Database.

SUPPLEMENTARY MATERIAL

The Supplementary Material for this article can be found online at: <https://www.frontiersin.org/articles/10.3389/fpls.2017.02268/full#supplementary-material>

- Boyle, J. F. (1995). A simple closure mechanism for a compact, large-diameter, gravity corer. *J. Paleolim.* 13, 85–87. doi: 10.1007/BF00678113
- Brázdil, R., Szabó, P., Stucki, P., Dobrovolný, P., Řezníčková, L., Kotyza, O., et al. (2017). The extraordinary windstorm of 7 December 1868 in the Czech Lands and its central European context. *Int. J. Climatol.* 37, 14–29. doi: 10.1002/joc.4973
- Čada, V., Morrissey, R. C., Michalová, Z., Bače, R., Janda, P., and Svoboda, M. (2016). Frequent severe natural disturbances and non-equilibrium landscape dynamics shaped the mountain spruce forest in central Europe. *For. Ecol. Manage.* 363, 169–178. doi: 10.1016/j.foreco.2015.12.023
- Cheddadi, R., Araújo, M. B., Maiorano, L., Edwards, M., Guisan, A., Carré, M., et al. (2016). Temperature range shifts for three European tree species over the last 10,000 years. *Front. Plant Sci.* 7:1581. doi: 10.3389/fpls.2016.01581
- Christen, J. A., and Pérez, E. S. (2009). A new robust statistical model for radiocarbon data. *Radiocarbon* 15, 1047–1059. doi: 10.1017/S003382220003410X
- Davis, M. B. (2000). Palynology after Y2K—understanding the source area of pollen in sediments. *Ann. Rev. Earth Planet. Sci.* 28, 1–18. doi: 10.1146/annurev.earth.28.1.1
- Ellenberg, H., and Leuschner, C. (1996). “Vegetation mitteleuropas mit den Alpen,” in *Ökologischer, dynamischer und historischer Sicht* (Stuttgart: Ulmer), 1–1095.
- Fægri, K., Kaland, P. E., and Kzywinski, K. (1989). *Textbook of Pollen Analysis*. New York, NY: Wiley.
- Feurdean, A., and Willis, K. J. (2008). Long-term variability of *Abies alba* in NW Romania: implication for its conservation management. *Divers. Distrib.* 14, 1004–1017. doi: 10.1111/j.1472-4642.2008.00514.x
- Feyen, L., and Dankers, R. (2009). Impact of global warming on streamflow drought in Europe. *J. Geophys. Res.* 114:D17116. doi: 10.1029/2008JD011438
- Fischer, A., Lindner, M., Abs, C., and Lasch, P. (2002). Vegetation dynamics in Central European forest ecosystems (near-natural as well as managed) after storm events. *Folia Geobot.* 37, 17–32. doi: 10.1007/BF02803188

- Foster, D. R., Swanson, F. J., Aber, J., Burke, I., Brokaw, N., Tilman, D., et al. (2003). The importance of land-use legacies to ecology and conservation. *Bioscience* 53, 77–87. doi: 10.1641/0006-3568(2003)053[0077:TIOULJ]2.0.CO;2
- Froyd, C. A., and Willis, K. J. (2008). Emerging issues in biodiversity and conservation management: the need for a palaeoecological perspective. *Quat. Sci. Rev.* 27, 1723–1732. doi: 10.1016/j.quascirev.2008.06.006
- Gamfeldt, L., Snäll, T., Bagchi, R., Jonsson, M., Gustafsson, L., Kjellander, P., et al. (2013). Higher levels of multiple ecosystem services are found in forests with more tree species. *Nat. Commun.* 4:1340. doi: 10.1038/ncomm.s2328
- Gao, X., and Giorgi, F. (2008). Increased aridity in the Mediterranean region under greenhouse gas forcing estimated from high resolution simulations with a regional climate model. *Glob. Planet. Change* 62, 195–209. doi: 10.1016/j.gloplacha.2008.02.002
- Gillson, L., and Willis, K. J. (2004). 'As earth's testimonies tell': wilderness conservation in a changing world. *Ecol. Lett.* 7, 990–998. doi: 10.1111/j.1461-0248.2004.00658.x
- Grimm, E. C. (1987). CONISS: a fortran 77 program for stratigraphically constrained cluster analysis by the method of incremental sum of squares. *Comput. Geosci.* 13, 13–35. doi: 10.1016/0098-3004(87)90022-7
- Grove, J. (2001). "The onset of the Little Ice Age," in *History and Climate: Memories of the Future?*, eds P. D. Jones, A. E. J. Ogilvie, T. D. Davies, and K. R. Briffa (New York, NY; Boston; Dordrecht; London; Moscow: Kluwer Academic/Plenum Publishers), 153–185.
- Hanewinkel, M., Cullmann, D. A., Schelhaas, M.-J., Nabuurs, G.J., and Zimmermann, K. E. (2012). Climate change may cause severe loss in the economic value of European forest land. *Nat. Clim. Change* 3, 203–207. doi: 10.1038/nclimate1687
- Heurich, M., and Englmaier, K. H. (2010). The development of tree species composition in the Rachel-Lusen region of the Bavarian Forest National Park. *Silva Gabreta* 16, 165–186. Available online at: http://www.npsumava.cz/gallery/11/3587-sg16_3_heurichenglmaier.pdf
- Holeksa, J., and Cybulski, M. (2001). Canopy gaps in a Carpathian subalpine spruce forest. *Forest Res.* 120, 331–348. doi: 10.1007/BF02796104
- Holeksa, J., Saniga, M., Szwagrzyk, J., Dziedzic, T., Ferenc, S., and Wodka, M. (2007). Altitudinal variability of stand structure and regeneration in the subalpine spruce forests of the Poľana biosphere reserve, Central Slovakia. *Eur. J. For. Res.* 126, 303–313. doi: 10.1007/s10342-006-0149-z
- Hrubý, P., Hejhal, P., Malý, K., Kočár, P., and Petr, L. (2014). *Centrální českomoravská vrchovina na prahu vrcholného středověku*. Brno: Masarykova univerzita.
- Iucn, P. (1994). *Guidelines for Protected Areas Management Categories*. Cambridge, UK; Gland: IUCN. 261.
- Jackson, S. T. (1997). "Documenting natural and human-caused plant invasions using paleoecological methods," in *Assessment and Management of Plant Invasions*, eds J. O. Luken and J. W. Thieret (New York, NY: Springer Verlag), 37–55.
- Janda, P., Trotsiuk, V., Mikoláš, M., Bače, R., Nagel, T. A., Seidl, R., et al. (2017). The historical disturbance regime of mountain Norway spruce forests in the Western Carpathians and its influence on current forest structure and composition. *For. Ecol. Manage.* 388, 67–78. doi: 10.1016/j.foreco.2016.08.014
- Jankovská, M. (2006). *Natural Regeneration and Vegetation Changes in Disturbed Norway Spruce Forests*. dissertation thesis, University of South Bohemia, České Budějovice.
- Knipping, M. (1989). *Zur spät- und postglazialen Vegetationsgeschichte des Oberpfälzer Waldes*. Berlin; Stuttgart: J. Cramer.
- Kozáková, R., Šamonil, R., Kuneš, P., Novák, J., Kočár, P., and Kočárová, R. (2011). Contrasting local and regional Holocene histories of *Abies alba* in the Czech Republic in relation to human impact: evidence from forestry, pollen and anthracological data. *Holocene* 21, 431–444. doi: 10.1177/0959683610385721
- Křenová, Z., and Hruška, J. (2012). Proper zonation – an essential tool for the future conservation of the Šumava National Park European. *Eur. J. Environ. Sci.* 2, 62–72. Available online at: <http://ejes.cz/index.php/ejes/article/view/81/35>
- Kulakowski, D. (2017). The central role of disturbances in mountain forests of Europe. *For. Ecol. Manage.* 388, 1–2. doi: 10.1016/j.foreco.2016.07.034
- Kuneš, P., Abraham, V., Kovářík, O., Kopecký, M., and PALYCZ contributors (2009). Czech quaternary palynological database – PALYCZ: a review and basic statistics of the data. *Preslia* 81, 209–238. Available online at: <http://www.preslia.cz/P093Kunes.pdf>
- Landres, P. B., Morgan, P., and Swanson, F. J. (1999). Overview of the use of natural variability concepts in managing ecological systems. *Ecol. Appl.* 9, 1179–1188.
- Loidi, J., and Fernández-González, F. (2012). Potential natural vegetation: reburial or reboring? *J. Veg. Sci.* 23, 596–604. doi: 10.1111/j.1654-1103.2012.01387.x
- Loidi, J., del Arco, M., Pérez de Paz, P. L., Asensi, A., Díez Garretas, B., Costa, M., et al. (2010). Understanding properly the "potential natural vegetation" concept. *J. Biogeogr.* 37, 2209–2211. doi: 10.1111/j.1365-2699.2010.02302.x
- Málek, J. (1981). Problematik der Ökologie der Tanne (*Abies alba* Mill.) und ihres Sterbens in der ČSSR. *Forest Res.* 100, 170–174. doi: 10.1007/BF02640631
- Manten, A. A. (1967). Lennart von Post and the foundation of modern palynology. *Rev. Palaeobot. Palynol.* 1, 11–22. doi: 10.1016/0034-6667(67)90105-4
- Mazier, F., Gaillard, M.-J., Kuneš, P., Sugita, S., Trondman, A.-K., and Broström, A. (2012). Testing the effect of site selection and parameter setting on REVEALS-model estimates of plant abundance using the Czech Quaternary palynological database. *Rev. Palaeobot. Palynol.* 187, 38–49. doi: 10.1016/j.revpalbo.2012.07.017
- Meyer, T., Kiener, H., and Křenová, Z. (2009). Wild heart of Europe. *Int. J. Wilderness.* 15, 33–40. Available online at: <http://ijw.wpengine.com/wp-content/uploads/2009/04/Dec09-IJW-vol-15-no-3small2.pdf>
- Mikyška, R., Deyl, M., Holub, J., Husová, M., Moravec, J., Neuhäusl R., and Neuhäuslová-Novotná, Z. (1968–1972). *Geobotanická mapa ČSSR 1. České země [Geobotanical map of the ČSSR 1. Czech Lands]*. Praha: Vegetace ČSSR, Ser. A, Academia.
- Müller, F. (1927). Paläofloristische untersuchungen dreier hochmoore des böhmischerwaldes. *Lotos* 75, 53–80.
- National Research Council (2005). *The Geological Record of Ecological Dynamics. Understanding the Biotic Effects of Future Environmental Change*. Washington, DC: National Academy Press.
- Neuhäuslová, Z., Blažková, D., Grulich, V., Husová, M., Chytrý, M., Jeník, J., et al. (1998). *Mapa potenciální Původní vegetace České republiky. Map of potential natural vegetation of the Czech Republic*. Praha: Academia.
- Nožička, J. (1957). *Přehled vývoje našich lesů*. Praha: Státní zemědělské nakladatelství.
- Prentice, I. C. (1985). Pollen representation, source area, and basin size: toward a unified theory of pollen analysis. *Quatern. Res.* 23, 76–86. doi: 10.1016/0033-5894(85)90073-0
- Průša, E. (2001). *Pěstování Lesu na Typologických Základech*. Praha: Lesnická práce. 593.
- R Core Team (2016). *R: A Language and Environment for Statistical Computing*. Vienna: R Foundation for Statistical Computing. Available online at: <https://www.R-project.org/>
- Reimer, P. J., Bard, E., Bayliss, A., Beck, J. W., Blackwell, P. G., Ramsey, C. B., et al. (2013). IntCal13 and Marine13 radiocarbon age calibration curves 0–50,000 years cal BP. *Radiocarbon* 55, 1869–1887. doi: 10.2458/azu_js_rc.55.16947
- Röder, J., Gossner, M. M., and Müller, J. (2010). Anthropol species richness in the Norway Spruce (*Picea abies* (L.) Karst) canopy along an elevation gradient. *For. Ecol. Manage.* 259, 1513–1521. doi: 10.1016/j.foreco.2010.01.027
- Spathef, P., van der Maaten, E., van der Maaten-Theunissen, M., Campioli, M., and Dobrowolska, D. (2014). Climate change impacts in European forests: the expert views of local observers. *Ann. For. Sci.* 71, 131–137. doi: 10.1007/s13595-013-0280-1
- Stalling, H. (1987). *Untersuchungen zur spät- und postglazialen Vegetationsgeschichte im Bayerischen Wald*. Dissertation thesis. Göttingen: Georg-August-University Göttingen.
- Stockmarr, J. (1972). Tablets with spores used in absolute pollen analysis. *Pollen Spores* 13, 614–621.
- Sugita, S. (1994). Pollen representation of vegetation in quaternary sediments: theory and method in patchy vegetation. *J. Ecol.* 82, 881–897. doi: 10.2307/2261452
- Sugita, S. (2007a). Theory of quantitative reconstruction of vegetation I: pollen from large sites REVEALS regional vegetation composition. *Holocene* 17, 229–241. doi: 10.1177/0959683607075837

- Sugita, S. (2007b). Theory of quantitative reconstruction of vegetation II: all you need is LOVE. *Holocene* 17, 243–257. doi: 10.1177/0959683607075838
- Svoboda, M., Fraver, S., Janda, P., Bače, R., and Zenáhlíková, J. (2010). Natural development and regeneration of a Central European montane spruce forest. *For. Ecol. Manage.* 260, 707–714. doi: 10.1016/j.foreco.2010.05.027
- Svoboda, M., Janda, P., Nagel, T. A., Fraver, S., Rejzek, J., and Bače, R. (2012). Disturbance history of an old-growth sub-alpine *Picea abies* stand in the Bohemian Forest, Czech Republic. *J. Veg. Sci.* 23, 86–97. doi: 10.1111/j.1654-1103.2011.01329.x
- Svoboda, M., Janda, P., Bače, R., Fraver, S., Nagel, T. A., Rejzek, J., et al. (2014). Landscape-level variability in historical disturbance in primary *Picea abies* mountain forests of the Eastern Carpathians, Romania. *J. Veg. Sci.* 25, 386–401. doi: 10.1111/jvs.12109
- Svobodová, H., Reille, M., and Goeury, C. (2001). Past vegetation dynamics of Vltavský luh, upper Vltava river valley in the Šumava mountains, Czech Republic. *Veget. Hist. Archaeobot.* 10, 185–199. doi: 10.1007/PL00006930
- Svobodová, H., Soukupová, L., and Reille, M. (2002). Diversified development of mountain mires, Bohemian Forest, Central Europe, in the last 13,000 years. *Quatern. Int.* 91, 123–135. doi: 10.1016/S1040-6182(01)00106-9
- Swetnam, T. W., Allen, C. D., and Betancourt, J. L. (1999). Applied historical ecology: using the past to manage for the future. *Ecol. Appl.* 9, 1189–1206. doi: 10.1890/1051-0761(1999)009[1189:AHEUTP]2.0.CO;2
- Szabó, P., Kuneš, P., Svobodová-Svitavská, H., Švarcová, M. G., Krížová, L., Suchánková, S., et al. (2017). Using historical ecology to reassess the conservation status of coniferous forests in central Europe. *Conserv. Biol.* 31, 150–160. doi: 10.1111/cobi.12763
- Tinner, W., and Lotter, A. F. (2005). Holocene expansion of *Fagus sylvatica* and *Abies alba* in Central Europe: where are we after eight decades of debate? *Quatern. Sci. Rev.* 25, 626–649. doi: 10.1016/j.quascirev.2005.03.017
- Tinner, W., Hubschmid, P., Wehrli, M., Ammann, B., and Conedera, M. (1999). Long-term forest fire ecology and dynamics in the southern Switzerland. *J. Ecol.* 87, 273–289. doi: 10.1046/j.1365-2745.1999.00346.x
- Tinner, W., Colombaroli, D., Heiri, O., Henne, P. D., Steinacher, M., Untenecker, J., et al. (2013). The past ecology of *Abies alba* provides new perspectives on future responses of silver fir forests to global warming. *Ecol. Monogr.* 83, 419–439. doi: 10.1890/12-2231.1
- Vacek, S., and Mayová, J. (2000). “K problematice vegetační stupňovitosti NP Šumava,” in *Monitoring, Výzkum a management ekosystému Národního parku Šumava. Sbor. z Celost. konf. Kostelec nad Černými lesy, 27–28 Listopadu 2000*, eds V. Podrázský, H. Ryšánková, S. Vacek, and I. Ulbrichová (Praha: ČZU), 138–141. Available online at: http://maxbot.botany.pl/cgi-bin/pubs/data/article_pdf?id=393
- van der Knaap, W. O., van Leeuwen, J. F. N., and Ammann, B. (2004). The first rise and fall of *Fagus sylvatica* and interactions with *Abies alba* at Faulenseemoos (Weiss Plateau) 6900–6000 cal yr BP. *Acta Palaeobotan.* 44, 249–266.
- Willis, K. J., and Birks, H. J. B. (2006). What is natural? The need for a long-term perspective in biodiversity conservation. *Science* 314, 1261–1265. doi: 10.1126/science.1122667
- Wright, H. E. Jr. (1967). A square-rod piston sampler for lake sediments. *J. Sediment. Petrol.* 37, 975–976. doi: 10.1306/74D71807-2B21-11D7-8648000102C1865D
- Zeppenfeld, T., Svoboda, M., DeRose, R. J., Heurich, M., Müller, J., Čížková, P., et al. (2015). Response of mountain *Picea abies* forests to stand-replacing bark beetle outbreaks: neighbourhood effects lead to self-replacement. *J. Appl. Ecol.* 52, 1402–1411. doi: 10.1111/1365-2664.12504

Conflict of Interest Statement: The authors declare that the research was conducted in the absence of any commercial or financial relationships that could be construed as a potential conflict of interest.

Copyright © 2018 Carter, Chiverrell, Clear, Kuosmanen, Moravcová, Svoboda, Svobodová-Svitavská, van Leeuwen, van der Knaap and Kuneš. This is an open-access article distributed under the terms of the Creative Commons Attribution License (CC BY). The use, distribution or reproduction in other forums is permitted, provided the original author(s) or licensor are credited and that the original publication in this journal is cited, in accordance with accepted academic practice. No use, distribution or reproduction is permitted which does not comply with these terms.



Temperature Range Shifts for Three European Tree Species over the Last 10,000 Years

Rachid Cheddadi^{1*}, Miguel B. Araújo^{2,3,4}, Luigi Maiorano⁵, Mary Edwards^{6,7}, Antoine Guisan^{8,9}, Matthieu Carré¹, Manuel Chevalier¹ and Peter B. Pearman^{10,11}

¹ Centre National de la Recherche Scientifique, Institut des Sciences de l'Évolution, University Montpellier II, Montpellier, France, ² Departamento de Biogeografía y Cambio Global, Museo Nacional de Ciencias Naturales, CSIC, Madrid, Spain, ³ Center for Macroecology, Evolution and Climate, Natural History Museum of Denmark, University of Copenhagen, Copenhagen, Denmark, ⁴ InBIO-CiBIO, University of Évora, Évora, Portugal, ⁵ Dipartimento di Biologia e Biotechnologie "Charles Darwin," Università di Roma "La Sapienza," Roma, Italy, ⁶ Geography and Environment, University of Southampton, Southampton, UK, ⁷ College of Natural Science and Mathematics, University of Alaska, Fairbanks, AK, USA, ⁸ Department of Ecology and Evolution, University of Lausanne, Lausanne, Switzerland, ⁹ Institute of Earth Science Dynamics, University of Lausanne, Lausanne, Switzerland, ¹⁰ Department of Plant Biology and Ecology, Faculty of Sciences and Technology, University of the Basque Country, UPV/EHU, Leioa, Spain, ¹¹ IKERBASQUE, Basque Foundation for Science, Bilbao, Spain

OPEN ACCESS

Edited by:

Valentí Rull,
Institute of Earth Sciences Jaume
Almera (ICTJA-CSIC), Spain

Reviewed by:

Donatella Magri,
Sapienza University of Rome, Italy
Rüdiger Grote,
Karlsruhe Institute of Technology,
Germany

*Correspondence:

Rachid Cheddadi
rachid.cheddadi@umontpellier.fr

Specialty section:

This article was submitted to
Agroecology and Land Use Systems,
a section of the journal
Frontiers in Plant Science

Received: 09 June 2016

Accepted: 06 October 2016

Published: 25 October 2016

Citation:

Cheddadi R, Araújo MB, Maiorano L,
Edwards M, Guisan A, Carré M,
Chevalier M and Pearman PB (2016)
Temperature Range Shifts for Three
European Tree Species over the Last
10,000 Years.
Front. Plant Sci. 7:1581.
doi: 10.3389/fpls.2016.01581

We quantified the degree to which the relationship between the geographic distribution of three major European tree species, *Abies alba*, *Fagus sylvatica* and *Picea abies* and January temperature (Tjan) has remained stable over the past 10,000 years. We used an extended data-set of fossil pollen records over Europe to reconstruct spatial variation in Tjan values for each 1000-year time slice between 10,000 and 3000 years BP (before present). We evaluated the relationships between the occurrences of the three species at each time slice and the spatially interpolated Tjan values, and compared these to their modern temperature ranges. Our results reveal that *F. sylvatica* and *P. abies* experienced Tjan ranges during the Holocene that differ from those of the present, while *A. alba* occurred over a Tjan range that is comparable to its modern one. Our data suggest the need for re-evaluation of the assumption of stable climate tolerances at a scale of several thousand years. The temperature range instability in our observed data independently validates similar results based exclusively on modeled Holocene temperatures. Our study complements previous studies that used modeled data by identifying variation in frequencies of occurrence of populations within the limits of suitable climate. However, substantial changes that were observed in the realized thermal niches over the Holocene tend to suggest that predicting future species distributions should not solely be based on modern realized niches, and needs to account for the past variation in the climate variables that drive species ranges.

Keywords: Holocene, past climate reconstruction, niche conservatism, *Abies*, *Fagus*, *Picea*

INTRODUCTION

Changes in climate may cause shifts in the geographic distribution of species (Parmesan and Yohe, 2003; Root et al., 2003), increase extinction rates (e.g., Thuiller et al., 2005), and alter provision of ecosystem services (Schröter et al., 2005). Adaptation of human societies to these global changes requires accurate predictions of the future potential distributions of key species, such as

endemic forest trees. Prediction of potential distributions of trees generally involves developing models of the relationship between current climate, distribution, and range dynamics (Guisan and Zimmermann, 2000; García-Valdés et al., 2013), then applying these models to data derived from models of potential future climate. These predictions rely on key aspects of the species climate requirements. In this context, one assumption for predicting species distributions, using niche-based models, is that species occupy all or most suitable geographic areas (Svenning and Skov, 2004). A second necessary assumption for these statistical models is that the species realized environmental niche (Hutchinson, 1957), as determined from empirical observations, remains stable over time, and space, a phenomenon called ecological niche conservatism (Wiens and Graham, 2005; Pearman et al., 2008). The validity of these assumptions remains a matter of contention.

One reason for uncertainty regarding niche conservatism is that species ecological flexibility and/or genetic adaptation can impact the observed degree of conservatism and the accuracy of predicted species distributions. Veloz et al. (2012) find at the generic level that between the late glacial period and today, the realized niches of *Fraxinus*, *Ostrya/Carpinus*, and *Ulmus* shifted substantially while the niches of other taxa, such as *Quercus*, *Picea*, and *Pinus strobus*, remained relatively stable. On the other hand, studies using current climate and species distributions to compare species realized niches between native and invasive ranges indicate that niches tend to remain stable during species invasions, but many exceptions (niche shifts) were also reported (Petitpierre et al., 2012; Guisan et al., 2014; Early and Sax, 2014). Additional studies suggest that over spans of decades or a 100 years, species environmental niches rarely change, but as time scales increase to millions of years, niche lability increases (Peterson, 2011).

The temporal niche lability of tree species may be partly due to adaptive evolutionary processes. Genetic modifications may be observed spatially (Heywood, 1991), however, they seldom develop over relatively short periods such as decades while they easily happen throughout several millennia, such as the Quaternary, with distinct and contrasting climate periods (Davis and Shaw, 2001; Davis et al., 2005). Molecular markers from the nuclear and organelle genomes have allowed reconstruction of the evolutionary history of plant species since the last glacial period (Taberlet et al., 1998; Petit et al., 2003). Using neutral markers, phylogeographic studies show that the modern spatial genetic structure over the range of many temperate tree species originated during the past few millennia (Hewitt, 2000, 2004; Petit et al., 2003). These phylogenetic studies show that there are strong interactions between past climate change, changing species ranges, and genetic constitution. While climate variability during the Holocene period was much reduced compared to the climate transitions between glacial and interglacials, species had to migrate and adapt nonetheless during the post-glacial recolonization process, which may have had an impact on their climate requirements and tolerances. The Holocene seems to be an ideal time period for investigating potential temperature shifts of tree species because (1) its reduced climate variability and relative favorability compared to the glacial period allowed taxa

to migrate to either track climate changes and potentially to adapt and (2) there are more fossil data-sets for species occurrences and past climates than for older Quaternary time periods.

This study uses observational data at the Holocene time scale to investigate whether or not some European tree species remained within their modern temperature range over the last 10,000 years. Obviously, temperature is only one component of the species niche. However, any shift of the modern range/climate relationship would challenge the assumption of niche conservatism. We examine whether January temperatures experienced by *Abies alba*, *Fagus sylvatica*, and *Picea abies* are similar to those experienced over approximately 10,000 years during the Holocene. Substantial changes in realized thermal niches over the last several millennia would demonstrate the difficulty of predicting future range shifts solely based on contemporary realized climatic niches and further reflect on the generality of the assumption of niche conservatism.

MATERIALS AND METHODS

Quantifying Past January Temperature

Studies exploring past changes in species realized niches have done so by relating historical species distributions to climate variables obtained from General Circulation Models (GCMs) (e.g., Pearman et al., 2007; Nogués-Bravo et al., 2008; Maiorano et al., 2013). Changes in these relationships have been studied either in time snapshots [usually 6000 and 21,000 years before present (BP)] or in transient simulations since the last glacial period. Notably, the goal of the simulations that produced the employed paleoclimate data was not to determine past climate but rather to examine distinct GCMs under different forcing conditions through comparison with reconstructed paleoclimate from observed data (i.e., Masson et al., 1999). There remains substantial disagreement among paleoclimate simulations and significant biases compared to observations exist, especially for rainfall (Braconnot et al., 2012), that may limit the suitability of these simulations for determining past climatic niches of species.

Here, we use January temperature (T_{jan}), quantitatively reconstructed over the past 10,000 years in Europe, in recognition of its ecological importance to fulfillment of chilling requirements for budburst and growth (Nienstaedt, 1967; Heide, 1993; Kramer, 1994, 1995; Harrington and Gould, 2015) and the influence of winter temperature on soil temperature, an important factor in determining treeline globally (Körner and Paulsen, 2004). Winter frost may damage needles and wood and, therefore, restrict the range of *A. alba* and *F. sylvatica* in areas where temperature descends below -10°C . *P. abies* is more frost tolerant than *F. sylvatica* and may withstand temperatures down to -17°C . Cold temperatures are a limiting factor for expansion of many tree species in the temperate latitudes, explaining about 80% of the variation in their range sizes (Pither, 2003). Cold temperatures also limit species distributions and diversity along elevation gradients worldwide (Körner and Paulsen, 2004). Furthermore, cold thermal limits of European Holarctic plants may be more conserved than warm limits (Pellissier et al., 2013), thus providing a conservative test for niche changes. Another important abiotic variable for plant species is water

availability as influence by precipitation. Palaeoecological studies show that annual precipitation and its seasonal distribution may have complex interactions with temperature in shaping ecosystems over the long term (Cheddadi and Khater, 2016). In the European temperate zone where *P. abies*, *A. alba*, and *F. sylvatica* occur, temperature is a limiting factor for growth (see i.e., Kramer, 1994 for *F. sylvatica*; Heide (1974) for *P. abies*, and Maxime and Hendrik, 2011 for both *A. alba* and *F. sylvatica*), but precipitation is not. In the present study we have focused on January temperature (T_{jan}) rather than on precipitation as it has a direct impact on the three focal species and its future increase will probably affect these species more than the expected up to 20% increase of annual precipitation (IPCC, 2014).

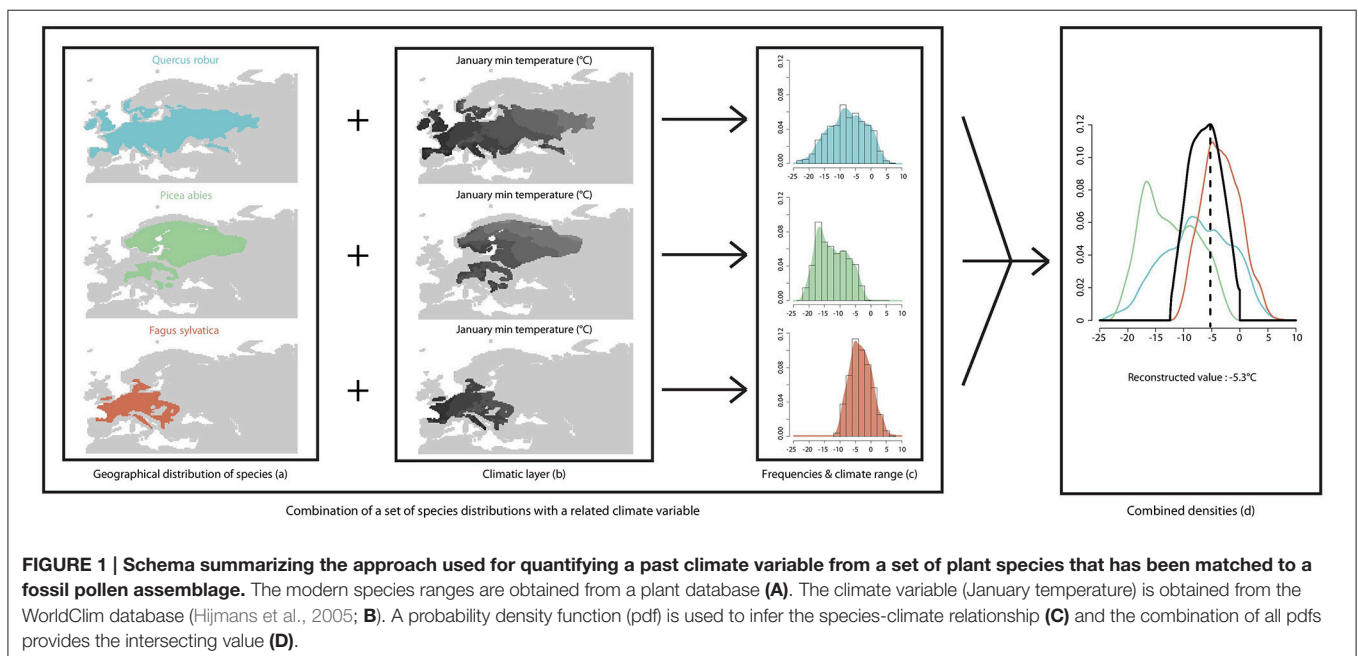
T_{jan} was calculated using fossil pollen records from a network of sediment cores from across Europe, combined with empirical probability density functions of plant taxa identified for the fossil samples, following the method described by Chevalier et al. (2014). Compared to other pollen-based reconstruction methods, this technique avoids the problem related to the lack of analogy between past and modern ecosystems (Jackson and Williams, 2004).

We express taxa-climate relationships (Figure 1) as probability density functions (*pdf*, Kühl et al., 2002) that are obtained from modern species distributions (Figure 1A) and values of the focal climate variable (T_{jan} , Figures 1B,C) in these distributions. Fossil pollen grains are often identified to a genus or a family level which does not allow an accurate identification of the originating species. In order to use the modern species distributions and their related climate, the pdf method requires an assignment of each taxon to a plant species. In the present study we assigned fossil taxa to modern plant species that have the widest climate range and occur in the area. For instance, *Pinus* pollen grains have been assigned to the species *P. sylvestris*

whose geographical range encompasses a wide temperature range. *Pinus* pollen grains cannot be identified to the species level which prevents the distinction between temperate and Mediterranean pines. Assigning a pollen grain to a species that has a restricted range (i.e., *P. pinaster* instead of *P. sylvestris*) would bias the climate reconstruction due to an unjustified reduction of the temperature range of the unknown species. Taxa pdfs (Figure 1D) for T_{jan} were built from a database of 270 georeferenced European plant species from published maps (Jalas and Suominen, 1973; Hultén and Fries, 1986) and from WorldClim 10' gridded, interpolated weather station data for modern climate (1950–2000 period; Hijmans et al., 2005). The instrumental modern climate data-set used in the present study is set within a warming trend that is related to ongoing anthropogenic climate change (IPCC, 2014). Between years 1861 and 2000 global temperature increased by about 0.6°C (Folland et al., 2001). Over a comparable time period (1901–2000), the winter temperature (DJF) in Europe recorded a warming trend of ~0.08°C per decade (Luterbacher et al., 2004), which is slightly higher than the global value. The human-induced temperature increase recorded over the last century (<1°C) has already affected the niche of many plant and animal species (Walther et al., 2002). However, this recent temperature increase is lower than the reconstructed amplitude of temperature change over the Holocene (Davis et al., 2003; Cheddadi and Bar-Hen, 2009).

T_{jan} was calculated from a pollen assemblage of n taxa in a fossil sample “ s ” as the temperature of maximum probability in the intersection of the n pdfs (Figure 1D), as follows:

$$T_{jan}(s) = \operatorname{argmax} \left[\left(\prod_{tax_1}^{tax_n} pdf_{tax_i, T_{jan}}^{W_i(s)} \right) (\sum W_i(s))^{-1} \right]$$



where:

$T_{jan}(s)$ is the reconstructed climate for sample s ;

pdf is the probability density function of plant *taxon* i (tax_i) to *taxon* n (tax_n) for the variable T_{jan} ; n is the number of taxa identified in a sample;

$W_i(s)$ is the weight associated with *taxon* i for sample s determined by the pollen percentage of *taxon* i . Pollen percentages were calculated after removing the pollen counts of the three taxa from the total pollen sum. $argmax$ is the function that returns the value for which a function is maximum.

This phenomenological, statistical method does not account for, or depend on, variation in ecological or environmental processes (competition, phenology, dispersal, or evolutionary adaptation, etc.) or their relative importance in structuring paleocommunities. Similarly, estimated variable values do not depend on or account for values that are estimated for preceding periods.

Average T_{jan} values were calculated for these records to represent fixed time slices every 1000 years (± 250 years). Fossil pollen records were selected from the European Pollen Database (EPD, <http://europeanpollendatabase.net>) for their time resolution and the quality of the associated calibrated age model. Pollen records with less than three radiometric datings or reversed dates were excluded as well as those with a sampling resolution that does not provide a series of at least one sample every 500 years over the covered period of time.

A conceptual difficulty of our climate reconstruction technique lies in its assumption that plant climate envelope is stable, which is what we aim to test. We partially circumvent this issue by excluding observations of the three focal tree species from the data-set used for paleoclimate reconstruction, so that any change in their thermal requirements would not affect the paleoclimate data. In order to evaluate the effect of the exclusion

of the three focal taxa, we computed the difference between T_{jan} reconstructed from a modern pollen data-set and the same pollen data-set excluding the focal three species (Figure 2). In order to estimate the impact of a shift on the reconstructed T_{jan} , we used the Holocene T_{jan} range of the three species in the reconstruction procedure and calculated the difference with T_{jan} based on the full set of species using a modern pollen data-set (Figure 2).

In this preliminary analysis we find that the reconstructed T_{jan} values remain robust to the exclusion of the three focal tree species from the suite of species used to make the climate reconstruction. Other geological or biological indicators of temperature, such as isotope ratios or chironomid flies, might be considered independent climate proxies, their sparse geographical distributions unfortunately do not allow for spatial climate gridding at the extent of the European continent. Moreover, complete independence of these potential proxies with terrestrial vegetation is unlikely. Similarly, data from GCM simulations of past climates have cryptic dependencies with plant distributions because of the need to specify boundary conditions that depend on vegetation albedo, biomass distribution, and the carbon cycle.

The T_{jan} values obtained in fossil records were spatially interpolated for each time slice (10 to 3 ka) over Europe onto a 0.5° longitude \times 0.5° latitude grid using universal kriging (R gstat package, Pebesma, 2004). The interpolated T_{jan} was then mapped as a smoothed surface using a spherical surface spline in tension (Smith and Wessel, 1990) within the generic mapping tools (GMT, Wessel et al., 2013; Figures 3A,B).

The number of time series from which T_{jan} is obtained increases from 10 to 3 ka, which may potentially affect the comparison of the estimated T_{jan} range through time. A similar issue has been raised and statistically tackled by weighting the

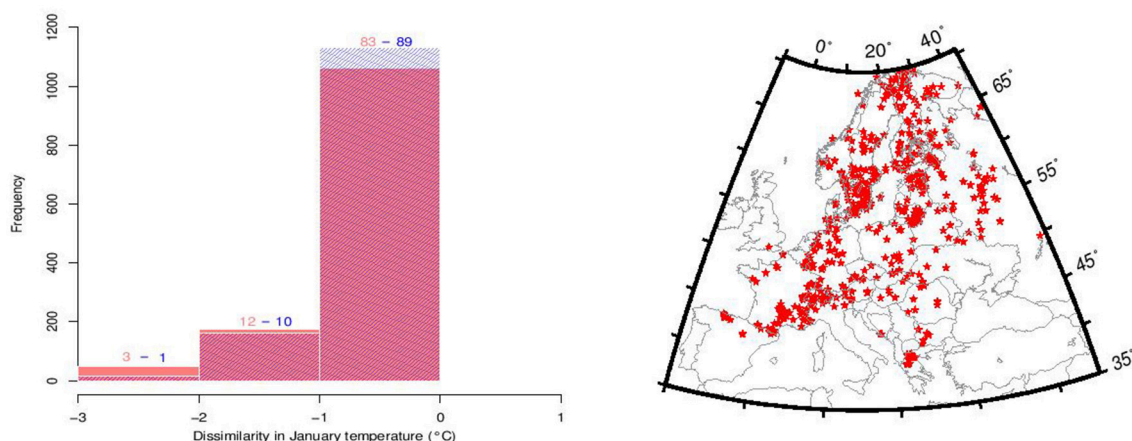


FIGURE 2 | Evaluation of the impact of *Abies alba*, *Fagus sylvatica*, and *Picea abies* and their Holocene thermal niche shift on the reconstructed T_{jan} values using dissimilarity between the modern T_{jan} (WorldClim, Hijmans et al., 2005) and (1) reconstructed T_{jan} from a data-set of 1132 modern pollen samples from which the three species were excluded (red histograms) and (2) the same modern pollen data-set including the three species but using their overall Holocene T_{jan} range (blue histograms) based on reconstructed T_{jan} between 10 and 3 ka (see Figure 3). Numbers over the histograms correspond to the percentages of pollen samples that deviate from 0. Between 83 and 89% of the reconstructed T_{jan} deviate by less than 1°C to the observed T_{jan} values from WorldClim (Hijmans et al., 2005). The map in the right panel shows the location of the modern pollen samples used for the dissimilarity analysis.

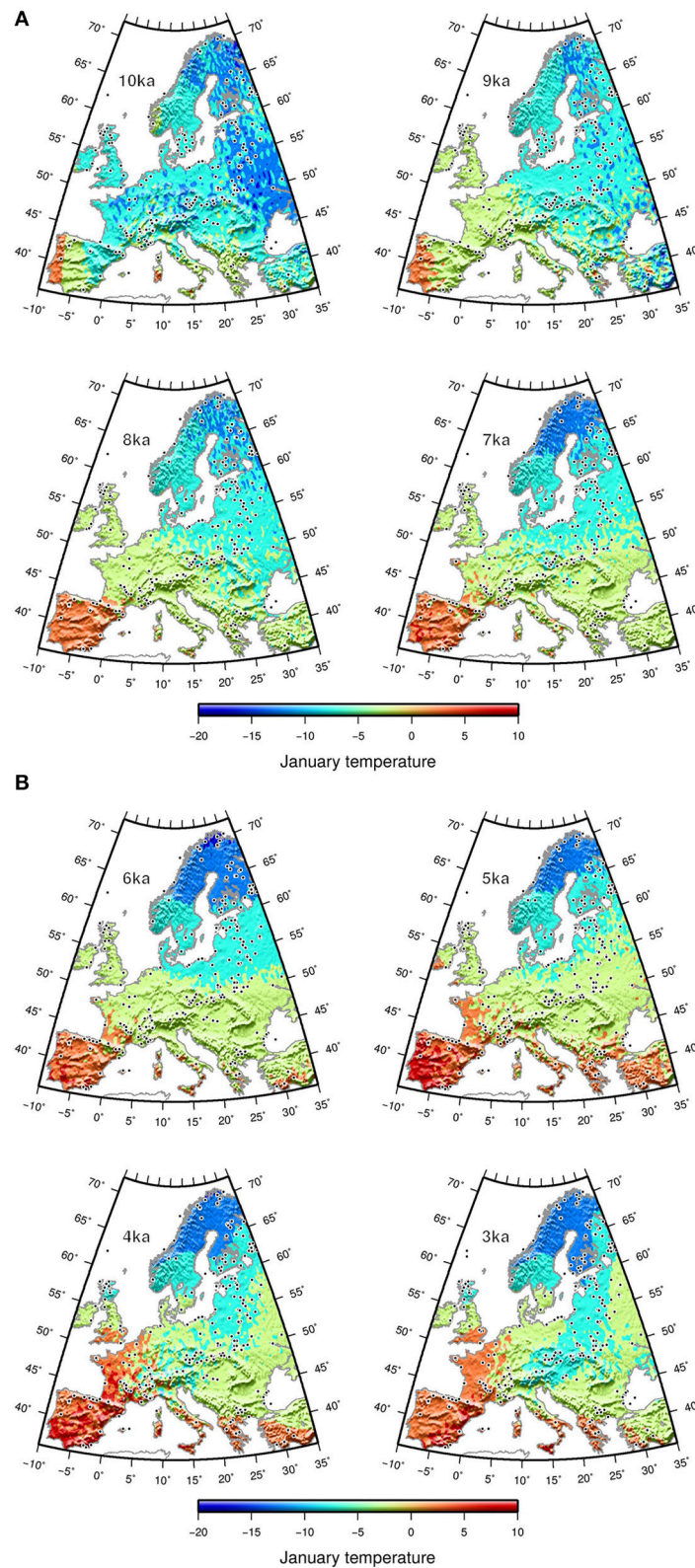


FIGURE 3 | Interpolated reconstructed mean January temperature (A) from 10 to 7 ka and (B) from 6 to 3 ka from fossil pollen data (black dots).

observed temperature values by the availability of climate over a gridded geographical space (Broennimann et al., 2012). The method in the latter work is not directly applicable to our data since these are non-gridded temperature values that are determined by the location of pollen cores and the age of samples. Therefore, we cannot project species range between 10 and 3 ka to a standardized climate space. However, we were able to generate an analogous normalization of the distribution of temperature by weighting each observation by a proportion that represented occupation of similar climate space, which we present for *Picea* at 10 ka, 3 ka, and today as an example (Figure 4). We weighted the reconstructed Tjan values by the relative frequencies of observations in relation to all cores with similar temperature values. Similar temperatures were determined by binning temperature values corresponding to all cores that represented a particular time slice. This normalization still integrates an unavoidable potential bias that is related to the availability of pollen cores in the Tjan gridded space in each bin.

Recovering Past Species Ranges

We reconstructed the past geographic distributions of *A. alba*, *F. sylvatica*, and *P. abies* at each time period using macrofossil data and pollen data. These species are ideal case studies because (1) they represent dominant arboreal species in Europe, and (2) they can be identified with a high degree of confidence to species in the fossil record. Unlike many other genera, *Abies*, *Fagus*, and *Picea* each has one dominant species in Europe, substantially reducing potential errors in the identification of fossil pollen taxa.

We restricted this study to the period prior to 3 ka to avoid human disturbances that strongly impacted European forests in the recent millennia (Kaplan et al., 2009). Therefore, changes observed in distributions of taxa in the past are primarily the result of climate change and ecological processes. The macrofossil data used for identifying species occurrences were obtained from published data-sets (*F. sylvatica*, Magri et al., 2006; *A. alba*, Terhürne-Berson et al., 2004 and *P. abies*, Latalowa and Van Der Knaap, 2006). Occurrences from pollen data were obtained from the EPD using a threshold of pollen percentage of 1% for detection of the three taxa. Since neither macroremains nor pollen of these three taxa were used for paleoclimate reconstructions, we assumed that the reconstructed geographic distributions are independent of the climate variables.

Recovering January Temperature Range for Each Species

The extent to which the distribution of Tjan values obtained from fossil data reliably represents the thermal range of a species depends on sample size and geographical distribution. The coring sites are reasonably well distributed over the whole of Europe, but the number of sites where occurrences are observed decreases between 3 and 10 ka. The sample size ranges from 375 at 3 ka for *P. abies*, to 12 at 10 ka for *A. alba* (Table 1) because the geographic distributions of European trees, including the focal three species, were dramatically reduced during glacial times and expanded progressively throughout Europe during the Holocene. As a result, species thermal ranges may be less accurately represented at 10 ka, which corresponds to early post-glacial recolonization.

We estimated the uncertainty related to random spatial sampling and to sample size using a Monte Carlo simulation. The modern spatial distribution of the focal species was randomly sampled to extract a Tjan distribution with the same sample sizes as available in the fossil data. Standard errors for Tjan medians were obtained after 1000 iterations and represented as error (Figure 5). The sampling uncertainty associated with Tjan medians was lower than 1°C for the three species at all time periods.

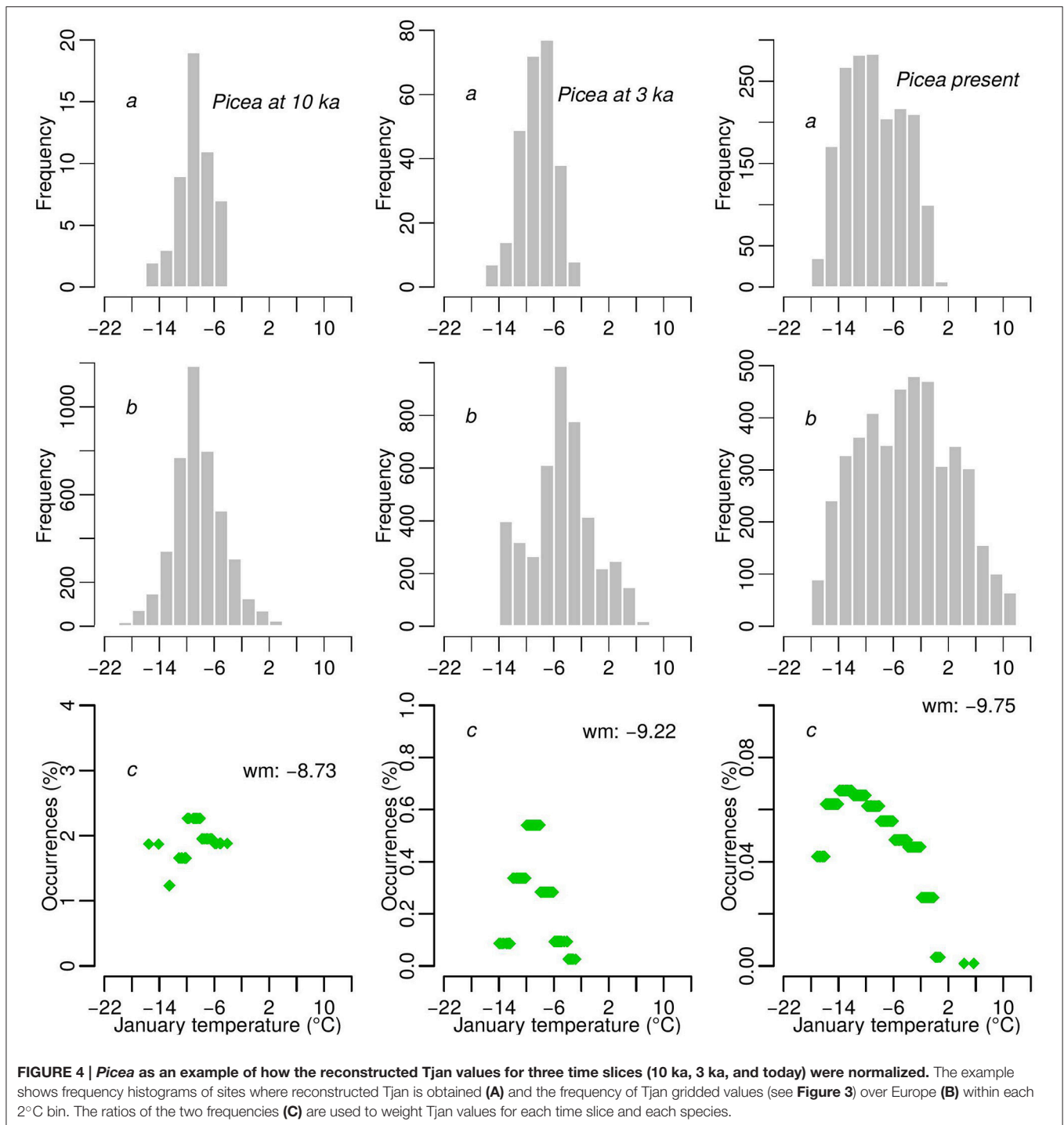
Several issues exist regarding the reconstruction of species past occurrences from fossil data. In general, fossil records allow the identification of *in situ* presence of a species, but tell less about whether the species was effectively absent. Undetected (thus probably small or sparse) populations may occur at a given site but be “silent” in the fossil record (e.g., trees not producing pollen; Hicks, 2006). Also, since tree plant species have different dispersal capacities, long generation time and their propagules may travel considerable distances from parent trees, it is generally accepted that there is “an inevitable time lag between the establishment of seedlings and the maturation of the trees to the stage that they are able to produce pollen” (Hicks, 2006). Reconstructions of broad-scale Holocene vegetation changes, including *Fagus* (Huntley et al., 1989), suggest that the bioclimatic response exhibits only a minor time lag. Although Svenning et al. (2008) argue that the expansion in Europe was delayed by several centuries, Tinner and Lotter (2006) conclude that, due to efficient animal dispersers, the lag was probably of minor importance in the overall postglacial migration process. To address both these issues, we considered that a species was present when it occurred within a broad time window of ± 250 years. In such a window, the potential time lag between the first arrival of many European tree species at a site and the establishment of a substantial population should be barely detectable (Tinner and Lotter, 2006).

RESULTS

Reconstructed January Temperature

The Tjan values reconstructed in the occupied grid cells yield frequency distributions of Tjan for each species at each time period, allowing us to estimate changes in the thermal range of the three species (Figure 5). Tjan distributions (Figures 5A–C) are generally not normal (Shapiro test, $p < 0.05$) and, thus, they are represented by their medians and the 0.25 and 0.75 quartiles. This interval corresponds to the core range of the species environmental distribution. The significance of differences between past and modern median Tjan values are derived from non-parametric Wilcoxon tests (Table 1).

Discarding the three taxa from the modern plant data-set to quantify Tjan does not affect significantly the reconstructed temperature values (Figure 2). About 83% of the values deviate with less than 1°C, while about 95% deviate less than 2°C in the negative values (Figure 2). More than 99% of the reconstructed positive values deviate by less than 1°C. In a test of temperature reconstruction in the reciprocal direction, use of the Tjan range from the Holocene to quantify modern Tjan values results in 89% of the values deviating less than 1°C and 99% of values less than 2°C when negative (Figure 2). These two dissimilarity tests show



(1) that the reconstruction method is robust and, therefore, that the reconstructed T_{jan} values are reliable and (2) that using a T_{jan} range of *P. abies*, *F. sylvatica*, and *A. alba*, as obtained for each species between 10 and 3 ka (Figure 5), to quantify T_{jan} has a very minor effect on the reconstructed values. This effect impacts mostly, if not exclusively, the reconstructed negative T_{jan} values.

The interpolated reconstructed T_{jan} values show T_{jan} ubiquitously lower than 10°C until 7 ka. Early warming ($T_{jan} > 0^\circ\text{C}$) in Europe first took place in the SW part of Europe (Iberian Peninsula), with a gradient of more than 10°C developing toward NE Europe (Figures 3A,B). Subsequently, warmer winters developed over southern Europe, a change corresponding to the onset of “Mediterranean” climate, with dry

TABLE 1 | Comparison of the medians of the reconstructed Tjan at different time slices in the past (10 to 3 ka and the full range as well) for each species with their modern range.

Time slices (ka)	<i>Picea abies</i>				<i>Fagus sylvatica</i>				<i>Abies alba</i>				Sites
	<i>p</i> -value	<i>p</i> -value (<i>w</i>)	OCC	SE	<i>p</i> -value	<i>p</i> -value (<i>w</i>)	OCC	SE	<i>p</i> -value	<i>p</i> -value (<i>w</i>)	OCC	SE	
10	0.86	0.7993	60	0.98	<10e-05	<10e-05	16	0.98	0.0033	0.0015	12	0.8	526
9	<10e-05	<10e-05	113	0.83	<10e-05	<10e-05	25	0.9	0.0003	<10e-05	27	0.68	596
8	<10e-05	<10e-05	155	0.75	<10e-05	<10e-05	40	0.82	0.3958	0.9483	57	0.59	639
7	<10e-05	<10e-05	186	0.7	<10e-05	<10e-05	73	0.76	0.7726	0.8620	93	0.53	671
6	<10e-05	<10e-05	247	0.66	<10e-05	<10e-05	110	0.7	0.0277	0.0564	110	0.48	706
5	<10e-05	<10e-05	294	0.62	0.0012	0.0019	136	0.66	0.0027	0.0060	130	0.45	764
4	<10e-05	<10e-05	335	0.59	<10e-05	<10e-05	185	0.62	0.2194	<10e-05	140	0.42	792
3	<10e-05	<10e-05	375	0.57	<10e-05	<10e-05	208	0.59	0.1741	0.0022	146	0.4	805
10–3 range	<10e-05	<10e-05			<10e-05	<10e-05			0.1995	0.2346			

We present Wilcoxon tests (*p*-value) and estimation of the standard error (SE) related to the number of sites where occurrences (OCC) are identified for the three studied species. Since the Tjan medians of all time slices (*n* = 9) for the three species have been compared to the same one (present), the *p*-value (α = 0.05) has been adjusted to α/n = 5.6e-3 in accordance with the Bonferroni criterion. The bold *p*-values are significant at this corrected threshold. *P*-value and *p*-value (*w*) correspond to the Wilcoxon test, with unweighted and weighted Tjan values respectively (see **Figure 4**).

summers and frost-free winters. Mountainous and other areas lacking pollen data may exhibit stronger interpolation deviation, potentially resulting in low Tjan values, such as those in Sicily and the Peloponnese area at 9 ka. The longitudinal gradient of the Early Holocene switched to a latitudinal gradient after 7 ka and remained so until 3 ka. The Tjan difference between the Mediterranean region and northern Scandinavia after 6 ka was as high as 15–20°C. This latitudinal distribution of Tjan across Europe seems to have persisted until today.

January Temperature Range of Focal Species

The overall Tjan range within all the areas recolonized during the Holocene by *P. abies* lies between approximately –16°C and 7°C while the modern range is between –16°C and slightly less than 6°C (**Figure 5A**). The Tjan at which *P. abies* populations are frequent today (the inter-quartile range) are about 3.5°C colder than at 5 ka, when *P. abies* occupied areas that tended to be relatively warm (**Figure 5A**). The recolonization of most of Scandinavia by *P. abies* took place after 4 ka (Tollefsrud et al., 2008), which explains the strong shift of the Tjan range toward lower values.

Unlike *Picea*, the main European *Fagus* populations today occupy, on average, warmer areas than at any time during the Holocene (**Figure 5B**). Nonetheless, half of the frequently occupied temperature range of the modern period overlaps with temperatures also occupied areas in the Holocene. We observe that during the early recolonization process (at 10 and 9 ka), *Fagus* populations occurred in areas with Tjan values that were generally lower than at other times during the Holocene. In contrast to *P. abies* and *F. sylvatica*, *A. alba* occurs in areas that are within its Holocene Tjan range (**Figure 5C**). Today the geographical range of the species spans a less extended temperature range than during the Holocene.

The Wilcoxon tests (**Table 1**) show that the medians of *P. abies* and *F. sylvatica* Tjan range differ substantially between modern values and those of the period 10 and 3 ka. This indicates shifts of

the thermal range of these two species between the Holocene and today. The thermal range for *A. alba* was significantly different from that of today during some periods but not in the overall Holocene range (**Table 1**, **Figure 5C**).

DISCUSSION

The use of observed data from fossil records instead of data from model simulations to evaluate the relationship between past species ranges and climate is a challenging issue. First, data on past climate and on species distributions should originate from two independent data-sets and both should have a spatial coverage that minimizes errors of spatial interpretation. Second, the methods for identifying species, recovering their past occurrences and reconstructing their contemporaneous climate values from different proxies should be accurate, reproducible, and have little error. Over the past decades, pollen data have proven to be excellent proxies for the reconstruction of past species distributions (Huntley and Birks, 1983) as well as past climates (Prentice et al., 1991). However, using fossil pollen data to evaluate the relationship between a species occurrence and any climate variable through time requires two important assumptions: First, fossil pollen data represent an image of an ecosystem that is in equilibrium with contemporaneous climate. Second, the observed changes in the past ecosystems are a result of individualistic responses of taxa to climate (Webb, 1986).

Paleoecologists also assume that species evolution is a slow process over the late-Quaternary because fossil data do not provide information on species genetic adaptation to changing climate but rather on species persistence *in situ*, their range expansion/contraction through migration and their extinction (Davis et al., 2005). Fossil pollen assemblages represent a static image of their originating ecosystem, one that prevents evaluating the level of competition between taxa. In the present study, we considered these fossil data as an instantaneous record of that species that occurred in various past ecosystems, each of which occupied portions of a common climate space.

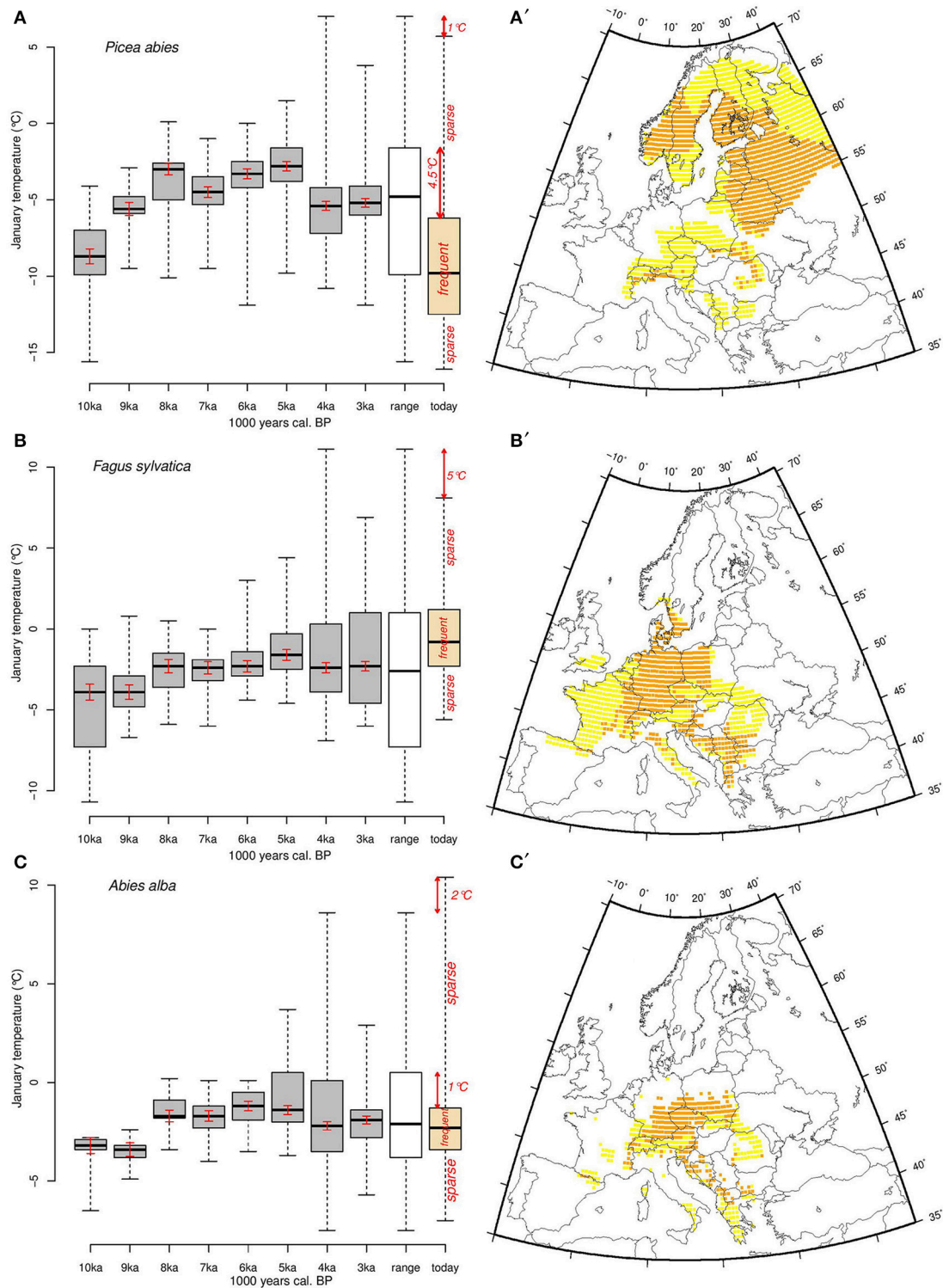


FIGURE 5 | Thermal amplitude of (A) *Picea abies*, (B) *Fagus sylvatica*, and (C) *Abies alba* for each 1000-year time slice between 10,000 and 3000 years cal. BP (gray boxplots), the Holocene overall (white boxplots), and the modern (orange boxplots) ranges, respectively. The black line is the median, the boxes represent the first and third quartiles (25 and 75th quartiles, respectively), and the whiskers represent the minimum and the maximum Tjan range. We consider the boxes and the whiskers as the Tjan ranges where populations are frequent and sparse, respectively. Red arrows indicate differences between current limits of Tjan distribution and those over the Holocene. Maps show today's areas of *Picea abies* (A'), *Fagus sylvatica* (B'), and *Abies alba* (C') where Tjan values correspond to the range between the first and third quartiles (orange, corresponding to areas where the species are most abundant) and more extreme values (yellow). The red bars inside the boxes correspond to the estimated uncertainty related to random spatial sampling and to sample size in Monte Carlo simulations.

Our results demonstrate that within Holocene ecosystems, the thermal ranges of *P. abies* and *F. sylvatica* differ significantly from the corresponding modern ones. These two species currently occur in areas where *Tjan* is either warmer (*F. sylvatica*) or cooler (*P. abies*) than the occupied regions of the Holocene. Conversely, *A. alba* is roughly within the same thermal range as during most of the Holocene. The finding that the thermal ranges of two species have varied during the Holocene is partially consistent with previous studies that used modeled Holocene temperatures (Maiorano et al., 2013).

Discrepancies between modeled distributions and ones observed in data on fossil material (e.g., Pearman et al., 2008) may be partially explained by the relationship between the numerical abundance and geographic distributions of species, which is a matter of continuing debate. The traditional view is that species are most abundant near their geographic range center and less so toward their range edge (Brown, 1984). However, when considering the geographic distribution of species based on their environmental niche (i.e., the niche-biotope duality, see Guisan et al., 2014), findings are less conclusive for the hypothesis that species should be most abundant at the center of their environmental distribution (Sexton et al., 2009). Here, in close analogy to abundance, we consider frequency of occurrence along a climate gradient, rather than in geographical space. Thus, we treat the *Tjan* median value of each tree species as the point of greatest frequency of population abundance.

Today *P. abies* is at its greatest abundance in areas where *Tjan* is between ca. -12 and -6°C (1st and 3rd quartiles, **Figures 5A,A'**). Assuming adequate plasticity and genetic variation, populations in these areas may potentially withstand a *Tjan* increase of about 4.5°C *in situ* (**Figure 5A**), while a similar temperature increase may have greater effects on populations that grow at the upper *Tjan* limit (mainly from Romania to the Dalmatian coast). The 1°C difference between the Holocene ranges and the modern one is not significant if we take into account the standard error related to the potential bias linked to the distribution of past species occurrences (**Table 1** and **Figure 5**). However, an increase of *Tjan* may have greater effects on *Picea* populations at the warm (southern) edge of the species range than on climatically central populations.

Fagus populations are frequent nowadays in areas where *Tjan* is between ca. -2.5 and 1.5°C (inter-quartile range, **Figures 5B,B'**), but currently occur infrequently in areas with *Tjan* values that are 5°C lower than those observed during the Holocene (**Figure 5B**). Unlike *P. abies*, *F. sylvatica* populations frequently occur today in areas that have *Tjan* values that are as high as those of the Holocene. Such thermal range occupancy suggests that, where it is frequent today, *Fagus* will likely be threatened by increasing temperature, while the sparse populations that occur at the cold edge of the distribution may withstand an increase of *Tjan* of up to 5°C . *F. sylvatica* is more sensitive to cold winter temperature and spring frost than *P. abies*, so climate warming may promote its expansion into areas where the range of the two taxa overlap, such as southern Sweden and/or potentially in the mid to high elevations in Poland and the Carpathians. Simulations for the next century show that *F. sylvatica* may have to migrate further north

while experiencing a loss of up to 29% of its current habitat (Kramer et al., 2010). This projection may well be valid since populations are most frequently located in areas that are at the highest *Tjan* values observed in the Holocene thermal range (**Figure 5B**). Furthermore, the species migration rate ($100\text{--}250\text{ m.yr}^{-1}$) estimated by Tinner and Lotter (2006) is lower than the velocity of the expected temperature change ($\sim 800\text{ m.yr}^{-1}$) for the temperate deciduous biome (Loarie et al., 2009). Nonetheless, the magnitudes of these velocities are highly dependent on the resolution of the underlying climate data-sets (Dobrowski et al., 2013).

The patterns shown by *A. alba* differ from those of *P. abies* and *F. sylvatica*. Unlike the other two species, the full modern *Tjan* range of *A. alba* is at its greatest extent since the early Holocene (**Figure 5C**). However, the most frequent populations occupy a much narrower *Tjan* range (ca. -3.5 to -1.5°C , **Figures 5C,C'**) than during the Holocene (ca. -4 to $+0.5^{\circ}\text{C}$), which suggests these environmentally central populations may be able to withstand a somewhat wider temperature range than they currently experience (**Figure 5C**). Conversely, there are sparse *A. alba* populations today that experience *Tjan* as high as $+10^{\circ}\text{C}$, which is about 2°C higher than for any known Holocene population (**Figure 5C**). Thus, the modern populations at the warmer end of the species distribution (Mediterranean mountains) may be threatened by further climate warming. While ecological niche models suggest that *A. alba* currently occupies less than 50% of its potential range (Svenning and Skov, 2004), our results suggest, in contrast, that this species currently occupies its full thermal range, and that the distribution of the populations within that thermal range may change as *Tjan* increases. This may occur through latitudinal migration, simple expansion of population density within other areas of the modern distribution (but without any further geographical expansion; see Figure 1E in Guisan et al., 2014), or expansion to fill sparsely and unevenly populated areas. The discrepancy with Svenning and Skov (2004) may be related to potential deviations during the interpolation of their climate data set, or the particular modeling algorithm they employ.

Ecological modelers and palaeoecologists both aim to address a crucial question: will major tree species withstand on-going global warming *in situ* (because they can tolerate a wider temperature range than what they currently encounter), migrate to areas that acquire suitable conditions, or simply decline. Species modeling approaches suggest that the impact of future climate change will be substantial in Europe (Thuiller et al., 2005). On the other hand, some fossil-based distribution data, such as for *A. alba*, suggest little risk will arise with climate warming (Tinner et al., 2013). In contrast, a recent palaeoecological study (Seppä et al., 2015) shows that the range of hazel (*Corylus avellana*) previously expanded about 4° northward from its current geographical limit in Fennoscandia as a response to a temperature increase of 2.5°C during the mid-Holocene, constituting an increase similar to some projections for response to on-going climate change. Species responses to climate warming may vary substantially and, thus, require focused study. While we concentrated on three tree species because of the direct correspondence between fossil pollen

taxa (identified to genus) and species-level identification (e.g., compared to the 22 European species *Quercus* that produce indistinguishable pollen), one might expect that the thermal ranges of additional tree species may have been different in the past. Additional gridded proxy data, other than pollen, as well as identification of fossil taxa using ancient DNA (Parducci and Petit, 2004) will be needed to address this issue.

Evaluating the climatic limits of species distributions through time is a key issue to understanding species responses to future climate change. Extended data-sets, such as those arising from fossil pollen, are sufficient for reconstructing past geographical distributions of many taxa and for estimating important climate variables. However, they do not contain any information about the adaptive evolution of species over the period of interest (i.e., the Holocene). When assessing the relationship between past species distributions and climate change, paleoecologists tend to assume that ecological responses, such as range shifts, migration rates, and recolonization, are the dominant processes that impact observed species distributions (Huntley et al., 1989; Huntley and Webb, 1989). However, other biotic responses such as phenotypic plasticity and genetic adaptation were also important during the Quaternary (Davis and Shaw, 2001). While evolutionary rates are likely slower than rates of ecological response to climate change, at least during the late Quaternary, promising developments in ancient DNA technology (Giguët-Covex et al., 2014) may help to determine whether or not species genetically adapted to past climate change.

Fossil records may indicate on-going and successful accommodation to climate when a species range remains in dynamic equilibrium with temperature over time (at least during the late-Quaternary period; Davis and Shaw, 2001). The assumption that species distributions in the past (or today) are at equilibrium with their contemporary climate has yet to be demonstrated. If species are not at equilibrium with climate, then there may be little justification to expect stasis in realized niches through space and time (Araújo and Peterson, 2012). Based on observed data, Araújo and Pearson (2005) suggest that assemblages of plants and breeding birds are closer to equilibrium with climate than other organisms and, therefore, their future ranges may be well predicted by niche-based models. Recent work based on fossil data, however, suggests significant potential disequilibrium between vegetation and climate at both leading and trailing edges of species ranges (Svenning and Sandel, 2013). This apparent disequilibrium arises in part from the estimated time lag of the response of individual species ranges to post-glacial warming (Webb, 1986). Thus, strong differences among species in the degree of distribution equilibrium may occur due to varying dispersal abilities, competition with other species, soil conditions, and other factors that may affect the ability of species distributions to track changing climate.

CONCLUSIONS

Modeling approaches are necessary to project how species distributions could change in the future. Here we show that fossil data provide valuable information on how temperature

changes might affect different parts of the range of a species in different ways. We demonstrate how fossil data can complement data on contemporary species distributions to provide valuable information on species tolerances to climate variation. Our results reveal changes in the thermal ranges of the three species with respect to an influential climate variable over the past 10,000 years. The results further suggest that differing impacts of future climate warming, depending on the density (sparsity) of populations. In parallel with approaches based on climate models, data on past species occurrences and reconstructed climates derived from them can provide independent estimates of whether species can cope with climate change and, potentially, what parts of their distributions will be the most threatened.

Nevertheless, the past reconstructions need to be constrained by an evaluation of the infra-specific adaptive ability of species, their dispersal capacity, their interspecific competitive ability, and the ecophysiological relationship of each species to different climate variables. Moreover, one climatic variable such as Tjan, may be considered as restrictive for evaluating the ranges of other species than our focal species. Therefore, other additional climate variables are necessary to better define the climatic niche of most plant species and their potential adaptive capacity through time. Water availability, through the annual amount of precipitation and its seasonal distribution, is a key variable for species spread, their persistence and populations expansion. Without an evaluation of these variables, the question remains as to whether a species is capable of withstanding a wider climatic range than that occupied currently and, thus, has portions of the full thermal range that remain unoccupied.

AUTHOR CONTRIBUTIONS

RC performed all data analysis, programming, computational work, figures, and tables and has written the original manuscript. PBP has improved several versions of the manuscript and contributed substantially, in a decisive way to its final version. MCa contributed to improving many statistical aspects of the study and particularly to estimating the errors through the Monte-Carlo simulations. MCh contributed to improving the climate reconstruction method. All co-authors have contributed to designing the study and refining its objectives in the frame of the EU ECOCHANGE project. MA, LM, ME, AG, MCa, and PBP have contributed to improving the manuscript at different stages.

ACKNOWLEDGMENTS

This work was funded by the EU ECOCHANGE project (Contract No. 066866 GOCE granted to AG, MA, ME, and RC). The original pollen data used in the present study were obtained from the European Pollen Database (<http://www.europeanpollendatabase.net>). We thank N. Zimmermann for helpful discussion throughout the project and especially during the Bonn meeting. This is ISEM contribution number 2016–206.

REFERENCES

- Araújo, M. B., and Pearson, R. G. (2005). Equilibrium of species' distributions with climate. *Ecography* 28, 693–695. doi: 10.1111/j.2005.0906-7590.04253.x
- Araújo, M. B., and Peterson, A. T. (2012). Uses and misuses of bioclimatic envelope modelling. *Ecology* 93, 1527–1539. doi: 10.1890/11-1930.1
- Braconnot, P., Harrison, S. P., Kageyama, M., Bartlein, P. J., Masson-Delmotte, V., Abe-Ouchi, A., et al. (2012). Evaluation of climate models using palaeoclimatic data. *Nat. Clim. Change* 2, 417–424. doi: 10.1038/nclimate1456
- Broennimann, O., Fitzpatrick, M. C., Pearman, P. B., Petitpierre, B., Pellissier, L., Yoccoz, N. G., et al. (2012). Measuring ecological niche overlap from occurrence and spatial environmental data. *Global Ecol. Biogeogr.* 21, 481–497. doi: 10.1111/j.1466-8238.2011.00698.x
- Brown, J. H. (1984). On the relationship between abundance and distribution of species. *Am. Nat.* 124, 255–279. doi: 10.1086/284267
- Cheddadi, R., and Bar-Hen, A. (2009). Spatial gradient of temperature and potential vegetation feedback across Europe during the late Quaternary. *Clim. Dyn.* 32, 371–379. doi: 10.1007/s00382-008-0405-7
- Cheddadi, R., and Khater, C. (2016). Climate change since the last glacial period in Lebanon and the persistence of Mediterranean species. *Q. Sci. Rev.* 150, 146–157. doi: 10.1016/j.quascirev.2016.08.010
- Chevalier, M., Cheddadi, R., and Chase, B. M. (2014). CREST (Climate REconstruction Software): a probability density function (PDF)-based quantitative climate reconstruction method. *Clim. Past* 10, 2081–2098. doi: 10.5194/cp-10-2081-2014
- Davis, M. B., and Shaw, R. G. (2001). Range shifts and adaptive responses to Quaternary climate change. *Science* 292, 673–679. doi: 10.1126/science.292.5517.673
- Davis, B. A. S., Brewer, S., Stevenson, A. C., Guiot, J., and Contributors, D. (2003). The temperature of Europe during the Holocene reconstructed from pollen data. *Q. Sci. Rev.* 22, 1701–1716. doi: 10.1016/S0277-3791(03)00173-2
- Davis, M. B., Shaw, R. G., and Etterson, J. R. (2005). Evolutionary responses to changing climate. *Ecology* 86, 1704–1714. doi: 10.1890/03-0788
- Dobrowski, S. Z., Abatzoglou, J., Swanson, A. K., Greenberg, J. A., Mynsberge, A. R., Holden, Z. A., et al. (2013). The climate velocity of the contiguous United States during the 20th century. *Glob. Change Biol.* 19, 241–251. doi: 10.1111/gcb.12026
- Early, R., and Sax, D. F. (2014). Climatic niche shifts between species' native and naturalized ranges raise concern for ecological forecasts during invasions and climate change. *Global Ecol. Biogeogr.* 23, 1356–1365. doi: 10.1111/geb.12208
- Folland, C. K., Rayner, N. A., Brown, S. J., Smith, T. M., Shen, S. S. P., Parker, D. E., et al. (2001). Global temperature change and its uncertainties since 1861.pdf. *Geophys. Res. Lett.* 28, 2621–2624. doi: 10.1029/2001GL012877
- García-Valdés, R., Zavala, M. A., Araújo, M. B., and Purves, D. W. (2013). Chasing a moving target: projecting non-equilibrium tree species responses to climate change. *J. Ecol.* 101, 441–453. doi: 10.1111/1365-2745.12049
- Giguët-Coxev, C., Pansu, J., Arnaud, F., Rey, P. J., Griggo, C., Gielly, L., et al. (2014). Long livestock farming history and human landscape shaping revealed by lake sediment DNA. *Nat. Commun.* 5, 1–7. doi: 10.1038/ncomms4211
- Guisan, A., Petitpierre, B., Broennimann, O., Daehler, C., and Kueffer, C. (2014). Unifying niche shift studies: insights from biological invasions. *Trends Ecol. Evol.* 29, 260–269. doi: 10.1016/j.tree.2014.02.009
- Guisan, A., and Zimmermann, N. E. (2000). Predictive habitat distribution models in ecology. *Ecol. Model.* 135, 147–186. doi: 10.1016/S0304-3800(00)00354-9
- Harrington, C. A., and Gould, P. J. (2015). Tradeoffs between chilling and forcing in satisfying dormancy requirements for Pacific Northwest tree species. *Front. Plant Sci.* 6, 1–12. doi: 10.3389/fpls.2015.00120
- Heide, O. M. (1974). Growth and dormancy in Norway spruce ecotypes (*Picea abies*) I. Interaction of photoperiod and temperature. *Physiol. Plant.* 30, 1–12. doi: 10.1111/j.1399-3054.1974.tb04983.x
- Heide, O. M. (1993). Dormancy release in beech buds (*Fagus sylvatica*) requires both chilling and long days. *Physiol. Plant.* 89, 187–191. doi: 10.1111/j.1399-3054.1993.tb01804.x
- Hewitt, G. (2000). The genetic legacy of the Quaternary ice ages. *Nature* 405, 907–913. doi: 10.1038/35016000
- Hewitt, G. M. (2004). Genetic consequences of climatic oscillations in the Quaternary. *Philos. Trans. R. Soc. Lond. Ser. B Biol. Sci.* 359, 183–195. doi: 10.1098/rstb.2003.1388
- Heywood, J. S. (1991). Spatial analysis of genetic variation in plant populations. *Annu. Rev. Ecol. Syst.* 22, 335–355. doi: 10.1146/annurev.es.22.110191.002003
- Hicks, S. (2006). When no pollen does not mean no trees. *Veg. Hist. Archaeobot.* 15, 253–261. doi: 10.1007/s00334-006-0063-9
- Hijmans, R. J., Cameron, S. E., Parra, J. L., Jones, P. G., and Jarvis, A. (2005). Very high resolution interpolated climate surfaces for global land areas. *Int. J. Clim.* 25, 1965–1978. doi: 10.1002/joc.1276
- Hultén, E., and Fries, M. (1986). *Atlas of North European Vascular Plants North of the Tropic of Cancer*. Koenigstein: Koeltz Scientific Books.
- Huntley, B., Bartlein, P. J., and Prentice, I. C. (1989). Climatic control of the distribution and abundance of Beech (*Fagus* L.) in Europe and North America. *J. Biogeogr.* 16, 551–560. doi: 10.2307/2845210
- Huntley, B., and Birks, H. J. B. (1983). *An Atlas of Past and Present Pollen Maps for Europe, 0-13,000 Years Ago*. Cambridge: Cambridge University Press. 667.
- Huntley, B., and Webb, T. III. (1989). Migration: species' response to climatic variations caused by changes in the earth's orbit. *J. Biogeogr.* 16, 5–19. doi: 10.2307/2845307
- Hutchinson, G. E. (1957). Concluding remarks. *Cold Spring Harb. Symp. Quant. Biol.* 22, 415–427. doi: 10.1101/SQB.1957.022.01.039
- IPCC (2014). "Climate change 2014: synthesis report," in *Contribution of Working Groups I, II and III to the Fifth Assessment Report of the Intergovernmental Panel on Climate Change*, eds R. K. Pachauri and L. A. Meyer (Geneva: IPCC), 151.
- Jackson, S. T., and Williams, J. W. (2004). Modern analogs in Quaternary paleoecology: here today, gone yesterday, gone tomorrow. *Annu. Rev. Earth Planet. Sci.* 32, 495–537. doi: 10.1146/annurev.earth.32.101802.120435
- Jalas, J., and Suominen, J. (1973). *Flora Europaea 2 Gymnospermae (Pinaceae to Ephedraceae)*. Cambridge University Press.
- Kaplan, J. O., Krumhardt, K. M., and Zimmermann, N. (2009). The prehistoric and preindustrial deforestation of Europe. *Quat. Sci. Rev.* 28, 3016–3034. doi: 10.1016/j.quascirev.2009.09.028
- Körner, C., and Paulsen, J. (2004). A world-wide study of high altitude treeline temperatures. *J. Biogeogr.* 31, 713–732. doi: 10.1111/j.1365-2699.2003.01043.x
- Kramer, K. (1994). Selecting a model to predict the onset of growth of *Fagus sylvatica*. *J. Appl. Ecol.* 31, 172–181. doi: 10.2307/2404609
- Kramer, K. (1995). Phenotypic plasticity of the phenology of seven European tree species in relation to climatic warming. *Plant Cell Environ.* 18, 93–104. doi: 10.1111/j.1365-3040.1995.tb00356.x
- Kramer, K., Degen, B., Buschbom, J., Hickler, T., Thuiller, W., Sykes, M. T., et al. (2010). Modelling exploration of the future of European Beech (*Fagus sylvatica* L.) under climate change-range, abundance, genetic diversity and adaptive response. *For. Ecol. Manag.* 259, 2213–2222. doi: 10.1016/j.foreco.2009.12.023
- Kühl, N., Gebhardt, C., Litt, T., and Hense, A. (2002). Probability density functions as botanical-climatological transfer functions for climate reconstruction. *Quat. Res.* 58, 381–392. doi: 10.1006/qres.2002.2380
- Latalowa, M., and Van Der Knaap, W. O. (2006). Late Quaternary expansion of Norway spruce *Picea abies* (L.) Karst. in Europe according to pollen data. *Quat. Sci. Rev.* 25, 2780–2805. doi: 10.1016/j.quascirev.2006.06.007
- Loarie, S. R., Duffy, P. B., Hamilton, H., Asner, G. P., Field, C. B., and Ackerly, D. D. (2009). The velocity of climate change. *Nature* 462, 1052–1055. doi: 10.1038/nature08649
- Luterbacher, J., Dietrich, D., Xoplaki, E., Grosjean, M., and Wanner, H. (2004). European seasonal and annual temperature variability, trends, and extremes since 1500. *Science* 303, 1499–1503. doi: 10.1126/science.1093877
- Magri, D., Vendramin, G. G., Comps, B., Dupanloup, I., Geburek, T., Gömöry, D., et al. (2006). A new scenario for the Quaternary history of European beech populations: palaeobotanical evidence and genetic consequences. *New Phytol.* 171, 199–221. doi: 10.1111/j.1469-8137.2006.01740.x
- Maiorano, L., Cheddadi, R., Zimmermann, N. E., Pellissier, L., Petitpierre, B., Pottier, J., et al. (2013). Building the niche through time: using 13,000 years of data to predict the effects of climate change on three tree species in Europe. *Glob. Ecol. Biogeogr.* 22, 302–317. doi: 10.1111/j.1466-8238.2012.00767.x
- Masson, V., Cheddadi, R., Braconnot, P., Joussaume, S., and Texier, D. (1999). Mid-Holocene climate in Europe: what can we infer from PMIP model-data comparisons? *Clim. Dyn.* 15, 163–182. doi: 10.1007/s003820050275
- Maxime, C., and Hendrik, D. (2011). Effects of climate on diameter growth of co-occurring *Fagus sylvatica* and *Abies alba* along an altitudinal gradient. *Trees* 25, 265–276. doi: 10.1007/s00468-010-0503-0

- Nienstaedt, H. (1967). Chilling requirements in seven *Picea* species. *Silvae Genetica* 16, 65–68.
- Nogués-Bravo, D., Rodríguez, J., Hortal, J., Batra, P., and Araújo, M. B. (2008). Climate change, humans, and the extinction of the mammoth. *PLOS Biol.* 6:e79. doi: 10.1371/journal.pbio.0060079
- Parducci, L., and Petit, R. J. (2004). Ancient DNA – unlocking plants' fossil secrets. *New Phytol.* 161, 335–339. doi: 10.1111/j.1469-8137.2004.00987.x
- Parmesan, C., and Yohe, G. (2003). A globally coherent fingerprint of climate change impacts across natural systems. *Nature* 421, 37–42. doi: 10.1038/nature01286
- Pearman, P. B., Guisan, A., Broennimann, O., and Randin, C. F. (2007). Niche dynamics in space and time. *Trends Ecol. Evol.* 23, 149–158. doi: 10.1016/j.tree.2007.11.005
- Pearman, P. B., Randin, C. F., Broennimann, O., Vittoz, P., van der Knaap, W. O., Engler, R., et al. (2008). Prediction of plant species distributions across six millennia. *Ecol. Lett.* 11, 357–369. doi: 10.1111/j.1461-0248.2007.01150.x
- Pebesma, E. J. (2004). Multivariable geostatistics in S: the gstat package. *Comput. Geosci.* 30, 683–691. doi: 10.1016/j.cageo.2004.03.012
- Pellissier, L., Bräthen, K. A., Vittoz, P., Yoccoz, N. G., Dubuis, A., Meier, E. S., et al. (2013). Thermal niches are more conserved at cold than warm limits in arctic-alpine plant species. *Glob. Ecol. Biogeogr.* 22, 933–941. doi: 10.1111/geb.12057
- Peterson, A. T. (2011). Ecological niche conservatism: a time-structured review of evidence. *J. Biogeogr.* 38, 817–827. doi: 10.1111/j.1365-2699.2010.02456.x
- Petitpierre, B., Kueffer, C., Broennimann, O., Randin, C., Daehler, C., and Guisan, A. (2012). Climatic niche shifts are rare among terrestrial plant invaders. *Science* 335, 1344–1348. doi: 10.1126/science.1215933
- Petit, R. J., Aguinagade, I., de Beaulieu, J.-L., Bittkau, C., Brewer, S., Cheddadi, R., et al. (2003). Glacial refugia: hotspots but not melting pots of genetic diversity. *Science* 300, 1563–1565. doi: 10.1126/science.1083264
- Pither, J. (2003). Climate tolerance and interspecific variation in geographic range size. *Proc. R. Soc. Lond. B* 270, 475–481. doi: 10.1098/rspb.2002.2275
- Prentice, I. C., Bartlein, P. J., and Webb, T. III. (1991). Vegetation and climate change in Eastern North America since the last glacial maximum. *Ecology* 72, 2038–2056. doi: 10.2307/1941558
- Root, T. L., Price, J. T., Hall, K. R., Schneider, S. H., Rosenzweig, C., and Pounds, J. A. (2003). Fingerprints of global warming on wild animals and plants. *Nature* 421, 57–60. doi: 10.1038/nature01333
- Schröter, D., Cramer, W., Leemans, R., Prentice, I. C., Araújo, M. B., Arnell, N. W., et al. (2005). Ecosystem service supply and vulnerability to global change in Europe. *Science* 310, 1333–1337. doi: 10.1126/science.1115233
- Seppä, H., Schurgers, G., Miller, P. A., Björne, A. E., Giesecke, T., Kühl, N., et al. (2015). Trees tracking a warmer climate: the holocene range shift of hazel (*Corylus avellana*) in northern Europe. *Holocene* 25, 53–56. doi: 10.1177/0959683614556377
- Sexton, J. P., McIntyre, P. J., Angert, A. L., and Rice, K. J. (2009). Evolution and ecology of species range limits. *Ann. Rev. Ecol. Evol. Syst.* 40, 415–436. doi: 10.1146/annurev.ecolsys.110308.120317
- Smith, W. H. F., and Wessel, P. (1990). Gridding with continuous curvature splines in tension. *Geophysics* 55, 293–305. doi: 10.1190/1.1442837
- Svenning, J. C., Normand, S., and Kageyama, M. (2008). Glacial refugia of temperate trees in Europe: insights from species distribution modelling. *J. Ecol.* 96, 1117–1127. doi: 10.1111/j.1365-2745.2008.01422.x
- Svenning, J. C., and Sandel, B. (2013). Disequilibrium vegetation dynamics under future climate change. *Am. J. Bot.* 100, 1266–1286. doi: 10.3732/ajb.1200469
- Svenning, J. C., and Skov, F. (2004). Limited filling of the potential range in European tree species. *Ecol. Lett.* 7, 565–573. doi: 10.1111/j.1461-0248.2004.00614.x
- Taberlet, P., Fumagalli, L., Wust-Saucy, A. G., and Cosson, J. (1998). Comparative phylogeography and postglacial colonization routes in Europe. *Mol. Ecol.* 7, 453–464. doi: 10.1046/j.1365-294x.1998.00289.x
- Terhürne-Berson, R., Litt, T., and Cheddadi, R. (2004). The spread of *Abies* throughout Europe since the last glacial period: combined macrofossil and pollen data. *Veg. Hist. Archaeobot.* 13, 257–268. doi: 10.1007/s00334-004-0049-4
- Thuiller, W., Lavorel, S., Araújo, M. B., Sykes, M. T., and Prentice, I. C. (2005). Climate change threats to plant diversity in Europe. *PNAS* 102, 8245–8250. doi: 10.1073/pnas.0409902102
- Tinner, W. D., Colombaroli, O., Heiri, P. D., Henne, M., Steinacher, J., Untenecker, E., et al. (2013). The past ecology of *Abies alba* provides new perspectives on future responses of silver fir forests to global warming. *Ecol. Monogr.* 83, 419–439. doi: 10.1890/12-2231.1
- Tinner, W., and Lotter, A. F. (2006). Holocene expansions of *Fagus sylvatica* and *Abies alba* in central Europe: where are we after eight decades of debate? *Quat. Sci. Rev.* 25, 526–549. doi: 10.1016/j.quascirev.2005.03.017
- Tollefsrud, M. M., Kissling, R., Gugerli, F., Johnsen, Ø., Skrøppa, T., Cheddadi, R., et al. (2008). Genetic consequences of glacial survival and postglacial colonization in Norway spruce: combined analysis of mitochondrial DNA and fossil pollen. *Mol. Ecol.* 17, 4134–4150. doi: 10.1111/j.1365-294X.2008.03893.x
- Veloz, S. D., Williams, J. W., Blois, J. L., He, F., Otto-Bliesner, B., and Liu, Z. (2012). No-analog climates and shifting realized niches during the late Quaternary: implications for 21st-century predictions by species distribution models. *Glob. Change Biol.* 18, 1698–1713. doi: 10.1111/j.1365-2486.2011.02635.x
- Walther, G.-R., Post, E., Convey, P., Menzel, A., Parmesan, C., Beebee, T. J., et al. (2002). Ecological responses to recent climate change. *Nature* 416, 389–395. doi: 10.1038/416389a
- Webb, T. III. (1986). Is vegetation in equilibrium with climate? How to interpret late-Quaternary pollen data. *Vegetatio* 67, 75–91. doi: 10.1007/BF00037359
- Wessel, P., Smith, W. H. F., Scharroo, R., Luis, L., and Wobbe, F. (2013). Generic mapping tools: improved version released, EOS trans. *AGU* 94, 409–410. doi: 10.1002/2013EO450001
- Wiens, J. J., and Graham, C. H. (2005). Niche conservatism: integrating evolution, ecology, and conservation biology. *Ann. Rev. Ecol. Evol.* 36, 519–539. doi: 10.1146/annurev.ecolsys.36.102803.095431

Conflict of Interest Statement: The authors declare that the research was conducted in the absence of any commercial or financial relationships that could be construed as a potential conflict of interest.

Copyright © 2016 Cheddadi, Araújo, Maiorano, Edwards, Guisan, Carré, Chevalier and Pearman. This is an open-access article distributed under the terms of the Creative Commons Attribution License (CC BY). The use, distribution or reproduction in other forums is permitted, provided the original author(s) or licensor are credited and that the original publication in this journal is cited, in accordance with accepted academic practice. No use, distribution or reproduction is permitted which does not comply with these terms.



Filling a Geographical Gap: New Paleocological Reconstructions From the Desert Southwest, USA

Andrea Brunelle^{1*}, Thomas A. Minckley², Jacqueline J. Shinker² and Josh Heyer¹

¹ Department of Geography, University of Utah, Salt Lake City, UT, United States, ² Department of Geography, University of Wyoming, Laramie, WY, United States

OPEN ACCESS

Edited by:

Jesse L. Morris,
Weber State University, United States

Reviewed by:

Michael-Shawn Fletcher,
University of Melbourne, Australia
Alberto Saez,
University of Barcelona, Spain

*Correspondence:

Andrea Brunelle
andrea.brunelle@geog.utah.edu

Specialty section:

This article was submitted to
Quaternary Science, Geomorphology
and Paleoenvironment,
a section of the journal
Frontiers in Earth Science

Received: 12 December 2017

Accepted: 05 July 2018

Published: 31 July 2018

Citation:

Brunelle A, Minckley TA, Shinker JJ
and Heyer J (2018) Filling a
Geographical Gap: New
Paleocological Reconstructions From
the Desert Southwest, USA.
Front. Earth Sci. 6:106.
doi: 10.3389/feart.2018.00106

In 1916 the time stamp for quantitative palynology was set with Lennart von Post's initial paper on pollen analysis and environmental change in the Scandinavian peat bogs. In the 1930s, Von Post provided a map of the known palynological reconstructions. This map showed many conspicuous gaps of geographic coverage that have endured to this day. In particular, environmental reconstruction in arid lands remain much less known, largely due to the paucity of depositional environments in these areas as well as challenges with preservation in regions either uniformly dry or subjected to strong wet/dry phases. Over the last decade we have examined linkages between desert wetland development and episodes of wet and arid conditions. Desert wetland, or *ciénegas*, are recharged by groundwater and appear to be sensitive to climate-driven groundwater fluctuations. These systems appear to “grow” during wet periods potentially associated with enhanced El Niño activity, suggesting an important linkage with groundwater dynamics and the quantity and frequency of winter precipitation delivery. Hydrologic conditions in *ciénegas* are also important controls on the preservation of pollen, where episodes of aridity coincide with periods of poor pollen preservation. We assess modern El Niño events, as analogs of past wet conditions, to provide context on the atmospheric controls for delivery of moisture into the desert southwest during winter. Our analysis shows that anomalously high and persistent moisture delivery into the region during El Niño events enables the growth of *ciénegas*, improves preservation of pollen and promotes the growth of fuels necessary to support wildfire. This paper examines *ciénega* sites located in the southwestern region of North America at the US/Mexico Border and discusses results that addresses a geographical gap identified by Von Post's original work in paleoenvironmental research.

Keywords: pollen, charcoal, *ciénega*, desert wetland, ENSO, El Niño

INTRODUCTION

The legacy of Lennart Von Post on quantitative paleoecology and palynology cannot be overstated. While Von Post did not invent palynology, he helped to cement this field of study through his foundational research conducted in Sweden and Norway during the late 1800s and early 1900s. Von Post's approach to paleoenvironmental reconstruction made its way to the American Deserts via the geochronological work of Ernst Antevs and American researcher Kirk Bryan (Manten, 1967; Smiley, 1974). While Antevs did not focus on pollen analysis himself, he was interested enough in the technique to opine on the naming of the methodology (Antevs, 1944) and his work was

critical to subsequent paleoenvironmental work in the desert landscapes of southwestern North America (hereinafter “southwestern deserts”).

Early pollen work in the southwestern deserts focused on woodland expansion (Clisby and Sears, 1956; Martin and Gray, 1962; Martin, 1963; Mehringer, 1965; Meyer, 1973). This initial research reported observations of periods where no pollen or low pollen abundances were recovered. These results altered the relative abundances of pollen types, which was interpreted to be caused by differential preservation and the individual researchers ability to identify degraded pollen grains. For example, through careful examination, the crumbled or degraded pollen grains of *Pinus*, *Artemisia*, Poaceae, and Amaranthaceae are easily distinguishable by the presence of distinct wall or annulated pore characteristic of the particular type. However, degradation and preservation issues reveal the difficult nature of arid land palynology. In short, the lack of perennial lacustrine environments results in discontinuous records of environmental change. Further, simple abundance in arid lands seems lower than one might experience in temperate environments. Subsequent research concentrated on macrobotanical records within woodrat middens (see Betancourt et al., 1990), instead of the ephemeral sedimentary nature of desert wetlands (however see Davis et al., 2002; Mensing et al., 2008).

In arid regions, environments suitable for pollen preservation are limited to riparian deposits, ciénegas or wetlands (Davis et al., 2002; Minckley and Brunelle, 2007), or on the deflated surfaces of former lake beds (Clisby and Sears, 1956; Martin, 1963; Meyer, 1973). Of these environments, ciénegas are proven archives of past environments and climate conditions as they collect charcoal, pollen, and macrofossils over thousands of years (Martin, 1963; Hall, 1985; Hendrickson and Minckley, 1985; Davis et al., 2002; Minckley and Brunelle, 2007; Brunelle et al., 2010; Pigati et al., 2014). The global distribution of desert wetland deposits has not been mapped, but they are considered to be widespread, though in other literature they are referred to as ground water deposits associated with hot or cold springs, seeps, or other wetland complexes (Pigati et al., 2014; Sáez et al., 2016). However, systematic studies of these complex systems are relatively recent, variously focusing on lithological, isotopic, or biological indicators (Minckley and Brunelle, 2007; Quade et al., 2008; Minckley et al., 2013a; Brunelle et al., 2014; Pigati et al., 2014 and references therein, Sáez et al., 2016).

Arid and semi-arid environments occupy 40% of the terrestrial land area on earth and in many cases represent areas where recent human population growth rates are high relative to more mesic regions (18.5% between 1990 and 2000; Hassan et al., 2005). The consumption of natural resources associated with rapid population growth places intense pressure on water resources, such as ciénegas. In addition to being a ready source of water, ciénegas provide crucial ecosystem services including erosion mitigation and prevention of the associated lowering of the water table. Ciénegas have also been identified as regions of high conservation priority for many reasons including endemism (Minckley, 1969, 1992; Hendrickson and Minckley, 1985; Abell, 2000). In Arizona, USA where wetland environments occupy ~2% of the land area, ciénegas are critical habitat for at least

19% of the threatened, candidate, or endangered species within the state (Baker et al., 2004). However, beyond species of concern, desert ciénegas and riparian corridors may increase regional biodiversity by up to 50% in some cases (Sabo et al., 2005).

Over the last decade, we examined sediment collected from ciénega systems located in the southwestern deserts to understand the hydrology, ecology, disturbance regimes, climatology, and environmental change from these critical systems. Our work builds on the legacies of scholars working in this region, including Antevs, Martin, and Mehringer (e.g., Antevs, 1962; Martin, 1963; Mehringer, 1967). Consideration of ciénegas as repositories of environmental history was largely untouched until Hendrickson and Minckley (1985) published “Ciénegas—Vanishing Climate Communities in the American Southwest.” Paleocological research of these sedimentary environments was largely unexplored until Davis et al. (2002) published a synthesis of several sites that examined changes in burning regime with European settlement. However, a large-scale evaluation of ciénega form and function has not yet been undertaken (see Pigati et al., 2014).

In this paper, we present data from four ciénega sites in the Arizona/New Mexico-Mexico borderlands using multiproxy analyses. Herein, we present data from previously published research as well as new records to provide a regional perspective on vegetation and disturbance history from the borderlands region. We detail our approach to handling differential pollen preservation and explain how sedimentary indicators may also provide evidence for hydrology as a control on pollen preservation. Despite the analytical challenges associated with ciénega sediments, the environmental record we present here shows regional coherence of wet-dry episodes. We show that pollen records from ciénegas provide insight to past climatological states related to variations in winter precipitation. For the desert Southwest, this is currently associated with quasi-periodic El Niño Southern Oscillation (ENSO) variations. In the tradition of Von Post, our first objective is to identify conditions in the sedimentological proxy data (e.g., pollen and charcoal) that record changes in ciénega systems attributed to climate. For our second objective, we identify modern episodes that are analogous to conditions found in the paleocological record (strong El Niño conditions) associated with ciénega growth (e.g., wet episodes) to assess the dominant atmospheric drivers related to enhanced winter precipitation in the arid southwest.

To address our first objective, we utilize indices of pollen preservation and charcoal abundance. We assess pollen preservation in ciénega systems of southwestern New Mexico and southeastern Arizona as well as the relationship to past ENSO variability based on our modern understanding of ENSO and southwestern North American hydroclimate teleconnections (Heyer et al., 2017). Further, we put forward past fire activity near the ciénegas was covariant with ENSO variability, similar to connections observed in historic southwestern forest fire research (Swetnam and Betancourt, 1990). Considering fuel availability produced during antecedent wet seasons is closely linked to wildfire in arid and semi-arid environments globally (Krawchuk and Moritz, 2011), we consider our linkage of

past fire activity and ENSO variability viable. To address our second objective, on the impact that El Niño events have on Southwestern climate, we use high-resolution modern climate data to assess teleconnections between moisture delivery and southwestern precipitation anomalies during winter and spring of strong El Niño events as a mechanism for sustained wet conditions that are conducive for pollen preservation in ciénegas.

REGIONAL DESCRIPTION

The southwestern deserts, particularly those in the Sonoran and Chihuahuan systems, have a high concentration of ciénegas (Hendrickson and Minckley, 1985; Minckley et al., 2013b; Cole and Cole, 2015). These wetlands are found in a variety of geomorphic contexts along riverine or stream channels, off-channel seeps, landslide backfill, and valley bottoms, to name a few. Often ciénegas are proximal to fault lines, which are common in the desert basin and range structures of western North America (Minckley, unpublished).

The modern climatic context of the arid southwest of North America is characterized as having bimodal precipitation (Mock, 1996; Shinker, 2010). Winter precipitation has broad spatial-scale patterns with persistent light precipitation delivered by midlatitude frontal systems (Mock, 1996; Comrie and Glenn, 1998; Shinker, 2010). In contrast, summer precipitation is highly variable spatially and typically short in duration associated with convective thunderstorms delivered via the North American Monsoon System (NAMS; Mock, 1996; Adams and Comrie, 1997; Sheppard et al., 2002; Diem and Brown, 2006; Shinker, 2010). The modern NAMS developed after climate started to warm and the Laurentide ice sheet began to collapse at the end of the last ice age. This warming led to the formation of summer thermal lows that provide a mechanism for drawing moisture from the Gulf of Mexico and southeastern Pacific (Spaulding, 1991; Adams and Comrie, 1997; Minckley et al., 2004). The bimodal nature of precipitation in the southwest, especially the extra precipitation in the summer associated with the NAMS, provides effective moisture at the surface related to water- and energy-balance components important for ecosystem and water resources related to vegetation and the ciénega systems of the southwest (Shinker and Bartlein, 2010).

In addition to the bimodal climate of the southwest, large-scale modes of variability such as ENSO impacts southwestern hydroclimate and ecosystems (Ropelewski and Halpert, 1986; Cole and Cook, 1998; Gershunov and Barnett, 1998a; Cayan et al., 1999; Dettinger et al., 2000). El Niño is the anomalous warming of the near-surface water off the western coast of South America that initiated about 5000 years ago (Enfield, 1992; Liu et al., 2014). Its atmospheric counterpart is the Southern Oscillation, which reflects changes in barometric pressure (Wallace and Gutzler, 1981; Enfield, 1992). Strong El Niño years in the modern record typically result in higher-than-normal winter precipitation in the southwestern United States; while strong La Niña typically causes lower-than-normal winter precipitation and is typically associated with regional drought (Shinker and Bartlein, 2009). Studies have identified a north-to-south precipitation dipole correlated with ENSO in the

western U.S., showing a strong relationship in the southwest between cool season (Oct-Mar) precipitation and El Niño events (Dettinger et al., 1998; Wise, 2010). Further, many studies have shown statistically significant correlations between ENSO and western North America precipitation, specifically in the southwest where spatially coherent correlations are found during the cool season (Dettinger et al., 1998; Heyer et al., 2017). However, various modes of ENSO are associated with different impacts on western NA hydroclimate (Ashok et al., 2007), and teleconnections can vary on decadal-to-centennial time scales (Gershunov and Barnett, 1998b), suggesting that southwest hydroclimate does not always respond to ENSO variability in a linear manner based on our modern understanding of southwest hydroclimate and ENSO correlations (Heyer et al., 2017). However, despite teleconnection variability (Gershunov and Barnett, 1998b), dipole variability (Wise, 2010) and different modes of ENSO (Ashok et al., 2007), paleo-sedimentary records suggest teleconnections between ENSO and southwest climate are similar to those observed in the modern record, and have persisted at century-millennial time scales (Barron and Anderson, 2010; Antinao and McDonald, 2013; Kirby et al., 2014; Hart et al., 2015). Further, paleoecological records have revealed the ENSO phenomenon is correlated with fire regimes of the southwest (Swetnam and Betancourt, 1990). Therefore, our research on San Bernardino Ciénega suggests that over centuries-to-millennial scales fire frequency trends are consistent with ENSO variability, with fire frequency increasing (decreasing) when El Niño (La Niña) was active (Brunelle et al., 2010).

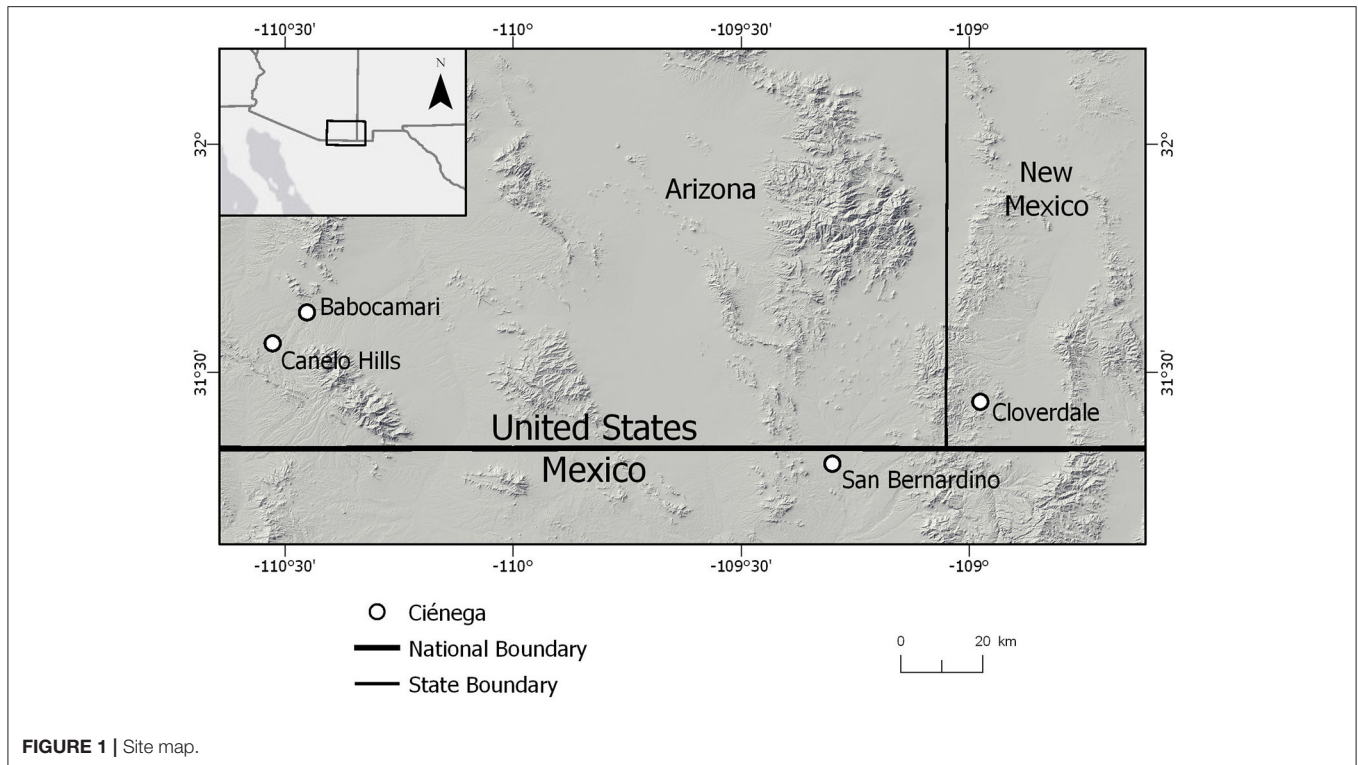
Our work has been focused on ciénegas near the US/Mexico borderlands region in southern Arizona and New Mexico (**Figure 1**) in the monsoon-dominated ecotone of the Sonoran and Chihuahuan deserts and in a region well correlated with ENSO activity (Wise, 2010; Heyer et al., 2017). Total annual precipitation is around 254 mm (Western Regional Climate Center, 2017). Summer temperatures are generally around 37°C while winter temperatures rarely fall below freezing.

SITE DESCRIPTIONS

San Bernardino Ciénega (31.3°N; 109.3°W, 1,160 m asl; **Figure 1**) is located in the drainage of Black Draw Wash/Rio de San Bernardino (RSB) of southeastern Arizona, USA and northeastern Sonora, MX near the ecotone of Chihuahuan and Sonoran grassland and desert scrub (Minckley and Brunelle, 2007; Minckley et al., 2009, 2011; Brunelle et al., 2010). Currently the ciénega surface is dry except for a few artificial impoundments and small perennial springs.

Cloverdale Ciénega is located in the Peloncillo Mountains, Coronado National Forest, NM (31°26.141' N, 108°58.517' W, 1,640 m asl; **Figure 1**). Cloverdale Ciénega is situated at the ecotone between Madrean woodland and grassland (Brunelle et al., 2014), making this location sensitive to changes in community composition over time. Currently, the Madrean woodlands form a mosaic of clustered tree stands interspersed with patches of shrub and grass (Brown, 1982).

Canelo Hills Ciénega (31° 33.833'N, 110° 31.711'W, 1,506 m asl; **Figure 1**) is a Nature Conservancy preserve located southeast



of Sonoita, Arizona on the east side of the Canelo Hills. The area is a Madrean grassland.

Babocamari Ciénega ($31^{\circ} 37.901'N$, $110^{\circ} 27.178'W$, 1,391 m asl; **Figure 1**) is southeast of Sonoita, Arizona and located between the Whetstone and Huachuca Mountains. The site is considered Madrean grassland.

METHODS

Field

San Bernardino

Sediments were collected from an active spring (Snail Spring), the incised channel wall of the Rio de San Bernardino arroyo (RSBA), and the ciénega surface of the San Bernardino National Wildlife Refuge (SBNWR). The RSBA samples were described and collected contiguously from a freshly exposed sediment face with a trowel. A 15-m long core was obtained from the SBNWR using a truck-mounted 5" (12.7 mm) hollow barrel auger (Minckley et al., 2007). The Snail Springs samples were collected using a modified Livingstone piston corer.

Cloverdale, Babocamari, and Canelo Hills Ciénegas

Sediment cores were collected using a vibracore system where manual probes indicated maximum sediment accumulation. The vibracore apparatus uses a cement leveling motor attached to a 3-inch aluminum tube inserted into the sediments until refusal (bedrock). Sediment was retained in the aluminum tube by placing an airtight cap on the top of the tube to create a vacuum, allowing the sediment

core to be removed from the ground without loss. The cores were transported in the aluminum tube to the University of Utah and split in the lab for description and sampling.

Laboratory and Analytical

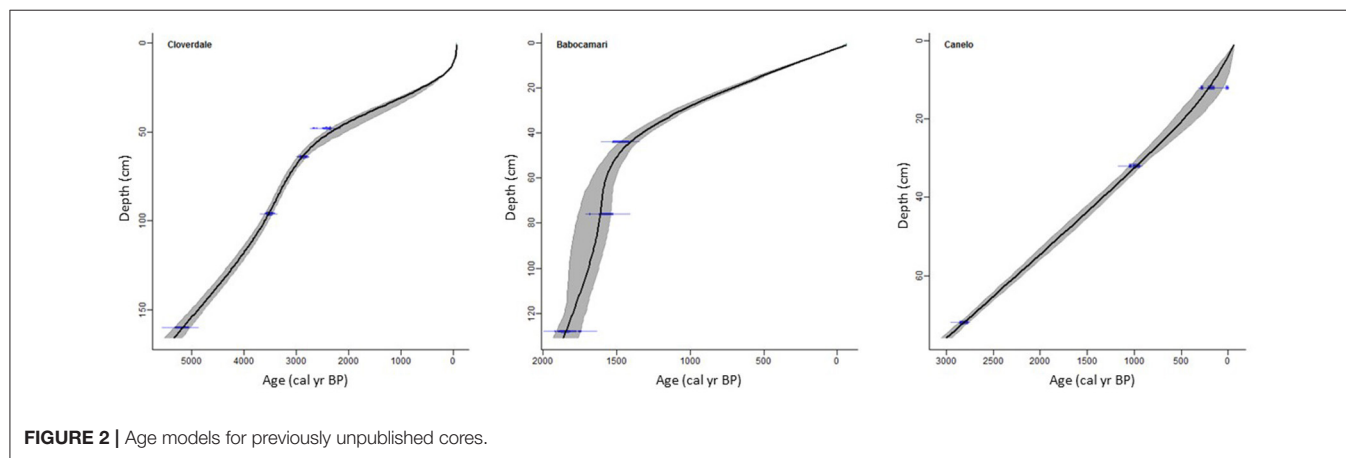
Once the cores were removed from the aluminum tube, the color and texture of the sediments were described. Every contiguous centimeter of the core was examined for charcoal analysis. For pollen analysis, samples were collected to acquire a minimum sample resolution of approximately every 200 years. The sediments were weakly stratified, massive, and organic.

Age-depth relationships were determined for the sediments based on AMS (accelerator mass spectrometry) dates on pollen concentrates, lead-210 chronology (when available), and the surface (collection year; **Table 1**). Ages are presented in calibrated years before present (cal yr BP) where 1950 CE is equal to year 0 cal yr BP. The age-depth models were generated in CLAM (Blaauw, 2010) using smoothing splines (**Figure 2**). The age model for San Bernardino was created using multiple linear regressions and was not rerun due to the multiple publications already based on the existing chronology (Brunelle et al., 2010 and citations therein).

Pollen extraction methods followed Faegri et al. (1989). For pollen analysis, we attempted to identify at least 300 terrestrial pollen grains to complete the rarefaction curve associated with pollen diversity (Maher, 1963). Pollen grains were identified at a magnification of 500X to the lowest possible taxonomic

TABLE 1 | Radiocarbon dates from the reported sites.

Depth	Core	Lab number	Method	Material	14C age	Calendar year	Error	Calibrated (CALIB 7.1) median probability
0–1	CC08C	–	Surface	–	–	–58	–	–
14–15	CC08C	–	Lead-210	Sediment	–	89	1	–
47–48	CC08C	CAIS 4477	AMS	Pollen	2,370	–	45	2,413
63–64	CC08C	CAIS 5469	AMS	Pollen	2,770	–	25	2,863
95–96	CC08C	CAIS 5470	AMS	Pollen	3,280	–	30	3,510
159–160	CC08C	CAIS 4478	AMS	Pollen	4,530	–	45	5,163
0–1	BAB10A	–	Surface	–	–	–60	–	–
43–44	BAB10A	CAIS 7339R	AMS	Pollen	1,580	–	24	1,468
75–76	BAB10A	CAIS 7340R	AMS	Pollen	1,663	–	24	1,564
127–128	BAB10A	CAIS 7341R	AMS	Pollen	1,899	–	30	1,848
0–1	CAN10A	–	Surface	–	–	–60	–	–
11–12	CAN10A	CAIS 7335	AMS	Pollen	190	–	25	180
31–32	CAN10A	CAIS 7336	AMS	Pollen	1,078	–	25	980
71–72	CAN10A	CAIS 7337	AMS	Pollen	2,720	–	25	2,814
0–1	RSB04	–	Surface	–	–	–54	–	–
40–42	RSB04	Beta-204829	AMS	Pollen	830	–	40	741
108–110	RSB04	Beta-204374	AMS	Pollen	1,200	–	40	1,128
155–160	RSB04	CAIS 1615	AMS	Pollen	1,700	–	45	1,609
175–180	RSB04	Beta-204828	AMS	Pollen	2,470	–	40	2,568
375–380	RSB04	Beta-203022	AMS	Pollen	3,900	–	40	4,335
346–347	SBNWR05	Beta-207161	AMS	Pollen	3,740	–	40	4,096
553–554	SBNWR05	Beta-207162	AMS	Pollen	3,920	–	40	4,354
667–668	SBNWR05	Beta-207163	AMS	Pollen	6,190	–	50	7,087



classification using published atlases (e.g., Erdtman, 1969; Kapp et al., 2000). Counts were converted to percentages based on the sum of total terrestrial grains and influx using the sedimentation rate calculated using the age models. In desert sediments, a 300-grain terrestrial count is not always obtainable because of poor preservation (Minckley and Brunelle, 2007; Minckley et al., 2011). Our standard has been to attempt 300-grain terrestrial counts or 300–1000 *Lycopodium* spore (exotic spore added as a tracer) tallies for each depth. If pollen counts do not exceed at least 100 terrestrial pollen grains we plot pollen presence instead of abundance to avoid artificial inflation of identifiable pollen

types as presenting ecological significance, an issue common in earlier studies as detailed in the Introduction.

A second way we avoid misinterpretation of desert pollen assemblages is by determining an index of pollen preservation (“preservation index”) where we consider the number of *Lycopodium* tracers to the total number of identified grains. Studying the way pollen has been preserved can help to determine changes in the deposition or preservation environment. This type of examination is a relatively underused technique (Tipping, 2000) that could be more widely used as an interpretive tool (Tweddle and Edwards, 2010). In our study, the preservation

index is used as an indicator of a decrease in water table height that would expose deposited grains to conditions of wetting and drying which are known to be consistent with deterioration (Campbell and Campbell, 1994; Tweddle and Edwards, 2010). The depth to water table in ciénega settings controls the water level at the surface. In turn, the water table is largely controlled by the amount of winter precipitation. High preservation indices are used to indicate wet (active) ciénega surfaces, while low indices indicate dry (inactive) surfaces.

Volumetric samples were taken from the sediments for charcoal analysis to reconstruct fire history. Sample volumes ranged from 1 to 10 cc based on the amount of charcoal found at various depths throughout the sections. Sample volume was adjusted to maintain a significant number of charcoal particles, but to reduce excessive counts ($>1,000$ particles). Methods and rationale follow Clark (1988) and Long et al. (1998). While taphonomic studies of large particle deposition on fluvial wetland surfaces have not been conducted, isotopic analysis of ciénega sediments indicates pooling and stagnation of surface waters (Minckley et al., 2009), suggesting sedimentation of charcoal fragments would be similar to those of lake and bog surfaces. Charcoal concentrations (particles/cm³) were converted to influx (particles/cm²/yr) using the age models.

Statistical Analyses

To compare ciénega CHAR record to regional charcoal variability, regional charcoal for Arizona, New Mexico, Southern Utah, and Southern Colorado (i.e., latitude >30 , latitude <38 , longitude ≤ 105 , longitude ≥ 113) were collected from the paleofire database (Blarquez et al., 2014), and used in correlative analyses. A total of 13 sites were included, of which all sites are from mid-upper elevations (i.e., $>2,300$ meters) with the exception of the Montezuma Well site (near 1,100 meters). Prior to comparing regional charcoal to ciénega charcoal, regional charcoal data were averaged (i.e., long-term average 10,000 cal yr BP—present) and standardized to z-scores. Charcoal data were then composited using a locally weighted scatterplot smoother and bootstrapping techniques (Blarquez et al., 2014).

Prior to correlation analyses, the CHAR and pollen preservation ratio data were decomposed into pseudoannual values and then reaggregated into 100-year bins to be comparable to the Moy et al. (2002) El Niño event frequency reconstruction. The time series of all the ciénega sites were then averaged to provide a comprehensive trend of the series. To quantitatively describe the relationships between the ENSO index (Moy et al., 2002) and the preservation ratio and CHAR time series, a Pearson product-moment correlation was run on the time series providing correlation coefficients and *p*-values.

Correlations were performed between data from 7,700 cal yr BP to present for mean-pollen preservation, and from 8,100 cal yr BP to present for mean-charcoal accumulation. Correlations were between ciénega sites mean-pollen preservation, ciénega sites mean-charcoal accumulation, regional standardized charcoal accumulation, and El Niño events/100 years (Moy et al., 2002). From 8,100 to 5,400 cal yr BP, only the San Bernardino ciénega site was active, with pollen preservation

and charcoal accumulation at or near zero, as expected considering El Niño event inactivity. Therefore, correlation analyses from 8,100 to 5,400 cal yr BP is not based on an actual average. However, we assume a lack of pollen preservation and charcoal accumulation at the inactive ciénega sites was due to a lack groundwater recharge, which may represent a reduction of persistent winter and spring precipitation potentially associated with reduced El Niño events (Scanlon et al., 2006; Heyer et al., 2017). We suggest if the other three ciénega sites had been active, then pollen preservation and charcoal accumulation would have been close to zero, similar to the San Bernardino ciénega. Thus, assuming the other ciénega sites would have also had pollen preservation and charcoal accumulation near zero, we only use pollen preservation and charcoal accumulation data from the San Bernardino ciénega to calculate the long term mean-pollen preservation (i.e., 7,700 cal yr BP—present) and mean-charcoal accumulation (i.e., 8,100 cal yr BP—present). From 5,300 to 0 cal yr BP at least two ciénega sites recorded data, allowing for a mean to be calculated.

Modern Climate Analog Approach

While proxy data such as charcoal, pollen and macrofossils provide a record of past ciénega variability from an ecological perspective, paleoecological data does not provide a record of the climatic mechanisms that caused such variability (Shinker et al., 2006). Therefore, understanding modern climate mechanisms and processes that cause variability in ciénegas and the sensitivity and range of ecological responses to such changes are fundamental to ecosystem management. We incorporate a modern climate analog technique (Mock and Shinker, 2013) in order to understand the climate processes and mechanisms associated with ENSO conditions that are evident in the sedimentological record from ciénega sites across the United States/Mexico borderlands. The modern climate analog technique (Mock and Shinker, 2013) relies on the principle of uniformitarianism and assumes that modern synoptic and dynamic climate processes operated similarly today as they did in the past. The modern climate analog approach is an effective way to identify climate mechanisms associated with past environmental changes (e.g., as seen in reconstructed sedimentary pollen analyses; Mock and Brunelle-Daines, 1999; Shinker et al., 2006; Shinker, 2014). A modern climate analog is a conceptual model that uses modern extremes (e.g., wet or dry episodes) as analogs of past events (e.g., vegetation disturbance associated with changes in ciénega hydrology) to identify possible synoptic and dynamic patterns that may have caused past extremes (Edwards et al., 2001; Shinker, 2014). Such conceptual models of dynamic processes can provide examples of modern climatic mechanisms as analogs of historic and past hydroclimatic variability (Mock and Brunelle-Daines, 1999; Shinker et al., 2006; Mock and Shinker, 2013; Shinker, 2014).

The first step in the modern climate analog approach is to identify conditions in the sedimentological proxy data that record a change in vegetation and subsequently represents changes in the ciénega system, which would have signaled a change in the

hydrological cycle. The next step is to use an environment-to-circulation approach (Yarnal, 1993; Barry and Carleton, 2001; Yarnal et al., 2001; Mock and Shinker, 2013; Shinker, 2014), which considers the surface conditions based on information gained from the proxy data collected from cienega sediments. We use the Multivariate ENSO Index (MEI, Wolter and Timlin, 2011) to identify analogous periods (seasons, years) of anomalous conditions and treat the selected cases as the modern analog for past hydrologic variability seen in the sedimentary pollen record. By identifying extremes (i.e., El Niño conditions) in the modern record, the environment-to-circulation approach helps identify potential dominant synoptic processes that created the persistent conditions leading to the ecological changes seen in the sedimentary record.

We use five strong El Niño events from the MEI (Wolter and Timlin, 2011) for the period 1979–2017 (the common period for the atmospheric circulation data we use). The selected El Niño years (cases) represent similar conditions (e.g., El Niño modes consistent with anomalous wet winter and spring conditions in the southwest) to those found in the sedimentary analyses. Once selected, the case years are used to calculate and map composite-anomaly values to assess the spatial configuration of climate processes during the selected anomalous case years (the modern climate analogs). We use climate data from the North American Regional Reanalysis (NARR) dataset (Mesinger et al., 2006), which spans 1979–2017. Use of the NARR dataset is advantageous for two reasons: (1) it provides a variety of climate variables that represent atmospheric synoptic processes (e.g., atmospheric pressure; moisture availability, and vertical motion) as well as surface conditions (e.g., precipitation rate and soil moisture); and (2) The spatial resolution (32-km grids) of the NARR is at a finer scale than large-scale GCMs. The 32-km resolution of the NARR is valuable for our area of geographic study because it captures topographic and climatic diversity of the southwest (Heyer et al., 2017). For each climate variable in the NARR dataset we use, the seasonal value (e.g., DJF) of the selected modern analog case years are averaged together (composited) and compared to the long-term mean (1981–2010) to create composite-anomaly values.

Finally, we map composite-anomaly values for selected modern climate analog case years to analyze and assess the spatial and temporal variability of our selected modern climate analogs for surface and atmospheric conditions that would support ecological change identified in the paleoecological record. Atmospheric variables (e.g., atmospheric pressure and specific humidity) are mapped at a continental scale to illustrate the large spatial scales in which such variables operate. Similarly, the surface variables (e.g., precipitation rate and soil moisture) are mapped at the local or regional level to illustrate the spatial heterogeneity of such processes.

RESULTS

Core Description

The sedimentary deposits were massive, organic rich clays with interbedded layers of silt and sand.

Age Models

San Bernardino Ciénega

The San Bernardino age model is presented in Minckley and Brunelle (2007); Blissett (2010), and Brunelle et al. (2010) and is based on a series of linear regressions using 8 radiocarbon dates.

Cloverdale Ciénega

The Cloverdale age model (Brunelle et al., 2014) is based on a smoothing spline (CLAM spar 0.1, goodness-of-fit = 22.4, Blaauw, 2010) based on the surface age, a lead-210 date and 4 radiocarbon dates (Figure 2).

Canelo Hills Ciénega

The Canelo Hills Ciénega age model is not previously published. It is based on a smoothing spline (CLAM spar 0.3, goodness-of-fit = 1.99, Blaauw, 2010) based on the surface age, and 3 radiocarbon dates (Figure 2).

Babocamari Ciénega

The Babocamari Ciénega age model is not previously published. It is based on a smoothing spline (CLAM spar 0.2, goodness-of-fit = 4.25, Blaauw, 2010) based on the surface age, and 3 radiocarbon dates (Figure 2).

Pollen

San Bernardino Ciénega

The pollen data represent changes in abundances of various taxa over the last ~8,000 cal yr BP (Figure 3). The *Lycopodium* curve indicates depths that have greater or lesser preservation. For example, the time period centered on 2,750 cal yr BP records a greater abundance of identified *Lycopodium* than pollen grains and reduced pollen preservation. Other interesting shifts in pollen types include the increase in Poaceae, Cyperaceae, and Typhaceae/Sparganium type after ~4,500 cal yr BP.

Cloverdale Ciénega

As with the SBNWR site, the amount of *Lycopodium* represents the preservation of the pollen grains for the last ~5,500 cal yr BP (Figure 4). At this site preservation is excellent from the beginning of the record until about 500 years ago. Other distinctive changes in the pollen include a decline and then subsequent increase in Cyperaceae centered on ~3,500 cal yr BP.

Canelo Hills Ciénega

The Canelo Hills record spans the last ~3,000 cal yr BP. Increased preservation as indicated by a decrease in *Lycopodium* improves from the beginning of the record toward present (Figure 5). Cyperaceae and grasses also increase toward present. Taxa extralocal to the cienega remain relatively constant with slight fluctuations (e.g., Amaranthaceae).

Babocamari Ciénega

The Babocamari record represent the last ~1,800 cal yr BP (Figure 6). Preservation is variable over time as indicated by increases and decreases in *Lycopodium*. Cyperaceae shows a strong increase toward present starting at ~900 cal yr BP. All other taxa remain relatively constant over the record.

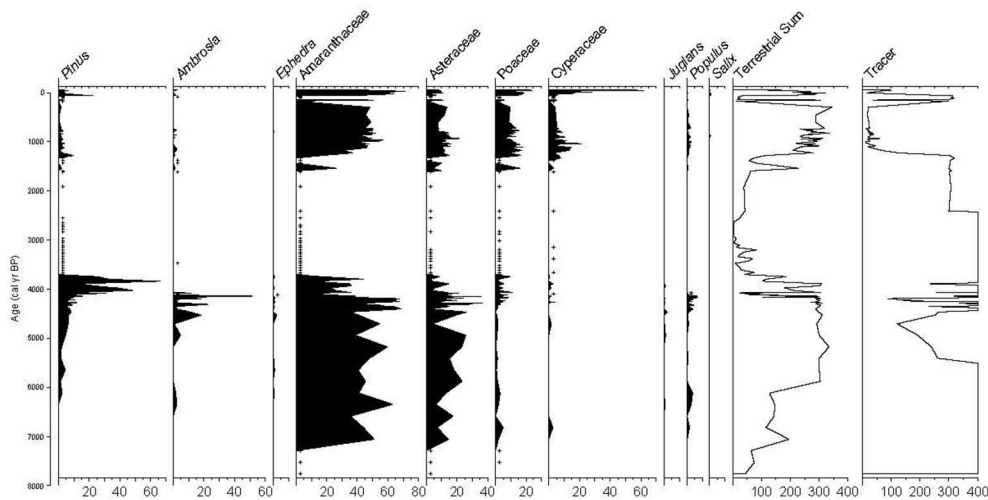


FIGURE 3 | San Bernardino pollen diagram. “+” symbol indicates counts of <100 terrestrial grains. Counts <100 are plotted as presence or absence to avoid over interpretation of sparse data.

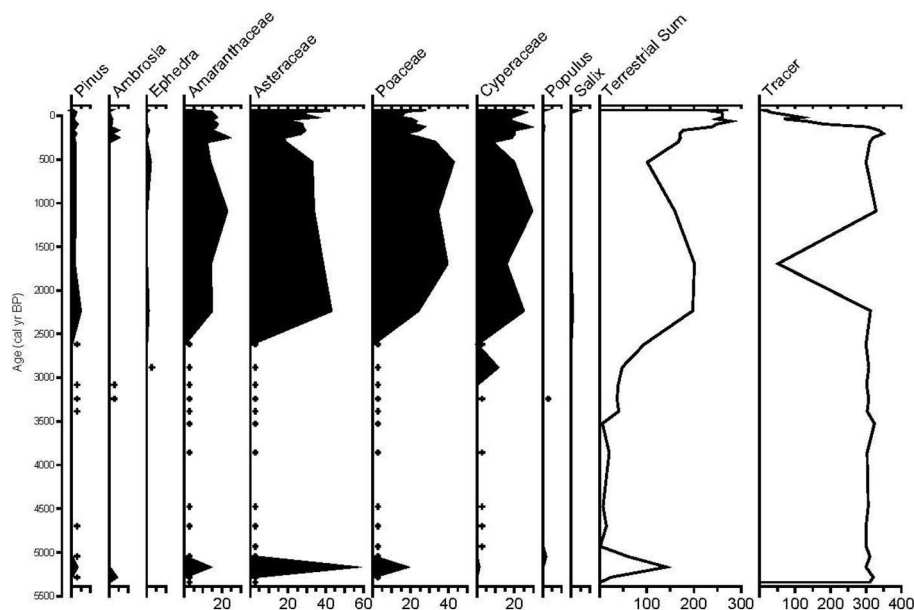


FIGURE 4 | Cloverdale pollen diagram. “+” symbol indicates counts of <100 terrestrial grains. Counts <100 are plotted as presence or absence to avoid over interpretation of sparse data.

Charcoal

San Bernardino Ciénega

The San Bernardino Ciénega charcoal record is the longest published fire history from the desert southwest (**Figure 7**). The record spans the last ~8,000 cal yr BP. From ~8,000 to ~5,000 cal yr BP there is essentially no charcoal in the SBNWR record. After ~5,000 cal yr BP the charcoal influx (CHAR) increases to a sustained level from 5,000 to 4,000 cal yr BP. After 4,000 cal yr BP the CHAR stabilizes around a new mean, increasing again around 1,500 cal yr BP.

Cloverdale Ciénega

The Cloverdale charcoal record initiates at ~5,000 cal yr BP and remains relatively constant for the entire record (**Figure 7**). There is a small decrease in CHAR centered on ~1,500 cal yr BP and it increases significantly in the last couple hundred years.

Canelo Ciénega

The Canelo Hills charcoal record represents the last ~3,000 cal yr BP (**Figure 7**). The CHAR slowly increases from the start of the record to present.

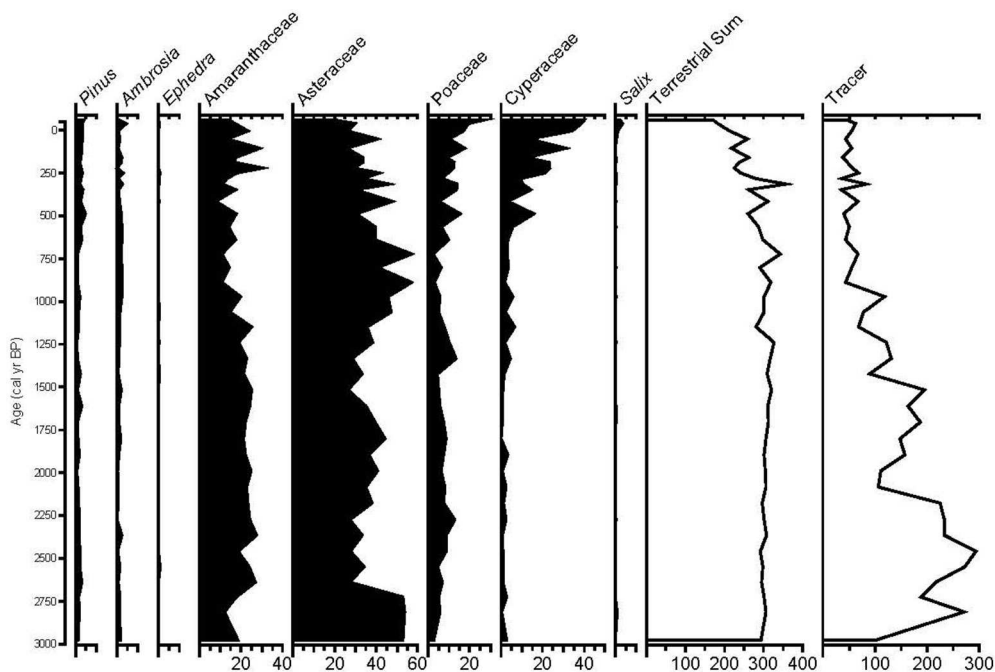


FIGURE 5 | Canelo Hills pollen diagram.

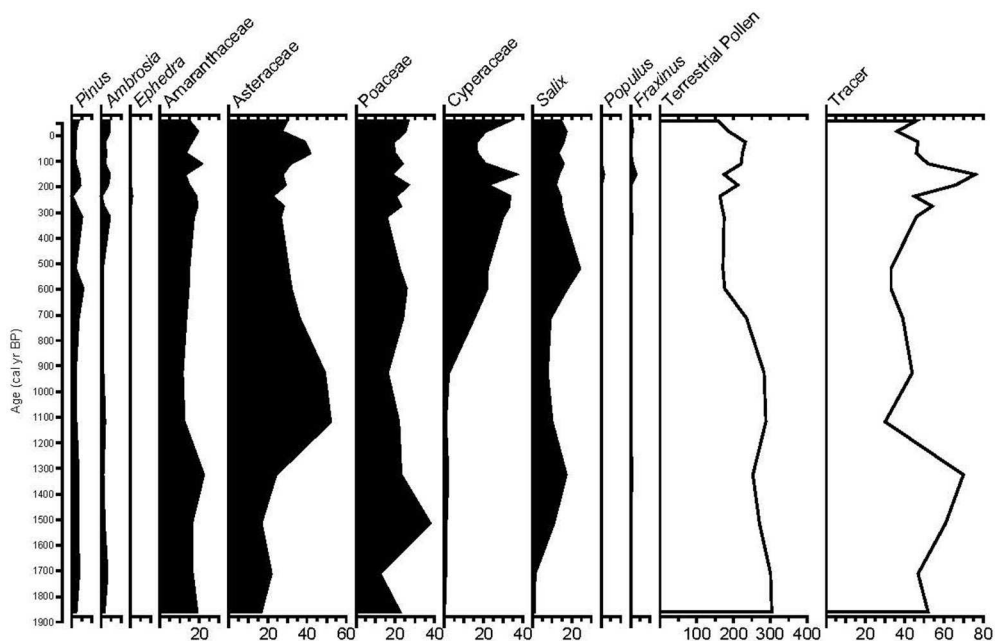


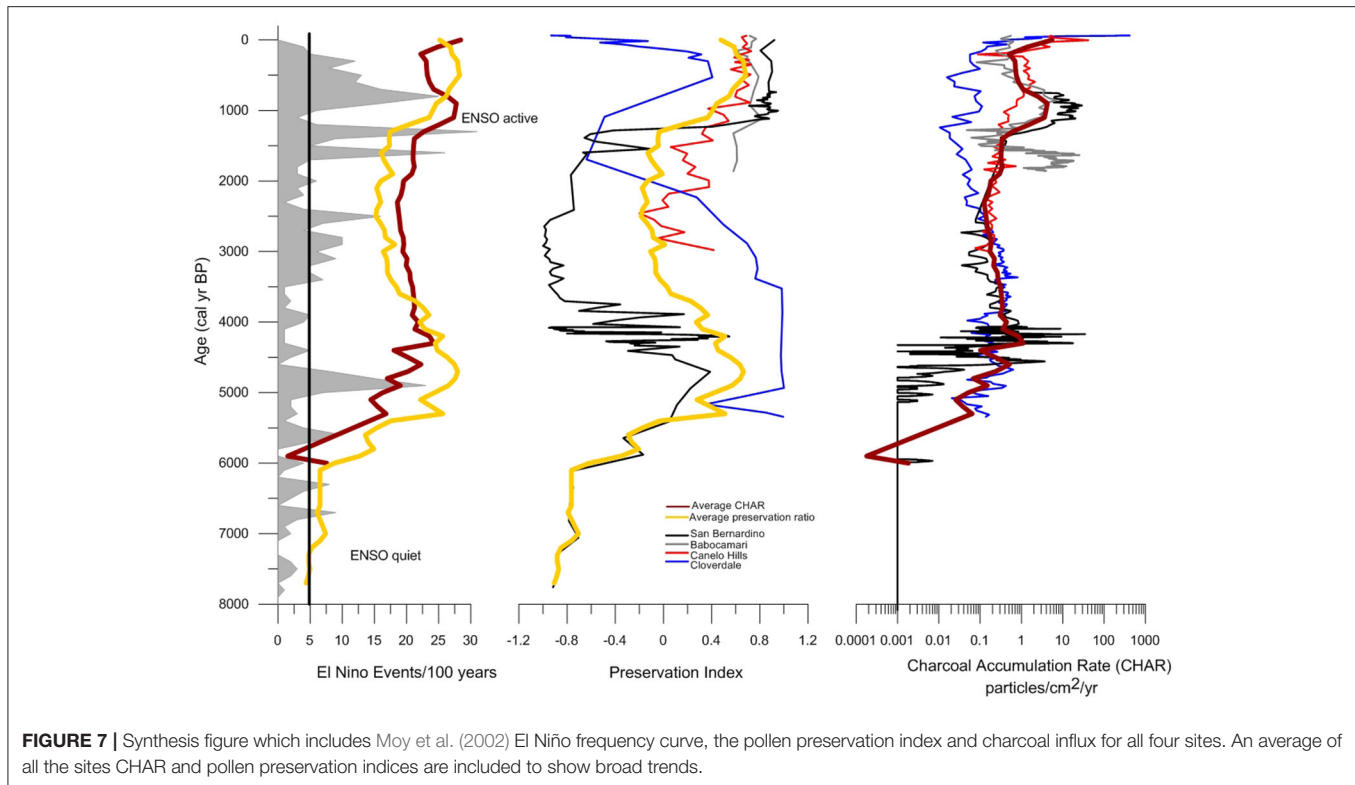
FIGURE 6 | Babocamari pollen diagram.

Babocamari Ciénega

The Babocamari record represents the last ~1,800 cal yr BP (Figure 7). The CHAR is relatively stable for the entire period and is of similar magnitude to the Canelo Hills and San Bernardino Ciénega records.

Modern Climate Analog

Our modern climate analog results illustrated in Figure 8 show composite-anomaly values based on the five strongest El Niño events from the Multivariate ENSO index (MEI) (Wolter and Timlin, 1993, 1998) and include 1982/1983; 1986/1987;



1991/1992; 1997/1998; and 2015/2016 compared to the long-term mean (1981–2010). We show winter (DJF) and spring (MAM) composite-anomaly values because these seasons represent the greatest impact of El Niño teleconnections in the region (Heyer et al., 2017). Additionally, winter and spring are important seasons for prolonged and persistent wet conditions that would support preservation of pollen in ciénegas.

During both winter and spring seasons, the southwest region experienced lower-than-normal atmospheric pressure at the 500 mb level (**Figure 8A**) indicative of persistent low pressure troughs. Such conditions are associated with counterclockwise flow of air around the region that deliver greater-than-normal moisture from the south via 850 mb specific humidity (**Figure 8B**). While the 500 mb Omega (vertical velocity) composite-anomaly maps (**Figure 8C**) indicate a mixture of weaker-than-normal (winter) and stronger-than-normal (spring) rising motions these motions are still associated with greater-than-normal moisture availability via specific humidity at the 850mb level. Both winter and spring months exhibit greater-than-normal precipitation values (**Figure 8D**) in our region of interest indicating persistent wet conditions through multiple seasons. The greater-than-normal precipitation along with lower-than-normal temperatures (not shown) contribute to the persistence of greater-than-normal soil moisture (**Figure 8E**) during both winter and spring months.

Statistical Relationships

The correlations between El Niño frequency and mean-pollen preservation ratios and mean-charcoal accumulation (CHAR) were compelling. The results show a correlation between El Niño

event frequency and CHAR and pollen preservation, however the correlation coefficient values strengthen when a lag in the data is considered. The optimal lag between El Niño frequency and CHAR is at 500 years while the optimal lag between El Niño frequency and pollen preservation ratios is at 300 years.

DISCUSSION

In this paper we present a quantitative approach for the interpretation of arid-land pollen sequences and introduce two new Southwestern desert sites. By merging the traditional summation and proportioning of terrestrial and non-terrestrial pollen, first demonstrated by Vonpost (1916) with a Boolean (presence/absence) and preservation evaluation, interpretations of absence or degradation can be placed in an ecological context. Ciénegas have been shown to be highly sensitive to hydrologic change and might be one of the few terrestrial ecosystems where state-changes have been identified (Scheffer et al., 2001; Scheffer and Carpenter, 2003; Folke et al., 2004; Heffernan, 2008; Minckley et al., 2011, 2013b). We utilize modern climate analogs of strong El Niño years to provide mechanisms for winter and spring moisture delivery into the region that would support ecological conditions of ciénega growth and pollen preservation.

Our interpretive approach allows us to address potential mechanisms driving ciénega development and controls on their growth related to regional climate and land-use (Brunelle et al., 2014). Winter and subsequent spring precipitation appears important to ciénega form and function through recharging groundwater systems that feed ciénega complexes. Without

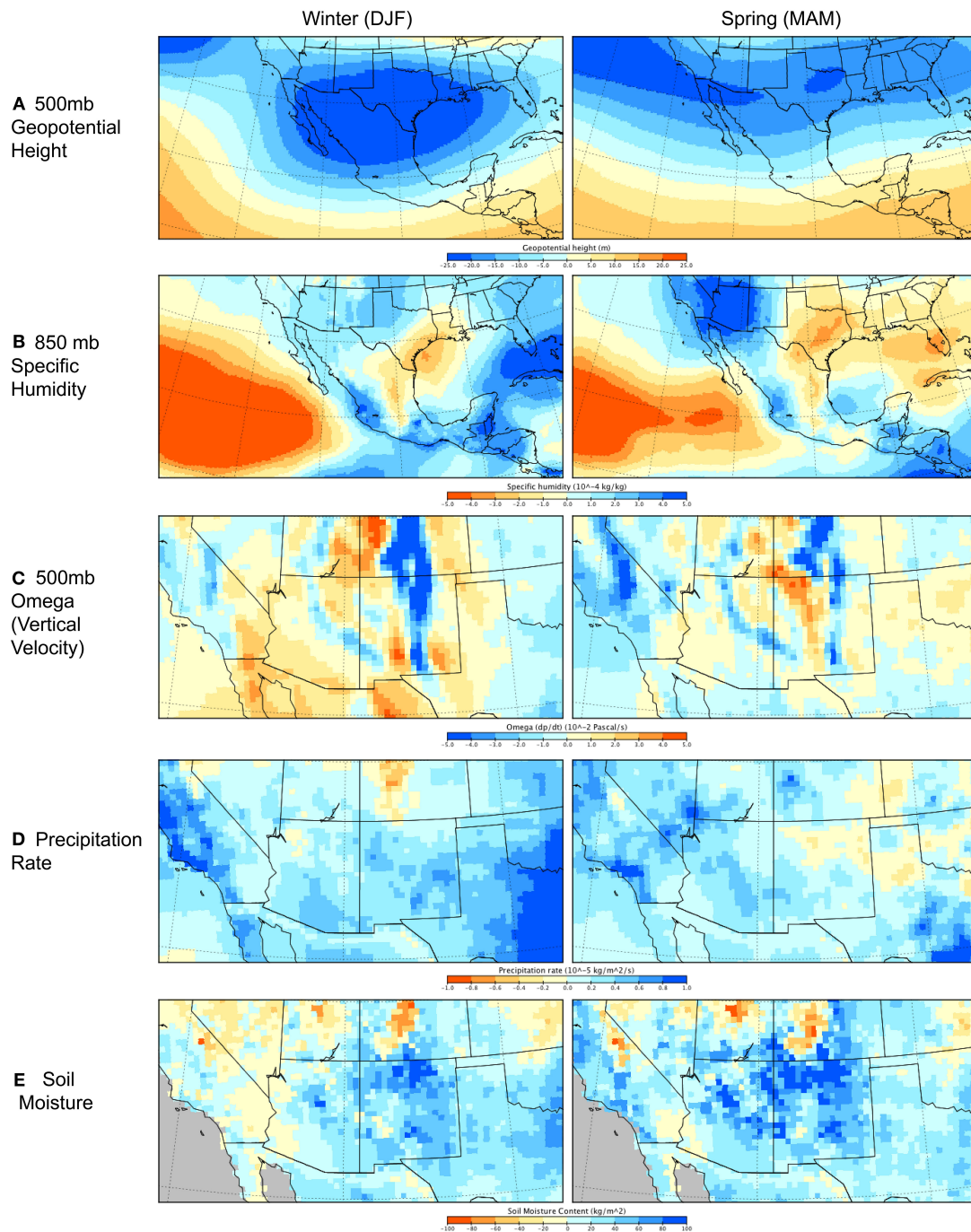


FIGURE 8 | Composite-anomaly maps for strong El Niño events 1982/1983; 1986/1987; 1991/1992; 1997/1998; and 2015/2016. Each map contains composite-anomaly values for winter (DJF) and spring (MAM) from the selected strong El Niño events compared to the long-term mean (1981–2010). **(A)** 500 mb geopotential height indicating anomalous ridges (red) or troughs (blue); **(B)** 850 mb specific humidity indicating moisture availability; **(C)** 500 mb omega (vertical velocity) indicating rising (blue) or sinking (red) motions; **(D)** Precipitation rate at the surface; and **(E)** Soil moisture.

critical inputs of winter and spring precipitation to support a water table emergence at the surface, ciénegas are intermittently dry or nonexistent. Groundwater lags have been shown to have long residence times of decades to centuries (Rodríguez et al., 2005; Wolaver et al., 2013) In the Southwest, winter and spring

precipitation is enhanced during El Niño events (Heyer et al., 2017). Scanlon et al. (2006) indicated that periods of frequent El Niño events result in three times as much groundwater recharge in the desert Southwest as compared to periods of frequent La Niña events. Flint et al. (2004) demonstrated with their

models that the southern part of the Great Basin gets 220% greater-than-mean recharge during El Niño years. These studies suggest a potential link between ENSO and ciénega state changes. Alternatively, groundwater discharge systems may also respond to local groundwater depletion via extraction in the present day (see Pigati et al., 2014; Sáez et al., 2016).

San Bernardino Ciénega

At San Bernardino Ciénega the pollen preservation ratio is low from the beginning of the record $\sim 8,000$ cal yr BP until $\sim 5,000$ cal yr BP (Minckley and Brunelle, 2007; Minckley et al., 2009, 2011). This transition in preservation coincides closely with our understanding of the initiation of ENSO active conditions (>5 El Niño events per 100 years; Moy et al., 2002). Prior to the onset of active ENSO, the site was an intermittent wetland based on the sediment characteristics and the presence of some aquatic-type pollen grains such as Cyperaceae (Figure 3). After $\sim 5,000$ cal yr BP preservation increases (Figure 7) as does the abundance of wetland pollen taxa (Figure 3). Not only does the pollen preservation ratio track the initiation of ENSO-active conditions at $\sim 5,000$ cal yr BP, but it also decreases during the “quiet active” ENSO period from $\sim 4,500$ to $2,000$ cal yr BP (fewer than 5 El Niño events per 100 years), increasing again with the increase in El Niño activity after $\sim 2,000$ cal yr BP.

The fire history at San Bernardino Ciénega also correlates closely with the timing of the initiation of active ENSO conditions (Figure 7). There is essentially no charcoal in the San Bernardino Ciénega record until before $5,000$ cal yr BP (Brunelle et al., 2010). Prior to $5,000$ cal yr BP, the majority of rainfall in the region would have been from summer monsoons. In the Southwest, increased winter precipitation results in increases in the production of spring flowering annuals, which creates fine herbaceous fuels during the summer (Swetnam and Betancourt, 1990; Bowers, 2005). The production of these fuels creates a fuel continuity which would normally not be present in arid Southwestern desert ecosystems. Prior to the onset of El Niño events, there would have been ignition in the desert with summer convective storms, but the lack of fine fuel associated with enhanced winter precipitation would have prevented fire spread. The absence of charcoal prior to $\sim 5,000$ cal yr BP does suggest minimal fire activity prior to that time. In addition to the step-wise increase in charcoal at $\sim 5,000$ cal yr BP, there is a second increase in charcoal influx at $\sim 1,500$ cal yr BP, coincident with when El Niño activity enters its most active phase (Figure 7). This suggests that once winter precipitation provided the fine fuel source and fuel connectivity, fire activity and charcoal production increased, connecting charcoal records and El Niño activity.

Cloverdale Ciénega

The Cloverdale Ciénega initiates when ENSO enters the active phase $\sim 5,000$ cal yr BP (Figure 7). We propose that the increase in groundwater recharge associated with El Niño-enhanced winter and spring precipitation allowed the water table to rise to the point of surface saturation/standing water and the ciénega to form. Scanlon et al. (2006) assert that groundwater recharge in the desert southwest is controlled by the occurrence of wet winters and springs associated with El Niño conditions. The

pollen preservation at Cloverdale Ciénega also improves with increased activity of El Niño events (Moy et al., 2002; Figure 7). Preservation decreases slightly with a small decrease in El Niño events $\sim 2,000$ cal yr BP, but then preservation increases with the subsequent increase in El Niño events. Wetland taxa like Cyperaceae decrease during the “quiet” El Niño period starting around $4,500$ cal yr BP possibly indicating a lowering of the water table (Minckley et al., 2013b; Figure 4). While the pollen preservation signal remains high for the remainder of the record, Cyperaceae percentages drop with the introduction of cattle to the site $\sim 1,600$ CE (Brunelle et al., 2014). This extensive use of the region for cattle grazing at this time led to woody plant encroachment and a shift in the vegetation community clearly recorded in the sedimentary pollen record (Brunelle et al., 2014).

The charcoal accumulation rate from Cloverdale Ciénega follows the general trends of El Niño frequency with a slight decline in charcoal accumulation associated with the quieter ENSO period (Figure 7). The charcoal record suggests a fire regime controlled by the presence of fine fuels, which would be enhanced by anomalous winter and spring moisture typical of strong El Niño events in the region (Figure 8, also see Heyer et al., 2017). The large increase in charcoal accumulation in the latest part of the record appears to be a decoupling of the natural fire regime and is likely associated with the encroachment of woody plants at this time (Brunelle et al., 2014). The decrease in complete combustion associated with woody fuels would lead to an increase in the production of charcoal (Marlon et al., 2006).

Canelo Hills Ciénega

The preservation ratio at Canelo Hills increases from the onset of the record at $\sim 3,000$ cal yr BP to present. The wetland record from Canelo Hills doesn't initiate until $\sim 3,000$ cal yr BP which is when El Niño enters a consistently active phase. The initiation of Canelo Hills is likely related to the winter precipitation recharge of the aquifer which then allowed water at the surface of the ciénega. In addition to an increase of preservation, Cyperaceae grains become increasingly more abundant from about 500 cal yr BP to present, likely indicating the expansion of the ciénega site. The charcoal accumulation rate slowly increases from the start of the record to present with dips coincident with decreases in the El Niño frequency curve. This again suggests a connection between El Niño years and fine fuel production and accumulation.

Babocamari Ciénega

Babocamari Ciénega is the youngest ciénega of the four sites, with a $\sim 1,800$ cal yr BP record. As with Cloverdale and Canelo Hills, there seems to be a strong connection between the state of ENSO and the initiation of the ciénega. Babocamari initiates after the very highest peaks in El Niño event frequency (Figure 7). There is strong support for the relationship between greater El Niño event frequency and increased groundwater recharge in the Southwestern deserts (e.g., Flint et al., 2004; Scanlon et al., 2006).

Also, like at Canelo Hills, we observe a relatively recent increase in Cyperaceae. At Babocamari the increase begins at about 900 cal yr BP, but then drops from ~ 150 to 50 cal yr BP ($1,800$ – $1,900$ CE). This decrease is likely associated with EuroAmerican impacts to the landscape (e.g., grazing,

water diversion, etc.), however we also see the recovery of the Cyperaceae wetland community in the most recent sample which likely reflects the restoration efforts underway at the ciénega.

Site Synthesis

Continuous records of environmental change reveal how environments respond to past natural perturbations, and provide insight into the trajectory and rate of change environments may experience in the future. Looking for a coherent pattern for the interpretation of desert wetland records is difficult, because unlike temperate lakes which can be produced from glaciation, ciénegas are controlled by local hydrologic conditions (Minckley et al., 2013b). In addition, during periods of disturbance or drought the sediments can be lost (Heffernan, 2008; Heffernan et al., 2008; Minckley et al., 2013b), so we lack a regional context that only multiple sites of similar age can provide. However, there are nested patterns in the data presented here. Wet-dry episodes seen in the longest record, San Bernardino Ciénega, are either repeated in the other records through temporal overlap of ecological histories recorded or the initiation of the younger records. This suggests that there is a regional climate linkage to the development, growth and senescence of these wetlands.

The relationship between fire and ENSO is well recorded in the regional upland forests records of the Southwest (Swetnam and Betancourt, 1990). To assess this relationship from the ciénega records, the average CHAR and pollen preservation ratios were calculated for the 4 sites. These averaged time series were then correlated with the El Niño frequency curve (Moy et al., 2002) to determine if statistically significant relationships exist [e.g., is the frequency of El Niño affecting the fire regime (CHAR) or state (wet vs. dry) of the wetland (as indicated by the pollen preservation ratio)]. When correlations were run on parallel time series (e.g., “no lag”), the correlation 95% confidence interval between El Niño frequency and CHAR was -0.04 to 0.38 with a p -value of 0.10 , and the correlation 95% confidence interval between El Niño and pollen preservation was 0.10 – 0.50 with a p -value of 0.05 (Table 2). These values do suggest that some of the variability in CHAR and pollen preservation are controlled by the frequency of El Niño. However, when one examines the CHAR and pollen preservation curves in comparison with the El Niño frequency curve (Figure 8) a temporal offset is evident. It is ecologically consistent that if there was a period of increased El Niño frequency that the increase in ciénega CHAR might follow with some lag. To better understand ciénega system lags, correlation analyses were performed at 100, 200, 300, 400, and 500 years. The analyses demonstrated that average ciénega CHAR correlates best with El Niño frequency at a lag of 500 years with a correlation 95% confidence interval of 0.26 – 0.62 and p -value of 0.000026 . The same exercise was conducted between El Niño and average ciénega pollen preservation data, with the optimal correlation 95% confidence interval of 0.25 – 0.61 and p -value of 0.00004 identified with a lag of 300 years (Table 2). Again, given the lag in groundwater recharge and emergence following a period of wet winters and springs (high El Niño frequency), and the lag in the drying of a ciénega system following a series of dry winters (low El Niño frequency), it is not surprising the best fit between the two time series included a several

TABLE 2 | Summary of correlation analyses and results.

Variables	95% Confidence interval	p -value
Mean-pollen preservation and mean-charcoal accumulation	0.22–0.59	0.0001
Mean-pollen preservation and El Nino events	0.10–0.50	0.005
Mean-pollen preservation and El Nino events 300 yr lag	0.25–0.61	0.00004
Mean-charcoal accumulation and El Nino events	–0.04–0.38	0.10
Mean-charcoal accumulation and El Nino events 500 yr lag	0.26–0.62	0.000026
Mean-charcoal accumulation and regional standardized charcoal	–0.28–0.16	0.57

hundred year lag. Also, the fact that we are dealing with multiple (likely imperfectly) age-modeled systems should be considered in the evaluation of the statistical correlations between these time series. The compelling result is the relatively high correlation values given the comparison of climatic forcings and ecological responses.

Another observation using the averaged CHAR data comes from the analysis of the averaged ciénega CHAR with the regional standardized CHAR. A 95% confidence interval of -0.26 to 0.15 , and a p -value of 0.57 (Table 2) indicate a lack of relationship between averaged ciénega CHAR and regional standardized CHAR. While ponderosa pine systems demonstrate a relationship with ENSO (Swetnam and Betancourt, 1990), many of the sites in the regional aggregate represent other forest types where fuel availability is less limited than the low elevation ciénega sites. In the American Southwest, upper elevation fire regimes are limited by moisture (low moisture and fire) whereas fire regimes in the deserts are limited by fuel availability (Krawchuk and Moritz, 2011). A Pearson's correlation between average ciénega pollen preservation and average ciénega CHAR reveal a 95% confidence interval of 0.22 – 0.59 and p -value of 0.0001 , suggesting fuel availability limited fire at our sites (Table 2). Further, the different controls on fire regime are strongly reflected in the lack of correlation between the average ciénega CHAR and the regional standardized CHAR (Table 2).

von Post (1946) identified the regions of the world where vegetation history was fairly well known. Conspicuously, temperate regions were well represented, while arid regions were largely blank. This map would be fairly similar today. Desert regions have limited depositional contexts where pollen data are preserved and, as such, quantifying past changes requires a degree of creativity. Our approach has been to take the traditional quantitative method as we have learned it and apply it as best we can in these contexts. However, palynology, as is necessarily practiced in arid environments, requires applying ecological knowledge to the variability within pollen counts (i.e., poor pollen preservation has meaning, and plotting percentages is not always appropriate). In doing so we can provide novel interpretations to the continuous history of place that sedimentary records provide us.

In addition to providing the general paleoenvironmental information for the sites presented here, there are four main interpretations that we make from these records. (1) The length of the sedimentary record provides information on groundwater levels (surface saturation via pollen preservation). (2) The pollen preservation index can be used to determine when sediments are continuously vs. intermittently wetted, which we propose as a proxy for winter precipitation. (3) Our evidence of fire history provides an indirect record of fuel connectivity away from the wetlands largely associated with fine fuel production. (4) Finally, our assessment of modern climate analogs during strong El Niño years provides a mechanism for consistent and persistent delivery of moisture into the region during winter and residual effective moisture during spring, which supports an active ciénega state, pollen preservation and production of fine fuels.

CONCLUSIONS

In the palynological tradition of Lennart Von Post, this paper utilized pollen data to understand the past environment in a poorly known region. We contribute two new ciénega reconstructions to the existing body of work of the relatively sparse paleoenvironmental record in the desert Southwest. Our objectives were to (1) identify conditions in the sedimentological proxy data (e.g., pollen and charcoal) that record changes in ciénega systems attributed to climate; and (2) to assess the dominant atmospheric drivers related to enhanced winter precipitation in ciénega systems. In addition to providing baseline information on the taxa present and fire regimes, we also detected connections between the frequency of El Niño events and sedimentary proxy.

We identified the pollen preservation index as a means to determine when sediments are continuously vs. intermittently wetted, which in this region is a proxy for winter precipitation. We also determined that the length of the sedimentary record provides information on groundwater levels (surface saturation) and the state and input of winter precipitation as well as persistence of effective moisture into spring months. Finally, fire history from ciénegas may be an indirect record of ENSO through the production of fine fuels. We propose that with continued analysis and the addition of more sites, desert ciénega records may be valuable in filling in the gaps of environmental reconstruction as an independent indicator of past El Niño activity.

By using modern climate analogs of strong El Niño events, we provide context for the teleconnections between such modes of variability and persistent wet conditions within desert Southwest

ciénegas. Since pollen preservation in ciénegas is dependent upon wet conditions and winter season precipitation associated with El Niño events that persist into spring in the Southwest, our modern climate analog results provide mechanisms for moisture delivery into the region that would support active ciénegas. This delivery is a function of persistent lower-than-normal pressure and higher-than-normal moisture availability delivered into the region from the subtropics. Our results are specific for the prolonged wetter-than-normal conditions that persist into spring during strong El Niño events. In other words, wetter-than-normal winters alone are not enough to provide moisture availability through subsequent spring months. Thus, analyses of prolonged wet ciénega conditions should consider the impact of persistence associated with multiple season anomalies, such as those that occur during strong El Niño events. Our results suggest that increased El Niño intensity or persistent El Niño events support enhanced and prolonged wet conditions from winter into spring months within ciénega ecosystems. Such persistence of moisture from winter through spring supports both pollen preservation as well as providing conditions conducive for establishment of fine fuels and increased fire activity.

AUTHOR CONTRIBUTIONS

AB and TM: field collection, lab analysis, data analysis, preliminary manuscript writing, editing, revisions; JS: modern climate analog analysis and writing, editing, revisions; JH: correlation analysis, regional charcoal analysis, writing, editing, revisions.

FUNDING

Funding for this research was provided by the EPA SCERP program.

ACKNOWLEDGMENTS

The authors would like to thank The Nature Conservancy for access to the Canelo Hills Ciénega and the Brophy family for access to the Babocamari Ciénega. We appreciate Dale Turner for his support and facilitation of this research over the years. In addition, we express our gratitude to Shawn Blissett and Jessica Spencer for field assistance and lab analysis of the cores. Thanks to Drs. Alberto Saez and Michael-Shawn Fletcher and the reviewers for their thoughtful suggestions on the manuscript and our editor Jesse Morris for his assistance in the publishing process.

REFERENCES

- Abell, R. A. (2000). *Freshwater Ecoregions of North America: A Conservation Assessment*. Island Press.
- Adams, D. K., Comrie, A. C. (1997). The North American monsoon. *Bull. Am. Meteorol. Soc.* 78, 2197–2213. doi: 10.1175/1520-0477(1997)078<2197:TNAM>2.0.CO;2
- Antevs, E. (1944). The right word? *Pollen Anal. Circ.* 6, 2–3.
- Antevs, E. (1962). Late quaternary climates in Arizona. *Am. Antiq.* 28, 193–198. doi: 10.2307/278377
- Antinao, J. L., and McDonald, E. (2013). An enhanced role for the tropical Pacific on the humid pleistocene–holocene transition in Southwestern North America. *Q. Sci.* 78, 319–341. doi: 10.1016/j.quascirev.2013.03.019
- Ashok, K., Behera, S. K., Rao, S. A., Weng, H., and Yamagata, T. (2007). El Niño–Modoki and its possible teleconnection. *J. Geophys. Res.* 112:C11007. doi: 10.1029/2006JC003798

- Baker, M. B. Jr., Ffolliott, P. F., DeBano, L. R., and Neary, D. G. (2004). *Riparian Areas of the Southwestern United States: Hydrology, Ecology, and Management*. Boca Raton, FL: Lewis.
- Barron, J. A., and Anderson, L. (2010). Enhanced Late Holocene ENSO/PDO expression along the margins of the eastern North Pacific. *Q. Int.* 235, 3–12. doi: 10.1016/j.quaint.2010.02.026
- Barry, R. G., and Carleton, A. M. (2001). *Synoptic and Dynamic Climatology*. London; New York, NY: Routledge.
- Betancourt, J. L., Vandevender, T. R., and Martin, P. S. (1990). *Packrat Middens: The Last 40,000 Years of Biotic Change*. Tucson, AZ: The University of Arizona Press.
- Blauw, M. (2010). Methods and code for “classical” age-modelling of radiocarbon sequences. *Q. Geochronol.* 5, 512–518. doi: 10.1016/j.quageo.2010.01.002
- Blarquez, O., Vanni re, B., Marlon J. R., Daniaux, A. L., Power, M. J., Brewer, S. et al. (2014). Paleofire: an R package to analyse sedimentary charcoal records from the Global Charcoal Database to reconstruct past biomass burning. *Comp. Geosci.* 72, 255–261. doi: 10.1016/j.jageo.2014.07.020
- Blissett, S. (2010). *A Late-Holocene Record of Fire, Vegetation and Climate from a Cienega in Sonora, Mexico*. Masters thesis, University of Utah.
- Bowers, J. E. (2005). El Ni o and displays of spring-flowering annuals in the Mojave and Sonoran deserts. *J. Torrey Bot. Soc.* 132, 38–49. doi: 10.3159/1095-5674(2005)132[38:ENADOS]2.0.CO;2
- Brown, D. E. (ed). (1982). *Biotic Communities: Southwestern United States and Northwestern Mexico*. University of Utah Press.
- Brunelle, A., Minckley, T. A., Blissett, S., Cobabe, S. K., and Guzman, B. L. (2010). A nearly 8000 year fire history from an arizona/sonora borderland cienega. *J. Arid Environ.* 74, 475–481. doi: 10.1016/j.jaridenv.2009.10.006
- Brunelle, A., Minckley, T. A., Delgadillo, J., and Blissett, S. (2014). A long-term perspective on woody plant encroachment in the desert southwest, new mexico, U.S.A. *J. Vegetat. Sci.* 25, 829–838. doi: 10.1111/jvs.12125
- Campbell, I. D., and Campbell, C. (1994). Pollen preservation: experimental wet-dry cycles in saline and desalinated sediments. *Palynology* 18, 5–10. doi: 10.1080/01916122.1994.9989434
- Cayan, D. R., Redmond, K. T., and Riddle, L. G. (1999). ENSO and hydrologic extremes in the Western United States. *J. Clim.* 12, 2881–2893. doi: 10.1175/1520-0442(1999)012<2881:EAHEIT>2.0.CO;2
- Clark, J. S. (1988). Particle motion and the theory of stratigraphic charcoal analysis: source area, transportation, deposition, and sampling. *Q. Res.* 30, 81–91. doi: 10.1016/0033-5894(88)90088-9
- Clisby, K. H., and Sears, P. B. (1956). San augustin plains–pleistocene climatic changes. *Science* 124, 537–539. doi: 10.1126/science.124.3221.537
- Cole, A., and Cole, C. (2015). An overview of aridland ci negas, with proposals for their classification, restoration and preservation. *New Mexico Botanist*, 28–56.
- Cole, J. E., and Cook, E. R., (1998). The changing relationship between ENSO variability and moisture balance in the continental United States. *Geophys. Res. Lett.* 25, 4529–4532. doi: 10.1029/1998GL00145
- Comrie, A. C., and Glenn, E. C. (1998). Principal components-based regionalization of precipitation regimes across the southwest United States and northern Mexico, with an application to monsoon precipitation variability. *Clim. Res.* 10, 201–215. doi: 10.3354/cr010201
- Davis, O. K., Minckley, T., Moutoux, T., Jull, T. and Kalin, B. (2002). The transformation of sonoran desert wetlands following the historic decrease of burning. *J. Arid Environ.* 50, 393–412. doi: 10.1006/jare.2001.0914
- Dettinger, M. D., Cayan, D. R., Diaz, H. F., and Meko, D. M. (1998). North–south precipitation patterns in western North America on interannual-to-decadal timescales. *J. Clim.* 11, 3095–3111. doi: 10.1175/1520-0442(1998)011<3095:NSPPIW>2.0.CO;2
- Dettinger, M. D., Cayan, D. R., McCabe, G. M., Marengo, J. A. (2000). “Multiscale streamflow variability associated with El Ni o/Southern Oscillation,” in *El Ni o and the Southern Oscillation-Multiscale Variability and Global and Regional Impacts*, eds H. F. Diaz, and V. Markgraf (Cambridge University Press), 113–146.
- Diem, J. E., Brown, D. P. (2006). Tropospheric moisture and monsoonal rainfall over the southwestern United States. *J. Geophys. Res.* 111, 1–12. doi: 10.1029/2005JD006836
- Edwards, M. E., Mock, C. J., Finney, B. P., Barber, V. A., and Bartlein, P. J. (2001). Potential analogues for paleoclimatic variations in eastern interior Alaska during the past 14,000 yr: atmospheric circulation controls of regional temperature and moisture responses. *Q. Sci. Rev.* 20, 189–202. doi: 10.1016/S0277-3791(00)00123-2
- Enfield, D. B. (1992). “El nino historical and paleoclimatic aspects of the southern oscillation,” in *El Nino: Historical and Paleoclimatic Aspects of the Southern Oscillation*, eds H. F. Diaz, and V. Markgraf (Cambridge: Cambridge University Press), 95–117.
- Erdtman, G. (1969). *Handbook of Palynology: Morphology, Taxonomy, Ecology*. Copenhagen: Macmillan.
- Fægri, K., Kaland, P. E., and Kzywinski, K. (1989). *Textbook of Pollen Analysis*. New York, NY: Wiley.
- Flint, A. L., Flint, L. E., and Hevesi, J. A. (2004). “Fundamental concepts of recharge in the desert southwest: a regional modeling perspective,” in *Groundwater Recharge in a Desert Environment: The Southwestern United States*, eds J. F. Hogan, F. M. Phillips, and B. R. Scanlon (American Geophysical Union Water and Science Application), 9.
- Folke, C., Carpenter, S., Walker, B., Scheffer, M., Elmqvist, T., Gunderson, L. and Holling, C. S. (2004). Regime shifts, resilience, and biodiversity in ecosystem management. *Ann. Rev. Ecol. Syst.* 35, 557–581. doi: 10.1146/annurev.ecolsys.35.021103.105711
- Gershunov, A., and Barnett, T. P. (1998a). Interdecadal modulation of ENSO teleconnections. *Bull. Am. Meteorol. Soc.* 79, 2715–2725. doi: 10.1175/1520-0477(1998)079<2715:IMOET>2.0.CO;2
- Gershunov, A., Barnett, T. P. (1998b). ENSO influence on intraseasonal extreme rainfall and temperature frequencies in the contiguous united states: observations and model results. *J. Clim.* 11, 1575–1586. doi: 10.1175/1520-0442(1998)011<3192:EIOIER>2.0.CO;2
- Hall, S. A. (1985). “Quaternary pollen analysis and vegetational history of the southwest,” in *Pollen Records of Late-Quaternary North American Sediments*, eds V. M. Bryant Jr, and R. G. Holloway (American Association of Stratigraphic Palynologists).
- Hart, I. A., Broughton, J. M. and R. Gruhn (2015). El Ni o controls Holocene rabbit and hare populations in Baja California. *Q. Res.* 84, 46–56. doi: 10.1016/j.yqres.2015.04.005
- Hassan et al. (2005). Available online at: <http://www.millenniumassessment.org/en/index.html>
- Heffernan, J. B. (2008). Wetlands as an alternative stable state in desert streams. *Ecology* 89, 1261–1271. doi: 10.1890/07-0915.1
- Heffernan, J. B., Sponseller, R. A. and Fisher, S. G. (2008). Consequences of a biogeomorphic regime shift for the hyporheic zone of a sonoran desert stream. *Freshw. Biol.* 53, 1954–1968. doi: 10.1111/j.1365-2427.2008.02019.x
- Hendrickson, D. and Minckley, W. L. (1985). Ci negas-vanishing climax communities of the american southwest. *Desert Plants* 6, 130–176.
- Heyer, J. P., Brewer, S. C., and Shinker, J. J. (2017). Using high-resolution reanalysis data to explore localized Western North America hydroclimate relationships with ENSO. *J. Clim.* 30, 5395–5417. doi: 10.1175/JCLI-D-16-0476.1
- Kapp, R. O., Davis, O. K. and King, J. E. (2000). *Guide to Pollen and Spores, 2nd Edn*. American Association of Stratigraphic Palynologists, 279.
- Kirby, M. E., Feakins, S. J., Hiner, C. A., Fantozzi, J., Zimmerman, S. R. H., Dingemans, T. and Mensing, S. A. (2014). Tropical Pacific forcing of Late-Holocene hydrologic variability in the coastal southwestern United States. *Q. Sci. Rev.* 102, 27–38. doi: 10.1016/j.quascirev.2014.08.005
- Krawchuk, M. A., and Moritz, M. A. (2011). Constraints on global fire activity vary across a resource gradient. *Ecology* 92, 121–132. doi: 10.1890/09-1843.1
- Liu, Z., Lu, Z., Wen, X., Otto-Bliesner, B. L., Timmermann, A., Cobb, K. M. (2014). Evolution and forcing mechanisms of El Ni o over the past 21,000 years. *Nature* 515, 550–553. doi: 10.1038/nature13963
- Long, C. J., Whitlock, C., Bartlein, P. J., Millsap, S. H. (1998). A 9000-year fire history from the Oregon Coast Range, based on a high-resolution charcoal study. *Can. J. For.* 28, 774–787. doi: 10.1139/x98-051
- Maher, L. J. (1963). Pollen analyses of surface materials from the southern san-juan mountains, colorado. *Geol. Soc. Am. Bull.* 74, 1485–1503. doi: 10.1130/0016-7606(1963)74[1485:PAOSMF]2.0.CO;2
- Manten, A. A. (1967). Lennart von post and the foundation of modern palynology. *Rev. Palaeobot. Palynol.* 1, 11–22. doi: 10.1016/0034-6667(67)90105-4
- Marlon, J., Bartlein, P. J., and Whitlock, C. (2006). Fire-fuel-climate linkages in the northwestern USA during the Holocene. *Holocene* 16, 1059–1071. doi: 10.1177/0959683606069396

- Martin, P. S. (1963). *The Last 10,000 Years: A Fossil Pollen Record of the American Southwest*. Tucson, AZ: The University of Arizona Press.
- Martin, P. S. and Gray, J. (1962). Pollen analysis and the cenozoic. *Science* 137, 103–111. doi: 10.1126/science.137.3524.103
- Mehring, P. J. (1965). Late pleistocene vegetation in the mohave desert of southern nevada. *J. Arizona Acad. Sci.* 3, 172–188. doi: 10.2307/40022772
- Mehring, P. J. (1967). “The environment of extinction of the late-Pleistocene megafauna,” in *The Arid Southwestern United States*, eds P. S. Martin and H. E. Wright Jr. (New Haven: Pleistocene Extinctions, Yale Univ. Press), 247–266.
- Mensing, S., Smith, J., Burkle Norman, K. and Allan, M. (2008). Extended drought in the great basin of western north america in the last two millennia reconstructed from pollen records. *Q. Int.* 188, 79–89. doi: 10.1016/j.quaint.2007.06.009
- Mesinger, F., DiMego, G., Kalnay, E., Mitchell, K., Shafran, P. C., Ebisuzaki, W., et al. (2006). North American regional analysis. *Bull. Am. Meteorol. Soc.* 87, 343–360. doi: 10.1175/BAMS-87-3-343
- Meyer, E. R. (1973). Late-quaternary paleoecology of cuatro cienegas basin, coahuila, mexico. *Ecology* 54, 983–995. doi: 10.2307/1935565
- Minckley, W. L. (1969). *Environments of the Bolson of Cuatro Ciénegas, Coahuila, Mexico*. Texas Western Press; The University of Texas at El Paso.
- Minckley, W. L. (1992). Three Decades near Cuatro Ciénegas, México: photographic documentation and a plea for area conservation. *J. Arizona-Nevada Acad. Sci.* 26, 89–118.
- Minckley, T. A., and Brunelle, A. (2007). Paleohydrology and growth of a desert cienega. *J. Arid Environ.* 69, 420–431. doi: 10.1016/j.jaridenv.2006.10.014
- Minckley, T. A., Bartlein, P. J., Shinker, J. J. (2004). “Paleoecological response to climate change in the Great Basin since the Last Glacial Maximum,” in *Early and Middle Holocene Archaeology of the Northern Great Basin*, eds D. L. Jenkins, T. J. Connolly, and C. M. Aikens (University of Oregon Anthropological Papers), 21–30.
- Minckley, T. A., Brunelle, A. and Blissett, S. (2011). Holocene sedimentary and environmental history of an in-channel wetland along the ecotone of the sonoran and chihuahuan desert grasslands. *Q. Int.* 235, 40–47. doi: 10.1016/j.quaint.2010.06.031
- Minckley, T. A., Brunelle, A. and Turner, D. (2013a). “A paleoenvironmental framework for understanding the development, stability and state-changes of cienegas in the american deserts,” in *Merging science and management in a rapidly changing world: biodiversity and management of the Madrean Archipelago III, 2012 May 1-5*, eds G. J. Gottfried, P. F. Ffolliott, B. S. Gebow, and L. G. Eskew (Fort Collins Colorado, CO; Tucson, AZ: U.S. Department of Agriculture, Forest Service, Rocky Mountain Research Station), 77–83.
- Minckley, T. A., Clementz, M., Brunelle, A. and Klopfenstein, G. A. (2009). Isotopic analysis of wetland development in the american southwest. *Holocene* 19, 737–744. doi: 10.1177/0959683609105297
- Minckley, T., Turner, D. and Weinstein, S. (2013b). The relevance of wetland conservation in arid regions: a re-examination of vanishing communities in the american southwest. *J. Arid Environ.* 88, 213–221. doi: 10.1016/j.jaridenv.2012.09.001
- Minckley, T. A., Whitlock, C., and Bartlein, P. J. (2007). Vegetation, fire, and climate history of the northwestern Great Basin during the last 14,000 years. *Q. Sci. Rev.* 26, 2167–2184. doi: 10.1016/j.quascirev.2007.04.009
- Mock, C. J. (1996). Climatic controls and spatial variations of precipitation in the western United States. *J. Clim.* 9, 1111–1125. doi: 10.1175/1520-0442(1996)009<1111:CCASVO>2.0.CO;2
- Mock, C. J., and Brunelle-Daines, A. R. (1999). A modern analog of western United States summer palaeoclimate 6,000 years before present. *Holocene* 9, 541–545. doi: 10.1191/095968399668724603
- Mock, C. J., Shinker, J. J. (2013). “Modern analog approaches in paleoclimatology,” in *The Encyclopedia of Quaternary Science*, Vol. 3, ed S. A. Elias (London: Elsevier), 102–112.
- Moy, C. M., Seltzer, G. O., Rodbell, D. T. and Anderson, D. M. (2002). Variability of el nino/southern oscillation activity at millennial timescales during the holocene epoch. *Nature*, 420, 162–165. doi: 10.1038/nature 01194
- Pigati, J. S., Rech, J. A., Quade, J., Bright, J. (2014). Desert wetlands in the geologic record. *Earth Sci. Rev.* 132, 67–81. doi: 10.1016/j.earscirev.2014.02.001
- Quade, J., Rech, J. A., Betancourt, J. L., Latorre, C., Quade, B., Rylander, K. A., and Fisher, T. (2008). Paleowetlands and regional climate change in the central Atacama Desert, northern Chile. *Q. Res.* 69, 343–360. doi: 10.1016/j.yqres.2008.01.003
- Rodríguez, A. A., Mijares, F. J. A., Ojeda, C. G., Morales, M. M., Hita, L. G., Zamarrón, G. H., et al. (2005). *Estudio Hidrogeológico de los Acuíferos el Hundido y Cuatrociénegas*. Secretaría de Medio Ambiente y Recursos Naturales, Instituto Mexicano de Tecnología del Agua, Comisión Nacional del Agua, Instituto Nacional de Ecología.
- Ropelewski, C. F., Halpert, M. S. (1986). North American precipitation and temperature patterns associated with the El Niño/Southern Oscillation (ENSO). *Month. Weat. Rev.* 114, 2352–2362. doi: 10.1175/1520-0493(1986)114<2352:NAPATP>2.0.CO;2
- Sabo, J. L., Sponseller, R., Dixon, M., Gade, K., Harms, T., Heffernan, J., and Welter, J. (2005). Riparian zones increase regional species richness by harboring different, not more, species. *Ecology* 86, 56–62. doi: 10.1890/04-0668
- Sáez, A., Godfrey, L. V., Herrera, C., Chong, G., Pueyo, J. J. (2016). Timing of wet episodes in Atacama Desert over the last 15 ka. The Groundwater Discharge Deposits (GWD) from Domeyko Range at 25°S. *Q. Sci. Rev.* 145, 82–93. doi: 10.1016/j.quascirev.2016.05.036
- Scanlon, B. R., Keese, K. E., Flint, A. L., Flint, L. E., Gaye, C. B., Edmunds, M., et al. (2006). Global synthesis of groundwater recharge in semiarid and arid regions. *Hydrol. Process.* 20, 3335–3370. doi: 10.1002/hyp.6335
- Scheffer, M. and Carpenter, S. R. (2003). Catastrophic regime shifts in ecosystems: linking theory to observation. *Trends Ecol. Evol.* 18, 648–656. doi: 10.1016/j.tree.2003.09.002
- Scheffer, M., Carpenter, S., Foley, J. A., Folke, C. and Walker, B. (2001). Catastrophic shifts in ecosystems. *Nature* 413, 591–596. doi: 10.1038/35098000
- Sheppard, P. R., Comrie, A. C., Packin, G. D., Angersbach, K., Hughes, M. K. (2002). The climate of the US Southwest. *Clim. Res.* 21, 219–238. doi: 10.3354/cr021219
- Shinker, J. J. (2010). Visualizing spatial heterogeneity of western U.S. *Clim. Variab. Earth Interact.* 14, 1–15. doi: 10.1175/2010EI323.1
- Shinker, J. J. (2014). Climatic controls of hydrologic extremes in south-interior intermountain west of Colorado, U.S.A. *Rocky Mount. Geol.* 49, 51–60. doi: 10.2113/gsrocky.49.1.51
- Shinker, J. J., Bartlein, P. J. (2009). Visualizing the large-scale patterns of ENSO-related climate anomalies in North America. *Earth Interactions* 13, 1–50. doi: 10.1175/2008EI244.1
- Shinker, J. J., Bartlein, P. J. (2010). Spatial variations of effective moisture in the western United States. *J. Geophys. Res. Lett.* 37:L02701. doi: 10.1029/2009GL041387
- Shinker, J. J., Bartlein, P. J., Shuman, B. (2006). Synoptic and dynamic climate controls of North American mid-continental aridity. *Q. Sci. Rev.* 25, 1401–1417. doi: 10.1016/j.quascirev.2005.12.012
- Smiley, T. (1974). A memorial to ernst valdemar antevs, 1888–1974. *Geol. Soc. Am.* 1–7.
- Spaulding, W. G. (1991). Pluvial climatic episodes in North America and North Africa: types and correlation with global climate. *Palaeogeogr. Palaeoclimatol. Palaeoecol.* 84, 217–227. doi: 10.1016/0031-0182(91)90045-S
- Swetnam, T. W. and Betancourt, J. L. (1990). Fire - southern oscillation relations in the southwestern united states. *Science* 249, 1017–1020. doi: 10.1126/science.249.4972.1017
- Tipping, R. (2000). “Pollen preservation analysis as a necessity in Holocene palynology,” in *Taphonomy and Interpretation: Symposia of the Association of Environmental Archaeologists*, Vol. 14, Oxbow Books, J. P. Huntley and S. Stallibrass (Oxford), 23–33.
- Tweddle, J. C., and Edwards, K. J. (2010). Pollen preservation zones as an interpretative tool in Holocene palynology. *Rev. Palaeobot. Palynol.* 161, 56–76. doi: 10.1016/j.revpalbo.2010.03.004
- Vonpost, L. (1916). Forest tree pollen in south swedish peat bog deposits, lecture to the 16th convention of scandinavian naturalists, kristiana (oslo). *Pollen et Spores* 9, 375–401.
- von Post, L. (1946). The prospect for pollen analysis in the study of the earth's climatic history. *New Phytol.* 45, 193–217. doi: 10.1111/j.1469-8137.1946.tb05056.x
- Wallace, J. M., Gutzler, D. S. (1981). Teleconnections in the geopotential height field during the northern hemisphere winter. *Month. Weat.*

- Rev. 109, 784–812. doi: 10.1175/1520-0493(1981)109<0784:TITGHF>2.0.CO;2
- Western Regional Climate Center, Monthly Climate Summary Data (2017). Available online at: <http://wrcc.dri.edu/climatedata/climsum/> (Accessed October 24, 2017).
- Wise, E. K. (2010). Spatiotemporal variability of the precipitation dipole transition zone in the northwestern United States. *Geophys. Res. Lett.* 37:L07706. doi: 10.1029/2009GL042193.
- Wolaver, B. D., Crossey, L. J., Karlstrom, K. E., Banner, J. L., Cardenas, M. B., GutiérrezOjeda, C., et al. (2013). Identifying origins of pathways for spring waters in a semiarid basin using He, Sr, and C isotopes: Cuatrociénegas Basin, Mexico. *Geosphere* 9, 113–125. doi: 10.1130/GES00849.1
- Wolter, K., and M. S. Timlin (1993). “Monitoring ENSO in COADS with a seasonally adjusted principal component index,” in *Proceedings of the 17th climate diagnostics workshop* (Norman, OK, NOAA/NMC/CAC, NSSL, Oklahoma Clim. Survey, CIMMS and the School of Meteor, University of Oklahoma), 52–57.
- Wolter, K., and M. S. Timlin (1998). Measuring the strength of ENSO events - how does 1997/98 rank? *Weather* 53, 315–324. doi: 10.1002/j.1477-8696.1998.tb06408.x
- Wolter, K., Timlin, M. S. (2011). El Niño/Southern Oscillation behaviour since 1871 as diagnosed in an extended multivariate ENSO index (MEI.ext). *Int. J. Climatol.* 31, 1074–1087. doi: 10.1002/joc.2336
- Yarnal, B. (1993). *Synoptic Climatology in Environmental Analysis: A Primer*. London:Belhaven Press, 195.
- Yarnal, B., Comrie, A. C., Frakes, B., Brown, D. P. (2001). Developments and prospects in synoptic climatology. *Int. J. Climatol.* 21, 1923–1950. doi: 10.1002/joc.675

Conflict of Interest Statement: The authors declare that the research was conducted in the absence of any commercial or financial relationships that could be construed as a potential conflict of interest.

The handling editor declared a shared affiliation, though no other collaboration, with one of the authors, AB.

Copyright © 2018 Brunelle, Minckley, Shinker and Heyer. This is an open-access article distributed under the terms of the Creative Commons Attribution License (CC BY). The use, distribution or reproduction in other forums is permitted, provided the original author(s) and the copyright owner(s) are credited and that the original publication in this journal is cited, in accordance with accepted academic practice. No use, distribution or reproduction is permitted which does not comply with these terms.



Long-Term Vegetation Dynamics in a Megadiverse Hotspot: The Ice-Age Record of a Pre-montane Forest of Central Ecuador

Encarni Montoya^{1,2*}, Hayley F. Keen¹, Carmen X. Luzuriaga³ and William D. Gosling^{1,4}

¹ School of Environment, Earth and Ecosystem Sciences, The Open University, Milton Keynes, United Kingdom, ² Instituto de Ciencias de la Tierra Jaume Almera, Consejo Superior de Investigaciones Científicas, Barcelona, Spain, ³ Estación Biológica de Pindo-Mirador, Universidad Tecnológica Equinoccial, Quito, Ecuador, ⁴ Institute for Biodiversity and Ecosystem Dynamics, University of Amsterdam, Amsterdam, Netherlands

OPEN ACCESS

Edited by:

Urs Feller,
University of Bern, Switzerland

Reviewed by:

Irene Tunno,
Lawrence Livermore National
Laboratory (DOE), United States
Walter Finsinger,
Centre National de la Recherche
Scientifique (CNRS), France
Juanma Rubiales,
Universidad Politécnica de Madrid
(UPM), Spain

*Correspondence:

Encarni Montoya
emontoya@ictja.csic.es;
encarnacionmontoya@gmail.com

Specialty section:

This article was submitted to
Agroecology and Land Use Systems,
a section of the journal
Frontiers in Plant Science

Received: 16 November 2017

Accepted: 01 February 2018

Published: 20 February 2018

Citation:

Montoya E, Keen HF, Luzuriaga CX
and Gosling WD (2018) Long-Term
Vegetation Dynamics in a
Megadiverse Hotspot: The Ice-Age
Record of a Pre-montane Forest
of Central Ecuador.
Front. Plant Sci. 9:196.
doi: 10.3389/fpls.2018.00196

Tropical ecosystems play a key role in many aspects of Earth system dynamics currently of global concern, including carbon sequestration and biodiversity. To accurately understand complex tropical systems it is necessary to parameterise key ecological aspects, such as rates of change (RoC), species turnover, dynamism, resilience, or stability. To obtain a long-term (>50 years) perspective on these ecological aspects we must turn to the fossil record. However, compared to temperate zones, collecting continuous sedimentary archives in the lowland tropics is often difficult due to the active landscape processes, with potentially frequent volcanic, tectonic, and/or fluvial events confounding sediment deposition, preservation, and recovery. Consequently, the nature, and drivers, of vegetation dynamics during the last glacial are barely known from many non-montane tropical landscapes. One of the first lowland Amazonian locations from which palaeoecological data were obtained was an outcrop near Mera (Ecuador). Mera was discovered, and analysed, by Paul Colinvaux in the 1980s, but his interpretation of the data as indicative of a forested glacial period were criticised based on the ecology and age control. Here we present new palaeoecological data from a lake located less than 10 km away from Mera. Sediment cores raised from Laguna Pindo (1250 masl; 1°27'S, 78°05'W) have been shown to span the late last glacial period [50–13 cal kyr BP (calibrated kiloyears before present)]. The palaeoecological information obtained from Laguna Pindo indicate that the region was characterised by a relatively stable plant community, formed by taxa nowadays common at both mid and high elevations. *Miconia* was the dominant taxon until around 30 cal kyr BP, when it was replaced by *Hedyosmum*, Asteraceae and *Ilex* among other taxa. Heat intolerant taxa including *Podocarpus*, *Alnus*, and *Myrica* peaked around the onset of the Last Glacial Maximum (c. 21 cal kyr BP). The results obtained from Laguna Pindo support Colinvaux's hypothesis that glacial cooling resulted in a reshuffling of taxa in the region but did not lead to a loss of the forest structure. Wide tolerances of the plant species

occurring to glacial temperature range and cloud formation have been suggested to explain Pindo forest stability. This scenario is radically different than the present situation, so vulnerability of the tropical pre-montane forest is highlighted to be increased in the next decades.

Keywords: diversity dynamics, eastern Andean flank, Last Glacial Maximum, neotropics, palaeoecology, stability, vulnerability, western equatorial Amazonia

INTRODUCTION

The degree to which the structure and composition of vegetation in tropical South America has been altered in response to high magnitude past global climate change has been long debated (Haffer, 1969; Liu and Colinvaux, 1985; Bush et al., 1990; Absy et al., 1991; Heine, 1994). Revealing the sensitivity of tropical forests to past climate change is the only way in which empirical data can be obtained into how this complex biodiverse region is likely to respond to projected future climate change (Cox et al., 2000; Myers et al., 2000; Malhi and Wright, 2004; IPCC, 2013). Furthermore, it is only by exploring the fossil record that we can parameterise the speed of change that the vegetation has experienced with in the past and consequently gain an idea of the rate at which it may be able to change in the future. Palaeoecology contains powerful tools, such as fossil pollen analysis, with which the dynamics of the vegetation communities through time can be unravelled (Von Post, 1916). The global Last Glacial Maximum (LGM) period (26.5–19 kyr BP; Clark et al., 2009) saw temperatures in the South American tropics of between 4 and 5°C and up to 8°C cooler than modern in the Andes (Bush et al., 2007), and 4–7°C cooler than the modern Amazon (Liu and Colinvaux, 1985; Bush et al., 1990). The LGM-to-modern warming to which tropical South America was subject to over the past 20 ka is, therefore, equivalent to the projected magnitude of change for the next century (IPCC, 2013). In addition, during the last glacial period precipitation (Mosblech et al., 2012) and landscape processes (Loughlin et al., 2018) are likely to have contributed to vegetation change. However, due to a paucity of study sites little is known about the structure and composition of tropical South American glacial vegetation and how it changed during the last glacial period (Colinvaux et al., 1996; Flantua et al., 2015).

The first evidence of glacial vegetation obtained through fossil pollen analysis comes from an outcrop on the Ecuadorian eastern Andean flank near the town of Mera (Liu and Colinvaux, 1985). The glacial sediments from the Mera section were interpreted as containing fossils from a mixture of lowland vegetation and other taxa that live nowadays at higher elevations, and were used to infer a temperature decrease of around 4.5°C compared to present-day. These data were received with scepticism by some researchers, especially regarding: (1) the chronology of the section (Heine, 1994), and (2) the tolerance range of ecological conditions of some of the taxa identified in the record (Gentry, 1993). In fact, some of these debates are still ongoing (Cárdenas et al., 2011a,b; Puyasena et al., 2011). The use of outcrops represents the primary source of sedimentary archives in a very geomorphologically active region (Hall et al., 2008; Lombardo,

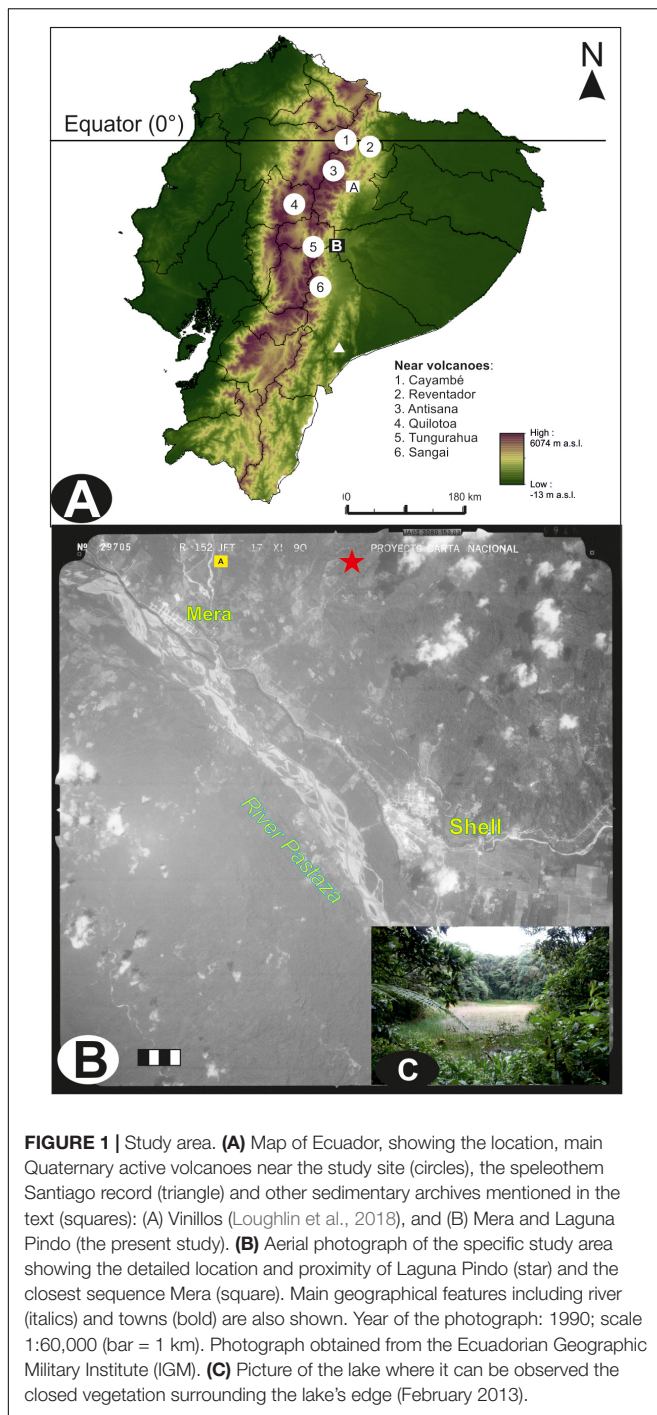
2014, 2016). However, outcrops often only represent a short time window and do not contain sediments extending up to the present so consequently interpretation can sometimes be challenging. In addition, outcrops on the eastern Andean flank normally contain interbedded layers of organic (pollen-rich) and inorganic (tephra-like) layers (Cárdenas et al., 2014; Loughlin et al., 2018). This mixture of processes that lead to the sediments' deposits can easily compromise the continuity of the record by containing numerous sedimentary gaps or hiatuses between the different layers, preventing the study of the vegetation changes in a continuous, dynamic fashion.

Here we present for the first time a continuous vegetation dynamics record from a lacustrine sequence of a mid-elevation Ecuadorian forest located within the diversity hotspot of the eastern Andean flank, in western Amazonia. The glacial dynamics will be explored based on pollen analysis, and supported by charcoal and stable isotope analyses. The aim is to reconstruct the full to late glacial vegetation dynamics, from around 50 to 13 cal kyr BP (calibrated kiloyears before present), as well as to derive potential palaeoclimatic and palaeoecological inferences. The study focuses on the potential changes that might have occurred around the LGM, and it was prompted by the lack of glacial lacustrine palaeoecological studies in the region and the unknown responses of its unique and endangered ecosystem to potential environmental changes. Emphasis will be placed on diversity and stability dynamics, as well as to identify the drivers that have triggered such dynamism. Final details about the sensitivity and resilience of the glacial forest that preceded the current plant community as well as the nature of the forest components will be discussed.

MATERIALS AND METHODS

Study Area

Laguna Pindo (1°27'S–78°05'W) is a small shallow lake (c. 1.2 m depth), roughly circular shaped (c. 40 m diameter), located in the Pastaza province near the town of Mera at an elevation of 1248 masl (**Figure 1**). Mean annual temperature is about 20.8°C with little seasonal variation, annual precipitation can reach up to 4800 mm per year (Ferdon, 1950; Hijmans et al., 2005). Currently the lake is not directly fed by an in-flow and has no visible out-flow; the lake receives water from surface run-off and via direct precipitation, with a rough estimation of a small catchment of around 2–3 km (**Figure 1**). The study site is positioned in the Andean foothills on a steep slope dropping down to the Pastaza river basin (**Figure 1**), there are no obvious geomorphological causes for the escarpment of



the lake and we hypothesise it is tectonic in origin (Matthews-Bird et al., 2017). The underlying geology of the eastern Andean flank is composed primarily of metamorphic rocks of Palaeozoic to Jurassic age (Aspden and Litherland, 1992; de Berc et al., 2005). The rocks were metamorphosed during the late Cretaceous and the Paleocene, and subsequently were overlain by volcanic/volcaniclastic formations of late Miocene to Quaternary origin (Bernal et al., 2011, 2012). Specifically, the inorganic sediment recovered at the bottom of the sequence has

been classified as basalt (Matthews-Bird et al., 2017). Laguna Pindo is a mid-elevation site at the transition between the high elevation *páramo* vegetation and lowland Amazonia rain forest. The site lies within an area classified as lower montane rain forest (Harling, 1979), or pre-montane forest (Sierra, 1999), just below the lower limit of the cloud forest. The lake is in an advanced stage of filling in, with abundant aquatic plants (*Eleocharis maculosa*, Cyperaceae) growing within the lake. The lake is completely surrounded by a closed belt of vegetation to the water's edge. The closed forest surrounding the site has a canopy of 15–25 m high; the dominant species belong to families of Melastomataceae, Araceae, Cecropiaceae, Euphorbiaceae, Myrtaceae, Rubiaceae, Myristicaceae, Asteraceae, and Mimosaceae. Lianas, epiphytes (Bromeliaceae, Orchidaceae), and tree ferns are also common (Jørgensen and León-Yáñez, 1999). A survey of the vegetation belt at the lake's edge is presented in Table 1. The lake is remote and currently beyond the influence of direct human activity such as agriculture and urbanisation, except for the presence of a biological station nearby.

Methodology

A sediment core was extracted from the deepest point of the lake in January 2013 using a cam-modified Livingstone piston corer (Livingstone, 1955; Colinvaux et al., 1999). The sediment core recovered had a total length of 924 cm. This study presents a multi-proxy investigation (sediment characteristics, pollen, charcoal, and stable isotope) of the lower section of the sediment core (514–924 cm), which has been dated to the last glacial period. Eighteen samples were selected through the entire sequence and sent to the NERC Radiocarbon Facility, SUERC, East Kilbride, Scotland for radiocarbon analysis by accelerator mass spectrometry (Table 2). An age-depth model was constructed using the statistical package “clam” in R (Blaauw, 2010) using the calibration curve SHCal.13.14c (Hogg et al., 2013).

Samples for pollen analysis (1 cc of wet sediment and 1 cm thickness) were processed using standard methods including KOH, HCl, and HF digestions, acetolysis and mounting/storing in glycerin jelly (Faegri and Iversen, 1989). *Lycopodium* tablets (University of Lund batch n° 124961; 12,542 spores/tablet) were added before chemical processing (Stockmarr, 1971). Counting was conducted until a minimum of 300 pollen and spores and the saturation of diversity (Rull, 1987). The pollen sum included all pollen types with the exception of aquatic plants (Cyperaceae, *Myriophyllum*, *Sagittaria*, *Utricularia*). Identification was based on the reference collection held at The Open University (United Kingdom), and regional floras and atlases (e.g., Roubik and Moreno, 1991; Colinvaux et al., 1999; Bush and Weng, 2006). Given the diversity of the study area, non-identified morphotypes were coded with the acronym UPP (Unidentified Pollen grain from Pindo). Charcoal particles were identified and counted in the same palynological slides, only particles >5 μm were considered and two different classes were established based on size: (1) small particles (>5–100 μm), indicative of regional fires due to easy dispersion by wind, and (2) big particles (>100 μm), indicative of fires occurred more in a local scale (Whitlock and Larsen, 2001).

TABLE 1 | List of main vegetation taxa currently present surrounding Laguna Pindo based on rough field survey by C. X. Luzuriaga in 2013 and Luzuriaga (2007).

Taxon	Family	Type
<i>Alchornea leptogyna</i>	Euphorbiaceae	Tree
<i>Aniba hostmanniana</i>	Lauraceae	Tree
<i>Anthurium</i> sp.	Araceae	Epiphyte
<i>Cabralea canjerana</i>	Meliaceae	Tree
<i>Calathea lutea</i>	Maranthaceae	Herb
<i>Cecropia engleriana</i>	Cecropiaceae	Tree
<i>Ceiba pentandra</i>	Bombacaceae	Tree
<i>Celtis guianensis</i>	Ulmaceae	Tree
<i>Clusia pallida</i>	Clusiaceae	Hemiepiphyte
<i>Cordia alliodora</i>	Boraginaceae	Tree
<i>Costus amazonicus</i>	Costaceae	Herb
<i>Croton lechleri</i>	Euphorbiaceae	Tree
<i>Dacryodes olivifera</i>	Burseraceae	Tree
<i>Eugenia</i> cf. <i>dibrachiata</i>	Myrtaceae	Tree
<i>Guadua angustifolia</i>	Poaceae	Tree
<i>Heliconia stricta</i>	Heliconiaceae	Herb
<i>Inga silanchensis</i>	Mimosaceae	Tree
<i>Inga velutina</i>	Mimosaceae	Tree
<i>Laetia procera</i>	Flacourtiaceae	Tree
<i>Macrolobium acaciifolium</i>	Caesalpiniaceae	Tree
<i>Matisia cordata</i>	Bombacaceae	Tree
<i>Miconia barbeyana</i>	Melastomataceae	Shrub–treelet–tree
<i>Miconia dielsi</i>	Melastomataceae	Shrub–tree
<i>Miconia splendens</i>	Melastomataceae	Shrub–treelet–tree
<i>Miconia</i> sp.	Melastomataceae	Shrub–treelet–tree
<i>Nectandra coeloclada</i>	Lauraceae	Tree
<i>Ocotea cernua</i>	Lauraceae	Tree
<i>Otoba parviflora</i>	Myristicaceae	Tree
<i>Palicourea guianensis</i>	Rubiaceae	Tree
<i>Piper aduncum</i>	Piperaceae	Shrub–treelet
<i>Pollalesta discolor</i>	Asteraceae	Tree
<i>Pourouma guianensis</i>	Cecropiaceae	Tree
<i>Pouteria multiflora</i>	Sapotaceae	Tree
<i>Sapium marmieri</i>	Euphorbiaceae	Tree
<i>Senna ruiziana</i>	Caesalpiniaceae	Tree
<i>Siparuna schimpffii</i>	Monimiaceae	Shrub–tree
<i>Socratea exorrhiza</i>	Arecaceae	Tree
<i>Saurauia prainiana</i>	Actinidiaceae	Shrub–treelet
<i>Syzygium jambos</i>	Myrtaceae	Tree
<i>Trema micrantha</i> -t*	Ulmaceae	Tree
<i>Turpinia occidentalis</i>	Staphyleaceae	Tree
<i>Viburnum ayavacense</i>	Caprifoliaceae	Shrub
<i>Vismia baccifera</i>	Clusiaceae	Tree
<i>Vochysia bracheliinae</i>	Vochysiaceae	Tree
<i>Wettinia maynensis</i>	Arecaceae	Tree
<i>Xanthosoma</i> sp.	Araceae	Herb
<i>Zanthoxylum kellermani</i>	Rutaceae	Tree

Family and plant type have been included following Jorgensen and León-Yáñez (1999). Asterisk "*" refers to visual ID in field only by common name (e.g., *Sapán negro*), caution must be taken.

Analysis of the stable isotopes $\delta^{13}\text{C}$ and $\delta^{15}\text{N}$ was performed at a 4–10 cm sampling interval. Samples for $\delta^{13}\text{C}$ and $\delta^{15}\text{N}$ were obtained from ~0.6 g sample aliquots that were homogenised and treated sequentially with 0.1 and 1 M HCl for 24 h, before being rinsed to neutrality with Milli-Q water ($18.2 \text{ M}\Omega \text{ cm}^{-1}$). Each step, involving a change of reagent or water, was preceded by centrifugation to prevent the loss of fine material in suspension. The isotopic composition ($\delta^{13}\text{C}$ and $\delta^{15}\text{N}$) of the dried re-homogenised residues was then determined using a Thermo Flash HT elemental analyser equipped with a Thermo zero-blank device coupled to a Thermo MAT 253 mass spectrometer (EA-MS). Results are expressed following the guidelines for the reporting of stable isotope measurement results (Coplen, 2011).

Pollen diagram, diversity measures, and cluster analyses were performed in R version 3.82 using the packages “vegan” 2.3-5 (Oksanen et al., 2013) and “rioja” (Juggins, 2017). For the cluster analysis the dataset used was the percentage data after square root transformation and the cluster method used was “average” (after calculating the dissimilarity). Zonation was obtained by CONISS using the broken stick method to determine the significant zones (Bennett, 1996). RoC as defined by Urrego et al. (2009) were calculated using the R package PaleoMas (Correa-Metrio et al., 2010). Diversity measures include N_0 (richness or species number, also called S), N_1 and N_2 , calculated following Hill (1973). For calculating the indices, the dataset used was the raw data without downweight of rare taxa in order to capture the total diversity values.

RESULTS

Sediment Description and Chronology

The sediment recovered from Laguna Pindo consists mostly of peat and clay with different levels of organic content, and frequent wood remains interbedded in the sediment. Based on the differences found, five sedimentary units were defined (Figure 2 and Table 3). The glacial interval was found in the sedimentary record from 514 cm downwards, corresponding to the Units 4 and 5, and the bottom section of Unit 3, delimited by the presence of a hiatus (Figure 2).

An age-depth model for Laguna Pindo was constructed in Clam.R based on eighteen radiocarbon dates samples (Table 2). The best fit was obtained with a linear interpolation (Figure 2), allowing the calculation of the RoC following Urrego et al. (2009) (Table 4). The sedimentation rate was found to be highly variable, ranging from 0.0009 to 0.25 cm yr^{-1} , with an average of 0.074 cm yr^{-1} (Figure 2). For the glacial interval, the sedimentation rate found was at least an order of magnitude slower compared to the Holocene section, ranging between 0.02 and 0.003 cm yr^{-1} for most of the interval, and showing the lowest value of $0.0009 \text{ cm yr}^{-1}$ for the upper part of the glacial section (late Glacial).

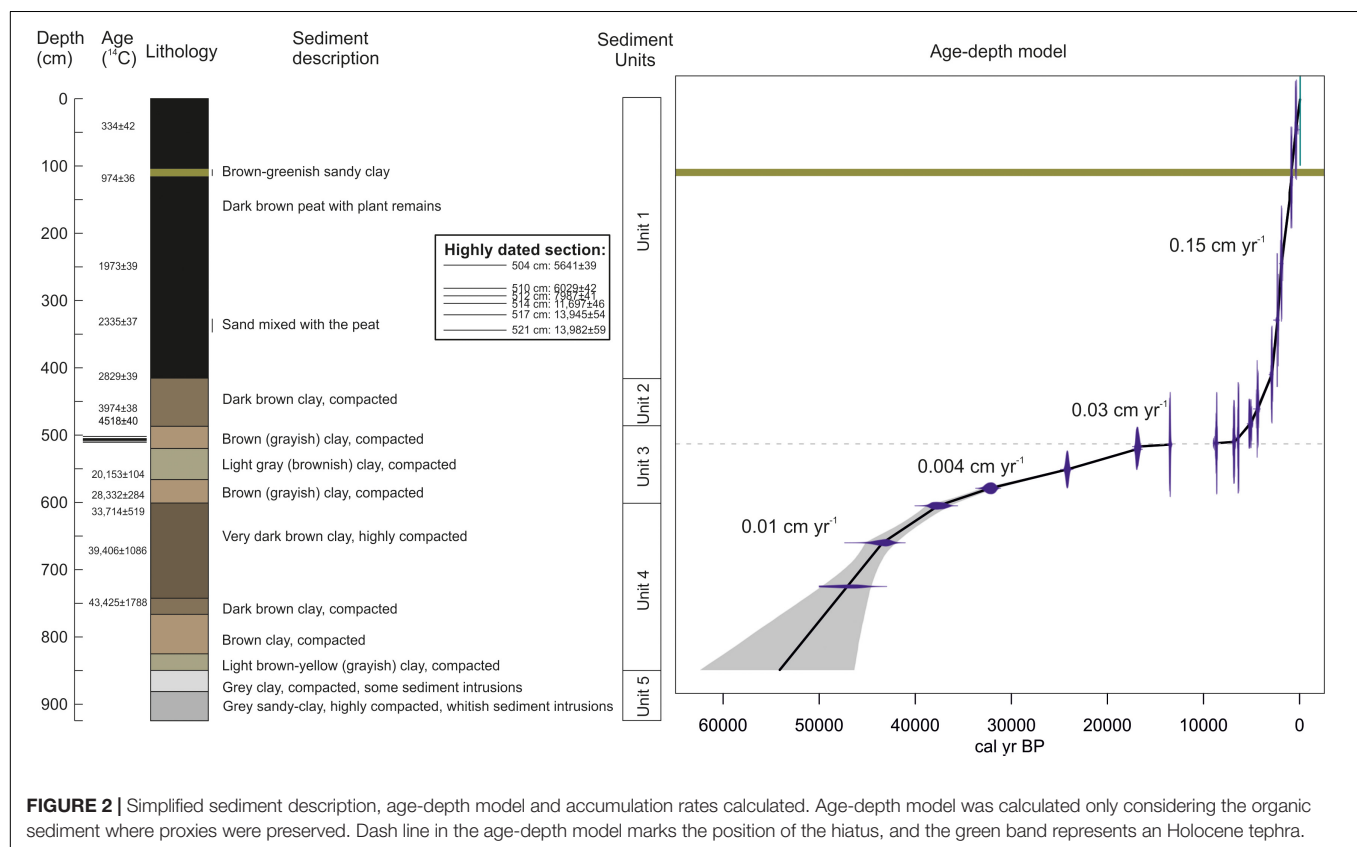
Pollen Zones

Pollen grains were found in Laguna Pindo until 822 cm depth, coinciding with the beginning of the sedimentary Unit

TABLE 2 | Conventional (yr BP) and calibrated (cal kyr BP) radiocarbon data used in construction of chronologies for Laguna Pindo.

Publication code	Depth (cm)	$\delta^{13}\text{C}_{\text{VPDB}} (\text{‰})^*$	^{14}C age (yr BP)	Calendar age (cal kyr BP) 2σ
SUERC-54395 ^b	46	-30.2	334 ± 42	289–470
SUERC-47634 ^b	117	-27.9	974 ± 36	769–923
SUERC-47635 ^b	245	-27.3	1973 ± 39	1812–1943
SUERC-47569 ^b	329	-24.9	2335 ± 37	2293–2361
SUERC-47572 ^b	410	-22.7	2829 ± 39	2781–2991
SUERC-48854 ^a	461	-28.7	3974 ± 45	4241–4447
SUERC-54385 ^a	483	-27.9	4518 ± 40	4969–5300
SUERC-54386 ^a	504	-27.8	5641 ± 39	6298–6454
SUERC-54387 ^a	510	-27.4	6029 ± 42	6717–6946
SUERC-61456 ^a	512	-28.4	7897 ± 41	8542–8784
SUERC-61457 ^a	514	-28.1	11,697 ± 46	13,387–13,580
SUERC-61458 ^a	517	-28.0	13,945 ± 54	16,581–17,073
SUERC-48855 ^a	521	-28.0	13,982 ± 59	16,618–17,138
SUERC-54388 ^a	551	-28.1	20,153 ± 104	23,907–24,450
SUERC-61459 ^a	579	-29.5	28,332 ± 284	31,449–32,998
SUERC-45933 ^b	605	-23.6	33,417 ± 519	36,354–38,781
SUERC-61505 ^a	660	-29.2	39,406 ± 1086	41,942–45,129
SUERC-56825 ^b	725	-26.7	43,425 ± 1788	44,725–49,907

* $\delta^{13}\text{C}$ values were measured on a dual inlet stable isotope mass spectrometer (Thermo Scientific Delta V Plus) and are representative of $\delta^{13}\text{C}$ in the pre-treated sample material. ^aBulk sediment samples; ^bwood remains' samples. Samples were 1 cm thick.



5 (Figure 2), which was barren for any biological remain. The pollen diagram of Laguna Pindo during the glacial interval delimits four significant zones based on differences in the most abundant taxa, only taxa occurring at percentages higher than

10% are represented (Figure 3). Charcoal particles have been calculated both as concentration and influx values. The two orders of magnitude difference in the sedimentation rate between the top and bottom of the sequence is generating an artefact in

TABLE 3 | Sedimentary units defined for Laguna Pindo core including main features.

Unit	Depth (cm)	Sediment	Colour	Features
Unit 1	0–414	Organic peat	10YR-2/2	The interval between 182 and 307 cm is characterised by numerous large wood remains Within this interval, a tephra is preserved at 105–114 cm depth (colour: 2.5YR-2/2), dated around 850 years ago and likely originated from Tungurahua or Quilotoa volcanoes event (Matthews-Bird et al., 2017)
Unit 2	414–482	Organic clay	2.5YR-3/3 2.5YR-3/1	Gradual change to upper unit (Unit 1)
Unit 3	482–601	Light clay	2.5YR-4/2 2.5YR-5/2 2.5YR-6/2 2.5YR-5/4	Very gradual transition colours, from darker to the extremes to lighter in the medial zone. Sediment compacted
Unit 4	601–850	Organic clay	10YR-2/2 10YR-3/2 10YR-4/2 10YR-3/2 10YR-4/2	Compacted sediment with occasional large wood remains
Unit 5	850–924	Inorganic clay	2.5YR-5/2 2.5YR-6/1 2.5YR-7/2 2.5YR-6/1 2.5YR-8/3	Highly compacted. XRF analysis of major elements located this sediment in a TAS diagram within the basalt domain (Matthews-Bird et al., 2017)

Munsell Colour Chart was used for defining the sediment colours.

TABLE 4 | Ecological metrics of Laguna Pindo glacial vegetation based on pollen data: rates of change (RoC) were calculated following Urrego et al. (2009), and diversity indices (N_0 , N_1 , N_2 , and the ratio N_2/N_0) following Hill (1973).

Age	RoC	N_0	N_1	N_2	N_2/N_0
13,487	NA	57	23.091	13.71	0.24
15,685	1.21×10^{-4}	45	24.697	17.54	0.39
16,783	4.03×10^{-4}	52	24.738	15.76	0.30
18,402	1.62×10^{-4}	47	26.729	18.25	0.39
20,809	1.91×10^{-4}	45	19.806	12.75	0.28
22,975	1.05×10^{-4}	51	23.592	14.97	0.29
25,614	1.15×10^{-4}	43	20.640	13.96	0.32
28,486	3.82×10^{-5}	50	22.840	14.36	0.29
31,358	1.51×10^{-4}	50	20.729	12.92	0.26
33,673	4.69×10^{-5}	50	19.781	11.42	0.23
40,875	5.48×10^{-5}	45	16.710	7.71	0.17
44,868	7.68×10^{-5}	50	23.269	14.07	0.28
47,135	9.18×10^{-5}	50	17.738	7.50	0.15
50,534	5.83×10^{-5}	56	16.611	7.52	0.13
52,574	3.77×10^{-4}	40	18.887	11.17	0.28

Sample age is reported in cal kyr BP.

the charcoal influx curve, which is masking the values attained at the top of the sequence (Figure 3). In this sense, results will be described following the concentration curve, although the interpretation of both curves will be provided in the next section.

Pollen Zone PIG-1: From 822 to 756 cm; >50–48.8 cal kyr BP

The oldest section of Laguna Pindo is marked by a decrease to the top of the zone of *Hedyosmum* and Asteraceae, and in a

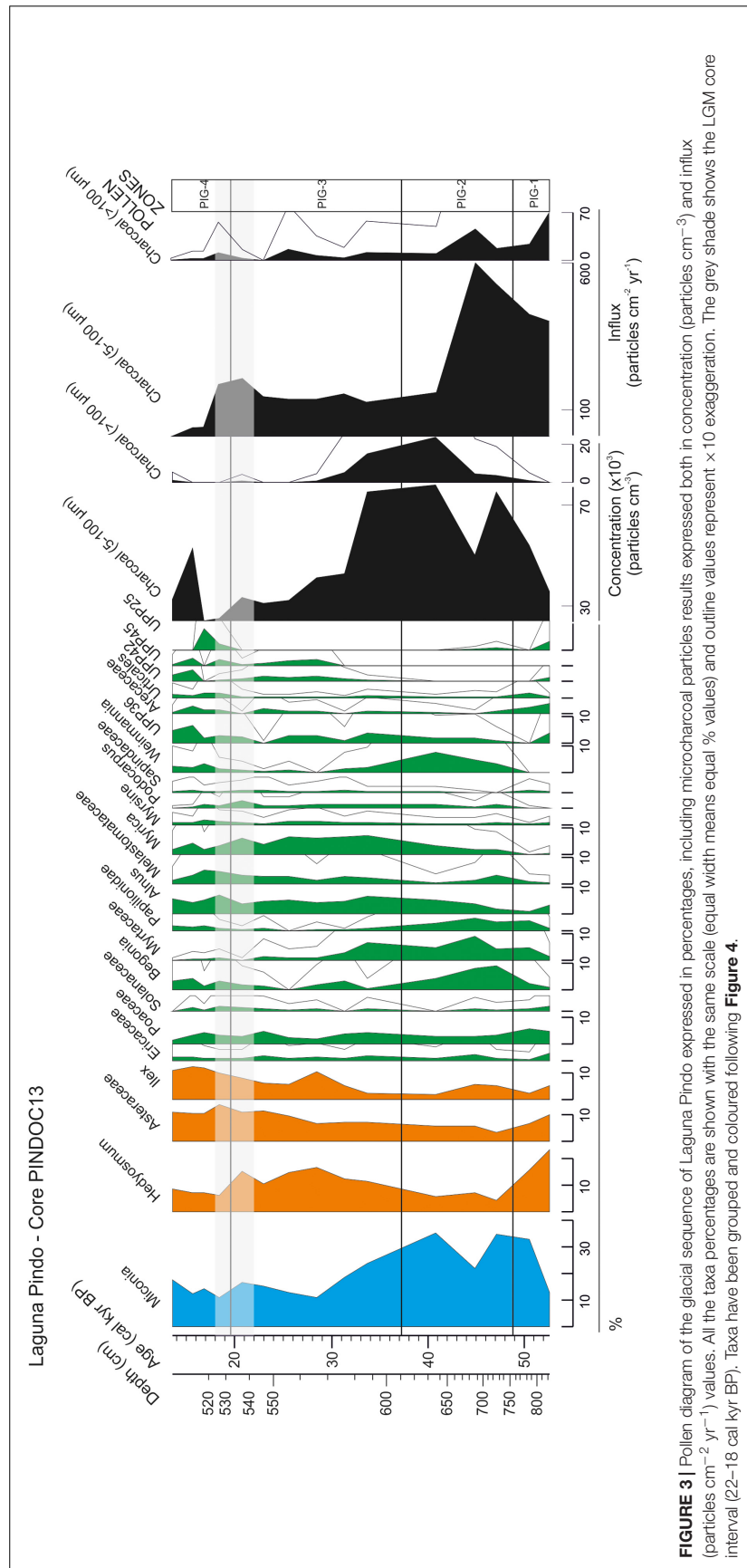
minor extent *Alnus* and some unidentified morphotypes such as UPP36, UPP42, and UPP25. At the same time, *Miconia* shows the opposite trend. Total pollen concentration ranges from 257,000 to 1,000,000 pollen grains cc^{-1} . The charcoal record during this interval is low (Figure 3).

Pollen Zone PIG-2: From 756 to 611 cm; 48.8–37.3 cal kyr BP

PIG-2 shows the inverse relationship between the dominant taxa of the previous zone *Hedyosmum* and *Miconia*, with low and high values, respectively (Figure 3). *Weinmannia* appears during this zone and *Alnus*, *Myrica*, *Myrsine*, *Podocarpus*, and UPP36 increase the abundance attained in the previous zone. On the contrary, taxa including Sapindaceae, Urticales, and unidentified UPP42 and UPP25 greatly decrease or disappears from the record. *Begonia*, *Ilex*, and Melastomataceae are also abundant at the beginning of the zone, but start decreasing towards the upper section. This zone is characterised in the upper half by the maximum values of charcoal, both small and big size (indicative of regional and local fires, respectively). Regarding pollen concentration, the values in this zone are also the highest of the record ranging from 436,000 to 1,279,000 pollen grains cc^{-1} .

Pollen Zone PIG-3: From 611 to 532 cm; 37.3–19.6 cal kyr BP

The most dramatic change of the vegetation surrounding Pindo during glacial time corresponds to the decrease observed in *Miconia* during this zone to values below 20%, until the middle of the section. Following the previous zone, *Hedyosmum* shows an opposite character to *Miconia*, evident in this zone with a subtle but solid increase. Coeval to the minimum value of



Miconia, a peak in *Ilex* is observed, followed by a steadier increase towards the top of the zone. UPP42 and UPP45 reappear during this zone, whereas Papilionidae, *Weinmannia*, and Myrtaceae decrease. The charcoal curve follows the high values attained at the end of the previous zone until approximately 32 cal kyr BP when they suddenly decrease to half of the particles abundance. Total pollen concentration in PIG-3 ranges from 277,000 to 905,000 pollen grains cc^{-1} .

Pollen Zone PIG-4: From 532 to 514 cm; 19.6–13.5 cal kyr BP

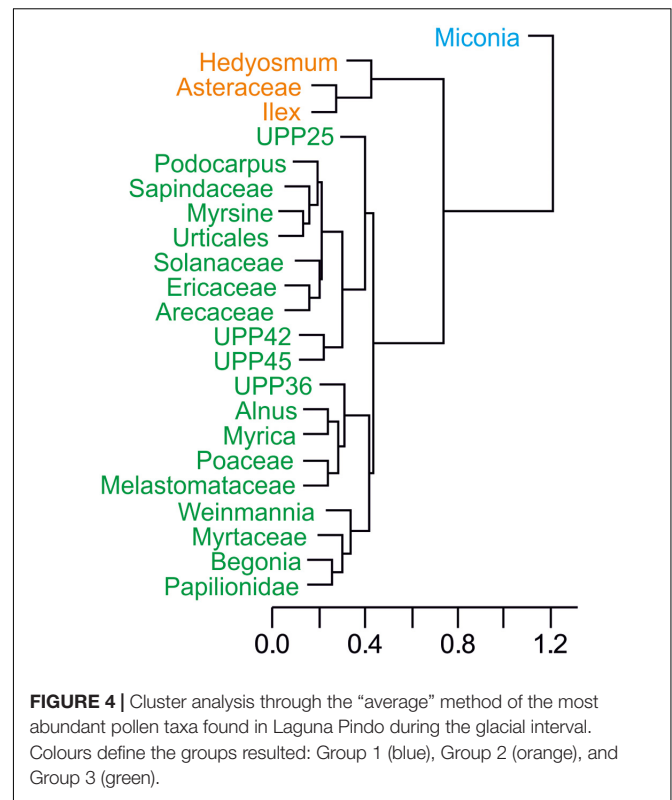
The post-LGM and late Glacial interval of Laguna Pindo is characterised by low values of both *Hedyosmum* and *Miconia* compared to the rest of the sequence. UPP25 peaks at the beginning of the zone and disappears again. Asteraceae and *Ilex* attain during this zone their highest values, and Myrtaceae shows its lowest abundance. Charcoal particles present in this zone are among the minimum values of the entire sequence, and the same occurs with the pollen concentration, ranging from 211,000 to 544,000 pollen grains cc^{-1} .

Additional Metrics for Plant Dynamics

Several tests were also run to get a better idea of the palynological dynamics. A cluster analysis of the represented taxa (percentages above 10%) was performed to see the grouping formed by the most abundant pollen morphotypes with similar distributions along the sequence (Figure 4). The plot shows three different groups well defined, with only *Miconia* belonging to the first group; *Hedyosmum*, Asteraceae, and *Ilex* forming the second group; and the rest of morphotypes (19) included in Group 3. Stable isotopes of C and N were plotted stratigraphically against age (Figure 5), providing values between -30 and -25‰ for $\delta^{13}\text{C}$, indicative of mostly C3 land plants, and between 0 and 5‰ for $\delta^{15}\text{N}$, representing a mixed primary production source formed by aquatic and terrestrial plants (Meyers and Teranes, 2001). $\delta^{13}\text{C}$ sees an increasing trend starting around 25 cal kyr BP. $\delta^{15}\text{N}$ shown an earlier increasing trend around 43 cal kyr BP including a brief drop around 19 cal kyr BP. Finally, some diversity metrics were calculated following Hill (1973), as previous works have highlighted their suitability for pollen data (Finsinger et al., 2017; Gosling et al., 2017). Based on a total of 134 recognisable pollen morphotypes for the glacial palynological assemblage of Laguna Pindo, samples N_0 vary between 40 and 57 morphotypes, N_1 and N_2 values rank from 17 up to 24 and from 7 to 18, respectively, and the ratio N_2/N_0 ranges between 0.13 and 0.39 (Table 4).

PALAEOECOLOGICAL INTERPRETATION AND DISCUSSION

In order to understand the ecological dynamics of the forests recorded in Laguna Pindo, a palaeoclimatic background is needed. Here, independent archives for temperature (Greenland ice core record) and precipitation (Santiago speleothem, Ecuador) reconstructions will be used and placed in a regional context (Figure 5). A palaeotemperature record from Greenland



is shown instead of the closer record of the Cariaco Basin (offshore Venezuela) as both are equally representatives of the North Atlantic Ocean palaeotemperature (Haug et al., 2001; Deplazes et al., 2013), and the Greenland ice record is expressed directly in temperature degrees (Alley, 2000). Vegetation dynamics will be compared with nearby records when possible and in addition, as Laguna Pindo is located in NW Amazonia at the boundary between Amazon and Andean forests just below the narrow band of cloud forests, comparison with long records retrieved in ecotonal areas from SW and NE Amazonia will be also contemplated.

Glacial Vegetation at Laguna Pindo

The small catchment size of Laguna Pindo and the persistent abundance of woody taxa (based on pollen and isotopic signals) throughout the glacial period suggest that the Mera region was continuously covered by forest during this period (Figures 3, 5). The large number of pollen taxa found in the glacial record from Laguna Pindo (>130 terrestrial morphotypes) reflects the high biodiversity that characterises western Amazonia and the eastern Andean flank. In this sense, the palynological assemblage of the glacial Pindo forest shows similar values of diversity (N_1) to modern pollen traps of tropical locations in Bolivia and Ghana (Gosling et al., 2017). It is noteworthy to highlight the high values of diversity obtained in such a present-day closed canopy to the shoreline and small catchment of the lake, an environmental setting prone to collect only evidence from a very local spatial scale (Figure 1; Jacobson and Bradshaw, 1981). In addition, it is interesting to observe that despite the homogeneous nature

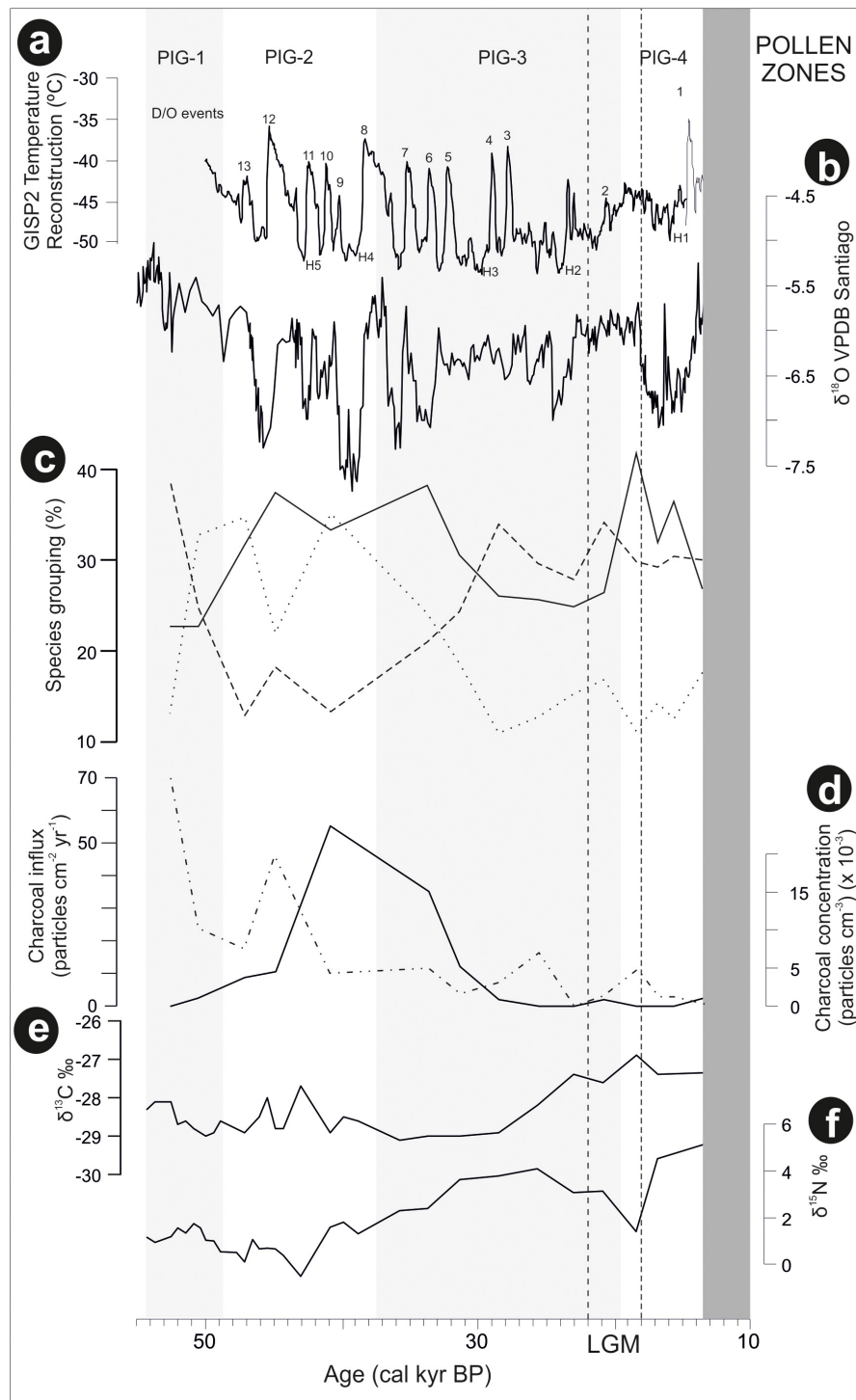


FIGURE 5 | Laguna Pindo metrics and additional data framed in a regional palaeoclimatic context (raw data downloaded from NOAA): **(a)** GISP2 temperature reconstruction of Greenland (Alley, 2000), in which are shown the Heinrich (H) and Dansgaard-Oeschger (D/O) events that occurred in the time interval under study; **(b)** precipitation reconstruction based on Santiago speleothem record (Mosblech et al., 2012); **(c)** percentages of the groups resulted in the cluster analysis of Laguna Pindo most abundant palynological taxa (Figure 4): with dotted, dashed, and continuous lines showing the different groups (Group 1, 2, and 3 of Figure 4, respectively); **(d)** local fires curve of Laguna Pindo based on big (>100 μm) charcoal particles, expressed in concentration and influx values (continuous and discontinuous lines, respectively); **(e)** $\delta^{13}\text{C}$ of Laguna Pindo, expressed in ‰; and **(f)** $\delta^{15}\text{N}$ of Laguna Pindo, expressed in ‰. The dark grey shade represents the hiatus of Laguna Pindo, calculated as the calibrated ages of the dated samples bracketing the sedimentary gap (at 512 and 514 cm depth), and the light grey bands mark the pollen zones obtained. Vertical dashed lines show the LGM core interval following Figure 3.

of the richness (N_0) values along the sequence, the maximum values for all the indices calculated were attained in a single sample, with an estimated age just at the end of the LGM (Table 4).

The forest taxa occurring had varied through time based on different climatic and ecological requirements, as forests have been doing since previous glacial-interglacial periods in the tropics and elsewhere (Bush et al., 2004a; Cárdenas et al., 2011a). In this sense, full to late glacial forest in Laguna Pindo was characterised by a mix of taxa that live nowadays in both mid and high elevations (>1000 masl). The continuous occurrence of taxa such as *Alnus*, *Hedyosmum*, *Myrica*, *Podocarpus*, and *Weinmannia* not present in today's forest (Table 1) suggest a colder climate than nowadays, whereas the presence of warm indicators like *Arecaceae* point to the existence of a no-analogue plant community (Williams and Jackson, 2007). Besides the mixed composition of the glacial forest, Laguna Pindo palynological record is in agreement with previous sequences in another important aspect, the community stability and tolerance during the glacial interval. RoC were calculated and provided very low results of magnitude around $\times 10^{-4}$ (Table 4). During full glacial conditions, the structure of the forest did not change compared to those observed nowadays, a pre-montane forest. The vegetation shift in composition is due to the coexistence during the ice age of taxa with different climatic requirements in the present-day.

Dynamics of Vegetation at Laguna Pindo

Laguna Pindo recorded a remarkably continuous lower montane forest cover during the last glaciation, despite several disturbance events or climatic episodes. Disturbance events likely occurred even in the absence of a clear imprint in the sedimentary archive. For instance, a high peak of local fires is located around 43–33 cal kyr BP, or slightly before (with peaks around 52 and 45 cal kyr BP) when expressed in influx values (Figures 3, 5). The occurrence of fires in the wet western Amazonia/eastern Andean flank prior to human arrival were probably caused by volcanic activity (Cárdenas et al., 2011a; Loughlin et al., 2018). However, during this interval no tephra have been observed in Laguna Pindo sequence coeval to the charcoal peak, although volcanic activity is known to have occurred in the region at this time (Keen, 2015; Loughlin et al., 2018). Consequently, a climatic origin for the fires recorded in Laguna Pindo cannot not be entirely ruled out because precipitation levels are thought to have fluctuated in the region throughout the last glacial and both periods with high charcoal in Laguna Pindo record are coeval with drier intervals in Santiago (Mosblech et al., 2012; Figure 5b). Regardless of the origin of the fires, the most conspicuous change observed in the vegetation occurred once these stopped, around 27 cal kyr BP also coeval to a drier interval in Santiago (Figures 5b,d), which occurred during a time period where the speleothem record was decoupled with insolation (Mosblech et al., 2012).

Based on the trends observed in the vegetation dynamics of the upper section of the sequence, late glacial interval was characterised in Laguna Pindo by a possible gradual change towards the Holocene (Figures 3, 5). In this sense, it can be

observed that the shifts in taxa abundance were mostly recorded prior or during LGM, and that the dynamics during the late Glacial were minor, until the record stopped at the beginning of the younger Dryas cold reversal (YD; 12.9–11.7 cal kyr BP). The smoothness observed in the diagram curves could be due to either insensitivity or time-lags of the taxa occurring along the lake shore during this time, or because the climatic change itself was mild at Pindo (i.e., not enough for crossing the tolerance thresholds of the occurring species). The nearby Santiago speleothem record (Figures 1, 5b) suggested a wet late glacial interval (Mosblech et al., 2012) whereas the palaeotemperature reconstruction of the Greenland ice record showed a more stable interval (Figure 5a), so it is suggested that both precipitation and temperature could have played a role in the late glacial dynamics of Pindo vegetation. In this sense it can be argued that wet conditions and a stable temperature trend without abrupt extreme values facilitated the late Glacial stability of the vegetation around Pindo, a location that receives >4000 mm yr⁻¹ and has a stable annual temperature around 20°C nowadays. Regarding temperature, comparing the palynological groups and the Greenland temperature reconstruction trends (Figures 5a,c), it can be observed, that, some changes did occur before the LGM. Thus, during the interval around 30–20 cal kyr BP and especially between Heinrich events H3 and H2, Group 1 (*Miconia*) and 2 (*Hedyosmum*, *Ilex*, and *Asteraceae*) attained their minimum and maximum values, respectively (Figure 5c). *Miconia* is a genus with more than 200 species with different ecological and climatic tolerances in Ecuador and is very abundant in the surroundings of Laguna Pindo in the present-day (Table 1; Jørgensen and León-Yáñez, 1999). However, some heat-intolerant taxa such as *Alnus*, *Podocarpus*, *Myrica*, and *Hedyosmum* peaked around the LGM core interval (22–18 cal kyr BP; Figure 3). Some of the changes in the abundances of *Miconia* and the heat intolerant taxa could be temperature-driven. If so, these shifts in abundances would be in agreement with Lago Consuelo record, a cloud forest location in the southern hemisphere (Peru/Bolivia), which also reported a gradual transition from glacial towards Holocene forests, and was preliminary interpreted in terms of temperature rather than precipitation as the major driver of vegetation changes (Bush et al., 2004b).

With respect to the different taxa sensitivity, the key factor to consider here is the proximity to the occurrence of environmental conditions' thresholds for the given species. Such ecological proximity could be modified through time due to ecosystem interactions, climatic shifts or feedbacks. Longer records have shown forest stability in more than one glaciation (Bush et al., 2004a). Considering the time scales of glacial versus interglacial duration, it is logical to think that the glacial vegetation was more adapted to cold conditions than to the warm characteristic of the Holocene. Moreover, Bush (2002) hypothesised that as the climate warms, the elevation of cloud formation on the Andean flank would have increased. In Lago Consuelo, the authors suggested a higher stability of glacial forest to dry events as a result of cloud cover formation (Urrego et al., 2010). Therefore, it is proposed here that the forest composition of Pindo during the glaciation was the result of complex environmental interactions, including at least these two factors: (i) the forest taxa had

climatic tolerances that include the temperature range (and other parameters like CO₂ levels) that occurred during the glaciation, and (ii) these lower temperatures of the glacial period facilitated the occurrence of clouds in the wet Laguna Pindo, buffering the effects of a decreased available moisture during the drier intervals. This way, the ecological or climatic threshold was not crossed even during the occurrence of abrupt events resulting in forest stability. The assumption of glacial tolerance range would imply a higher sensitivity to climate change of the forest during interglacials such as the present one. Holocene palaeoecological studies have manifested a high dynamism of plant communities through the entire Amazon basin (e.g., Flantua et al., 2016). Given the current projections on climate change, it is expected that cloud coverage of the eastern Andean flank will continue moving upwards and narrowing as the temperature rises (Bush, 2002; IPCC, 2013). The cloud migration would progressively intensify the vulnerability of large areas of pre-montane and cloud forests, as the buffering effect of the cloud cover moves to higher elevations. The lack of buffer, together with an increased human impact (i.e., increment in land use involving deforestation), would have dramatic consequences for the already threatened biodiversity hotspot of the Ecuadorian eastern Andean flank.

Dynamics of Glacial Vegetation in the Eastern Andean Flank

The first evidence of non-Andean glacial age forests in tropical South America was from a sedimentary sequence obtained by Paul Colinvaux near the town of Mera, Ecuador (Liu and Colinvaux, 1985) just around 10 km from Laguna Pindo (Figure 1). The Mera record was an outcrop exposed by road cutting where a temperature drop of about 4.5°C relative to modern was estimated based on the pollen assemblage found (Liu and Colinvaux, 1985). The estimate of cooling was based on the occurrence of heat-intolerant taxa such as *Alnus*, *Hedyosmum*, and *Podocarpus*. Based on the Mera palynological record, it was suggested that during glacial times tropical forests did not disappear, but were reconfigured and included taxa today only found at much higher elevations. The taxa mixture implied that forests species behaved individually, and not grouped by associations and/or belts, a view those days still not widely accepted outside North America (Whittaker, 1951; van der Hammen, 1974; Davis et al., 1986). Moreover, the glacial forest persistence hypothesis resulting from Mera directly confronted the biogeographic hypothesis of glacial refugia proposed by Haffer (1969) (Colinvaux, 1998; Colinvaux et al., 2000).

The controversial nature of the fossil pollen record from Mera by Liu and Colinvaux (1985) about the structure and composition of the glacial tropical vegetation resulted in several challenges to the interpretation. First of all, the outcrop section contained a large amount of unidentified taxa, as Neotropical palynology was still in its infancy (Colinvaux et al., 1999). Second, the volcanic nature of the inorganic sediment could allow transportation of material from elsewhere, including wood remains of the coniferous tree *Podocarpus* that were found interbedded in Mera's sediments (Gentry, 1993). Third, this potentially transported material could be

much older than the age reported by radiocarbon dating due to contamination and then the record could not be glacial (Heine, 1994). And finally, the uniqueness of a single-site results located within one of the defined refuge areas prevented a general statement of glacial cooling instead of aridity as the main driver of vegetation changes during the ice-age in the tropical forests of South America (Haffer, 1969). Most of these concerns were addressed by the finding of a second glacial record from another outcrop located at San Juan Bosco, just 160 km to the south from Mera, and the setup of modern pollen traps systematic sampling in different locations of Ecuador and Brazil (Bush et al., 1990, 2001; Bush, 1991; Bush and Weng, 2006). San Juan Bosco record showed a mixed assemblage of pollen grains from taxa nowadays living in mid and high elevations as Mera did (Bush et al., 1990). However, the outcrop nature of the record still compromised the potential occurrence of reworked material from volcanic events transportation and hence contamination with older sediments (Heine, 1994).

Subsequent palaeoecological records recovered from lowland tropical sites in South America have supported Liu and Colinvaux's assertion that taxa currently found at higher, colder elevations coexisted with modern "warm" lowland taxa in the lowlands during the last glacial period (Haberle and Maslin, 1999; van't Veer et al., 2000; Bush et al., 2004b; Whitney et al., 2011). The closest of the other glacial records to the Mera and San Juan Bosco sites is Vinillos, which is 100 km north of Pindo (Figure 1), and is also characterised by a very similar pollen glacial forest assemblage (Loughlin et al., 2018). Finally, the glacial palynological assemblage is not restricted to the last glaciation, as it has been found in previous glacial stadials as well in the region (Cárdenas et al., 2011a). However, all these evidence share the outcrop nature of the record, with the dubious provenance of the sediments, the dating limitations and the potential contamination problems. Laguna Pindo is the first lacustrine record on the westernmost edge of the equatorial Amazonia that registers the last glacial dynamics. By being lacustrine in origin and with such a small catchment, scepticism about the continuity of the sediment, the spatial scale information of the data provided and the volcanic transport contamination can be finally ruled out. Given the volume of the glacial records obtained so far for the Ecuadorian Andean flank, there is a general agreement on the heat intolerant taxa found mixed with current heat tolerant were common and abundant during the last ice age in the eastern Andean flank in western Amazonia.

CONCLUSION

Laguna Pindo sequence contains the story of a pre-montane forest in the biodiversity hotspot of the eastern Andean flank of Ecuador during the last glaciation, for the first time obtained from a continuous lacustrine record. The glacial forest of Laguna Pindo has been described as a mix of taxa living nowadays in mid and high elevations. Heat-intolerant taxa including *Podocarpus*, *Alnus*, or *Myrica* showed maximum values around the start

of the LGM, replacing the previous dominant taxon, *Miconia*. However, the forest was characterised by stability, in contrast to the Holocene dynamism of Amazon plant communities (Flantua et al., 2016). This stability can be understood in terms of forest structure, being a pre-montane forest during full glacial conditions as it is nowadays, instead of compositional, based on the different climatic and ecological requirements of the occurring species. Wide tolerance ranges to glacial conditions and cloud formation have been proposed as key drivers to maintain Pindo stability. Given the ongoing climate change and the potential scenarios projected, it is more than likely that eventually the clouds that act as buffer of unfavourable climatic events such as droughts will disappear and move upwards, increasing the vulnerability of these tropical forests. Hence, it is essential to adopt management strategies and conservation measures in order to keep the currently desired ecosystem services of this biodiversity hotspot. Finally, the mature or “old-grown” forest concept in the eastern Andean flank or western Amazonia should be revised in order to establish accurate future projections and resilience estimates.

AUTHOR CONTRIBUTIONS

EM and WG lead the field work to recover the sediments. HK analysed the charcoal record and created the GIS figure in **Figure 1**. CL provided a vegetation inventory survey. All authors participate in the discussion during the writing of the manuscript, which was lead by EM.

REFERENCES

- Absy, M., Clief, A., Fournier, M., Martin, L., Servant, M., Sifeddine, A., et al. (1991). Mise en évidence de quatre phases d'ouverture de la forêt dense dans le sud-est de l'Amazonie au cours des 60,000 dernières années: première comparaison avec d'autres régions tropicales. *C. R. Acad. Sci. Paris* 312, 673–678.
- Alley, R. B. (2000). The Younger Dryas cold interval as viewed from central Greenland. *Quat. Sci. Rev.* 19, 213–226. doi: 10.1016/S0277-3791(99)00062-1
- Aspden, J. A., and Litherland, M. (1992). The geology and Mesozoic collisional history of the cordillera real, Ecuador. *Tectonophysics* 205, 187–204. doi: 10.1016/0040-1951(92)90426-7
- Bennett, K. D. (1996). Determination of the number of zones in a biostratigraphical sequence. *New Phytol.* 132, 155–170. doi: 10.1111/j.1469-8137.1996.tb04521.x
- Bernal, C., Christophoul, F., Darrozes, J., Soula, J., Baby, P., and Burgos, J. (2011). Late glacial and Holocene avulsions of the Río Pastaza megafan (Ecuador-Peru): frequency and controlling factors. *Int. J. Earth Sci.* 100, 1759–1782. doi: 10.1007/s00531-010-0555-9
- Bernal, C., Christophoul, F., Soula, J., Darrozes, J., Bourrel, L., Laraque, A., et al. (2012). Gradual diversions of the Río Pastaza in the Ecuadorian piedmont of the Andes from 1906 to 2008: role of tectonics, alluvial fan aggradation, and ENSO events. *Int. J. Earth Sci.* 101, 1913–1928. doi: 10.1007/s00531-012-0752-9
- Blauw, M. (2010). Methods and code for “classical” age-modelling of radiocarbon sequences. *Quat. Geochronol.* 5, 512–518. doi: 10.1016/j.quageo.2010.01.002
- Bush, M. B. (1991). Modern pollen-rain data from South and Central America: a test of the feasibility of fine-resolution lowland tropical palynology. *Holocene* 1, 162–167. doi: 10.1177/095968369100100209
- Bush, M. B. (2002). Distributional change and conservation on the Andean flank: a palaeoecological perspective. *Glob. Ecol. Biogeogr.* 11, 463–467. doi: 10.1046/j.1466-822X.2002.00305.x

FUNDING

This study has been developed under the auspices of project FORSENS, funded by the Natural Environment Research Council of United Kingdom (grant NE/J018562/1 to EM). Radiocarbon dating was supported by the NERC Radiocarbon Facility NRCF010001 (allocation number 1682.1112) awarded to FORSENS project by EM and performed by Pauline Gulliver (NRCF East Kilbride).

ACKNOWLEDGMENTS

Field sampling was performed thanks to the required permits for research investigations provided by the Ecuadorian Ministry of Environment (ref. 14-2012-IC-FLO-DPAP-MA), with the support of Susana León-Yáñez. Frazer Matthews-Bird helped with core sampling and the core recovery was possible at Laguna Pindo thanks to the Universidad Tecnológica Equinoccial de Ecuador (UTE), the local Council of the Province Pastaza, and the Estación Biológica de Pindo Mirador staff, with special emphasis in Doña Gloria Quichimbo. Special thanks to Emily Sear, Mabs Gilmour, and Simona Nicoara for the technical support, and Stephen Brooks, Mark Bush, and Iain Gilmour for their participation in the project. The work and suggestions of three anonymous referees and the editor Urs Feller greatly improved the quality of the manuscript. This paper is in memorial of Paul Colinvaux, who could not find the Ecuadorian lake of his dreams in the search of the Ice-Age in the American Equator.

- Bush, M. B., Colinvaux, P. A., Wiemann, M. C., Piperno, D. R., and Liu, K.-B. (1990). Late Pleistocene temperature depression and vegetation change in Ecuadorian Amazonia. *Quat. Res.* 34, 330–345. doi: 10.1016/0033-5894(90)90045-M
- Bush, M. B., De Oliveira, P. E., Colinvaux, P. A., Miller, M. C., and Moreno, J. E. (2004a). Amazonian paleoecological histories: one hill, three watersheds. *Palaeogeogr. Palaeoclimatol. Palaeoecol.* 214, 359–393. doi: 10.1016/S0031-0182(04)00401-8
- Bush, M. B., Hanselman, J. A., and Hooghiemstra, H. (2007). “Andean montane forests and climate change,” in *Tropical Rainforest Responses to Climatic Change*, 2nd Edn, eds M. B. Bush, J. R. Flenley, and W. D. Gosling (Chichester: Springer-Praxis), 35–60. doi: 10.1007/978-3-540-48842-2
- Bush, M. B., Moreno, E., de Oliveira, P. E., Asanza, E., and Colinvaux, P. A. (2001). The influence of biogeographic and ecological heterogeneity of Amazonian pollen spectra. *J. Trop. Ecol.* 17, 729–743. doi: 10.1017/S0266467401001547
- Bush, M. B., Silman, M. R., and Urrego, D. H. (2004b). 48,000 years of climate and forest change in a biodiversity hotspot. *Science* 303, 827–829. doi: 10.1007/s00267-010-9602-3
- Bush, M. B., and Weng, M. B. (2006). Introducing a new (freeware) tool for palynology. *J. Biogeogr.* 34, 377–380. doi: 10.1111/j.1365-2699.2006.01645.x
- Cárdenas, M. L., Gosling, W. D., Pennington, R. T., Poole, I., Sherlock, S. C., and Mothes, P. (2014). Forests of the tropical eastern Andean flank during the middle Pleistocene. *Palaeogeogr. Palaeoclimatol. Palaeoecol.* 393, 76–89. doi: 10.1016/j.palaeo.2013.10.009
- Cárdenas, M. L., Gosling, W. D., Sherlock, S. C., Poole, I., Pennington, R. T., and Mothes, P. (2011b). Response to comment on “The response of vegetation on the Andean flank in western Amazonia to Pleistocene climate change”. *Science* 333:1825. doi: 10.1126/science.1207525
- Cárdenas, M. L., Gosling, W. D., Sherlock, S. C., Poole, I., Pennington, R. T., and Mothes, P. (2011a). The response of vegetation on the Andean flank

- in western Amazonia to Pleistocene climate change. *Science* 331, 1055–1058. doi: 10.1126/science.1197947
- Clark, P. U., Dyke, A. S., Shakun, J. D., Carlson, A. E., Clark, J., Wohlfarth, B., et al. (2009). The last glacial maximum. *Science* 325, 710–714. doi: 10.1126/science.1172873
- Colinvaux, P. A. (1998). A new vicariance model for Amazonian endemics. *Glob. Ecol. Biogeogr. Lett.* 7, 95–96. doi: 10.2307/2997812
- Colinvaux, P. A., De Oliveira, P. E., and Bush, M. B. (2000). Amazonian and neotropical plant communities on glacial time-scales: the failure of the aridity and refuge hypothesis. *Quat. Sci. Rev.* 19, 141–169. doi: 10.1016/S0277-3791(99)00059-1
- Colinvaux, P. A., De Oliveira, P. E., and Moreno, J. E. (1999). *Amazon Pollen Manual and Atlas*. Amsterdam: Harwood Academic Publishers.
- Colinvaux, P. A., De Oliveira, P. E., Moreno, J. E., Miller, M. C., and Bush, M. B. (1996). A long pollen record from lowland Amazonia: forest and cooling in glacial times. *Science* 274, 85–88. doi: 10.1126/science.274.5284.85
- Coplen, T. B. (2011). Guidelines and recommended terms for expression of stable-isotope-ratio and gas-ratio measurement results. *Rapid Commun. Mass Spectrom.* 25, 2538–2560. doi: 10.1002/rcm.5129
- Correa-Metrio, A., Cabrera, K. R., and Bush, M. B. (2010). Quantifying ecological change through discriminant analysis: a paleoecological example from the Peruvian Amazon. *J. Veg. Sci.* 21, 695–704. doi: 10.1111/j.1654-1103.2010.01178.x
- Cox, P. M., Betts, R. A., Jones, C. D., Spall, S. A., and Totterdell, I. J. (2000). Acceleration of global warming due to carbon-cycle feedbacks in a coupled climate model. *Nature* 408, 184–187. doi: 10.1038/35041539
- Davis, M. B., Woods, K. D., and Futyma, R. P. (1986). Dispersal versus climate: expansion of *Fagus* and *Tsuga* into the upper Great Lakes region. *Vegetatio* 67, 93–103. doi: 10.1007/BF00037360
- de Berc, S. B., Soula, J., Baby, P., Souris, M., Christophoul, F., et al. (2005). Geomorphic evidence of active deformation and uplift in a modern continental wedge-top-foredeep transition: example of the eastern Ecuadorian Andes. *Tectonophysics* 399, 351–380. doi: 10.1016/j.tecto.2004.12.030
- Deplazes, G., Lückge, A., Peterson, L. C., Timmermann, A., Hamann, Y., Huguen, K. A., et al. (2013). Links between tropical rainfall and North Atlantic climate during the last glacial period. *Nat. Geosci.* 6, 213–217. doi: 10.1038/ngeo1712
- Faegri, K., and Iversen, J. (1989). *Textbook of Pollen Analysis*, 4th Edn, eds K. Faegri, P. E. Kaland, and K. Krzywinski. New York, NY: John Wiley & Sons, 328.
- Ferdon, E. N. J. (1950). *Studies of Ecuadorian Geography*. Los Angeles, CA: University of Southern California.
- Finsinger, W., Morales-Molino, C., Galka, M., Valsecchi, V., Bojovic, S., and Tinner, W. (2017). Holocene vegetation and fire dynamics at Crveni Potok, a small mire in the Dinaric Alps (Tara National Park, Serbia). *Quat. Sci. Rev.* 167, 63–77. doi: 10.1016/j.quascirev.2017.04.032
- Flantua, S. G. A., Hooghiemstra, H., Grimm, E. C., Behling, H., Bush, M. B., González-Arango, C., et al. (2015). Updated site compilation of the Latin American Pollen Database. *Rev. Palaeobot. Palynol.* 223, 104–115. doi: 10.1016/j.revpalbo.2015.09.008
- Flantua, S. G. A., Hooghiemstra, H., Vuille, M., Behling, H., Carson, J., Gosling, W., et al. (2016). Climate variability and human impact on the environment in South America during the last 2000 years: synthesis and perspectives. *Clim. Past* 12, 483–523. doi: 10.5194/cp-12-483-2016
- Gentry, A. H. (1993). *A Field Guide to the Families and Genera of Woody Plant of Northwest South America (Colombia, Ecuador, Peru) with Supplementary Notes on Herbaceous Taxa*. Washington, DC: Conservation International.
- Gosling, W. D., Julier, A. C. M., Adu-Breda, S., Djagbletey, G. D., Fraser, W. T., Jardine, P. E., et al. (2017). Pollen-vegetation richness and diversity relationships in the tropics. *Veg. Hist. Archaeobot.* doi: 10.1007/s00334-017-0642-y
- Haberle, S. G., and Maslin, M. A. (1999). Late Quaternary vegetation and climate change in the Amazon basin based on a 50,000-year pollen record from the Amazon Fan, ODP Site 932. *Quat. Res.* 51, 27–38. doi: 10.1006/qres.1998.2020
- Haffer, J. (1969). Speciation in Amazonian forest birds. *Science* 165, 131–137. doi: 10.1126/science.165.3889.131
- Hall, M. L., Samaniego, P., Le Pennec, J. L., and Johnson, J. B. (2008). Ecuadorian Andes volcanism: a review of Late Pliocene to recent activity. *J. Volcanol. Geotherm. Res.* 176, 1–6. doi: 10.1016/j.jvolgeores.2008.06.012
- Harling, G. (1979). “The vegetation types of Ecuador: a brief survey,” in *Tropical Botany*, eds K. Larsen and L. B. Holm Nielsen (London: Academic Press), 165–174.
- Haug, G., Hughen, K. A., Sigman, D. M., Peterson, L. C., and Röhl, U. (2001). Southward migration of the Intertropical convergence zone through the holocene. *Science* 293, 1304–1308. doi: 10.1126/science.1059725
- Heine, K. (1994). The Mera site revisited: ice-age Amazon in the light of new evidence. *Quat. Int.* 21, 113–119. doi: 10.1016/1040-6182(94)90025-6
- Hijmans, R. J., Cameron, S. E., Parra, J. L., Jones, P. G., and Jarvis, A. (2005). Very high resolution interpolated climate surfaces for global land areas. *Int. J. Climatol.* 25, 1965–1978. doi: 10.1002/joc.1276
- Hill, M. O. (1973). Diversity and evenness: a unifying notation and its consequences. *Ecology* 54, 427–432. doi: 10.2307/1934352
- Hogg, A. G., Hua, Q., Blackwell, P. G., Niu, M., Buck, C. E., Guilderson, T. P., et al. (2013). SHCal13 Southern Hemisphere calibration, 0–50,000 cal yr BP. *Radiocarbon* 55, 1889–1903. doi: 10.2458/azu_js_rc.55.16783
- IPCC (2013). *Climate Change 2013: The Physical Science Basis. Contribution of Working Group I to the Fifth Assessment Report of the Intergovernmental Panel on Climate Change*, eds T. F. Stocker, D. Qin, G.-K. Plattner, M. Tignor, S. K. Allen, J. Boschung, et al. Cambridge: Cambridge University Press, 1535.
- Jacobson, G. L., and Bradshaw, R. H. W. (1981). The selection of sites for paleovegetational studies. *Quat. Res.* 16, 80–96. doi: 10.1016/0033-5894(81)90129-0
- Jørgensen, P. M., and León-Yáñez, S. (eds). (1999). *Catalogue of the Vascular Plants of Ecuador*. St. Louis, MO: Missouri Botanical Garden Press.
- Juggins, S. (2017). *rioja: Analysis of Quaternary Science Data, R Package Version (0.9-15)*. Available at: <http://cran.r-project.org/package=rioja>
- Keen, H. F. (2015). *Past Environmental Change in the Amazon Basin*. Ph.D. thesis, The Open University, Milton Keynes.
- Liu, K.-B., and Colinvaux, P. A. (1985). Forest changes in the Amazon basin during the last glacial maximum. *Nature* 318, 556–557. doi: 10.1038/318556a0
- Livingstone, D. A. (1955). A lightweight piston sampler for lake sediments. *Ecology* 36, 137–139. doi: 10.2307/1931439
- Lombardo, U. (2014). Neotectonics, flooding patterns and landscape evolution in southern Amazonia. *Earth Surf. Dyn.* 2, 493–511. doi: 10.5194/esurf-2-493-2014
- Lombardo, U. (2016). Alluvial plain dynamics in the southern Amazonian foreland basin. *Earth Surf. Dyn.* 7, 453–467. doi: 10.5194/esd-7-453-2016
- Loughlin, N. J. D., Gosling, W. D., Coe, A. L., Gulliver, P., Mothes, P., and Montoya, E. (2018). Landscape-scale drivers of glacial ecosystem change in the montane forests of the eastern Andean flank. *Palaeogeogr. Palaeoclimatol. Palaeoecol.* 489, 198–208. doi: 10.1016/j.palaeo.2017.10.011
- Luzuriaga, C. X. (2007). *Diagnóstico de Flora Estación Biológica Pindo-Mirador*. Quito: Universidad Tecnológica Equinoccial.
- Malhi, Y., and Wright, J. (2004). Spatial patterns and recent trends in the climate of tropical rainforest regions. *Philos. Trans. R. Soc. Lond. B Biol. Sci.* 359, 311–329. doi: 10.1098/rstb.2003.1433
- Matthews-Bird, F., Brooks, S. J., Gosling, W. D., Gulliver, P., Mothes, P., and Montoya, E. (2017). Aquatic community response to volcanic eruptions on the Ecuadorian Andean flank: evidence from the paleoecological record. *J. Paleolimnol.* 58, 437–453. doi: 10.1007/s10933-017-0001-0
- Meyers, P. A., and Teranes, J. L. (2001). “Sediment organic matter,” in *Tracking Environmental Change Using Lake Sediments. Physical and Geochemical Methods*, Vol. 2, eds J. P. Smol, H. J. B. Birks, and W. M. Last (Dordrecht: Kluwer), 239–270. doi: 10.1007/0-306-47670-3_9
- Mosblech, N. A. S., Bush, M. B., Gosling, W. D., Hodell, D., Thomas, L., van Calsteren, P., et al. (2012). North Atlantic forcing of Amazonian precipitation during the last ice age. *Nat. Geosci.* 5, 817–820. doi: 10.1038/ngeo1588
- Myers, N., Mittermeier, R. A., Mittermeier, C. G., da Fonseca, G. A. B., and Kent, J. (2000). Biodiversity hotspots for conservation priorities. *Nature* 403, 853–858. doi: 10.1038/35002501
- Oksanen, J., Guillaume Blanchet, F. R. K., Legendre, P., Minchin, P. R., O'Hara, B. R., Simpson, G. L., et al. (2013). *Vegan: Community Ecology Package. R Package Version 2.0-10*. Available at: <https://cran.r-project.org/package=vegan>
- Puyasena, S. W., Dalling, J. W., Jaramillo, C., and Turner, B. L. (2011). Comment on “The response of vegetation on the Andean flank in Western Amazonia to Pleistocene climate change”. *Science* 333:1825. doi: 10.1126/science.1207525

- Roubik, D. W., and Moreno, J. E. P. (1991). *Pollen and Spores of Barro Colorado Island. Monographs in Systematic Botany*. St. Louis, MO: Missouri Botanical Garden.
- Rull, V. (1987). A note on pollen counting in palaeoecology. *Pollen Spores* 29, 471–480.
- Sierra, R. (1999). *Propuesta Preliminar de un Sistema de Clasificación de Vegetación Para el Ecuador Continental*. Quito: Proyecto INEFAN/GEF-BIRF y EcoCiencia. doi: 10.13140/2.1.4520.9287
- Stockmarr, J. (1971). Tablets with spores used in absolute pollen analysis. *Pollen Spores* 16, 615–621.
- Urrego, D. H., Bush, M. B., Silman, M. R., Correa-Metrio, A., Ledru, M. P., Mayle, F. E., et al. (2009). “Millennial-scale ecological changes in tropical South America since the Last Glacial Maximum,” in *Past Climate Variability from the Last Glacial Maximum to the Holocene in South America and Surrounding Regions*, eds F. Vimeux, F. Sylvestre, and M. Khodri (Paris: Springer).
- Urrego, D. H., Bush, M. B., and Silman, M. S. (2010). A long history of cloud and forest migration from Lake Consuelo, Peru. *Quat. Res.* 73, 364–373. doi: 10.1016/j.yqres.2009.10.005
- van der Hammen, T. (1974). Pleistocene changes of vegetation and climate in tropical South America. *J. Biogeogr.* 1, 3–26. doi: 10.2307/3038066
- van't Veer, R., Islebe, G. A., and Hooghiemstra, H. (2000). Climate change during the Younger Dryas chron in northern South America: a test of the evidence. *Quat. Sci. Rev.* 19, 1821–1835. doi: 10.1016/S0277-3791(00)00093-7
- Von Post, L. (1916). Om skogsträdpollen i sydsvenska torfmosslagerföljder. *Geol. Fören. Stockh. Förhandlingar* 38, 384–390.
- Whitlock, C., and Larsen, C. (2001). “Charcoal as a fire proxy,” in *Tracking Environmental Change Using Lake Sediments. Terrestrial, Algal, and Siliceous Indicators*, Vol. 3, eds J. P. Smol, H. J. B. Birks, and W. M. Last (Dordrecht: Kluwer), 75–98. doi: 10.1007/0-306-47668-1_5
- Whitney, B. S., Mayle, F. E., Punyasena, S. W., Fitzpatrick, K. A., Burn, M. J., Guillen, R., et al. (2011). A 45 kyr palaeoclimate record from the lowland interior of tropical South America. *Palaeogeogr. Palaeoclimatol. Palaeoecol.* 307, 177–192. doi: 10.1016/j.palaeo.2011.05.012
- Whittaker, R. H. (1951). A criticism of the plant association and climatic climax concepts. *Northwest Sci.* 25, 17–31.
- Williams, J. W., and Jackson, S. T. (2007). Novel climates, no-analog communities, and ecological surprises. *Front. Ecol. Environ.* 5, 475–482. doi: 10.1890/070037

Conflict of Interest Statement: The authors declare that the research was conducted in the absence of any commercial or financial relationships that could be construed as a potential conflict of interest.

Copyright © 2018 Montoya, Keen, Luzuriaga and Gosling. This is an open-access article distributed under the terms of the Creative Commons Attribution License (CC BY). The use, distribution or reproduction in other forums is permitted, provided the original author(s) and the copyright owner are credited and that the original publication in this journal is cited, in accordance with accepted academic practice. No use, distribution or reproduction is permitted which does not comply with these terms.



First Pollen Record in South America. Commentary: Die Zeichenschrift der Pollenstatistik

Vera Markgraf^{1,2*}

¹ Institute of Arctic and Alpine Research, University of Colorado, Boulder, CO, USA, ² School of Earth Sciences and Environmental Sustainability, Northern Arizona University, Flagstaff, AZ, USA

Keywords: South America, Tierra del Fuego, pollen records, von Post, history of palynology

A commentary on

Die Zeichenschrift der Pollenstatistik

by Von Post, L. (1929). *Geol. Fören. För.* 51, 543–565. doi: 10.1080/11035892909449566

OPEN ACCESS

Edited by:

Valentí Rull,
Institute of Earth Sciences Jaume
Almera, Spain

Reviewed by:

Ana María Borromei,
National Scientific and Technical
Research Council, Argentina
Silvina Stutz,
National Scientific and Technical
Research Council (CONICET) and
Universidad Nacional de Mar del
Plata, Argentina

*Correspondence:

Vera Markgraf
vera.markgraf@colorado.edu

Specialty section:

This article was submitted to
Quaternary Science, Geomorphology
and Paleoenvironment,
a section of the journal
Frontiers in Earth Science

Received: 12 October 2016

Accepted: 07 November 2016

Published: 22 November 2016

Citation:

Markgraf V (2016) First Pollen Record
in South America. Commentary: Die
Zeichenschrift der Pollenstatistik.
Front. Earth Sci. 4:100.
doi: 10.3389/feart.2016.00100

By the end of the 1920's, pollen analysis had become an actively growing field of research with scientists throughout Northern and Central Europe producing pollen diagrams. Erdtman (1924) even had ventured farther afield studying peats from southern New Zealand. At this point, Von Post (1929) apparently felt the need to re-iterate some of the basic principles of pollen analysis, a technique he had introduced in 1916, including questions of which taxa should be represented in the pollen sum, use of absolute versus percentage data and type of symbols to graphically depict the different pollen taxa. Among the examples of diagrams Von Post (1929) presented in this publication were pollen diagrams from two 150 cm long cores from a bog at the eastern end of Lago Fagnano in Tierra del Fuego, Argentina, a site that has since become submerged following an earthquake in the 1940's. A characteristic volcanic ash layer allowed correlation between the two cores, one from the center of the bog, the other from the margin. The material was given to von Post by C. Caldenius, who between 1925 and 1928 had mapped and analyzed glacial deposits on the Argentine side of the Andes from 42 to 53°S (Caldenius, 1932). Von Post (1929) analyses of the pollen assemblages of those two cores represent the very first vegetation history record from South America (see Markgraf, 1993). As such it pointed to the global applicability of the technique, which certainly was one of von Post's reasons for including the Tierra del Fuego records in this study (Von Post, 1929, p. 561). Given the focus of the paper, Von Post's (1929) other reason to present the pollen data was to discuss questions about pollen sum and pollen symbols to be used in diagrams from very different environments. The pollen types reproduced in the diagrams by 6 and 7 levels, respectively, are *Nothofagus*, Ericaceae, Gramineae and Cyperaceae (Figure 1), mentioning also the presence of several other herbaceous and tree pollen types. In contrast to the European pollen records available in the 1920s, primarily showing successions of diverse tree pollen types, the Tierra del Fuego pollen assemblages were dominated by only one tree pollen type, *Nothofagus*, abundant in the upper levels while non-arboreal taxa dominated the lower levels. Hence von Post concluded that non-arboreal taxa had to be included in the pollen sum, at that time generally assumed to represent strictly local, site-related conditions, irrelevant in discussions on regional vegetation histories. Differences in the pollen numbers between the central and the marginal peat core indicated to him, however, that Ericaceae had to represent a local signal. Despite of this, he decided to include Ericaceae in the diagram—after applying the adequate pollen sum calculation (p. 560: “sobald man die richtige Berechnungsweise gefunden hat!”). The Ericaceae percentages thus were calculated out-of-sum which was based on *Nothofagus*, Gramineae and Cyperaceae (Figure 1).

Interpreting the shift in pollen assemblages, from steppe taxa to forest, Von Post (1929) concluded that it represented a change from warmer and drier to cooler and wetter climates. Pollen morphological differentiation based on pore number of the three *Nothofagus* species, presently

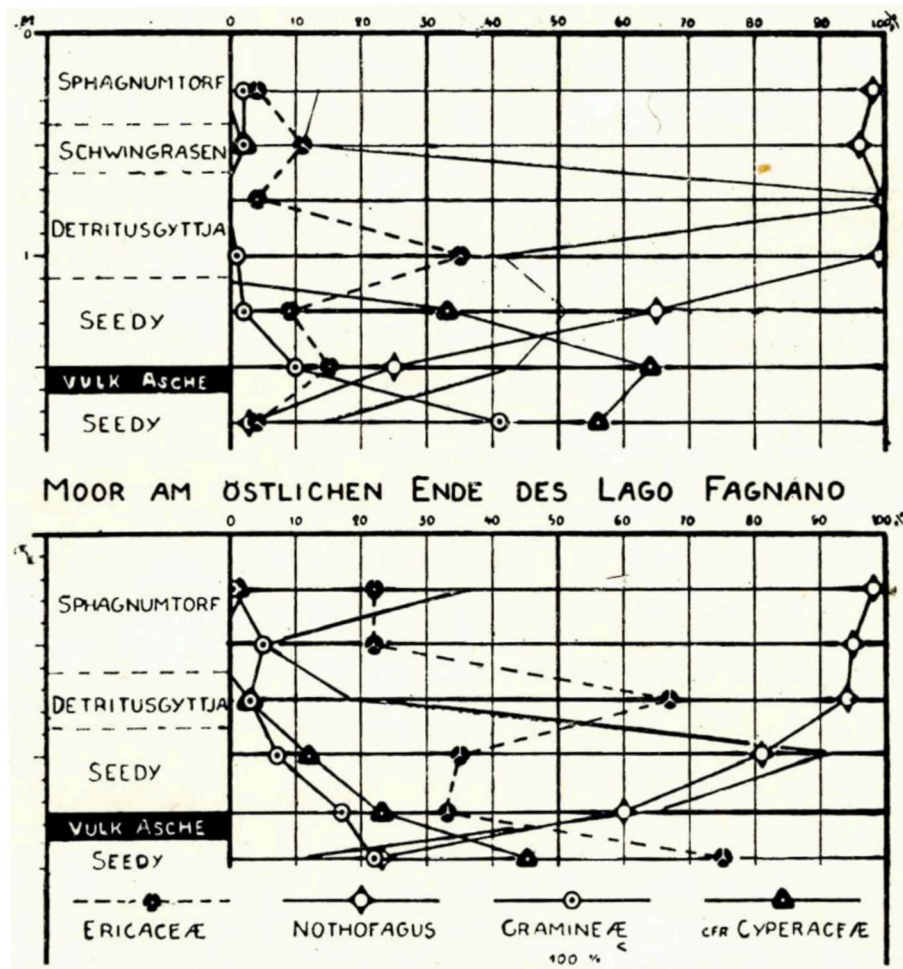


FIGURE 1 | Two diagrams from a bog at the eastern end of Lago Fagnano, Tierra del Fuego, Argentina (Von Post, 1929, p. 559; reproduced by Auer, 1949, p. 177). The same diagram was replotted, excluding Cyperaceae from the pollen sum and published by Markgraf (1983).

growing in the region, allowed further detail in interpreting the vegetation succession, related to changes in climate.

At the same time, between 1928 and 1929, the Geographical Society of Finland supported a scientific expedition to Tierra del Fuego. One of the scientists, Auer (1933), followed in von Post's footsteps analyzing the pollen content of peat cores from 33 sites, ranging from the western rainforest region to the eastern steppe. Presence of three characteristic volcanic ashes in the cores, analyzed geochemically by Salmi (1941), allowed correlations between the records that led Auer (1948, 1949) to propose tephrochronology as a new dating technique for postglacial sediments. Several of these records show treeless conditions followed by forest expansion at the base near the oldest of the three volcanic ashes. The shift from steppe to forest in Von Post's (1929) analyses near the youngest of the ash layers has also been found in several other cores (Auer, 1933).

This initial shift from treeless to forest conditions in Tierra del Fuego, just above the oldest volcanic ash layer, was assumed

coeval with the postglacial expansion of forest in Northern Europe, on the basis of (1) today's climate conditions in both regions was considered comparable and (2) the similarity of climatic trends as interpreted from the pollen assemblage successions (Auer, 1933, 1949). Using the Blytt-Sernander (Blytt, 1876; Sernander, 1908) Scandinavian climate succession model and its nomenclature, dated by the Baltic Sea varve chronology (De Geer, 1912; Sauramo, 1929), this initial postglacial vegetation change in the Tierra del Fuego records was dated to the beginning of the Boreal period, i.e. about 7000 years BC (ca 9000 C 14 years BP) (Auer, 1949, p. 136). Despite these somewhat questionable assumptions, the shift from treeless conditions to *Nothofagus* forest was subsequently radiocarbon dated on material from one of the original cores analyzed by Auer (1933) (Bahia Beaubasin, Isla Clarence, site 23, diagram 41, Auer, 1933) and actually gave the age of 8820 ± 290 C14 years BP (Jungner, 1979; Markgraf, 1983).

Since those early explorations, South America in general and the southern portion of South America specifically have

produced a wealth of paleoecological data (reviews e.g., Markgraf, 1993; Markgraf and Huber, 2010).

It was the pioneering research of these earlier scientists, many of them from Scandinavian countries, that subsequent research could build upon. Improved coring technology resulted in the recovery of materials going back to the times when full-glacial age ice had begun to recede from the Andean forelands. Radiocarbon dating, higher analytical resolution, multi-proxy analysis of the records and simplification of the diagrams, and no longer using the confusing symbols proposed by Von Post (1916, 1929) represented advances in reconstructing past environmental history of southern South America. Advanced

radiocarbon dating combined with other dating techniques (i.e. thermoluminescence, paleomagnetic) made correlations realistic, including intra-hemispheric correlations (Markgraf, 2001). Given the restrictions of the early studies, including difficulty in traveling in these remote regions, it is truly amazing how much was accomplished and how many far-reaching ideas had been proposed, that subsequent research could only confirm.

AUTHOR CONTRIBUTIONS

The author confirms being the sole contributor of this work and approved it for publication.

REFERENCES

- Auer, V. (1933). Verschiebungen der Wald- und Steppengebiete Feuerlands in postglazialer Zeit. *Acta Geogr.* 5, 1–313.
- Auer, V. (1948). Las capas volcánicas como nuevo método de cronología postglacial en Fuegopatagonia. *Gaea VIII*, 311–336.
- Auer, V. (1949). Las capas volcánicas como base de la cronología postglacial en Fuegopatagonia. *Rev. Invest. Agricol. Buenos Aires III*, 49–208.
- Blytt, A. (1876). *Essay on Immigration of the Norwegian Flora during Alternating Rainy and Dry Periods*. Christiania; Oslo: Alb. Cammermeyer.
- Caldenius, C. (1932). Las glaciaciones cuaternarias de la Patagonia y Tierra del Fuego. *Geogr. Ann.* 14, 1–164. doi: 10.2307/519583
- De Geer, H. (1912). Geochronologie der letzten 12 000 Jahre. *Geol. Rundsch.* 3, 457–471.
- Erdtman, G. (1924). Studies in micropalaeontology IV: peat from Chatham Islands and Otago District. *Geol. Fören. För.* 46, 679–681.
- Jungner, H. (1979). *Radiocarbon Dates I*. Radiocarbon Dating Laboratory, University of Helsinki, Report no. 1:77.
- Markgraf, V. (1983). Late and postglacial vegetational and paleoclimatic changes in subantarctic, temperate, and arid environments in Argentina. *Palynology* 7, 43–70. doi: 10.1080/01916122.1983.9989252
- Markgraf, V. (1993). Paleoenvironments and paleoclimates in Tierra del Fuego and southernmost Patagonia, South America. *Palaeogeogr. Palaeoclimatol. Palaeoecol.* 102, 53–68. doi: 10.1016/0031-0182(93)90005-4
- Markgraf, V. (2001). *Interhemispheric Climate Change*. San Diego, CA: Academic Press.
- Markgraf, V., and Huber, U. (2010). Late and postglacial vegetation and fire history in Southern Patagonia and Tierra del Fuego. *Palaeogeogr. Palaeoclimatol. Palaeoecol.* 297, 351–366. doi: 10.1016/j.palaeo.2010.08.013
- Salmi, M. (1941). Die postglazialen Eruptionsschichten Patagoniens und Feuerlands. *Ann. Acad. Sci. Fenn. A III* 2, 1–115.
- Sauramo, M. (1929). *The Quaternary Geology of Finland*. Helsinki: Helsingfors Publisher.
- Sernander, R. (1908). On the evidence of postglacial changes of climate furnished by the peat-mosses of northern Europe. *Geol. Fören. För.* 30, 456–478. doi: 10.1080/11035890809445601
- Von Post, L. (1916). Om skogsträdpollen i sydsvenska torfmosselagerföljder. *Geol. Fören. För.* 38, 384–390.
- Von Post, L. (1929). Die Zeichenschrift der Pollenstatistik. *Geol. Fören. För.* 51, 543–565. doi: 10.1080/11035892909449566

Conflict of Interest Statement: The author declares that the research was conducted in the absence of any commercial or financial relationships that could be construed as a potential conflict of interest.

Copyright © 2016 Markgraf. This is an open-access article distributed under the terms of the Creative Commons Attribution License (CC BY). The use, distribution or reproduction in other forums is permitted, provided the original author(s) or licensor are credited and that the original publication in this journal is cited, in accordance with accepted academic practice. No use, distribution or reproduction is permitted which does not comply with these terms.



Modulation of Fire Regimes by Vegetation and Site Type in Southwestern Patagonia Since 13 ka

Patricio I. Moreno^{1*}, Isabel Vilanova², Rodrigo P. Villa-Martínez³ and Jean P. Francois⁴

¹ Departamento de Ciencias Ecológicas, Universidad de Chile, Santiago, Chile, ² CONICET-Museo Argentino de Ciencias Naturales, Buenos Aires, Argentina, ³ CIGA, Universidad de Magallanes, Punta Arenas, Chile, ⁴ Departamento de Ciencias Geográficas Universidad de Playa Ancha, Valparaíso, Chile

OPEN ACCESS

Edited by:

Thomas Giesecke,
Georg-August-Universität Göttingen,
Germany

Reviewed by:

Nadia Solovieva,
University College London,
United Kingdom
Vincent Montade,
Georg-August-Universität Göttingen,
Germany

Thomas A. Minckley,
University of Wyoming, United States

*Correspondence:

Patricio I. Moreno
pimoreno@uchile.cl

Specialty section:

This article was submitted to
Paleoecology,
a section of the journal
Frontiers in Ecology and Evolution

Received: 12 December 2017

Accepted: 19 March 2018

Published: 09 April 2018

Citation:

Moreno PI, Vilanova I,
Villa-Martínez RP and Francois JP
(2018) Modulation of Fire Regimes by
Vegetation and Site Type in
Southwestern Patagonia Since 13 ka.
Front. Ecol. Evol. 6:34.
doi: 10.3389/fevo.2018.00034

The degree to which vegetation and site type have influenced fire regimes through the Holocene has not been investigated in detail in the temperate ecosystems of southern Patagonia. Here we present a first attempt using a paired-basin approach to study the evolution of fire regimes in sectors dominated by humid *Nothofagus* forests and the xeric Patagonian steppe in the Magallanes region of Chilean Patagonia (51°S). We analyzed sediment cores from two small lakes and a bog located within the same climate zone on opposite sides of the forest-steppe ecotone, ~28 km apart. The position of this biological boundary east of the Andes is controlled by the strength and position of the southern westerly winds, which constitute the sole source of precipitation throughout western Patagonia. Our results indicate that fires have occurred in the study region repeated times over the last ~13,000 years at bi- and tridecadal timescales. Sectors currently dominated by Patagonian steppe feature high frequency and low magnitude of local fires, and vice versa in humid forests. Climate-driven expansion of *Nothofagus* scrubland/woodland into steppe environments over the last ~4,200 years increased the magnitude and lowered the frequency of fire events, culminating with peak *Nothofagus* abundance, fire magnitude and frequency during the last millennium. We also detect divergences between lake-based vs. bog-based paleofire histories among paired sites located within the Patagonian steppe, ~12 km apart, which we attribute to local burning of the bog at times of lowered water table. This divergence suggests to us that bog-based vegetation and fire histories exacerbate a local, azonal, signal blurring extra-local or regional regimes, thus accounting for some discrepancies in the Quaternary paleovegetation/paleoclimate literature of southern Patagonia.

Keywords: fire regime, vegetation dynamics, paleoclimate, Patagonia, lake sediments

INTRODUCTION

Fire regimes have shaped the structure, composition and functioning of nearly all terrestrial ecosystems at global scale, affecting sedimentary and geomorphic processes (Kean et al., 2011), atmospheric chemistry (Galanter et al., 2000), radiative balance (Zhang and Wang, 2011), and the global carbon cycle (Van Der Werf et al., 2004). Fire regimes have changed in the past in response to shifts in mean climate state and variability, vegetation type, land-use changes, and are expected to change during the twenty first century as a consequence of climate change and anthropogenic

pressure on the landscapes (Krawchuk et al., 2009). Hence, it becomes a necessity to improve our understanding of the linkages between climate, vegetation type, fire regimes, and human perturbations to predict the potential consequences of future climate change, and for increasing societal preparedness and resilience.

Global-scale studies have postulated that wildfires in forest ecosystems are limited by the desiccation of fuels during warm/dry intervals, considering that abundant and spatially/temporally continuous biomass is available for burning (Krawchuk et al., 2009). This concept, known as the varying constraint hypothesis, also states that wildfire occurrence in drier landscapes dominated by grasslands and sparse scrublands is constrained by the amount and continuity of fine fuels rather than the occurrence of warm/dry intervals. Syntheses and analyses of biomass burning at global scale over the last 21,000 years have revealed a monotonic increase in fires with temperature given intermediate moisture levels (Daniau et al., 2012). These large-scale spatial and temporal patterns can be tested at the landscape level and multidecadal time scales using detailed fire histories from contrasting physiognomic units, ideally from the same region and subject to the same climatic forcing.

Fire histories extending beyond instrumental records or historical accounts have been developed with high temporal and spatial precision using fire-scar chronologies from tree rings and, with lower precision but larger time spans, from stratigraphic records. Charcoal particles and organic compounds released during combustion are preserved in multiple settings across the landscape, including soils, lake sediments, wetland and aeolian deposits, glaciers, etc. Sedimentary records from small closed-basin lakes offer the opportunity to develop continuous time series of past vegetation, charcoal particles as a proxy for paleofire, and environmental change at relatively small spatial (a few km²) and temporal scales (decadal to millennial). This allows exploring the modulation of fire regimes by vegetation type through time, space and climatic states.

Southern South America is an interesting region to explore the linkages between climate, vegetation and fire regimes, and their likely evolution under future climate scenarios. Large-scale fires in recent years highlight the vulnerability of natural and managed landscapes to a widespread (and ongoing) megadrought (Garreaud et al., 2017). Lightning strikes, Native American burning and volcanism provide likely sources of ignition in pre-European time throughout the region, the geographic and stratigraphic dimension of which is unconstrained or partially constrained by available data. Regional vegetation and fire syntheses in this region have relied primarily on records retrieved from bogs (Huber et al., 2004; Whitlock et al., 2007; Power et al., 2008), many of which exhibit limited stratigraphic and chronologic control, non-contiguous sampling and coarse temporal resolution. A broad-scale synthesis of fire patterns between 34° and 54°S (Whitlock et al., 2007) identified widespread enhancement of fire activity between 12 and 9.5 ka (ka = 1,000 calendar years before 1950 CE), a generalized decline and spatial heterogeneity between 9.5 and 6 ka, and intensification of that variability during the last 3,000 years.

These results were interpreted as multi-millennial changes in the Southern Westerly Winds (SWW), a pattern that Fletcher and Moreno (2012) subsequently interpreted as a zonally symmetric decline in SWW strength in the southern mid-latitudes. A global synthesis and analysis of charcoal records by Power et al. (2008) produced regional paleofire curves through standardization, transformation and rescaling of individual site data. The South American summary curve is fully compatible with the patterns identified by Whitlock et al. (2007) and indicates positive anomalies in fire activity during the early Holocene, a subsequent decline and negative anomalies during the mid-Holocene, and renewed fire activity over the last ~4,000 years. One complication in those records, however, is that terrestrial vegetation growing on the bog surfaces may impose a biased palynological and paleofire history, blurring the interpretation of extra-local and regional vegetation, fire-regimes and climate change.

In this paper we examine the impact of vegetation type on local fire regimes at multidecadal scale and fine spatial resolution during the last ~13,000 years using, for the first time, continuous pollen and macroscopic charcoal records from two lakes and a bog located in mixed evergreen-deciduous *Nothofagus* forests and the xeric steppe in southwestern Patagonia. These data allow testing the applicability of the varying constraint hypothesis to vegetation and fire-regime changes from multidecadal to millennial timescales during the Holocene.

STUDY AREA

Southwestern Patagonia (50–55°S) is a key region in the southern middle latitudes for deciphering the evolution of the SWW and their impact on terrestrial ecosystems during and since the last glaciation. The SWW supply abundant precipitation on the windward side of the Andes, as moisture-laden air masses are forced to ascend the cordillera causing copious orographic rains. The descent and acceleration of moisture-deprived air masses causes a rain shadow effect east of the Andes, which accentuates farther east in the extra-Andean plains. The interplay between the SWW and the Andes cordillera generates a vast diversity of environments along west-to-east, north-to-south and altitudinal axes, and from sea level to the high Andes, influencing the structure and composition of the land biota, as well as the frequency and magnitude of disturbance regimes, including fire. A west-to-east transect across the Andes at latitude 51°S (Villa-Martínez and Moreno, 2007) shows Magellanic Moorland communities along the windswept hyperhumid sectors adjacent to the Pacific coast, this unit is replaced by Evergreen Magellanic forests dominated by *Nothofagus betuloides* further east, Deciduous forests dominated by *N. pumilio* and *N. antarctica*, and Patagonian Steppe east of the Andes. This zonation reflects an eastward decline in precipitation of westerly origin that spills through the Andes, in conjunction with enhanced seasonality, continentality and the aforementioned rainshadow effect. The Andean treeline gives way to sparsely vegetated high-Andean grassland and scrubland at ~700 m.a.s.l. (Lara et al., 2005) in response to colder conditions and prolonged snow cover.

The interface between *Nothofagus* forests and the Patagonian steppe is an extensive biogeographical boundary in southern South America, spanning over 2,000 km along the eastern flank of the Andes Cordillera (e.g., Pisano, 1954; Schmithüsen, 1956; Dimitri, 1972; Donoso, 1998). Palynological studies in areas located within or near the forest-steppe ecotone in southwestern Patagonia (~45° and 56°S) have related past variations of this boundary with fluctuations in the position and/or intensity of the SWW (Schäbitz, 1991; Heusser, 1993, 1994, 1995; Huber and Markgraf, 2003; Villa-Martínez and Moreno, 2007; Mancini, 2009; Moreno et al., 2009, 2010; Wille and Schäbitz, 2009). These studies document the spread of *Nothofagus* trees eastward into areas formerly occupied by the Patagonian steppe, driven by a regional increase in moisture during the Holocene. The timing, structure, and magnitude of this phenomenon vary across the Andes, distance from the Pacific coast, and among different site types (lakes vs. bogs).

STUDY SITES

Lago Cipreses (51°17'6.15"S, 72°51'13.48"W, 1.1 ha, 110 m.a.s.l.) is a small closed-basin lake located on a bedrock depression along the southwestern portion of Lago Toro, ~85 meters above the current surface of Lago Toro (25 m.a.s.l.) (**Figure 1**). The site is surrounded by mixed forests dominated by the evergreen tree *Nothofagus betuloides* and the deciduous *N. pumilio*, along with the hygrophilous trees *Drimys winteri*, *Lomatia ferruginea* and the conifer *Pilgerodendron uviferum*. The records from Lago Cipreses span uninterrupted since ~14.3 ka (ka = 1,000 cal. yr BP) (Moreno et al., 2018). Lago Guanaco (51°52'S, 72°52'W, 200 m.a.s.l.) is a small closed-basin lake (~2 ha) located on a bedrock basin ~1.5 km north of Lago Sarmiento (**Figure 1**) and ~28 km north of Lago Cipreses, in Torres del Paine National Park (TPNP) (**Figure 1**). The sedimentary record from Lago Guanaco covers the last 12,600 years (Moreno et al., 2010). Vega Ñandú (50°55'58"S, 72°45'55"W; 4 ha, 200 m elevation) is a small mire located ~12 km north of Lago Guanaco in TPNP (**Figure 1**). Vega Ñandú is situated on a narrow W-E oriented ravine that runs perpendicular to the Río Paine valley, about 50 m above the valley floor. The Vega Ñandú record spans continuously since 12.2 ka to the present (Villa-Martínez and Moreno, 2007). In sum, Lago Cipreses is located on the wet (western) side of the forest/steppe ecotone, whereas Lago Guanaco and Vega Ñandú lie on the dry (eastern) side of the ecotone, the exact position of which has been modified by intensive disturbance by European-set fires and livestock grazing since the nineteenth century (Villa-Martínez and Moreno, 2007; Moreno et al., 2009).

METHODS

We obtained sediment cores using a 5-cm diameter Wright square-rod piston corer (Wright et al., 1984). In the case of Lago Cipreses and L. Guanaco we cored from an anchored raft equipped with 10-cm diameter aluminum casing on the deepest sectors of the lakes. We retrieved the water-sediment interface with a Plexiglas piston corer, which we sampled on site at 1

cm-thick intervals. In the case of Vega Ñandú we obtained the upper meter with a D-section Russian corer and the remaining section with a Wright square-rod piston corer. All sedimentary material was sent to the Quaternary paleoecology laboratory at Universidad de Chile and stored in a cold room at 4°C. We documented the core stratigraphies with the aid of X-radiographs and textural descriptions of the sediments (Villa-Martínez and Moreno, 2007; Moreno et al., 2010, 2018).

The chronology of Lago Cipreses cores is constrained by 15 ²¹⁰Pb dates and 23 AMS radiocarbon dates performed on bulk lake sediment associated to salient features on the litho- and pollen stratigraphy. In the case of Lago Guanaco we obtained 18 AMS radiocarbon dates on bulk lake sediments and mollusk shells, and in Vega Ñandú 12 AMS radiocarbon dates. We developed Bayesian age models for each site using Bacon for R (Blaauw and Christen, 2011).

We obtained 1-cm thick, 2-cc samples for pollen analysis. All samples were processed following conventional physical and chemical methods that include deflocculation with 10% KOH, sieving (<120 μm), treatment with 40% HF for 30 min in hot water bath, acetolysis and ultrasound (Faegri and Iversen, 1989). The pollen analyses were performed at 400× and 1,000× magnification. Reference material and relevant literature were used to facilitate the identification of pollen, spores (Heusser, 1971; Villagrán, 1980), and microalgal remains. We counted at least 300 pollen grains per level including upland trees, shrubs and herbs (terrestrial pollen sum). The abundance of paludal/aquatic taxa and pteridophytes were added to separate sums, and their percentage values were calculated with reference to the supersums "total pollen" (terrestrial pollen+aquatics) and "total pollen and spores" (total pollen+pteridophytes) respectively. *Nothofagus* in this study refers to the palynomorph *Nothofagus dombeyi* type, which includes three tree species (*N. betuloides*, *N. pumilio*, *N. antarctica*) that occur in different plant communities throughout SW Patagonia, from sea level to the upper treeline and from the hyperhumid Pacific coast to the forest/steppe ecotone east of the Andes.

We processed macroscopic charcoal samples following the methodology described by Whitlock and Anderson (2003) on the basis of 2-cc sediment samples taken at contiguous 1-cm intervals, deflocculated with 10% KOH and washed through 106-μm mesh screens. Particles were counted in gridded petri dishes under a Zeiss KL1500 LCD stereomicroscope at 50–100× magnification. We conducted time series analysis using CharAnalysis to detect charcoal peaks from the background, and deconvolute a local fire history (Higuera et al., 2009). We interpolated the macroscopic charcoal record at 33-year time windows, the highest median time step between adjacent samples of the three sites (see results section), and defined background charcoal with a lowess robust to outliers and smoothing windows between 500 and 1,000 years, and detected the peaks component with a locally defined threshold that separates the 99th percentile distribution of positive residuals, utilizing a Gaussian mixture model. We calculated the frequency of fire events per 1,000 year overlapping time windows and charcoal peak magnitude.

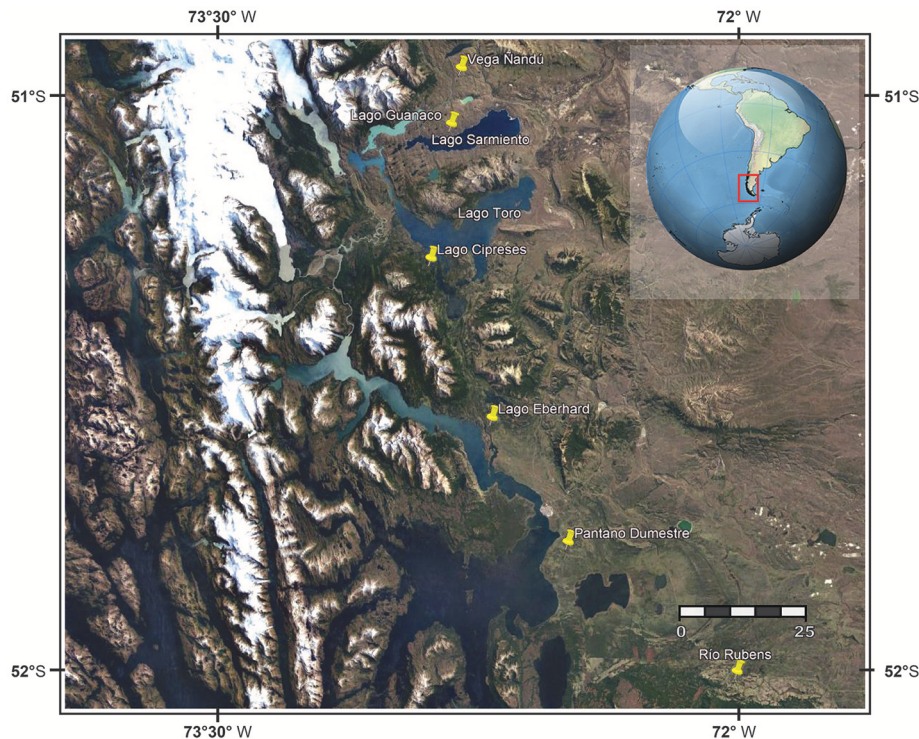


FIGURE 1 | Satellite image of the study area obtained from Google Earth showing the location of the sites discussed in the main text.

RESULTS

This study is based on sediment cores from Lago Cipreses (cores PS0710SC1 + PS0710AT1-3, 365 cm depth) reported in Moreno et al. (2018), Lago Guanaco (cores PS0404SC + PS0711GT1-7, 519 cm depth) reported in Moreno et al. (2010), and Vega Nandú (cores PS0405RC1A + PS0303AT1-4, 400 cm depth) reported in Villa-Martínez and Moreno (2007). These consist of organic silts in the case of Lago Cipreses and Lago Guanaco, and various transitions from organic mud and peat in the case of Vega Nandú. The age models suggest continuous high-sediment accumulation rates since 14.3, 12.6, and 12.2 ka, respectively (**Figure 2**). The palynological/macrosopic charcoal records from Lago Cipreses, L. Guanaco and Vega Nandú feature median time steps between adjacent samples of 33/33, 40/24, and 67/29 years, respectively, allowing a detailed examination of vegetation, fire-regime and climate changes from *Nothofagus* forests currently dominated by evergreen and deciduous species to a xeric steppe in TPNP.

The Lago Cipreses record shows low *Nothofagus* abundance (mean: 13%) prior to 12.7 ka, along with shrubs, herbs, and ferns (Poaceae, Asteraceae, Ericaceae, *Blechnum*), followed by a rapid increase that culminates during a relatively stable plateau (mean *Nothofagus*: 83%) that persists since 11 ka (**Figure 3**). The pollen record from Lago Guanaco shows dominance of shrubs and herbs during much of the record. We observe a gradual rise in *Nothofagus* at 7.8 ka, accompanied by an increase in its hemiparasite *Misodendrum* starting at 6.8 ka

(**Figure 3**). Superimposed upon this trend we detect rapid pulses of arboreal expansion at 4, 2.7, 1.4, and 0.6 ka. The *Nothofagus* rise led to maximum abundance between ~0.6 and 0.1 ka (57%), followed by deforestation by Chilean/European settlers. The Vega Nandú record shows similar trends to those observed in Lago Guanaco, with larger-amplitude fluctuations and peak *Nothofagus* abundance between 2.4 and 2.1 ka (**Figure 3**). *Nothofagus* exhibits a gradual decline between 2.1 and 0.15 ka and an abrupt decrease associated with European disturbance since then.

The Charcoal Accumulation Rate (CHAR) record from Lago Cipreses features multiple short-lived, large-magnitude increases which correspond with episodes of forest fragmentation and proliferation of understory shrubs, herbs, and ferns (Moreno et al., 2018), with peak frequencies typically at or below 1 event/500 years and frequency maxima at 11 ka, between 9 and 8 ka, and between 5.6 and 3 ka (**Figure 4**). The Lago Guanaco CHAR record shows intermediate values between 13 and 12 ka, low values between 12 and 4 ka with multiple small-magnitude peaks, a rising trend that starts at 4 ka and leads to a variable high-stand with the largest-magnitude peaks over the last 3,000 years (**Figure 4**). Peak frequency maxima are evident between 13 and 10 ka and during the last millennium. Vega Nandú features predominance of low CHAR values, punctuated by multiple millennial-scale maxima with increasing peak magnitude that culminates at 2 ka. We note a clustering of high-frequency intervals between 12 and 9 ka (**Figure 4**).

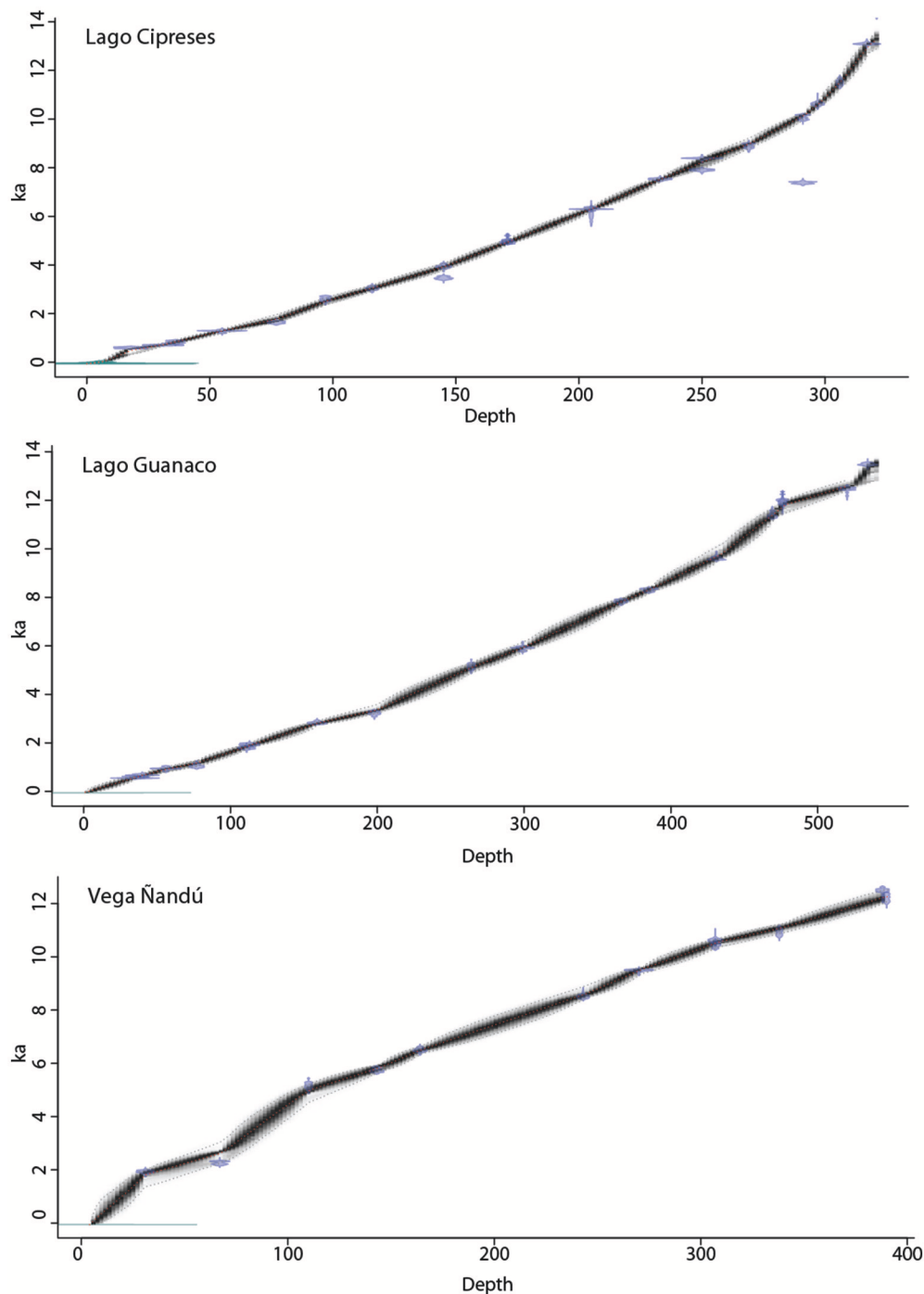
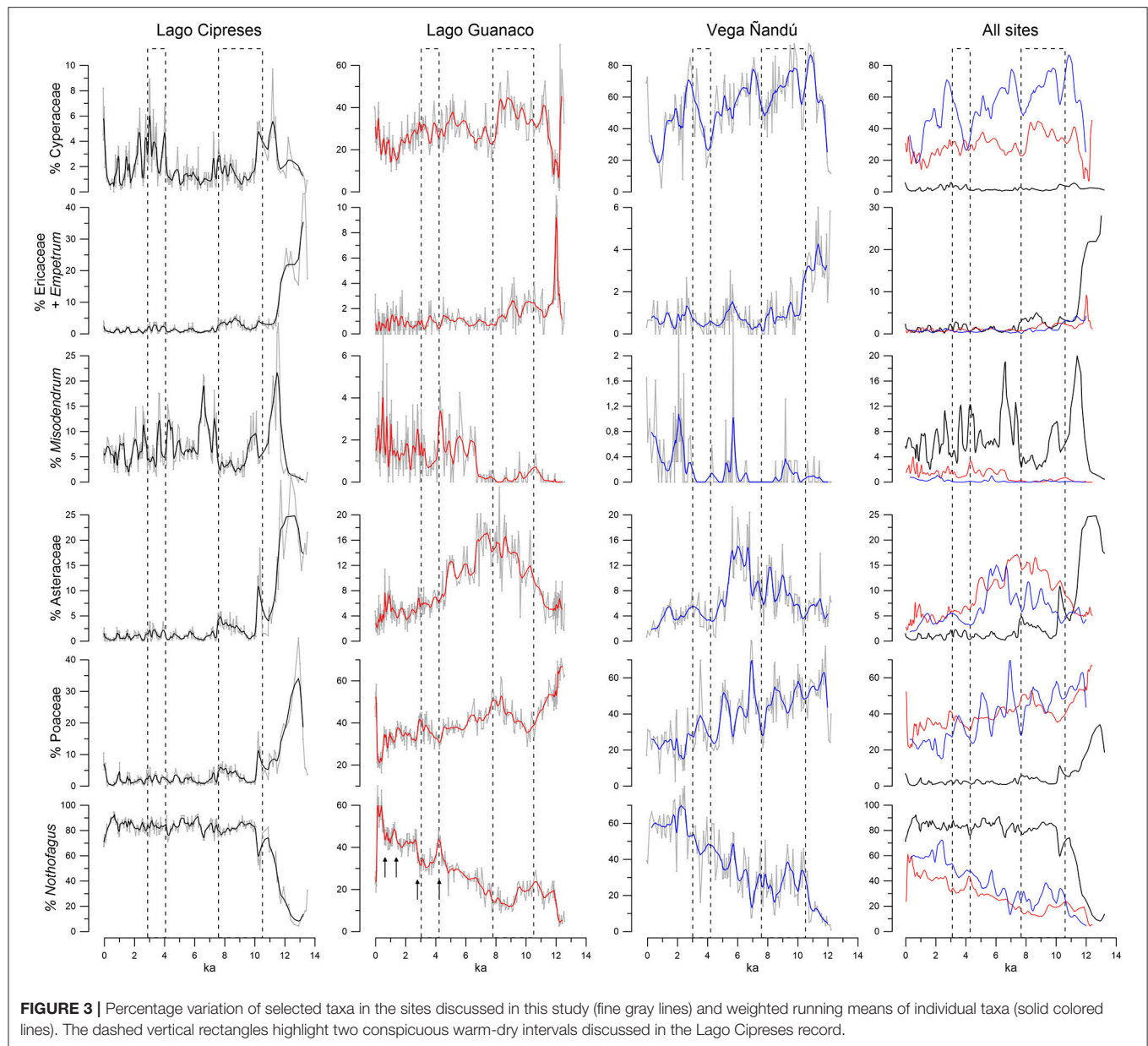


FIGURE 2 | Age models of the sites discussed in this study constructed with the Bacon package for R. The probability distribution of the individual calibrated radiocarbon dates are shown in blue. The 95% confidence of the age model is shown in gray, the median probability age of the age model is shown with a red line.

DISCUSSION

We detect prominent changes in vegetation and fire regimes in southwestern Patagonia since 13 ka (**Figure 3**). In the case of Lago Cipreses, closed-canopy *Nothofagus* forests have persisted since 11 ka with centennial-scale episodes of canopy

opening, proliferation and diversification of understory shrubs and herbs, lake-level declines and paleofires (Moreno et al., 2018). Occurrence of paleofires in this humid sector dominated by *Nothofagus* forests is restricted to episodic but recurrent centennial-scale negative anomalies in hydroclimate during the last 11,000 years (Moreno et al., 2018). Sites located in TPNP



show dominance of shrubs and herbs (Poaceae, Asteraceae, Ericaceae), along with a gradual and persistent increase in *Nothofagus* since 7.8 ka that reached its maximum during the last two millennia. All sites show onset of Chilean/European disturbance during the mid- to late nineteenth century, with deforestation and spread of exotic herbs (*Rumex*, and possibly *Plantago* and Asteraceae subfamily Cichorioidae) (Figure 4). These data indicate that forest vegetation established early during the Holocene in the Lago Cipreses sector (Figure 3) and that the forest-steppe ecotone must have lain somewhere between Lago Toro and Lago Sarmiento through much of the Holocene, i.e., between 10 and 26 km north of Lago Cipreses (Figure 1). We note that the difference in mean *Nothofagus* abundance between Lago Cipreses (80%) and Lago Guanaco (17%) was

highest during the interval between 11 and 7.8 ka ($\Delta = 63\%$) (Figure 3), establishing a steep gradient in arboreal pollen during the early Holocene. This gradient declined and reached its minimum during the Little Ice Age ($\Delta = 30\%$ between 0.6 and 0.1 ka) (Figure 3) through a series of gradual (between 7.8 and 5 ka) and rapid (5, 2.7, 0.6 ka) increments, oscillations (between 2 and 0.6 ka) and abrupt reversals (between 4 and 2.7 ka). We interpret these changes as a sustained encroachment of *Nothofagus* scrubland and woodland, punctuated by rapid pulses of arboreal expansion at 4, 2.7, 1.4, and 0.6 ka, into areas formerly dominated by steppe vegetation. Because the distribution of arboreal vegetation in this sector of southwestern Patagonia is controlled by the amount of precipitation of westerly origin, we interpret increases in *Nothofagus* as enhanced influence

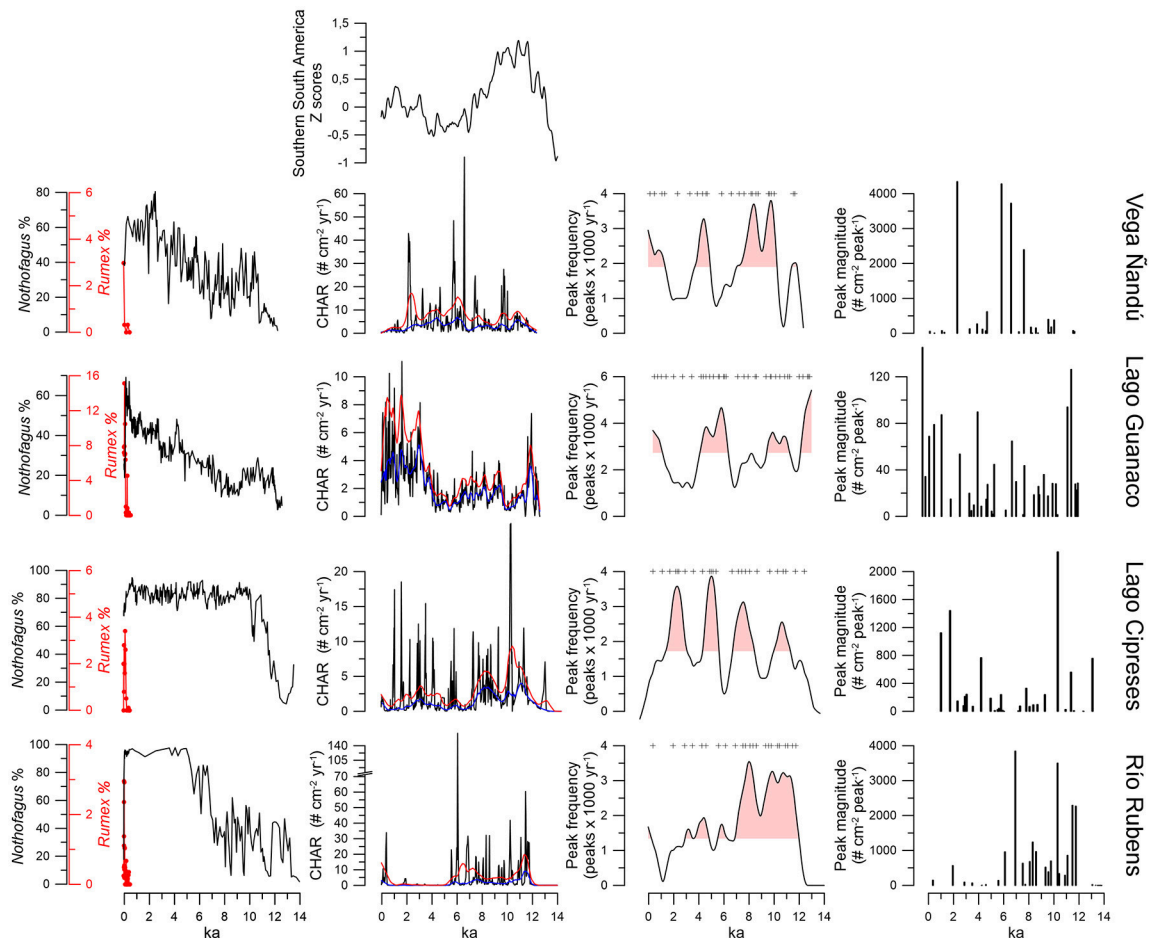


FIGURE 4 | Comparison of the *Nothofagus* and *Rumex* percentages from Lago Cipreses, Lago Guanaco, Vega Nandú, and Río Rubens, along with their corresponding macroscopic charcoal records and results of CharAnalysis. The black line corresponds to CHAR, the blue line denotes the calculated background, and the red line a locally defined threshold value. The red filling denotes frequency values above the mean in each site, the + symbol represents statistically significant charcoal peaks, the histogram indicates the magnitude of the statistically significant charcoal peaks. Also shown is the charcoal synthesis curve from southern South America normalized to the modern (1–0.1 ka interval) values.

of the SWW at this latitude since 7.8 ka (Moreno et al., 2010).

By virtue of being a fen with a vegetated surface, the Vega Nandú palynological record incorporates a local (azonal) signal to an airborne extralocal or zonal pollen rain (Villa-Martínez and Moreno, 2007; Moreno et al., 2009). When compared to Lago Guanaco this record not only shows persistently higher abundance of Cyperaceae (Figure 3), owing to the minerotrophic and shallow nature of this wetland, but also higher abundance and larger-amplitude fluctuations of *Nothofagus* superimposed on the trends shared with the Lago Guanaco record. One explanation for this behavior is that the species *Nothofagus antarctica*, which establishes the arboreal limit in the forest-steppe ecotone east of the Andes and also thrives in waterlogged substrates, may have grown on the surface of Vega Nandú increasing its pollen abundance and variability in the sedimentary record (Figure 3). We note that peak *Nothofagus* abundance in the Vega Nandú

record was achieved between 2.4 and 2.1 ka, whereas in Lago Guanaco this occurred between ~0.6 and 0.1 ka (Figure 3). This difference could represent the decline of local *Nothofagus* populations growing on the surface of Vega Nandú in response to a rise in water table during a series of precipitation increases recorded in Lago Guanaco between ~1.5 and 0.1 ka.

Local fires have taken place repeated times over the last 13,000 years with important variations in the frequency and magnitude of events (Figure 4). Likely sources of ignition for these fires include lightning strikes, Native American burning and volcanism. Lightning in western Patagonia is associated to postfrontal convection with a primary maximum along the coast and a secondary maximum along the eastern Andean slopes (Garreaud et al., 2014). To date, unfortunately, we have no proxy for past density of lightning strikes in the stratigraphic record. Because radiocarbon-dated archeological sites in Patagonia suggest that Native Americans have been

present in the region consistently since 13 ka (Méndez, 2013), we take this potential source of ignition as a latent driver and assume no major differences in forested vs. landscapes through time along the ~40 km distance separating our study sites. Explosive volcanism can be ruled out as the main driving mechanism for fire occurrence considering that up to five tephras are present in the records (Villa-Martínez and Moreno, 2007; Moreno et al., 2010), and the number of fires in each record is substantially higher than those potentially triggering events. Hence, we consider climate conditions as the main driver of fire activity in this sector of southern Patagonia, and consider lightning strikes and human activities as equally plausible sources of ignition in our study sites since 13 ka.

In Lago Cipreses we observe relatively low fire frequency (overall mean: 1.72 events* 1,000 years⁻¹) and relatively high fire magnitudes, as expected from the local abundance of coarse fuels. Fire occurrence in this forested sector of southwestern Patagonia has been intermittent and is associated with centennial- and millennial-scale warm/dry episodes (Figure 4). Frequency maxima occur at 11, 8, 6, and 3 ka, followed by a steady decline until the present. The frequency of local fire events in Lago Guanaco is higher than in Lago Cipreses (overall mean: 2.73 events* 1,000 years⁻¹), with lower-magnitude events (Figure 4). Frequency maxima occur at 13, 11–9, 5.5–4 ka and during the last millennium. We observe a trend toward larger-magnitude events from 4 ka onward, in conjunction with successive increases and culmination in the abundance of *Nothofagus* (Figure 4). These results suggest that rapid generation and desiccation of fine fuels (shrubs, herbs) in a steppe environment allowed the occurrence of frequent, low-magnitude fires, and that ambient moisture was sufficiently low through most of the record to enable combustion. Increasing levels and continuity of coarse woody fuels since 4 ka, as suggested by the increase in *Nothofagus*, led to higher frequency of events that peaked at 0.3 ka. Vega Nándú, on the other hand, shows an overall mean of 1.92 local fire events/1,000 years, with a clustering of high-frequency intervals between 10–9, 5.5 ka, and during the last 1,400 years, along with very large magnitude events between 8 and 2 ka (Figure 4). We note a divergence in fire regimes between Vega Nándú and Lago Guanaco despite being located in the same moisture and vegetation zone within the TPNP area, aspect we attribute to local burning of vegetation and/or organic deposits at the surface of Vega Nándú. Ground and underground fires in wetlands is a common phenomenon in southwestern Patagonia at times of lowered water table, as the fire fronts sweep through the landscape aided by strong summer winds. Thus, taphonomic processes in bogs can potentially overprint extralocal or regional signals, overemphasizing a local or azonal signal.

We carried out time series analysis of the macroscopic charcoal record from Río Rubens bog (Huber et al., 2004) to compare with our records (Figure 4), interpolating samples at 33-year intervals. High CHAR values are evident prior to ~5.5 ka, with a broad maximum in fire frequency between 11.5–7.5 ka and very large-magnitude events between 12–6 ka. This was contemporaneous with dominance of steppe herbs

and shrubs during the minerotrophic phase of the site (Huber et al., 2004). Fires become absent or rare after ~5.5 ka, coeval with increased arboreal abundance (Figure 4) and a shift to ombrotrophic conditions. Renewed fire activity over the past ~400 years overlaps with European settlement and appearance of *Rumex*. We observe that bog sites (Vega Nándú and Río Rubens) share high fire frequency intervals between 10–8 ka and at ~4.5 ka, along with very large-magnitude fire events between 8–6 ka (Figure 4). Lake records show a similar, though much diminished peak in fire frequency and substantially lower magnitude of events during the same interval, even in the case Lago Cipreses which shows dominance of forest vegetation. From this comparison we conclude that charcoal records from bogs tend to overestimate fire occurrence by surface burning at times of lowered precipitation and water table.

Regional Implications

Broad-scale syntheses show a conspicuous enhancement of fire activity during the early Holocene in southern South America (Whitlock et al., 2007; Power et al., 2008) (Figure 4), and southwestern Patagonia in particular (Huber et al., 2004), followed by a generalized decline and spatial heterogeneity between 9.5 and 6 ka, and intensification of that variability during the last 3,000 years. We observe that these signals are not prominent features in the macroscopic charcoal records from Lago Cipreses, L. Guanaco and Vega Nándú (Figure 4), suggesting that the broad scale signal revealed by the regional synthesis of (predominantly) microscopic charcoal records is modulated by contingencies at smaller spatial scales. Our charcoal records from TPNP, however, do show multiple maxima in the frequency of local fires during the early Holocene (11–7.5 ka), compatible with Huber et al. (2004)'s observation of high fire activity during this interval (Figure 4). Also, the southern South American charcoal curve (Power et al., 2008) shows a sustained rise from the lowest Holocene values starting at 4 ka, in agreement with the Lago Guanaco CHAR record (Figure 4).

Previously published macroscopic charcoal records from Lago Eberhard and Pantano Dumestre (Moreno et al., 2012), located 35 and 65 km SE from Lago Cipreses respectively (Figure 1), show a major increase in fire frequency at the beginning of the Holocene (11.5 ka). Unlike Lago Eberhard, the Pantano Dumestre record shows a major increase in the magnitude of local fires contemporaneous with a regressive lake phase that led to terrestrialization of the site and forest encroachment early during the Holocene. These findings, along with the previous discussion, suggest to us that macroscopic charcoal records from bogs and fens, e.g., the Río Rubens site (Figure 4) (Huber et al., 2004) yield a paleofire signal skewed toward surface burning of the bogs themselves, blurring the extralocal or regional fire-regime signal. We acknowledge, however, that our conclusions are based only on a few detailed time series of continuous/contiguously sampled macroscopic charcoal records from small closed-basin lakes.

We posit that taphonomic differences could account, to a large extent, for the apparent divergence in vegetation and climate histories among previously published records from lakes and bogs in southwestern Patagonia. One of those divergences is evident between the pollen records from Cerro Frías (Mancini, 2009) and Lago Guanaco, sites separated by 70 km along the eastern Andean slopes of southwestern Patagonia. The Cerro Frías record shows continuous deposition in a Cyperaceae fen since 12 ka and a steady increase in *Nothofagus* between ~11 and 3 ka, in agreement with the lake-sediment-based pollen record from Lago Guanaco. *Nothofagus* attained its maximum at 3 ka in Cerro Frías and then started a sustained decline until its minimum Holocene values during the recent centuries (Mancini, 2009). The Lago Guanaco record, on the other hand, shows rapid increases at 2.7 and 0.6 ka which led to a *Nothofagus* maximum between 0.6 and 0.1 ka (Figures 3, 4). These results were interpreted as a decline in temperature (Mancini, 2009) and precipitation (Tonello et al., 2009) over the last ~3,000 years in the case of the Cerro Frías record, and as an increase in precipitation in Lago Guanaco (Moreno et al., 2009, 2010), coherent with the Vega Ñandú (Villa-Martínez and Moreno, 2007) and Lago Cipreses (Moreno et al., 2018) records. These interpretations were, in turn, attributed to weaker (Cerro Frías) or stronger (Lago Guanaco, Vega Ñandú, Lago Cipreses) SWW influence over the last 3,000 years for sites located only 70 km apart. We posit that the differences between the Lago Guanaco and Cerro Frías pollen records could represent a decline in *Nothofagus* trees growing on the surface of the Cerro Frías fen, driven by a rise in local water table associated with increased precipitation of SWW origin during the last 3,000 years, as illustrated by the Lago Guanaco, Vega Ñandú and Lago Cipreses records.

REFERENCES

- Blaauw, M., and Christen, J. A. (2011). Flexible paleoclimate age-depth models using an autoregressive gamma process. *Bayes. Anal.* 6, 457–474. doi: 10.1214/11-BA618
- Daniau, A. L., Bartlein, P. J., Harrison, S. P., Prentice, I. C., Brewer, S., Friedlingstein, P., et al. (2012). Predictability of biomass burning in response to climate changes. *Glob. Biogeochem. Cycles* 26:GB4007. doi: 10.1029/2011GB004249
- Dimitri, M. J. (1972). *La Región de los Bosques Andino-Patagónicos*. Sinopsis General, Colección Científica del INTA, Buenos Aires. 254 pages.
- Donoso, C. (1998). *Bosques Templados de Chile y Argentina*. Variación, estructura y dinámica. Santiago, Chile. 483 pages.
- Fægri, K., and Iversen, J. (1989). *Textbook of Pollen Analysis*. Chichester: John Wiley & Sons.
- Fletcher, M. S., and Moreno, P. I. (2012). Have the Southern Westerlies changed in a zonally symmetric manner over the last 14,000 years? A hemisphere-wide take on a controversial problem. *Quat. Int.* 253, 32–46. doi: 10.1016/j.quaint.2011.04.042
- Galanter, M., Levy, H., and Carmichael, G. R. (2000). Impacts of biomass burning on tropospheric CO, NO_x, and O₃. *J. Geophys. Res. Atmos.* 105, 6633–6653. doi: 10.1029/1999JD901113
- Garreaud, R., Alvarez-Garretón, C., Barichivich, J., Boisier, J. P., Christie, D., Galleguillos, M., et al. (2017). The 2010–2015 mega drought in Central Chile: Impacts on regional hydroclimate and vegetation. *Hydrol. Earth Syst. Sci. Discuss.* 2017, 1–37. doi: 10.5194/hess-2017-191

SUMMARY AND CONCLUDING REMARKS

The data shown in this paper suggests that vegetation type exerts an important influence on fire regimes (local fire event frequency and magnitude) through the Holocene along a short transect (~28 km) through the forest-steppe ecotone in southwestern Patagonia. We also detect significant differences between vegetation and fire histories developed from a lake and a bog in TPNP, and conclude that differences in taphonomic processes produce a signal skewed toward local (azonal) conditions in the case of bogs.

Our lake-sedimentary data are consistent with findings based on relative area burned over a 25-year period along a latitudinal transect of 3,300 km through southwestern South America (between 25°S and 56°S) (Holz et al., 2012). Our findings expand upon those results and suggest that vegetation differences at the landscape level have also determined the nature of climate-fire relationships at timescales ranging from multi-decadal to multi-millennial.

AUTHOR CONTRIBUTIONS

PM and RV-M designed the study and carried out initial analyses. IV developed the pollen record from Lago Cipreses. RV-M developed the pollen record from Vega Ñandú. JF developed the pollen and charcoal record from Lago Guanaco. PM wrote the paper with contributions from all coauthors.

FUNDING

ICM P05-002 and NC120066, Fondecyt 1151469, Fondap 15110009, DRI USA2013-0035.

- Garreaud, R. D., Nicora, M. G., and Bürgesser, R. E., Ávila, E.E. (2014). Lightning in western patagonia. *J. Geophys. Res. Atmos.* 119, 4471–4485. doi: 10.1002/2013JD021160
- Heusser, C. J. (1971). *Pollen and Spores from Chile*. Tucson, AZ: University of Arizona Press.
- Heusser, C. J. (1993). Late-glacial of southern South America. *Q. Sci. Rev.* 12, 345–350. doi: 10.1016/0277-3791(93)90042-K
- Heusser, C. J. (1994). Paleoindians and fire during the late quaternary in Southern South-America. *Rev. Chil. Hist. Nat.* 67, 435–443.
- Heusser, C. J. (1995). Three late quaternary pollen diagrams from southern Patagonia and their paleoecological implications. *Palaeogeogr. Palaeoclimatol. Palaeoecol.* 118, 1–24.
- Higuera, P. E., Brubaker, L. B., Anderson, P. M., Hu, F. S., and Brown, T. A. (2009). Vegetation mediated the impacts of postglacial climate change on fire regimes in the south-central Brooks Range, Alaska. *Ecol. Monogr.* 79, 201–219. doi: 10.1890/07-2019.1
- Holz, A., Kitzberger, T., Paritsis, J., and Veblen, T. T. (2012). Ecological and climatic controls of modern wildfire activity patterns across southwestern South America. *Ecosphere* 3, 1–25. doi: 10.1890/ES12-00234.1
- Huber, U. M., and Markgraf, V. (2003). European impact on fire regimes and vegetation dynamics at the steppe-forest ecotone of southern Patagonia. *Holocene* 13, 567–579. doi: 10.1191/0959683603hl647rp
- Huber, U., Markgraf, V., and Schabitz, F. (2004). Geographical & temporal trends in Late Quaternary fire histories of Fuego-Patagonia, South America. *Quat. Sci. Rev.* 23, 1079–1097. doi: 10.1016/j.quascirev.2003.11.002

- Kean, J. W., Staley, D. M., and Cannon, S. H. (2011). *In situ* measurements of post-fire debris flows in southern California: comparisons of the timing and magnitude of 24 debris-flow events with rainfall and soil moisture conditions. *J. Geophys. Res. Earth Surface* 116:F04019. doi: 10.1029/2011JF002005
- Krawchuk, M. A., Moritz, M. A., Parisien, M.-A., Van Dorn, J., and Hayhoe, K. (2009). Global pyrogeography: the current and future distribution of wildfire. *PLoS ONE* 4:e5102. doi: 10.1371/journal.pone.0005102
- Lara, A., Villalba, R., Wolodarsky-Franke, A., Aravena, J. C., Luckman, B. H., and Cuq, E. (2005). Spatial and temporal variation in *Nothofagus pumilio* growth at tree line along its latitudinal range (35 degrees 40'–55 degrees S) in the Chilean Andes. *J. Biogeogr.* 32, 879–893. doi: 10.1111/j.1365-2699.2005.01191.x
- Mancini, M. V. (2009). Holocene vegetation and climate changes from a peat pollen record of the forest – steppe ecotone, Southwest of Patagonia (Argentina). *Quat. Sci. Rev.* 28, 1490–1497. doi: 10.1016/j.quascirev.2009.01.017
- Méndez, C. (2013). Terminal Pleistocene/early Holocene 14C dates from archaeological sites in Chile: critical chronological issues for the initial peopling of the region. *Quat. Int.* 301, 60–73. doi: 10.1016/j.quaint.2012.04.003
- Moreno, P. I., Francois, J. P., Villa-Martínez, R., and Moy, C. M. (2009). Millennial-scale variability in Southern Hemisphere westerly wind activity over the last 5000 years in SW Patagonia. *Quat. Sci. Rev.* 28, 25–38. doi: 10.1016/j.quascirev.2008.10.009
- Moreno, P. I., Francois, J. P., Villa-Martínez, R., and Moy, C. M. (2010). Covariability of the Southern Westerlies and atmospheric CO₂ during the Holocene. *Geology* 39, 727–730. doi: 10.1130/G30962.1
- Moreno, P. I., Vilanova, I., Villa-Martínez, R., Dunbar, R. B., Mucciarone, D. A., Kaplan, M. R., et al. (2018). Onset and evolution of southern annular mode-like changes at centennial timescale. *Sci. Rep.* 8:3458. doi: 10.1038/s41598-018-21836-6
- Moreno, P. I., Villa-Martínez, R., Cardenas, M. L., and Sagredo, E. A. (2012). Deglacial changes of the southern margin of the southern westerly winds revealed by terrestrial records from SW Patagonia (52 degrees S). *Quat. Sci. Rev.* 41, 1–21. doi: 10.1016/j.quascirev.2012.02.002
- Pisano, E. (1954). La vegetación de las distintas zonas geográficas chilenas. *Rev. Geogr. Chile Terra Aust.* 11, 95–107.
- Power, M. J., Marlon, J., Ortiz, N., Bartlein, P. J., Harrison, S. P., Mayle, F. E., et al. (2008). Changes in fire regimes since the Last Glacial Maximum: an assessment based on a global synthesis and analysis of charcoal data. *Clim. Dynam.* 30, 887–907. doi: 10.1007/s00382-007-0334-x
- Schäbitz, F. (1991). Holocene vegetation and climate in southern Santa Cruz, Argentina. *Bamberger Geograph. Schr.* 11, 235–244.
- Schmithüsen, J. (1956). *Die Raumlische Ordnung der chilenischen Vegetation. Bonner Geographische Abhandlungen*, Vol. 17. Munich: Stollfuss, 1–86.
- Tonello, M. S., Mancini, M. V., and Seppä, H. (2009). Quantitative reconstruction of Holocene precipitation changes in southern Patagonia. *Quat. Res.* 72, 410–420. doi: 10.1016/j.yqres.2009.06.011
- van der Werf, G. R., Randerson, J. T., Collatz, G. J., Giglio, L., Kasibhatla, P. S., Arellano, A. F., et al. (2004). Continental-scale partitioning of fire emissions during the 1997 to 2001 El Niño/La Niña period. *Science* 303, 73–76. doi: 10.1126/science.1090753
- Villagrán, C. (1980). Vegetationsgeschichtliche und pflanzensoziologische Untersuchungen im Vicente Perez Rosales Nationalpark (Chile). *Diss. Bot.* 54, 1–165.
- Villa-Martínez, R., and Moreno, P. I. (2007). Pollen evidence for variations in the southern margin of the westerly winds in SW Patagonia over the last 12,600 years. *Quat. Res.* 68, 400–409. doi: 10.1016/j.yqres.2007.07.003
- Wille, M., and Schäbitz, F. (2009). Late-glacial and Holocene climate dynamics at the steppe/forest ecotone in southernmost Patagonia, Argentina: the pollen record from a fen near Brazo Sur, Lago Argentino. *Veget. Hist. Archaeobot.* 18, 225–234. doi: 10.1007/s00334-008-0194-2
- Whitlock, C., and Anderson, R. S. (2003). “Fire history reconstructions based on sediment records from lakes and wetlands,” in *Fire and Climatic Change in Temperate Ecosystems of the western Americas*, eds T. T. Veblen, W. L. Baker, G. Montenegro, and T. W. Swetnam (New York, NY: Springer), 265–295.
- Whitlock, C., Moreno, P. I., and Bartlein, P. (2007). Climatic controls of Holocene fire patterns in southern South America. *Quat. Res.* 68, 28–36. doi: 10.1016/j.yqres.2007.01.012
- Wright, H. E. J., Mann, D. H., and Glaser, P. H. (1984). Piston corers for peat and lake sediments. *Ecology* 65, 657–659. doi: 10.2307/1941430
- Zhang, H., and Wang, Z. (2011). Advances in the study of black carbon effects on climate. *Adv. Clim. Change Res.* 2, 23–30. doi: 10.3724/SP.J.1248.2011.00023

Conflict of Interest Statement: The authors declare that the research was conducted in the absence of any commercial or financial relationships that could be construed as a potential conflict of interest.

The reviewer VM and handling Editor declared their shared affiliation.

Copyright © 2018 Moreno, Vilanova, Villa-Martínez and Francois. This is an open-access article distributed under the terms of the Creative Commons Attribution License (CC BY). The use, distribution or reproduction in other forums is permitted, provided the original author(s) and the copyright owner are credited and that the original publication in this journal is cited, in accordance with accepted academic practice. No use, distribution or reproduction is permitted which does not comply with these terms.



Holocene Dynamics of Temperate Rainforests in West-Central Patagonia

Virginia Iglesias^{1*}, Simon G. Haberle², Andrés Holz³ and Cathy Whitlock^{1,4}

¹ Montana Institute on Ecosystems, Montana State University, Bozeman, MT, United States, ² School of Culture, History and Language, Australian National University, Canberra, ACT, Australia, ³ Department of Geography, Portland State University, Portland, OR, United States, ⁴ Department of Earth Sciences, Montana State University, Bozeman, MT, United States

OPEN ACCESS

Edited by:

Valentí Rull,
Instituto de Ciencias de la Tierra
Jaume Almera (CSIC), Spain

Reviewed by:

Antonio Maldonado,
Centro de Estudios Avanzados en
Zonas Áridas, Chile
Colin Long,
University of Wisconsin–Oshkosh,
United States

*Correspondence:

Virginia Iglesias
virginia.iglesias@msu.montana.edu

Specialty section:

This article was submitted to
Paleoecology,
a section of the journal
Frontiers in Ecology and Evolution

Received: 23 October 2017

Accepted: 28 December 2017

Published: 26 January 2018

Citation:

Iglesias V, Haberle SG, Holz A and
Whitlock C (2018) Holocene Dynamics
of Temperate Rainforests in
West-Central Patagonia.
Front. Ecol. Evol. 5:177.
doi: 10.3389/fevo.2017.00177

Analyses of long-term ecosystem dynamics offer insights into the conditions that have led to stability vs. rapid change in the past and the importance of disturbance in regulating community composition. In this study, we (1) used lithology, pollen, and charcoal data from Mallín Casanova (47°S) to reconstruct the wetland, vegetation, and fire history of west-central Patagonia; and (2) compared the records with independent paleoenvironmental and archeological information to assess the effects of past climate and human activity on ecosystem dynamics. Pollen data indicate that *Nothofagus-Pilgerodendron* forests were established by 9,000 cal yr BP. Although the biodiversity of the understory increased between 8,480 and 5,630 cal yr BP, forests remained relatively unchanged from 9,000 to 2,000 cal yr BP. The charcoal record registers high fire-episode frequency in the early Holocene followed by low biomass burning between 6,500 and 2,000 cal yr BP. Covarying trends in charcoal, bog development, and Neoglacial advances suggest that climate was the primary driver of these changes. After 2,000 cal yr BP, the proxy data indicate (a) increased fire-episode frequency; (b) centennial-scale shifts in bog and forest composition; (c) the emergence of vegetation-fire linkages not recorded in previous times; and (d) paludification in the last 500 years possibly associated with forest loss. Our results therefore suggest that *Nothofagus-Pilgerodendron* dominance was maintained through much of the Holocene despite long-term changes in climate and fire. Unparalleled fluctuations in local ecosystems during the last two millennia were governed by disturbance-vegetation-hydrology feedbacks likely triggered by greater climate variability and deforestation.

Keywords: anthropogenic impact, charcoal, climate, pollen, stability, vegetation, Holocene, forest

INTRODUCTION

Instrumental and tree-ring records from the southern Andes show a strong warming trend during the last 50 years coupled with a decline in precipitation (Villalba et al., 2003). With rising temperatures, glaciers in the North and South Patagonian icefields are receding up to 100 times faster than at any time since the Little Ice Age (Glasser et al., 2011). These trends are projected to continue in the coming decades and lead to increased moisture deficits, further ice recession, tree mortality, and greater risk of fires (Cabr   et al., 2016).

Paleoenvironmental data from Patagonia suggest that past changes in climate and land use have profoundly influenced not only the water balances and disturbance regimes, but also the composition and distribution of vegetation (e.g., Huber et al., 2004; Markgraf et al., 2013). Prior to ca. 18,000 cal yr BP, cold, dry and windy conditions were associated with extensive glaciation in western Patagonia and led to the extirpation of several plant species over much of their former range (Barreda et al., 2007). Open steppe/heath prevailed in unglaciated areas, and trees either migrated to northern latitudes or survived in local refugia (Pastorino and Gallo, 2002). Higher temperatures and a shift in dominance from year-round Antarctic air during glacial times to more humid Pacific winds in the Holocene (Heusser, 2003) promoted the reorganization of vegetation (e.g., Iglesias et al., 2014). In particular, *Nothofagus*-dominated forests expanded throughout the western Andes. This increase in woody fuel allowed a progressive rise in regional fire activity that peaked between 10,000 and 7,000 cal yr BP (Whitlock et al., 2006). The Late Holocene was characterized by fluctuations in moisture availability that resulted in spatial and temporal variability in vegetation composition and probability of fire (Fletcher and Moreno, 2012). In recent centuries, deforestation has affected forest diversity and soil structure, and these changes threaten ecosystem services, including carbon storage, forage production, and water supply (Veblen et al., 2011). In this study, we reconstruct the Holocene vegetation and fire history in west-central Patagonia (Mallín Casanova 47°38'36.86"S; 72°58'30.81"W; 126 m elev), and assess the impact of climate, fire, and volcanic eruptions on vegetation and wetland dynamics. By analyzing the long-term history of this site, we offer insights into the conditions that have driven change in terrestrial and wetland communities in the past.

STUDY AREA

Lake Casanova and the surrounding ombrotrophic *Sphagnum* bog (Mallín Casanova) are situated in the Baker River watershed, between the North and South Patagonian icefields (Figure 1). The rugged topography of the area results from Pleistocene glaciation and postglacial alluvial and slope activity (Niemeyer et al., 1984; Sernageomin, 2002). Precipitation is associated with frontal storm systems that migrate eastwards along the path of the Southern Westerlies (Garreaud et al., 2013). Uplift of low-level winds over the Andes produces year-round orographic precipitation on the west side of the mountains (e.g., 4,300 mm yr⁻¹ on San Pedro island; Dirección Meteorológica de Chile, 2017). Conversely, forced subsidence on the leeward slopes causes adiabatic warming of the air masses, resulting in increasingly drier conditions toward the east (e.g., 800 mm yr⁻¹ in Cochrane; Dirección Meteorológica de Chile, 2017).

The present-day west-to-east precipitation gradient leads to a transition from evergreen cool rainforests of *Nothofagus nitida*-*N. betuloides*-*Pilgerodendron* in the lowland (precipitation \geq 1,500 mm yr⁻¹) to deciduous forests of *Nothofagus pumilio* (precipitation = 1,500–400 mm yr⁻¹) at higher elevations to steppe characterized by a matrix of tussock grasses, herbs, and

cushion shrubs (precipitation < 500 mm yr⁻¹). M. Casanova is surrounded by *N. betuloides*-*Pilgerodendron* forest with open shrub/grassland and *Sphagnum* peatland (precipitation = 3,000 mm yr⁻¹). The presence of burned trees on the bog and homogeneous stand structure attest to the effects of recent fires (Holz et al., 2012), which burned both tree crowns and surface fuels. These mixed-severity fires are associated with interannual moisture variability (Holz and Veblen, 2009, 2012). Since ca. 1930 AD, the wetland has been surrounded by *Estancia Casanova*, a small family farm (Holz and Veblen, 2011).

METHODS

A 1-m-long, 80-mm-diameter piston sampler was used to collect a 350-cm-long sediment core from Mallín Casanova at the southeastern margin of the lake. The record provides evidence of environmental change from the beginning of sediment deposition at the wetland to present day. Core segments were transported to the Australian National University, Canberra, where they were split into working and archival halves and subsampled. Description of the sedimentary structures and biological components was performed visually following Schnurrenberger et al. (2001). Magnetic susceptibility (SI) was measured at 1-cm contiguous intervals to assess changes in inorganic sediment input to the wetland (Gedye et al., 2000).

Eight charcoal samples were submitted for AMS radiocarbon dating to the W. M. Keck Carbon Cycle AMS facility (University of California, Irvine) and calibrated with the ShCal13 calibration curve (Hogg et al., 2013; Table 1). Chronologies were developed by modeling depth as a function of the explicitly combined probability distribution of each calibrated date and prior expectations about temporal variability in sediment accumulation rates (Blaauw and Christen, 2011). Specifically, the prior distribution for sediment accumulation rates had a mean of 0.05 cm yr⁻¹ and a shape equal to 1.5. Depths were adjusted by removing volcanic ashes >1 cm in thickness on the assumption that these layers were deposited in a negligible span of time.

Past vegetation dynamics were inferred from changes in pollen abundance through time. Standard techniques were employed to extract pollen residues from 0.5 cm⁻³ sediment samples at 2–5 cm intervals (Faegri and Iversen, 1989). Pollen identification was based on published atlases (Heusser, 1971; Markgraf and D'Antoni, 1978) and a modern reference collection, and performed at 250 and 400x magnification. Pollen percentages (both terrestrial and aquatic) were calculated as a function of the sum of terrestrial pollen types, which in all cases exceeded 250 grains per sample to ensure replicability (Iglesias et al., 2016b).

Empetrum and Caryophyllaceae were excluded from the terrestrial pollen sum. Modern pollen-vegetation studies suggest that, due to the very limited pollen dispersal capabilities of these taxa, they are depicted in the pollen rain only when locally present in the landscape (Fletcher and Thomas, 2007; Iglesias et al., 2016b). This high fidelity is likely to be reinforced in peat deposits, where local vegetation is overrepresented in the pollen spectrum (Janssen, 1973). For these reasons, we assumed that variations in the pollen abundance of *Empetrum*

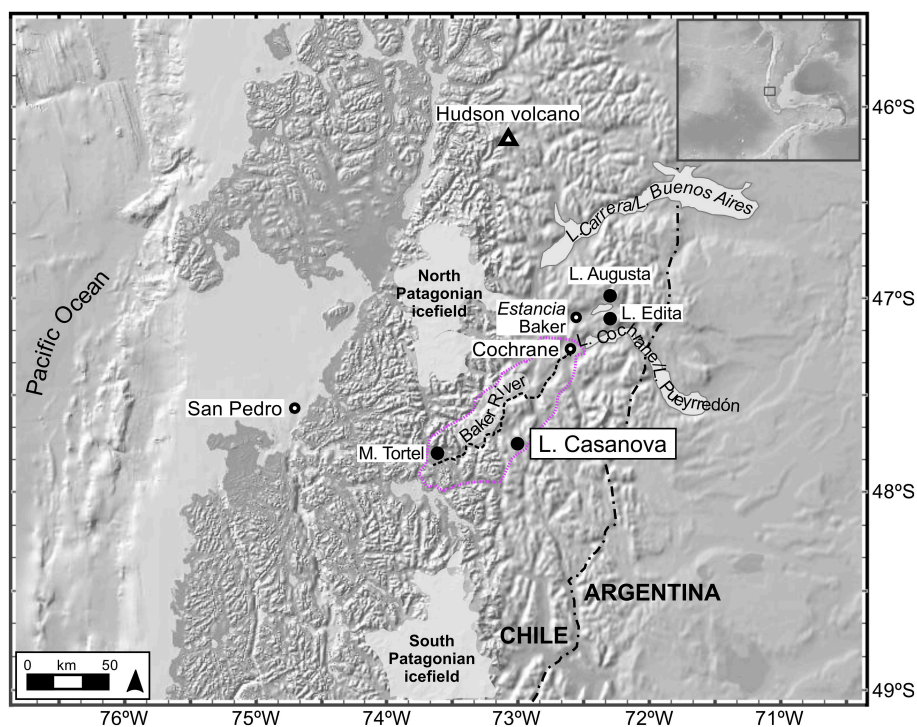


FIGURE 1 | Study area and location of L. Casanova and other sites mentioned in the manuscript. M. Casanova is the ombrotrophic *Sphagnum* bog surrounding the lake. The coring site is located southeast of L. Casanova. The approximate boundaries of the Baker River watershed are shown in color.

TABLE 1 | Radiocarbon and calibrated dates from M. Casanova.

Depth (cm)	Lab. no.	Radiocarbon age (^{14}C yr BP)	Age error (yr)	Calibrated age (cal yr BP; 1 sigma range) ^a
0	NA	Inferred	NA	−57 to (−47)
10	83174	−525	15	Invalid age for calibration curve ^b
37	83175	745	30	574 to 674
62	83176	1,410	40	1,194 to 1,311
93	83177	1,785	40	1,607 to 1,705
143	83178	3,685	30	3,897 to 4,065
242	83179	6,370	40	7,178 to 7,310
312	83180	7,165	50	7,874 to 8,001
333	83181	8,720	40	9,553 to 9,664

^aRelative area under probability distribution = 1.000 (Hogg et al., 2013).

^bNot included in the chronology.

¹³C values were not measured.

and Caryophyllaceae probably reflected changes in wetland composition rather than changes in terrestrial vegetation at the watershed-scale (Huber et al., 2004), although we recognize that both taxa have wider ecological distributions.

For this study, pollen types exceeding 3% of the terrestrial pollen sum are discussed in detail, while poorly represented taxa were grouped according to their ecological affinities. *Nothofagus dombeyi*-type includes *N. pumilio*, *N. dombeyi*, *N. nitida*, *N. betuloides*, and *N. antarctica*. Currently, only *N. betuloides* and *N. antarctica* grow in the study area. Cupressaceae

pollen is attributed to *Pilgerodendron uviferum*, although *Fitzroya cupressoides* and, less likely, *Austrocedrus chilensis* may have been long-distance contributors. Pollen from *Hydrangea*, *Eucryphia/Caldcluvia*-type, Myrtaceae, *Weinmannia*, *Coriaria*, *Drimys*, *Pseudopanax*, and *Saxegothea* are grouped into “Other rainforest taxa.” “Other shrubs” includes *Schinus*, *Embothrium*, *Escallonia*, Verbenaceae, Rhamnaceae, and *Berberis*. “Other grassland taxa” corresponds to pollen from xerophytic shrubs and herbs, such as *Acaena*, *Phacelia*, and *Mulinum*. Selected pollen percentages were plotted as a function of time. The resulting pollen diagram was zoned by visual inspection to aid in the description of the stratigraphic changes.

In order to obtain a local high-resolution fire reconstruction, macroscopic charcoal (i.e., particles > 125 μm in diameter) was extracted from contiguous 1-cm thick samples and quantified under a binocular dissecting microscope (Whitlock and Larsen, 2001). Changes in sediment accumulation rates and sampling variability were accounted for by converting charcoal concentrations to charcoal accumulation rates (CHAR; particles $\text{cm}^{-2} \text{yr}^{-1}$) and interpolating the data to the median time resolution.

A locally weighted scatterplot smoother was used to isolate the high-frequency component of the charcoal time series (i.e., positive residuals of the model) from the long-term trends in CHAR (i.e., “background charcoal”). Comparison of the charcoal data and fire scars in tree rings of *P. uviferum* shows high correlation coefficients and suggests that the CHAR times series constitutes a record of biomass burning within 10 km of

the bog (Holz et al., 2012). Large CHAR values (i.e., positive residuals of the model that exceeded the 95th percentile of a locally fit Gaussian distribution; “charcoal peaks”) were tested for significance with a Poisson distribution and interpreted as local fire episodes (i.e., fire events occurring within the time span of the charcoal peak; Higuera et al., 2009). Local fire episodes were summarized as fire-episode frequency (i.e., fire episodes $1,000 \text{ years}^{-1}$).

To explore the relationship between variations in fire and climate, we calculated the probability of fire episodes occurring at times of regional glacier advance or retreat as:

$$(1) \text{ Pr}(\text{fire}_{\text{gl}}) = \text{Sum}(\text{Fire episodes}_{\text{gl}}) * \text{Total samples}_{\text{gl}}^{-1} \text{ and} \\ (2) \text{ Pr}(\text{fire}_{\text{non-gl}}) = \text{Sum}(\text{Fire episodes}_{\text{non-gl}}) * \text{Total} \\ \text{samples}_{\text{non-gl}}^{-1}, \text{ respectively,}$$

with $\text{Pr}(\text{fire}_{\text{gl}})$: probability of fire at times of glacier advances; $\text{Sum}(\text{Fire episodes}_{\text{gl}})$: total number of fire episodes at times of glacier advances; $\text{Total samples}_{\text{gl}}$: number of sample at times of glacier advances; $\text{Pr}(\text{fire}_{\text{non-gl}})$: probability of fire at times of glacier retreat; $\text{Sum}(\text{Fire episodes}_{\text{non-gl}})$: total number of fire episodes at times of glacier retreat and $\text{Total samples}_{\text{non-gl}}$: number of sample at times of glacier retreat. Times of glacier advances and retreat were obtained from Aniya (2013). A Chi-squared test for proportions was used to assess if the probabilities of fire at times of glacier advances and retreat were statistically different at the 0.05 alpha-level (Table 2).

Long-term changes in community composition were inferred from a dissimilarity matrix produced for the terrestrial taxa tallied in the pollen samples. Specifically, we calculated the squared chord distance (SCD) between every sample and the first sample of the record (i.e., 344 cm depth; 9,840 cal yr BP) as an assessment of their dissimilarity from the oldest pollen assemblages. We interpreted this time series as a measure of long-term trends in the stability of the vegetation. Under the premise that stable ecosystems remain mostly unchanged over time or fluctuate around an equilibrium point, our null hypothesis was that SCDs would be equal to the median Holocene SCD. SCDs larger than the median would provide evidence of statistically significant change in vegetation composition. In order to account for change in sampling effort, rates of change between pairs of consecutive samples were also estimated. Rates of change were defined as:

$$(3) \text{ Rate of change}_{(t)} = \text{abs}[(\text{SCD}_{(t)} - \text{SCD}_{(t-1)}) / \\ (\text{Age}_{(t)} - \text{Age}_{(t-1)})]$$

TABLE 2 | Probability of fire episodes at times of glacier advances or glacial retreat.

	Glacier advance	Glacier retreat
9,950 cal yr BP—present	0.02	0.05
Before 2,000 cal yr BP	0.01	0.04
After 2,000 cal yr BP	0.03	0.09

Rates of change of zero would result from the comparison of identical samples (i.e., no temporal changes in composition = stable plant communities), while non-zero values would be indicative of changes in vegetation composition or unstable communities between times t and $t-1$. Because we acknowledge the possibility of sampling errors, we bootstrapped confidence intervals for the median Holocene SCD and for rates of change equal to zero. SCDs and rates of change were visually compared with charcoal data, climate variability inferred from independent proxies, and the archeological and historical record. The same procedure was applied to aquatic taxa and interpreted as a proxy of wetland dynamics.

Spectral analysis was conducted on the terrestrial SCD time series to detect possible changes in the periodicity of oscillations in vegetation composition. Specifically, a dynamic Lomb-Scargle periodogram was used to identify periodic signals in the unevenly spaced time series (Press and Rybicki, 1989). All analyses and figures were performed with R (R Core Team, 2015).

RESULTS

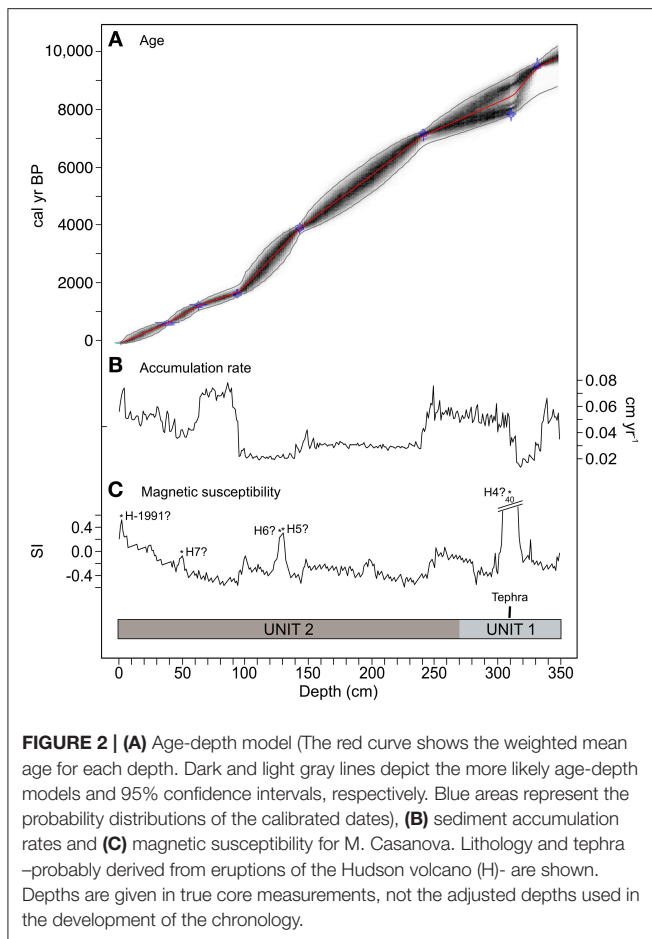
Chronology

Seven AMS radiocarbon dates and the inferred age of the top sample were used in the construction of a calibrated age-depth model (Table 1). The radiocarbon age corresponding to the sample extracted at 10-cm depth ($-525 \pm 15 \text{ }^{14}\text{C yr BP}$) was judged to be anomalously young and not included in age model development. The estimated age-depth relationship was relatively linear, suggesting quite stable sediment accumulation rates ($0.01\text{--}0.07 \text{ cm yr}^{-1}$; Figure 2).

Lithology

Two lithological units were visually identified in the core from M. Casanova (Figure 2). The basal unit (Unit 1: 350–275 cm depth; 9,950–7,840 cal yr BP) was composed of fine clay. With the exception of two peaks at 326 and 310 cm depth (9,220 and 8,520 cal yr BP; 0.19 and 39.62 SI, respectively), magnetic susceptibility was always negative (median = -0.18 SI), suggesting that the sediment was mainly composed of diamagnetic minerals, such as quartz, calcite, and/or organic matter. A large peak in magnetic susceptibility at 310 cm depth corresponds with a 4-cm-thick tephra, possibly derived from the H4 eruption of the Hudson volcano. H4 tephra deposits are widespread in Patagonia. AMS radiocarbon dates place the mean age of this tephra at 8,440 cal yr BP in lake cores and 7,891 cal yr BP in outcrops, bog, and soil samples (Stern et al., 2016). Due to this systematic difference between radiocarbon dates, which has been attributed to the percolation of humic acids in soils and bogs (Bertrand et al., 2012) as well as to ^{14}C reservoir effects in lakes (Stern et al., 2016), the age of this tephra was not employed in the development of the core chronology.

The uppermost unit (Unit 2: 275–0 cm depth; 7,840 cal yr BP–present) was characterized by brown fibrous peat, low magnetic susceptibility (median = 0.20 SI), and overall low sedimentation rates (median = 0.03 cm yr^{-1}). Gray-brown fine material was observed at 258 and 251 cm depth (7,510 and 7,320 cal yr BP, respectively). Weakly positive magnetic susceptibility values at



those depths, as well as in the 136–131 and 27–0 cm depth segments (3,630–3,400 and 450 cal yr BP–present, respectively) indicate the presence of paramagnetic minerals (e.g., iron oxides, iron carbonates, and/or iron silicates). Although no lithological changes were visually identified in this unit, it is possible that magnetic enrichment of these three segments resulted from the deposition of basaltic to andesitic tephra produced during the H5 (pooled mean age = 3,840 cal yr BP), H6 (pooled mean age = 2,740 cal yr BP) and 1991 AD eruptions of the Hudson volcano (Haberle and Lumley, 1998).

Pollen and Charcoal Records

The pollen record from M. Casanova was visually divided in five pollen zones to aid in the description of vegetation and fire history reconstructions (Figures 3, 4). Pollen data are publicly available at Neotoma Paleocology Database (www.neotomadb.org), and charcoal data have been deposited in the Global Charcoal Database (www.gpwg.org).

Zone MC-1 (350–308 cm depth; 9,950–8,480 cal yr BP) was dominated by *N. dombeyi*-type (72–86%), Poaceae (<11%) and Cupressaceae (<11%). Other rainforest taxa, Other shrubs, and Other grassland taxa, including Asteraceae and Amaranthaceae, were poorly represented in the pollen assemblage (1% in all cases). The vegetation probably resembled present-day *Nothofagus/Pilgerodendron* forest, and was relative stable (rates of

change <0.003% yr⁻¹; Haberle and Bennett, 2001). Aquatic and wetland pollen and spores were virtually absent (<0.7%; rates of change <0.005% yr⁻¹), suggesting that the wetland was poorly developed at the time, or that the modern lake extended to the coring site. CHAR levels oscillated between 0 and 0.49 particles cm⁻² yr⁻¹, and local fire-episode frequency steadily declined from 4.8 episodes 1,000 yr⁻¹ at 9,950 cal yr BP to 1.7 episodes 1,000 yr⁻¹ at the top of the zone.

Zone MC-2 (308–195 cm depth; 8,480–5,630 cal yr BP) continued to be dominated by *N. dombeyi*-type (65–88%) and Cupressaceae (15–19%), but pollen from *Misodendron* (<12.3%), *Maytenus* (<3%), Other shrubs (<3%), and Other grassland taxa (<2%) was higher than before. This increase in palynological richness implies diversification of the understory and/or opening of the *Nothofagus/Pilgerodendron* forest. High rates of change in terrestrial SCDs point to fast changes in vegetation composition at the 8,320–8,150 and 7,660–7,510 cal yr BP periods. These fluctuations are evidenced by pronounced variability in *N. dombeyi*-type pollen percentages. *Empetrum*, *Myriophyllum*, and Cyperaceae rose up to 4%, but the aquatic rates of change remained low (<0.01% yr⁻¹). CHAR was lower than before (<0.15 particles cm⁻² yr⁻¹), and fire-episode frequency declined to 0.1 after reaching a local maximum of 3.5 fire episodes 1,000 yr⁻¹ at 7,100 cal yr BP.

Zone MC-3 (195–101 cm depth; 5,630–2,000 cal yr BP). *N. dombeyi*-type increased to 85.4% at expense of *Misodendron* (<3%), Cupressaceae (<12%), Other rainforest taxa (<2.5%), *Maytenus* (<0.6%), and Other shrubs (<1.5%). Vegetation-pollen calibrations indicate that the vegetation was dominated by closed *Nothofagus/Pilgerodendron* forest (rates of change <0.003% yr⁻¹; Haberle and Bennett, 2001). *Empetrum* pollen and *Sphagnum* spores rose and reached peaks of 112 and 23% of the total terrestrial sum, respectively, suggesting the establishment of the modern *Sphagnum* bog at the beginning of this zone. Although *Sphagnum* values were erratic, modern studies suggest that the presence of spores in the sediment is indicative of moss accumulation (Halsey et al., 2000). Terrestrial rates of change remained stable throughout the zone while aquatic SCDs began to slowly rise at ca. 5,000 cal yr BP. CHAR declined to <0.08 particles cm⁻² yr⁻¹, and so did local fire-episode frequency, which ranged between 0 and 2 fire episodes 1,000 yr⁻¹.

Zone MC-4 (101–31 cm depth; 2,000–530 cal yr BP). *N. dombeyi*-type (<77%), *Misodendron* (>1.6%), and Other rainforest taxa (<2%) declined, and *Podocarpus* and Cupressaceae pollen percentages were higher than before (<47.4 and <27.3%, respectively). CHAR and fire-episode frequency increased to 0.19 particles cm⁻² yr⁻¹ and 4.8 fire episodes 1000 yr⁻¹, respectively, suggesting that the forest supported more frequent and possibly more severe fires than before. Terrestrial and aquatic SCDs greater than the Holocene median and high rates of change imply large and rapid variations in terrestrial and bog vegetation throughout the period. Dynamic spectral analysis of terrestrial SCDs shows high power at 300- and 700-year periods during the last 2000 years (Figure 5).

Zone MC-5 (31–0 cm depth; 530 cal yr BP–present) was characterized by rapid fluctuations in pollen percentages of

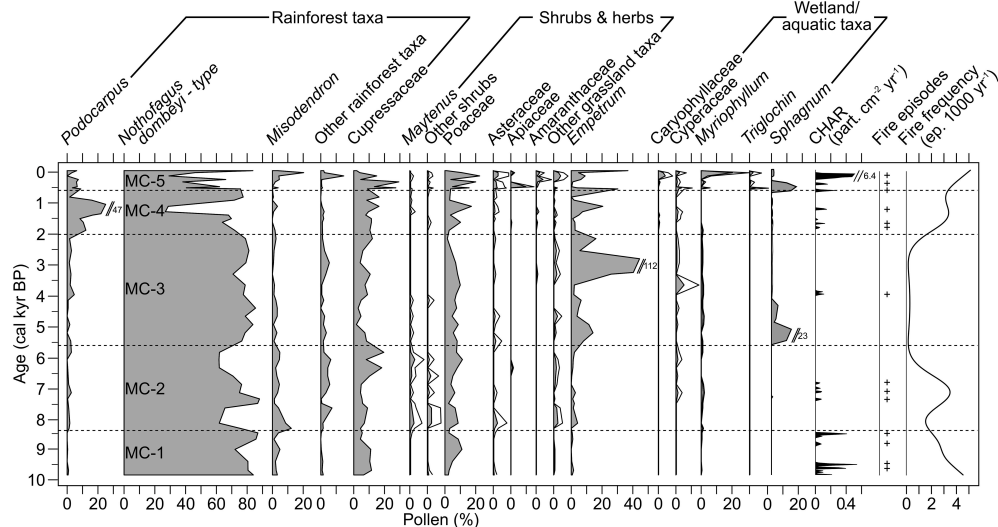


FIGURE 3 | Pollen percentages of selected taxa and macroscopic charcoal data from M. Casanova. Exaggeration curves depict 3* taxa percentages.

most taxa (terrestrial rates of change $>0.003\% \text{ yr}^{-1}$). Overall, *Podocarpus* and *N. dombeyi*-type declined to $>3.4\%$ and $>26.8\%$, respectively, while Cupressaceae ($<29.3\%$), Poaceae ($<22.6\%$), Apiaceae ($<9.8\%$), and Other grassland taxa ($<7\%$) increased. This pollen assemblage compares well with modern samples from the forest/grassland ecotone found in the wet Chonos archipelago in westernmost Patagonia ($44\text{--}47^\circ\text{S}$; Haberle and Bennett, 2001). CHAR ($0\text{--}6.4 \text{ particles cm}^{-2} \text{ yr}^{-2}$), pollen of Caryophyllaceae ($<5\%$), Cyperaceae ($<3\%$), *Myriophyllum* ($<21\%$), and *Triglochin* ($<3\%$), terrestrial rates of change, and aquatic SCDs reached their highest Holocene values. Fire-episode frequency increased to Zone 1 levels ($4.8 \text{ fire episodes } 1,000 \text{ yr}^{-1}$).

DISCUSSION AND CONCLUSIONS

Vegetation and Fire History of West-Central Patagonia

During the Last Glacial Maximum (LGM; $23,000\text{--}19,000 \text{ cal yr BP}$), sea-surface temperatures off the coast of Chile were $\sim 6^\circ\text{C}$ lower than at present (Lamy et al., 2004; Kaiser et al., 2007). Reconstructions of glacier extent suggest that the North and South Patagonian icefields along with their outlet glaciers coalesced to form a $>1200\text{-m}$ -thick ice sheet (Caldenius, 1932; Glasser et al., 2008; $\sim 38\text{--}56^\circ$). Rapid thinning of the ice sheet at $17,500 \text{ cal yr BP}$ was associated with changes in atmospheric circulation and regional warming, and resulted in ice-free conditions in the study area by $15,000 \text{ cal yr BP}$ (Hulton et al., 2002; Boex et al., 2013).

As the glaciers retreated, deep glacially-carved valleys filled with a system of lakes. Present-day Lake General Carrera/Lake Buenos Aires and Lake Cochrane/Lake Pueyrredón (Figure 1) are the remnants of a glacial lake that extended between 46 and 48°S . Dammed in the west by the icefields and mountains, the glacial lakes drained into the Atlantic Ocean (Clapperton, 1993).

Between $12,800$ and $8,000 \text{ cal yr BP}$, the water breached the ice dam resulting in a regional drainage reversal toward the west. The watershed of the Baker River, where M. Casanova is located, adopted its modern configuration at this time (Turner et al., 2005; Bell, 2008).

In late-glacial times ($17,500\text{--}10,000 \text{ cal yr BP}$), rising winter and annual insolation coupled with changes in atmospheric circulation led to increasingly higher temperatures in Antarctica (Figure 4A) and southern South America, forcing a poleward shift of the Southern Westerlies to a position south of the study region (Rojas et al., 2009). This trend toward warmer conditions and longer growing seasons peaked in the early Holocene and favored the expansion of tree populations throughout western Patagonia (Moreno, 2004; Iglesias et al., 2016a). Initial tree expansion was time transgressive, occurring as early as $16,500 \text{ cal yr BP}$ at 41°S (Whitlock et al., 2006), at $15,000$ at $44\text{--}45^\circ\text{S}$ (Haberle and Bennett, 2004; Massaferro et al., 2005), at $12,500$ at 46°S (Lumley and Switsur, 1993), and not until $7,000 \text{ cal yr BP}$ at 52°S (Markgraf and Huber, 2010). This north-to-south pattern represents a response to changes in effective moisture associated with warming and a southward shift of the westerly storm tracks (Iglesias et al., 2016a). It is possible that poorly developed soils and the presence of ice in high-elevation valleys (Aniya, 2013) were contributing factors to the late colonization of areas adjacent to the Patagonian icefields.

Pollen data from Lake Augusta (Villa-Martínez et al., 2012) and Lake Edita (Henríquez et al., 2016) located on the eastern flanks of the Andes at 47°S (Figure 1) indicate that expansion of *Nothofagus* began with ice recession and continued until $9,000 \text{ cal yr BP}$. At M. Casanova, *Nothofagus* (possibly *N. betuloides*) and Cupressaceae (likely *Pilgerodendron*) dominated mountain slopes before $8,480 \text{ cal yr BP}$ (Figure 3). Deposition of fine clay and low percentages of aquatic pollen and spore percentages ($<0.7\%$) suggest the presence of open water.

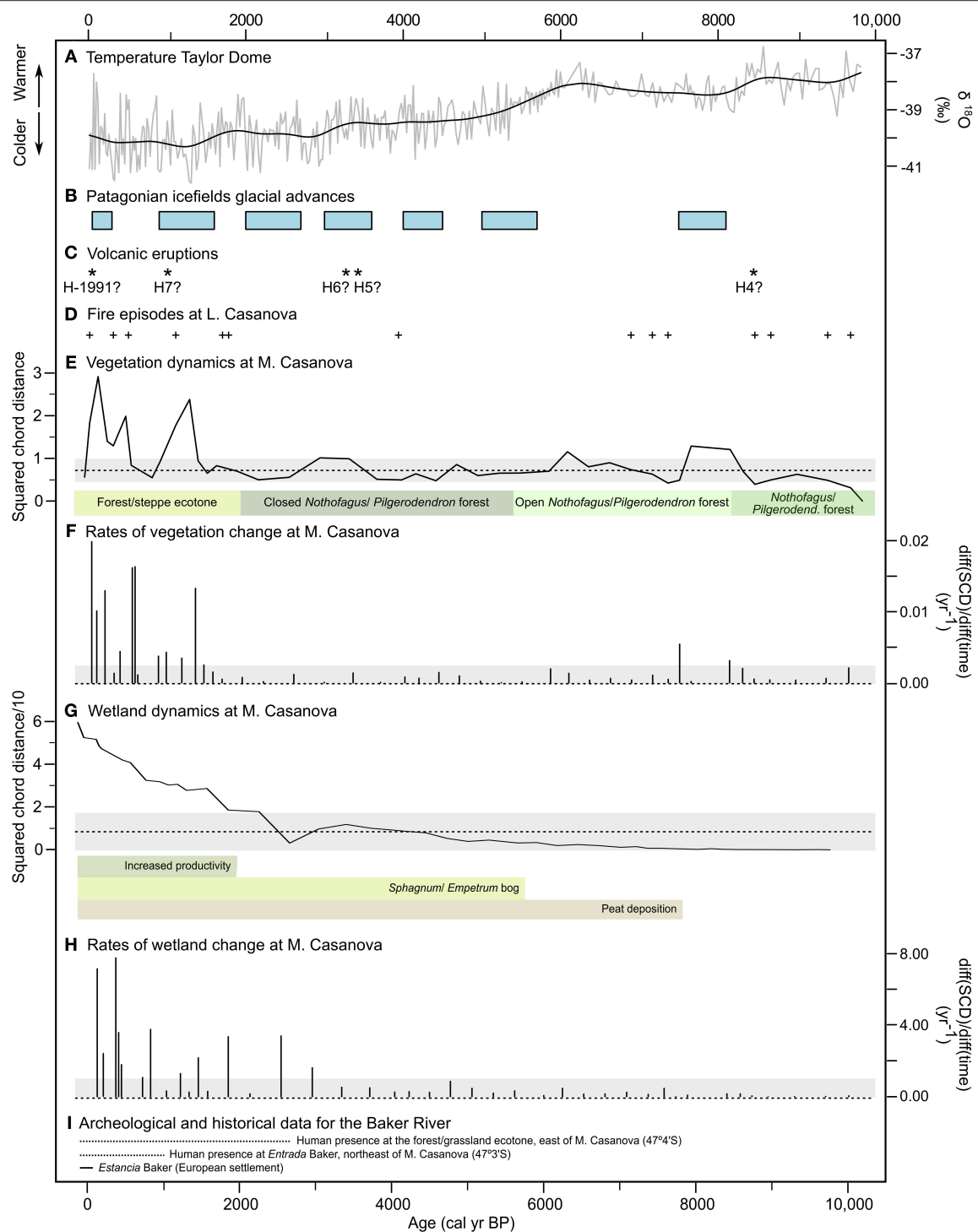
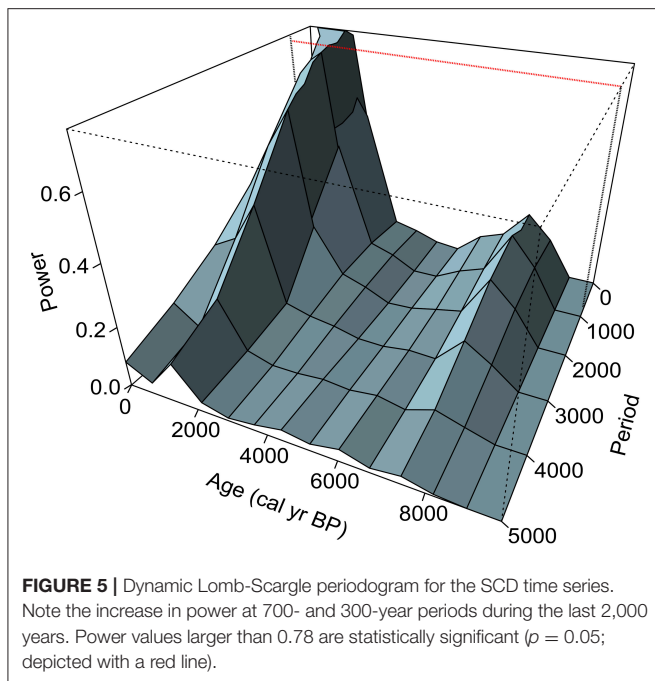


FIGURE 4 | (A) $\delta^{18}\text{O}$ record from Taylor Dome (Groote et al., 1993). **(B)** Holocene glacial advances of the Patagonian icefields (Aniya, 2013). **(C)** Possible events of tephra deposition associated with known eruptions of the Hudson volcano. **(D)** Reconstructed fire episodes from M. Casanova charcoal data. Long-term dynamics in **(E)** vegetation and **(G)** wetland composition as inferred from the squared chord distance (SCD) between every pollen sample and the first sample of the record. The median Holocene SCDs (dashed line) and their confidence intervals (gray shading) are shown. Pollen zones and wetland characteristics (as interpreted from changes in lithology, sedimentation rates, magnetic susceptibility, and the presence/absence of *Sphagnum* spores) are indicated. Estimated rates of change in **(F)** vegetation and **(H)** wetland composition inferred from pollen data. Confidence intervals for 0 yr^{-1} (i.e., no change) are depicted in gray. **(I)** Archeological and historical information for the study area (Martinic, 1977; Mena and Jackson, 1991; Fuentes-Mucherl et al., 2012).



Fire frequencies declined from 4.8 episodes $1,000 \text{ yr}^{-1}$ at 9,840 cal yr BP to 1.7 episodes $1,000 \text{ yr}^{-1}$ at 8,500 cal yr BP (Figure 3). Frequent fires prior to 9,000 cal yr BP are consistent with charcoal records throughout western Patagonia. Frequent burning at the time is attributed to increasing fuel loads coupled with an early onset of the fire season and higher probability of lightning (Haberle and Bennett, 2004; Moreno, 2004; Whitlock et al., 2007; de Porras et al., 2012; Villa-Martínez et al., 2012; Markgraf et al., 2013; Iglesias and Whitlock, 2014). Although it is possible that anthropogenic ignitions were an additional cause of fire, these early-Holocene fire episodes pre-date archeological evidence of humans in the study area.

Between 8,480 and 5,630 cal yr BP, vegetation continued to be dominated by *Nothofagus* forest. Higher-than-before pollen percentages of *Maytenus* and other shrubs and herbs, however, point to a more diverse understory and/or forest openings (Figure 3). CHAR was lower than before ($<0.15 \text{ particles cm}^{-2} \text{ yr}^{-1}$), and fire-episode frequency declined to 0.1 fire episodes $1,000 \text{ yr}^{-1}$ after reaching a maximum of 3.5 fire episodes $1,000 \text{ yr}^{-1}$ at 7,100 cal yr BP. Forest expansion and reduced fire activity have been inferred at sites on both sides of the Andes (e.g., Haberle and Bennett, 2004; Moreno, 2004; Markgraf et al., 2007; Abarzúa and Moreno, 2008; Wille and Schäbitz, 2009; de Porras et al., 2012; Iglesias et al., 2016a) in association with the onset of effectively wetter conditions during the mid-Holocene (Berger and Loutre, 1991; Liu et al., 2003).

Increasingly cooler/wetter conditions during the late Holocene (5,800 cal yr BP-present) supported advances of outlet glaciers from the Patagonian icefields (Aniya, 2013; Figure 4) and aquifer recharge in southern Patagonia (51°S ; Larson et al., 2008). At 5,630 cal yr BP, closed forest prevailed in the M. Casanova watershed, and fire activity declined sharply and

remained very low until 2,000 cal yr BP ($\text{CHAR} < 0.08 \text{ particles cm}^{-2} \text{ yr}^{-1}$). Similar trends toward closed forest and reduced fires are observed south of the study site (e.g., Villa-Martínez and Moreno, 2007; Mancini, 2009; Moreno et al., 2009; Wille and Schäbitz, 2009; Echeverría et al., 2014). These conditions contrast with steppe expansion at 44°S (de Porras et al., 2012, 2014) and may be explained by a southward shift and/or weakening of the northern margin of the Southern Westerlies, which would have prevented storm tracks—and therefore precipitation and lightning—from reaching northern Patagonia (Lamy et al., 2010).

Peat accumulation started at the coring site at 7,840 cal yr BP (Figure 2). A rapid increase of *Empetrum* pollen and *Sphagnum* spores at 5,800 cal yr BP, nonetheless, suggests that maximum development of the ombrotrophic bog did not occur until the onset of effectively more humid conditions between 5,800 and 2,000 cal yr BP (Figure 3). The rise of *Empetrum* pollen to its Holocene maximum at 3,500–2,700 cal yr BP is associated with peaks in magnetic susceptibility possibly derived from the H5 and H6 eruptions. This association suggests that *Empetrum* populations resisted the effects of tephra deposition on soil permeability and geochemistry. Low CHAR at times of *Empetrum-Sphagnum* bog expansion has also been reported in Fuego-Patagonia (50°S) during the Holocene (Huber and Markgraf, 2003). Huber et al. (2004) interpret the relationship between low fire occurrence and *Sphagnum* growth as evidence of infrequent burning of forest and bog during periods of higher effective moisture conducive to peat accumulation.

Between 2,000 and 530 cal yr BP, rising lake levels and forest expansion south of 44°S have been recorded east and west of the Andes and are attributed to higher effective moisture (Mancini, 2009; de Porras et al., 2014; Echeverría et al., 2014; Iglesias et al., 2016a). At M. Casanova, faster peat accumulation and lower-than-before magnetic susceptibility (Figure 2) suggest increased bog productivity (Figure 4). Higher effective moisture may also explain the expansion of *Podocarpus* on poorly drained fluvio-glacial deposits west of the lake or at higher elevations in the study area between 2,000 and 1,000 cal yr BP (Pérez et al., 2016; Figure 3). Rising CHAR at M. Casanova (Figure 3) is consistent with fire-history reconstructions throughout Patagonia that suggest increased biomass burning during this period (Szeicz et al., 2003; Haberle and Bennett, 2004; Villa-Martínez and Moreno, 2007; de Porras et al., 2014; Iglesias and Whitlock, 2014).

The last 530 years are characterized by changes in bog hydrology at M. Casanova, including the establishment of Caryophyllaceae, *Triglochin*, and other wetland plants, and rapid deposition of peaty sediments (Figures 2–4). The presence of submersed aquatic taxa, such as *Myriophyllum*, indicates that areas of the bog were flooded at times. High percentages of Asteraceae, Apiaceae, Amaranthaceae, and other herbaceous taxa and a decline in arboreal pollen suggest a loss of forest cover in recent centuries (Figure 3). Frequent fires (up to 5 fire episodes $1,000 \text{ yr}^{-1}$; Figure 3) would have favored the expansion of disturbance-adapted taxa (e.g., Amaranthaceae and herbs) at expense of less-tolerant trees. A decline of arboreal taxa in the last 500 years has also been reported north (44°S ; Haberle and Bennett, 2004; de Porras et al., 2014) and south of the study

area (50–55°S; Huber et al., 2004; Mancini, 2009). Deforestation through burning and, more recently, logging probably reduced evapotranspiration and facilitated paludification (Holz and Veblen, 2011).

Effects of Climate, Disturbance, and Human Impact on Ecosystem Stability

Paleoenvironmental data from L. Augusta (47°S) suggest that *Nothofagus* forests prevailed relatively unchanged in the watershed from the time of their establishment at ca. 9,800 cal yr BP to European arrival in the area in the twentieth century. Villa-Martínez et al. (2012) attribute this stability to the high tolerance of *N. pumilio*, the dominant tree, to changes in precipitation. The pollen record from M. Casanova shows that *Nothofagus-Pilgerodendron* forests have existed in the study area for about 9,000 years despite long-term changes in climate and fire (Figure 3). Rates of change statistically equal to zero indicate that terrestrial pollen percentages did not vary significantly over the period from 9,000 to 1,400 cal yr BP (Figure 4). The temporal and taxonomic resolution of the pollen time series, however, does not allow examining whether this stability resulted from *Nothofagus*' resistance to environmental change, its rapid recovery after disturbance (i.e., resilience), or trade-offs in the *Nothofagus* species [i.e., deciduous, fire-adapted *N. antarctica* vs. deciduous, obligate-seeder, fire-sensitive *N. pumilio* vs. evergreen, obligate-seeder, fire-sensitive *N. betuloides* and *N. nitida* (Correa, 1984), all of which grow at this latitude and whose pollen cannot be differentiated].

Two periods of rapid change before 1,400 cal yr BP were identified in the terrestrial SCD series. One occurred between 8,320 and 8,150 cal yr BP, when shrub taxa, Asteroideae, herbs, and grasses expanded at the expense of *Nothofagus*. The other one took place from 7,660 to 7,510 cal yr BP as a result of a pronounced increase in *Nothofagus*, and was coeval with the start of peat accumulation in the wetland (Figure 4). A reorganization of the ecosystem toward more open vegetation occurred between these two periods of rapid change (8,150–7,660 cal yr BP) and coincided with renewed glaciation in the Patagonian icefields (Aniya, 2013; Bourgois et al., 2016), suggesting that low temperatures probably limited seedling survival. Additionally, tephra from the H4 eruption of the Hudson volcano (Figures 2, 4) may have promoted the acidification of the soils and precluded tree establishment in the study area. It is possible, however, that the change in pollen composition registered from 7,660 to 7,510 cal yr BP did not reflect changes in terrestrial vegetation but rather a shift in depositional environments (i.e., shift from fine clay to peat; Figure 2).

Charcoal times series from the Baker River watershed (i.e., Mallín Tortel [47°48'S, 73°28'W] and M. Casanova; Holz et al., 2012) show synchronous changes in fire activity in the last 7,000 years, including a pronounced rise in biomass burning at 2,000 cal yr BP. Comparison of reconstructed fire episodes at M. Casanova and the glacial record from the Patagonian icefields indicates that the probability of fire was significantly lower during times of ice advance (Table 2; Figure 4). Increased effective moisture and/or lower temperatures are likely to have

favored ice expansion and bog productivity and suppressed fire activity (Figure 4).

During the last 2,000 years, fire-episode frequency was as high as that of the early Holocene (>3 fire episodes $1,000 \text{ yr}^{-1}$), despite wetter and/or cooler conditions (Table 2; Figure 4). The large SCDs indicate that, in contrast with the early- and mid-Holocene wetland and vegetation history, the bog has been highly variable since ca. 1,800 cal yr BP, while *Nothofagus-Pilgerodendron* forests have experienced pronounced and rapid departures from the long-term median composition after ca. 1,400 cal yr BP (Figure 4). The frequency spectrum of terrestrial squared chord distances reveals statistically significant power at centennial-scales during the last 2,000 years (300-year cycles; Figure 5), indicating that changes in vegetation occurred in a quasi-periodic manner. This periodicity matches that reconstructed for late-Holocene fire episodes (Figure 3), pointing to fire-induced forest loss followed by forest recovery/fuel accumulation and renewed fire activity in ca. 300-year cycles. These shifts in local ecosystem dynamics could have been an abrupt response to human impact and/or resulted from nonlinear climate-vegetation-fire linkages.

Humans arrived in Patagonia ca. 18,500 years ago (Dillehay et al., 2015) and lived throughout the region as small, dispersed groups until 7,000 cal yr BP, when population densities increased (Pérez et al., 2016). Resource availability in highly variable ecosystems would have been unpredictable, and when combined with the greater demands from growing human populations (Pérez et al., 2016), would have motivated the use of the Baker River watershed. The increasing presence of people in the area in the last two millennia may have therefore been an adaptation strategy in response to reduced resources per capita. Higher human population densities, in turn, possibly reinforced climate-disturbance-vegetation feedbacks operating at the local scale.

Comparison of reconstructed patterns of human occupation and environmental records from the central Patagonian Andes in Chile (44°S) suggests that hunter-gatherers likely increased the probability of fire, particularly in the last 3,000 years (Méndez et al., 2016). For example, Holz and Veblen (2011) reported burning of *Pilgerodendron* stands primarily by the Kawésqar canoeing group to secure dry firewood and canoe-building material. Similarly, fires set by aboriginal peoples to hunt guanacos (*Lama guanicoe*) and rheas (*Rhea* spp.) in northern Patagonia (~41–43°S) were described by early European explorers and missionaries (Musters, 1871; Cox, 1963).

The shift in vegetation, fire activity and hydrology observed at M. Casanova after ca. 2,000 cal yr BP may therefore be partly anthropogenic. Faunal and lithic analyses from a small rock shelter in the Chacabuco Valley to the east (47°4'48"S, 72°16'20"; ca. 40 km from the study site) suggest use of the forest/grassland ecotone as early as 2,800 cal yr BP (Fuentes-Mucherl et al., 2012). Conversely, archeological evidence from the Baker River watershed shows human presence only after 1,000 cal yr BP (Mena and Jackson, 1991), and permanent settlement is not recorded until the establishment of the *Estancia* Baker by European ranchers in 1902 AD (ca. 35 km from the study site; Martinic, 1977). The late settlement record in this watershed, however, may reflect a lack of older

archeological data, rather than an absence of people before Europeans.

The possibility of human ignitions at M. Casanova does not rule out climate as a driving force of change in local ecosystem dynamics reconstructed for the last 2,000 years that include (a) high fire activity; (b) unprecedented variability in bog composition; (c) emergence of regular fluctuations in the relative abundance of trees and shrubs that seem related to post-fire regeneration; and (d) paludification in association with forest loss. Decadal- and centennial-scale climate variability in the mid- and high latitudes of Patagonia has been ascribed to the Southern Annular Mode (Moreno et al., 2014), El Niño-Southern Oscillation (Whitlock et al., 2006), and to changes in solar irradiance associated with the Vries/Suess solar cycle (Lüdecke et al., 2015). Heightened moisture variability probably favored fires, and well-drained, acidic, tephra-rich soils may have slowed the post-fire regeneration of sensitive taxa. Fire, whether natural or anthropogenic in origin, led to forest loss in the last 500 years, which, in turn, contributed to paludification. Thus, the long-term trend toward cooler, effectively wetter conditions,

combined with extreme wet and dry events and more frequent disturbance created a unique set of conditions that led to unprecedented change at M. Casanova starting at ca. 2,000 cal yr BP.

AUTHOR CONTRIBUTIONS

VI and SH: Designed research; SH and CW: Contributed reagents; VI: Counted pollen samples and analyzed data; VI, SH, AH, and CW: Interpreted results; VI: Wrote the paper; SH, AH, and CW: Edited the manuscript.

ACKNOWLEDGMENTS

This work was supported by grants from the National Science Foundation (0966472, 0956552, 0602166), the National Geographic Society (7988-06), and the Department of Archaeology and Natural History at the Australian National University. We thank Philip Roberts for counting charcoal samples.

REFERENCES

- Abarzúa, A., and Moreno, P. I. (2008). Changing fire regimes in the temperate rainforest region of southern Chile over the last 16,000 yr. *Quat. Res.* 69, 62–71. doi: 10.1016/j.yqres.2007.09.004
- Aniya, M. (2013). Holocene glaciations of Hielo Patagónico (Patagonia Icefield), South America: a brief review. *Geochem. J.* 47, 97–105. doi: 10.2343/geochemj.10171
- Barreda, V., Anzotegui, L. M., Prieto, A. R., Aceñolaza, P., Bianchi, M. M., Borromei, A. M., et al. (2007). Diversificación y cambios de las angiospermas durante el Neógeno en Argentina. *Ameghiniana* 11, 173–191.
- Bell, C. M. (2008). Punctuated drainage of an ice-dammed quaternary lake in Southern South America. *Geogr. Ann.* 90, 1–17. doi: 10.1111/j.1468-0459.2008.00330.x
- Berger, A., and Loutre, M. F. (1991). Insolation values for the climate of the last 10 million years. *Quat. Sci. Rev.* 10, 297–317. doi: 10.1016/0277-3791(91)90033-Q
- Bertrand, S., Araneda, A., Vargas, P., Jana, P., Fagel, N., and Urrutia, R. (2012). Using the N/C ratio to correct bulk Chilean Patagonia. *Quat. Geochronol.* 12, 23–29. doi: 10.1016/j.quageo.2012.06.003
- Blaauw, M., and Christen, J. A. (2011). Flexible paleoclimate age-depth models using an autoregressive gamma process. *Bayesian Anal.* 6, 457–474. doi: 10.1214/11-BA618
- Boex, J., Fogwill, C., Harrison, S., Glasser, N. F., Hein, A., Schnable, C., et al. (2013). Rapid thinning of the late Pleistocene Patagonian Ice Sheet followed migration of the Southern Westerlies. *Nat. Sci. Rep.* 3:2118. doi: 10.1038/srep02118
- Bourgeois, J., Cisternas, M. E., Braucher, R., Bourles, D., and Frutos, J. (2016). Geomorphic records along the General Carrera (Chile)-Buenos Aires (Argentina) glacial lake (46–48S), climate inferences, and glacial rebound for the past 7–9 ka. *J. Geol.* 124, 27–53. doi: 10.1086/684252
- Cabré, M. F., Solman, S., and Núñez, M. (2016). Regional climate change scenarios over southern South America for future climate (2080–2099) using the MM5 Model. Mean, interannual variability and uncertainties. *Atmósfera* 29, 35–60. doi: 10.20937/ATM.2016.29.01.04
- Caldenius, C. C. (1932). Las glaciaciones cuaternarias en la Patagonia y Tierra del Fuego. *Geografiska Annaler*, 14, 1–164 (English summary 144–157).
- Clapperton, C. M. (1993). *Quaternary Geology and Geomorphology of South America*. Amsterdam: Elsevier.
- Correa, M. E. (1984). *Flora Patagónica*. Buenos Aires: Instituto Nacional de Tecnología Agropecuaria.
- Cox, G. (1963). Viajes a las regiones septentrionales de Patagonia 1862–1863. *Anal. Univ. Chile* 23, 3–239.
- de Porras, M. E., Maldonado, A., Abarzúa, A. M., Cárdenas, M. L., Francois, J. P., Martel-Cea, A., et al. (2012). Postglacial vegetation, fire and climate dynamics at Central Chilean Patagonia (Lake Shaman, 44°S). *Quat. Sci. Rev.* 50, 71–85. doi: 10.1016/j.quascirev.2012.06.015
- de Porras, M. E., Maldonado, A., Quintana, F., Martel-Cea, A., Reyes, O., and Méndez, C. (2014). Environmental and climatic changes at central Chilean Patagonia since the Late Glacial (Mallín El Embudo, 44°S). *Clim. Past* 10, 1063–1078. doi: 10.5194/cp-10-1063-2014
- Dillehay, T. D., Ocampo, C., Saavedra, J., Sawakuchi, A. O., Vega, R. M., Pino, M., et al. (2015). New archaeological evidence for an early human presence at Monte Verde, Chile. *PLoS ONE* 10:e0141923. doi: 10.1371/journal.pone.0141923
- Dirección Meteorológica de Chile (2017). *Climatología*. Available online at: <http://www.meteochile.cl/PortalDMC-web/index.xhtml> (Accessed May 31, 2017).
- Echeverría, M. E., Sottile, G. D., Mancini, M. V., and Fontana, S. L. (2014). *Nothofagus* forest dynamics and palaeoenvironmental variations during the mid and late Holocene, in southwest Patagonia. *Holocene* 24, 957–969. doi: 10.1177/0959683614534742
- Fægri, K., and Iversen, J. (1989). *Textbook of Pollen Analysis*. London: Wiley & Sons.
- Fletcher, M., and Moreno, P. I. (2012). Have the Southern Westerlies changed in a zonally symmetric manner over the last 14,000 years? A hemisphere-wide take on a controversial problem. *Quat. Int.* 253, 32–46. doi: 10.1016/j.quaint.2011.04.042
- Fletcher, M.-S., and Thomas, I. (2007). Modern pollen-vegetation calibration relationships in western Tasmania, Australia. *Rev. Palaeobot. Palynol.* 146, 146–168. doi: 10.1016/j.revpalbo.2007.03.002
- Fuentes-Muchel, F., Mena, F., Blanco, J., and Contreras, C. (2012). Excavaciones en Alero Gianella, curso medio del valle de Chacabuco (Andes centro patagónicos). *Magallania* 40, 259–265. doi: 10.4067/S0718-22442012000200013
- Garreaud, R. D., Lopez, P., Minvielle, M., and Rojas, M. (2013). Large scale control on the Patagonian climate. *J. Clim.* 26, 215–230. doi: 10.1175/JCLI-D-12-00001.1
- Gedye, S. J., Jones, R. T., Tinner, W., Ammann, B., and Oldfield, F. (2000). The use of mineral magnetism in the reconstruction of fire history: a case study from Lago di Origgio, Swiss Alps. *Palaeogeogr. Palaeoclimatol. Palaeoecol.* 164, 101–110. doi: 10.1016/S0031-0182(00)00178-4
- Glasser, N. F., Harrison, S., Jansson, K. N., Anderson, K., and Cowley, A. (2011). Global sea-level contribution from the Patagonian Icefields since the Little Ice Age maximum. *Nat. Geosci.* 4, 303–307. doi: 10.1038/ngeo1122

- Glasser, N. F., Jansson, K. N., Harrison, S., and Kleman, J. (2008). The glacial geomorphology and Pleistocene history of South America between 38 degrees S and 56 degrees S. *Quat. Sci. Rev.* 27, 365–390. doi: 10.1016/j.quascirev.2007.11.011
- Groote, P. M., Stuiver, M., White, J. W. C., Johnsen, S. J., and Jouzel, J. (1993). Comparison of oxygen isotope records from the GISP2 and GRIP Greenland ice cores. *Nature* 366, 552–554. doi: 10.1038/366552a0
- Haberle, S. G., and Bennett, K. D. (2001). Modern pollen rain and lake mud-water interface geochemistry along environmental gradients in southern Chile. *Rev. Palaeobot. Palynol.* 117, 93–107. doi: 10.1016/S0034-6667(01)00079-3
- Haberle, S. G., and Bennett, K. D. (2004). Postglacial formation and dynamics of North Patagonian Rainforest in the Chonos Archipelago, Southern Chile. *Quat. Sci. Rev.* 23, 2433–2452. doi: 10.1016/j.quascirev.2004.03.001
- Haberle, S. G., and Lumley, S. H. (1998). Age and origin of tephra recorded in postglacial lake sediments to the west of the southern Andes, 44°S to 47°S. *J. Volcanol. Geotherm. Res.* 84, 239–256. doi: 10.1016/S0377-0273(98)00037-7
- Halsey, L. A., Vitt, D. H., and Gignac, L. D. (2000). *Sphagnum*-dominated peatlands in North America since the last glacial maximum: their occurrence and extent. *Bryologist* 103, 334–352. doi: 10.1639/0007-2745(2000)103[0334:SDPINA]2.0.CO;2
- Henríquez, W. I., Villa-Martínez, R., Vilanova, I., de Pol-Holz, R., and Moreno, P. I. (2016). The last glacial termination on the eastern flank of the Patagonian Andes (47°S). *Clim. Past* 13, 879–895. doi: 10.5194/cp-13-879-2017
- Heusser, C. J. (1971). *Pollen and Spores of Chile: Modern types of the Pteridophyta, Gymnospermae, and Angiospermae*. Tucson, AZ: University of Arizona Press.
- Heusser, C. J. (2003). *Ice Age in the Southern Andes: A Chronicle of Paleoenvironmental Events*. Amsterdam: Elsevier.
- Higuera, P. E., Brubaker, L. B., Anderson, P. M., Hu, F. S., and Brown, T. A. (2009). Vegetation mediated the impacts of postglacial climatic change on fire regimes in the south central Brooks Range, Alaska. *Ecol. Monogr.* 79, 201–219. doi: 10.1890/07-2019.1
- Hogg, A. G., Hua, Q., Blackwell, P. G., Buck, C. E., Guilderson, T. P., Heaton, T. J., et al. (2013). ShCal13 Southern Hemisphere calibration, 0–50,000 cal yr BP. *Radiocarbon* 55, 1889–1903. doi: 10.2458/azu_js_rc.55.16783
- Holz, A., Haberle, S., Veblen, T. T., De Pol-Holz, R., and Southon, J. (2012). Fire history in western Patagonia from paired tree-ring fire-scar and charcoal records. *Clim. Past* 8, 451–466. doi: 10.5194/cp-8-451-2012
- Holz, A., and Veblen, T. T. (2009). *Pilgerodendron uviferum*: the southernmost tree-ring fire recorder species. *Ecoscience* 16, 322–329. doi: 10.2980/16-3-3262
- Holz, A., and Veblen, T. T. (2011). The amplifying effects of humans on fire regimes in temperate rainforests in western Patagonia. *Palaeogeogr. Palaeoclimatol. Palaeoecol.* 311, 82–92. doi: 10.1016/j.palaeo.2011.08.008
- Holz, A., and Veblen, T. T. (2012). Wildfire activity in rainforests in western Patagonia linked to the Southern Annular Mode. *Int. J. Wildland Fire* 21, 114–126. doi: 10.1071/WF10121
- Huber, U. M., and Markgraf, V. (2003). European impact on fire regimes and vegetation dynamics at the steppe-forest ecotone of southern Patagonia. *Holocene* 13, 567–579. doi: 10.1191/0959683603hl647rp
- Huber, U. M., Markgraf, V., and Schabitz, F. (2004). Geographical and temporal trends in Late Quaternary fire history in Fuego-Patagonia, South America. *Quat. Sci. Rev.* 23, 1079–1097. doi: 10.1016/j.quascirev.2003.11.002
- Hulton, N. R. J., Purves, R. S., McCulloch, R. D., Sugden, D. E., and Bentley, M. J. (2002). The Last Glacial Maximum and deglaciation in southern South America. *Quat. Sci. Rev.* 21, 233–241. doi: 10.1016/S0277-3791(01)00103-2
- Iglesias, V., Markgraf, V., and Whitlock, C. (2016a). 17,000 years of vegetation, fire and climate change in the eastern foothills of the Andes (lat. 44°S). *Palaeogeogr. Palaeoclimatol. Palaeoecol.* 457, 195–208. doi: 10.1016/j.palaeo.2016.06.008
- Iglesias, V., Quintana, F., Nanavati, W., and Whitlock, C. (2016b). Interpreting modern and fossil pollen data along a steep environmental gradient in northern Patagonia. *Sage* 27, 1008–1018. doi: 10.1177/0959683616678467
- Iglesias, V., and Whitlock, C. (2014). Fire responses to postglacial climate change and human impact in northern Patagonia (41–43°S). *Proc. Natl. Acad. Sci. U.S.A.* 111, E5545–E5554. doi: 10.1073/pnas.1410443111
- Iglesias, V., Whitlock, C., Markgraf, V., and Bianchi, M. M. (2014). Postglacial history of the Patagonian forest/steppe ecotone (41–43°S). *Quat. Sci. Rev.* 94, 120–135. doi: 10.1016/j.quascirev.2014.04.014
- Janssen, C. R. (1973). “Local and regional pollen deposition,” in *Quaternary Plant Ecology*, eds H. J. P. Birks and R. G. West (New York, NY: Wiley & Sons), 31–42.
- Kaiser, J., Lamy, F., Arz, H. W., and Hebbeln, D. (2007). Dynamics of the millennial-scale sea surface temperature and Patagonian Ice Sheet fluctuations in southern Chile during the last 70 kyr (ODP Site 1233). *Quat. Int.* 161, 77–89. doi: 10.1016/j.quaint.2006.10.024
- Lamy, F., Kaiser, J., Ninnemann, U., Hebbeln, D., Arz, H. W., and Stoner, J. (2004). Antarctic Timing of Surface Water Changes off Chile and Patagonian Ice Sheet Response. *Science* 304, 1959–1962. doi: 10.1126/science.1097863
- Lamy, F., Kilian, R., Arz, H., Francois, J. P., Kaiser, J., Prangem, M., et al. (2010). Holocene changes in the positions and intensity of the southern westerly wind belt. *Nat. Geosci.* 3, 695–699. doi: 10.1038/ngeo959
- Larson, S. A., Moy, C. M., Dunbar, R. B., and Moreno, P. I. (2008). Lacustrine carbonate records of climate variability in SW Patagonia. *AGU Fall Meeting, PP41C-1466*. San Francisco.
- Liu, Z., Brady, E., and Lynch-Stieglitz, J. (2003). Global ocean response to orbital forcing in the Holocene. *Paleoceanography* 18, 1041–1060. doi: 10.1029/2002PA000819
- Lüdecke, H.-J., Weiss, C. O., and Hempelmamm, A. (2015). Paleoclimate forcing by the solar DeVries/Suess cycle. *Clim. Past Discuss.* 11, 279–305. doi: 10.5194/cpd-11-279-2015
- Lumley, S. H., and Switsur, R. (1993). Late Quaternary chronology of the Taitao Peninsula, southern Chile. *J. Quat. Sci.* 8, 161–165. doi: 10.1002/jqs.3390080208
- Mancini, M. V. (2009). Holocene vegetation and climate changes from a peat pollen record of the forest-steppe ecotone, southwest of Patagonia (Argentina). *Quat. Sci. Rev.* 28, 1490–1497. doi: 10.1016/j.quascirev.2009.01.017
- Markgraf, V., and D’Antoni, H. L. (1978). *Pollen Flora of Argentina*. Tucson, AZ: University of Arizona Press.
- Markgraf, V., and Huber, U. (2010). Late and postglacial vegetation and fire history in Southern Patagonia and Tierra del Fuego. *Palaeogeogr. Palaeoclimatol. Palaeoecol.* 297, 351–366. doi: 10.1016/j.palaeo.2010.08.013
- Markgraf, V., Iglesias, V., and Whitlock, C. (2013). Late and postglacial vegetation and fire history from Cordón Serrucho Norte, northern Patagonia. *Palaeogeogr. Palaeoclimatol. Palaeoecol.* 371, 109–118. doi: 10.1016/j.palaeo.2012.12.023
- Markgraf, V., Whitlock, C., Haberle, S. (2007). Vegetation and fire history during the last 18,000 cal yr B.P. in Southern Patagonia: Mallin Pollux, Coyhaique, Province Aisen (45°41’30” S, 71°50’30” W, 640 m elevation). *Palaeogeogr. Palaeoclimatol. Palaeoecol.* 254, 492–507. doi: 10.1016/j.palaeo.2007.07.008
- Martinic, M. B. (1977). Ocupación y colonización de la Región Septentrional del Antiguo Territorio de Magallanes, entre los paralelos 47° y 49 Sur. *Anales del Instituto Patagónico* 8, 5–57.
- Massaferro, J., Brooks, S. J., and Haberle, S. G. (2005). The dynamics of chironomid assemblages and vegetation during the Late Quaternary at Laguna Facil, Chonos Archipelago, southern Chile. *Quat. Sci. Rev.* 24, 2510–2522. doi: 10.1016/j.quascirev.2005.03.010
- Mena, F., and Jackson, D. (1991). Tecnología y subsistencia en el alero entrada Baker, región de Aisen, Chile. *Anales del Instituto Patagónico Serrano de Ciencias Sociales* 20, 169–204.
- Méndez, C., de Porras, M. E., Maldonado, A., Reyes, O., Nuevo Delaunay, A., and García, J.-L. (2016). Human effects in Holocene fire dynamics of central western Patagonia (~44°S, Chile). *Front. Ecol. Evol.* 4:100. doi: 10.3389/fevo.2016.00100
- Moreno, P. I. (2004). Millennial-scale climate variability in northwest Patagonia over the last 15,000 yr. *J. Quat. Sci.* 19, 35–47. doi: 10.1002/jqs.813
- Moreno, P. I., François, J. P., Villa-Martínez, R. P., and Moy, C. M. (2009). Millennial-scale variability in Southern Hemisphere westerly wind activity over the last 5000 years in SW Patagonia. *Quat. Sci. Rev.* 28, 25–38. doi: 10.1016/j.quascirev.2008.10.009
- Moreno, P. I., Vilanova, I., Villa-Martínez, R., Garreaud, R. D., Rojas, M., and De Pol-Holz, R. (2014). Southern Annular Mode-like changes in southwestern Patagonia at centennial timescales over the last three millennia. *Nat. Commun.* 5:4375. doi: 10.1038/ncomms5375
- Musters, G. C. (1871). *At Home with the Patagonians: A Year’s Wanderings over Untrodden Ground from the Straits of Magellan to the Río Negro*. London: Murray.
- Niemeyer, H. R., Skarmeta, J. M., Fuenzalida, R. P., and Espinosa, W. N. (1984). *Hojas Peninsula de Taitao y Puerto Aisen, Región Aisen del General Carlos Ibañez del Campo*. Santiago: Servicio Nacional de Minería.

- Pastorino, M., and Gallo, L. (2002). Quaternary evolutionary history of *Austrocedrus chilensis*, a cypress native to the Andean Patagonian forest. *J. Biogeogr.* 29, 1167–1178. doi: 10.1046/j.1365-2699.2002.00731.x
- Pérez, S. I., Postillone, M. B., Rindel, D., Gobbo, D., Gonzalez, P. N., and Bernal, V. (2016). Peopling time, spatial occupation and demography of the Late Pleistocene-Holocene human population from Patagonia. *Quat. Int.* 425, 214–223. doi: 10.1016/j.quaint.2016.05.004
- Press, W. H., and Rybicki, G. B. (1989). Fast algorithm for spectral analysis of unevenly sampled data. *Astrophys. J.* 388, 277–280. doi: 10.1086/167197
- R Core Team (2015). *R: A Language and Environment for Statistical Computing*. Vienna: R Foundation for Statistical Computing.
- Rojas, M., Pi, M., Kageyama, M., Crucifix, M., Hewitt, C., Abe-Ouchi, A., et al. (2009). The southern westerlies during the last glacial maximum in PMIP2 simulations. *Clim. Dyn.* 32, 525–548. doi: 10.1007/s00382-008-0421-7
- Schnurrenberger, D. B., Kelts, K. R., Johnson, T. C., Shane, L. C. K., and Ito, E. (2001). National lacustrine core repository (LacCore). *J. Paleolimnol.* 25, 123–127. doi: 10.1023/A:1008171027125
- Sernageomin (2002). *Carta Geológica de Chile, N°75, Escala: 1,000,000, Hoja 3*. Servicio Nacional de Geología y Minería, Subdirección Nacional de Geología, Chile.
- Stern, C. R., Moreno, P. I., Henríquez, W. I., Villa-Martínez, R., Sagredo, E., Aravena, J. C., et al. (2016). Holocene tephrochronology around Cochrane (~47°S), southern Chile. *Andean Geol.* 43, 1–19. doi: 10.5027/andgeoV43n1-a01
- Szeicz, J. M., Haberle, S. G., and Bennett, K. D. (2003). Dynamics of north Patagonian rainforests from fine-resolution pollen, charcoal and tree-ring analysis, Chonos Archipelago, southern Chile. *Austral Ecol.* 28, 413–422. doi: 10.1046/j.1442-9993.2003.01299.x
- Turner, K. J., Fogwill, C. J., McCulloch, R. D., and Sugden, D. E. (2005). Deglaciation of the eastern flank of the North Patagonian Icefield and associated continental-scale lake diversions. *Geogr. Ann.* 87, 363–374. doi: 10.1111/j.0435-3676.2005.00263.x
- Veblen, T. T., Holz, A., Paritsis, J., Raffaele, E., Kitzberger, T., and Blackhall, M. (2011). Adapting to global environmental change in Patagonia: what role for disturbance ecology? *Austral. Ecol.* 36, 891–903. doi: 10.1111/j.1442-9993.2010.02236.x
- Villalba, R., Lara, A., Boninsegna, J. A., Masiokas, M., Delgado, S., Aravena, J. C., et al. (2003). Large-scale temperature changes across the southern Andes: 20th century variations in the context of the past 400 years. *Clim. Change* 59, 177–232. doi: 10.1023/A:1024452701153
- Villa-Martínez, R., Moreno, P. I., and Valenzuela, M. A. (2012). Deglacial and postglacial vegetation changes on the eastern slopes of the central Patagonian Andes (47 degrees S). *Quat. Sci. Rev.* 32, 86–99. doi: 10.1016/j.quascirev.2011.11.008
- Villa-Martínez, R. P., and Moreno, P. I. (2007). Pollen evidence for variations in the southern margin of the westerly winds in SW Patagonia over the last 12,600 years. *Quat. Res.* 68, 400–409. doi: 10.1016/j.yqres.2007.07.003
- Whitlock, C., Bianchi, M. M., Bartlein, P. J., Markgraf, V., Marlon, J., Walsh, M., et al. (2006). Postglacial vegetation, climate, and fire history along the east side of the Andes (lat. 41–42.5° S), Argentina. *Quat. Res.* 66, 187–201. doi: 10.1016/j.yqres.2006.04.004
- Whitlock, C., and Larsen, C. P. S. (2001). “Charcoal as a fire proxy,” in *Tracking Environmental Change Using Lake Sediments: Terrestrial, Algal, and Siliceous indicators*, Vol. 3, eds J. P. Smol, H. J. P. Birks and W. M. Last (Dordrecht: Kluwer Academic Publishers), 75–97.
- Whitlock, C., Moreno, P. I., and Bartlein, P. J. (2007). Climatic controls of Holocene fire patterns in southern South America. *Quat. Res.* 68, 28–36. doi: 10.1016/j.yqres.2007.01.012
- Wille, M., and Schäbitz, F. (2009). Late-glacial and Holocene climate dynamics at the steppe/forest ecotone in southernmost Patagonia, Argentina: the pollen record from a fen near Brazo Sur, Lago Argentino. *Veg. Hist. Archaeobot.* 18, 225–234. doi: 10.1007/s00334-008-0194-2

Conflict of Interest Statement: The authors declare that the research was conducted in the absence of any commercial or financial relationships that could be construed as a potential conflict of interest.

Copyright © 2018 Iglesias, Haberle, Holz and Whitlock. This is an open-access article distributed under the terms of the Creative Commons Attribution License (CC BY). The use, distribution or reproduction in other forums is permitted, provided the original author(s) and the copyright owner are credited and that the original publication in this journal is cited, in accordance with accepted academic practice. No use, distribution or reproduction is permitted which does not comply with these terms.



Environmental Drivers of Holocene Forest Development in the Middle Atlas, Morocco

Jennifer F. E. Campbell¹, William J. Fletcher^{1*}, Sebastien Joannin², Philip D. Hughes¹, Mustapha Rhanem³ and Christoph Zielhofer⁴

¹ Department of Geography, School of Environment, Education and Development, University of Manchester, Manchester, United Kingdom, ² Institut des Sciences de l'Évolution de Montpellier, UMR 5554 Centre National de la Recherche Scientifique, Montpellier University, Montpellier, France, ³ Unité de Botanique et Écologie Montagnarde, Faculté des Sciences, Département de Biologie, Moulay Ismail University, Meknès, Morocco, ⁴ Institute of Geography, Leipzig University, Leipzig, Germany

OPEN ACCESS

Edited by:

Thomas Giesecke,
University of Göttingen, Germany

Reviewed by:

Henry Lamb,
Aberystwyth University,
United Kingdom
Cesar Morales Del Molino,
Université de Bordeaux, France

*Correspondence:

William J. Fletcher
will.fletcher@manchester.ac.uk

Specialty section:

This article was submitted to
Paleoecology,
a section of the journal
Frontiers in Ecology and Evolution

Received: 27 July 2017

Accepted: 07 September 2017

Published: 27 September 2017

Citation:

Campbell JFE, Fletcher WJ, Joannin S, Hughes PD, Rhanem M and Zielhofer C (2017) Environmental Drivers of Holocene Forest Development in the Middle Atlas, Morocco. *Front. Ecol. Evol.* 5:113. doi: 10.3389/fevo.2017.00113

In semi-arid regions subject to rising temperatures and drought, palaeoecological insights into past vegetation dynamics under a range of boundary conditions are needed to develop our understanding of environmental responses to climatic changes. Here, we present a new high-resolution record of vegetation history and fire activity spanning the last 12,000 years from Lake Sidi Ali in the southern Middle Atlas Mountains, Morocco. The record is underpinned by a robust AMS radiocarbon and ²¹⁰Pb/¹³⁷Cs chronology and multi-proxy approach allowing direct comparison of vegetation, hydroclimate, and catchment tracers. The record reveals the persistence of steppic landscapes until 10,340 cal yr BP, prevailing sclerophyll woodland with evergreen *Quercus* until 6,300 cal yr BP, predominance of montane conifers (*Cedrus* and Cupressaceae) until 1,300 cal yr BP with *matorralization* and increased fire activity from 4,320 cal yr BP, and major reduction of forest cover after 1,300 cal yr BP. Detailed comparisons between the pollen record of Lake Sidi Ali (2,080 m a.s.l.) and previously published data from nearby Tigalmamine (1,626 m a.s.l.) highlight common patterns of vegetation change in response to Holocene climatic and anthropogenic drivers, as well as local differences relating to elevation and bioclimate contrasts between the sites. Variability in evergreen *Quercus* and *Cedrus* at both sites supports a Holocene summer temperature maximum between 9,000 and 7,000 cal yr BP in contrast with previous large-scale pollen-based climate reconstructions, and furthermore indicates pervasive millennial temperature variability. Millennial-scale cooling episodes are inferred from *Cedrus* expansion around 10,200, 8,200, 6,100, 4,500, 3,000, and 1,700 cal yr BP, and during the Little Ice Age (400 cal yr BP). A two-part trajectory of Late Holocene forest decline is evident, with gradual decline from 4,320 cal yr BP linked to synergism between pastoralism, increased fire and low winter rainfall, and a marked reduction from 1,300 cal yr BP, attributed to intensification of human activity around the Early Muslim conquest of Morocco. This trajectory, however, does not mask vegetation responses to millennial climate variability. The findings reveal the sensitive response of Middle Atlas forests to rapid climate changes and underscore the exposure of the montane forest ecosystems to future warming.

Keywords: palynology, vegetation history, Northwest Africa, Lake Sidi Ali, Tigalmamine, millennial-scale variability, microcharcoal, fire history

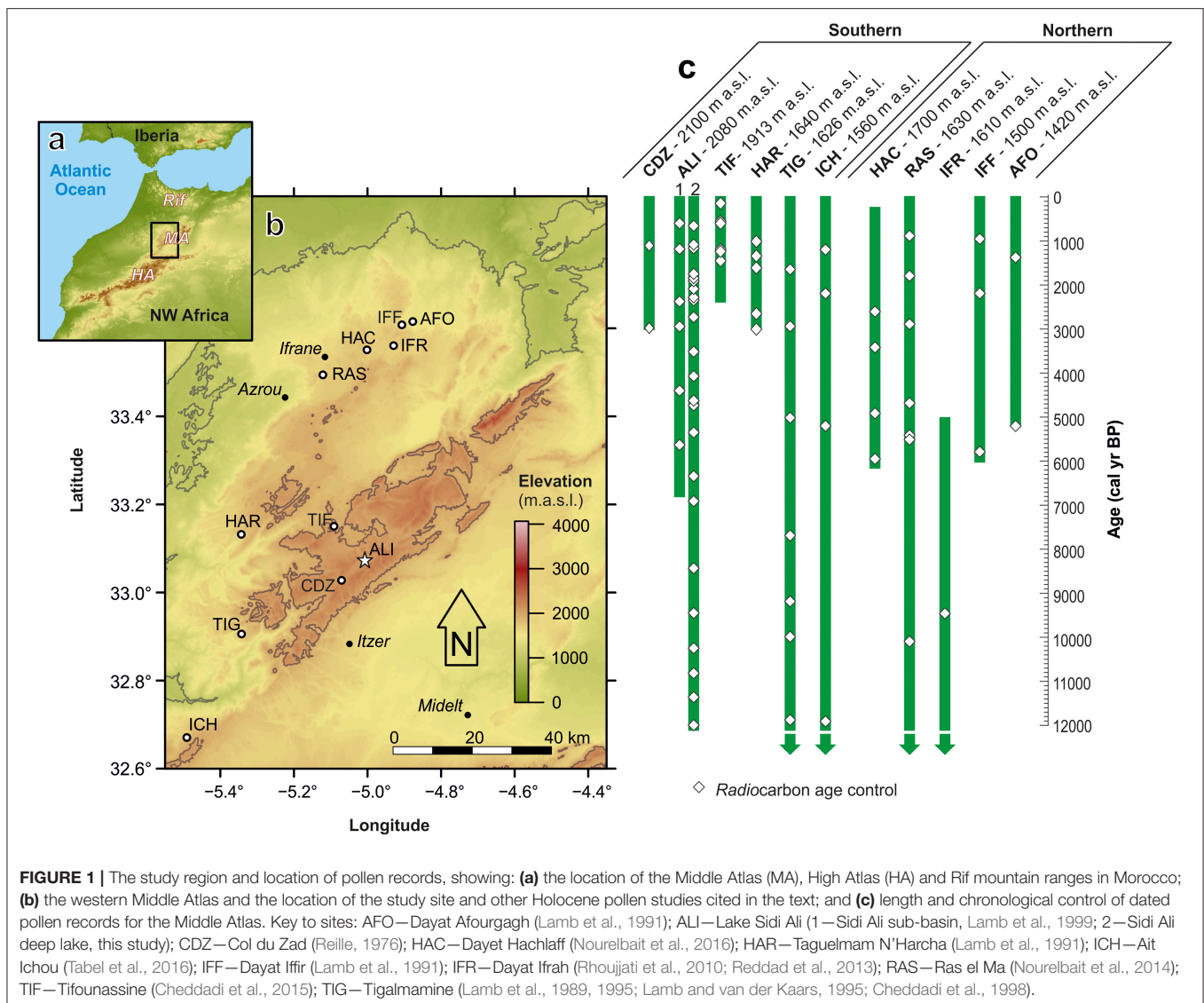
INTRODUCTION

Background and Rationale

Northwest Africa is a key region for exploring changes in forest vegetation cover and composition in response to past climate changes. Future climate change projections highlight the exposure of Northwest Africa to increased heat and drought stress (Born et al., 2008; Diffenbaugh and Scherer, 2011; Lelieveld et al., 2016). This exposure underlines the need for understanding the resilience of keystone forest species such as *Cedrus atlantica* and the ecosystem functions they support (e.g., nutrient cycling, carbon sequestration, reducing soil erosion) in the face of global change (Parmesan, 2006; Dawson et al., 2011; Moritz and Agudo, 2013). The biological and bioclimatic diversity of the region, particularly as contained within the Atlas mountain ranges (Ozenda, 1975; Medail and Quezel, 1997), furthermore provides a valuable “test-bed” for understanding the wider response of

Mediterranean and semi-arid environments and ecosystems to climatic perturbations.

The Middle Atlas range in Morocco presents a diversity of perennial and seasonal wetlands suitable for palaeoecological analysis and represents a focal area of current research investigation. Pioneering palynological investigations at Col du Zad (Reille, 1976) yielded the first insights into past changes in the vegetation cover of the Middle Atlas (**Figure 1**), including fluctuations in the local population of *Cedrus atlantica* during the last ca 3,000 calendar years before present (cal yr BP). Studies at Tigalmamine on a marginal core (Lamb et al., 1989) and deep lake core (Lamb and van der Kaars, 1995) contributed the first well constrained environmental reconstructions spanning the full Holocene, and highlighted a Holocene succession of environmental changes at the site including an Early Holocene transition from grasslands to evergreen *Quercus* forest and the subsequent Late Holocene establishment of *Cedrus*. The studies also supported fundamental insights into palaeoclimatic linkages



between Northwest Africa and the Atlantic region, linking lake-level lowering in the Middle Atlas with North Atlantic cooling events (Lamb et al., 1995). Alongside palaeoclimatic insights, key information emerged about the scale and nature of human impacts, through the complementary study of Holocene deposits at Taguelmam N'Harcha, Dayat Iffir, and Dayat Afoughagh (Lamb et al., 1991). The studies indicate a history of low intensity human impact on the Middle Atlas landscape during the last five millennia, intensification of impacts around 2,000 cal yr BP and a significant reduction of *Cedrus* populations at Taguelmam N'Harcha at 1,400 cal yr BP. A 7,000 cal yr record from Lake Sidi Ali (Lamb et al., 1999) adopted a multiproxy approach and examined interactions between climate, catchment processes and lake status associated with the transition from evergreen *Quercus*- to *Cedrus*-dominated forest and subsequent forest decline during the last 3,000 cal yr.

The Middle Atlas has recently experienced a resurgence of palaeoecological activity, including contributions to the understanding of longer term environmental change since the last glacial including past fire activity at Lake Ifrah (Rhoujjati et al., 2010; Reddad et al., 2013), although the core does not include the last 5,000 years. Recent studies have contributed further knowledge regarding patterns and processes of Holocene vegetation change in the northwestern Middle Atlas at Ras el Ma and Dayat Hachlaf (Nourelbait et al., 2014, 2016; Tabel et al., 2016), and forthcoming data for the Holocene are indicated for Lake Tifounassine (Cheddadi et al., 2015). At Dayat Hachlaf, forested conditions with *Quercus* (undifferentiated) and *Pinus* are recorded throughout the record from 6,000 cal yr BP, and include a shift in forest composition around 3,500 cal yr BP, with the expansion of *Cedrus* (Nourelbait et al., 2016). In contrast, the nearby record of Ras el Ma documents a late development of forest with *Quercus* and *Cedrus* only after 5,000 cal yr BP (Nourelbait et al., 2014). In the southwestern Middle Atlas, the pollen record of Ait Ichou documents the transition from steppic to forested vegetation at 6,800 cal yr BP (Tabel et al., 2016). Comparison of Late Holocene records from the Middle Atlas and Rif support similar trajectories of increasing human impact during the last 2,000 years (Cheddadi et al., 2015). Overall, the growing number of studies from the Middle Atlas highlight important spatial and temporal variability in the patterns of forest development, and point to multiple drivers of environmental change (climate, human activity, fire).

In light of the available information, key research areas regarding the dynamics of montane vegetation in the Middle Atlas require further investigation and are highly relevant in the context of future climate change. These include:

- (i) The nature and timing of vegetation changes during the Holocene, including spatial and altitudinal patterns in the forest cover and composition;
- (ii) The exposure of forest ecosystems to long-term and rapid climate changes of the Holocene (e.g., Mayewski et al., 2004) and/or resilience in the face of climatic perturbation (Aranbarri et al., 2014);

- (iii) The spatiotemporal characteristics of Holocene fire regimes and the role of fire as an agent of Holocene vegetation change;
- (iv) The role of human agency in Holocene land cover changes, the resilience of the natural vegetation cover, and human-environment interactions (Blondel, 2006).

Ultimately, robust exploration of these research areas requires palaeoecological data with high temporal resolution (centennial-scale sampling or better), robust radiometric chronological control, and, ideally, a multi-proxy approach with co-registration of independent climate tracers in the same cores.

The focus of this study is Aguelmam (Lake) Sidi Ali. As the largest and deepest perennial lake in the Middle Atlas, the site offers great potential for addressing key regional palaeoenvironmental and palaeoclimatic questions. The first coring efforts at the site focused on a marginal sub-basin, yielding a sediment record spanning the last ca. 7,000 cal yr BP (Barker et al., 1994; Lamb et al., 1999). These previous studies reveal signals of recurrent centennial-scale water-level fluctuations in the diatom assemblages (Barker et al., 1994), and long-term catchment impacts on lake status linked to vegetation change and human impact (Lamb et al., 1999). The studies clearly highlight the merits of a multiproxy palaeolimnological approach (Birks and Birks, 2006), and also provide first indications of some of the particular challenges at Lake Sidi Ali, notably for radiocarbon dating in the hardwater karstic setting, for disentangling climate and catchment influences on the lake system, and for elucidating climatic and anthropogenic drivers of change.

New research activity at Lake Sidi Ali since 2012 has focused on drilling of the main (deep) lake basin, recovery of longer cores extending across the full Holocene, and development of a robust radiometric deposition model (Fletcher et al., 2017). Reliance on $^{210}\text{Pb}/^{137}\text{Cs}$ analysis and 26 AMS radiocarbon dates on terrestrial pollen concentrates and macrofossils circumvents the problem of hardwater errors for bulk radiocarbon dates (Fletcher et al., 2017) and underpins the high-resolution and multiproxy palaeolimnological study (Zielhofer et al., 2017a). Key findings include the detection of pervasive variability in Atlantic-derived winter precipitation, and a Mid Holocene shift in prevailing climate pattern reflecting the emergence of centennial dynamics resembling the North Atlantic Oscillation (NAO-like) after 5,000 cal yr BP (Zielhofer et al., 2017a). The main horizon of anthropogenic catchment disturbance is also constrained by geochemical and sedimentological data to 1,400 cal yr BP (Zielhofer et al., 2017a), and is supported by evidence for a relatively old, soil-derived pollen component in some dating samples (Fletcher et al., 2017). New research also reveals that Lake Sidi Ali acts as a receptor for remote (Saharan) dust, providing indications of millennial-scale fluctuations in dust mobilization across the end of the African Humid Period (Zielhofer et al., 2017b). Overall, this context provides an ideal opportunity to evaluate vegetation dynamics on a range of timescales (orbital, millennial, centennial), and to test the coupling of vegetation and hydroclimate proxies.

Here, we present a new record of vegetation and fire activity from Lake Sidi Ali in the Middle Atlas with sub-centennial resolution (60 year average), and undertake a detailed comparison with the deep lake record of Tigalmamine (Lamb and van der Kaars, 1995), the only other full Holocene pollen record in the Middle Atlas with a comparable (110 year average) sampling resolution as well as robust age control incorporating correction for hardwater errors. Specifically, we seek to address several key questions about the environmental drivers of vegetation change in the Middle Atlas. First, regarding vegetation-climate relationships, is there evidence for an Early Holocene summer temperature maximum consistent with insolation forcing and climate models (Renssen et al., 2009), or a cool Early Holocene, as suggested by large-scale pollen-based reconstructions for the Western Mediterranean (Davis et al., 2003; Mauri et al., 2015)? Is there evidence for vegetation response to millennial-scale variability in Holocene climate, as previously reported for the Western and Central Mediterranean (Fletcher et al., 2013; Jaouadi et al., 2016) but for which evidence is generally lacking in the Middle Atlas (cf. Lamb et al., 1995)? Second, regarding fire ecology in the Middle Atlas landscape, how did fire activity develop with respect to Holocene changes in climate, biomass, and human activity? Was fire activity at this high elevation site limited by fuel availability or climate (Linstädter and Zielhofer, 2010), and did constraints change through the Holocene in parallel with neighboring regions (Gil-Romera et al., 2010)? Finally, regarding the origins of the currently degraded forest landscape, was the trajectory of human impact gradual and multi-millennial (e.g., Tinner et al., 2013) or incremental, with distinct thresholds of major impact (e.g., Morales-Molino et al., 2017)? Moreover, did the transition to an anthropogenic landscape mask climate responses in the vegetation, or were impacts of pervasive Holocene climatic fluctuations and historical climate changes evident?

Study Area

The Middle Atlas range is an intracontinental fold-thrust belt that extends for around 250 km in northern Morocco along a primarily SW-NE alignment (Arbolea et al., 2004) and reaches elevations in excess of 3,300 m.a.s.l. in the eastern sector. The dominant geology of the Middle Atlas is Mesozoic limestones giving rise to significant karstification of the landscapes. A legacy of Plio-Pleistocene volcanism is also highly evident in regional landforms (De Waele and Melis, 2009). Located on one of the main regional SW-NE trending lineaments, Lake Sidi Ali (33° 03' N, 05° 00' W) is one of the largest (surface area of up to 2.8 km²), highest (2,080 m.a.s.l.) and deepest (up to 40 m water depth) lakes in the karstic uplands of the western Middle Atlas Mountains in Morocco. The lake is located within a small closed catchment (~14 km²) that reaches up to around 2,400 m.a.s.l. in elevation. The lake lies in a structural depression at the contact between Middle Jurassic limestones and Lower Jurassic dolomites. In September 2012, the lake displayed a maximum water depth of 38 m and anaerobic conditions at the hypolimnion (Zielhofer et al., 2017a). A shallow sub-basin to the SW is partly separated from the main basin by early Quaternary basalt flows. The two basins are linked when lake levels are at their highest (Lamb et al.,

1999); they are currently separated due to lake lowering trends in recent decades (Menjour et al., 2016; **Figure 2**). There are no significant surface inlet or outlet streams, and lake levels are sensitive to annual precipitation variability (Sayad et al., 2011).

Located at the southern margins of the Middle Atlas, Lake Sidi Ali is situated near the transition between the Atlantic, Mediterranean and Saharan climatic zones (Knippertz et al., 2003; Born et al., 2010). The regional climate is Mediterranean with summer drought influenced by the sub-tropical high-pressure belt and humid winters impacted by the Atlantic westerly circulation. Across the Middle Atlas, a strong NW to SE gradient of increasing aridity is evident, with high rainfall due to orographic effects at the NW margins of the Middle Atlas near Ifrane, and drying associated with subsequent Foehn effects as northwesterly air masses cross the SW-NE ridges of the Middle Atlas (Rhanem, 2009). The local climate station at Lake Sidi Ali documents a mean annual temperature of 10.3°C, mean temperature of the coldest month (January) of 2.0°C and mean temperature of the warmest month (July) of 19.7°C. A mean annual precipitation of 430 mm was recorded between 1982 and 2009, with maxima in spring (April–May) and late autumn/winter (November–December), as well as torrential summer storms associated with convection along the Atlas-Sahara margins.

The vegetation of the Middle Atlas displays a characteristic series of altitudinal vegetation levels associated with temperature and moisture availability across the thermo- to oromediterranean bioclimates (Benabid, 1982; **Figure 3**). The current forest vegetation surrounding Lake Sidi Ali corresponds to the high-altitude, semi-arid *Cedrus* series (Achhal et al., 1980) with *Cedrus atlantica* (Endl.) Manetti ex Carrière, *Quercus rotundifolia* Lam. (synonym *Quercus ilex* subsp. *ballota* (Desf.) Samp.), *Juniperus thurifera* L., *Crataegus* sp., *Acer monspessulanum* L. and *Fraxinus dimorpha* Coss. and Durieu accompanied by *Berberis* sp., *Ribes uva-crispa* L., and *Ephedra major* Host on locally rocky substrates (**Figure 3**). The forest surrounding the lake is rather sparse and degraded, and has an open character that gives way to scrub with spiny, cushion-form xerophytes (primarily Fabaceae spp.), along with an array of herbaceous taxa, including Asteraceae spp., Brassicaceae spp., *Plantago* spp., and *Rumex* spp. In common with many areas across its Maghrebian range (Linares et al., 2012), *Cedrus atlantica* trees near the site show signs of degradation (logging, grazing pressure, and cutting for firewood) and die-back (loss of foliage, crown dieback, mortality) (**Figure 4**).

Tigalmamine (32° 54' N 05° 21' W, 1,626 m a.s.l.), studied by Lamb and van der Kaars (1995) and a source of secondary data for this study, is part of a cluster of lakes located ca. 50 km to the southwest of Lake Sidi Ali and 450 m lower in elevation. The study site was 0.6 km² in area and around 16 m water depth at the date of coring, with an above ground catchment area of ~3.5 km² (Lamb and van der Kaars, 1995). Tigalmamine experiences a similar temperature regime to Lake Sidi Ali (mean 10°C, mean temperature of the coldest month (January) of 2.5°C and mean temperature of the warmest month (July) of 20°C) and significantly higher rainfall (930 mm/yr) (Cheddadi et al., 1998). The surrounding forest vegetation is characteristic of the

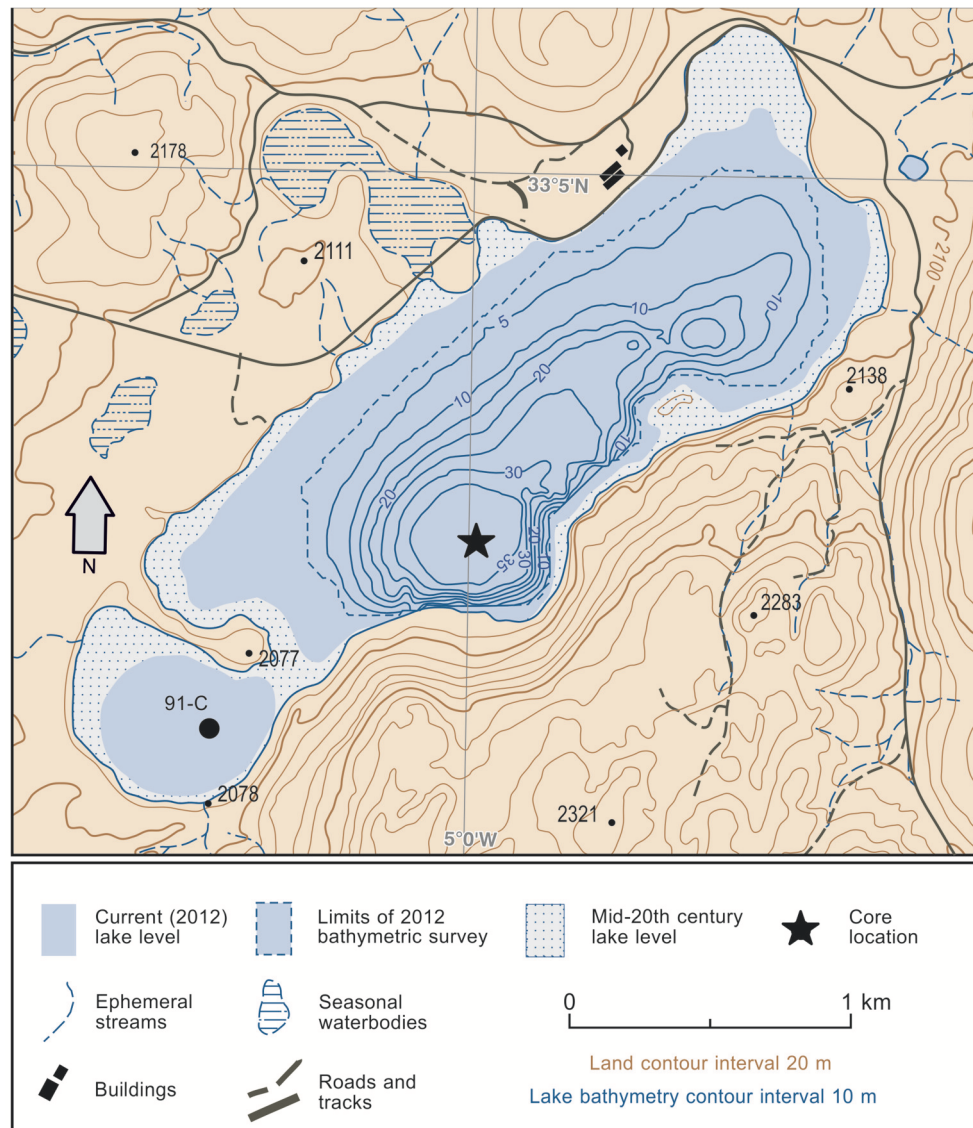


FIGURE 2 | Topographic setting and bathymetry of Lake Sidi Ali, showing the drilling position of core sequence ALI 01-10 (Zielhofer et al., 2017a and this study) and core 91-C (Barker et al., 1994; Lamb et al., 1999).

upper mediterranean level (**Figure 3**), dominated by *Quercus rotundifolia* with *Quercus canariensis* Willd. and *Cedrus atlantica* along with *Ilex aquifolium* L. and *Crataegus* spp. (Lamb et al., 1989).

MATERIALS AND METHODS

Sediment cores were recovered at Lake Sidi Ali from a floating platform located at the deepest part of the main lake basin (**Figure 2**) using a UWITEC piston corer with plastic liners. A 19.56 m core (ALI 01-10) was recovered in 10 drives from a single borehole. Careful measurement on the steel depth cable was used to control the depth of the 10 sequential drives. A core-catcher device prevents material from falling out of the

core chamber. Total depth of the borehole was determined by the capability of the equipment, and does not represent the base of the sediment infill of the lake. The reported depths represent a corrected depth scale that accounts for core expansion in the liners. Full details of the bathymetric and seismic surveys and coring procedure are given in Zielhofer et al. (2017a).

The ALI 01-10 cores comprise horizontally bedded, faintly laminated, calcareous to lime silicic gyttja without any hiatus or major sedimentological shifts (**Figure 5**). Due to rare terrestrial macrofossils in the core, a dating strategy focusing on systematic AMS radiocarbon dating of pollen concentrates was implemented (Fletcher et al., 2017). Dates on pollen concentrates ($n = 23$), terrestrial macrofossils ($n = 3$) and $^{210}\text{Pb}/^{137}\text{Cs}$

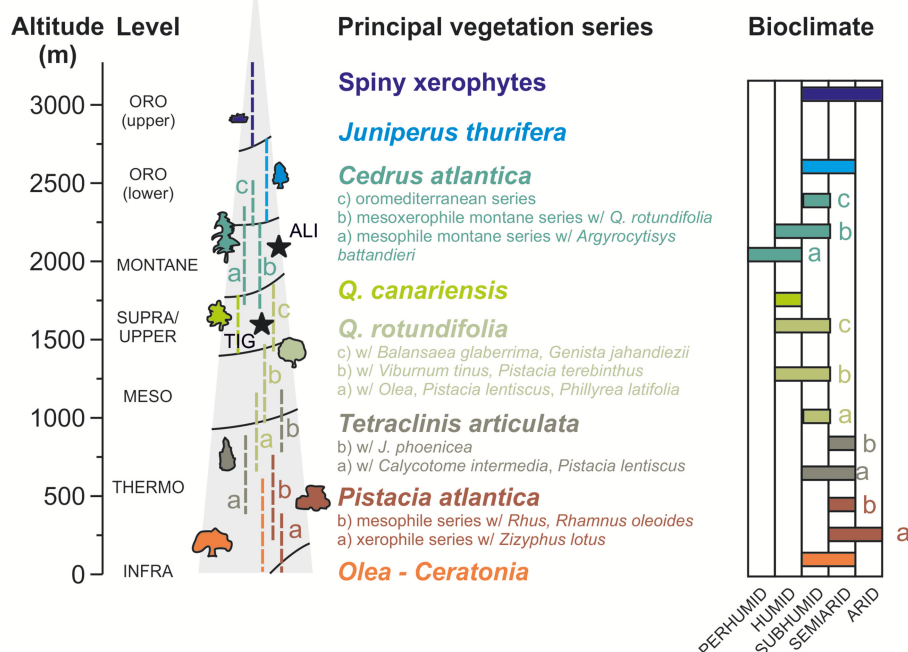


FIGURE 3 | Altitudinal distribution of the principal vegetation series of the Middle Atlas and their associated bioclimates, derived from Benabid (1982), showing the position of Lake Sidi Ali (ALI) and Tigalmamine (TIG).

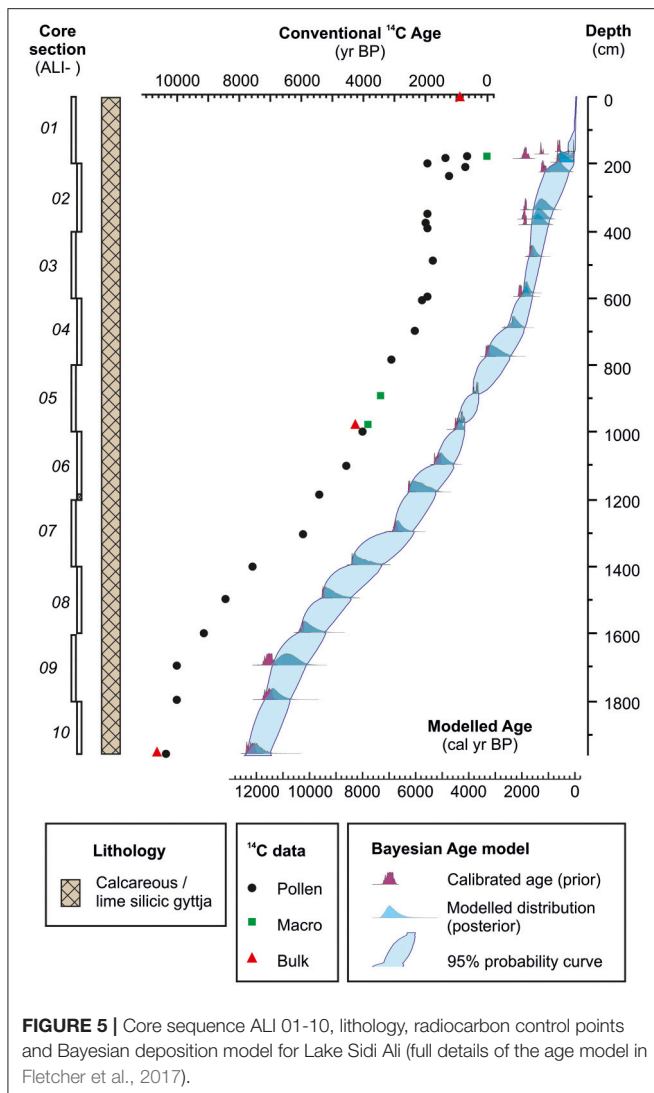


FIGURE 4 | Vegetation cover in the Lake Sidi Ali catchment in 2014. *Cedrus atlantica* trees showing signs of crown and/or branch dieback as well as dead individuals are common, interspersed with young healthy specimens of *Quercus rotundifolia*. (Credit: W. Fletcher).

constraints on the upper sediments were used to generate a realistic Poisson-process Bayesian deposition model (Bronk Ramsey, 2008; **Figure 5**). The deposition interval spans the last 12,000 cal yr BP. Long-term average sedimentation rates at this deep-lake location exceed 0.15 cm/yr (1.5 m/ka), offering great potential for high resolution proxy analysis spanning the entire Holocene.

Volumetric 1 cm³ samples were prepared for pollen analysis at regular, 10 cm intervals, yielding a total of 201 samples and an average temporal resolution of 60 years. A series of standard preparation treatments were employed, specifically: (i) addition of *Lycopodium* tablets to enable the calculation of pollen concentrations (Stockmarr, 1971); (ii) KOH digestion to remove humic acids; (iii) sieving at 180 μ m to remove coarse material; (iv) removal of siliceous material using either HF digestion or dense-media separation with sodium polytungstate (SPT); and (v) acetolysis to destroy cellulose. At stage (iv) SPT was selectively applied to improve concentration of organic material in the upper part of the sequence, following rigorous testing to ensure that no bias is imparted in terms of pollen type recovery (Campbell et al., 2016). Residues were dehydrated in alcohol and mounted using silicon oil. A minimum of 300 terrestrial grains were counted for each sample using transmitted light microscopy at high magnification (400–1,000x). Non-pollen palynomorphs (NPPs) observed during the pollen counts were recorded. Pollen taxa were identified with reference to pollen atlases and keys (Moore et al., 1991; Reille, 1992; Beug, 2004). *Lygeum spartum* is an unusual example of a single species within the Poaceae family that is easily distinguished due to its large size (longest dimension 50–70 μ m), elongated elliptical/ovoid form (length/width ratio >2) and lateral pore position (Giner et al., 2002; Abdeddaim-Boughanmi and Kaid-Harche, 2009).

Pollen percentages are calculated on the basis of a main sum of total land pollen (TLP) excluding aquatics and spores. Percentages of aquatic pollen and spores are expressed on the basis of the main sum of TLP plus the individual



pollen/spore count. Pollen assemblage zones (PAZs) are defined based on changes in the TLP percentages, with a hierarchical division of major PAZs reflecting higher order shifts in dominant taxa and sub-zones reflecting lower order fluctuations in the pollen spectra. The PAZs were determined by numerical zonation by optimal splitting by information content (Bennett, 1996) including twenty-two taxa occurring at >3% in at least one sample (*Acer*, *Apiaceae*, *Artemisia*, *Astragalus* type, *Brassicaceae*, *Caryophyllaceae*, *Cedrus*, *Chenopodiaceae*, *Coronilla* type, *Cupressaceae*, deciduous *Quercus*, *Ephedra*, evergreen *Quercus*, *Fraxinus*, *Olea*, *Phillyrea*, *Pinus*, *Pistacia*, *Plantago*, *Poaceae*, *Rumex*, *Ulex* type). Statistically significant PAZs exceeding a broken-stick model were retained (Bennett, 1996). Sub-zones were subsequently selected by eye so as to best facilitate the description of the pollen record. The arboreal/non-arboreal (AP/NAP) pollen ratio was also calculated as a proxy for forest cover that is not constrained by the limitations of closed percentage data (Magri, 1994).

In addition to pollen percentages, pollen concentration and pollen accumulation rates (PARs, expressed as grains $\text{cm}^{-2} \text{yr}^{-1}$) were calculated. PARs are a useful tool for understanding the behavior of individual taxa, while avoiding the classical problem of interdependence of percentage abundance values (Jensen et al., 2007). The PAR for each taxon is independent of other taxa within the record, and therefore may provide a better representation of the local abundance of the individual taxa (Seppä and Hicks, 2006).

Taxon-specific concentrations (X_C , expressed in grains $\cdot \text{cm}^{-3}$) were calculated as follows:

$$X_C = (N_X \cdot T_L) / (N_L \cdot V)$$

Where N_X is number of the individual taxon counted, T_L is the number of *Lycopodium* added, N_L is the number of *Lycopodium* counted, and V is the volume of the sample in cm^3 . PAR were subsequently calculated using the concentrations and sedimentation rates derived from the age-depth model:

$$X_{\text{PAR}} = X_C \times \text{SR}$$

Where X_{PAR} is the pollen accumulation rate of the taxa (expressed in grains $\cdot \text{cm}^{-2} \text{yr}^{-1}$), X_C is the concentration of the taxa (in grains $\cdot \text{cm}^{-3}$) and SR is the sedimentation rate (in $\text{cm} \cdot \text{yr}^{-1}$).

Microscopic charcoal analysis was conducted on the same slides as the pollen analysis. A sum of 200 charcoal particles and *Lycopodium* spores was counted in each sample, to reach an accurate estimate of particles for the entire sample (Finsinger and Tinner, 2005). Charcoal concentration (CHAC) and accumulation rate (CHAR) are calculated in the same way as for pollen concentration and PAR.

Comparative pollen data for the central lake core C-86 at Tigalmamine (Lamb and van der Kaars, 1995) were downloaded from the European Pollen Database (EPD, Fyfe et al., 2009). We reproduce the published age model for C-86 using linear interpolation between the seven hardwater-corrected calcite dates (see Table 1 of Lamb and van der Kaars, 1995: 402) but recalibrate the corrected radiocarbon ages using the IntCal13 calibration curve (Reimer et al., 2013). Following Lamb and van der Kaars (1995), the dates on organic material are excluded as they may be subject to hardwater errors. Select pollen curves are reproduced graphically in this study from the pollen diagram of the Sidi Ali marginal basin core C-91 (Lamb et al., 1999). We harmonize the pollen nomenclature of these works with our own, equating *Quercus rotundifolia* with evergreen *Quercus* type, *Quercus canariensis* with deciduous *Quercus* type, and Gramineae with Poaceae.

To highlight millennial-scale trends, data for select curves from Lake Sidi Ali and Tigalmamine were resampled to a regular sample spacing of 60 years and a lowpass filter was applied at 1,000 yr ($T_0/T = 0.06$) using the statistics software PAST (Hammer et al., 2001).

TABLE 1 | Definition and main characteristics of the pollen assemblage zones (PAZs) (boldface) and sub-zones for cores ALI 01–10.

PAZ	Sub-zones	Depth (cm)	Age (cal yr BP)	Age (AD/BC)	Main features	AP/NAP ratio (PAZ mean)
5		379–7	1,300–(–50)*	650 AD–2000 AD	Reduced <i>Cedrus</i>, increased <i>Artemisia</i>, <i>Poaceae</i> and <i>Plantago</i> types	1.2
	5c	138–7	30–(–50)	1920 AD–2000 AD	Increase in spiny xerophytes (<i>Astragalus</i> , <i>Coronilla</i> , <i>Ulex</i> types) and <i>Plantago</i> types	1.1
	5b	229–138	580–30	1370 AD–1920 AD	Increase in <i>Cedrus</i> , evergreen <i>Quercus</i> and <i>Olea</i> , decline in spiny xerophytes (<i>Astragalus</i> , <i>Coronilla</i> , <i>Ulex</i> types), <i>Artemisia</i> and <i>Plantago</i> types	1.3
	5a	379–229	1,300–580	650 AD–1370 AD	Decrease in <i>Cedrus</i> and Cupressaceae, increase in <i>Poaceae</i> , <i>Artemisia</i> , Chenopodiaceae and <i>Rumex</i> , peak <i>Plantago</i> types	1.1
4		993–379	4,320–1,300	4350 BC–650 AD	High abundance of Cupressaceae and <i>Cedrus</i> with evergreen and deciduous <i>Quercus</i>, rise in spiny xerophytes	2.4
	4e	556–379	1,690–1,300	260 AD–650 AD	Increase in Cupressaceae, decrease in <i>Cedrus</i>	1.9
	4d	642–556	1,990–1,690	40 BC–260 AD	Increase in <i>Cedrus</i> , decrease in Cupressaceae	2.7
	4c	757–642	2,730–1,990	780 BC–40 BC	Increase in Cupressaceae, decrease in <i>Cedrus</i>	2.3
	4b	831–757	3,280–2,730	1330 BC–780 BC	Increase in <i>Cedrus</i> , decrease in Cupressaceae	2.3
	4a	993–831	4,320–3,280	2370 BC–1330 BC	Increasing Cupressaceae, decreasing <i>Cedrus</i> , minor peak in deciduous <i>Quercus</i> , increase in spiny xerophytes (<i>Astragalus</i> , <i>Coronilla</i> , <i>Ulex</i> types), Brassicaceae and <i>Rumex</i> , decrease in <i>Poaceae</i>	2.8
3		1,260–993	6,300–4,320	4350 BC–2370 BC	High abundance of <i>Cedrus</i>, with evergreen <i>Quercus</i>, deciduous <i>Quercus</i> and <i>Poaceae</i>	2.7
	3c	1,132–993	5,280–4,320	3330 BC–2370 BC	Peak <i>Cedrus</i> , rise in deciduous <i>Quercus</i>	2.9
	3b	1,186–1,132	5,790–5,280	3840 BC–3330 BC	Decline in <i>Cedrus</i> and Cupressaceae, declining evergreen <i>Quercus</i> , increase in <i>Olea</i> and <i>Acer</i> , with <i>Phillyrea</i> and <i>Pistacia</i>	2.6
	3a	1,260–1,186	6,300–5,790	4350 BC–3840 BC	Increase in <i>Cedrus</i> and Cupressaceae, declining evergreen <i>Quercus</i> and <i>Artemisia</i>	2.3
2		1,642–1,260	10,340–6,300	8390 BC–4350 BC	High abundance of evergreen <i>Quercus</i>, <i>Poaceae</i> and declining <i>Artemisia</i>, fluctuations in <i>Cedrus</i> and Cupressaceae	1.6
	2d	1,398–1,260	7,980–6,300	6030 BC–4350 BC	Peak evergreen <i>Quercus</i> , declining <i>Artemisia</i> , with <i>Poaceae</i> , <i>Phillyrea</i> , <i>Pistacia</i> and <i>Fraxinus</i>	1.9
	2c	1,455–1,398	8,640–7,980	6690 BC–6030 BC	Peak in <i>Cedrus</i> and Cupressaceae, reduced evergreen <i>Quercus</i> and <i>Poaceae</i>	2.1
	2b	1,598–1,455	9,980–8,640	8030 BC–6690 BC	High evergreen <i>Quercus</i> , <i>Artemisia</i> and <i>Poaceae</i> , with <i>Phillyrea</i> , <i>Pistacia</i> and <i>Fraxinus</i>	1.2
	2a	1,642–1,598	10,340–9,980	8390 BC–8030 BC	Rising evergreen <i>Quercus</i> , high <i>Poaceae</i> , with peak in <i>Cedrus</i> and Cupressaceae	1.4
1		1,962–1,642	12,000–10,340	10050 BC–8390 BC	High abundance of <i>Artemisia</i>, <i>Poaceae</i>, <i>Pistacia</i>, increasing evergreen <i>Quercus</i>	0.6
	1b	1,924–1,642	11,810–10,340	9860 BC–8390 BC	High <i>Artemisia</i> and <i>Poaceae</i> , with evergreen <i>Quercus</i> , <i>Pistacia</i> , <i>Lygeum spartum</i> , and Cupressaceae	0.7
	1a	1,962–1,924	12,000–11,810	10050 BC–9860 BC	Peak <i>Artemisia</i> and <i>Poaceae</i> , with <i>Pistacia</i> , <i>Lygeum spartum</i> , and Cupressaceae	0.5

*Coretop defined as 2012 AD; uppermost sample modeled age –52.4 cal BP (2002 AD).

RESULTS

Pollen

Core ALI 01–10 contains well-preserved and abundant pollen. The dominant feature of the Holocene record is the long-term transition from herbaceous- to arboreal-dominated spectra associated with a succession of dominant pollen types (*Artemisia*, *Poaceae*, *Quercus* evergreen type, *Cedrus*, and Cupressaceae) across five major pollen assemblage zones (PAZ-1 to PAZ-5) and several sub-zones (Figure 6, Table 1). Pollen concentration

values and PARs confirm the main changes in pollen percentages throughout the record (Figure 7). Specifically, high PARs support the following sequence of dominant pollen types: *Artemisia* and *Poaceae* (PAZ-1); *Poaceae* and evergreen *Quercus*, with episodic increases in *Cedrus* and Cupressaceae (PAZ-2); *Cedrus* (PAZ-3); *Cedrus* and Cupressaceae (PAZ-4); and finally a reduction in all woody taxa (PAZ-5). Alongside terrestrial pollen, chlorophyte algae (*Botryococcus* and *Pediastrum*) are abundant in some intervals, with high values for both taxa in PAZ-1b, PAZ-2, and PAZ-3, and spikes in *Pediastrum* abundance in PAZ-5.

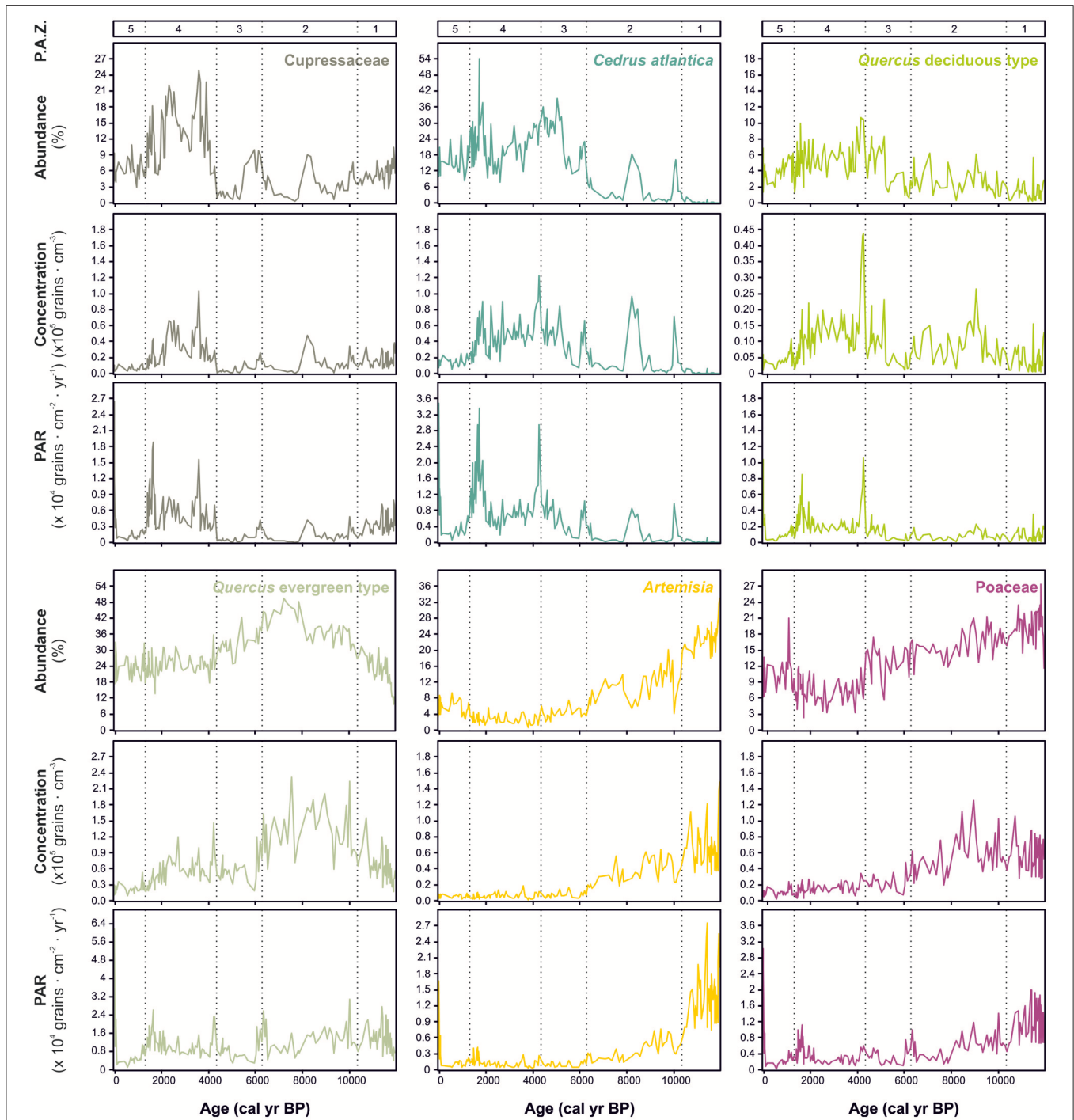


FIGURE 7 | Comparison of percentage, concentration and pollen accumulation rate (PAR) values for six main taxa at Lake Sidi Ali plotted against age with pollen assemblage zones (PAZs) indicated.

Only a modest assemblage of submerged (e.g., *Myriophyllum*) and marginal (e.g., *Typha/Sparganium*) aquatic pollen types is documented. Overall, pollen concentrations (typically $\sim 2 \times 10^5$ grains cm^{-3}) and PARs (typically around $\sim 5 \times 10^4$ grain $\text{cm}^{-2} \text{yr}^{-1}$) are high throughout the core.

Microcharcoal

Microcharcoal is recorded throughout the sequence and CHAC values vary between the PAZs, specifically: low in PAZ-1; moderate and fairly stable in PAZ-2; low in PAZ-3; high, dynamic, fluctuating in PAZ-4; low in PAZ-5, excluding a

sub-recent peak (**Figure 6**). CHAR values, taking into account sedimentation rates, display low values in PAZ-1 to PAZ-3, and show the highest values in in PAZ-4 and PAZ-5.

DISCUSSION

Vegetation Signals at Lake Sidi Ali

Due to the large surface to catchment ratio and closed hydrological system at Lake Sidi Ali, the pollen signal should be dominated by a well-mixed atmospheric pollen rain without over-representation of local or lake-marginal vegetation, making it an ideal site to study regional vegetation responses to climate. Considering the size of the basin, it is anticipated that pollen will be recruited from long distances (up to 20 km) (Prentice, 1985). Furthermore, upslope transport of pollen from lower elevations is typical of montane locations (Markgraf, 1980). This phenomenon is evident in modern surface pollen samples from the Lake Sidi Ali catchment (Bell and Fletcher, 2016), which contain taxa such as *Olea*, *Phillyrea*, and deciduous *Quercus* that grow at lower elevations in thermo-, meso-, and supra/upper-mediterranean bioclimates, respectively (**Figure 3**). The interpretation therefore considers that pollen source areas will be very large and will integrate signals across several altitudinal levels. High pollen concentrations and PARs may indicate focusing of organic matter into the deepest part of the lake (**Figure 2**). While the PARs provide valuable confirmation of the main vegetation changes, they may not necessarily be independent of lake level changes or represent true productivity values of surrounding vegetation (Giesecke and Fontana, 2008).

The new pollen data show excellent replication of the original pollen record of Lamb et al. (1999) allowing for some centennial-scale temporal offsets probably relating to the weaker chronological control on core 91-C (**Figure 8**). Three phases of *Cedrus* expansion are clearly recognized (**Figure 8**, shaded bars), as well as strong similarities in the curves for other important terrestrial (*Artemisia*, evergreen *Quercus*) and aquatic (*Myriophyllum*, *Pediastrum*) types. Some differences are noted; for example, higher abundances of Cupressaceae and deciduous *Quercus* are recorded in cores ALI 01-10, which may reflect differences in dominant transport vectors to the marginal and deep-lake core sites.

Comparison of Vegetation and Lake Proxies

Select results of the multiproxy approach at Lake Sidi Ali are shown in **Figure 9**. Inferences about past winter rainfall are based on the oxygen isotope composition of benthic ostracods, with enrichment in ^{18}O on orbital- to multi-centennial timescales associated with reduced influence of isotopically light, winter-season Atlantic moisture sources (Zielhofer et al., 2017a) within an overall highly evaporative closed-lake context (positive $\delta^{18}\text{O}$ values). Changes in lake status (Unit 1 to Unit 5) are based on sedimentological proxies for terrestrial sediment supply (magnetic susceptibility, K concentrations) and lake sediment composition (calcium carbonate, CaCO_3 , and total organic carbon, TOC) (**Figure 9**). Lake-level inferences are further supported by sulfur and iron (S/Fe) ratios and ostracod

abundances providing insights into hypolimnion conditions, as well as a preliminary diatom dataset and the derived planktonic/littoral (P/L) ratios (Zielhofer et al., 2017a). In general, low lake level phases (aerobic hypolimnion) correspond to higher precipitation of CaCO_3 , high ostracod abundances and enhanced magnetic susceptibility, while high lake level phases (anaerobic hypolimnion) are inferred from higher TOC-values, enhanced S/Fe ratios and high P/L ratios (Zielhofer et al., 2017a).

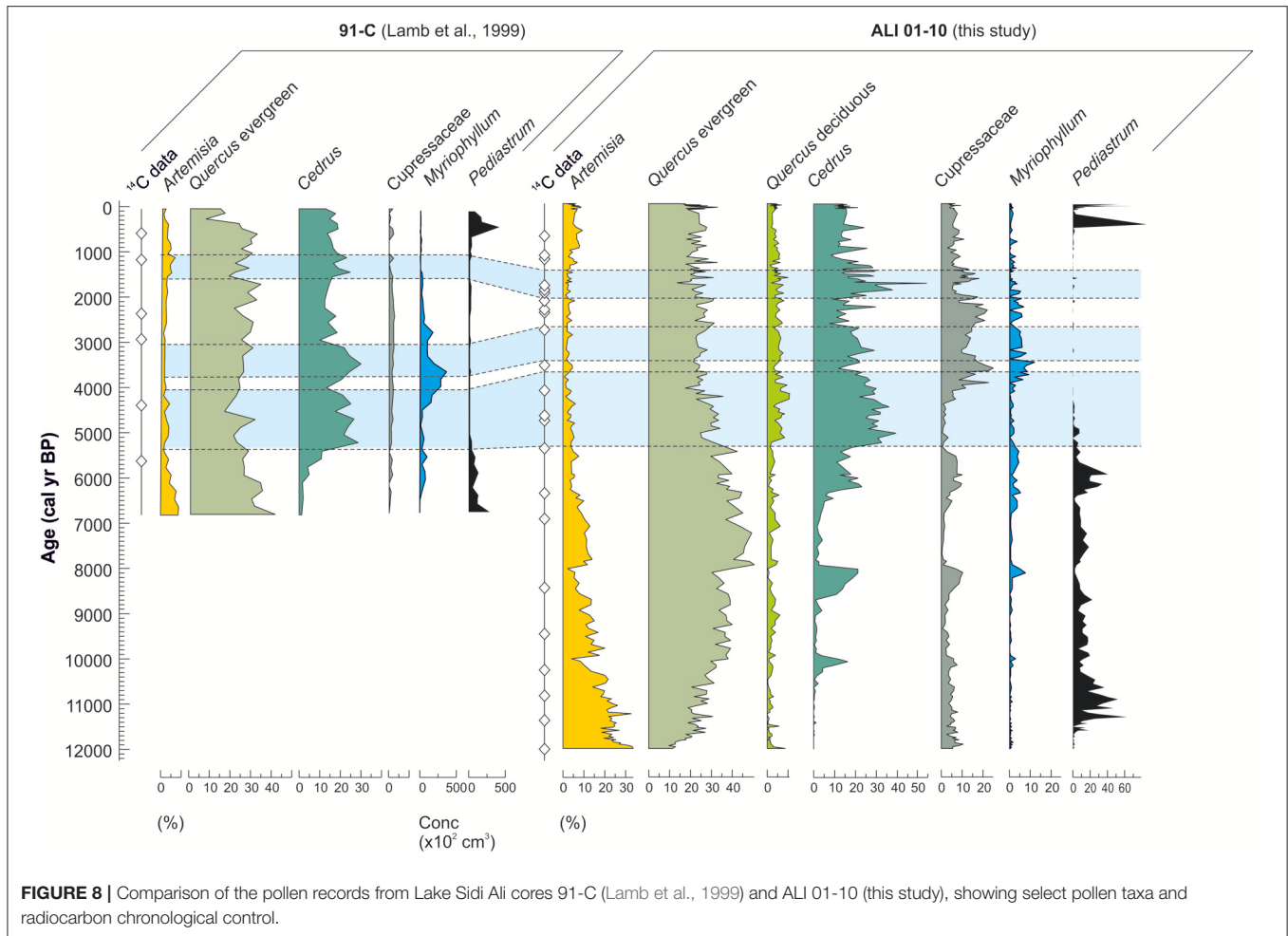
The compilation of proxies highlights how some vegetation and fire activity changes correspond to changes in lake status, including:

- (i) The transition from steppe to wooded landscape in the Early Holocene (PAZ-1 to PAZ-2) and increasing CHAC accompanies indicators of rising/high lake levels from Unit 1 to Unit 3.
- (ii) Maximum forest development (highest AP/NAP), the Holocene *Cedrus* maximum (PAZ-3c) and low CHAC and CHAR correspond with high lake level in Mid Holocene Unit 4b.
- (iii) Shifts in forest composition (higher Cupressaceae, PAZ-4) and increased fire regime (fluctuating high CHAR) accompany the transition from high to low lake level (Unit 4b to 4c) at the transition to the Late Holocene, along with increased abundance of *Myriophyllum*.
- (iv) Forest cover decrease (low AP/NAP, PAZ-5) accompany indicators of catchment disturbance and soil erosion in Unit 5 along with highest Holocene CHAR peak.

Nevertheless, a broad contrast is apparent between prevailing high winter rainfall and high lake levels during the early Holocene and predominance of steppic and sclerophyll vegetation types in the pollen record. We interpret this contrast to reflect different predominant seasonal (winter/summer) sensitivity of the hydrological and vegetation proxies, and explore the detailed environmental and climatic implications of the record in the next section.

Environmental Changes at Lake Sidi Ali PAZ-1 (12,000–10,340 cal yr BP)

PAZ-1 reflects an open, non-forested landscape with *Artemisia* and Poaceae around Lake Sidi Ali during the Pleistocene-Holocene transition and first centuries of the Holocene. AP percentages below 20% are consistent with frequencies observed in surface samples from non-forested areas of the Middle and High Atlas at present (Bell and Fletcher, 2016). *Artemisia*-dominated vegetation does not have analogs in the Lake Sidi Ali area today, but is dominant in more arid environments with high continentality. In the Moulouya Basin (located to the east of the Middle Atlas), *Artemisia herba-alba* Asso is typical on poorly drained fine substrates—subject to some seasonal waterlogging—as part of an edaphic mosaic of steppe vegetation, alongside *Stipa tenacissima* L. (Poaceae) on rocky slopes and halophytic Chenopodiaceae where there is significant soil salinity (Emberger, 1939; Rhanem, 2009). Recurrent observations of *Lygeum spartum* in the pollen record, which develops on arid, saline soils, further point to high continentality and seasonal



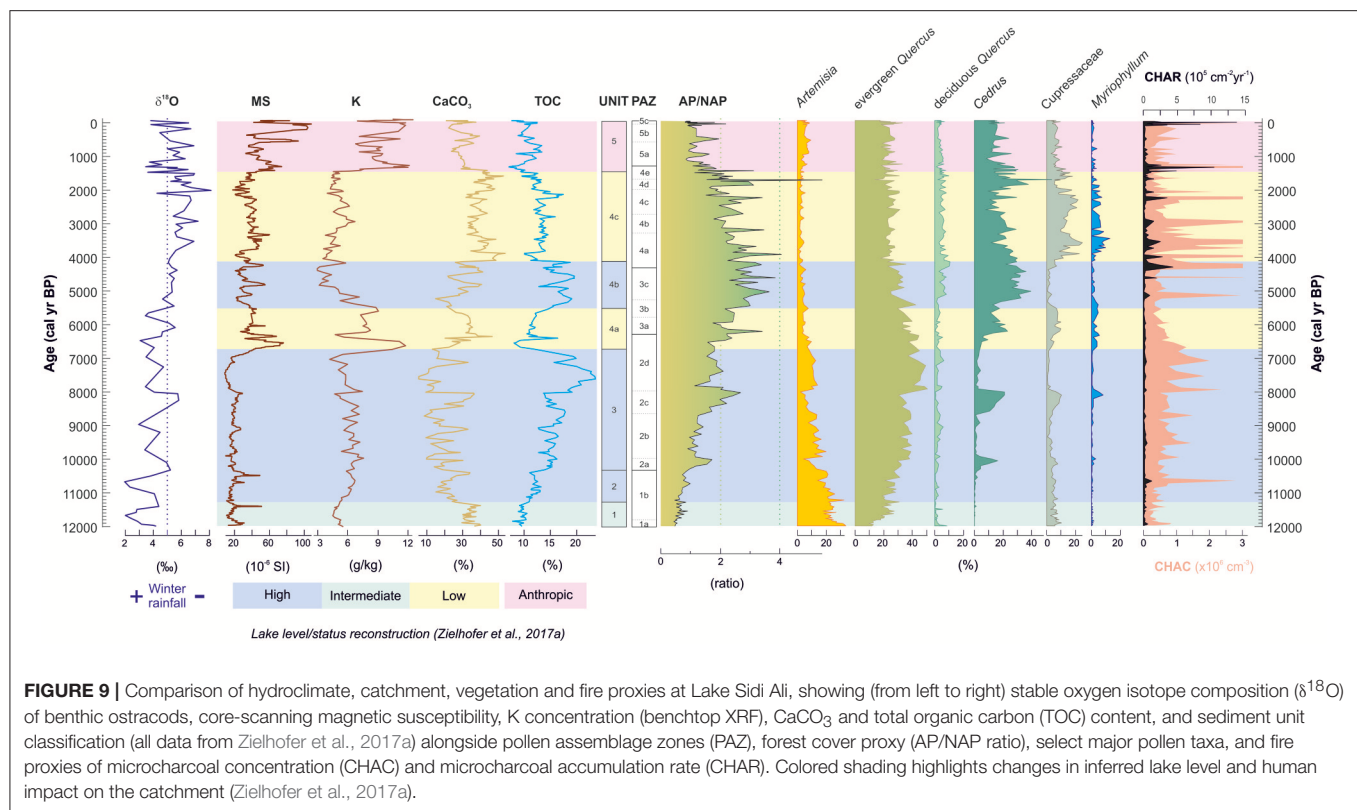
aridity. Although non-arboreal vegetation was dominant, the moderate presence of shrubby sclerophylls (notably *Pistacia*) reflects pre-steppic woody formations developing under warm and dry conditions, probably at lower elevations. Low frequencies of evergreen *Quercus* may represent long-distance transport, although increasing values from 11,810 cal yr BP (PAZ-1b) suggest incipient afforestation processes in the Lake Sidi Ali sector.

A rapid increase in algal productivity is implied by the increasing, high abundances of colonial green algae (*Botryococcus* and *Pediastrum*) in PAZ-1b. Although very widely distributed, *Botryococcus* is commonly associated with seasonally cold climates in montane environments (Rull et al., 2008), and is favored by warm summer temperatures. Blooms of *Pediastrum* may similarly occur in response to several factors, but warm summer temperatures and possible nutrient enrichment associated with snowmelt at the onset of Holocene hydroclimatic conditions may be implicated here. Regional fire activity appears low despite prevailing arid conditions, pointing to fuel limitation as a primary constraint on wildfire at this time. Overall, the contrast between, on the one hand, inferred moderate to high lake levels and high winter precipitation (Figure 9) and, on the other,

vegetation indications of semi-arid to arid bioclimate may be explained by very strong seasonal extremes, with concentration of precipitation as snowfall in the winter and warm dry summers.

PAZ-2 (10,340–6,300 cal yr BP)

PAZ-2 reflects the development of an open sclerophyll woodland with evergreen *Quercus* and, probably at lower elevations, *Phillyrea*. *Pistacia* continued to play a role in the regional vegetation, again probably at lower elevations and somewhat reduced in importance compared with PAZ-1. Afforestation in PAZ-2 represents an extension of processes commencing in PAZ-1b and suggests an increase in moisture availability permitting arboreal development near the bioclimatic margins for tree growth. It is important to note that the evergreen *Quercus* pollen morphology (syn. *Quercus ilex*-type) in the Middle Atlas derives from *Quercus rotundifolia*. This sclerophyll tree occurs across an enormous altitudinal range in Morocco (300–2,800 m.a.s.l.) and is remarkable in its ecological plasticity (Barbero et al., 1992). It is tolerant of drought and high continentality, and is abundant across the meso- to montane-mediterranean vegetation levels in subhumid and semiarid bioclimates (Peguero-Pina et al., 2014). While the taxonomic status of the “*rotundifolia*”



morphotype is debated, it clearly represents a distinct ecotype with enhanced drought resistant functional traits compared with *Q. ilex* (Barbero et al., 1992). Evergreen *Quercus* pollen reaches maximum percentages and PARs in PAZ-2, indicating an important degree of drought stress under warm, summer-dry conditions in the Early Holocene. Parallel indications of summer warmth are provided by the abundant lake algae, *Botryococcus*, pointing to high lake productivity. Microcharcoal points to a moderate, stable background fire activity without exceptional fire episodes, gradually increasing in line with rising forest cover and lake level. These features suggest a continued role of fuel limitation at the regional scale.

Within PAZ-2, two well-defined episodes marked by increased *Cedrus* and Cupressaceae pollen (PAZ-2a and PAZ-2c) occurred, commencing at 10,340 cal yr BP and 8,640 cal yr BP, respectively. *Cedrus* peaks exceed 15 and 20%, respectively, during these episodes. In the study of soil surface samples from the Sidi Ali catchment (Bell and Fletcher, 2016), *Cedrus* percentages exceeding 7% were generally observed only in the immediate vicinity of *Cedrus* trees. The inferred low pollen dispersal of *Cedrus*, similar to that reported for the eastern Mediterranean species *Cedrus libani* A.Rich (Hajar et al., 2008), supports the interpretation of local presence of *Cedrus* stands in the Sidi Ali catchment during these episodes. Nevertheless, as the pollen transport pathways will be different for the lake basin and surface samples, notably with a greater contribution of a well-mixed atmospheric pollen rain into the lake basin, a longer-distance signal reflecting enhanced pollen production in select distant locales, or integrating across more numerous and productive

patches in the wider landscape, cannot be ruled out. These episodes are also distinguished by isotope-inferred decreases in winter rainfall (Figure 9), increases in the submerged macrophyte *Myriophyllum*, and reductions in *Pediastrum*. Noting the general correlation between *Myriophyllum* and lower-lake-level phases (Figure 9), these changes suggest a combination of winter drying, lake level lowering and aquatic vegetation changes at the same time as summer cooling and reduced bioclimatic drought inferred from the expansion of montane conifers. Broadly, these indicators point to “cool summer, dry winter” episodes with diverse ecological impacts.

PAZ-3 (6,300–4,320 cal yr BP)

PAZ-3 represents a Mid Holocene transition in forest composition characterized by a decline in evergreen *Quercus* and the expansion of *Cedrus*. The floristic changes suggest a climatic transition toward generally cooler and more humid conditions favoring the development of montane conifer forest. A step-wise expansion of *Cedrus* is evident, initially accompanied by Cupressaceae at 6,300 cal yr BP (sub-zone PAZ-3a), and later accompanied by deciduous *Quercus* at 5,380 cal yr BP (PAZ-3c). The two phases of expansion leading to the dominance of *Cedrus* are separated by a minor regression during which warm-tolerant taxa *Pistacia*, *Phillyrea*, and *Olea* increased (PAZ-3b). The PAZ-3a to PAZ-3b sequence, with contrasting expression of conifer and sclerophyll vegetation suggests the continuation of the dynamics prevailing in PAZ-2 and the superimposed impacts of cool-warm cycles onto the long-term transition from sclerophyll

to conifer dominance. In this respect, *Cedrus* expansion in PAZ-3a in association with isotope-inferred winter rainfall decline suggests a further “cool summer, dry winter” interval centered around 6,100 cal yr BP. In contrast to the prevailing dynamics evident in PAZ-2, where *Cedrus* appears to have undergone local extirpation during unfavorable episodes (PAZ-2b, PAZ-2d), long-term conditions from 6,300 cal yr BP onwards permitted the development of a resilient local population of *Cedrus* at Lake Sidi Ali. Indeed, even the floristic characteristics during the minor regression of *Cedrus* in PAZ-3b point to slightly less arid bioclimate than that prevailing in PAZ-2b and PAZ-2d, reflected in the Holocene maximum representation of both *Olea* (a remote signal of thermophilous woody cover at low elevations) and *Acer* (probably a local component of summer-green vegetation on the lake margins).

Subsequently, maximum arboreal development for the Holocene was attained during a fairly stable interval with high values of *Cedrus* accompanied by increased deciduous *Quercus* between 5,280 and 4,320 cal yr BP (PAZ-3c). In concert with high lake levels (Unit 4b), these features suggest the Holocene interval of most humid bioclimate in the Middle Atlas. With regard to the isotope record, this humid interval does not appear to have been caused by especially high winter rainfall and is associated instead with intermediate isotopic values close to the long-term average (Figure 9). Rather, humidity signals at this time may result from the long-term (orbitally-driven) reduction in summer temperature and reduction in seasonal extremes (reduced summer drought, reduced concentration of precipitation in the winter season) leading to more favorable growing season conditions for moisture-sensitive taxa. The combined signals suggest development of moisture-demanding forest vegetation series with *Cedrus* in the montane belt around Lake Sidi Ali, and with deciduous *Quercus* at lower elevations (supra/upper mediterranean level). Alternatively, specimens of deciduous *Quercus* may have established alongside *Cedrus* in the Sidi Ali sector; however, the rather modest increase of this taxon in PAZ-3 in the context of recurring low values throughout the record may accord more strongly with a remote signal than a shift in local floristic composition. Low fire activity throughout PAZ-3 in the context of maximum arboreal development and floristic and limnological indications of humid bioclimate suggests a transition away from prevailing fuel-limitation during the Early Holocene toward a climate-limited fire dynamic after 6,300 cal yr BP.

PAZ-4 (4,320–1,300 cal yr BP)

PAZ-4 documents the continued dominance of montane conifer forest with *Cedrus* and, notably, Cupressaceae. PAZ-4 also reveals a modest, progressive opening of the forest cover from 4,320 cal yr BP onwards with increases in shrubby taxa and reduction of AP/NAP ratios. These changes accompanied lower lake level status and weakened influence of winter rainfall (Figure 9) and suggest a transition to generally drier conditions. A considerable decline in lake algae and increase in aquatic macrophytes (*Myriophyllum*), may also reflect either shallower lake levels and/or enhanced nutrient status (Lamb et al., 1999). At the same time, certain grazing resistant and waste ground taxa—notably,

Astragalus, *Ulex* and *Coronilla* types, reflecting spiny cushion form shrubs, along with Brassicaceae—may point to early signals of pastoral activity at this time. From 4,320 cal yr BP, a shift in fire activity is also evident, with frequent high amplitude fire episodes. This enhanced fire dynamic developed in the context of high forest cover and a shift to drier conditions, consistent with climate-limited fire dynamics from the Mid Holocene (PAZ-3) onwards. The association of high fire frequency and early anthropogenic signals in PAZ-4 suggests that anthropogenic triggers for fire lighting may be implicated.

PAZ-4 subzones suggest a competitive dynamic between *Cedrus* and Cupressaceae in response to moisture increases (*Cedrus*) and decreases (Cupressaceae) under a generally cooler prevailing temperature regime than during the Early Holocene. The Late Holocene maxima in Cupressaceae (PAZ-4a, PAZ-4c, PAZ-4e) probably represent local populations of *Juniperus thurifera*, the most prevalent Cupressaceae species around Lake Sidi Ali today. However, as Cupressaceae pollen is identifiable only to family level, the record may integrate several taxa with a range of thermic preferences, from the high mountain juniper, *J. thurifera*, and the fairly widespread *J. oxycedrus*, to warm climate taxa such as *J. phoenicea* and the western Mediterranean endemic, *Tetraclinis articulata* (Emberger, 1939). All taxa are, however, generally associated with semiarid conditions, supporting the inference of a drier affinity than *Cedrus*.

PAZ-5 (1,300 cal yr BP to Present)

PAZ-5 reflects an opening and degradation of the forest cover that affected *Cedrus* and Cupressaceae most strongly. The pollen spectra imply a prevalence of open ground areas with herbaceous vegetation, with Poaceae, *Artemisia*, Chenopodiaceae, *Plantago* types and *Rumex*. Following a major fire episode around 1,300 cal yr BP, fire activity appears generally low and stable, which may be a consequence of the opening of the vegetation cover and low flammable material due to grazing. The signals of deforestation are strongly supported by proxies for erosion and terrestrial input to the lake (Figure 9), and may have caused a pulse in nutrients promoting *Pediastrum* blooms. Within PAZ-5, three distinct phases are detected, reflecting a modest oscillation in arboreal cover (AP/NAP ratios, Table 1) with lowest arboreal cover and maximum *Plantago* between 1,300 cal yr BP and 580 cal yr BP (PAZ-5a), a subsequent increase in *Cedrus* and evergreen *Quercus* after 580 cal yr BP (PAZ-5b), and a final reduction in the twentieth century (PAZ-5c). Although this pattern occurs within an anthropogenically-modified environment, it may reflect climatic influence on arboreal vegetation, particularly decreased drought stress during the Little Ice Age interval as documented in Middle Atlas *Cedrus atlantica* tree-ring widths (Esper et al., 2007).

Local and Regional Patterns of Long-Term Ecological Change

In order to differentiate local and regional signals, and examine vegetation development at two different elevations, it is informative to compare the Lake Sidi Ali and Tigalmamine records in detail. Key pollen taxa and AP/NAP ratios (Figure 10) highlight both commonalities and contrasts in vegetation history

between these two sites located within 50 km distance. Key common features include:

- (i) Peak abundance of *Artemisia* at the Pleistocene-Holocene transition and a parallel reduction during the Early Holocene, reflecting the gradual disappearance of regional steppic vegetation.
- (ii) An Early Holocene maximum of evergreen *Quercus* at both sites, reflecting the maximum regional development of drought tolerant sclerophyll forest.
- (iii) A Mid Holocene maximum for moisture-demanding taxa between ca. 5,000 and 4,000 cal yr BP with *Cedrus* at Lake Sidi Ali and deciduous *Quercus* at Tigalmamine.
- (iv) An important role of *Cedrus* at both sites from 4,000 cal yr BP onwards.

Broadly, these parallels suggest a prevailing common influence of long-term regional climatic drivers. Essentially, they may be explained by a long-term cooling from an Early Holocene thermal maximum toward present, consistent with both summer insolation forcing (Berger and Loutre, 1991) and climate simulations (Renssen et al., 2009), accompanied by gradual reduction of seasonal temperature extremes and reduced temperature-driven summer drought stress associated with the precession cycle (Bosmans et al., 2015). At Lake Sidi Ali, a long-term reduction in the contribution of winter rainfall to the lake water is inferred (Figure 9, Zielhofer et al., 2017a), which might be assumed to counterbalance the positive effect of cooling on moisture availability for plant growth. However,

in a high-insolation mountain setting with significant snowfall, winter precipitation may be subject to rapid melting and sublimation effects and hence of limited bioavailability during the growth season. While winter precipitation may ultimately help to recharge groundwater, only deep-rooting taxa (such as evergreen *Quercus*) will be able to take advantage of this water source to mitigate against summer drought, while shallow rooting taxa (e.g., *Cedrus*) depend on edaphic moisture sources and are more exposed to extended summer drought (Aussenac, 1984).

The interaction of these factors allows a model for regional environmental change related to long-term climatic drivers to be proposed. During the Early Holocene, a combination of cold, wet winters and hot, dry summers promoted the development of deep-rooting sclerophyll taxa and the persistence of steppic vegetation where aridity was too great. During the Mid Holocene, a “Goldilocks interval” where winter precipitation was moderately high, summer temperatures moderately warm and summer drought less intense promoted the maximum development of moisture demanding trees, similar to the phenomenon of the mesophytic forest maximum identified in SE Iberia mountain regions (Carrión, 2002; Carrión et al., 2003). During the Late Holocene, lower summer temperatures and reduced temperature-driven drought stress favored cool-tolerant and shallow-rooting forest taxa despite hydrological aridity resulting from reduced winter precipitation.

The specific timing and character of local vegetation responses to this long-term evolution will have been modulated by the

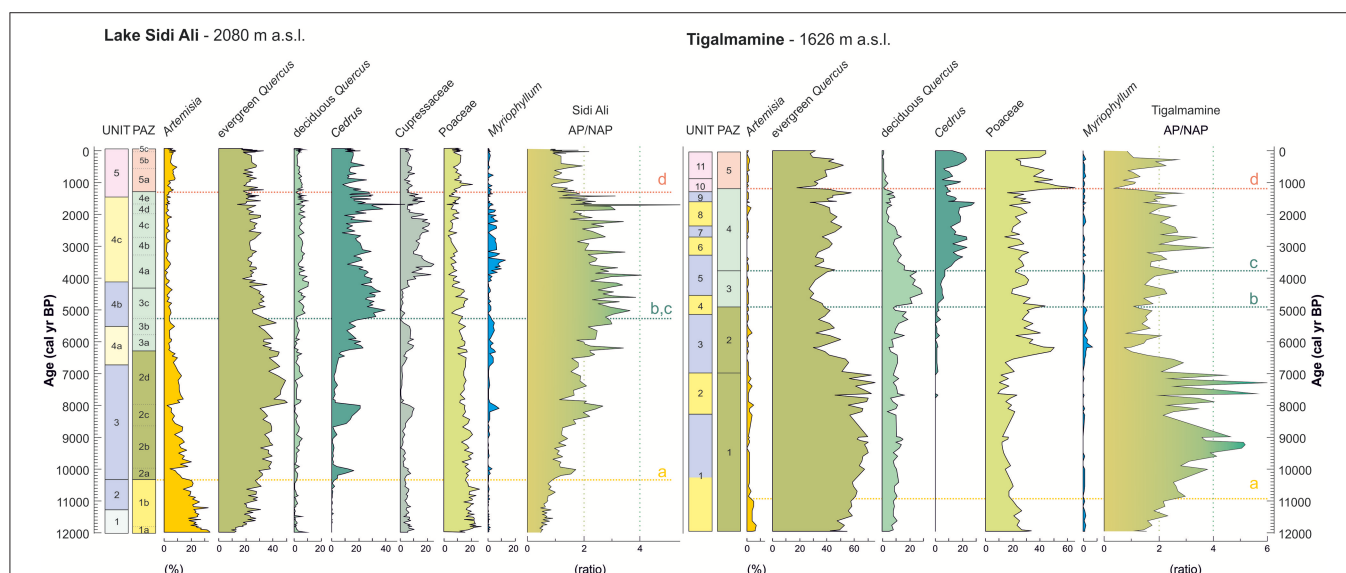


FIGURE 10 | Comparison of key pollen taxa and AP/NAP ratios for Lake Sidi Ali (this study) and Tigalmamine (Lamb and van der Kaars, 1995). Lake Sidi Ali sedimentological units color-coded according to inferred lake level and status (see key in Figure 9). Tigalmamine lithological units are similarly color-coded for shallow (yellow), deep-water (blue) and anthropic (red) facies following unit descriptions and interpretation in Lamb and van der Kaars (1995). PAZ labels color-coded according to the dominant vegetation: *Artemisia* (yellow), evergreen *Quercus* (olive green), deciduous *Quercus* and *Cedrus* (pale green), non-arboreal and anthropogenic indicators (red). Dashed lines highlight similar assemblage changes at both sites: (a) Early Holocene *Artemisia* decline and evergreen *Quercus* rise; (b) Mid Holocene deciduous *Quercus* rise; (c) transgressive Mid to Late Holocene *Cedrus* expansion; (d) inferred Late Holocene anthropogenic forest decline.

specific geographical and bioclimatic settings of the sites. Notable differences for Lake Sidi Ali and Tigalmamine (**Figure 10**) include:

- (i) An important role of Cupressaceae at Lake Sidi Ali, particularly during the Late Holocene, while Cupressaceae is insignificant in Tigalmamine pollen record (<1%).
- (ii) Delayed expansion of *Cedrus* at Tigalmamine compared with Lake Sidi Ali.
- (iii) Maximum forest development (AP/NAP ratios, **Figure 10**) was attained at Tigalmamine during the Early Holocene, but only during the Mid to Late Holocene at Lake Sidi Ali, with an opposed, corollary pattern for Poaceae.

These differences can be understood firstly with respect to the elevation of the sites. The elevation difference of >450 m should account for a moderate prevailing temperature difference between the sites due to the normal lapse rate of 0.6°C per 100 m. This difference is reflected nicely in the contrasting forest composition during the Mid Holocene under prevailing humid bioclimatic conditions (*Cedrus* at higher elevation vs. deciduous *Quercus* at lower elevation), and during the drier Late Holocene (*Cedrus* with Cupressaceae vs. evergreen *Quercus* with *Cedrus*). These patterns are coherent with characteristic vegetation differences along elevation gradients at present (**Figure 3**). Between the Mid and Late Holocene, the shift in vegetation composition can furthermore be understood to reflect an effective lowering of the regional vegetation levels in response to gradual cooling. The delayed expansion of *Cedrus* at the lower elevation site also points to local threshold responses to gradual cooling, with suitable conditions for *Cedrus* forest development reached earlier at higher elevations.

Secondly, Lake Sidi Ali is a significantly drier location (current semi-arid to subhumid bioclimate) than Tigalmamine (subhumid to humid bioclimate), primarily due to weaker influence of Atlantic-derived winter rainfall. As this difference is primarily linked to topographical controls arising from the NE-SW alignment of the Middle Atlas, it is likely to have remained fairly constant throughout the Holocene. In contrast, Mediterranean-sourced precipitation during the spring and autumn, and convective storms in summer, may play a more important role at Sidi Ali. A broadly consistent difference in aridity likely explains the important role of *Artemisia* steppe at the Pleistocene-Holocene transition and its greater persistence into the Early Holocene at Sidi Ali. *Artemisia*-rich steppe was dominant also at Tigalmamine during the Late Pleistocene (Lamb et al., 1989), but the expansion of sclerophyll woodland was more advanced by the onset of the Holocene. Similarly, greater aridity may also explain the weaker development of forest at Sidi Ali during the Early Holocene. Although evergreen *Quercus* was favored at both sites, a greater impact of high Early Holocene winter rainfall was probably effective at the more humid site. This may have been compounded by increased ecological challenges at the higher elevation site for colonization by seedlings.

The interplay of regional climatic changes and local conditions should have explanatory power for interpreting other existing and forthcoming Middle Atlas records. For example, at the nearby site of Ait Ichou (Tabel et al., 2016), located farther

to the SW at similar elevation to Tigalmamine and in an intermediate bioclimatic setting between Lake Sidi Ali and Tigalmamine, common features with both records are observed. The site documents a synchronous Mid Holocene maximum with mesophytic deciduous *Quercus* and a Late Holocene expansion of *Cedrus*, reflecting similarities in forest composition changes with Tigalmamine related to gradual Holocene cooling. However, a Mid to Late Holocene maximum in forest development occurred that is similar to trends at Lake Sidi Ali, along with a strong persistence of *Artemisia* steppe into the Early Holocene; both features may be related to the drier setting that did not permit a strong response to enhanced Early Holocene winter rainfall.

In common with other Mediterranean climate regions, human impact and fire also appear to have played a role in the Holocene vegetation development, and within the study area many similarities are apparent in these factors. Broadly, at Lake Sidi Ali two phases of impact are recognized, with signals of *matorralization* (increase of shrubs) and enhanced fire activity apparent from around 4,300 cal yr BP, followed by a stronger horizon of impact with forest decline around 1,500–1,100 cal yr BP. These early responses have parallels at Ait Ichou, where development of *Cistus* scrub and increased burning is recorded around 4,500 cal yr BP. The coincidence of these changes and independent evidence for winter drying and lake level lowering at Lake Sidi Ali point to synergistic impacts of pastoral activities of the indigeneous Berber peoples of the Atlas and climate changes at the onset of the Late Holocene. Similar early signals were suggested for sites in the northern Middle Atlas (Afourgagh, Iffir) (Lamb et al., 1991), but predate the suggested 2,000 cal yr BP horizon of human impact reported for Ras el Ma, Tifounassine and sites in the Rif (Cheddadi et al., 2015). Important similarities with fire activity in SE Iberia (Gil-Romera et al., 2010) are noted, notably modest fire activity during the Early Holocene in a fuel-load limited system, low fire activity during a humid Mid Holocene associated with the installation of *Cedrus* at Lake Sidi Ali and a mesophytic tree maximum in SE Iberia, and dynamic fire activity during the Late Holocene in the context of drying and increased human activity.

The second phase, marked by strong forest cover reduction and *Cedrus* decline in the first millennium AD, is evident at all sites in the southern Middle Atlas, including Lake Sidi Ali, Tigalmamine (Lamb et al., 1995), Ait Ichou (Tabel et al., 2016), Taguelmam n'Harcha (Lamb et al., 1991), and Col du Zad (Reille, 1976). The timing at Sidi Ali (PAZ-5 boundary, 1,300 cal yr BP, or 650 AD) suggests a possible association with more intensive use of forest resources in the Middle Atlas following the Early Muslim conquest of Northwest Africa in the mid seventh century AD (Abun-Nasr, 1987). As such, the forest decline in the southern Middle Atlas may be part of a wider phase of significant first millennium AD anthropogenic impact in mountain environments extending to the High Atlas (McGregor et al., 2009; Fletcher and Hughes, 2017). The two-phase forest decline at Sidi Ali represents an valuable example of the wider phenomenon of montane conifer forest decline in the face of intensification of human pressure on Mediterranean mountain environments and changes in fire activity, which includes *Abies alba* in Italy (Tinner et al., 2013), and *Pinus nigra* and *P. sylvestris*

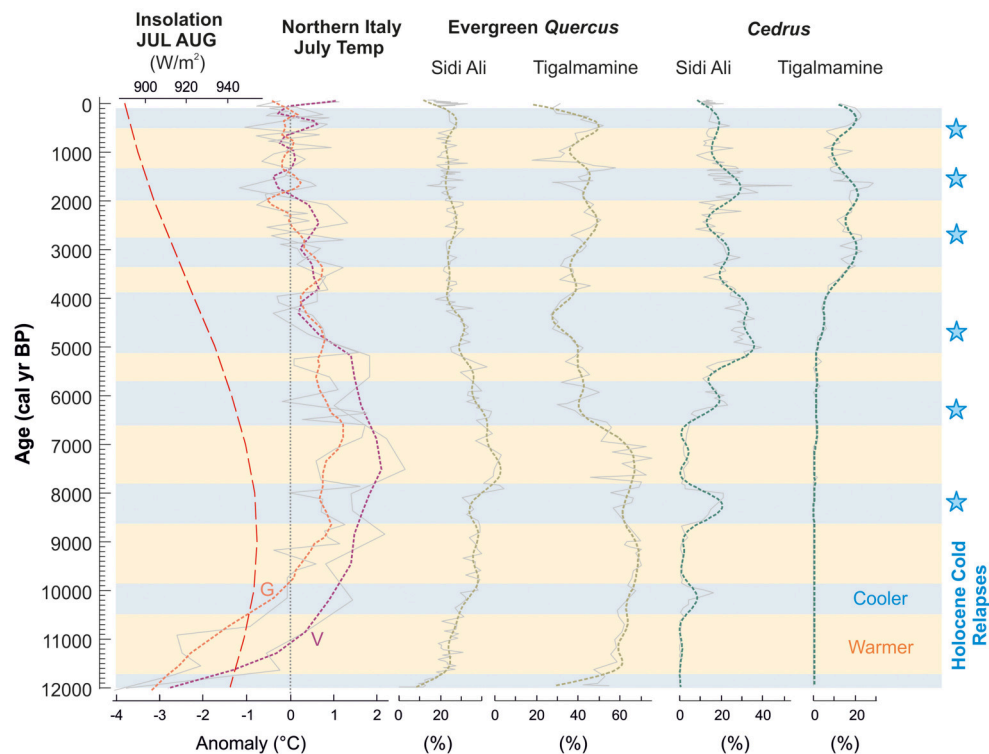


FIGURE 11 | Inferred summer temperature variability in the Middle Atlas, Morocco, showing: orbital insolation parameter for combined July and August insolation at 30°N (Berger and Loutre, 1991); chironomid-based summer temperature reconstructions from Gemini (G) and Verdarolo (V) in northern Italy (Samartin et al., 2017); pollen curves for warm-tolerant (evergreen *Quercus*) and cool-tolerant (*Cedrus*) trees at Lakes Lake Sidi Ali (this study) and Tigalmamine (Lamb and van der Kaars, 1995). Dashed lines through the pollen curves show results of lowpass filter (1,000 year) removing centennial variability. Stars indicate global Holocene “cold relapses” (Wanner et al., 2011).

in Iberia (Rubiales et al., 2012; Morales-Molino et al., 2017). The details of the temporal, cultural and climatic context appear regionally-specific, and a synthetic treatment of the shared and unique features of the historical trajectories of these vulnerable organisms could be a valuable future research avenue.

Impacts of Long-Term and Millennial-Scale Summer Temperature Changes

The important role of two climate-sensitive species at Lake Sidi Ali and Tigalmamine supports the investigation of common trends and patterns of millennial-scale variability. As discussed above, the contrasting rooting depths of *Cedrus atlantica* and *Quercus rotundifolia* relate to different strategies for maintaining photosynthetic activity during summer drought. *Cedrus atlantica* develops an extensive shallow root system and tolerates drought through gradual reduction of stomatal conductance to reduce transpiration, maintaining photosynthetic activity under considerable hydric stress. However, lack of transpiration blockage can lead to difficulties under prolonged, severe drought (Aussenac, 1984). In contrast, *Quercus rotundifolia* develops deep rooting structures to access groundwater reserves and maintain high rates of transpiration in combination with stomatal closure under extreme stress (David et al., 2004; Cubera and

Moreno, 2007; Vaz et al., 2010). These different strategies leave *Cedrus* more vulnerable to extended temperature-driven summer drought and low soil moisture. This phenomenon is implicated in current dieback of *Cedrus* in NW Africa (Linares et al., 2011; Rhanem, 2011) and encroachment of *Quercus rotundifolia* into cedar forest areas (Figure 4). Field observations highlight the current decline at the lower limits of the species' elevation range and a healthy state toward the upper limits, further supporting temperature-driven abiotic stress as a key driver of ongoing dieback (Rhanem, 2011).

Figure 11 highlights opposed trends on long-term and millennial timescales between warm-tolerant evergreen *Quercus* and cool-preferring *Cedrus*. We find that the long-term trend is in good agreement with orbital forcing during summer (July, August) (Berger and Loutre, 1991) and with the chironomid-based temperature reconstructions of Samartin et al. (2017) for Mediterranean northern Italy. Millennial phases of warmer and cooler bioclimate are also inferred and again these show good coherence with signals in Mediterranean northern Italy. Despite the remote location of the Verdarolo and Gemini reconstructions, similarities with NW Africa would be anticipated from significant correlations in July temperatures between the regions ($r = 0.3\text{--}0.5$, Samartin et al., 2017). The millennial patterns of warmer and cooler temperatures also show

coherent signals with respect to well-known Holocene cooling intervals, such as multi-centennial summer cooling around the short-lived 8.2 ka event (Rohling and Pälike, 2005), and the so-called “cold relapses” around 8,200, 6,300, 4,700, 2,700, 1,550, and 550 cal yr BP identified in global records by Wanner et al. (2011). It is noteworthy that the last of these relapses, associated with the Northern Hemisphere Little Ice Age, is evident in *Cedrus* expansion at both sites, weakly at Lake Sidi Ali and more strongly at Tigalmamine, even though this climatic shift occurred after the main horizon of anthropogenic impact on the landscape. In contrast to lowland Mediterranean areas, where precipitation changes are implicated as the main driver of millennial-scale vegetation changes, including forest declines (Fletcher et al., 2013) and *matorral*-steppe fluctuations (Jaouadi et al., 2016), we suggest that the temperature component of millennial-scale climate variability may have been a key driver in the Middle Atlas, impacting directly on growing season bioclimate and modulating the intensity of summer drought.

The match between the records of evergreen *Quercus* at Lake Sidi Ali and Tigalmamine and the Italian records supports an Early Holocene summer thermal maximum between 9,000 and

7,000 cal yr BP in the Middle Atlas, interrupted by a multi-centennial interval of summer cooling around 8,000 cal yr BP. More widely, an important role of Early Holocene high summer temperatures is implicated in strong development of evergreen *Quercus* in the Alboran Sea basin regions of S Iberia and N Morocco (Fletcher and Goñi, 2008; Combourieu Nebout et al., 2009) and southern Portugal (Fletcher et al., 2007). High temperatures during the Early Holocene are also implicated in the maximum depletion in speleothem ^{13}C by 9,500 cal yr BP at La Mine Cave in Tunisia associated with enhanced soil microbial activity above the cave (Genty et al., 2006). The summer thermal maximum inferred from the Middle Atlas pollen records is coherent with insolation forcing and model predictions (Renssen et al., 2009). In contrast, it does not support the results of large-scale pollen-based climate reconstructions (Davis et al., 2003; Mauri et al., 2015) which produce cool Early Holocene temperatures for the SW European/W Mediterranean sector. The challenge for pollen-based reconstructions in the Mediterranean climate zone is the interaction of temperature and precipitation changes in determining bioclimatic moisture availability for vegetation development, and hence the truly independent reconstruction of either temperature or precipitation. In this case, the multiproxy approach at Lake Sidi Ali indicates high lake levels and strong influence of winter precipitation during the Early Holocene (particularly evident in anaerobic hypolimnion conditions favoring organic preservation and light oxygen isotope signatures; Figure 9). As such, an alternative scenario that the vegetation changes essentially reflect a shift from low to high precipitation changes can be rejected, with a caveat relating to possible enhancement of summer precipitation over the Holocene in line with precession forcing (Bosmans et al., 2015). More widely, another challenge for continental-scale reconstructions will be the merging of signals from *Quercus rotundifolia* (extensive across NW Africa and S Iberia) and *Quercus ilex* (in NW, central and E Mediterranean sectors), given the very different tolerances for high continentality of these species.

Implications for Future Change

The pollen records of Lake Sidi Ali and Tigalmamine reveal the significant exposure of forest vegetation to pervasive millennial climate changes in the Middle Atlas. This finding contrasts with other areas of the western Mediterranean where vegetation resilience in the face of rapid climate changes has been identified, such as the continental interior of eastern Iberia (Aranbarri et al., 2014). The picture reinforces the view of high sensitivity of mountain regions to climatic changes, as predicted for the Twenty-first century (Nogués-Bravo et al., 2007). Importantly, fluctuations in the relative abundance of evergreen *Quercus* and *Cedrus* (Figure 12) persisted even in an anthropogenically altered landscape. Indeed, from a Holocene perspective, the current decline of *Cedrus atlantica* may be understood partly as a response to a quasi-periodic Holocene fluctuation in climate and less favorable conditions since the end of the Little Ice Age. However, the pollen records also indicate that total forest cover is at the lowest level since the onset of the Holocene, increasing the vulnerability of *Cedrus* to regional extirpation due to reduced

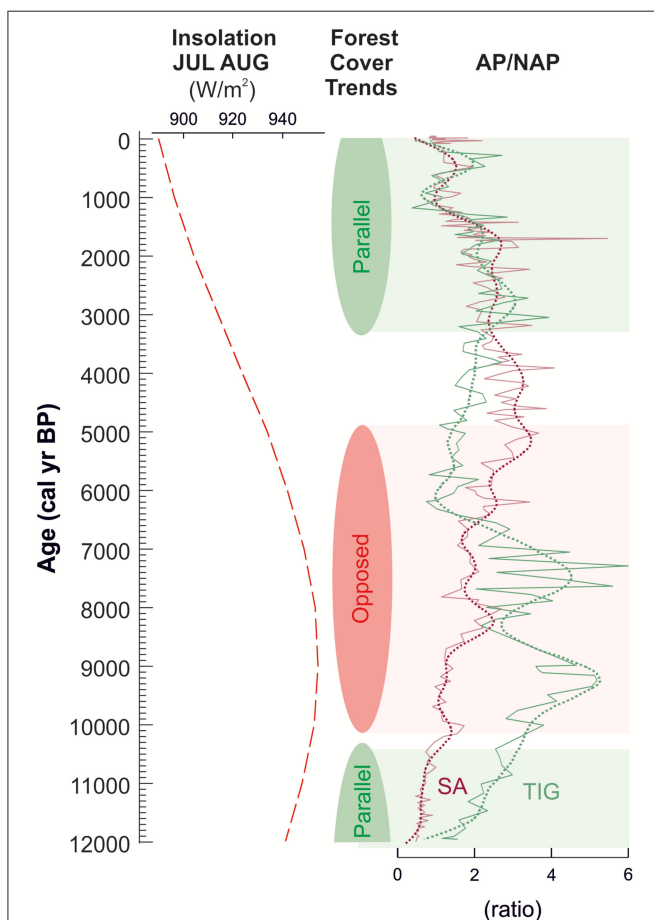


FIGURE 12 | Holocene millennial trends in forest cover at Lake Sidi Ali (SA) and Tigalmamine (TIG), highlighting intervals of parallel (green shading) and opposed (red shading) patterns of expansion and decline.

population size and range fragmentation. Moreover, projected increases in summer heat stress in the context of anthropogenic global change will exacerbate the natural trend, pushing the species toward extinction from many areas of its current range (Cheddadi et al., 2009).

The Holocene perspective on total forest cover at Lake Sidi Ali and Tigalmamine (**Figure 12**) highlights a second implication of future warming. Similar trends of forest increase following the Pleistocene-Holocene transition and Late Holocene decline during the last 3,000 years are observed at both sites, consistent with broadly parallel trajectories of climatic and anthropogenic forcing (**Figure 12**, green shaded intervals). However, the patterns diverge during the Early Holocene, especially near the Early Holocene summer thermal maximum, when forest cover changes in response to millennial fluctuations were opposed in direction (**Figure 12**, red shading). This is most clearly evident for two inferred warm phases centered around 9,500 and 7,500 cal yr BP (**Figure 12**). We suggest that under a prevailing high summer temperature regime, forest vegetation at the site receiving higher winter rainfall (Tigalmamine) could respond positively to millennial intervals of summer warming, while the same warming intervals lead to forest declines at the drier site (Lake Sidi Ali). Our findings are similar to long-term observations in the Canadian Cordillera (Schwörer et al., 2017), where Holocene forest dynamics were modulated by millennial temperature changes, but the development of closed forest was limited by topographical and geomorphological controls on moisture availability. Our findings suggest that in a warmer future, forest response to climate will be spatially complex. Higher temperatures will exacerbate differences in moisture availability associated with topography and elevation, leading to divergent patterns of productivity, biomass and carbon sequestration within the region.

CONCLUSIONS

The high-resolution and robustly-dated pollen record from Lake Sidi Ali documents the Holocene vegetation history at a high elevation site in the southern Middle Atlas and provides multiple insights into the environmental drivers of ecological change. Five main vegetation phases are identified, of which the first four appear climatically-driven, namely: (i) *Artemisia* steppe between 12,000 and 10,340 cal yr BP under a semi-arid, continental regime, (ii) open sclerophyll woodland with evergreen *Quercus* between 10,340 and 6,300 cal yr B under a warm, subhumid regime with marked summer drought, (iii) transition to *Cedrus* forest between 6,300 and 4,320 ca yr BP under a cool, humid to subhumid regime with reduced summer drought, and (iv) gradual decline of cold-tolerant montane conifer forests with *Cedrus* and Cupressaceae between 4,320 and 1,300 cal yr BP under a cool, subhumid to semiarid regime. The succession of changes points to a primary influence of long-term climatic drivers including gradual reduction in seasonal extremes of winter precipitation and summer drought, consistent with lake level and rainfall proxies from the same core. Associated changes in fire activity suggest a shift from

fuel-load limitation to climate-limitation from the Early to Mid Holocene, and reveal a significant increase in fire activity in the Late Holocene. Anthropogenic impact may be implicated in processes of *matorralization* and enhanced fire activity from 4,320 cal yr BP, but the timing coincides with lake level lowering and reduced winter rain during the Late Holocene and synergistic climate-human impacts may be implicated. The fifth phase (v) reflects opening and degradation of the forest cover from 1,300 cal yr BP, and probably marks a horizon of more intense human impact, evident across the southern Middle Atlas (Reille, 1976; Lamb et al., 1991; Tabel et al., 2016).

The detailed comparison of the pollen records from Lake Sidi Ali and Tigalmamine (Lamb and van der Kaars, 1995) on their respective age models provides valuable insights into forest cover and composition at two different altitudes within the same southern Middle Atlas region. The main phases of vegetation change are replicated, but elevation and precipitation differences contribute to site specific patterns. Notably, the Mid Holocene interval of maximum bioclimatic humidity (dated from 5,280 to 4,320 cal yr BP at Lake Sidi Ali) is reflected in a *Cedrus* maximum at higher elevation and a deciduous *Quercus* (*Q. canariensis*) maximum at lower elevation. Throughout the Holocene, similar dynamics are observed at the sites in terms of fluctuating, opposed evergreen *Quercus* and *Cedrus* abundances. These dynamics can be understood in terms of the different drought tolerance mechanisms for these taxa, and may be predominantly controlled by summer temperature influence on moisture availability. The inferred summer temperature changes suggest a Holocene summer temperature maximum between 9,000 and 7,000 cal yr BP (Samartin et al., 2017) and pervasive millennial-scale climate variability. Millennial cooling episodes favoring expansion of *Cedrus* were centered around 10,200, 8,200, 6,100, 4,500, 3,000, and 1,700 cal yr BP, as well as during the Little Ice Age (400 cal yr BP). These climate-driven fluctuations persist through the Late Holocene, despite opening of the forest cover and intensification of human impact.

The results demonstrate the sensitive response of Middle Atlas forests to rapid climate changes, and underscore the important influence of temperature regime on vegetation dynamics in this mountain region. The negative implications of temperature increase for *Cedrus* are reinforced (Cheddadi et al., 2009) and spatial complexity of future changes in forest cover and productivity appear likely in light of divergent trends of forest cover during the Early to Mid Holocene thermal maximum.

AUTHOR CONTRIBUTIONS

JC undertook pollen and charcoal analyses and wrote the first draft of the manuscript. WF designed the study and revised the final version of the manuscript. SJ undertook pollen and charcoal analyses. PH and MR provided scientific input to the project conception and interpretation of the data. CZ was responsible for the fieldwork, provided multiproxy data and scientific input to the data interpretation. All authors contributed to the preparation and revision of the manuscript.

ACKNOWLEDGMENTS

This study was funded by the Natural Environment Research Council UK (New Investigator Award NE/K000608/1), the German Research Foundation (grant no. DFG ZI 721/9-1), and a School of Environment, Education and Development PhD scholarship to JC. We gratefully acknowledge fieldwork support from the Institut National des Sciences de l'Archéologie

et du Patrimoine (INSAP, Rabat), Caidad d'Azrou and the Centre National d'Hydrobiologie et de Pisciculture. We thank John Moore and Jonathan Yarwood of the Physical Geography Laboratories (University of Manchester) for technical support. We are grateful to Steffen Mischke for helpful comments on the draft manuscript, and to Henry Lamb and Cesar Morales Del Molino whose constructive reviews helped improve the final manuscript.

REFERENCES

- Abdeddaim-Boughanmi, K., and Kaid-Harche, M. (2009). Structure, ultrastructure of the anther, pollen microsporogenesis and morphology of pollen grains of two populations of *Lygeum spartum* L. Algeria. *A. J. Agric. Biol. Sci.* 4, 201–205. doi: 10.3844/ajabssp.2009.201.205
- Abun-Nasr, J. M. (ed.) (1987). *A History of the Maghrib in the Islamic Period*. Cambridge: Cambridge University Press.
- Achhal, A., Akabli, O., Barbero, M., Benabid, A., M'hirit, A., Peyre, C., et al. (1980). A propos de la valeur bioclimatique et dynamique de quelques essences forestières au Maroc. *Ecol. Mediterr.* 5, 211–249.
- Aranbarri, J., González-Sampériz, P., Valero-Garcés, B., Moreno, A., Gil-Romera, G., Sevilla-Callejo, M., et al. (2014). Rapid climatic changes and resilient vegetation during the Lateglacial and Holocene in a continental region of south-western Europe. *Glob. Planet. Change* 114, 50–65. doi: 10.1016/j.gloplacha.2014.01.003
- Arbolea, M. L., Teixell, A., Charroud, M., and Julivert, M. (2004). A structural transect through the High and Middle Atlas of Morocco. *J. Afr. Earth Sci.* 39, 319–327. doi: 10.1016/j.jafrearsci.2004.07.036
- Aussenac, G. (1984). Le Cèdre, essai d'interprétation bioclimatique et écophysiologique. *Bull. Soc. Bot. France Actual. Bot.* 131, 385–398. doi: 10.1080/01811789.1984.10826679
- Barbero, M., Loisel, R., and Quézel, P. (1992). Biogeography, ecology and history of mediterranean *Quercus ilex* ecosystems. *Vegetatio* 99, 19–34. doi: 10.1007/BF00118207
- Barker, P. A., Roberts, N., Lamb, H. F., van der Kaars, S., and Benkaddour, A. (1994). Interpretation of Holocene lake-level change from diatom assemblages in Lake Sidi Ali, Middle Atlas, Morocco. *J. Paleolimnol.* 12, 223–234. doi: 10.1007/BF00678022
- Bell, B. A., and Fletcher, W. J. (2016). Modern surface pollen assemblages from the Middle and High Atlas, Morocco: insights into pollen representation and transport. *Grana* 55, 286–301. doi: 10.1080/00173134.2015.1108996
- Benabid, A. (1982). Bref aperçu sur la zonation altitudinale de la végétation climacique du Maroc. *Ecol. Mediterr.* 8, 301–315.
- Bennett, K. D. (1996). Determination of the number of zones in a biostratigraphical sequence. *New Phytol.* 132, 155–170. doi: 10.1111/j.1469-8137.1996.tb04521.x
- Berger, A., and Loutre, M. F. (1991). Insolation values for the climate of the last 10 million years. *Q. Sci. Rev.* 10, 297–317. doi: 10.1016/0277-3791(91)90033-Q
- Beug, H.-J. (2004). *Leitfaden der Pollenbestimmung für Mitteleuropa und Angrenzende Gebiete*. Munich: Verlag Dr. Friedrich Pfeil.
- Birks, H. H., and Birks, H. J. B. (2006). Multi-proxy studies in palaeolimnology. *Veg. Hist. Archaeobot.* 15, 235–251. doi: 10.1007/s00334-006-0066-6
- Blondel, J. (2006). The 'design' of Mediterranean landscapes: a millennial story of humans and ecological systems during the historic period. *Hum. Ecol.* 34, 713–729. doi: 10.1007/s10745-006-9030-4
- Born, K., Fink, A. H., and Knippertz, P. (2010). "Meteorological processes influencing the weather and climate of Morocco," in *Impacts of Global Change on the Hydrological Cycle in West and Northwest Africa*, eds P. Speth, M. Christoph, and B. Dieckrüger (Berlin: Heidelberg: Springer), 150–163.
- Born, K., Fink, A. H., and Paeth, H. (2008). Dry and wet periods in the northwestern Maghreb for present day and future climate conditions. *Meteorolog. Z.* 17, 533–551. doi: 10.1127/0941-2948/2008/0313
- Bosmans, J. H. C., Drijfhout, S. S., Tuentner, E., Hilgen, F. J., Lourens, L. J., and Rohling, E. J. (2015). Precession and obliquity forcing of the freshwater budget over the Mediterranean. *Q. Sci. Rev.* 123, 16–30. doi: 10.1016/j.quascirev.2015.06.008
- Bronk Ramsey, C. (2008). Deposition models for chronological records. *Q. Sci. Rev.* 27, 42–60. doi: 10.1016/j.quascirev.2007.01.019
- Campbell, J. F. E., Fletcher, W. J., Hughes, P. D., and Shuttleworth, E. L. (2016). A comparison of pollen extraction methods confirms dense-media separation as a reliable method of pollen preparation. *J. Q. Sci.* 31, 631–640. doi: 10.1002/jqs.2886
- Carrión, J. S. (2002). Patterns and processes of Late Quaternary environmental change in a montane region of southwestern Europe. *Q. Sci. Rev.* 21, 2047–2066. doi: 10.1016/S0277-3791(02)00010-0
- Carrión, J. S., Sánchez-Gómez, P., Mota, J. F., Yll, R., and Chaín, C. (2003). Holocene vegetation dynamics, fire and grazing in the Sierra de Gádor, southern Spain. *Holocene* 13, 839–849. doi: 10.1191/0959683603hl662rp
- Cheddadi, R., Fady, B., François, L., Hajar, L., Suc, J. P., Huang, K., et al. (2009). Putative glacial refugia of *Cedrus atlantica* deduced from Quaternary pollen records and modern genetic diversity. *J. Biogeogr.* 36, 1361–1371. doi: 10.1111/j.1365-2699.2008.02063.x
- Cheddadi, R., Lamb, H. F., Guiot, J., and van der Kaars, S. (1998). Holocene climatic change in Morocco: a quantitative reconstruction from pollen data. *Clim. Dyn.* 14, 883–890. doi: 10.1007/s003820050262
- Cheddadi, R., Nourelbait, M., Bouaissa, O., Tabel, J., Rhoujjati, A., López-Sáez, J. A., et al. (2015). A history of human impact on Moroccan mountain landscapes. *Afr. Archaeol. Rev.* 32, 233–248. doi: 10.1007/s10437-015-9186-7
- Comboudieu Nebout, N., Peyron, O., Dormoy, I., Desprat, S., Beaudouin, C., Kotthoff, U., et al. (2009). Rapid climatic variability in the west Mediterranean during the last 25000 years from high resolution pollen data. *Clim. Past* 5, 503–521. doi: 10.5194/cp-5-503-2009
- Cubera, E., and Moreno, G. (2007). Effect of single *Quercus ilex* trees upon spatial and seasonal changes in soil water content in dehesas of central western Spain. *Ann. For. Sci.* 64, 355–364. doi: 10.1051/forest:2007012
- David, T. S., Ferreira, M. I., Cohen, S., Pereira, J. S., and David, J. S. (2004). Constraints on transpiration from an evergreen oak tree in southern Portugal. *Agric. Forest Meteorol.* 122, 193–205. doi: 10.1016/j.agrformet.2003.09.014
- Davis, B. A., Brewer, S., Stevenson, A. C., and Guiot, J. (2003). The temperature of Europe during the Holocene reconstructed from pollen data. *Q. Sci. Rev.* 22, 1701–1716. doi: 10.1016/S0277-3791(03)00173-2
- Dawson, T. P., Jackson, S. T., House, J. I., Prentice, I. C., and Mace, G. M. (2011). Beyond predictions: biodiversity conservation in a changing climate. *Science* 332, 53–58. doi: 10.1126/science.1200303
- De Waele, J., and Melis, M. T. (2009). Geomorphology and geomorphological heritage of the Ifrane–Azrou region (Middle Atlas, Morocco). *Environ. Geol.* 58, 587–599. doi: 10.1007/s00254-008-1533-4
- Diffenbaugh, N. S., and Scherer, M. (2011). Observational and model evidence of global emergence of permanent, unprecedented heat in the 20th and 21st centuries. *Clim. Change* 107, 615–624. doi: 10.1007/s10584-011-0112-y
- Emberger, L. (1939). *Aperçu Général sur la Végétation du Maroc: Commentaire de la Carte Phytogéographique du Maroc 1: 1500000*. Berne: H. Huber.
- Espér, J., Frank, D., Büntgen, U., Verstege, A., Luterbacher, J., and Xoplaki, E. (2007). Long-term drought severity variations in Morocco. *Geophys. Res. Lett.* 34:L17702. doi: 10.1029/2007GL030844
- Finsinger, W., and Tinner, W. (2005). Minimum count sums for charcoal concentration estimates in pollen slides: accuracy and potential errors. *Holocene* 15, 293–297. doi: 10.1191/0959683605hl808rr

- Fletcher, W. J., Boski, T., and Moura, D. (2007). Palynological evidence for environmental and climatic change in the lower Guadiana valley, Portugal, during the last 13 000 years. *Holocene* 17, 481–494. doi: 10.1177/0959683607070727
- Fletcher, W. J., Debret, M., and Goñi, M. F. S. (2013). Mid-Holocene emergence of a low-frequency millennial oscillation in western Mediterranean climate: implications for past dynamics of the North Atlantic atmospheric westerlies. *Holocene* 23, 153–166. doi: 10.1177/0959683612460783
- Fletcher, W. J., and Goñi, M. F. S. (2008). Orbital and sub-orbital-scale climate impacts on vegetation of the western Mediterranean basin over the last 48,000 yr. *Q. Res.* 70, 451–464. doi: 10.1016/j.yqres.2008.07.002
- Fletcher, W. J., and Hughes, P. D. (2017). Anthropogenic trigger for Late Holocene soil erosion in the Jebel Toubkal, High Atlas, Morocco. *Catena* 149, 713–726. doi: 10.1016/j.catena.2016.03.025
- Fletcher, W. J., Zielhofer, C., Mischke, S., Bryant, C., Xu, X., and Fink, D. (2017). AMS radiocarbon dating of pollen concentrates in a karstic lake system. *Q. Geochronol.* 39, 112–123. doi: 10.1016/j.quageo.2017.02.006
- Fyfe, R. M., de Beaulieu, J. L., Binney, H., Bradshaw, R. H., Brewer, S., Le Flao, A., et al. (2009). The European Pollen Database: past efforts and current activities. *Veg. Hist. Archaeobot.* 18, 417–424. doi: 10.1007/s00334-009-0215-9
- Genty, D., Blamart, D., Ghaleb, B., Plagnes, V., Causse, C., Bakalowicz, M., et al. (2006). Timing and dynamics of the last deglaciation from European and North African $\delta^{13}\text{C}$ stalagmite profiles—comparison with Chinese and South Hemisphere stalagmites. *Q. Sci. Rev.* 25, 2118–2142. doi: 10.1016/j.quascirev.2006.01.030
- Giesecke, T., and Fontana, S. L. (2008). Revisiting pollen accumulation rates from Swedish lake sediments. *Holocene* 18, 293–305. doi: 10.1177/0959683607086767
- Gil-Romera, G., Carrión, J. S., Pausas, J. G., Sevilla-Callejo, M., Lamb, H. F., Fernández, S., et al. (2010). Holocene fire activity and vegetation response in South-Eastern Iberia. *Q. Sci. Rev.* 29, 1082–1092. doi: 10.1016/j.quascirev.2010.01.006
- Giner, M. M., García, J. S. C., and Camacho, C. N. (2002). Seasonal fluctuations of the airborne pollen spectrum in Murcia (SE Spain). *Aerobiologia* 18, 141–151. doi: 10.1023/A:1020652525493
- Hajar, L., Khater, C., and Cheddadi, R. (2008). Vegetation changes during the late Pleistocene and Holocene in Lebanon: a pollen record from the Bekaa Valley. *Holocene* 18, 1089–1099. doi: 10.1177/0959683608095580
- Hammer, Ø., Harper, D. A. T., and Ryan, P. D. (2001). PAST: paleontological statistics software package for education and data analysis. *Palaeontol. Electron.* 4, 1–9.
- Jaouadi, S., Lebreton, V., Bout-Roumzeilles, V., Siani, G., Lakhdar, R., Bousoffara, R., et al. (2016). Environmental changes, climate and anthropogenic impact in south-east Tunisia during the last 8 kyr. *Clim. Past* 12, 1339–1359. doi: 10.5194/cp-12-1339-2016
- Jensen, C., Vorren, K. D., and Mørkved, B. (2007). Annual pollen accumulation rate (PAR) at the boreal and alpine forest-line of north-western Norway, with special emphasis on *Pinus sylvestris* and *Betula pubescens*. *Rev. Palaeobot. Palynol.* 144, 337–361. doi: 10.1016/j.revpalbo.2006.08.006
- Knippertz, P., Christoph, M., and Speth, P. (2003). Long-term precipitation variability in Morocco and the link to the large-scale circulation in recent and future climates. *Meteorol. Atmos. Phys.* 83, 67–88. doi: 10.1007/s00703-002-0561-y
- Lamb, H. F., Damblon, F., and Maxted, R. W. (1991). Human impact on the vegetation of the Middle Atlas, Morocco, during the last 5000 years. *J. Biogeogr.* 18, 519–532. doi: 10.2307/2845688
- Lamb, H. F., Eicher, U., and Switsur, V. R. (1989). An 18,000-year record of vegetation, lake-level and climatic change from Tigalmamine, Middle Atlas, Morocco. *J. Biogeogr.* 16, 65–74. doi: 10.2307/2845311
- Lamb, H. F., Gasse, F., and Benkaddour, A. (1995). Relation between century-scale Holocene arid intervals in tropical and temperate zones. *Nature* 373, 134–137. doi: 10.1038/373134a0
- Lamb, H. F., and van der Kaars, S. (1995). Vegetational response to Holocene climatic change: pollen and palaeolimnological data from the Middle Atlas, Morocco. *Holocene* 5, 400–408. doi: 10.1177/095968369500500402
- Lamb, H., Roberts, N., Leng, M., Barker, P., Benkaddour, A., and van der Kaars, S. (1999). Lake evolution in a semi-arid montane environment: response to catchment change and hydroclimatic variation. *J. Paleolimnol.* 21, 325–343. doi: 10.1023/A:1008099602205
- Lelieveld, J., Proestos, Y., Hadjinicolaou, P., Tanarhte, M., Tyrilis, E., and Zittis, G. (2016). Strongly increasing heat extremes in the Middle East and North Africa (MENA) in the 21st century. *Clim. Change* 137, 245–260. doi: 10.1007/s10584-016-1665-6
- Linares, J. C., Pazo-Sarria, R., Taïqui, L., Camarero, J. J., Ochoa, V., Lechuga, V., et al. (2012). Efectos de las tendencias climáticas y la degradación del hábitat sobre el decaimiento de los cedrales (*Cedrus atlantica*) del norte de Marruecos. *Revista Ecosistemas* 21, 7–14. doi: 10.7818/ECOS.2012.21-3.02
- Linares, J. C., Taïqui, L., and Camarero, J. J. (2011). Increasing drought sensitivity and decline of Atlas cedar (*Cedrus atlantica*) in the Moroccan Middle Atlas forests. *Forests* 2, 777–796. doi: 10.3390/f2030777
- Linstädter, A., and Zielhofer, C. (2010). Regional fire history shows abrupt responses of Mediterranean ecosystems to centennial-scale climate change (Olea–Pistacia woodlands, NE Morocco). *J. Arid Environ.* 74, 101–110. doi: 10.1016/j.jaridenv.2009.07.006
- Magri, D. (1994). Late-Quaternary changes of plant biomass as recorded by pollen-stratigraphical data: a discussion of the problem at Valle di Castiglione, Italy. *Rev. Palaeobot. Palynol.* 81, 313–325. doi: 10.1016/0034-6667(94)90115-5
- Markgraf, V. (1980). Pollen dispersal in a mountain area. *Grana* 19, 127–146. doi: 10.1080/00173138009424995
- Mauri, A., Davis, B. A. S., Collins, P. M., and Kaplan, J. O. (2015). The climate of Europe during the Holocene: a gridded pollen-based reconstruction and its multi-proxy evaluation. *Q. Sci. Rev.* 112, 109–127. doi: 10.1016/j.quascirev.2015.01.013
- Mayewski, P. A., Rohling, E. E., Stager, J. C., Karlén, W., Maasch, K. A., Meeker, L. D., et al. (2004). Holocene climate variability. *Q. Res.* 62, 243–255. doi: 10.1016/j.yqres.2004.07.001
- McGregor, H. V., Dupont, L., Stuut, J. B. W., and Kuhlmann, H. (2009). Vegetation change, goats, and religion: a 2000-year history of land use in southern Morocco. *Q. Sci. Rev.* 28, 1434–1448. doi: 10.1016/j.quascirev.2009.02.012
- Medail, F., and Quezel, P. (1997). Hot-spots analysis for conservation of plant biodiversity in the Mediterranean Basin. *Ann. Missouri Bot. Garden* 84, 112–127. doi: 10.2307/2399957
- Menjour, F., Amraoui, F., and Rémml, T. (2016). “Assessment of the spatio-temporal evolution of Aguelmam Sidi Ali Lake using multitemporal Landsat Imagery (Middle Atlas-Morocco),” in *6th International Conference on Cartography and GIS*, eds T. Bandrova and M. Konecny (Sofia: Bulgarian Cartographic Association), 588–597.
- Moore, P. D., Webb, J. A., and Collison, M. E. (1991). *Pollen Analysis*. Oxford: Blackwell Scientific Publications.
- Morales-Molino, C., Tinner, W., García-Antón, M., and Colombaroli, D. (2017). The historical demise of *Pinus nigra* forests in the Northern Iberian Plateau (south-western Europe). *J. Ecol.* 105, 634–646. doi: 10.1111/1365-2745.12702
- Moritz, C., and Agudo, R. (2013). The future of species under climate change: resilience or decline? *Science* 341, 504–508. doi: 10.1126/science.1237190
- Nogués-Bravo, D., Araújo, M. B., Errea, M. P., and Martínez-Rica, J. P. (2007). Exposure of global mountain systems to climate warming during the 21st Century. *Glob. Environ. Change* 17, 420–428. doi: 10.1016/j.gloenvcha.2006.11.007
- Nourelbait, M., Rhoujjati, A., Benkaddour, A., Carré, M., Eynaud, F., Martínez, P., et al. (2016). Climate change and ecosystems dynamics over the last 6000 years in the Middle Atlas, Morocco. *Clim. Past* 12, 1029–1042. doi: 10.5194/cp-12-1029-2016
- Nourelbait, M., Rhoujjati, A., Eynaud, F., Benkaddour, A., Dezileau, L., Wainer, K., et al. (2014). An 18 000-year pollen and sedimentary record from the cedar forests of the Middle Atlas, Morocco. *J. Q. Sci.* 29, 423–432. doi: 10.1002/jqs.2708
- Ozenda, P. (1975). Sur les étages de végétation dans les montagnes du bassin méditerranéen. *Docum. Cartogr. Ecol.* 16, 1–32.
- Parmesan, C. (2006). Ecological and evolutionary responses to recent climate change. *Annu. Rev. Ecol. Evol. Syst.* 37, 637–669. doi: 10.1146/annurev.ecolsys.37.091305.110100

- Peguero-Pina, J. J., Sancho-Knapik, D., Barrón, E., Camarero, J. J., Vilagrosa, A., and Gil-Pelegrín, E. (2014). Morphological and physiological divergences within *Quercus ilex* support the existence of different ecotypes depending on climatic dryness. *Ann. Bot.* 114, 301–313 doi: 10.1093/aob/mcu108
- Prentice, I. C. (1985). Pollen representation, source area, and basin size: toward a unified theory of pollen analysis. *Q. Res.* 23, 76–86. doi: 10.1016/0033-5894(85)90073-0
- Reddad, H., Etabaai, I., Rhoujjati, A., Taieb, M., Thevenon, F., and Damnati, B. (2013). Fire activity in North West Africa during the last 30,000 cal years BP inferred from a charcoal record from Lake Ifrah (Middle atlas–Morocco): climatic implications. *J. Afr. Earth Sci.* 84, 47–53. doi: 10.1016/j.jafrearsci.2013.03.007
- Reille, M. (1976). Analyse pollinique de sédiments postglaciaires dans le Moyen-Atlas et le Haut-Atlas marocains: premiers résultats. *Ecol. Mediterr.* 2, 153–170.
- Reille, M. (1992). *Pollen et Spores d'Europe et d'Afrique du Nord*. Marseille: Laboratoire de Botanique historique et Palynologie.
- Reimer, P. J., Bard, E., Bayliss, A., Beck, J. W., Blackwell, P. G., Ramsey, C. B., et al. (2013). IntCal13 and Marine13 radiocarbon age calibration curves 0–50,000 years cal BP. *Radiocarbon* 55, 1869–1887. doi: 10.2458/azu_js_rc.55.16947
- Renssen, H., Seppä, H., Heiri, O., Roche, D. M., Goosse, H., and Fichetef, T. (2009). The spatial and temporal complexity of the Holocene thermal maximum. *Nat. Geosci.* 2, 411–414. doi: 10.1038/ngeo513
- Rhanem, M. (2009). L'alfa (*Stipa tenacissima* L.) dans la plaine de Midelt (haut bassin versant de la Moulouya, Maroc)—Éléments de climatologie. *Physio-Géo*. 3, 1–20.
- Rhanem, M. (2011). Aridification du climat régional et remontée de la limite inférieure du cèdre de l'Atlas (*Cedrus atlantica* Manetti) aux confins de la plaine de Midelt (Maroc). *Physio-Géo* 5, 143–165.
- Rhoujjati, A., Cheddadi, R., Taïeb, M., Baali, A., and Ortu, E. (2010). Environmental changes over the past c. 29,000 years in the Middle Atlas (Morocco): a record from Lake Ifrah. *J. Arid Environ.* 74, 737–745. doi: 10.1016/j.jaridenv.2009.09.006
- Rohling, E. J., and Pälike, H. (2005). Centennial-scale climate cooling with a sudden cold event around 8,200 years ago. *Nature* 434, 975–979. doi: 10.1038/nature03421
- Rubiales, J. M., Morales-Molino, C., Álvarez, S. G., and García-Antón, M. (2012). Negative responses of highland pines to anthropogenic activities in inland Spain: a palaeoecological perspective. *Veg. Hist. Archaeobot.* 21, 397–412. doi: 10.1007/s00334-011-0330-2
- Rull, V., López-Sáez, J. A., and Vegas-Vilarrúbia, T. (2008). Contribution of non-pollen palynomorphs to the paleolimnological study of a high-altitude Andean lake (Laguna Verde Alta, Venezuela). *J. Paleolimnol.* 40, 399–411. doi: 10.1007/s10933-007-9169-z
- Samartin, S., Heiri, O., Joos, F., Renssen, H., Franke, J., Brönnimann, S., et al. (2017). Warm Mediterranean Mid Holocene summers inferred from fossil midge assemblages. *Nat. Geosci.* 10, 207–212. doi: 10.1038/ngeo2891
- Sayad, A., Chakiri, S., Martin, C., Bejjaji, Z., and Echarfaoui, H. (2011). Effet des conditions climatiques sur le niveau du lac Sidi Ali (Moyen Atlas, Maroc). *Physio-Géo*. 5, 251–268.
- Schwörer, C., Gavin, D. G., Walker, I. R., and Hu, F. S. (2017). Holocene tree line changes in the Canadian Cordillera are controlled by climate and topography. *J. Biogeogr.* 44, 1148–1159. doi: 10.1111/jbi.12904
- Seppä, H., and Hicks, S. (2006). Integration of modern and past pollen accumulation rate (PAR) records across the arctic tree-line: a method for more precise vegetation reconstructions. *Q. Sci. Rev.* 25, 1501–1516. doi: 10.1016/j.quascirev.2005.12.002
- Stockmarr, J. (1971). Tablets with spores used in absolute pollen analysis. *Pollen Spores* 13, 615–621.
- Tabel, J., Khater, C., Rhoujjati, A., Dezileau, L., Bouimetarhan, I., Carre, M., et al. (2016). Environmental changes over the past 25 000 years in the southern Middle Atlas, Morocco. *J. Q. Sci.* 31, 93–102. doi: 10.1002/jqs.2841
- Tinner, W., Colombaroli, D., Heiri, O., Henne, P. D., Steinacher, M., Untenecker, J., et al. (2013). The past ecology of *Abies alba* provides new perspectives on future responses of silver fir forests to global warming. *Ecol. Monogr.* 83, 419–439. doi: 10.1890/12-2231.1
- Vaz, M., Pereira, J. S., Gazarini, L. C., David, T. S., David, J. S., Rodrigues, A., et al. (2010). Drought-induced photosynthetic inhibition and autumn recovery in two Mediterranean oak species (*Quercus ilex* and *Quercus suber*). *Tree Physiol.* 30, 946–956. doi: 10.1093/treephys/tpq044
- Wanner, H., Solomina, O., Grosjean, M., Ritz, S. P., and Jetel, M. (2011). Structure and origin of Holocene cold events. *Q. Sci. Rev.* 30, 3109–3123. doi: 10.1016/j.quascirev.2011.07.010
- Zielhofer, C., Fletcher, W. J., Mischke, S., De Batist, M., Campbell, J. F., Joannin, S., et al. (2017a). Atlantic forcing of Western Mediterranean winter rain minima during the last 12,000 years. *Q. Sci. Rev.* 157, 29–51. doi: 10.1016/j.quascirev.2016.11.037
- Zielhofer, C., von Suchodoletz, H., Fletcher, W. J., Schneider, B., Dietze, E., Schlegel, M., et al. (2017b). Millennial-scale fluctuations in Saharan dust supply across the decline of the African Humid Period. *Q. Sci. Rev.* 171, 119–135. doi: 10.1016/j.quascirev.2017.07.010

Conflict of Interest Statement: The authors declare that the research was conducted in the absence of any commercial or financial relationships that could be construed as a potential conflict of interest.

Copyright © 2017 Campbell, Fletcher, Joannin, Hughes, Rhanem and Zielhofer. This is an open-access article distributed under the terms of the Creative Commons Attribution License (CC BY). The use, distribution or reproduction in other forums is permitted, provided the original author(s) or licensor are credited and that the original publication in this journal is cited, in accordance with accepted academic practice. No use, distribution or reproduction is permitted which does not comply with these terms.



Pollen, People and Place: Multidisciplinary Perspectives on Ecosystem Change at Amboseli, Kenya

Esther N. Githumbi^{1*}, Rebecca Kariuki¹, Anna Shoemaker², Colin J. Courtney-Mustaphi^{1,2}, Maxmillian Chuhilla³, Suzi Richer^{1,4}, Paul Lane^{2,5} and Rob Marchant¹

¹ Environment Department, York Institute for Tropical Ecosystems, University of York, York, United Kingdom, ² Department of Archaeology and Ancient History, Uppsala University, Uppsala, Sweden, ³ Department of History, University of Dar es Salaam, Dar es Salaam, Tanzania, ⁴ Department of Archaeology, University of York, York, United Kingdom, ⁵ School of Geography, Archaeology and Environmental Studies, University of the Witwatersrand, Johannesburg, South Africa

OPEN ACCESS

Edited by:

Encarni Montoya,
Instituto de Ciencias de la Tierra
Jaume Almera (CSIC), Spain

Reviewed by:

Charlotte Sarah Miller,
Zentrum für Marine
Umweltwissenschaften, Universität
Bremen, Germany
Alberto Saez,
University of Barcelona, Spain

*Correspondence:

Esther N. Githumbi
esthergithumbi@gmail.com

Specialty section:

This article was submitted to
Quaternary Science, Geomorphology
and Paleoenvironment,
a section of the journal
Frontiers in Earth Science

Received: 28 September 2017

Accepted: 26 December 2017

Published: 25 January 2018

Citation:

Githumbi EN, Kariuki R, Shoemaker A,
Courtney-Mustaphi CJ, Chuhilla M,
Richer S, Lane P and Marchant R
(2018) Pollen, People and Place:
Multidisciplinary Perspectives on
Ecosystem Change at Amboseli,
Kenya. *Front. Earth Sci.* 5:113.
doi: 10.3389/feart.2017.00113

This study presents a multidisciplinary perspective for understanding environmental change and emerging socio-ecological interactions across the Amboseli region of southwestern Kenya. We focus on late Holocene (<5,000 cal yr. BP) changes and continuities reconstructed from sedimentary, archeological, historical records and socio-ecological models. We utilize multi-disciplinary approaches to understand environmental-ecosystem-social interactions over the *longue durée* and use this to simulate different land use scenarios supporting conservation and sustainable livelihoods using a socio-ecological model. Today the semi-arid Amboseli landscape supports a large livestock and wildlife population, sustained by a wide variety of plants and extensive rangelands regulated by seasonal rainfall and human activity. Our data provide insight into how large-scale and long-term interactions of climate, people, livestock, wildlife and external connections have shaped the ecosystems across the Amboseli landscape. Environmental conditions were dry between ~5,000 and 2,000 cal yr. BP, followed by two wet periods at ~2,100–1,500 and 1,400–800 cal yr. BP with short dry periods; the most recent centuries were characterized by variable climate with alternative dry and wet phases with high spatial heterogeneity. Most evident in paleo and historical records is the changing woody to grass cover ratio, driven by changes in climate and fire regimes entwined with fluctuating elephant, cattle and wild ungulate populations moderated by human activity, including elephant ivory trade intensification. Archeological perspectives on the occupation of different groups (hunter-gatherers, pastoralists, and farmers) in Amboseli region and the relationships between them are discussed. An overview of the known history of humans and elephants, expanding networks of trade, and the arrival and integration of metallurgy, livestock and domesticated crops in the wider region is provided. In recent decades, increased runoff and flooding have resulted in the expansion of wetlands and a reduction of woody vegetation, compounding problems created by increased enclosure and privatization of these landscapes. However, most

of the wetlands outside of the protected area are drying up because of the intensified water extraction by the communities surrounding the National Park and on the adjacent mountains areas, who have increased in numbers, become sedentary and diversified land use around the wetlands.

Keywords: Africa, groundwater, land cover, land use, paleovegetation, protected areas, vegetation, wetlands

INTRODUCTION

Palynological expeditions have been undertaken in East Africa for over 80 years with the first publication of results, by Dubois and Dubois, appearing in 1939 (Van Zinderen and Coetzee, 1988) followed in 1948 by Hedberg and his “Swedish East Africa Expedition” which collected samples from Lake Victoria, Lake Tanganyika, Mt. Kenya and the Ruwenzori Mountains (Fries and Fries, 1948). Early palynological work in eastern Africa described Pleistocene to Holocene-aged lacustrine and peat sediment sequences, largely collected from mesic and wet regions in montane western Uganda (Osmaston, 1958, 1965; Livingstone, 1962, 1967; Morrison, 1968) and the Kenyan highlands (Cherangani Hills, Van Zinderen, 1962; Mount Kenya, Coetzee, 1964, 1967). These early studies focused on Afromontane taxa timing and response to climatic variability during the Late Pleistocene glacial retreat and subsequent broad-scale at the Late Pleistocene-Early Holocene transition (Livingstone, 1967; Morrison, 1968). Further research used pollen data to chart anthropogenic deforestation of Afromontane forests to explain vegetation changes (Morrison and Hamilton, 1974; Hamilton, 1982; Hamilton et al., 1986; Perrott, 1987). Pollen results from longer sequences found that these forests had previously expanded, as Afromontane glaciers coverage increased leading into the global Last Glacial Maximum (Bonnefille and Riollet, 1988). Montane vegetation patterns were described as altitudinal bands (Mackinder, 1900; Fries and Fries, 1948; Hedberg, 1951), but further examination of pollen records and forest biogeographies showed a high degree of complexity in montane forests from the lower montane to forest-ericaceous zone transitions and non-linearity in vegetation responses to climatic variability (Bussmann and Beck, 1995a,b; Hemp, 2006a,b; Platts et al., 2013). A review by Van Zinderen and Coetzee (1988) broadly summarizes the last 32,000 cal yr. BP of East Africa as warm and humid (32,000–20,000 cal yr. BP), cool and dry from 20,000 to 14,000 cal yr. BP, warm and dry until 12,000 cal yr. BP, warm and humid from 12,000 cal yr. BP to 4,000 cal yr. BP and then regionally arid from 4,000 cal yr. BP.

Examinations of climate and anthropogenic modifications to montane forests in East Africa remains an important topic to which modern ecology, geoarcheology, and pollen studies continue to contribute (Finch and Marchant, 2011; Heckmann, 2014; Heckmann et al., 2014; Finch et al., 2016). The increase in the number of paleorecords and proxies in recent years, as well as wide-ranging reference collections, has led to interpretations that are more complex as well as a better understanding of the drivers of the changes observed in the records. Notable topics of interest have been the influences of increasing atmospheric CO₂ concentrations on vegetation changes over the latter

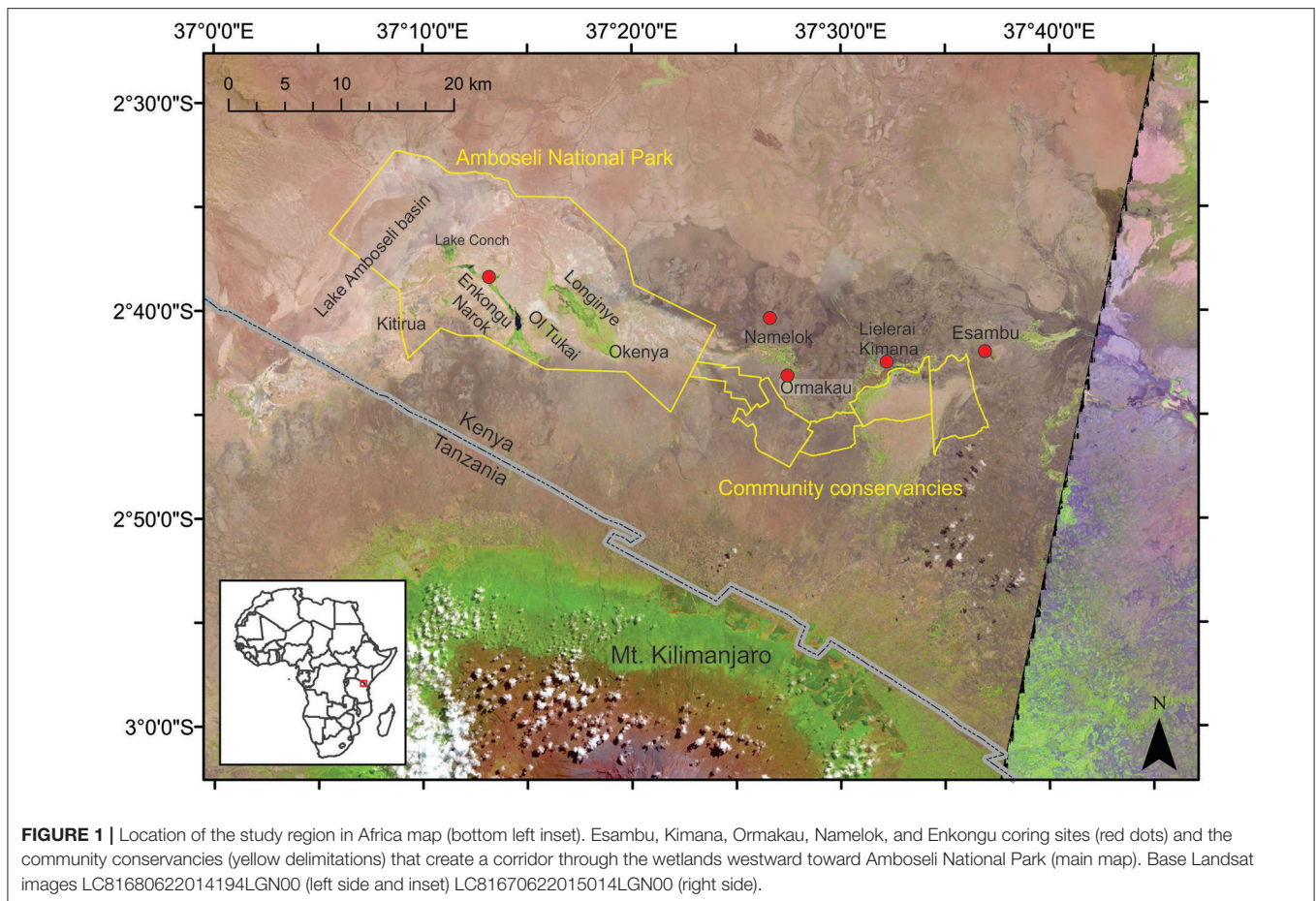
millennia of the Late Pleistocene and into the Holocene (Jolly and Haxeltine, 1997), and the effects of disturbances like fire (Bussmann, 2001; Hemp and Beck, 2001; Rucina et al., 2010; Finch et al., 2016). Further palynological investigations have focused on long-term deposits in lakes that provide Late Quaternary vegetation histories (DeBusk, 1998; Nelson et al., 2012) and on small lakes and wetland sites to reveal high-resolution environmental histories from the late Holocene to present (Muiruri, 2008; Rucina et al., 2010; Colombaroli et al., in press). Although few in number, there is a growing number of co-located study sites linking high-resolution paleoenvironmental data with archeological sites to build concise descriptions of human-environmental interactions during the late Holocene (Robertshaw, 1997; Lejju et al., 2003, 2005; Taylor et al., 2005; Iles et al., 2014).

Building on these previous studies, this paper summarizes the integrated results of several studies of the Amboseli area of southern Kenya, equatorial eastern Africa (**Figure 1**). By combining newly collated and analyzed palynological, archeological and historical data sets with longitudinal socio-ecological data generated by previous research we provide fresh insights into the origins and drivers of spatial heterogeneity in this semi-arid savannah ecosystem and its temporal variability over the last several thousand years. In particular, we first review (I) pollen-based reconstructions of Holocene vegetation and environmental change in Amboseli, and (II) archeological and historical evidence for changes and continuities in livelihood strategies and land use management practices within Amboseli, and between Mt Kilimanjaro and Amboseli communities, before going on to (III) combine insights drawn from different data sources to model impacts of land use choices in Amboseli with data from the last 50 years. Given the rapidity of land cover change in the area and current challenges surrounding human-ecosystem-climate interactions in Amboseli, a particular concern is to demonstrate how knowledge of the historical ecology of this landscape can contribute to sustainable land use management and conservation, which forms the focus of our concluding discussion.

Physiography of Amboseli

Located north of Kilimanjaro (**Figure 1**), the Amboseli basin formed through isostatic down warping of country rock due to the mass of the Kilimanjaro volcano upon the crust (Pickford, 1986). Regional lithology can be divided into three major groups (Touber et al., 1983):

1. The Precambrian metamorphic basement rocks present across much of the northern region (Williams, 1972).
2. Late Pleistocene lacustrine-derived plain and clayey, alkaline soils of the Amboseli Lake bed, which were deposited under



wetter-than-present conditions; these soils are comprised of impure limestone, marls, and local diatomite, with sepiolitic clays near springs and minor inputs of volcanic ash (Williams, 1972; Stoessell and Hay, 1978; Hay and Stoessell, 1984).

3. Tertiary to Quaternary volcanic rocks and lavas around the footsteps of Mt. Kilimanjaro and reworked Pleistocene pyroclastic deposits elsewhere in the southern part of the region.

Hydrology in Amboseli is controlled by climate, geology, and topography. Groundwater originates from Kilimanjaro and supply is controlled by fractures, rock porosity, and drainage network. Rainfall within the lower elevations of the Amboseli watershed is currently about 350 mm per year concentrated within two rainy seasons (November to January and March to May), with a negative evapotranspiration-precipitation budget with warm mean temperatures (21–25°C) and a range of 12–35°C (Meijerink and Van Wijngaarden, 1997; Altmann et al., 2002; Worden et al., 2003). Hydrological models estimate that spring discharge could exist at 1,450 m asl on the slopes of Mt. Kilimanjaro (Meijerink and Van Wijngaarden, 1997), and wetlands persist currently at elevations between 1,150 and 1,250 m asl. Lake Amboseli (1,125 m asl) is recharged by diffuse flows from groundwater seepage and minor surface flow from the Namanga and Sinet Rivers (Meijerink and Van Wijngaarden,

1997). Currently, the lake ephemerally fills with shallow water, but geological evidence suggests the lake was much larger and deeper during most of the Late Pleistocene (100,000–20,000 cal yr. BP) concomitant with higher water levels at Lake Challa (Williams, 1972; Moernaut et al., 2010). Since the end of the Last Glacial Maximum, eastern Africa has experienced high hydroclimatic variability evidenced by fluctuating lake levels owing to wetter intervals and arid phases (Nicholson and Yin, 2001; Kiage and Liu, 2006; Verschuren and Charman, 2008; Moernaut et al., 2010; Tierney et al., 2011) likely resulting in highly variable water depths at Lake Amboseli with the possibility of intermittent desiccation (Stager and Johnson, 2008). To date, however, there are no detailed paleolimnological studies of Lake Amboseli either to constrain the ages of the lacustrine deposits or to reconstruct past water depth through paleo shoreline mapping. Boreholes (Williams, 1972) have not ascertained the maximum depth of the lacustrine deposits above the basement metamorphic rocks.

Currently, the Amboseli groundwater levels have been increasing since the 1950s, caused by neo-tectonism increasing the outflow of the deeper diffuse part of the flow system and increased runoff caused by overgrazing in the catchment, without a corresponding increase in long-term rainfall (Meijerink and Van Wijngaarden, 1997). This contributed to localized tree

mortalities (*Acacia*) due to increased salt concentration and hydric soils but, not enough water to re-fill of the Lake Amboseli Basin. Riverine wetlands persist on flat topographies where river flows can overbank as flow slows down and broadens and hydric soils are maintained by high groundwater levels. Some of these wetlands, such as Kimana, are supplemented by groundwater seeps and springs, whereas others are primarily sourced from them, e.g., Enkongu.

Controls on the characteristics of wetlands result from interactions between local and regional environmental drivers. For Amboseli, regional-scale drivers include hydroclimatic variability, degree of forest cover and land use type on Kilimanjaro. Local-scale drivers include micro-topographic gradients, animals and anthropogenic activity, which contribute to the geohydrology through trampling, wading and wallowing, creation of wells and digging into springs. As well as influencing vegetation in the catchment, these processes can change surface and subsurface hydrology and forest-atmosphere exchanges in montane elevations. High wildlife and livestock grazing intensities in the area have been suggested as drivers of watershed vegetation changes and increased surface channeling during short wet periods (Meijerink and Van Wijngaarden, 1997; Western and Maitumo, 2004). The changing nature of the agro-pastoral-protected area economic system in the region has also contributed to land cover and wetland changes (Western and Van Praet, 1973; Worden et al., 2003).

Paleoenvironmental Prospects in Semi-arid Amboseli

Pollen records provide information of past vegetation compositional changes and can be used to explore interacting environmental and anthropogenic drivers of land cover change. Currently, there are 14 records of late Holocene vegetation change in semi-arid savannah ecosystems of eastern Africa (Table 1). Amboseli, being a semi-arid region and prone to both multi-year wetter and drier phases, poses multiple challenges and opportunities for paleoenvironmental reconstructions (Pigati et al., 2014). Sedimentological and glacial studies from the highlands of Kilimanjaro provide a long-term context for change in the lowlands (Thompson et al., 2002; Zech, 2006; Zech et al., 2011; Schüller et al., 2012), but offer limited insights regarding environmental change at a local scale in Amboseli, or at a fine temporal scale, both of which are of interest to various stakeholders, including current inhabitants, conservation workers, land managers, and demographers.

Paleobotanical studies of semi-arid ecosystem deposits from older analogous sedimentary sequences, such as those of Olduvai, can be used to interpret current changes at Amboseli. Wetland deposits on low gradient landscapes exposed in 1.85 million year old rock at Olduvai Gorge, Tanzania, suggest that permanently saturated ground from groundwater seepage can persist through arid climate periods and fill with shallow standing water during wetter climates (Ashley et al., 2016). At Olduvai, these landscape features are associated with bone deposit evidence suggesting continued potential for exploitation by mammal and proto-human populations (Magill et al., 2012a,b; Ashley et al., 2016).

One inference from such studies is that the spatial complexity of the landscape combined with temporal complexity provides an environment that is rich in research potential yet patchy. Paleoenvironmental records therefore require integration of different data sets to capture more of the spatiotemporal variability necessary for understanding these environmental complexities in relation to human land use and land cover modifications.

Paleoenvironmental studies have been published on ecosystem change in the lowlands surrounding Mt. Kilimanjaro, including Lake Challa (Blaauw et al., 2010; Nelson et al., 2012; Barker et al., 2013) and Namelok wetland (Rucina et al., 2010). These studies provide evidence of late Holocene environmental change at a decadal to centennial scale and are being complemented by ongoing sedimentological (Githumbi et al., 2016) and multidisciplinary historical ecology studies (Courtney-Mustaphi et al., 2015). Several spatially isolated, perennial and ephemeral wetlands persist across Amboseli today (Table 2). These wetlands are topographically divided at 1,250 m asl causing groundwater and channelized flowing westward to Lake Amboseli or eastward toward the Chyulu Hills.

The wetlands are maintained by groundwater seepage, springs and runoff. Wetland hydro geomorphology is modified by wetting and drying cycles, herbivores (Laws, 1968; Murray-Rust, 1972; McCarthy et al., 1998; Deocampo, 2002), and anthropogenic modifications (Murray-Rust, 1972; Rapp et al., 1972; Payton et al., 1992). Hydrology, topography, pedology, lithology, vegetation, and land-use types and intensities (Poesen et al., 2010) control surface channeling, uphill gully erosion and erosion. These interacting long-term processes include top-down hydroclimatic controls and local scale bottom-up controls of micro-topography, geology, animals, and people, forming a very complex and heterogeneous landscape. These processes present two main challenges for paleoenvironmental reconstruction studies: interruptions in sediment accumulation rates and reworking of previously deposited sediments. Hydroclimatic conditions can result in periods of lower water levels (regression) leading to no deposition and/or subaqueous or subaerial redeposition of sediments resulting in stratigraphic hiatuses. Bioturbation by mega herbivores, invertebrates and plants can also contribute to crosscutting and reworking of sediments. Bioturbation by plant roots and formation of rhizoliths are common characteristics of sedimentary deposits from the margin of paleowetlands in arid environments (Mount and Cohen, 1984; Liutkus and Ashley, 2003; Liutkus et al., 2005).

Methodology

This paper applied a quantitative and qualitative multi-proxy approach. They study involved radiocarbon dating, pollen and charcoal analysis, archeological surveys, analysis of documentary and oral historical sources and agent based modeling (ABM). Through combined pollen and charcoal analysis, and archeological and historical research we were able to track the extent to which humans, climate, livestock and wildlife have shaped the course of ecosystem dynamics in the Amboseli landscape. Charcoal and pollen samples were analyzed to get an in-depth understanding of the interactions and dynamics

TABLE 1 | Main data from paleovegetation studies derived from woody savannah ecosystems in eastern Africa.

Site	Coordinates	Elevation (m asl)	Age (cal yr. BP)	Deposit	Proxies	References
Kanderi	–3.363167, 38.672500	490	1,400	Palustrine	Pollen	Gillson, 2004
Challa	–3.315319, 37.697170	886	25,000	Lacustrine	Pollen groups, macro-, microcharcoal	Nelson et al., 2012
Ziwani	–3.390177, 37.788068	910	350	Palustrine	Pollen, microcharcoal	Gillson, 2006
Loboi	0.365034, 36.045882	1,010	700	Palustrine	Pollen, geochemistry	Ashley et al., 2004
Enkongu Narok	–2.704661, 37.260777	1,136	2,000	Palustrine	Pollen, macrocharcoal, LOI	Githumbi, 2017
Simbi	–0.367568, 34.628954	1,146	1,200 (and 5,000)	Lacustrine	Pollen, macrocharcoal, grass cuticles, phytoliths	Mworia-Maitima, 1997; Colombaroli et al., in press
Namelok	–2.706910, 37.456199	1,160	2,700	Palustrine	Pollen	Rucina et al., 2010
Ormakau	–2.717633, 37.456183	1,173	2,700	Palustrine	Macrocharcoal	Githumbi, 2017
Esambu	–2.711914, 37.554358	1,196	5,000	Palustrine	Pollen, macrocharcoal	Githumbi et al., 2017
Marura	0.022312, 36.918494	1,770	2,200	Palustrine	Pollen, NPP, microcharcoal	Muiruri, 2008
Rumuruti	0.319504, 36.596227	1,800	1,200	Palustrine	Pollen, NPP, microcharcoal	Muiruri, 2008
Naivasha	–0.768564, 36.410367	1,880	1,100	Lacustrine	Pollen	Lamb et al., 2003
Loitigon	0.737778, 36.465556	1,900	6,800	Fluvial, soil	Pollen, charcoal, organic carbon	Taylor et al., 2005
Kimana	2.748833, 37.515367	1,222	1,200	Palustrine	Pollen, macrocharcoal, LOI, PSD, ITRAX-XRF	Githumbi, 2017

LOI, Loss on ignition analysis; NPP, non-pollen palynomorphs; PSD, particle size distributions; XRF, X-ray fluorescence; Microcharcoal, pollen slide counts of charcoal; macrocharcoal, wet sieved charcoal counts (> 125 μ m).

TABLE 2 | List of important wetlands in eastern Amboseli, arranged by elevation.

Name	Coordinates	Elevation	Area (ha)	Inflow	Outflow	Vegetation
WESTWARD FLOW						
Namelok	–2.706, 37.456	1,180–1,150	1,000	Spring, channel	Evaporative	Poaceae, Cyperaceae, <i>Typha</i> , <i>Acacia</i>
Loginya	–2.703, 37.315	1,138–1,130	2,000	Spring	Channel	Cyperaceae
OI-Tukai Orok	–2.682, 37.265	1,135	450	Groundwater seep	Evaporative	Cyperaceae
Enkongu Narok	–2.704, 37.260	1,134	710	Spring	Channel	Cyperaceae
Lake Amboseli	–2.630, 37.110	1,125	15,600	Channel	Evaporative, infiltration	Barren, Poaceae, Cyperaceae
EASTWARD FLOW						
Lielera Kimana	–2.272, 37.527	1,220	800	Spring, seep, channel	Channel	Poaceae, Cyperaceae, <i>Typha</i> , <i>Acacia</i>
Lenkati	–2.739, 37.514	1,060	750	Channel	Channel, evaporative	Poaceae, Cyperaceae, <i>Typha</i> , <i>Acacia</i>
Olgarua Esoitpus	–2.739, 37.753	1,040–1,025	300	Channel or springs	Evaporative, channel	Poaceae, Cyperaceae

Areal estimates based on hydric soil fringe of wetlands using Google Earth imagery collected on 24 February 2016.

in the landscape. While pollen and charcoal analysis provided a deep understanding over a longue durée, historical methods were useful for understanding contemporary and more recent dynamics.

Coring

Site selection for this study was based on the depth and availability of a sedimentary archive. A suitable coring spot was determined by probing with fiberglass rods to locate the thickest sediment accumulation. The cores were retrieved using a Russian D-shaped corer (Jowsey, 1966) in 50 cm drives with 10 cm overlapped sections. Cores were transferred to PVC tubes, wrapped in plastic film and aluminum foil, shipped to the University of York, UK, and refrigerated at 4°C. Sediment cores were collected from seven locations (Table 3) in different Amboseli wetlands, of which five sites have been radiocarbon dated (Figure 2 and Table S1). Pollen analysis was carried out on

4 cores and 138 pollen types identified from Esambu, Namelok, Enkongu and Kimana swamps.

Radiocarbon Dating

Bulk sediment samples were sampled from the sediment cores for radiocarbon dating, as there were no macrofossils present to pick for dating except one *Acacia* spp. wood fragment from the Esambu sediment. The bulk sediment samples were picked from each of the cores for radiocarbon dating at Direct AMS, the NERC Radiocarbon Facility-East Kilbride and the SUERC AMS Laboratory for ^{14}C analysis. Six samples were selected from the Esambu sediment core; four from Namelok, seven samples were picked from the Kimana core, six from the Ormakau core and six from the Enkongu site. The samples were selected from sections where there was a change in sedimentary features such as texture and color. The number of samples selected for dating were limited by budgetary constraints.

TABLE 3 | List of sediment cores collected from Amboseli wetlands using a hand-operated, D-shaped barrel (5 cm diameter) Russian peat corer (Jowsey, 1966).

Core name	Core length (cm)	Coring year	Basal age (cal yr. BP)	No. of dates	Coordinates	Elevation (m asl)	Sediments
Enkongu Narok	195	2009	2,002	6	−2.704661, 37.260777	1,136	Massive organic silty gyttja, low organic content at base
Olondare	250	2009	NA	0	−2.703064, 37.314742	1,138	Massive organic silty gyttja
Isinet	420	2009	NA	0	−2.748964, 37.514486	1,222	Massive organic silty gyttja
Esambu	247.5	2009	4,500	5	−2.711914, 37.554358	1,196	Massive organic silty gyttja, low organic content at base
Namelok	400	2005	2,500	4	−2.706910, 37.456199	1,161	Massive organic silty gyttja
Ormakau	304	2014	2,700	5	−2.717633, 37.456183	1,173	Massive organic silty gyttja
Kimana Sanctuary	384	2014	1,500	4	2.748833, 37.515367	1,222	Massive organic silty gyttja

The IntCal13 curve (Reimer et al., 2013) was used to calibrate the dates and presented in calibrated year BP (AD 1950) with the year 1950 chosen as it was around the time the first ^{14}C dates were obtained (Birks et al., 2012). An age-depth model was developed for each site using BACON (Blaauw et al., 2010). The priors set were different for each age-depth model, for Kimana the minimum depth was set as 0 cm and maximum depth as 384 cm, the accumulation mean (acc.mean) was changed to 2 yr/cm as suggested by BACON during the analysis, a run of cal BP and calibrated ^{14}C dates were used to run the model with 77.5 sections, acc.shape:1.5, mem.strength:4 and mem.mean:0.7 to produce the age-depth model. The Enkongu priors were set as minimum depth = 0 cm, maximum depth = 195 cm, acc.shape:1.5, acc.mean:20, mem.strength:4 and mem.mean:0.7. The Ormakau priors were set at minimum depth = 0 cm, maximum depth = 304 cm, acc.shape:1.5, acc.mean:10, mem.strength:4 and mem.mean:0.7 and 61.5 sections using a run of cal BP and calibrated ^{14}C dates. The Esambu age-depth model was developed with minimum depth = 0 cm, maximum depth = 247.5 cm, acc.shape:1.5, acc.mean:20, mem.strength:4 and mem.mean:0.7 and 49 sections using a run of cal BP and calibrated ^{14}C dates. An age-depth model was developed for Namelok, the priors were; minimum depth = 0 cm, maximum depth = 400 cm, acc.shape:1.5, acc.mean:10, mem.strength:4 and mem.mean:0.7 and 75 sections using a run of cal BP and calibrated ^{14}C dates.

Pollen Analysis

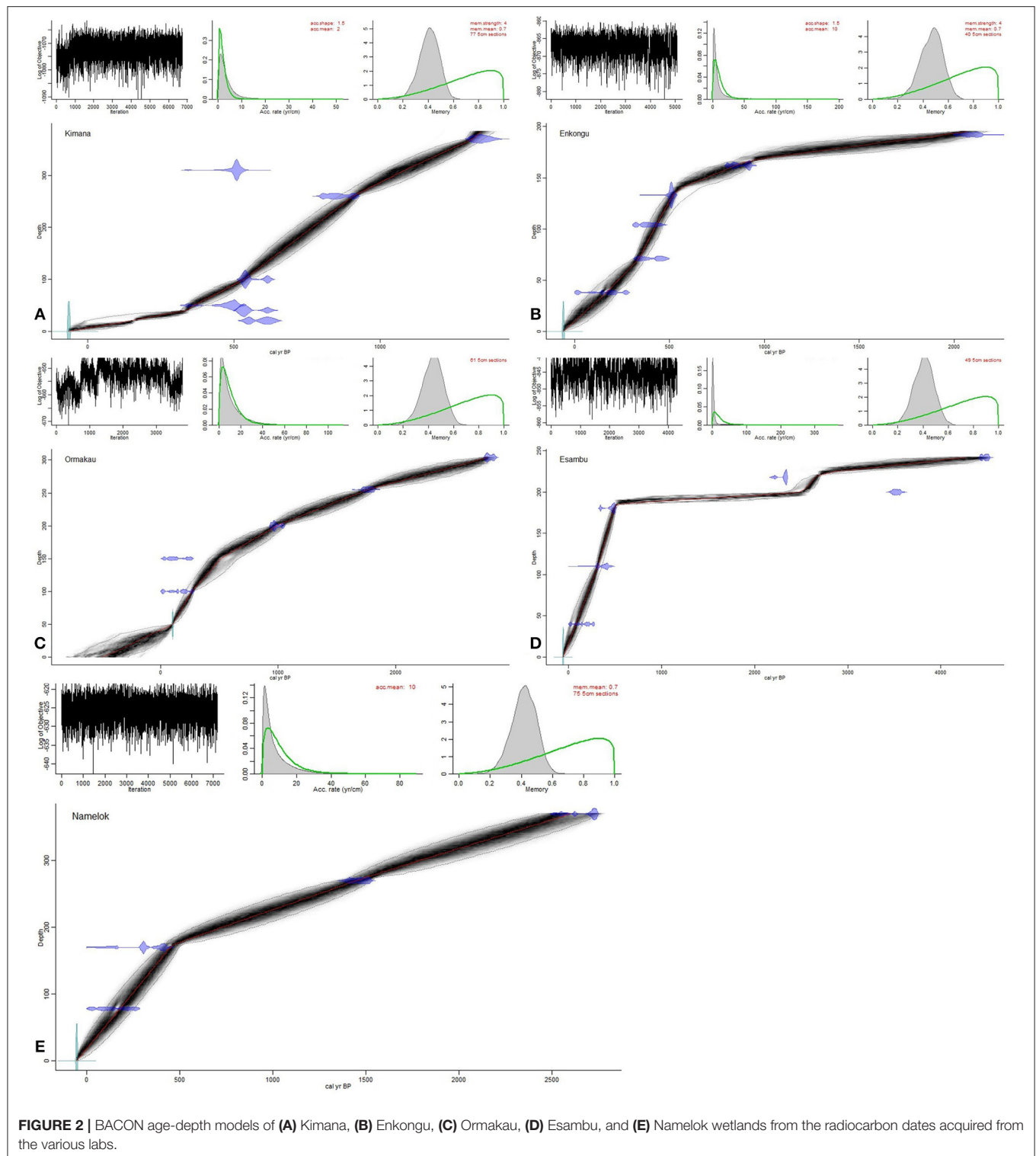
A 1 cm³ sub-sample was obtained every 20 cm for pollen and spore analysis from Kimana, every 10 cm from Namelok, every 5 cm from Enkongu and every 2.5 cm from Esambu following the standard protocol (Moore et al., 1991). Pollen analysis was not carried out on the Ormakau sediment core. An exotic marker (*Lycopodium* spores) was added prior to pollen analysis to aid in calculation of absolute concentrations (Stockmarr, 1971). The 1 cm³ was sampled into 100 ml beakers together with the one *Lycopodium* tablet with a known number of spores (9,666 spores) added to each sample. 10 ml of HCl (to remove the calcium carbonate in the samples) was added to the samples, vortexed to encourage mixing of the sample with the acid and placed on a hot water bath for 2 min. Samples were then centrifuged

at 3,000 revolutions per minute (rpm) for 3 min and the liquid decanted. Seven milliliter of distilled water was added to each sample, vortexed, centrifuged and the liquid decanted. This was done twice to remove all the HCl. Seven milliliter of distilled water was added to each sample, vortexed, centrifuged and the liquid decanted. This was done twice to remove all the HCl.

Twenty milliliter of 10% KOH (to digest organic matter) was added to the samples, which were then gently boiled while mixing on a hot plate to facilitate peptisation for 5 min, and then left to cool. The samples were sieved (to remove large unwanted particles) through 250 m mesh screens into 15 ml polypropylene centrifuge tubes and centrifuged for 1 min at 2,000 rpm and the liquid decanted. Samples were then washed twice with deionized water by adding 2–3 ml deionized water, thoroughly shaking the samples, topping up with water and centrifuging at 2,000 rpm for 1 min.

If carbonates were still present 1 ml ethanol and 1 ml H₂O were added and the sample vortexed. Seven ml of 96% Glacial acetic acid was added and carefully mixed into the mixture and left for 8–12 h. Samples were then washed with deionized water to prepare for acetolysis. During acetolysis samples were washed twice with acetic acid, i.e., 4 ml, Acetic acid was added to the samples and centrifuged at 2,000 rpm for 1 min and the clear liquid decanted. Acetolysis mixture 96% H₂SO₄: Acetic anhydride at a ratio of 1:9 was added to the samples, which were heated in aluminum block heater to 100°C. The acetolysis mixture digests the cellulose covering the pollen making the exine features distinct. The tubes were vortexed and heated further for 10 min. Samples were centrifuged and decanted to remove acetolysis mixture and washed twice in deionized water.

Heavy liquid separation using Sodium polytungstate (3NaWO₄.9WO₃.H₂O with $d = 2$) was carried out to separate the pollen from the remaining organic material. Three ml of the heavy liquid was added to samples and vortexed, water was carefully added using a glass rod to prevent mixture of the two liquids, the mixture was centrifuged at 3,000 rpm for 1 min and an organic suspension layer appeared at the boundary between the heavy liquid and water before the organic suspension was then carefully transferred to another test tube and samples were washed twice in deionized water. Prepared samples were transferred to residue tubes using 96% alcohol, centrifuged and



decanted. Glycerine (same volume as residue) was then added to the sample and the tubes left to evaporate in stove at 60°C. Pollen samples were mounted onto the pollen slides where the identification and enumeration of the pollen, spores and micro charcoal was carried out at a magnification of 400–1,000 and

from each slide a minimum of 300 pollen grains, excluding Poaceae and Cyperaceae, using a Leica DM4000B. The pollen grains were identified using images and descriptions from the African Pollen Database and published atlases (Hamilton, 1976; Hamilton and Perrott, 1980).

For each of the sites, a b-stick analysis was carried out to determine the suitable number of pollen zones. The zones were then delineated by carrying out a constrained incremental sum of squares (CONISS) analysis.

Charcoal Analysis

Subsamples of 1 cm³ of sediment were extracted at 1 cm intervals from the Kimana and Ormakau cores, every 0.5 cm from the Enkongu Narok core, and between 1 and 5 cm from the Esambu core. Macrocharcoal analysis was not carried out on the Namelok sediment core. The samples were soaked in sodium hexametaphosphate solution and a drop of hydrogen peroxide to disaggregate the samples and aid in the separation of the organic material and the clay particles (Bamber, 1982; Schlachter and Horn, 2010; Whitlock et al., 2010). Samples were wet sieved through a 125 µm mesh, the retained charcoal were identified by visual inspection and probed with a metal needle, and pieces were tallied under a Zeiss Axio Zoom V16 microscope at 10–40 X magnifications. All pieces above 125 µm were counted and the counts converted to charcoal concentration values, i.e., number of particles per unit of volume (pieces/cm⁻³) and charcoal concentration rates (number/cm²/yr⁻¹).

Archeological and Historical Synthesis

This paper provides an overview of the literature pertaining to human occupation of the Amboseli area and pastoralism in East Africa more generally in the mid to late Holocene. Both primary (archival documents, oral histories, preliminary data on archeological surveys and excavations) and secondary sources were consulted to generate insight on human-environmental interaction in the pre-colonial and colonial era (Chuhila, 2016; Shoemaker, in prep). More detailed results on archeological research in Amboseli investigating change and continuity in pastoral livelihoods over the last thousand years is forthcoming (Shoemaker, in prep). Further examination of the history of twentieth century land use change on Kilimanjaro is available in Chuhila 2016. Yet rather than summarizing these archeological and historical studies, which were guided by complimentary but not identical research questions, this section instead explores *potential* ways that people *may* have directly and indirectly modified the vegetation and water catchment system in the wider Amboseli region, and how livelihood adaptations *may* have responded to changing wetland environments over the last c. 5,000 years. In order to avoid overly reducing the complexities of ecosystem dynamics on this landscape, or evoking environmentally deterministic explanations for livelihood change, this section is necessarily vague. The complications of combining and interpreting paleoenvironmental and archeological records are fully acknowledged. Yet, as the incompleteness of paleoenvironmental and archeological records will never be resolved, this must not preclude attempts to understand their interaction. The integration of historical, archeological and paleoenvironmental data in contemporary human-environmental models is critical, and this section is in contribution to their *ongoing* synthesis.

Modeling

We developed an ABM to understand the interactions between biophysical and socio-economic drivers of land use change by exploring the role of rainfall, socio-economic circumstances, and governance factors, in driving land use decisions by pastoralists and the impact of land use change on wildlife densities across the Amboseli landscape from 1950 to present. Coupled biophysical and socio-economic data can be used to link the interaction between natural and human factors (Boone et al., 2011). The biophysical variables (i.e., the availability of grazing resources) were simulated by the LPJ-GUESS (Smith et al., 2001) dynamic global vegetation model and were provided as an input to link together with other socio-economic variables in the ABM. LPJ-GUESS is a deterministic, process-based vegetation model that simulates plant physiological and biogeochemical processes as a function of changing climates (Lindeskog et al., 2013; Pachzelt et al., 2013; Bodin et al., 2016). It is driven by temperature, rainfall and atmospheric CO₂ concentrations, with simulations run at both daily and annual time steps at a spatial resolution of 0.5 degrees (Bodin et al., 2016). Vegetation is represented as plant functional types distinguished by bioclimatic limits, morphology, phenology, photosynthetic pathway and life history strategy (Ahlström et al., 2015; Jönsson et al., 2015). The plant functional types compete for water and light (Lehsten et al., 2016) and their changing distribution at regional and functional scales is simulated (Quillet et al., 2010; Scheiter et al., 2013). ABMs can be used for linking the biophysical and socio-economic components of social-ecological systems characterized by multiple, stochastic and non-linear interactions (Matthews and Bakam, 2007; Rounsevell et al., 2012; Bert et al., 2014). Applications of ABMs offers a mechanism for incorporating human decision-making criteria on land use change at multiple scales (Matthews et al., 2007; Schindler, 2013; Bert et al., 2014).

The period for the ABM is from 1950 to present. Long-term mean rainfall from Climatic Research Unit (CRU) was used in LPJ-GUESS to simulate vegetation biomass for Amboseli for the period between 1950 and 2005 at 0.5 × 0.5 degree resolution. The simulated biomass was converted to kilograms per kilometers squared and used as input data in the ABM to simulate the biomass available to wildlife and livestock. To parameterize other ecological and socio-economic variables used in the ABM, we used data on animal densities, grazing rates, income levels, household densities and irrigation probabilities from literature focussed on pastoralists/agropastoralists in Amboseli (De Leeuw and Tothill, 1990; BurnSilver, 2009; Nkedianye et al., 2009) and from the 2009 Kenya census (KNBS, 2010). For each parameter, we used the mean and standard deviation to incorporate stochasticity in the ABM. To capture multiple land use change behaviors observed in Amboseli in the ABM, we applied the principle of pattern oriented modeling (POM) (Grimm et al., 2005) in the model design. We used insights from semi-structured interviews conducted with pastoralists in Amboseli in January and February 2016. The interviews focussed on the history and drivers of land use types, land tenure, livelihood strategies and land management.

The ABM was built in NetLogo (version 6.0.2; Wilensky, 1999). The model design adopted the “pattern oriented modeling” (Grimm et al., 2005) approach, using multiple land use change behaviors observed in the Amboseli ecosystem as a guide. Some of these system behaviors include: (1) pastoralism is hampered in subdivided rangelands that are densely populated, (2) high rainfall areas are the first to be converted to rain fed agriculture, (3) there is a high probability of irrigated agro pastoralism near wetlands, and (4) with high wildlife density and significant benefit from wildlife conservation initiatives, landowners are likely to use their land for conservation. Using empirical data from local community experts in Amboseli, from literature (De Leeuw and Tothill, 1990; BurnSilver, 2009; Nkedianye et al., 2009; Okello et al., 2016), and the latest (2009) Kenyan census, we derived parameters and values for socio-economic and some ecological factors such as income levels per land use types, household density, number of tropical livestock units and wildlife density. The influence of grazing resources and socio-economic factors on land use type and the impact of adopted land use types on wildlife was then simulated.

RESULTS AND DISCUSSION

Amboseli Chronology

Five wetlands (Figure 2) across Amboseli have been radiocarbon dated to provide a chronological framework for past ecosystem histories. Although the sites have complex age-depth relationships, and were treated with large chronological uncertainty regarding their interpretation, there are coherent patterns of paleoenvironmental change at individual sites and across the sites.

Five dates from Kimana wetland when modeled give the basal date of Kimana core to be ~1,200 cal yr. BP. The model recognizes the age from 310 cm as an outlier as it is younger than the depths from the two levels above it (Figure 2A). The Enkongu core has a basal date of ~2,000 cal yr. BP modeled from the six radiocarbon dates. There is an age reversal where the sample from 100 cm was older than the samples from two lower depths, as a result three dates were noted as outliers and not modeled (Figure 2B). At Ormakau, the six dates are modeled to give a basal date of ~2,700 cal yr. BP with one date left out of the model (118 from 150 cm) which was also recognized as an outlier due to being younger than the two dates above it (Figure 2C). Linear interpolation of the six Esambu radiocarbon dates show that the sediment record spans from ~4,974 cal yr. BP (Figure 2D). The Namelok age-depth model (Figure 2E) incorporated all four radiocarbon dates spanning from ~2,594 cal yr BP to present.

There are several probable causes for the abrupt changes in sedimentation rates, the potential hiatus or reversed ages observed in these cores: they may have an erosional cause resulting from the change from dominantly semi-arid conditions to increased moisture, or a depositional cause by increased aridity with subsequent cessation or very low sediment accumulation. Significant bioturbation by the wildlife that utilize these semi-arid wetlands could also disturb the stratigraphic order of the sediments. Despite these chronological challenges, coherent and

repeatable age-depth models can be constructed from the sites and the proxy evidence appears similarly robust with coherent signals of change detected through the sedimentary sequences.

Amboseli Vegetation Dynamics since the Mid-holocene

The pollen data from Esambu, Namelok and Enkongu (Figure 3) are summarized into broad ecological groups that enable comparison between the sites and engender linkages to other stands of evidence. Across the landscape sedges (*Cyperaceae* and *Typha* sp.), grasses (*Cenchrus ciliaris*, *Cynodon dactylon*, *Digitaria ciliaris*, and *Pennisetum* sp.), shrub and tree species in the adjacent riverine areas (*Acacia* spp., *Amaranthaceae*, *Balanites* spp., *Commiphora* spp., *Euphorbia* spp., and *Tabernaemontana elegans*) currently dominate the wetlands. The assemblage indicates that vegetation mosaics had different compositions in the past, and in what follows contrasts between these will be treated as successive discrete time periods that characterize the main phases of environmental change.

Between ~5,000 and 2,000 cal yr. BP, as seen in ESAM1 (Figure 3), the local Esambu ecosystem was a semi-arid woodland environment with *Amaranthaceae*/*Chenopodiaceae* and *Acacia* spp. as the dominant taxa followed by *Asteraceae* and *Capparis* sp. Low abundances of aquatic and semi-aquatic taxa (i.e., *Cyperaceae*, *Nymphaea* sp., *Typha* sp., and *Tapura* sp.) indicate that the Esambu wetland was much more restricted than today. There was a high presence of non-pollen palynomorphs (NPP) abundance and the most dominant species suggest a high herbivore density, implying wild herbivores were concentrated within a relatively small area to access water and grazing. The Namelok record also suggests that the vegetation around the wetland was more open from ~3,000 to 2,100 cal yr. BP with low abundance of tree taxa coupled with an increase in the abundance of shrubs and herbaceous taxa. Charcoal concentration at Esambu (Figure 4) was very low suggesting few fires, due to the reduced fuel connectivity because of the low vegetation cover.

From ~2,000 to 400 cal yr. BP (ESAM2) there was increased moisture and fuel connectivity linked to macrophyte expansion around the Esambu wetland margin. There was an increase in pollen diversity with increased shrub and woodland (*Balanites* sp. and *Cordia* sp.) and aquatic taxa as well as *Afromontane* taxa (*Celtis* sp., *Commiphora* sp., *Croton* sp., *Juniperus* sp., *Olea* sp., and *Schefflera* sp.) on the adjacent highlands. The Namelok record (Figure 3) captures an arid phase maintaining the open semi-arid shrubs and low aquatic taxa abundance between ~2,100 and 1,700 cal yr. BP (NAM2). From ~1,700 to 1,200 cal yr. BP, the Namelok record (NAM3) indicates a mesic phase with the increase of herbaceous taxa and *Syzygium* sp., followed by a decrease in *Syzygium* sp. coupled with an increase in *Acacia* spp., *Amaranthaceae*/*Chenopodiaceae*, *Euphorbia* sp. and particularly *Poaceae* up to ~700 cal yr. BP. The Enkongu record (ENK1 and ENK2) indicates that the period between ~2,000 to 900 cal yr. BP was relatively mesic compared to the rest of the record, dominated by aquatic taxa, *Poaceae*, *Asteraceae*, *Amaranthaceae*, *Solanum* sp. and *Maesa* sp. forming a woodland

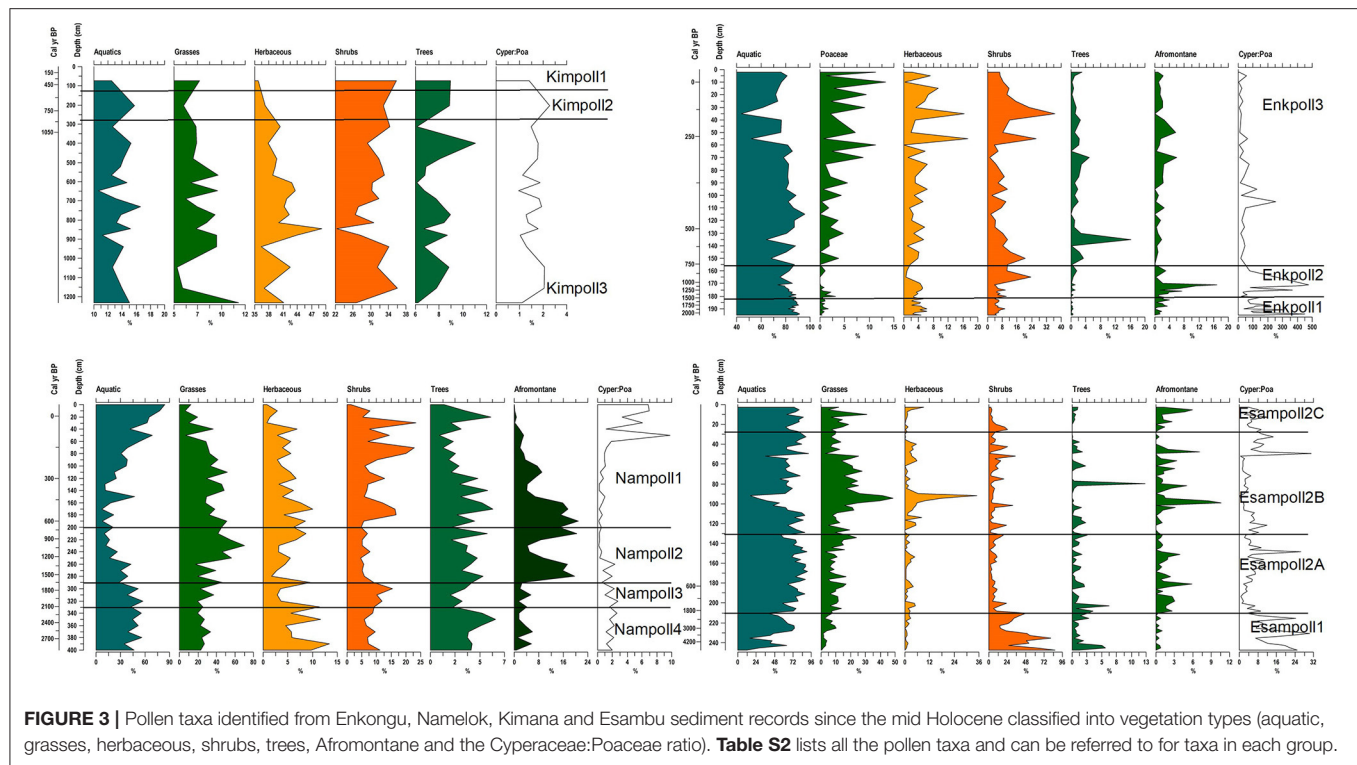


FIGURE 3 | Pollen taxa identified from Enkongu, Namelok, Kimana and Esambu sediment records since the mid Holocene classified into vegetation types (aquatic, grasses, herbaceous, shrubs, trees, Afromontane and the Cyperaceae:Poaceae ratio). **Table S2** lists all the pollen taxa and can be referred to for taxa in each group.

savannah where woody taxa dominated over the non-woody taxa. There was an increase in charcoal concentration relative to the previous period suggesting greater fire frequency as the increased shrub and herbaceous taxa increased fuel load and connectivity. From ~700 cal yr. BP, there was a significant increase in the Cyperaceae and Poaceae abundance, in the Esambu record Cyperaceae, Poaceae and *Typha* sp. (aquatic taxa and grasses) dominate ESAM3. Within the Namelok record (NAM4) Asteraceae, *Cissampelos* sp., and *Syzygium* sp. decreased with increases in *Acacia* spp., Amaranthaceae/Chenopodiaceae, Cyperaceae and particularly Poaceae from 500 cal yr. BP. Within Enkongu (ENK3), the dominating taxa are the shrubs Amaranthaceae/Chenopodiaceae, *Commelina* sp., *Solanum* spp. and Asteraceae while the Poaceae abundance significantly increases.

Across the sites, the last ~500 cal yr. BP is identified as a significant period with drastic differences in macro charcoal records (Figures 3, 4). There is a significant decrease in macro charcoal concentration in the Esambu record however within the Kimana record there is a significant increase in the macro charcoal concentration (Figure 4). The pollen records point to increased standing water (~400 cal yr. BP) and within the recent past (100 cal yr. BP to present) an intensification of human modifications to the channels and wetland area for agriculture within the Esambu wetland. The Cyperaceae: Poaceae ratios (Figure 3) can be used as an indicator of water level where an increase in only Cyperaceae is due to falling water levels exposing sediment and providing a greater habitat for expansion of marginal wetland plants. Within the last ~500 cal yr. BP, the Cyperaceae: Poaceae ratio (Figure 3) indicates a consistently

open landscape after a drop in the water level, reducing the size of the wetland at Enkongu. The Namelok record shows a previously open landscape and a continued reduction in the size of the open water area while Esambu shows a fluctuating extent of open water area.

Livelihood Strategies in Amboseli from the Mid Holocene

Archeological evidence suggests that many of the changes in vegetation in East Africa during Late Holocene were influenced by changes in human land use (Table 4). The following sections outline regional and local archeological and historical records to provide further detail concerning possible anthropogenic landscape modifications in Amboseli. Also considered are the potential ways that people in Amboseli responded to environmental changes.

Late Stone Age >c. 4,500 BP

In the early-mid Holocene, Late Stone Age (LSA) hunter-gatherer groups occupied eastern Africa including the Rift Valley in Kenya and Tanzania and adjacent highlands (Kusimba, 2013). Archeological evidence in the Central Rift suggests that LSA hunter-gatherer groups used rock shelters at forest-grassland ecotones and open-air savannahs (Mehlman, 1979; Ambrose, 1984, 1998; Marean, 1992; Kusimba, 1999, 2001). Faunal assemblages indicate hunting of forest-savannah game, though honey was also an important food (Ambrose, 1984; Marean, 1992). Little is known about LSA hunter-gatherer plant use in east Africa, but ethnographic analogies suggest people would have been consuming, tending, and transplanting

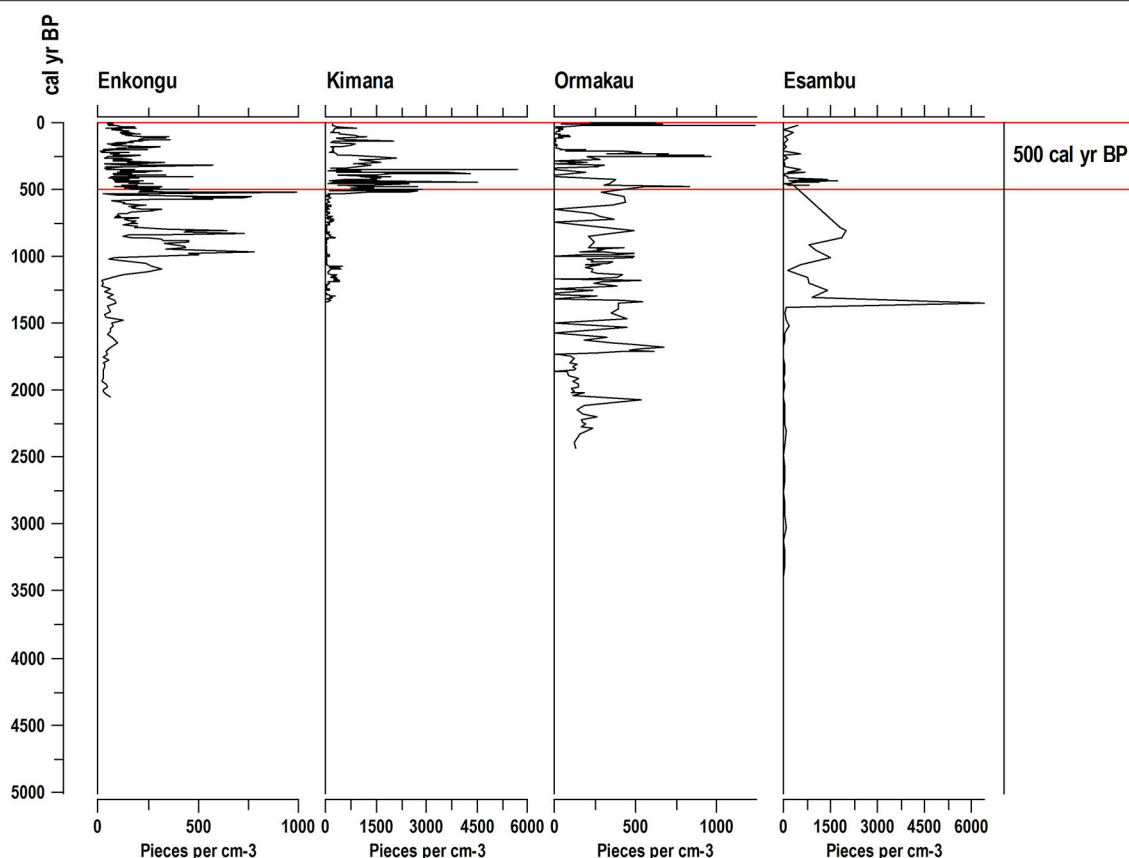


FIGURE 4 | Macrocharcoal records from the Esambu, Kimana, Ormakau and Enkongu sediment records since the mid Holocene. The ~500 cal yr BP zone where macrocharcoal concentration changes differ significantly across the sites is highlighted.

TABLE 4 | Outline chronology of different archeological periods and material traditions in eastern Africa (after Lane, 2013).

Age BP (kyr)	Archeological periodization	Selected LSA stone tool industries	Pastoralist and other ceramic traditions	Dominant subsistence strategies and other trends
0	Historically documented ethnic groups	None	Variable—named after contemporary pastoralist, farming and foraging ethnic groups	Major inter-sectional and inter-ethnic reconfigurations ~200 cal yr. BP. Specialized pastoralism and settled agriculture widespread, with encapsulated pockets of hunting-and-gathering
1	Later IA (LIA) and Pastoral IA (PIA)	Indeterminate quartz and obsidian based	Kisima from c. 750–200 BP (PIA) Lanet/Sirikwa from c. 1,200–300 BP (PIA) Diverse LIA ceramic traditions	Specialized pastoralism Mixed herding and horticulture First use of metals among herders ~1,200 BP
2	Early Iron Age (EIA), Late Pastoral Neolithic	Indeterminate quartz and obsidian based	Urewe c. 2,500–1,000 BP Akira c. 1,900–1,200 BP Maringishu to c. 1,700 BP Kwale c. 1,800–1,400 BP Tana/Triangular Incised Ware—c. 1,400–1,000 BP	Early farming and iron using Mixed pastoral economies shift to more mixed herding-hunting economies and fluid ethnic boundaries ~1,900–1,200 BP
3	Pastoral Neolithic Traditions (Savanna Pastoral Neolithic (SPN) and Elmenteitan	Elmenteitan SPN	Narosura c. 2,800–1,400 BP Elmenteitan c. 3,300–1,300 BP	Possible formation of a “static” frontier between herders and hunter-gatherers ~3,000–1,900 BP, and first occurrence of “specialized” pastoralism
4.5	Initial Pastoral Neolithic (PN). Overlaps with later LSA	Eburran 5 LSA-“Bone harpoon” sites	Nderit & Ilert c. 4,800–1,500 BP Wayi Line	Era of initial “moving frontiers” of pastoralism, ~4,800–3,000 BP
6	Later LSA	Eburran 4 Kansyore	Aceramic Kansyore	Immediate return Hunting-Gathering Delayed return of Hunting-Fishing-Gathering

wild plants to varying degrees (Marshall, 2001; Marlowe and Berbesque, 2009). On the shores of Lake Turkana and Lake Victoria, hunter-fisher-gatherer peoples also intensively exploited lacustrine resources including fish and shellfish (Robbins, 1972; Lane et al., 2006, 2007; Dale and Ashley, 2010; Prendergast and Lane, 2010; Prendergast and Beyin, in press).

Prior to the adoption of crops and livestock, regional aridity caused forests to recede to higher elevations, grassy savannah expanded as lake levels fell, and rainfall decreased from ~ 5,000 cal yr. BP (Ricketts and Johnson, 1996; Damnati, 2000; Gasse, 2000; Marchant and Hooghiemstra, 2004; Russell and Johnson, 2005). In the Central Rift, LSA hunter-gatherers may have shifted settlement locations to higher elevations as savannah-montane forest ecotonal areas advanced in elevation (Ambrose and Sikes, 1991). In Amboseli, the Esambu pollen record from this study suggests that while the local ecosystem was dry, the permanent water availability of the wetlands still served to attract herbivores in relatively dense concentrations. During this period of intense aridity, Amboseli wetlands were perhaps one of a few permanent sources of water in an otherwise dry landscape. These wetlands may have been of particular importance to hunter-gatherers and wildlife at this time. Conversely, during the mid-Holocene Dry Phase foragers may have preferentially occupied higher elevation zones, such as on nearby Mt. Kilimanjaro. More intensive surveys and excavations focused on elucidating the history of Holocene hunter-gatherers in Amboseli is required to clarify these issues.

Regionally, evidence suggests that some pre-pastoral LSA foragers engaged in moderate delayed-return subsistence strategies (Dale and Ashley, 2010), and fire was quite possibly used in Amboseli as a tool for landscape management from an early time. Contemporary hunter-gatherers in southern Africa are known to strategically burn grasslands (Lee, 1979), for example, as periodic burning in savannah environments serves to reduce and break up homogenous bush cover, promoting the productivity and diversity of biomes (Butz, 2009; Bond and Parr, 2010; Kamau and Medley, 2014). There are no known securely dated LSA hunter-gatherer occupation sites in Amboseli, however, making it difficult to surmise the behavior of early-mid Holocene inhabitants. It is likely that early foragers in Amboseli incorporated wild edible plant foods into their diets, consuming a variety of the starchy tuberous roots, fruits, legumes, grains, and leafy greens that occur in the landscape today (Altmann et al., 1987). It is possible that fishing also formed a component of hunter-gatherer diets in Amboseli at some time in the past. Catfish and other fish bones have been found in the dried Amboseli lakebed (Foley, 1981), and fish currently persist in the wetlands; although, they are not exploited as is the case in some wetlands of Tanzania (Hamidu et al., 2017). Hunting and scavenging of terrestrial fauna, also potentially contributed to LSA forager livelihoods in Amboseli.

Pastoral Neolithic (c. 4.5–1.5 ka BP)

Livelihood strategies based on domesticates began emerging as early as c. 4,800 years ago in northern Kenya, and by c. 4,100 cal. BP in south-central Kenya and northern Tanzania, marking the beginning of the Pastoral Neolithic (PN) in these areas (Lane,

2011a; Crowther et al., in press). Pottery wares such as Nderit and Ileret are found in association with wild fauna and the rare caprine dating to this time, indicating the nominal incorporation of domesticates into hunter-fisher-gatherer livelihoods (Gifford-Gonzalez, 2000). The transition to pastoralism in East Africa was neither immediate, nor comprehensive (Lane, 2004; Prendergast and Beyin, in press). Overall, during the mid-5th–4th millennium BP, domestic taxa constituted increasingly larger proportions of faunal assemblages and new technological traditions emerged, including the Savannah Pastoral Neolithic (SPN) (Marshall, 1990). SPN encompasses a diversity of archeological contexts associated with the onset of pastoralism in eastern Africa that bear certain material signifiers, such as Narosura ceramics and stone bowls (Wandibba, 1980; Robertshaw and Collett, 1983).

Around Amboseli, the earliest and closest archeological evidence for pastoralist habitation comes from an SPN site on the lower western slopes of Mt. Kilimanjaro (4,100 cal yr. BP) (Mturi, 1986). On the Galana River in nearby Tsavo livestock also appear in archeological deposits dated to c. 3,800 BP (Wright, 2005, 2007). At present, evidence for PN occupation of Amboseli is entirely based on survey finds, including ceramics bearing affinity to Narosura and Akira pottery wares and a fragmented stone bowl (Foley, 1981; Weissbrod, 2010; Shoemaker, in prep), making inferences about settlement and subsistence strategies difficult. The cultural provenience of Akira ware is also not well established (Ashley and Grillo, 2015), though radiocarbon dates from the type site Guji 2 range between 1,255 and 1,695 cal yr. BP (Bower et al., 1977), spanning the Pastoral Neolithic–Iron Age time period. The association elsewhere between Akira with PN sites containing predominantly wild faunal assemblages has led to the suggestion that Akira pottery was produced by hunter-gatherer groups, and its wide distribution perhaps indicates its value as a trade good (Robertshaw, 1990). Akira ware may also be associated with a “final phase” of SPN expansion wherein wild resources were more wholly embraced (Bower, 1991).

Transitions to pastoral livelihoods were nevertheless underway before the end of the Mid-Holocene Dry Phase in East Africa. Early herders in Kenya contended with novel epizootic challenges and comparative aridity, factors which may have contributed to the lag in time between the first appearance of domesticates and the emergence of specialized pastoralism (Gifford-Gonzalez, 1998, 2000). Lake levels in northern Kenya appear to have been returning to higher stands around 3,300 cal yr. BP (Garcin et al., 2012), though the Esambu and Namelok pollen records from this study (Figure 3) indicate that wetter conditions did not prevail in Amboseli until after 2000 years ago. Long-term trends in aridity are not the sole considerations; the improved predictability and volume of bimodal rainfall regimes after 3000 years ago may have also encouraged specialized pastoralism across the region (Western and Finch, 1986; Marshall, 1990, 1994; Bower, 1991). However, the processes by which pastoralists became woven into the socio-economic fabric of East Africa were not entirely dependent on weather patterns. Livestock herding emerged and reproduced in multiple and dynamic ways across a myriad of landscapes during the span of millennia, and while the climatic context of this history is important, it did not determine it.

There is also increasing recognition that PN herders were not only responsive to environmental factors but that the arrival of livestock in East Africa also conditioned “emerging ecosystems” (Milton, 2003; Hobbs et al., 2006), with new species compositions and relative abundances driven by human interventions that had not previously existed. The soil nutrient and water retention enhancing properties of livestock dung, for instance, are known to lead to distinct successions of vegetation on abandoned pastoral settlements (Dunne et al., 1978; Western and Dunne, 1979; Reid and Ellis, 1995; Muchiru et al., 2009; Boles and Lane, 2016). There may have also been an acceleration of anthropogenic burning activity and a decline in dense bushland and woodland vegetation due to interventions by emergent herders in the latter half of the Holocene. After the inception of herding, the burning of vegetation in Amboseli may have served to improve the quality of pasture (Archibald and Bond, 2004), and to moderate tsetse-harboring woodlands and bushlands (Gifford-Gonzalez, 2000). The introduction of livestock to Amboseli would certainly have exerted considerable influence on the ecological development of the wetlands and surrounding environs. The timing and local circumstances under which livestock were adopted in Amboseli are still under evaluation, however. What is known is that the wetlands of Amboseli remained a source of permanent water on the landscape, no doubt attracting wildlife and livestock to some degree.

Emergence of Farming Communities (c. 2 ka BP)

Current evidence suggests that from around 2,000 years ago the first farming communities begin to be established in the western part of the region, spreading steadily eastwards and likely co-existing with established PN and LSA groups (Lane, 2004). In regional archeological terminology, the arrival of the first farmers marks the start of the Iron Age, traditionally distinguished (Oliver, 1966) by knowledge of iron working, the introduction of proto-Bantu languages, new pottery types, and the cultivation of African root (yams) and cereal (sorghum, pearl millet, finger millet) crops, supplemented by various legumes (De Langhe et al., 1995; Fuller and Hildebrand, 2013). Indian Ocean maritime exchange between Southeast Asia and Africa's eastern coast in the latter part of the (~1,500–1,000 cal yr. BP), if not earlier, was also responsible for the introduction of additional crops and animal species (De Langhe, 2007; Fuller and Boivin, 2009; Fuller et al., 2011a,b; Boivin et al., 2013, 2014; Prendergast et al., 2017; Crowther et al., in press).

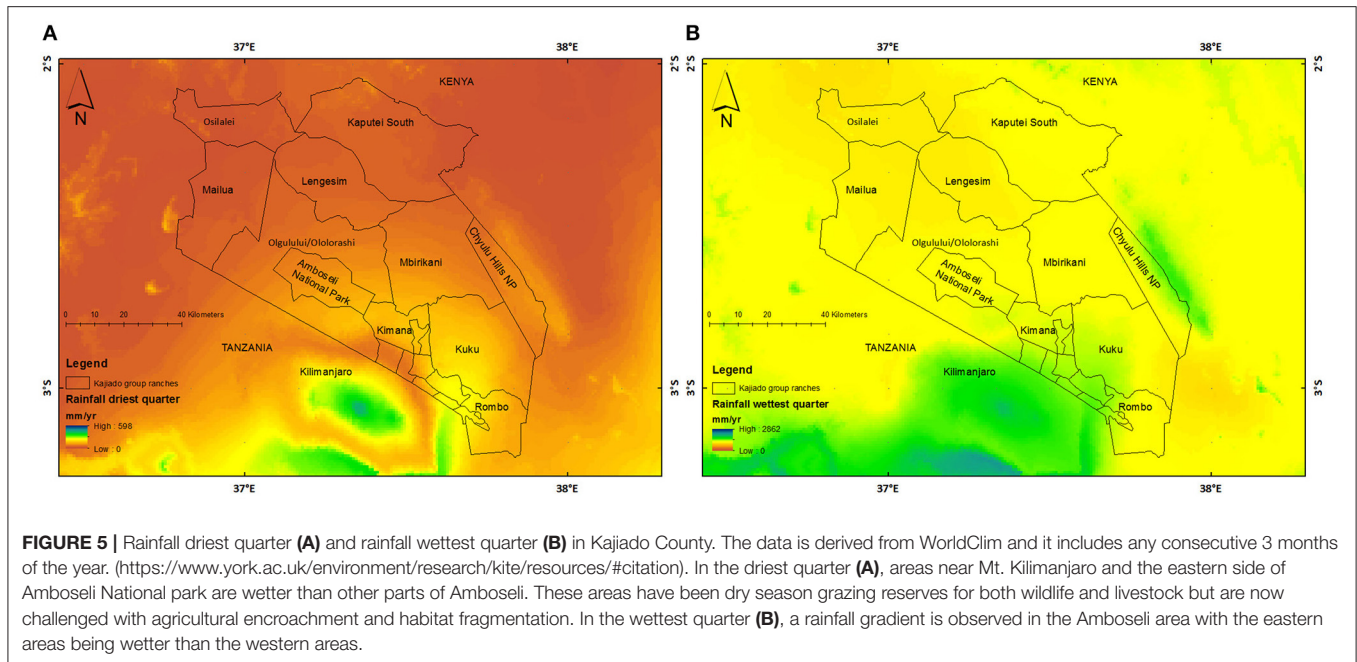
Direct evidence for iron production (e.g., slag, tuyères) has not yet been recovered in the Amboseli area; although various Iron Age pottery wares and habitation sites are certainly present (Soper, 1976; Shoemaker, in prep). Furthermore, while the low-rainfall in the Amboseli basin (Figure 5) suggests this would not have been a viable area for agriculture, the potential for cultivation immediately surrounding the wetlands or at higher-rainfall altitudinal, zones within the Amboseli ecosystem cannot be dismissed. The Esambu and Namelok pollen records (Figure 3) show periods of increased precipitation where there is increased shrub and tree taxa (Nampoll4 and Esampoll1). Finds of grinding-stones, stone rings (potentially used as digging stick weights) and Early Iron Age Kware pottery provide indirect

evidence for farming and iron manufacturing communities on the northwestern slopes of Mt. Kilimanjaro going back as far as two millennia (Fosbrooke and Sassoon, 1965; Odner, 1971). Still, the higher precipitation rates on the southern and eastern slopes of Mt. Kilimanjaro were probably more attractive to agricultural settlement than the northern and western slopes, which lie in the rain shadow of the mountain (Stump and Tagseth, 2009). Livestock herding and foraging inhabitants of Amboseli would have been well situated to trade with iron working and farming communities on Mt. Kilimanjaro and in other highland areas to the southeast.

Concurrent with the arrival of Iron Age farming communities, there is some evidence to suggest a transition in pastoral economies in the Central Rift Valley between 1,900 and 1,300 cal yr. BP with herders shifting away from specialized pastoralism toward more highly mobile settlement strategies and a greater reliance on wild foods (Bower, 1991). Settlement sites in southwestern Kenya also appear to become smaller in comparison to earlier PN occupations (Robertshaw, 1990), perhaps being a factor of increased mobility. There is no indication that PN diets or mobility patterns changed substantially on the Galana River in Tsavo during the second millennium BP, however, (Wright, 2007), highlighting the potential diversity of pastoral adaptations during this time.

With the adoption of agriculture and metallurgy in the wider region after 2,000 cal yr. BP came opportunities for the intensification of trade and interactions between pastoralists, foragers, farmers and iron working communities in Amboseli. As documented elsewhere (Lane, 2011a; Crowther et al., in press), a dynamic mosaic of livelihoods including foraging, hunting, specialized herding, farming, and combinations thereof would have existed in the wider Amboseli area. Specialized relationships between farmers and herders may have even facilitated new, more intensive management and production systems by pastoralists and agriculturalists (Robertshaw, 1990; Davies, 2015). Unfortunately, compared to the coastal strip (Helm, 2000) and the Lower Pangani Valley to the south (Walz, 2010), little is known about the scale and dimensions of economic activity in Amboseli during the earliest Iron Age.

As agricultural and iron producing communities in East Africa emerged, a transformation in the capacity for people to modify their environments to suit their habitation (i.e., human niche construction) occurred (Boivin et al., 2016). Introductions of novel agricultural crops to the region would have also brought new pathogens, non-domesticated “weed” species, and some pre-existing taxa would have thrived on the biomes emerging on cultivated plots (Baker, 1991). The degree to which regional vegetation was modified by iron working is still under investigation though iron manufacturing in East Africa required charcoal, the production of which can be, though certainly not always, be linked to reductions in forest cover (Iles, 2016). Anthropogenically driven transformations of flora and fauna, potentially including land clearance and soil erosion on Mt. Kilimanjaro may have intensified, as has been observed in the Pare Mountain bloc over the last 2,000 years (Heckmann, 2014), with a spike in human landscape modifications occurring ~500 cal yr. BP, and c. 200 cal yr. BP (Finch et al., 2016). The impacts



of such anthropogenic activities and potential modifications to the water catchment system may be responsible in part for the apparent shift in the hydrology and biota of the wetlands in Amboseli 500 years ago, though the mechanisms of this have yet to be discerned. The increased opening up of the landscape implied by increase in Poaceae and Cyperaceae accompanied by an increase in local fires suggested by the macro charcoal is one such indication of anthropogenic driven change.

The Later Iron Age (c. 0.5 ka BP–1900 CE)

During the last thousand years, there is mounting evidence that major socioeconomic and environmental changes were underway in the wider Amboseli region. A change in land use was taking place in locales across the region by the mid-first millennium BP, if not earlier, in the form of irrigation agriculture (Stump and Tagseth, 2009). Progressive anthropogenic land modification linked to agriculture was already occurring ~600 cal yr. BP in North Pare (Heckmann, 2014). In South Pare, greater levels of forest disturbance and an increase in pioneer taxa in the last 500 years similarly indicates intensive anthropogenic activity at montane elevations (Finch et al., 2016). Taken together, these lines of evidence suggest a certain intensification in agricultural activity over the last 500 years in the wider area.

Also occurring over the last 500 years was the introduction to Africa of domesticated plants, including maize, from the Americas as part of the “Columbian Exchange” (Crosby, 2003). Maize is now one of the most important crops consumed in Amboseli, although the date and pathway of its introduction to East Africa is largely unknown. “New World” crops such as maize likely arrived at trading ports along the Swahili coast with the Portuguese. Historical sources indicate maize was present on Zanzibar by 1643 (White, 1949), and being sold at markets in Pare by 1861 (Von der Decken, 1869). Paleocological records

find maize considerably earlier at Lake Naivasha ~500 cal yr. BP (Lamb et al., 2003), in the South Pare Mountains by ~400 cal yr. BP (Finch et al., 2016), and on the Laikipia Plateau by ~200 yr. cal BP (Taylor et al., 2005). The trajectory of maize cultivation on Mt. Kilimanjaro remains to be discovered, though it was present in the Loitokitok area in the nineteenth century (Meyer, 1900).

The hunting of elephants in the interior of eastern and southern Africa to supply external ivory markets has also been ongoing for centuries (Alpers, 1992; Håkansson, 2004; Shalem, 2005). This trade in ivory from the Swahili coast intensified considerably during the nineteenth century (Beachey, 1967; Cutler, 1985; Håkansson, 2004; Lane, 2010). With increasing involvement in the long-distance ivory trade, an expansion of irrigation agriculture and centralization of Chagga-speaking polities is suggested to have occurred on Mt Kilimanjaro’s southern and eastern slopes (Stahl, 1964; Håkansson, 2008), resulting in the amalgamation of previously semi-autonomous clans of diverse ethnic origins, including Maa-speaking groups (Chuhila, 2016). Cattle, as “the lifeblood of political relationships” in the regional economy were in high demand in the nineteenth century (Håkansson, 2008). The entangled consumption of livestock and crops 200 years ago with the ivory trade elevated their status from mostly of significance to local and regional exchange, to that of international commerce.

The depopulation of elephants in Amboseli due to hunting may have also induced ecosystem shifts. In nearby Tsavo, for instance, an increase in elephant hunting has been suggested to have caused an expansion in scrub vegetation (Kusimba, 2009), although this link has not been conclusively established. Available paleocological records from Kanderi Wetland (Gillson, 2004) indicate a marked phase transition from woodland to grassland in the Tsavo area commencing ~420 cal yr. BP and lasting to ~180 cal yr. BP, after which there was a return to more

wooded conditions. Gillson (2004) tentatively attributes the opening up of the Tsavo landscape around 420 cal yr. BP to increased herbivory, probably elephant, but notes that phase transitions from grassland to woodland may be attributed to factors other than a decline in herbivore density. Elephants are known to exert a great deal of control over the vegetation in Amboseli, as has been shown by the loss of trees and shrubs in Amboseli National Park since the mid-1960s (Western, 2006). As rising numbers of elephants have come to seek refuge in the protected space, *Acacia xanthophloea* and *Acacia tortilis* woodlands have been heavily grazed and impeded from recovery (Western and Maitumo, 2004). However, very little is known about the local circumstances under which elephant populations were hunted in Amboseli over the last 500 years, making it difficult to evaluate the hypothesis that woodlands expanded over this time due to the removal of elephants. The exact extent of defaunation of elephants in the interior of East Africa is under investigation (Coutu et al., 2016). More information is available for the nineteenth century. Various historical sources indicate that elephants were rarely seen in the area east of Kilimanjaro in the late 1800s (Wimmelbücker, 2009, pp. 130–131). While it is conceivable that elephant populations were similarly depleted in Amboseli, it is also possible that elephant numbers increased here at this time, as these animals sought refuge from comparatively more extensive hunting activity to the east. Early European traveler accounts reveal that Amboseli was known to have had wild animals in abundance, but they also indicate that ivory hunters were present in the area (Rebmann, 1848; Thomson, 1885). Either way elephants with large tusks existed in the Kilimanjaro region in the nineteenth century, suggesting that herds had not been entirely decimated. This is best attested by a pair of tusks with a combined weight of just under 200 kg from a large bull elephant reportedly killed on the mountain in 1898, before being transported to Zanzibar and ultimately landing up in the Natural History Museum in London (Kunz, 1926), where they remain.

It is evident that adding to all of these transformations would have been the accumulation of landscape transformations driven by pastoral activity in Amboseli over the course of millennia. Herders continued to influence the spatial and temporal availability of soil nutrients across the region, with implications for the composition and distribution of plant and animal taxa. Anthropogenic transformations in Amboseli were not on a linear trajectory however, major disruptions occurring due to droughts, pathogens, and socio-economic upheavals introduced hiatuses and reversals in long-term trends.

The intensification and transformation of slavery and slave trading which occurred during the nineteenth century in East Africa (Alpers, 1975; Sheriff, 1987; Glassman, 1995) may have been a particularly insidious cause of turbulence in the wider region. In the Taita district of Kenya, Kusimba and Kusimba (2005) suggest that people relocated from the lowland plains to defensive rock shelters to protect themselves from slave raiding. There is little to indicate slave trading had a similar impact in Amboseli, though recognizing slavery in archeological contexts is challenging (Alexander, 2001; Lane, 2011b). Historical sources do

indicate that early nineteenth century Maa-speaking pastoralists who are ancestrally linked to the current inhabitants of Amboseli were involved in the slave trade however (Krapf, 1854).

Considerable disruption and social upheaval among various livestock herding groups certainly occurred between 1840 and 1870 during the so-called Iloikop Wars (Waller, 1979; Galaty, 1993; Jennings, 2003). Maasai in Amboseli today recount that during the 1800s groups of Maasai, many of them from Tanzania, moved into Amboseli and the pastoralists they encountered were assimilated, migrated elsewhere, or killed. Regional paleoenvironmental reconstructions are now also indicating a drought of acute severity at the turn of the nineteenth century (Verschuren et al., 2000) with a number of social consequences for pastoral communities (Sobania, 1980; Anderson, 2016; Petek and Lane, 2016). It may be no coincidence that the Loikop Wars began toward the end of the 1830s, coinciding with the recovery of lake levels immediately following the intense drought and a corresponding recovery of rangeland (Anderson, 2016). Another period of drought in northeastern Tanzania in the 1830s may have further catalyzed Maasai movements north into Kenya (Wimmelbücker, 2009). The impacts of such a severe drought on societies in East Africa must have been radical, causing widespread famine, and the loss of livestock and human lives on a grand scale, and probably major migrations. This great drought at the end of the eighteenth century may have created the conditions for the emergence or perhaps re-instigation of the Maasai in the following years.

Another disturbance to pastoral livelihoods occurred in Amboseli in the late 1800s when devastation was brought to livestock herders across East Africa in the form of bovine pleuropneumonia, rinderpest, smallpox epidemics, and failed rains (Ofcansky, 1981; Waller, 1988). Cattle losses are estimated as high as 90%, while Maasai mortality rates have been suggested to have been up to 50% of the population overall (Leys, 1924). European traveler accounts indicate that stockless Maasai had taken up the cultivation of beans, maize and cassava in the Loitokitok area of Mt Kilimanjaro, though there were still pastoralists tending their herds in the Amboseli basin (Meyer, 1900; Bernsten, 1976).

Amboseli in the Colonial Era, c. 1900

At the turn of the twentieth century, the colonial encounter began in Amboseli ushering in an era of socio-economic sanctions and geo-political borders inconsistently enforced by two colonial governments varying in their motivations to maximize the potential of “Maasailand.” The general trend during the twentieth century in Amboseli was toward the confinement of livestock and herders within ever diminishing parcels of land (BurnSilver and Mwangi, 2007). Rangelands that were once flexibly and communally managed became increasingly fenced and settled (Western and Manzollilo-Nightingale, 2003; Mwangi, 2006; BurnSilver et al., 2007). There has also been an increase in the area of land cultivated using irrigation, particularly around the wetlands of Amboseli (Campbell et al., 2003). These changes have disrupted previous patterns of mobility and presented challenges to pastoralists living in Amboseli.

In the early colonial period Maasai people received little support to develop their livestock production sector and were at times actively hindered by the colonial administration (Dresang and Sharkansky, 1975; Spencer, 1983; Rutten, 1992); consequently, diversification of livelihoods toward agriculture proved attractive. In addition, as European settlers appropriated large swaths of East Africa (Hughes, 2006) and as populations rose, conditions were created for the scarcity of land, prompting the influx of farmers from other areas into the Amboseli region (Rutten, 1992, pp. 189, 191). The conversion of land for growing cash crops such as coffee for export also diminished the level of food security in the Kilimanjaro region (Wimmelbucker, 2009, p. 395), further encouraging the development of agriculture in lowland areas that had previously not been cultivated to the same degree (Chuhila, 2016).

The trend toward the influx of agriculturalists was not linear: in the 1950s, for instance, there was a reduction in cultivation throughout Kajiado District due to the eviction of Kikuyu families suspected to be connected to Mau Mau, though in this same decade irrigation farming projects were underway in Loitokitok and Kimana (Rutten, 1992). Irrigation farming schemes were common in the years following World War II as colonial authorities turned their attention to the development of semi-arid rangelands such as Amboseli (e.g., Swynnerton, 1955; ALDEV, 1962). Policies were implemented that aimed to facilitate the conversion of rangelands to farmlands, and enhance the productivity of the Maasai livestock economy through destocking and sedentarization, policies that have had enduring and often negative impacts on pastoral livelihoods and resources in Amboseli (Overton, 1989).

Another major development in the later colonial era was the increased pressure on the government to protect Amboseli wildlife from livestock, leading to interventions with little regard for consultation with local pastoralists (Lindsay, 1989). According to colonial administration reports from the 1950s, it was perceived that competition between pastoralists and wildlife had reached an untenable level. A narrative was put forth at this time that continued grazing in the Amboseli National Reserve would result in depletion of the area's resources and wildlife. For example, Donald Ker, a Kenyan hunter, safari guide, and conservationist of British descent, warned in 1955 that there had been an increase in the number of Maasai herds and that due to overstocking the Maasai must be relocated to new grazing and watering zones outside the central basin (Ker, 1955). Ker observed "many of the indigenous herds of game have been forced to leave what is now a dust-covered desert for grazing grounds many miles away, and travel back to their natural watering places to find them occupied by vast herds of Maasai stock during day-time, so that most of the grass-eating animals are compelled to drink at night or perish (1955)." In the late 1950s government authorities attempted to move livestock concentrations away from the central basin by constructing boreholes and dams in peripheral areas and regulating livestock grazing patterns (Lindsay, 1989). In 1974 a 488 km² portion of the Amboseli basin was gazetted as a National Park, and Maasai access to this area was severely restricted.

Estimates of livestock populations between 1948 and 1984 indicate the number of cattle in Kajiado District has fluctuated a great deal but over the long term the population remained stable (Grandin, 1991), yet per capita livestock holdings have been falling steadily in Amboseli since the 1960s (Western and Manzollillo-Nightingale, 2003). Change in economic and population dynamics coupled with severe successive droughts for the pastoralist Maasai in the Amboseli ecosystem over the last 25 years has resulted in a 3.5-fold increase in crop cultivation supplemented by irrigation (Norman, 2010). Agriculture is more profitable than pastoralism or conservation, and much of the farming in Amboseli is dependent on the wetlands (Okello, 2005). Gaps in our knowledge regarding the wetlands, especially their hydrology, biodiversity and ecosystem functions hinder their sustainable management.

Modeling Recent Socio-Ecological Changes in Amboseli

Paleoecological, archeological, historical and ecological research has determined that many challenges currently facing pastoral systems in sub-Saharan Africa are attributable to environmental factors, caused by climate variability and habitat fragmentation, driven by land use change (Hailegiorgis et al., 2010). Climatic variability affects the availability of pasture and distribution of water points (Hailegiorgis et al., 2010) with pasture production being influenced by rainfall seasonality and storm patterns independent of total rainfall (Western and Manzollillo-Nightingale, 2003). In Amboseli, rainfall is highly variable across months and between years (Altmann et al., 2002; Figure 5), and droughts are a common occurrence (BurnSilver et al., 2007). This leads pastoralists to adapt different coping mechanisms that largely involve changing their land use types or diversifying their livelihoods. Ongoing modeling research seeks to understand the feedback between land use change and the ecology of Amboseli by exploring pastoral land use change decisions under different climatic and land tenure scenarios.

The high rates of pastoral land use change in Amboseli are driven by interacting biophysical, political and socio-economic factors operating at different time scales. The colonial and independent governments in Kenya perceived pastoralism as an inefficient method of managing livestock in Kenyan rangelands (Seno and Shaw, 2002; Western and Manzollillo-Nightingale, 2003; Mwangi and Ostrom, 2009) and advocated for policies that supported communal group ranch subdivision (Seno and Shaw, 2002; BurnSilver et al., 2007; Mwangi and Ostrom, 2009; Sundstrom et al., 2012). Private land ownership was perceived to bring economic development and a national level policy in their support was formulated in 1983 (BurnSilver et al., 2007). Around the same time, poor leadership and management of group ranch resources led to dissatisfaction among group members prompting the subdivision of most Kajiado group ranches from the mid-1970s (Galaty, 1993; Sundstrom et al., 2012). Additionally, between 1973 and 1984, immigrant communities from Central and Eastern Kenya, as well as Maasai herders, further influenced land use change in

Amboseli by farming on the slopes of Kilimanjaro leading to rapid expansion of irrigated and rainfed agriculture (Campbell et al., 2003).

Livestock activities by pastoralists are well adapted to the variable habitat and shifting patch dynamics of arid and semi-arid areas (Bulte et al., 2008). Pastoralists' land use decisions are based on prevailing environmental and socio-economic factors and have differential impacts on the ecology and wildlife structure of dry areas. When deciding their livelihood strategies, contemporary pastoralists diversify their economic options and reduce their drought vulnerability using different strategies, such as agriculture, wage employment, diversification of livestock production and diversification of wildlife based revenues (Western and Manziolillo-Nightingale, 2003; Homewood et al., 2009; Reid et al., 2014). Most (92%) of Amboseli is classified as arid or semi-arid and droughts are characterized by the failure of either or both the short and long rains (BurnSilver et al., 2007). After experiencing severe droughts in 1977 and 1984, most pastoralists in Amboseli settled near the wetlands and practiced agriculture as a temporary survival solution and as a strategy to rebuild their herds (BurnSilver et al., 2007). Though they planned to go back to pastoralism, most became sedentary and shifted to agro-pastoralism (BurnSilver et al., 2007). Agriculture was perceived to have significantly higher and immediate income compared to wildlife conservation, which has minimal direct benefits for most households (Okello and D'Amour, 2008). Readily available water and pastoralists willing to lease their land to farming communities further promoted commercial agriculture around the Amboseli wetlands (Okello and Kioko, 2011). Additionally, wetter parts of Kajiado, which formed dry season grazing zones for livestock, had been taken up by agriculture posing a challenge to livestock herding (Western and Manziolillo-Nightingale, 2003). From these activities, a gradient of pastoral land use across the Amboseli landscape ensued with agro-pastoralism practiced around wetlands, pastoralism on subdivided lands and extensive pastoralism in the interior, dry rangelands zones (Homewood et al., 2009).

Similar trends of sedentarization have been observed in other pastoral areas in East Africa over the last ~100 cal yr. BP. The pastoral Pokot community of northwestern Kenya have changed from extensive livestock grazing land use to more sedentary and diversified livelihoods such as rain-fed agriculture, livestock marketing and honey production (Bollig, 2016; Greiner and Mwaka, 2016). Like in Amboseli, sedentarization among the Pokot began in fertile and wet areas, largely the highlands, and spread to the lowlands (Greiner et al., 2013). Agriculture was unsuccessfully introduced in the lowlands in the 1980s; however, by the 1990s, it had expanded to the lowlands where about 30% of households presently practice it (Greiner and Mwaka, 2016). In Loliondo, located in Ngorongoro District of northern Tanzania, most pastoralists have adopted agriculture combined with traditional pastoralism with peak levels of agriculture expansion documented in the 1970s (McCabe et al., 2010). Interestingly, most of the households adopt agriculture by choice and not out of necessity (McCabe et al., 2010; Greiner and Mwaka, 2016).

Understanding these interactions between natural factors and human activities in Amboseli is challenging because the system is dynamic, complex and constantly evolving. Our model outcomes show land use types as number of grids in kilometer squared (**Figure 6**). Actors are taken to be autonomous with an ability to interact with each other and with their environment (Valbuena et al., 2010). The dominant land use types are livestock grazing, smallholder agriculture, livestock grazing with conservation activities and urban or built-up areas. They overlap across the Amboseli landscape but show some underlying trends based on key drivers of change. On the whole, communal land tenure is predominated by livestock grazing while, the levels of livestock grazing and agriculture do not differ much on private land tenure (**Figures 6A,B**). During a wet year, the prevalence of agriculture rises in communal and private land, where in the communal land there are fewer numbers of grids with agriculture land use compared to private land. Availability of financial support from Non-Governmental Organizations (NGOs) and investors supporting wildlife conservation initiatives shows a trade-off between conservation and other land use types where pastoralists are willing to use their land for wildlife conservation if the conservation budget increases (**Figures 6C–F**). Consequently, wildlife density is correlated with livestock grazing and conservation land use and increases as the wildlife budget increase. Wildlife density is also slightly higher on wet years relative to dry years and where there is no support for conservation; it is inversely related to livestock grazing and agriculture in both communal and private land tenure. The interaction between rainfall and conservation budget show that on a wet year, when the conservation budget is small, agriculture levels are high but reduce as the conservation budget increases. We note that the proportion of land used for urban areas remains constant as the conservation budget increases. However, this is because, in the model, urban areas are largely dependent on current household density in Amboseli, which is static.

By combining insights from vegetation data, interviews with local communities and other secondary data sources, our model shows the interaction of rainfall, land tenure types and availability of conservation budget in shaping land use patterns among pastoralists in Amboseli. It also shows the impact of land use choices on wildlife densities and how that relationship changes in different rainfall years and across land ownership types. Though our socio-ecological model treats different land use types independently, it also shows that the ability of pastoral communities to depend entirely on livestock grazing for their subsistence is declining, leading them to diversify their livelihoods and employ different strategies on and off their land.

Outcomes and Next Steps

The Late Holocene social-ecological history of Amboseli is characterized by a diversification in anthropogenic consequences for the landscape that we have traced in this paper from around the initial inception of pastoralist livelihoods c.4000 years ago to the emergence of agriculture, through the colonial period and into present times. These livelihood strategies emerged upon a context of a longer history of hunter-gatherer use of the animal, plant and water natural capital of Amboseli. As noted above,

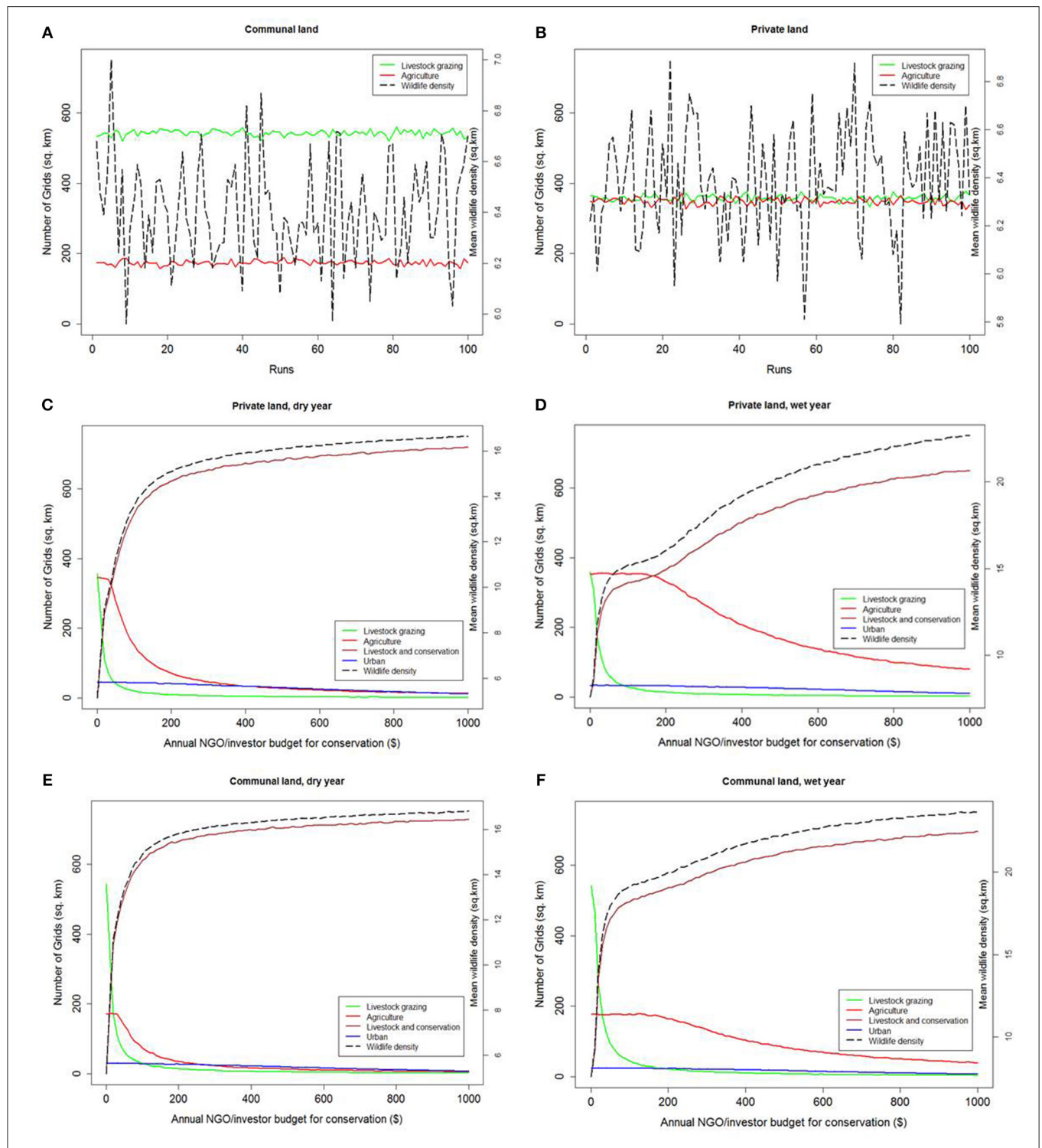


FIGURE 6 | The relationship between land use types and wildlife densities as simulated from a socio-ecological model. **(A,B)** Show the trends between livestock grazing, agriculture and wildlife densities in community and private land tenure in Amboseli. **(C,D)** Compare the relationship between land use types and wildlife density in private land between dry and wet rainfall years as Non-Governmental Organizations (NGOs) or investors into conservation initiatives in Amboseli invest more money. **(E,F)** Compare land use trends, monetary investment into conservation initiatives and wildlife density between dry and wet rainfall years in community land.

the temporal and spatial scale of the environmental effects of early herders in sub-Saharan Africa are only just beginning to be understood. However, despite the older assumption that livestock unilaterally denude the environments in which they live (Sinclair and Fryxell, 1985; Schlesinger et al., 1990), we have demonstrated that heterogeneous, dynamic, and biodiverse East African savannah ecologies have existed with pastoralists as active participants for millennia. After two millennia of what was likely relatively low-density livestock herding and continuing hunting and gathering by different social groups, the cultivation of diverse African and other domesticated crops began around the margins of the ecosystem, most notably on the slopes of Kilimanjaro, creating a mosaic of ethnic groups, land use strategies and settlement systems. These dynamic groups engaged in exchange relationships with each other and were linked to wider networks. The latter most conspicuously involved commodities trade, such as ivory, from at least the late second millennium CE, and connected Amboseli inhabitants to neighboring and distant regions that included the Indian Ocean and, ultimately, also the Atlantic world system. From the late nineteenth century, colonial era policies disrupted and transformed livelihoods and land use practices in East Africa. Pastoralism has nonetheless continued to the present and remains the food production system that culturally and economically defines Amboseli.

Most socio-ecological systems have undergone massive climatic, landscape and institutional changes over the last century (Goldman and Riosmena, 2013) and recent studies have shown that their adaptive and resilient nature plays an important role in mediating impacts of environmental changes and allowing social responses that sustain production (Anderson and Bollig, 2016). Pastoralists in Amboseli never stop practicing livestock grazing entirely despite the environmental, socio-economic and political challenges they face. Instead, they apply different pastoral and agro-pastoral land use strategies. Like most pastoral systems in East African drylands, livestock grazing remains the main land use type (Seno and Shaw, 2002; Homewood et al., 2009) and plays a major role in Amboseli's culture and economy (Sundstrom et al., 2012). Over the past decades, populations have increased markedly and the introduction of intensive agriculture surrounding the Amboseli wetlands has resulted in unprecedented change. Given the rapidity of land cover change and challenges surrounding human-ecosystem-climate interactions, there is increasing interest in exploiting the potential of paleoenvironmental and archeological records characterizing these changes to contextualize processes governing long-term dynamics and development of the ecosystem.

As outlined above, a comprehensive understanding of interactions between environmental change, social use and the important drivers that have determined ecosystem composition and structure within the Amboseli ecosystem since ~5,000 cal yr. BP is emerging. Further extensive archeological surveys and intensive archival work are needed to enhance and fill in the gaps about the movement of people and animals as well as the decisions influencing their behavior. Long-term investment is needed from all stakeholders, i.e., the local communities, the local and national government, the conservation and tourism industry as well as researchers, to continue in the development

of adaptive and sustainable management plans for current and future Amboseli communities.

Undoubtedly, finer resolution data will improve our understanding of past socio-ecological dynamics within the landscape, especially due to the different responses that have been observed, likely indicating local and regional drivers of change. However, alongside gaining a greater comprehension of events that have occurred in the past the next step is also to build on the combined datasets and the insights from them by fully exploring their application to present-day and future issues. One such issue that has formed a theme throughout this paper concerns the longevity and adaptive capacity of the pastoralist lifestyle in Amboseli. However, this is thought to be increasingly under threat from factors such as competing land uses, changing weather patterns and climate, the increasing move to sedentarization, degradation of the wider landscape and restrictions on access to labor as more children go into (and stay in) education and/or then move away (Seno and Tome, 2013).

The current predictions for population growth in Kenya suggest that numbers will almost double by 2050 (United Nations, Department of Economic and Social Affairs, Population Division, 2017); climate change projections suggest that temperatures on the African continent are expected to rise faster than the rest of the world (Adhikari et al., 2015); and rainfall patterns will be substantially altered (Platts et al., 2015). These predictions lead to questions such as what are the implications of these changes to pastoralism in Amboseli? Will pastoralists continue to adapt and change? Will a tipping point be reached and when? We cannot know the answers to these questions from the data and insights presented alone, but this does not mean that they are of no relevance.

The final technique that we utilized was ABM. This approach was used to help understand the complex and shifting biophysical and socio-economic factors affecting pastoral livelihoods in the very recent past. However, by continuing to work alongside modelers there is potential to combine techniques such as ABM or Bayesian modeling with the datasets from the past in order to interrogate them predictively for the future. Combining the different datasets presented here has already *illustrated* the adaptive capacity of pastoralists over the *longue durée* changing environmental and social pressures, the next step is to *actively use* these insights within models with specific questions in mind. This would not only provide estimates and models that are potentially useful to a range of stakeholders, e.g., the Amboseli community, planners, conservation specialists etc., but they would also allow us (as researchers) to pose research questions—at what point may a pastoralist lifestyle become unviable in Amboseli or will it thrive? What are likely to be the factor/s driving these changes? The Amboseli landscape has seen a long history of change, affected by both local and regional factors, and we are only just coming to comprehend this complexity using the interdisciplinary approach taken here. Landscape evolution does not stop at the end of a paleoecological core or an oral history account, but it continues to evolve, we need to find nuanced methods for linking these valuable historical insights into the current, and informing the future, management of the these important conservation *and* pastoral landscapes.

AUTHOR CONTRIBUTIONS

Primary research on the paleoecological records of Amboseli was undertaken by EG, CC-M, supervised by RM; primary research on the archeology of Amboseli was undertaken by AS, supervised by PL; MC, and AS undertook the historical research relating to Kilimanjaro and RK developed the socio-ecological models, supervised by RM. All authors contributed to the drafting and writing of the manuscript. All authors approved it for publication.

ACKNOWLEDGMENTS

We gratefully acknowledge those who helped in sediment collection and processing, such as Veronica Muiruri, Rahab Kinyanjui, Rebecca Muthoni and Stephen Rucina from the National Museums of Kenya; and Nik Petek, Geert van der Plas and Aynalem Zenebe from the REAL project. John Kanyingi helped survey wetland areas of Amboseli. We thank Rebecca Muthoni and Lauren Shotter for collecting data in the laboratory. We thank David Western, and the wider African Conservation Centre, for continued discussions on the Amboseli research. National Commission issued permits for this research for Science, Technology and Innovation permits

NACOSTI/P/14/6965/1096. This research was partially funded by a European Commission Marie Skłodowska-Curie Initial Training Network grant to PL and RM titled “Resilience in East African Landscapes (REAL)” (FP7-PEOPLE-2013-ITN project number 606879). CCM was supported through the “Adaptation and Resilience to Climate Change (ARCC)” project under the Sustainability and resilience—tackling climate and environmental changes programme funded by Vetenskapsrådet, Sida and Formas (2016-06355) awarded to PL and RM. The British Institute in Eastern Africa are thanked for their continued support.

SUPPLEMENTARY MATERIAL

The Supplementary Material for this article can be found online at: <https://www.frontiersin.org/articles/10.3389/feart.2017.00113/full#supplementary-material>

Table S1 | Radiocarbon dates from four Amboseli sites with lab ID and sample information. Bulk sediment was dated at all the sites except at *Esambu 180.5 cm.

Table S2 | Table containing a list of all the pollen identified from the four Amboseli records, i.e., Enkongu, Kimana, Esambu and Namelok. The taxa identified, family and Plant Function Type are listed. Pioneer and disturbance taxa are highlighted. **X** means present **N** means absent. Classification into groups is based on <http://www.africanplants.senckenberg.de/root/index.php>

REFERENCES

- Adhikari, U., Nejadhashemi, A. P., and Woznicki, S. A. (2015). Climate change and eastern Africa: a review of impact on major crops. *Food Energy Sec.* 4, 110–132. doi: 10.1002/fes3.61
- Ahlström, A., Xia, J., Arneth, A., Luo, Y., and Smith, B. (2015). Importance of vegetation dynamics for future terrestrial carbon cycling. *Environ. Res. Lett.* 10:054019. doi: 10.1088/1748-9326/10/5/054019
- ALDEV (1962). *African Land Development in Kenya 1946-62*. Nairobi: English Press.
- Alexander, J. (2001). Islam, archaeology and slavery in Africa. *World Archaeol.* 33, 44–60. doi: 10.1080/00438240120047627
- Alpers, E. A. (1975). *Ivory and Slaves in East Central Africa: Changing Patterns of Internal Trade to the Late Nineteenth Century*. London: Heinemann.
- Alpers, E. A. (1992). “The ivory trade in Africa. An historical overview,” in *Elephant: The Animal and its Ivory in African Culture*, ed D. Ross (Los Angeles CA: University of California), 349–360.
- Altmann, J., Alberts, S. C., Altmann, S. A., and Roy, S. B. (2002). Dramatic change in local climate patterns in the Amboseli basin, Kenya. *Afr. J. Ecol.* 40, 248–251. doi: 10.1046/j.1365-2028.2002.00366.x
- Altmann, S. A., Post, D. G., and Klein, D. F. (1987). Nutrients and toxins of plants in Amboseli, Kenya. *Afr. J. Ecol.* 25, 279–293. doi: 10.1111/j.1365-2028.1987.tb01119.x
- Ambrose, S. (1984). “The introduction of pastoral adaptations to the highlands of east africa,” in *From Hunters to Farmers: The Causes and Consequences of Food Production in Africa*, eds J. D. Clark and S. A. Brandt (Berkeley, CA: University of California Press), 212–239.
- Ambrose, S. (1998). Chronology of the later stone age and food production in East Africa. *J. Archaeol. Sci.* 25, 377–392. doi: 10.1006/jasc.1997.0277
- Ambrose, S. H., and Sikes, N. E. (1991). Soil carbon isotope evidence for Holocene habitat change in the Kenya Rift Valley. *Science* 253:1402. doi: 10.1126/science.253.5026.1402
- Anderson, D. M. (2016). The beginning of time? Evidence for catastrophic drought in Baringo in the early nineteenth century. *J. East Afr. Stud.* 10, 45–66. doi: 10.1080/17531055.2015.1134532
- Anderson, D. M., and Bollig, M. (2016). Resilience and collapse: histories, ecologies, conflicts and identities in the Baringo-Bogoria basin, Kenya. *J. East Afr. Stud.* 10, 1–20. doi: 10.1080/17531055.2016.1150240
- Archibald, S., and Bond, W. J. (2004). Grazer movements: spatial and temporal responses to burning in a tallgrass African savannah. *Int. J. Wildland Fire* 13, 377–385. doi: 10.1071/WF03070
- Ashley, C. Z., and Grillo, K. M. (2015). Archaeological ceramics from eastern Africa: past approaches and future directions. *Azania* 50, 460–480. doi: 10.1080/0067270X.2015.1102939
- Ashley, G. M., Maitima-Mworia, J., Muasya, A. M., Owen, R. B., Driese, S. G., Hover, V. C., et al. (2004). Sedimentation and recent history of a freshwater wetland in a semi-arid environment: Lobo Swamp, Kenya, East Africa. *Sedimentology* 51, 1301–1321. doi: 10.1111/j.1365-3091.2004.00671.x
- Ashley, G. M., Wet, C. B., Barboni, D., and Magill, C. R. (2016). Subtle signatures of seeps: record of groundwater in a dryland, DK, Olduvai Gorge, Tanzania. *Depositional Rec.* 2, 4–21. doi: 10.1002/dep2.11
- Baker, H. G. (1991). The continuing evolution of weeds. *Econ. Bot.* 45, 445–449. doi: 10.1007/BF02930705
- Bamber, R. N. (1982). Sodium hexametaphosphate as an aid in benthic sample sorting. *Mar. Environ. Res.* 7, 251–255. doi: 10.1016/0141-1136(82)90017-4
- Barker, P. A., Hurrell, E. R., Leng, M. J., Plessen, B., Wolff, C., Conley, D. J., et al. (2013). Carbon cycling within an East African lake revealed by the carbon isotope composition of diatom silica: a 25-ka record from Lake Challa, Mt. Kilimanjaro. *Quat Sci. Rev.* 66, 55–63. doi: 10.1016/j.quascirev.2012.07.016
- Beachey, R. W. (1967). The East African ivory trade in the nineteenth century. *J. Afr. Hist.* 8, 269–290. doi: 10.1017/S0021853700007052
- Bernsten, J. L. (1976). The maasai and their neighbours: variables of interaction. *Afr. Econ. Hist.* 2, 1–11.
- Bert, F. E., Rovere, S. L., Macal, C. M., North, M. J., and Podestà, G. P. (2014). Lessons from a comprehensive validation of an agent based-model: the experience of the Pampas Model of Argentinean agricultural systems. *Ecol. Modell.* 273, 284–298. doi: 10.1016/j.ecolmodel.2013.11.024
- Birks, H., Lotter, A. F., Juggins, S., and Smol, J. P. (2012). *Tracking Environmental Change Using Lake Sediments: Data Handling and Numerical Techniques*, Vol. 5. Springer Netherlands.

- Blaauw, M., van Geel, B., Kristen, I., Plessen, B., Lyaruu, A., Engstrom, D. R., et al. (2010). High-resolution ^{14}C dating of a 25,000-year lake-sediment record from equatorial East Africa. *Quat. Sci. Rev.* 30, 3043–3059. doi: 10.1016/j.quascirev.2011.07.014
- Bodin, P., Olin, S., Pugh, T. A. M., and Arneth, A. (2016). Accounting for interannual variability in agricultural intensification: the potential of crop selection in Sub-Saharan Africa. *Agric. Sys.* 148, 159–168. doi: 10.1016/j.agry.2016.07.012
- Boivin, N., Crowther, A., Helm, R., and Fuller, D. Q. (2013). East Africa and Madagascar in the Indian Ocean world. *J. World Prehist.* 26, 213–281. doi: 10.1007/s10963-013-9067-4
- Boivin, N., Crowther, A., Prendergast, M., and Fuller, D. Q. (2014). Indian Ocean food globalisation and Africa. *Afr. Archaeol. Rev.* 31, 547–581. doi: 10.1007/s10437-014-9173-4
- Boivin, N., Zeder, M. A., Fuller, D. Q., Crowther, A., Larson, G., Erlandson, J. M., et al. (2016). Ecological consequences of human niche construction: examining long-term anthropogenic shaping of global species distributions. *Proc. Natl. Acad. Sci. U.S.A.* 113, 6388–6396. doi: 10.1073/pnas.1525200113
- Boles, O. J. C., and Lane, P. J. (2016). The Green, Green Grass of Home: an archaeo-ecological approach to pastoralist settlement in central Kenya. *Azania* 51, 507–530. doi: 10.1080/0067270X.2016.1249587
- Bollig, M. (2016). Adaptive cycles in the savannah: pastoral specialization and diversification in northern Kenya. *J. East Afr. Stud.* 10, 21–44. doi: 10.1080/17531055.2016.1141568
- Bond, W. J., and Parr, C. L. (2010). Beyond the forest edge: ecology, diversity and conservation of the grassy biomes. *Biol. Cons.* 143, 2395–2404. doi: 10.1016/j.biocon.2009.12.012
- Bonnefille, R., and Riollet, G. (1988). The Kashiru pollen sequence (Burundi) palaeoclimatic implications for the last 40,000 yr. B.P. in tropical Africa. *Quat. Res.* 30, 19–13. doi: 10.1016/0033-5894(88)90085-3
- Boone, R., Galvin, K., BurnSilver, S., Thornton, P., Ojima, D., and Jawson, J. (2011). Using coupled simulation models to link pastoral decision making and ecosystem services. *Ecol. Soc.* 16:6. doi: 10.5751/ES-04035-160206
- Bower, J. R. (1991). The Pastoral Neolithic of East Africa. *J. World Prehis.* 5, 49–82. doi: 10.1007/BF00974732
- Bower, J. R. F., Nelson, C. M., Waibel, A. F., and Wandibba, S. (1977). The University of Massachusetts' later stone age/pastoral 'Neolithic' comparative study in Central Kenya: an overview. *Azania* 12, 119–146.
- Bulte, E. H., Boone, R. B., Stringer, R., and Thornton, P. K. (2008). Elephants or onions? Paying for nature in Amboseli, Kenya. *Environ. Dev. Econ.* 13, 395–414. doi: 10.1017/S1355770X08004312
- BurnSilver, S. B. (2009). "Pathways of continuity and change: maasai livelihoods in Amboseli, Kajiado District, Kenya," in *Staying Maasai?*, eds K. Homewood, P. Kristjansson, and P. C. Trench (New York, NY: Springer), 161–207.
- BurnSilver, S., and Mwangi, E. (2007). *Beyond Group Ranch Subdivision: Collective Action for Livestock Mobility, Ecological Viability and Livelihoods*. Washington, DC: International Food Policy Research Institute.
- BurnSilver, S., Worden, J., and Boone, R. B. (2007). "Processes of fragmentation in the amboseli ecosystem, Southern Kajiado District, Kenya," in *Fragmentation of Semi-Arid and Arid Landscapes: Consequences for Human and Natural Systems*, eds K. Galvin, R. Reid, R. Behnke, and T. Hobbs (New York, NY: Verlag Publishers), 225–254.
- Bussmann, R. W. (2001). Succession and regeneration patterns of East African mountain forests: a review. *Syst. Geogr. Plants.* 1, 959–974. doi: 10.2307/3668731
- Bussmann, R. W., and Beck, E. (1995a). The forests of Mount Kenya (Kenya), a phytosociological synopsis. *Phytocoenologia* 25, 467–560. doi: 10.1127/phyto/25/1995/467
- Bussmann, R. W., and Beck, E. (1995b). Regeneration and succession processes in the Cedar-Forests (*Juniperion procerae*) of Mt. Kenya. *Ecotropica* 1, 79–84.
- Butz, R. J. (2009). Traditional fire management: historical fire regimes and land use change in pastoral East Africa. *Int. J. Wildland Fire* 18, 442–450. doi: 10.1071/WF07067
- Campbell, D. J., Lusch, D. P., Smucker, T. A., and Wangui, E. E. (2003). *Land Use Change Impacts and Dynamics (LUCID)*. Project working paper 19. ILRI, Nairobi, Kenya.
- Chuhila, M. J. (2016). *Coming down the Mountain: History of Land Use Change in Kilimanjaro, ca. 1920 to 2000s*. Ph.D. thesis, University of Warwick.
- Coetzee, J. A. (1964). Evidence for a considerable depression of the vegetation belts during the Upper Pleistocene on the East African mountains. *Nature* 204, 564–566.
- Coetzee, J. A. (1967). "Pollen analytical studies in East and Southern Africa," in *Palaeoecology of Africa and of the Surrounding Islands and Antarctica*, ed E. M. van Zinderen Bakker (Amsterdam: CRC Press, Taylor and Francis Group), 1–146.
- Colombaroli, D., van der Plas, G., Rucina, S., and Verschuren, D. (in press). Determinants of savanna-fire dynamics in the eastern Lake Victoria catchment (western Kenya) during the last 1200 years. *Quat. Int.* doi: 10.1016/j.quaint.2016.06.028
- Courtney-Mustaphi, C. J., Shoemaker, A. C., Githumbi, E. N., Kariuki, R., Muriuki, R. M., Rucina, S., et al. (2015). Historical ecology perspectives of changes in Amboseli, Kenya. *GLP* 12, 26–29. Available online at: <https://glp.earth/how-we-work/glp-newsletters/glp-newsletter-issue-no-12-november-2015>
- Coutu, A. N., Lee-Thorp, J., Collins, J. M., and Lane, P. J. (2016). Mapping the elephants of the 19th Century East African Ivory trade with a multi-isotope approach. *PLoS ONE* 11:e0163606. doi: 10.1371/journal.pone.0163606
- Crosby, A. (2003) [1972]. *The Columbian Exchange: Biological and Cultural Consequences of 1492*. Westport, CN: Praeger.
- Crowther, A., Prendergast, M. E., Fuller, D. Q., and Boivin, N. (in press). Subsistence mosaics, forager-farmer interactions, and the transition to food production in eastern Africa. *Quat. Int.* doi: 10.1016/j.quaint.2017.01.014
- Cutler, A. (1985). *The Craft of Ivory: Sources, Techniques, and Uses in the Mediterranean World, AD 200–1400*. Washington, DC: Dumbarton Oaks.
- Dale, D., and Ashley, C. Z. (2010). Holocene hunter-fisher-gatherer communities: new perspectives on Kanyore-using communities of western Kenya. *Azania* 45, 24–48. doi: 10.1080/00672700903291716
- Damnati, B. (2000). Holocene lake records in the Northern Hemisphere of Africa. *J. Afr. Earth Sci.* 31, 253–262. doi: 10.1016/S0899-5362(00)00089-0
- Davies, M. I. J. (2015). Economic specialisation, resource variability, and the origins of intensive agriculture in Eastern Africa. *Rural Landscapes Soc. Environ. Hist.* 2, 1–18. doi: 10.16993/r.laf
- DeBusk, G. H. (1998). A 37,500-year pollen record from Lake Malawi and implications for the biogeography of Afrotropical forests. *J. Biogeogr.* 25, 479–500. doi: 10.1046/j.1365-2699.1998.2530479.x
- De Langhe, E. (2007). "The establishment of traditional plantain cultivation in the African rain forest: a working hypothesis," in *Rethinking Agriculture: Archaeological and Ethnoarchaeological Perspectives*, eds T. P. Denham, J. Iriarte, and L. Vrydaghs (Walnut Creek: Left Coast Press), 361–370.
- De Langhe, E., Swennen, R., and Vuylsteke, D. (1995). Plantain in the Early Bantu World. *Azania* 29, 147–160.
- De Leeuw, P. N., and Tothill, J. C. (1990). *The Concept of Rangeland Carrying Capacity in Sub-Saharan Africa: Myth or Reality*. London: Overseas Development Institute, Pastoral Development Network.
- Deocampo, D. M. (2002). Sedimentary structures generated by *Hippopotamus amphibius* in a lake-margin wetland, Ngorongoro Crater, Tanzania. *Palaios* 17, 212–217. doi: 10.1669/0883-1351(2002)017<0212:SSGBHA>2.0.CO;2
- Dresang, D. L., and Sharkansky, I. (1975). Sequences of Change and the Political Economy of public Corporations: Kenya. *J. Polit.* 37, 163–186. doi: 10.2307/2128895
- Dunne, T., Dietrich, W. E., and Brunengo, M. J. (1978). Recent and past erosion rates in semi-arid Kenya. *Z. Geomorphol.* 29, 130–140.
- Finch, J., and Marchant, R. (2011). A palaeoecological investigation into the role of fire and human activity in the development of montane grasslands in East Africa. *Veg. Hist. Archaeobot.* 20, 109–124. doi: 10.1007/s00334-010-0276-9
- Finch, J., Marchant, R., and Courtney-Mustaphi, C. J. (2016). Ecosystem change in the South Pare Mountain bloc, Eastern Arc Mountains of Tanzania. *Holocene* 27, 796–810. doi: 10.1177/0959683616675937
- Foley, R. (1981). *Off-Site Archaeology and Human Adaptation in Eastern Africa: An Analysis of Regional Artefact Density in the Amboseli, Southern Kenya*. Cambridge: Cambridge Monographs in African Archaeology 3. BAR International Series 97.
- Fosbrooke, H. A., and Sassoon, H. (1965). Archaeological Remains on Kilimanjaro. *Tanganyika Notes Records* 64, 62–64.
- Fries, R. E., and Fries, T. C. E. (1948). "Phytogeographical researches on Mt. Kenya and Mt. Aberdare, British East Africa" in *Kungl. Svenska Vetenskapsakademiens*

- Handlingar, *Tbedje Serien* (Stockholm: Band 25. No 5. Almqvist & Wiksell Boktryckeri-a.-b.), 1–83.
- Fuller, D. Q., and Boivin, N. (2009). “Crops, cattle and commensals across the Indian Ocean: current and potential archaeobiological evidence,” in *Plantés et Sociétés, Études océan Indien* 42–43, ed G. Lefèvre (Paris: CEROI-INALCO), 3–46.
- Fuller, D. Q., Boivin, N., Hoogervorst, T., and Allaby, R. (2011b). Across the Indian Ocean: the prehistoric movement of plants and animals. *Antiquity* 84, 544–558. doi: 10.1017/S0003598X00067934
- Fuller, D. Q., and Hildebrand, E. A. (2013). “Domesticating plants in Africa,” in *The Oxford Handbook of African Archaeology*, eds P. Mitchell and P. J. Lane (Oxford: University of Oxford Press), 507–525.
- Fuller, D. Q., van Etten, J., Manning, K., Castillo, C., Kingwell-Banham, E., Weisskopf, A., et al. (2011a). The contribution of rice agriculture and livestock pastoralism to prehistoric methane levels: an archaeological assessment. *Holocene* 21, 743–759. doi: 10.1177/0959683611398052
- Galaty, J. G. (1993). “Maasai expansion and the New East African Pastoralism,” in *Being Maasai: Ethnicity and Identity in East Africa*, eds R. Spear and J. Waller (London: Curry), 61–86.
- Garcin, Y., Melnick, D., Strecker, M. R., Olago, D., and Tiercelin, J. J. (2012). East African mid-Holocene wet-dry transition recorded in palaeo-shorelines of Lake Turkana, northern Kenya Rift. *Earth Planet Sci. Lett.* 331, 322–334. doi: 10.1016/j.epsl.2012.03.016
- Gasse, F. (2000). Hydrological changes in the African tropics since the Last Glacial Maximum. *Quat. Sci. Rev.* 19, 189–211. doi: 10.1016/S0277-3791(99)00061-X
- Gifford-Gonzalez, D. P. (1998). Early pastoralists in East Africa: ecological and social dimensions. *J. Anthropol. Archaeol.* 17, 166–200. doi: 10.1006/jaar.1998.0322
- Gifford-Gonzalez, D. P. (2000). Animal disease challenges to the emergence of pastoralism in sub-Saharan Africa. *Afr. Archaeol. Rev.* 17, 95–139. doi: 10.1023/A:1006601020217
- Gillson, L. (2004). Testing non-equilibrium theories in savannahs: 1400 years of vegetation change in Tsavo National Park, Kenya. *Ecol. Comp.* 1, 281–298. doi: 10.1016/j.ecocom.2004.06.001
- Gillson, L. (2006). A ‘large infrequent disturbance’ in an East African savannah. *Afr. J. Ecol.* 44, 458–467. doi: 10.1111/j.1365-2028.2006.00662.x
- Githumbi, E. (2017). *Holocene Environmental and Human Interactions in East Africa*. Unpublished Ph.D., thesis, University of York, Dordrecht.
- Githumbi, E., Courtney-Mustaphi, C., and Marchant, R. (2016). Holocene ecosystem, social and landscape dynamics in East Africa. *Quat. Int.* 404, 199–200. doi: 10.1016/j.quaint.2015.08.175
- Githumbi, E., Courtney-Mustaphi, C., Yun, K. J., Muiruri, V., Rucina, S. R., and Marchant, R. (2017). *Late Holocene Wetland Transgression and 500 Years of Vegetation and Fire Variability in the Semi-Arid Amboseli Landscape, Southern Kenya*. Dordrecht: AMBIO.
- Glassman, J. (1995). *Feasts and Riots: Revelry, Rebellion, and Popular Consciousness on the Swahili Coast, 1856–888*. London: James Currey.
- Goldman, M. J., and Riosmena, F. (2013). Adaptive capacity in Tanzanian Maasailand: changing strategies to cope with drought in fragmented landscapes. *Glob. Environ. Chang.* 23, 588–597. doi: 10.1016/j.gloenvcha.2013.02.010
- Grandin, B. E. (1991). “The Maasai: socio-historical context and group Ranches,” in *Maasai Herding – An Analysis of the Livestock Production System of Maasai Pastoralists in Eastern Kajiado District, Kenya*, eds S. Bekure, P. N. de Leeuw, B. E. Grandin, and P. J. H. Neate (Addis Ababa: International Livestock Centre for Africa), 21–39.
- Greiner, C., Alvarez, M., and Becker, M. (2013). From cattle to corn: attributes of emerging farming systems of former pastoral nomads in East Pokot, Kenya. *Soc. Nat. Resour.* 26, 1478–1490. doi: 10.1080/08941920.2013.791901
- Greiner, C., and Mwaka, I. (2016). Agricultural change at the margins: adaptation and intensification in a Kenyan dryland. *J. East Afr. Stud.* 10, 130–149. doi: 10.1080/17531055.2015.1134488
- Grimm, V., Berger, U., Bastiansen, F., Eliassen, S., Ginot, V., Giske, J., et al. (2005). A standard protocol for describing individual-based and agent-based models. *Ecol. Model.* 198, 115–126. doi: 10.1016/j.ecolmodel.2006.04.023
- Hailegiorgis, A. B., Kennedy, W. G., Rouleau, M., Bassett, J. K., Coletti, M., Balan, G. C., et al. (2010). *An Agent Based Model of Climate Change and Conflict among Pastoralists in East Africa*. Doctoral dissertation, International Environmental Modelling and Software Society.
- Håkansson, N. T. (2004). The human ecology of world systems in East Africa: the impact of the ivory trade. *Hum. Ecol.* 32, 561–591. doi: 10.1007/s10745-004-6097-7
- Håkansson, N. T. (2008). “The decentralized landscape: regional wealth and the expansion of production in Northern Tanzania before the eve of colonialism,” in *Economics and the Transformation of Landscape*, eds L. Cliggett and C. A. Pool (Lanham: Altamira Press), 239–265.
- Hamidu, A. S., Shirima, D. D., Courtney-Mustaphi, C. J., Marchant, R., and Munishi, P. K. T. (2017). The impact of land use and land cover change on biodiversity within and adjacent Kibasira Swamp in Kilombero valley, Tanzania. *Afr. J. Ecol.* doi: 10.1111/aje.12488. [Epub ahead of print].
- Hamilton, A. C. (1976). Identification of East African Urticales Pollen. *Pollen Et Spores* 18, 27–66.
- Hamilton, A. C. (1982). *Environmental History of East Africa: A Study of the Quaternary*. London: Academic Press.
- Hamilton, A. C., and Perrott, R. (1980). “Modern pollen deposition on a tropical african mountain,” in *Pollen Et Spores, Chapter Modern Pol*, Vol. 22 (Amsterdam), 437–468.
- Hamilton, A., Taylor, D., and Vogel, J. C. (1986). Early forest clearance and environmental degradation in south-west Uganda. *Nature* 320, 164–167. doi: 10.1038/320164a0
- Hay, R. L., and Stoessell, R. K. (1984). Sepiolite in the Amboseli Basin of Kenya: a new interpretation. *Dev. Sed.* 37, 125–136. doi: 10.1016/S0070-4571(08)70032-3
- Heckmann, M. (2014). Farmers, smelters and caravans: two thousand years of land use and soil erosion in North Pare, NE Tanzania. *Catena* 113, 187–201. doi: 10.1016/j.catena.2013.07.010
- Heckmann, M., Muiruri, V., Boom, A., and Marchant, R. (2014). Human-environment interactions in an agricultural landscape: a 1400-yr. sediment and pollen record from North Pare, NE Tanzania. *Palaeogeog. Palaeoclim. Palaeoecol.* 406, 49–61 doi: 10.1016/j.palaeo.2014.04.005
- Hedberg, O. (1951). Vegetation belts of the East African mountains. *Svensk Botanisk Tidskrift* 45, 140–202.
- Helm, R. (2000). *Conflicting Histories: The Archaeology of Iron-Working, Farming Communities in the Central and Southern Coast Region of Kenya*. Unpublished Ph.D., thesis, University of Bristol.
- Hemp, A. (2006a). Continuum or zonation? Altitudinal gradients in the forest vegetation of Mt. Kilimanjaro. *Plant Ecol.* 184, 27–42. doi: 10.1007/s11258-005-9049-4
- Hemp, A. (2006b). Vegetation of Kilimanjaro: hidden endemics and missing bamboo. *Afr. J. Ecol.* 44, 305–328. doi: 10.1111/j.1365-2028.2006.00679.x
- Hemp, A., and Beck, E. (2001). *Erica excelsa* as a fire-tolerating component of Mt. Kilimanjaro’s forests. *Phytocoenologia* 31, 449–475. doi: 10.1127/phyto/31/2001/449
- Hobbs, R. J., Arico, S., Aronson, J., Baron, J. S., Bridgewater, P., Cramer, V. A., et al. (2006). Novel ecosystems: theoretical and management aspects of the new ecological world order. *Global Ecol Biogeog.* 15, 1–7. doi: 10.1111/j.1466-822X.2006.00212.x
- Homewood, K., Kristjanson, P., and Trench, P. (2009). *Staying Maasai: Livelihoods, Conservation and Development in East African rangelands*, Vol. 5. New York, NY: Springer Science & Business Media.
- Hughes, L. (2006). *Moving the Maasai: A Colonial Misadventure*. Basingstoke: Palgrave Macmillan.
- Iles, L. (2016). The role of metallurgy in transforming global forests. *J. Archaeol. Meth. Theory.* 23, 1219–1241. doi: 10.1007/s10816-015-9266-7
- Iles, L., Robertshaw, P., and Young, R. (2014). A furnace and associated iron working remains at Munsu, Uganda. *Azania* 49, 45–63. doi: 10.1080/0067270X.2013.877619
- Jennings, C. C. (2003). “They called themselves Iloikop: rethinking pastoralist history in nineteenth-century East Africa,” in *Sources and Methods in African History: Spoken, Written, Unearthed*, eds T. Falola and C. C. Jennings (Rochester, NY: University of Rochester Press), 173–194.
- Jolly, D., and Haxeltine, A. (1997). Effect of low glacial atmospheric CO₂ on tropical African montane vegetation. *Science* 276, 786–788. doi: 10.1126/science.276.5313.786

- Jönsson, A. M., Lagergren, F., and Smith, B. (2015). Forest management facing climate change—an ecosystem model analysis of adaptation strategies. *Mitig. Adapt. Strat. Glob. Change* 20, 201–220. doi: 10.1007/s11027-013-9487-6
- Jowsey, P. C. (1966). An improved peat sampler. *New Phytol.* 65, 245–248. doi: 10.1111/j.1469-8137.1966.tb06356.x
- Kamau, P. N., and Medley, K. E. (2014). Anthropogenic fires and local livelihoods at Chyulu Hills, Kenya. *Landscape Urban Plan.* 124, 76–84. doi: 10.1016/j.landurbplan.2014.01.010
- Kenya National Bureau of Statistics (KNBS) (2010). *Kenya 2009 Population and Housing Census Highlights KNBS Government of Kenya, Nairobi*. Nairobi: Kenya National Bureau of Statistics.
- Ker, D. (1955). *Letter to the Editor – The East African Standard*. Nairobi: The East African Standard.
- Kiage, L. M., and Liu, K. B. (2006). Late Quaternary paleoenvironmental changes in East Africa: a review of multiproxy evidence from palynology, lake sediments, and associated records. *Prog. Phys. Geog.* 30, 633–658. doi: 10.1177/0309133306071146
- Krapf, J. L. (1854). *Vocabulary of the Engutuk Eloikob or the Wakuafi-Nation in the Interior of Equatorial East Africa*. Tübingen: L. F. Fues.
- Kunz, G. F. (1926). *Ivory and the Elephant in Art, in Archaeology and in Science*. New York, NY: Doubleday.
- Kusimba, C. M. (2009). “Landscape at two scales: economy and trade in East Africa,” in *Politics and Power: Archaeological Perspectives on the Landscapes of Early States*, eds S. E. Falconer and C. L. Redman (Tucson: University of Arizona Press), 163–178.
- Kusimba, C. M., and Kusimba S. B., (2005). “Mosaics and Interactions: East Africa, 2000 B. P. to the Present,” in *African Archaeology: A Critical Introduction*, ed A. B. Stahl (Oxford: Blackwell), 392–419.
- Kusimba, S. B. (1999). Hunter-gatherer land use patterns in later stone age East Africa. *J. Anthropol. Archaeol.* 18, 165–200. doi: 10.1006/jaar.1998.0335
- Kusimba, S. B. (2001). The Pleistocene Later Stone Age in East Africa: excavations and lithic assemblages from Lukenya Hill. *Afr. Archaeol. Rev.* 18, 77–123. doi: 10.1023/A:1011032025300
- Kusimba, S. B. (2013). “Hunter-gatherer-fishers of eastern and South-Central Africa since 20,000 years ago,” in *The Oxford Handbook of African Archaeology*, eds P. Mitchell and P. J. Lane (Oxford: Oxford University Press), 461–472.
- Lamb, H., Darbyshire, I., and Verschuren, D. (2003). Vegetation response to rainfall variation and human impact in central Kenya during the past 1100 years. *Holocene* 13, 285–292. doi: 10.1191/0959683603hl618rr
- Lane, P. J. (2004). The ‘moving frontier’ and the transition to food production in Kenya. *Azania* 39, 243–264. doi: 10.1080/00672700409480402
- Lane, P. J. (2010). Developing landscape historical ecologies in Eastern Africa: an outline of current research and potential future directions. *Afr. Stud.* 69, 299–322. doi: 10.1080/00020184.2010.499203
- Lane, P. J. (2011a). An outline of the later Holocene archaeology and pre-colonial history of the Ewaso Basin, Kenya. *Smithson. Contrib. Zool.* 632, 11–30. doi: 10.5479/si.00810282.632.11
- Lane, P. J. (2011b). “Slavery and slave trading in Eastern Africa: exploring the intersections of historical sources and archaeological evidence,” in *Slavery in Africa: Archaeology and Memory*, eds P. J. Lane and K. C. MacDonald (London: Oxford University Press), 281–314.
- Lane, P. J. (2013). “Trajectories to pastoralism in northern and central Kenya: an overview of the archaeological and environmental evidence,” in *Pastoralism in Africa: Past Present and Future*, eds M. Bollig and H. P. Wotzka (Oxford: Berghahn Books), 104–143.
- Lane, P. J., Ashley, C., and Oteyo, G. (2006). New dates from Kanyore and Urewe wares from northern Nyanza, Kenya. *Azania*. 41, 123–138. doi: 10.1080/00672700609480438
- Lane, P. J., Seitsonen, O., Harvey, P., Mire, S., and Odede, F. (2007). The transition to farming in eastern Africa: new faunal and dating evidence from Wadh Lang'o and Usenge, Kenya. *Antiquity* 81, 62–81. doi: 10.1017/S0003598X00094849
- Laws, R. M. (1968). Interactions between elephant and *Hippopotamus* populations and their environments. *East Afr. Agric. For.* 33, 140–147.
- Lee, R. B. (1979). *The !Kung San: Men, Women, and Work in a Foraging Society*. Cambridge: Cambridge University Press.
- Lehsten, V., Arneth, A., Spessa, A., Thonicke, K., and Moustakas, A. (2016). The effect of fire on tree–grass coexistence in savannahs: a simulation study. *Int. J. Wildland Fire* 25, 137–146. doi: 10.1071/WF14205
- Lejju, B. J., Robertshaw, P., and Taylor, D. (2003). Vegetation history and archaeology at Munsu, western Uganda. *Azania* 38, 155–165. doi: 10.1080/00672700309480363
- Lejju, B. J., Taylor, D., and Robertshaw, P. (2005). Late-Holocene environmental variability at Munsu archaeological site, Uganda: a multicore, multiproxy approach. *Holocene* 15, 1044–1061. doi: 10.1191/0959683605hl877ra
- Leys, N. (1924). *Kenya*. London: Frank Cass and Company Ltd. Reprinted 1973.
- Lindeskog, M., Arneth, A., Bondeau, A., Waha, K., Seaquist, J., Olin, S., et al. (2013). Implications of accounting for land use in simulations of ecosystem carbon cycling in Africa. *Earth Syst. Dyn.* 4, 385–407. doi: 10.5194/esd-4-385-2013
- Lindsay, W. K. (1989). “Integrating parks and pastoralists: some lessons from Amboseli,” in *Conservation in Africa: People, Policies and Practice*, eds D. Anderson and R. Grove (Cambridge: Cambridge University Press), 149–167.
- Liutkus, C. M., and Ashley, G. M. (2003). Facies model of a semiarid freshwater wetland, Olduvai Gorge, Tanzania. *J. Sed. Res.* 73, 691–705. doi: 10.1306/021303730691
- Liutkus, C. M., Wright, J. D., Ashley, G. M., and Sikes, N. E. (2005). Paleoenvironmental interpretation of lake-margin deposits using $\delta^{13}\text{C}$ and $\delta^{18}\text{O}$ results from early Pleistocene carbonate rhizoliths, Olduvai Gorge, Tanzania. *Geology* 33, 377–380. doi: 10.1130/G21132.1
- Livingstone, D. A. (1962). Age of deglaciation in the ruwenzori range, Uganda. *Nature* 194, 859–860. doi: 10.1038/194859b0
- Livingstone, D. A. (1967). Postglacial vegetation of the Ruwenzori Mountains in equatorial Africa. *Ecol. Monogr.* 37, 25–52. doi: 10.2307/1948481
- Mackinder, H. J. (1900). A journey to the summit of Mount Kenya, British East Africa. *Geogr. J.* 15, 453–476. doi: 10.2307/1774261
- Magill, C. R., Ashley, G. M., and Freeman, K. H. (2012a). Ecosystem variability and early human habitats in eastern Africa. *Proc. Natl Acad. Sci. U.S.A.* 110, 1167–1174. doi: 10.1073/pnas.1206276110
- Magill, C. R., Ashley, G. M., and Freeman, K. H. (2012b). Water, plants, and early human habitats in eastern Africa. *Proc. Natl Acad. Sci. U.S.A.* 110, 1175–1180. doi: 10.1073/pnas.1209405109
- Marchant, R. A., and Hooghiemstra, H. (2004). Rapid environmental change in African and South American tropics around 4000 years before present: a review. *Earth Sci. Rev.* 66, 217–260. doi: 10.1016/j.earscirev.2004.01.003
- Marean, C. W. (1992). Hunter to Herder: large mammal remains from the Hunter-gatherer Occupation at Enkapune ya Muto Rock-shelter. *Afr. Archaeol. Rev.* 10, 65–127. doi: 10.1007/BF01117697
- Marlowe, F. W., and Berbesque, J. C. (2009). Tubers as fallback foods and their impact on Hadza hunter-gatherers. *Am. J. Phys. Anthropol.* 140, 751–758. doi: 10.1002/ajpa.21040
- Marshall, F. (1990). Origins of specialized pastoral production in East Africa. *Am. Anthropol.* 92, 873–894. doi: 10.1525/aa.1990.92.4.02a00020
- Marshall, F. (1994). “Archaeological perspectives on East African pastoralism,” in *African Pastoralist Systems*, eds E. Fratkin, J. Galvin and E. Roth (Boulder: Lynne-Reinner), 17–44.
- Marshall, F. (2001). Agriculture and use of wild and weedy greens by the *Piik ap Oom* Okiek of Kenya. *Econ. Bot.* 55, 32–46. doi: 10.1007/BF02864544
- Matthews, R. B., and Bakam, I. (2007). “A combined agent-based and biophysical modelling approach to address GHG mitigation policy issues,” in *MODSIM International Congress on Modelling and Simulation* (Christchurch).
- Matthews, R. B., Gilbert, N. G., Roach, A., Polhill, J. G., and Gotts, N. M. (2007). Agent-based land-use models: a review of applications. *Landsc. Ecol.* 22, 1447–1459. doi: 10.1007/s10980-007-9135-1
- McCabe, J. T., Leslie, P. W., and DeLuca, L. (2010). Adopting cultivation to remain pastoralists: the diversification of Maasai livelihoods in northern Tanzania. *Hum. Ecol.* 38, 321–334. doi: 10.1007/s10745-010-9312-8
- McCarthy, T. S., Ellery, W. N., and Bloem, A. (1998). Some observations on the geomorphological impact of hippopotamus (*Hippopotamus amphibius* L.) in the Okavango Delta, Botswana. *Afr. J. Ecol.* 36, 44–56. doi: 10.1046/j.1365-2028.1998.89-89089.x
- Mehlman, M. J. (1979). Mumba Hohle Revisited: the relevance of a forgotten excavation to some current issues in East African prehistory. *World Archaeol.* 11, 80–94. doi: 10.1080/00438243.1979.9979751
- Meijerink, A. M. J., and Van Wijngaarden, W. (1997). “Contribution to the groundwater hydrology of the Amboseli ecosystem, Kenya,” in *Groundwater/Surface Water Ecotones: Biological and Hydrological Interactions*

- and Management Options, eds J. Gilbert, J. Mathieu, and F. Fournier (Cambridge: Cambridge University Press), 111–118.
- Meyer, H. (1900). *Der Kilimanjaro*. Berlin: Reimer-Vohsen.
- Milton, S. J. (2003). 'Emerging ecosystems': a washing-stone for ecologists, economists and sociologists? *S. Afr. J. Sci.* 99, 404–406. Available online at: <https://hdl.handle.net/10520/EJC97706>
- Moernaut, J., Verschuren, D., Charlet, F., Kristen, I., Fagot, M., and De Batist, M. (2010). The seismic-stratigraphic record of lake-level fluctuations in Lake Challa: hydrological stability and change in equatorial East Africa over the last 140kyr. *Earth Plan Sci Lett.* 290, 214–223. doi: 10.1016/j.epsl.2009.12.023
- Moore, P. D., Webb, J. A., and Collison, M. E. (1991). *Pollen Analysis*. Oxford: Blackwell publishers.
- Morrison, M. E. S. (1968). Vegetation and climate in the uplands of southwestern Uganda during the Later Pleistocene Period, I. Muchoya Swamp, Kigezi District. *J. Ecol.* 56, 363–384. doi: 10.2307/2258239
- Morrison, M. E. S., and Hamilton, A. C. (1974). Vegetation and climate in the uplands of southwestern Uganda during the later Pleistocene Period: II. Forest clearance and other vegetational changes in the Rukiga Highlands during the past 8000 Years. *Ecology* 62, 1–31.
- Mount, J. F., and Cohen, A. S. (1984). Petrology and geochemistry of rhizoliths from Plio-Pleistocene fluvial and marginal lacustrine deposits, east Lake Turkana, Kenya. *J. Sed. Res.* 54, 263–275.
- Mturi, A. A. (1986). The Pastoral Neolithic of West Kilimanjaro. *Azania* 21, 53–63. doi: 10.1080/00672708609511367
- Muchiru, A. N., Western, D., and Reid, R. S. (2009). The impact of abandoned pastoral settlements on plant and nutrient succession in an African savanna ecosystem. *J. Arid. Environ.* 73, 322–331. doi: 10.1016/j.jaridenv.2008.09.018
- Muiruri, V. M. (2008). *Detecting Environmental Change and Anthropogenic Activities on the Laikipia Plateau, Kenya*. Master's degree, Earth Sciences Department, Palynology Section, National Museums of Kenya, Nairobi, and Department of Botany, University of Free State South Africa.
- Murray-Rust, D. H. (1972). Soil erosion and reservoir sedimentation in a grazing area west of Arusha, northern Tanzania. *Geografiska Ann. Series A. Phys. Geog.* 54, 325–343. doi: 10.1080/04353676.1972.11879872
- Mwangi, E. (2006). The footprints of history: path dependence in the transformation of property rights in Kenya's Maasailand. *J. Inst. Ecol.* 2, 157–180. doi: 10.1017/S1744137406000324
- Mwangi, E., and Ostrom, E. (2009). "A century of institutions and ecology in East Africa's rangelands: linking institutional robustness with the ecological resilience of Kenya's maasailand," in *Institutions and Sustainability: Political Economy of Agriculture and the Environment - Essays in Honour of Konrad Hagedorn*, eds V. Beckmann and M. Padmanabhan (Dordrecht: Springer).
- Mworia-Maitima, J. (1997). Prehistoric fires and land-cover change in western Kenya: evidences from pollen, charcoal, grass cuticles and grass phytoliths. *Holocene* 7, 409–417. doi: 10.1177/095968369700700404
- Nelson, D. M., Verschuren, D., Urban, M. A., and Hu, F. S. (2012). Long-term variability and rainfall control of savannah fire regimes in equatorial East Africa. *Glob. Change Biol.* 18, 3160–3170. doi: 10.1111/j.1365-2486.2012.02766.x
- Nicholson, S. E., and Yin, X. (2001). Rainfall conditions in equatorial East Africa during the nineteenth century as inferred from the record of Lake Victoria. *Clim. Change* 48, 387–398. doi: 10.1023/A:1010736008362
- Nkedianye, D., Radeny, M., Kristjanson, P., and Herrero, M. (2009). "Assessing returns to land and changing livelihood strategies in Kitengela," in *Staying Maasai?*, eds K. Homewood, P. Kristjanson, and P. C. Trench (New York, NY: Springer), 115–149.
- Norman, R. (2010). *Kimana Wetlands Spring and Water Use Inventory*. Nairobi: African Wildlife Institution.
- Odner, K. (1971). A preliminary report on an archaeological survey on the slopes of Kilimanjaro. *Azania* 6, 131–149. doi: 10.1080/00672707109511549
- Ofcansky, T. P. (1981). The 1889–1897 rinderpest epidemic and the rise of British and German colonialism in eastern and southern Africa. *J. Afr. Stud.* 8, 31–38.
- Okello, M. M. (2005). Land use changes and human–wildlife conflicts in the Amboseli Area, Kenya. *Hum. Dim. Wildlife* 10, 19–28. doi: 10.1080/10871200590904851
- Okello, M. M., and D'Amour, D. E. (2008). Agricultural expansion within Kimana electric fences and implications for natural resource conservation around Amboseli National Park, Kenya. *J. Arid. Environ.* 72, 2179–2192. doi: 10.1016/j.jaridenv.2008.07.008
- Okello, M. M., and Kioko, J. M. (2011). A field study in the status and threats of cultivation in Kimana and Ilchala swamps in Amboseli dispersal area, Kenya. *Nat. Resour.* 2, 197–211. doi: 10.4236/nr.2011.24026
- Okello, M. M., Kiringe, J. W., Njumbi, S. J., and Isiche, J. (2016). Prevalence of human elephant conflicts in Amboseli ecosystem, Kenya: current opinions of local community. *Int. J. Biodivers. Conserv.* 8, 60–71. doi: 10.5897/IJBC2015.0865
- Oliver, R. (1966). The problem of the Bantu expansion. *J. Afr. Hist.* 7, 361–376. doi: 10.1017/S0021853700006472
- Osmaston, H. A. (1958). *Pollen Analysis in the Study of the Past Vegetation and Climate of Ruwenzori and its Neighbourhood*. Unpublished BSc., thesis, Oxford University.
- Osmaston, H. A. (1965). *The Past and Present Climate and Vegetation of the Ruwenzori and its Neighbourhood*. Unpublished DPhil, thesis, University of Oxford, Oxford, UK.
- Overton, J. D. (1989). Social control and social engineering: African Reserves in Kenya 1895–1920. *Environ. Plann D Soc. Space* 8, 163–174.
- Pachzelt, A., Rammig, A., Higgins, S., and Hickler, T. (2013). Coupling a physiological grazer population model with a generalized model for vegetation dynamics. *Ecol. Model.* 263, 92–102. doi: 10.1016/j.ecolmodel.2013.04.025
- Payton, R. W., Christiansson, C., Shishira, E. K., Yanda, P., and Eriksson, M. G. (1992). Landform, soils and erosion in the northeastern Irangi Hills, Kondoa, Tanzania. *Geografiska Ann. Series A. Phys. Geog.* 74, 65–79. doi: 10.1080/04353676.1992.11880351
- Perrott, R. A. (1987). Early forest clearance and the environment in south-west Uganda. *Nature* 325, 89–90. doi: 10.1038/325089b0
- Petek, N., and Lane, P. (2016). Ethnogenesis and surplus food production: communities and identity building among nineteenth- and early twentieth-century Ilchamus, Lake Baringo, Kenya. *World Archaeol.* 49, 40–60. doi: 10.1080/00438243.2016.1259583
- Pickford, M. (1986). "Sedimentation and fossil preservation in the Nyanza Rift System, Kenya," in *Sedimentation in the African Rifts*, eds L. E. Frostick, R. W. Renaut, I. Reid, and J. J. Tiercelin (Oxford: Blackwell Scientific Publications), 339–363.
- Pigati, J. S., Rech, J. A., Quade, J., and Bright, J. (2014). Desert wetlands in the geologic record. *Earth Sci. Rev.* 132, 67–81. doi: 10.1016/j.earscirev.2014.02.001
- Platts, P. J., Gereau, R. E., Burgess, N. D., and Marchant, R. (2013). Spatial heterogeneity of climate change in an Afromontane centre of endemism. *Ecography* 36, 518–530. doi: 10.1111/j.1600-0587.2012.07805.x
- Platts, P. J., Omeny, P., and Marchant, R. (2015). AFRICLIM: high-resolution climate projections for ecological applications in Africa. *Afr. J. Ecol.* 53, 103–108. doi: 10.1111/aje.12180
- Poesen, J. W. A., Torri, D. B., and Vanwalleghe, T. (2010). "Gully erosion: procedures to adopt when modelling soil erosion," in *Landscapes Affected by Gully*, eds R. P. C. Morgan and M. A. Nearing (Chichester: John Wiley & Sons), 360–386.
- Prendergast, M. E., and Beyin, A. (in press). Fishing in a fluctuating landscape: terminal Pleistocene and early Holocene subsistence strategies in the Lake Turkana Basin, Kenya. *Quat Int.* doi: 10.1016/j.quaint.2017.04.022
- Prendergast, M. E., and Lane, P. J. (2010). Middle Holocene Fishing Strategies in East Africa: zooarchaeological analysis of Pundo, a Kanyore shell midden in northern Nyanza (Kenya). *Int. J. Osteoarchaeol.* 20, 88–112. doi: 10.1002/oa.1014
- Prendergast, M., Quintana Morales, E., Crowther, A., Horton, M. C., and Boivin, N. (2017). Dietary diversity on the Swahili coast: the fauna from two Zanzibar trading locales. *Int. J. Osteoarchaeol.* 27, 621–637. doi: 10.1002/oa.2585
- Quillet, A., Peng, C., and Garneau, M. (2010). Toward dynamic global vegetation models for simulating vegetation–climate interactions and feedbacks: recent developments, limitations, and future challenges. *Environ. Rev.* 18, 333–353. doi: 10.1139/A10-016
- Rapp, A., Axelsson, V., Berry, L., and Murray-Rust, D. H. (1972). Soil erosion and sediment transport in the Morogoro River catchment, Tanzania. *Geografiska Ann. Series A. Phys. Geog.* 54, 125–155. doi: 10.1080/04353676.1972.11879863

- Rebmann, J. (1848). "Tagebuch des missionars vom 14 February 1848-16," in *Veröffentlichungen des Archivs der Stadt Gerlingen: Band 3* (Gerlingen: Herausgegeben vom Stadtarchiv Gerlingen), 1997.
- Reid, R. S., and Ellis, J. E. (1995). Impacts of pastoralists on woodlands in South Turkana, Kenya: livestock-mediated tree recruitment. *Ecol. Appl.* 5, 978–992. doi: 10.2307/2269349
- Reid, R. S., Fernández-Giménez, M. E., and Galvin, K. A. (2014). Dynamics and resilience of rangelands and pastoral peoples around the globe. *Ann. Rev. Environ. Resour.* 39, 217–242. doi: 10.1146/annurev-environ-020713-163329
- Reimer, P. J., Bard, E., Bayliss, A., Beck, J. W., Blackwell, P. G., Ramsey, C. B., et al. (2013). IntCal13 and Marine13 Radiocarbon Age Calibration Curves 0–50,000 Years cal BP. *Radiocarbon*. 55, 1869–1887. doi: 10.2458/azu_js_rc.55.16947
- Ricketts, R. D., and Johnson, T. C. (1996). Climate change in the Turkana basin as deduced from a 4000-year long delta 0–18 record. *Earth Planet. Sci. Lett.* 142, 7–17. doi: 10.1016/0012-821X(96)00094-5
- Robbins, L. (1972). Archaeology in the Turkana District, Kenya. *Science* 176, 359–366. doi: 10.1126/science.176.4033.359
- Robertshaw, P. (1997). Munsu earthworks: a preliminary report on recent excavations. *Azania* 32, 1–20. doi: 10.1080/00672709709511585
- Robertshaw, P. T. (1990). "Early Pastoralists and their Herds in the Loita-Mara Region," in *Early Pastoralists of Southwestern Kenya*, ed P. T. Robertshaw (Nairobi: British Institute in Eastern Africa), 293–302.
- Robertshaw, P. T., and Collett, D. T. (1983). The identification of pastoral peoples in the archaeological record: an example from East Africa. *World Archaeol.* 15, 67–78. doi: 10.1080/00438243.1983.9979885
- Rounsevell, M. D. A., Robinson, D. T., and Murray-Rust, D. (2012). From actors to agents in socio-ecological systems models. *Philos. Trans. R. Soc. B* 367, 259–269. doi: 10.1098/rstb.2011.0187
- Rucina, S. M., Muiruri, V. M., Downton, L., and Marchant, R. (2010). Late-Holocene savannah dynamics in the Amboseli Basin, Kenya. *Holocene* 20, 667–677. doi: 10.1177/0959683609358910
- Russell, J. M., and Johnson, T. C. (2005). A high-resolution geochemical record from Lake Edwards, Uganda Congo and the timing and causes of tropical African drought during the late Holocene. *Quat. Sci. Rev.* 24, 1375–1389. doi: 10.1016/j.quascirev.2004.10.003
- Rutten, M. M. E. M. (1992). *Selling Wealth to Buy Poverty: The Process of Individualization of Land Ownership among the Maasai Pastoralists of Kajiado District, Kenya*. Saarbrücken: Verlag Breitenbach Publishers.
- Scheiter, S., Langan, L., and Higgins, S. I. (2013). Next-generation dynamic global vegetation models: learning from community ecology. *New Phytol.* 198, 957–969. doi: 10.1111/nph.12210
- Schindler, J. (2013). About the uncertainties in model design and their effects: an illustration with a land-use model. *J. Artif. Soc. Soc. Simul.* 16:6. doi: 10.18564/jasss.2274
- Schlachter, K. J., and Horn, S. P. (2010). Sample preparation methods and replicability in macroscopic charcoal analyses. *J. Paleolim.* 44, 701–708. doi: 10.1007/s10933-009-9305-z
- Schlesinger, W. H., Reynolds, J. F., Cunningham, G. L., Huenneke, L. K., Jarrell, W. M., Virginia, R. A., et al. (1990). Biological feedbacks in global desertification. *Science* 247, 1043–1048. doi: 10.1126/science.247.4946.1043
- Schüler, L., Hemp, A., Zech, W., and Behling, H. (2012). Vegetation, climate and fire-dynamics in East Africa inferred from the Maundi crater pollen record from Mt Kilimanjaro during the last glacial–interglacial cycle. *Quat. Sci. Rev.* 39, 1–13. doi: 10.1016/j.quascirev.2012.02.003
- Seno, S. K., and Shaw, W. W. (2002). Land tenure policies, Maasai traditions, and wildlife conservation in Kenya. *Soc. Nat. Resour.* 15, 79–88. doi: 10.1080/089419202317174039
- Seno, S. K., and Tome, S. (2013). Socio-economic and ecological viability of pastoralism in Loitokitok District, Southern Kenya. *Nomadic Ppl.* 17, 66–86. doi: 10.3167/np.2013.170104
- Shalem, A. (2005). "Trade in and the availability of ivory: the picture given by the medieval sources," in *The Ivories of Muslim Spain: Papers from a Symposium Held in Copenhagen from the 18th to the 20th of November 2003*, eds K. von Folsach and J. Meyer (Copenhagen: The David Collection), 25–36.
- Sheriff, A. (1987). *Slaves, Spices and Ivory in Zanzibar: Integration of an East African Commercial Empire into the World Economy 1770–1873*. London: James Currey.
- Sinclair, A. R. E., and Fryxell, J. M. (1985). The Sahel of Africa: ecology of a disaster. *Can. J. Zool.* 63, 987–994. doi: 10.1139/z85-147
- Smith, B., Prentice, I. C., and Sykes, M. T. (2001). Representation of vegetation dynamics in the modelling of terrestrial ecosystems: comparing two contrasting approaches within European climate space. *Global Ecol. Biogeog.* 10, 621–637. doi: 10.1046/j.1466-822X.2001.00256.x
- Sobania, N. P. (1980). *The Historical Traditions of the Peoples of the Eastern Lake Turkana Basin c.1840–1925*. Ph.D., thesis, SOAS, University of London.
- Soper, R. (1976). Archaeological Sites in the Chyulu Hills, Kenya. *Azania* 11, 83–116. doi: 10.1080/00672707609511232
- Spencer, I. (1983). "Pastoralism and Colonial Policy in Kenya, 1895–1929," in *Imperialism, Colonialism, and Hunger: East and Central Africa*, ed R. Rotberg (Lexington: D.C. Heath), 113–140.
- Stager, J. C., and Johnson, T. C. (2008). The late Pleistocene desiccation of Lake Victoria and the origin of its endemic biota. *Hydrobiologia* 596, 5–16. doi: 10.1007/s10750-007-9158-2
- Stahl, K. M. (1964). *The History of the Chagga People of Kilimanjaro*. The Hague: Mouton.
- Stockmarr, J. (1971). Tablets with spores used in absolute pollen analysis. *Pollen Spores* 13, 615–621.
- Stoessell, R. K., and Hay, R. L. (1978). The geochemical origin of sepiolite and kerolite at Amboseli, Kenya. *Contrib. Mineral. Pet.* 65, 255–267. doi: 10.1007/BF00375511
- Stump, D., and Tagseth, M. (2009). "The history of pre-colonial and early colonial agriculture on Kilimanjaro: a review," in *Culture, History and Identity: Landscapes of Inhabitation in the Mount Kilimanjaro Area, Tanzania*, BAR International Series 1966, ed T. Clack (Oxford: Archaeopress), 107–124.
- Sundstrom, S., Tynon, J. F., and Western, D. (2012). Rangeland privatization and the Maasai experience: social capital and the implications for traditional resource management in Southern Kenya. *Soc. Nat. Resour.* 25, 483–498. doi: 10.1080/08941920.2011.580420
- Swynnerton, R. J. M. (1955). *A Plan to Intensify the Development of African Agriculture in Kenya*, Government Printer. Nairobi: Colony and Protectorate of Kenya.
- Taylor, D., Lane, P. J., Muiruri, V., Rutledge, A., Gaj McKeever, R., Nolan, T., et al. (2005). Mid-to late-Holocene vegetation dynamics on the Laikipia Plateau, Kenya. *Holocene* 15, 837–846. doi: 10.1191/0959683605h1857ra
- Thompson, L. G., Mosley-Thompson, E., Davis, M. E., Henderson, K. A., Brecher, H. H., Zagorodnov, V. S., et al. (2002). Kilimanjaro ice core records: evidence of Holocene climate change in tropical Africa. *Science* 298, 598–593. doi: 10.1126/science.1073198
- Thomson, J. (1885). *Through Masai Land*. London: Sampson Low.
- Tierney, J. E., Russell, J. M., Damsté, J. S. S., Huang, Y., and Verschuren, D. (2011). Late Quaternary behaviour of the East African monsoon and the importance of the Congo Air Boundary. *Quat. Sci. Rev.* 30, 798–807. doi: 10.1016/j.quascirev.2011.01.017
- Touber, L., van der Pouw, B. J., and van Engelen, V. W. (1983). *Soils and Vegetation of the Amboseli - Kibwezi area*. Reconnaissance Soil Survey Report R6. Kenya Soil Survey, Nairobi.
- United Nations, Department of Economic and Social Affairs, Population Division (2017). *World Population Prospects: The 2017 Revision, Key Findings and Advance Tables*. Working Paper No. ESA/P/WP/248.
- Valbuena, D., Verburg, P. H., Bregt, A. K., and Ligtnerberg, A. (2010). An agent-based approach to model land–use change at a regional scale. *Landscape Ecol.* 25, 185–199. doi: 10.1007/s10980-009-9380-6
- Van Zinderen, B. E. M. (1962). A late-glacial and postglacial climatic correlation between East Africa and Europe. *Nature* 194, 201–203. doi: 10.1038/194201a0
- Van Zinderen, B. E. M., and Coetzee, J. A. (1988). A review of Late Quaternary pollen studies in East, Central and Southern Africa. *Rev. Palaeobot. Palynol.* 55, 155–174. doi: 10.1016/0034-6667(88)90083-8
- Verschuren, D., and Charman, D. (2008). "Latitudinal linkages in late-holocene moisture-balance variation," in *Natural Climate Variability and Global Warming*, eds R. W. Battarbee and H. A. Binney (Oxford: Wiley-Blackwell), 189–231.

- Verschuren, D., Laird, K. R., and Cumming, B. F. (2000). Rainfall and drought in equatorial East Africa during the past 1,100 years. *Nature* 403, 410–414. doi: 10.1038/35000179
- Von der Decken, C. C. (1869). *Reisen in Ost-Afrika in den Jahren 1859 bis 1865*. Leipzig: C. F. Winter'sche Verlagshandlung.
- Waller, R. (1979). *The Lords of East Africa: The Maasai in the mid-Nineteenth Century, c1840–1885*. Ph.D., thesis, Cambridge.
- Waller, R. (1988). 'Emutai': crisis and response in Maasailand, 1883–1902," in *Ecology of Survival*, eds D. Johnson and D. M. Anderson (Boulder: Westview), 73–113.
- Walz, J. R. (2010). *Route to a Regional Past: An Archaeology of the Lower Pangani (Ruvu) Basin, Tanzania, 500–1900 C. E.* Unpublished Ph.D., thesis, University of Florida.
- Wandibba, S. (1980). "The application of attribute analysis to the study of Later Stone Age/Neolithic pottery ceramics in Kenya," in *Proceedings of the Eighth Panafrican Congress of Prehistory and Quaternary Studies, Nairobi*, eds R. E. Leakey and B. Ogot (Nairobi: The International Louis Leakey Memorial Institute for African Prehistory), 283–285.
- Weissbrod, L. (2010). *The Small Animals of Maasai Settlements: Ethnoarchaeological Investigations of the Commensalism Model*. Unpublished Ph.D., dissertation, Washington University.
- Western, D. (2006). A half a century of habitat change in Amboseli National Park, Kenya. *Afr. J. Ecol.* 45, 302–310. doi: 10.1111/j.1365-2028.2006.00710.x
- Western, D., and Dunne, T. (1979). Environmental aspects of settlement site decisions among pastoral Maasai. *Hum. Ecol.* 7, 75–97. doi: 10.1007/BF00889353
- Western, D., and Finch, V. (1986). Cattle and pastoralism: survival and production in arid lands. *Hum. Ecol.* 14, 77–94. doi: 10.1007/BF00889211
- Western, D., and Maitumo, D. (2004). Woodland loss and restoration in a savannah park: a 20-year experiment. *Afr. J. Ecol.* 42, 111–121. doi: 10.1111/j.1365-2028.2004.00506.x
- Western, D., and Manziillo-Nightingale, D. L. (2003). *Environmental Change and the Vulnerability of Pastoralists to Drought: A Case Study of the Maasai in Amboseli, Kenya*. New York, NY: Cambridge University Press.
- Western, D., and Van Praet, C. (1973). Cyclical Changes in the Habitat and Climate of an East African Ecosystem. *Nature* 241, 104–106. doi: 10.1038/241104a0
- White, A. C. A. (1949). Maize names as indicators of economic contacts. *Uganda J.* 13, 61–81.
- Whitlock, C., Higuera, P., McWethy, D. B., and Briles, C. E. (2010). Paleocological perspectives on fire ecology: revisiting the fire-regime concept. *Open Ecol.* 3, 6–23. doi: 10.2174/1874213001003020006
- Wilensky, U. (1999). *NetLogo*. Evanston, IL: Center for Connected Learning and Computer-Based Modeling, Northwestern University. Available online at: <http://ccl.northwestern.edu/netlogo/>
- Williams, L. A. J. (1972). *Geology of the Amboseli Area*, Vol. 90. Nairobi: Geological Survey of Kenya, Ministry of Natural Resources, Republic of Kenya.
- Wimmelbucker, L. (2009). "Local memories of famine," in *Culture, History, and Identity: Landscapes of Inhabitation in the Mount Kilimanjaro Area, Tanzania: Essays in Honour of Paramount Chief Thomas Lenana Mlangi Marealle II (1915–2007)*, ed T. Clack (Oxford: BAR International), 171–193.
- Worden, J., Reid, R., and Gichohi, H. (2003). *Land-Use Impacts on Large Wildlife and Livestock in the Swamps of the Greater Amboseli Ecosystem, Kajiado District, Kenya - Part 1, Text and Tables*. LUCID working paper series number 27.
- Wright, D. K. (2005). New perspectives on early regional interaction networks of East African traded; a view from Tsavo National Park, Kenya. *Afr. Archaeol. Rev.* 22, 111–140. doi: 10.1007/s10437-005-8041-7
- Wright, D. K. (2007). Tethered mobility and riparian resource exploitation among Neolithic hunters and herders in the Galana River basin, Kenyan coastal lowlands. *Environ. Archaeol.* 12, 25–47. doi: 10.1179/174963107x172732
- Zech, M. (2006). Evidence for Late Pleistocene climate changes from buried soils on the southern slopes of Mt. Kilimanjaro, Tanzania. *Palaeogeog. Palaeoclim.* 242, 303–312. doi: 10.1016/j.palaeo.2006.06.008
- Zech, M., Leiber, K., Zech, W., Poetsch, T., and Hemp, A. (2011). Late Quaternary soil genesis and vegetation history on the northern slopes of Mt. Kilimanjaro, East Africa. *Quat Int.* 243, 327–336. doi: 10.1016/j.quaint.2011.05.020

Conflict of Interest Statement: The authors declare that the research was conducted in the absence of any commercial or financial relationships that could be construed as a potential conflict of interest.

Copyright © 2018 Githumbi, Kariuki, Shoemaker, Courtney-Mustaphi, Chuhilla, Richer, Lane and Marchant. This is an open-access article distributed under the terms of the Creative Commons Attribution License (CC BY). The use, distribution or reproduction in other forums is permitted, provided the original author(s) or licensor are credited and that the original publication in this journal is cited, in accordance with accepted academic practice. No use, distribution or reproduction is permitted which does not comply with these terms.



Palynology and the Ecology of the New Zealand Conifers

Matt S. McGlone^{1*}, Sarah J. Richardson¹, Olivia R. Burge¹, George L. W. Perry² and Janet M. Wilmshurst^{1,2}

¹ Manaaki Whenua-Landcare Research, Lincoln, New Zealand, ² School of Environment, University of Auckland, Auckland, New Zealand

OPEN ACCESS

Edited by:

Jesse L. Morris,
University of Utah, United States

Reviewed by:

Li Wu,
Anhui Normal University, China
Thomas A. Minckley,
University of Wyoming, United States

*Correspondence:

Matt S. McGlone
mcglonem@landcareresearch.co.nz

Specialty section:

This article was submitted to
Quaternary Science, Geomorphology
and Paleoenvironment,
a section of the journal
Frontiers in Earth Science

Received: 03 September 2017

Accepted: 03 November 2017

Published: 16 November 2017

Citation:

McGlone MS, Richardson SJ,
Burge OR, Perry GLW and
Wilmshurst JM (2017) Palynology and
the Ecology of the New Zealand
Conifers. *Front. Earth Sci.* 5:94.
doi: 10.3389/feart.2017.00094

The New Zealand conifers (20 species of trees and shrubs in the Araucariaceae, Podocarpaceae, and Cupressaceae) are often regarded as ancient Gondwanan elements, but mostly originated much later. Often thought of as tall trees of humid, warm forests, they are present throughout in alpine shrublands, tree lines, bogs, swamps, and in dry, frost-prone regions. The tall conifers rarely form purely coniferous forest and mostly occur as an emergent stratum above evergreen angiosperm trees. During Maori settlement in the thirteenth century, fire-sensitive trees succumbed rapidly, most of the drier forests being lost. As these were also the more conifer-rich forests, ecological research has been skewed toward conifer dynamics of forests wetter and cooler than the pre-human norm. Conifers are well represented in the pollen record and we here review their late Quaternary history in the light of what is known about their current ecology with the intention of countering this bias. During glacial episodes, all trees were scarce south of c. 40° S, and extensive conifer-dominant forest was confined to the northern third of the North Island. Drought- and cold-resistant *Halocarpus bidwillii* and *Phyllocladus alpinus* formed widespread scrub in the south. During the deglacial, beginning 18,000 years ago, tall conifers underwent explosive spread to dominate the forest biomass throughout. Conifer dominance lessened in favor of angiosperms in the wetter western lowland forests over the Holocene but the dryland eastern forests persisted largely unchanged until settlement. Mid to late Holocene climate change favored the more rapidly growing Nothofagaceae which replaced the previous conifer-angiosperm low forest or shrubland in tree line ecotones and montane areas. The key to this dynamic conifer history appears to be their bimodal ability to withstand stress, and dominate on poor soils and in cool, dry regions but, in wetter, warmer locations, to slowly grow thorough competing broadleaves to occupy an exposed, emergent stratum where their inherent stress resistance ensures little effective angiosperm competition.

Keywords: conifer, history, New Zealand, glaciation, palynology, Holocene, ecology, niche

INTRODUCTION

In 1935, Lucy Cranwell—a young New Zealand researcher attending the VI International Botanical Congress in Amsterdam—was invited to work with Lennart von Post on the pollen analysis of peat sequences collected from southern New Zealand by the Swedish glaciologist Carl Caldenius (Cameron, 2000). Their resulting paper on the postglacial history of the far south of the South Island (Cranwell and von Post, 1936) was the first such effort for Australasia and provided

a compelling narrative of vegetation and climate change that was adopted by ecologists and Quaternary researchers alike. Several decades later, palynologist Bill Harris—who had worked for Lucy Cranwell—asked whether “... the two techniques, that of the ecologist, and that of the palynologist can be mutually helpful...” (Harris, 1963), and this question remains relevant both in New Zealand and elsewhere (Rull, 2010; Reitalu et al., 2014). Palaeoecology and neoecology often appear to be proceeding on quite different tracks, publishing in different journals and addressing quite separate themes. The purpose of this paper is to address Bill Harris’s question with particular emphasis on the history of the New Zealand conifers, and to assess progress in integrating the two disciplines over the 80 years since Lucy Cranwell and Lennart von Post’s pioneering publication.

New Zealand conifers offer an excellent opportunity to integrate the rapidly developing understanding of their ecology and biogeography with insights derived from nearly a century of palynological research. The 20 conifer species in New Zealand (**Table 1**; **Figure 1**) are represented by three distinct families: Araucariaceae (1 genus, 1 species), Cupressaceae (1 genus, 2 species) and Podocarpaceae (including the synapomorphic Phyllocladaceae; 8 genera, 16 species). Six of the most abundant of the tree conifer species are easily identified by their pollen (**Table 1**); many of the conifer species are emergent; and all are wind-pollinated. These traits have resulted in a detailed representation of conifer taxa in the terrestrial and marine pollen records from across the entire geological

sequence in New Zealand, allowing the long-term dynamics of conifers to be confidently reconstructed. In contrast, many of the angiosperm trees and shrubs in New Zealand are insect pollinated, have poorly dispersed pollen that is mostly identifiable to genus level, and tend to be under-represented in the pollen records relative to their local abundance (Macphail and McQueen, 1983). The New Zealand conifer pollen records therefore provide an ideal setting to expand understanding of conifer history, biogeography, and ecology.

Ecological studies of New Zealand conifers have focused on their forest dynamics at small spatial and limited time scales (sub-millennial) although progress has also been made in understanding their physiology, and soil preferences and climate drivers at a national level. In contrast, pollen analytical studies typically address time scales ranging from hundreds to millions of years, are often carried out by researchers with a geological or geographic background, and the major preoccupation has been interpreting pollen sequences in terms of climate or landscape change. This mismatch means integration of ecological and palynological data has been somewhat neglected.

Conifers are abundant in New Zealand forests and shrublands (Ogden and Stewart, 1995). They are found from tree line to the lowlands, from the driest to the wettest regions and from the northern tip of the North Island to Stewart Island in the far south, absent only from some of the offshore islands of the archipelago (**Table 1**). They include the tallest tree (50 m)

TABLE 1 | New Zealand conifer species: ecological parameters.

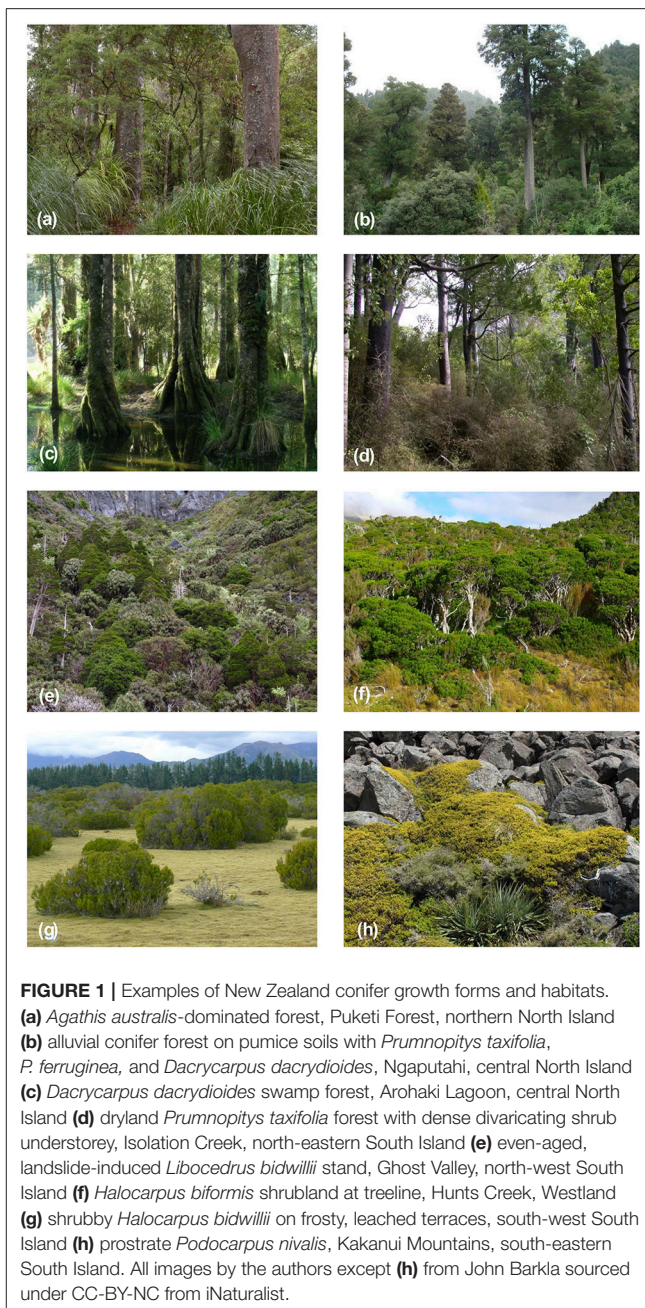
Species	Max height ^a	Max age ^b	Dist.	Alt. range	Moist forest	Dryland forest	Infertile soils	Wetland-wet soils	In alpine ecotone
<i>Agathis australis</i> *	40	1,700	NN	L-M	•		•		
<i>Libocedrus bidwillii</i>	20	805	N, S	M-S	•				•
<i>Libocedrus plumosa</i>	25	–	NN	L	•				
<i>Dacrycarpus dacrydioides</i> *	50	775	N, S, St	L-M	•	•		•	
<i>Dacrydium cupressinum</i> *	40	1,200	N, S, St	L-M	•		•	•	
<i>Halocarpus bidwillii</i>	5	280	N, S, St	L-A		•	•	•	•
<i>Halocarpus biformis</i>	10	1,000	N, S, St	L-S			•	•	•
<i>Halocarpus kirkii</i>	25	–	NN	L	•		•		
<i>Lepidothamnus intermedius</i>	15	247+	N, S, St	L-S			•	•	•
<i>Lepidothamnus laxifolius</i>	0.1	Clonal	N, S, St	L-A			•	•	•
<i>Manoao colensoi</i> *	15	800	N, S	L-M			•	•	
<i>Phyllocladus alpinus</i>	12	260	N, S	Mostly M-A	•	•	•	•	•
<i>Phyllocladus toatoa</i>	20	441	NN	L-M	•		•	•	
<i>Phyllocladus trichomanoides</i>	25	>300	N, S	L-M	•		•		
<i>Podocarpus acutifolius</i>	10	–	S	L-M	•				
<i>Podocarpus laetus</i>	24	625	N, S, St	L-S	•	•	•		•
<i>Podocarpus nivalis</i>	3	Clonal	N, S	M-A					•
<i>Podocarpus totara</i>	35	1,000	N, S, St	L-S	•	•			
<i>Prumnopitys ferruginea</i> *	30	770	N, S, St	L-M	•				
<i>Prumnopitys taxifolia</i> *	30	1,400	N, S, St	L-M	•	•			

*Unique pollen type in New Zealand; •Taxon favors this environment. NN, northern North Island; N, North Island; S, South Island; St, Stewart Island. L, lowland; M, montane; S, subalpine; A, alpine. ^aMcGlone et al. (2010), ^bData from: Wardle (1991), Ogden and Stewart (1995) updated by data compiled by the authors for the NZ Plant Traits Database.

and also sprawling, prostrate shrubs. Many of the conifers are large, emergent trees and often dominate forest biomass. Several (*Agathis australis*, *Prumnopitys taxifolia*, *Podocarpus totara*, *Dacrycarpus dacrydioides*, and *Dacrydium cupressinum*) yield valuable timber, which underpinned the New Zealand economy in the first few decades of European settlement and continued to be exploited until the closing decades of the twentieth century. Understandably, these ubiquitous, dominant and valuable trees have been a focus of biogeographic and ecological research in New Zealand, and debates over their origin, ecological role and, in particular, regeneration dynamics, have continued unabated over the last 120 years.

Leonard Cockayne was the first New Zealand ecologist and, in *The Vegetation of New Zealand* (Cockayne, 1928), formulated ideas about the ecology of the conifers, many of which remain current. However, more controversially, drawing on both ecological and macrofossil evidence he argued that conifer and angiosperm species were locked in a longstanding evolutionary conflict. The historical tendency, as he saw it, was for conifer retreat in the face of angiosperm competition and, although disturbance and poor soils could give them a temporary advantage from time to time, his opinion was that eventually they would become relic: "...a remnant merely of ancient conifer forests which have been in the process of gradual extinction by certain broad-leaved dicotyledonous trees—a process of extreme slowness" (Cockayne, 1928, p. 21). Cockayne's ideas were championed by Robbins (1962) who, after a descriptive survey of the conifer-angiosperm forests of the North Island, likewise claimed the angiosperm forest "represents a broadleaf forest climax which is surely replacing a more ancient podocarp forest climax, remnants of which still remain mingled with the broadleaf forest" (p. 34). This view has persisted that the conifers and other older broadleaved genera represent an unchanging rainforest element from a Gondwana predating the 80–85 Ma separation of the ancestral Zealandia continental fragment (Kirkpatrick and DellaSala, 2011). The popular conservation literature often refers to the conifer-rich lowland forests of New Zealand as "dinosaur forest" (<http://www.aucklandbotanicgardens.co.nz/whats-on/events/dinosaurs-in-the-gardens/>). A recent publication on the fossil history of the Southern Hemisphere rainforests referred to their characteristic taxa as "southern wet forest survivors" (Kooymann et al., 2014), thus emphasizing their antiquity and embattled persistence. It has been claimed that the conifers—because of their antiquity and slow adaptation to Pleistocene climates—are photosynthetically adapted to function at higher temperatures than are optimal for present day New Zealand (Hawkins and Sweet, 1989). It is not unreasonable to see this presumption of "primitiveness" as implicitly guiding the tenor of much ecological discussion about southern conifers, which becomes focussed on their survival in an "advanced" angiosperm dominated world.

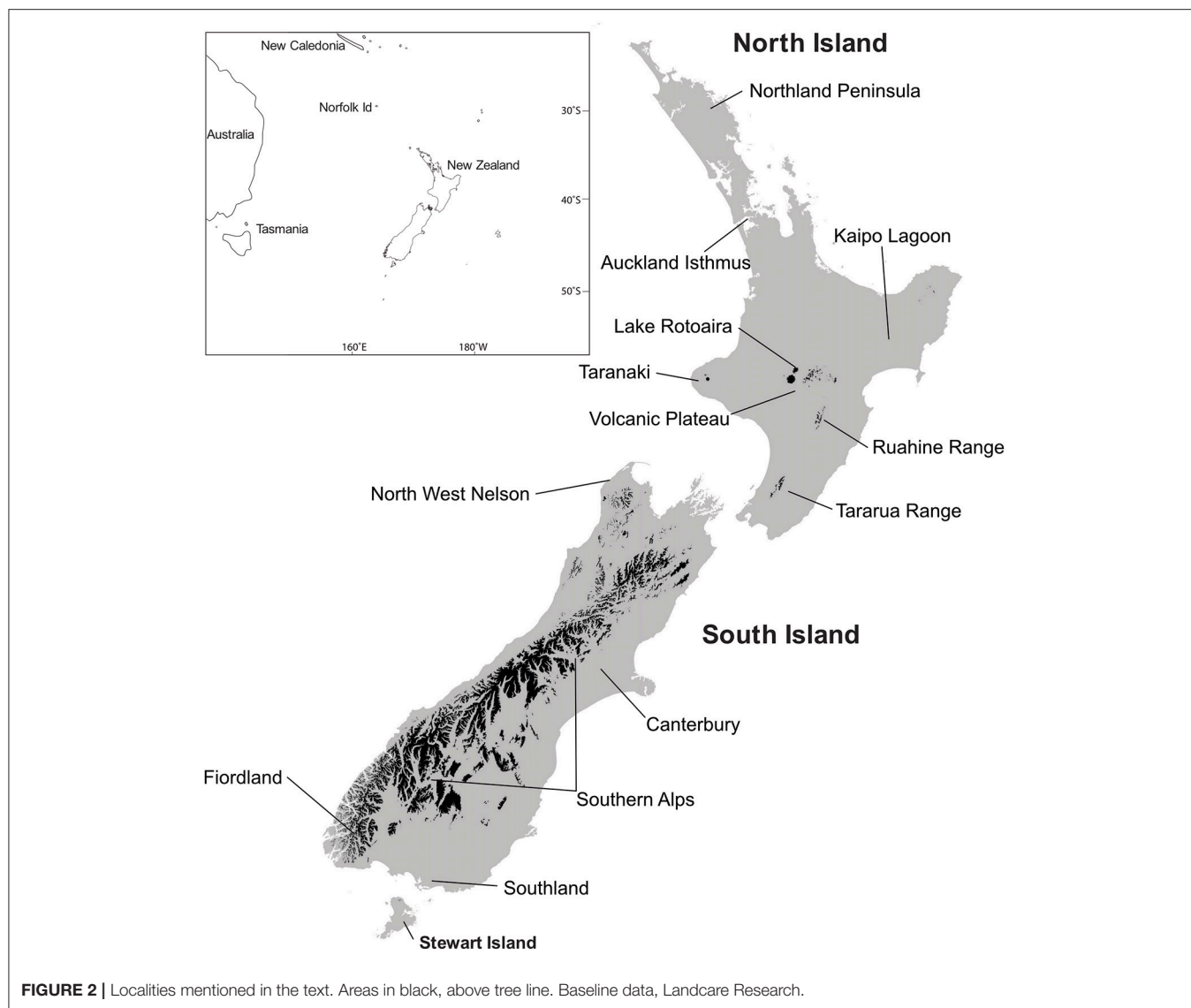
Here we provide an overview of the reaction of New Zealand conifers to climate and landscape transformation during and after the Last Glacial Maximum (LGM), including the impact of recent human arrival and the introduction of fire. We then use this background to explore to what extent the long-term perspective provided by pollen analytical data can shed light on



their current ecology and if, the concept of southern conifers as besieged relics is either valid or useful.

NEW ZEALAND VEGETATION CHANGE OVER THE LAST 30,000 YEARS

General locations are given in Figure 2 and Figures 3, 4 and 5–9 provide representative pollen diagrams illustrating the changes discussed. Table 2 summarizes the typical climatic regimes of important conifer-dominant vegetation types in relation to their current and past distributions.



Last Glacial Maximum

The LGM (29 to 19 ka) (ka = thousands of calibrated radiocarbon years before 1950 CE) was the coldest period of the present glacial-interglacial cycle (Lorrey et al., 2012). During this period mean annual temperatures fell by 4–7°C (Newnham et al., 2013), glaciers advanced throughout the Southern Alps, extending below current sea level in the west. Overall precipitation was lower, perhaps by as much as a third (Alloway et al., 1992) and the prevailing westerly airflow meant that the rain shadow region east of the axial ranges became semiarid. The plains of the interior south-eastern South Island have been described as approximating a polar desert (McIntosh et al., 1990).

Last Glacial Maximum (LGM) pollen sequences (Figure 3) show a forested or partly forested northern third of the North Island (above c. latitude 38°). In Northland, although Nothofagaceae were the dominant tree cover (with abundant *Lophozonia menziesii* and *Fuscospora truncata*), tall conifers played an important role, particularly *Dacrydium cupressinum*

(Newnham, 1992; Wright et al., 1995; Elliot, 1998; Newnham et al., 2017). From the Auckland Isthmus southwards, tall forest became sparser or confined to the coast while in the central districts of the North Island and the north of the South Island, conifer shrubland to low forest of *Phyllocladus alpinus* and *Halocarpus bidwillii* formed a mosaic with Nothofagaceae forest patches, broadleaved shrubland, and grassland. The western districts of the South Island, even those adjacent to the glacier fronts, had angiosperm shrubland-grassland cover, but also patches of low conifer forest, and sparse stands of tall conifers (Vandergoes et al., 2005). This vegetation type extended to coastal Fiordland in the far south of the mainland (Pickrill et al., 1992). In eastern lowland districts, grassland, low-growing angiosperm shrubland and sparse prostrate shrubs and herbfield were the main cover and conifers of any type were rare or absent over large areas although maintaining a regional presence (Moar, 1980; McGlone, 2002).

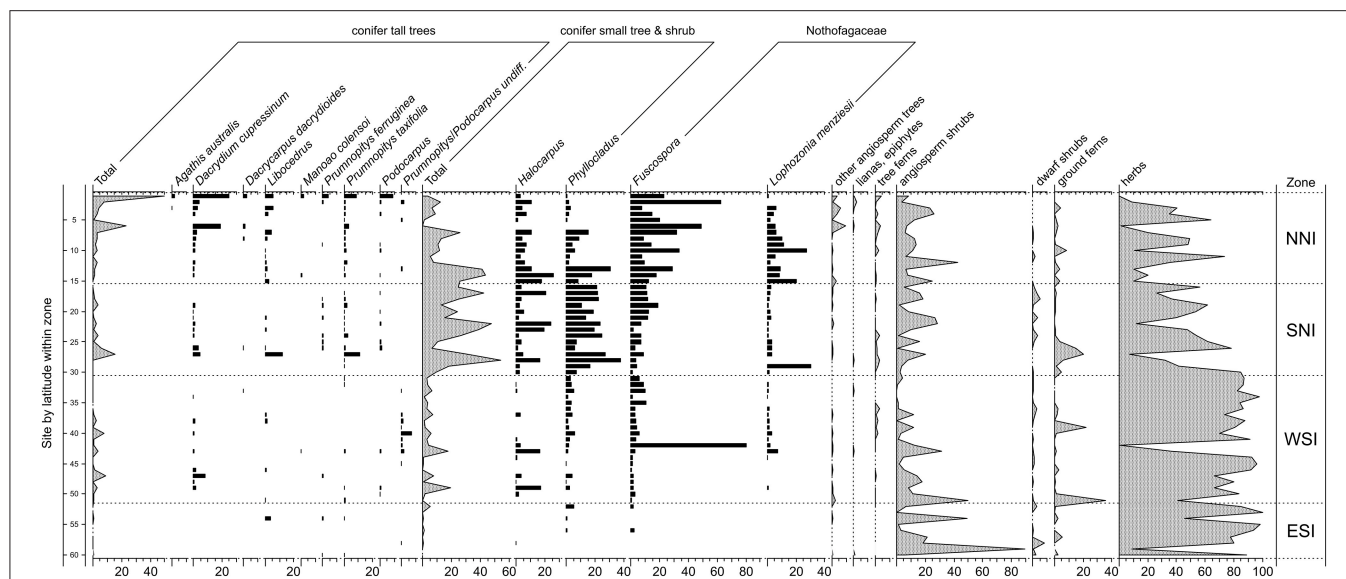


FIGURE 3 | Pollen and spore results for representative samples within sites dating to the LGM. In descending order of increasing latitude within broad zones: northern North Island (NNI—north of latitude 37° S); southern North Island (SNI—south of 37° S but including the overlapping portion of the South Island); western South Island (WSI—west of the Southern Alps); eastern South Island (ESI—east of the Southern Alps). Pollen sum: all terrestrial types excluding ferns, lycopods, and wetland forbs, rushes, and sedges. After McGlone et al. (2010).

The Deglaciation (18 to 11.6 Ka)

A hemispheric warming and rapid retreat of glaciers began at about 17–18 ka following the last LGM advance at around 19 ka (Moreno et al., 2015; Darvill et al., 2016). Conifer-angiosperm forest spread in the central and northern North Island from 17 to 14 ka replacing previous forest-scrub-grassland mosaics (Figures 4–6). For instance, lowland forest expanded in the Auckland Isthmus between 15.5 and 14 ka (Sandiford et al., 2002, 2003; Newnham et al., 2007; Augustinus et al., 2011); at Kaipo Lagoon in the montane North Island, 16.5–14 ka (Newnham and Lowe, 2000), in lowland Taranaki at 15 ka (McGlone and Neall, 1994); and at Lake Rotoaira on the montane central Volcanic Plateau 16.5–15 ka (McGlone and Topping, 1977, 1983).

In the South Island, stands of forests expanded in what was still a largely grass and shrub covered landscape (Figures 4, 7–9). Northwest Nelson saw expansion of conifer forest at around 14.5 ka (Jara et al., 2015), and at Okarito on the west coast, between 15 and 14.5 ka (Vandergoes et al., 2005); at Cass Basin in inland Canterbury, 15.7–14.5 ka (McGlone et al., 2004) and at Clarks Junction, eastern South Island, 15.5–13.5 ka (McGlone et al., 2003). A minor reversal of this warming trend occurred between 14.5 and 12.9 ka with glacial readvances in the Southern Alps (Darvill et al., 2016). By this time, dense tall conifer forest had occupied all but the driest eastern districts of the North Island and extensive stands were present in the lowland South Island throughout. These early deglacial forest pollen spectra were dominated by *Prumnopitys taxifolia* (Figures 5–9) but with significant input from *Phyllocladus*, *Libocedrus* and, in places, the Nothofagaceous *Lophozonia menziesii* and the deciduous angiosperm tree *Plagianthus regius* were common. These trees are all frost-hardy (Bannister, 2007)

and can tolerate a certain amount of drought, in sharp contrast to the angiosperms that became abundant in the early Holocene (e.g., *Ascarina*, *Metrosideros*) (Leathwick and Whitehead, 2001; Hall and McGlone, 2006).

The Holocene

The beginning of the Holocene period at 11.7 ka, marks the transition to true interglacial climates. Warming continued in New Zealand with increasing rainfall in the west, and the period between c. 11 and 8 ka was characterized by a greatly weakened westerly airflow (Shulmeister et al., 2004). The intensely oceanic climate promoted the spread of the small tree *Ascarina lucida* which cannot tolerate dry air or frost (McGlone and Moar, 1977; Martin and Ogden, 2005). A forest dynamic model was used to explore the climatic implications of a deglacial-Holocene pollen sequence from a montane rainfall spill-over area of the Southern Alps. Warmer than present winters, somewhat cooler summers, and less but more evenly spread rainfall were predicted for the early Holocene (McGlone et al., 2004).

In northern districts of the North Island, and western districts throughout, conifer forests with abundant *Dacrydium cupressinum*, *Prumnopitys ferruginea*, and *Dacrycarpus dacrydioides* and tree ferns dominated (Figures 4, 5). In rain-shadow eastern districts *Prumnopitys taxifolia* and *Podocarpus* spp. spread in lowland to montane locations (McGlone, 2002; McGlone et al., 2004), but low forest of *Phyllocladus alpinus* and *Halocarpus bidwillii* occupied the drier, frosty inland basins and hill slopes (McGlone and Moar, 1998). Stewart Island at the far south of the South Island was the last region where lowland conifers spread (Figures 4, 9, Toitoti). The early postglacial forests on Stewart Island were

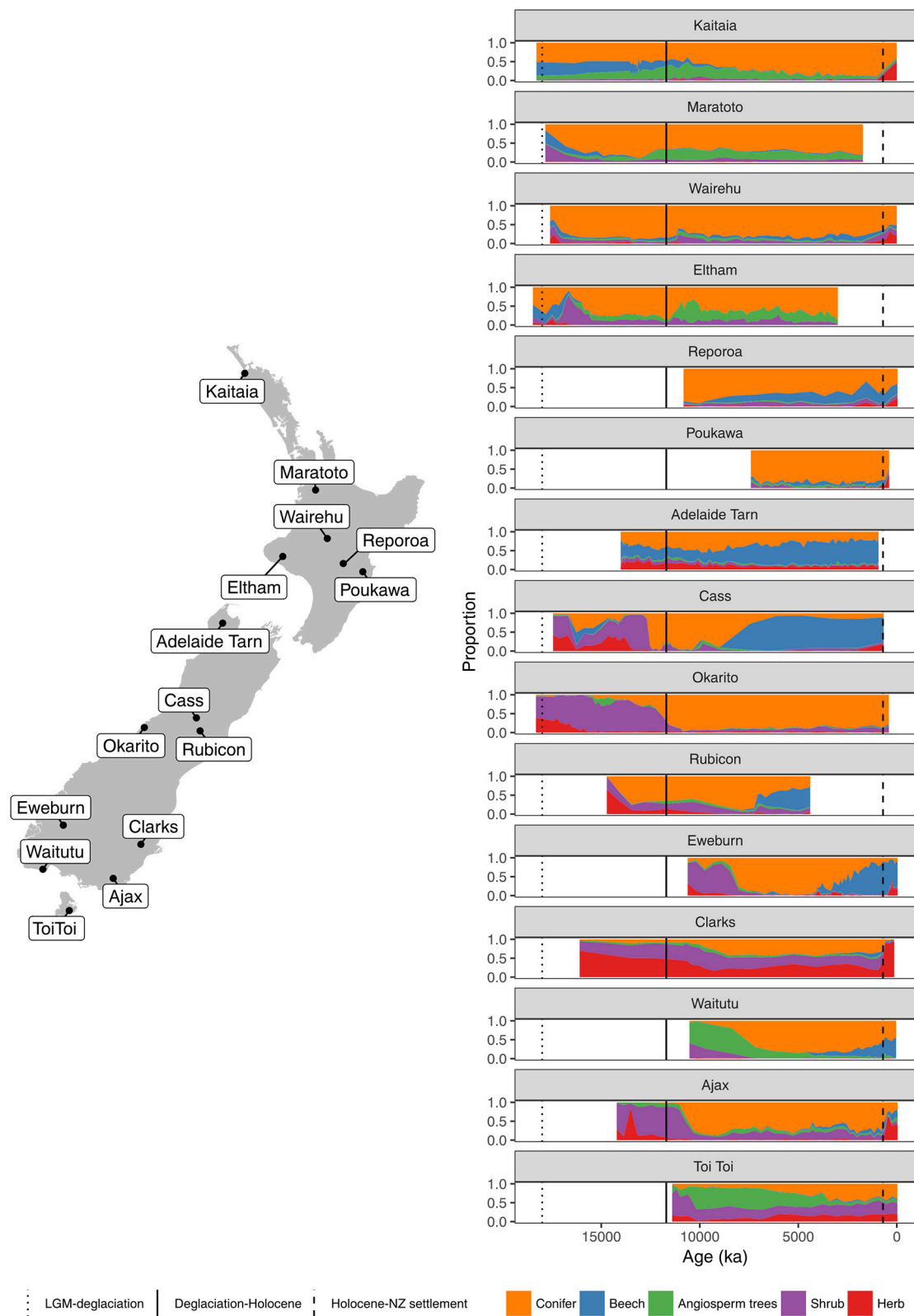


FIGURE 4 | Summary percentage pollen diagrams (sum: all terrestrial types excluding ferns, lycopods and wetland forbs, rushes, and sedges) and site locations.

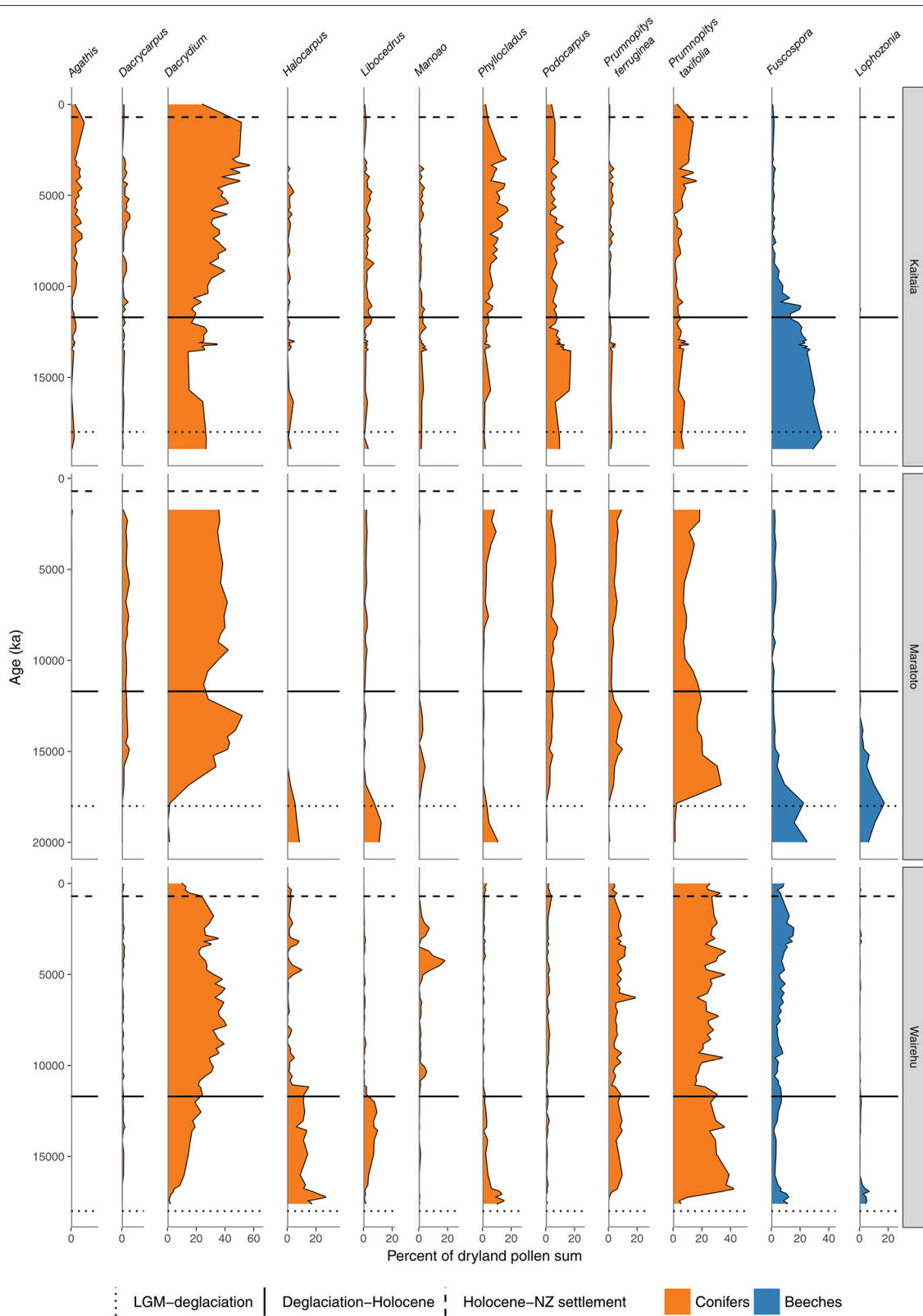


FIGURE 5 | Conifer and Nothofagaceae pollen sequences. Kaitia bog, Northland (Elliot, 1998). Lake Maratoto, Hamilton Basin (McGlone, 2001a). Wairehu, Rotoaira Basin (McGlone and Topping, 1977).

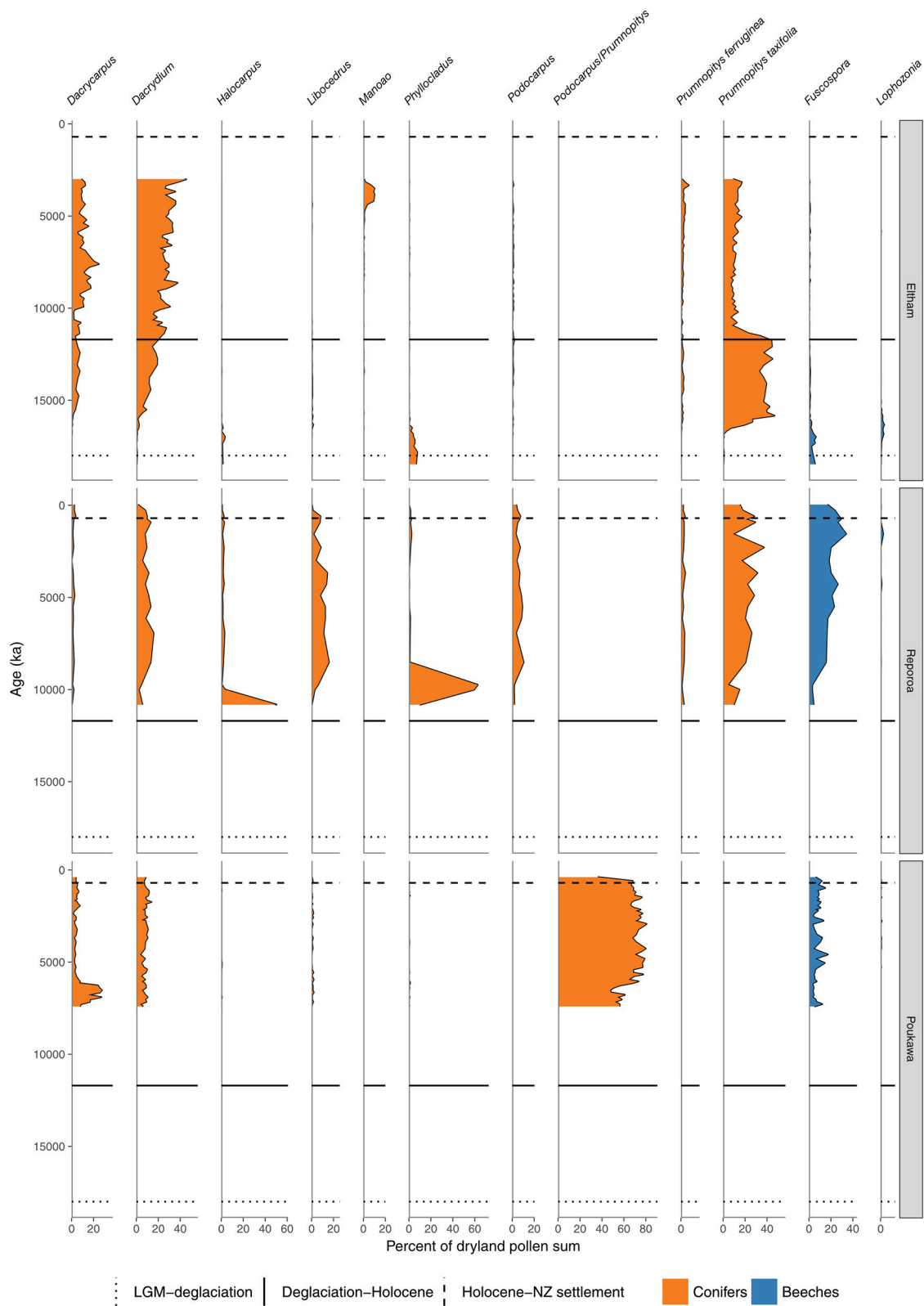


FIGURE 6 | Conifer and Nothofagaceae pollen sequences (cont.). Eltham Bog, Taranaki (McGlone and Neall, 1994). Reporoa Bog, upland central North Island (Rogers and McGlone, 1989). Lake Poukawa, Hawkes Bay (McGlone, 2002).

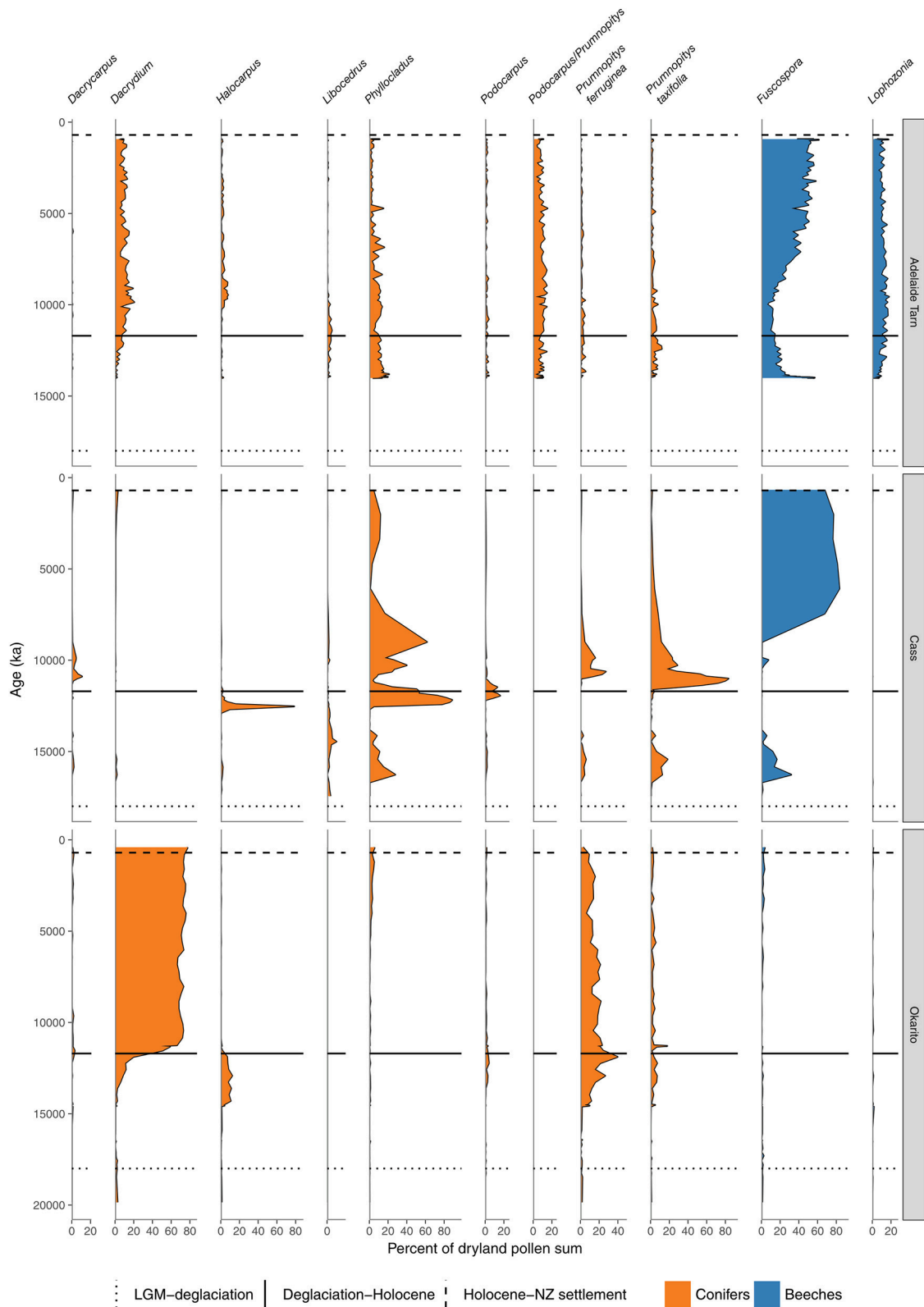


FIGURE 7 | Conifer and Nothofagaceae pollen sequences (cont.). Adelaide Tarn, treeline, Northwest Nelson (Jara et al., 2015). Cass Basin, Kettlehole Tarn, inland Canterbury (McGlone et al., 2004). Okarito bog, central West Coast (Newnham et al., 2007).

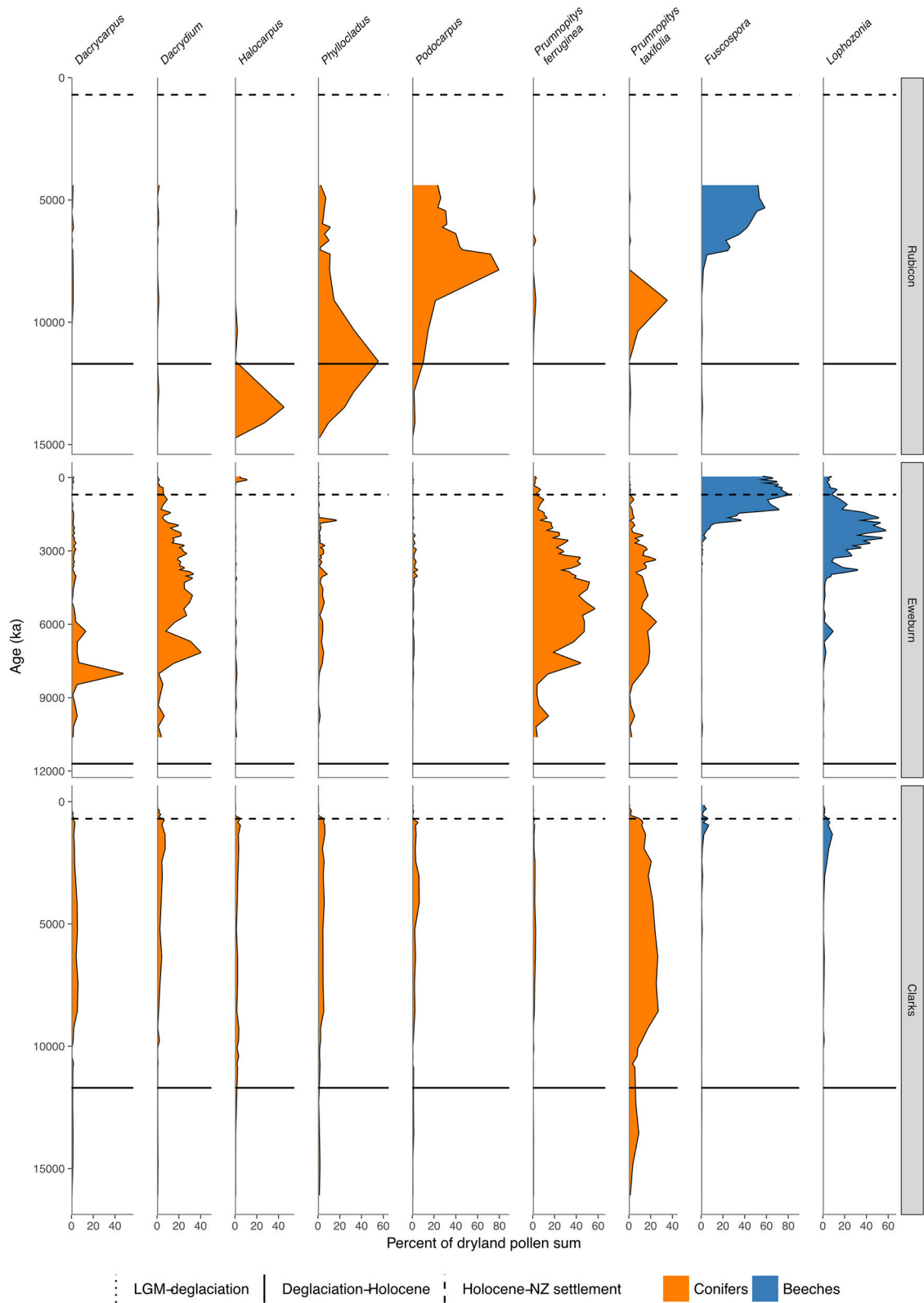


FIGURE 8 | Conifer and Nothofagaceae pollen sequences (cont.). Rubicon River, inland Canterbury (Moar, 1973). Eweburn Bog, Southland (Wilmshurst et al., 2002). Clarks Junction, Otago (McGlone et al., 2003).

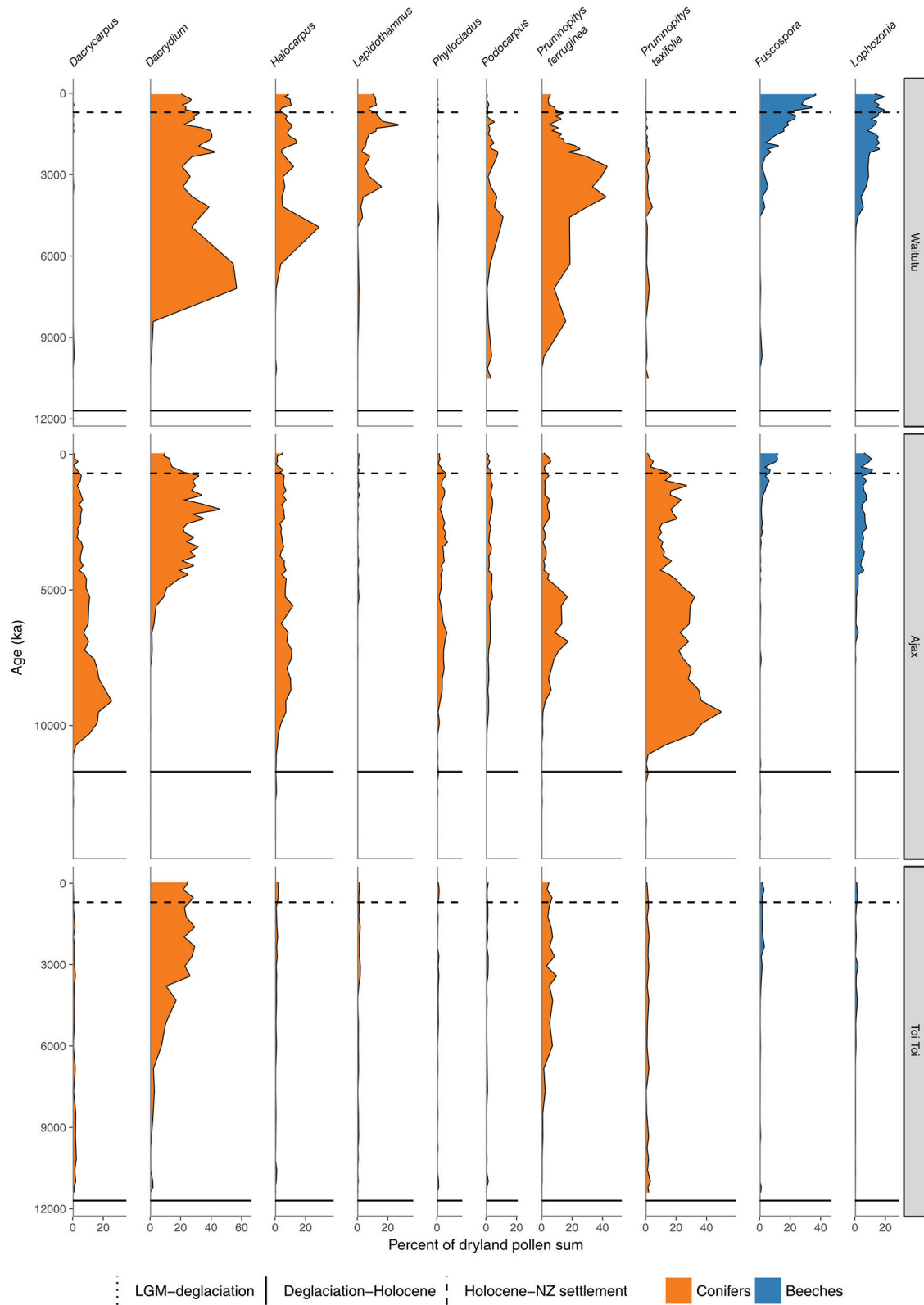


FIGURE 9 | Conifer and Nothofagaceae pollen sequences. Waitutu, Fiordland (Turney et al., 2017). Ajax Bog, Southland (McGlone et al., 2003). Toi Toi Flat, Stewart Island (McGlone and Wilson, 1996).

TABLE 2 | Climate regimes for major conifer associations past and present.

Climate regime	Characteristic vegetation	Current distribution	Past distribution
S: warm, relatively dry, long W: mild, wet	Conifer-broadleaved, most tall conifers present, <i>Agathis</i> in north	Northland, lowland central NI	Mid- to late Holocene, NNI
S: mild, moderate to abundant rainfall W: mild, wet	Conifer-broadleaved, most tall conifers present, <i>Dacrydium</i> and <i>Dacrycarpus</i> abundant	Western districts of southern NI and SI	Early deglacial onwards in west throughout
S: mild, excessively cloudy and humid W: mild, wet	Broadleaved canopy trees and tree fern dominant	Coastal, damp gullies	Coastal far southern districts, early Holocene
S: cool, but with warm clear spells, wet to very wet. Short W: cold	Nothofagaceae with subdominant <i>Phyllocladus alpinus</i> in places	Upper montane and treeline throughout	Mid to late Holocene, Northland early postglacial
S: cool, cloudy; moist to very wet. W: mild	Conifer scrub, <i>Phyllocladus alpinus</i> , <i>Halocarpus bidwillii</i> , and broadleaved scrub	Upper montane and treeline in central Southern Alps, Taranaki	Widespread in axial ranges early to mid Holocene. Lowland western districts LGM
S: warm, dry. Short W: cold	Conifer-broadleaved, dominant <i>Prumnopitys taxifolia</i> , <i>Podocarpus laetus</i> , <i>Dacrycarpus</i> . <i>Kunzea</i> stands	Eastern dryland rainshadow	Widespread in early deglacial in North
S: warm, very dry. Short. W: very cold and dry	<i>Phyllocladus alpinus</i> conifer scrub dominant, small-leaved angiosperm scrub	Southeastern SI interior basins and montane slopes	Widespread during LGM in NI

Climate data after Leathwick et al. (2003). S, summer (January mean temperatures): warm, 18°C+; mild, 18–14°C; cool, 13.9–10°C; cold, below 10°C. W, winter (July mean temperatures): mild, 8°C+; cool, 8–5°C; cold, 4.9–0; very cold, below zero. NI, North Island; SI, South Island.

entirely dominated by broadleaved angiosperms and tree ferns. Although Stewart Island was connected to the mainland well into the early postglacial, neither Nothofagaceae nor *Phyllocladus alpinus*, both abundant on the adjacent mainland, are present on the island, suggesting climatic factors or climate-moderated competition prevented their establishment while land connections existed.

The Mid to Late Holocene

The intensely oceanic climates of the early Holocene gave way from 8 ka onwards to more seasonal regimes characterized by longer, cooler winters and shorter, but warmer, summers. Increased south-westerly wind flow over New Zealand brought increased winter rainfall (McGlone et al., 2004). This increased seasonality strongly favored some trees over others. In the far North, it is only post 8 ka that *Agathis australis*—the giant Araucarian forest dominant (Figure 1)—becomes universally common in the pollen rain (Ogden et al., 1992) at about the same time that *Prumnopitys taxifolia*, *Podocarpus* spp., *Phyllocladus* spp., and *Libocedrus plumosa* became also more prominent (Elliot, 1998; Newnham, 1999; Elliot et al., 2005) (Figure 5). Some caution is needed in interpreting *Agathis* fossil records as pollen and macrofossil occurrences may not match because of differential preservation, and thus fluctuations during the mid to late Holocene may simply reflect changing wetland watertables (D'Costa et al., 2009). In the very far southern Stewart Island, the conifers *Dacrydium cupressinum*, *Prumnopitys ferruginea*, *Halocarpus biformis*, and *Lepidothamnus* spp. began their spread into the previously dominant *Metrosideros*-*Weinmannia* broadleaf forests from about 6 ka onwards (McGlone and Wilson, 1996; Figure 9). On the adjacent south-eastern South Island mainland, *Phyllocladus* and *Podocarpus* low forest occupied the dry interior basin-and-range country only after 8 ka (McGlone et al., 1995, 1997).

The mid to late Holocene saw spread of Nothofagaceae in most districts (McGlone et al., 1996). There are two exceptions. The Northland Peninsula and the Auckland Isthmus had extensive Nothofagaceae forest, mostly *Fuscospora truncata* and *Lophozonia menziesii* during the LGM and early postglacial but this was replaced during the early Holocene by *Agathis*-*podocarp*-broadleaved communities (Elliot, 1998; Newnham et al., 2017). *Lophozonia menziesii* formed part of the lowland deglacial forests in the central North Island but was eliminated before the beginning of the Holocene by conifer-broadleaved forests (Newnham et al., 1989, 1999; Alloway et al., 1992). Nothofagaceae at the LGM occurred only in scattered patches in the far south but had a more substantial presence in coastal areas of the north-west of the South Island (Marra and Leschen, 2004). *Fuscospora* spread appears to have started more-or-less synchronously throughout the uplands of the central and southern North Island and northern South Island during the early Holocene (Figures 4, 6–9). *Fuscospora* forests are currently the most common cover of the uplands and axial ranges of the central and southern North Island and northern South Island, but only became treeline dominants from about 9 to 3 ka, depending on the site (Rogers and McGlone, 1989; McGlone et al., 1996; Jara et al., 2015). *Fuscospora cliffortioides*—the most abundant tree line forest tree—almost invariably spread into pre-existing alpine forests and shrubland of *Libocedrus bidwillii*, *Phyllocladus alpinus*, and *Halocarpus* spp.

Lophozonia spread after c. 7–6 ka across the south of the South Island in widely separated areas mainly upland treeline sites, but including montane-lowland conifer-broadleaved forest (McGlone et al., 2003). Where *Lophozonia* took part in these mid to late Holocene successions in lowland to lower montane settings, it mostly spread into conifer-broadleaved forest where *Prumnopitys ferruginea* or *Dacrydium cupressinum* were abundant (see Eweburn, Figure 8). In these lowland-montane

sites, *Fuscospora* spp. follow the initial invasion or spread by *Lophozonia*.

Late Holocene and Polynesian Fire

Fire occurred frequently on the large, raised restiad bogs of northern New Zealand (Newnham, 1992; Battersby et al., 2017; Haenfling et al., 2017) but elsewhere was sporadic. Along the rain-shadow regions in the ranges to the east of the Southern Alps fires burnt from time to time, inducing a patchy landscape of conifer low forest, shrubland and grassland (Burrows et al., 1993; Burrows, 1996; Wardle, 2001b; Pugh and Shulmeister, 2010). Fire frequency may have increased at around 3 ka in some eastern parts of the North and South Islands but was still infrequent (McGlone and Moar, 1998; Ogden et al., 1998; Horrocks et al., 2001; Woodward et al., 2014). Few New Zealand woody plants have significant adaptations to fire (Perry et al., 2014) and conifers in particular appear to be highly vulnerable to fire. A notable exception is *Halocarpus bidwillii*, which has thick bark and can recover through basal resprouting after fire (Wardle, 1991). Polynesian fires beginning in the late thirteenth century, ultimately removed about 40% of the montane and lowland forest cover (McWethy et al., 2010; Perry et al., 2014). This forest loss was concentrated among conifer-rich lowland forests where c. 30% of this type was lost in the North Island, and nearly 90% in the South Island (Perry et al., 2012a). Some offshore islands were thought never to have had conifer forest, but pre-Polynesian pollen sequences have demonstrated that they did (Wilmshurst et al., 2014).

A GLACIAL-INTERGLACIAL PERSPECTIVE ON THE ENVIRONMENTAL NICHE OF THE NEW ZEALAND CONIFERS

Ecological Niche

An outline of the ecological niche of the conifers has been given in **Table 1**, and in **Table 2** we summarize how the changing climate and seasonality over a glacial-interglacial cycle has shifted the distribution of broadly defined conifer vegetation groupings. The loss of 80% of New Zealand's lowland forests since human settlement, along with nearly all the forest from rain shadow eastern districts, has left wet conifer-broadleaved forests and montane to alpine Nothofagaceae dominant forests as the most common forest types. Our understanding of their niches derives mainly from ecological observations made in dense, wet forests—which do not fully cover the environmental range of most of the species—and correlations between environmental variables and their abundance in these same forests. Nevertheless, a number of statements can be made about New Zealand conifer ecological niches (see Coomes and Bellingham, 2011) which are likely to be robust.

New Zealand conifers are slow growing and long-lived in comparison with competing angiosperms (Ogden and Stewart, 1995) and markedly taller. Despite conifers making up only 8% of the tree flora, 33% of the trees growing 20 m or more in height are conifers. As a group, the conifers are markedly frost-tolerant, most resisting frosts of -7°C or more,

and the three most frost-tolerant trees and shrubs in the flora (*Halocarpus bidwillii*, *Phyllocladus alpinus*, and *Podocarpus nivalis*) are conifers (Bannister, 2007). With regard to low rainfall and drought, *Prumnopitys taxifolia*, *Podocarpus laetus* (formerly *P. hallii*), *P. totara*, and *Dacrycarpus dacrydioides* are among a small group of trees singled out as currently having their maximum abundance under wet climate regimes, but also being capable of tolerating dry, warm lowland sites (Leathwick and Whitehead, 2001). *Agathis australis*, grows best under drier summer conditions and can tolerate severe drought (Macinnis-Ng et al., 2016). In particular, these species can tolerate low atmospheric deficits. *Dacrydium cupressinum* and *Prumnopitys ferruginea* are, on the other hand, far less tolerant of both dry soils and atmospheric deficits. Some species have an ambiguous relationship to drought: *Dacrycarpus dacrydioides* can tolerate warm, dry lowland situations (Leathwick and Whitehead, 2001) but physiological measures show it has a very low tolerance of water deficit (Brodribb and Cochard, 2009) and remaining stands are often associated with wet soils (**Figure 1**).

New Zealand conifers are generally regarded as being tolerant of poor soils (Coomes and Bellingham, 2011; de Jonge et al., 2012), and have an affinity for leached, low nutrient, acid or poorly drained soils that form in ever-wet environments and some (*Dacrydium cupressinum*, *Dacrycarpus dacrydioides*, *Lepidothamnus intermedius*, *Manoao colensoi*, *Libocedrus plumosa*, *Halocarpus bidwillii*, *H. biformis*) are characteristic of such sites (Richardson et al., 2005b). Where the climate supports tall trees, conifers usually dominate the tree biomass as there are only three tall angiosperm trees that tolerate wetlands (*Elaeocarpus hookerianus*, *Laurelia novae-zelandiae* and *Syzygium maire*; McGlone, 2009). Pollen diagrams confirm this and peat sites usually show conifer sequences with *Dacrycarpus dacrydioides* at the fertile, often swamp or lagoon beginning of the sequence, and *Dacrydium cupressinum*, *Manoao colensoi*, *Lepidothamnus intermedius*, and *Halocarpus bidwillii* at the infertile bog later stages (McGlone, 2009). However, in some situations conifers are quick to colonize fertile soils after disturbance, losing ground to angiosperm broadleaves as the succession proceeds, and this is most apparent in the pollen record after large-scale volcanic disturbance (Wilmshurst and McGlone, 1996; Horrocks and Ogden, 1998) but it also occurs after smaller scale disturbances (Bray, 1989; Carswell et al., 2007; de Jonge et al., 2012).

This tolerance of frost, drought, dry air and low nutrient or water-saturated soils can to a certain extent be attributed to their narrow, embolism-resistant tracheids, conservative hydraulic systems and thick, narrow leaves which lead to slow growth relative to competing angiosperms but much greater stress tolerance of poor soils, cold and drought (Sperry et al., 2006). This combination of attributes is the key to conifer niche over both long and short timescales. Despite slow growth rates, longevity ensures that the crowns of New Zealand forest conifers eventually rise well above the continuous lower broadleaved canopy. They therefore spend most of their life span with their crowns exposed to high solar radiation, higher wind speeds and low humidity which induce a drying effect exacerbated by the physiological water transport stress that scales with height

(Koch et al., 2004). For instance, tropical emergent trees transpire most of the water used in the forest they form part of (Kunert et al., 2017). A second, related fact is that New Zealand conifers within a conifer/broadleaf tract are often most abundant on ridges and steeper slopes exposing their canopies to windier, less humid conditions and drier soils. Just a handful of tall angiosperms compete in this supracanopy emergent space (e.g., *Laurelia novae-zelandiae*, *Metrosideros robusta*, *Knightia excelsa*, *Fuscospora fusca*, and *F. truncata*), and it has been argued that the angiosperm and conifer components of the forests they co-occur in are largely independent of each other (Ogden, 1985; Lusk, 2002).

Regeneration

New Zealand conifers have long been believed to face severe regeneration problems (Cockayne, 1928; Holloway, 1954; Robbins, 1962; Wardle, 1963; Veblen and Stewart, 1982; Smale et al., 2016). Most are bird-dispersed and dispersal seems not a critical issue. The wind-dispersed *Agathis australis* and *Libocedrus* spp. appear to have more limitations, and the montane to alpine *Libocedrus biddiwillii* has a markedly discontinuous distribution (Wardle, 2011), but even so they regenerate well after disturbance (Veblen and Stewart, 1982; Stewart and Beveridge, 2010). The essential problem faced by the conifers in lowland forests is establishment in openings that quickly fill with tree ferns and fast-growing and/or vegetatively resprouting angiosperm trees. This difficulty is compounded by conifers rarely recruiting under closed canopies (Ogden and Stewart, 1995). A marked feature of most New Zealand conifers is distinct juvenile foliage or growth forms (Dorken and Parsons, 2016)—most strikingly with the divaricate branched juvenile *Prumnopitys taxifolia*, the drooping foliage of *Dacrydium cupressinum* and the pyramidal “ricker” juvenile of *Agathis australis*. It is at least plausible that these monopodial juvenile growth forms compensate for slow biomass accumulation by favoring a single stem axis while the often elongated, planar or dispersed leaves maximize photosynthesis in a complex light environment. Although the New Zealand conifers are generally considered to be shade-intolerant (Cameron, 1954; Ebbett and Ogden, 1998), experimental studies suggest that this intolerance varies between taxa. Lusk et al. (2009) report little relationship between light availability and seedling presence of *Dacrydium cupressinum* and *Prumnopitys ferruginea* in forest stands in the central North Island. Observations in a northern North Island conifer-broadleaved forest showed that while the conifers had much the same shade tolerance as their angiosperm competitors, they grew more slowly and it was only at forest edges that their greater stress tolerance allowed them to overcome this regeneration handicap (Lusk et al., 2015). Conifer regeneration in drier regions is poorly known. However, we can postulate that drier, relatively infertile sites have sparser understoreys and ground-layers, providing better opportunities for conifer regeneration (Wardle, 1963; Burns and Leathwick, 1996) and the greater stress tolerance of the adult trees permit them to dominate.

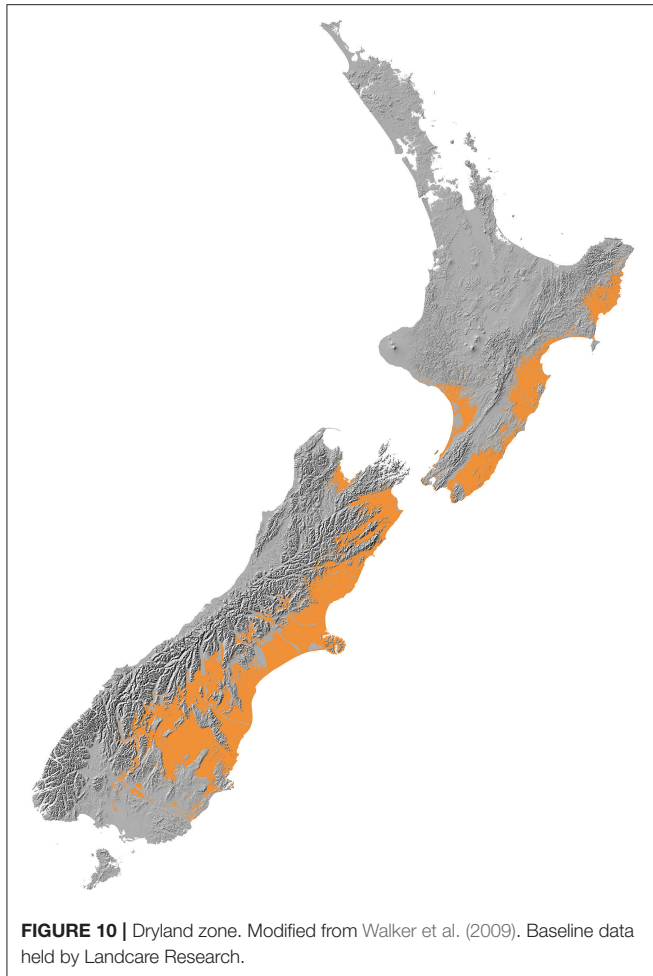
John Ogden proposed an influential model in which successive generations of conifers form a lesser proportion of a

conifer-broadleaved forest due to recruitment difficulties until a large-scale disturbance resets the forest with thickly stocked conifer stands (Ogden, 1985). Some recent data suggests higher conifer mortality and slower replacement in central North Island forests affected by volcanic eruptions consistent with this model (Smale et al., 2016), but complexities of forest history make sweeping generalizations inadvisable. For instance, broad scale analyses of North Island forests have shown some of the largest conifers have lower mortality rates than angiosperm trees (Richardson et al., 2009), and selective logging of conifers from wide tracts of conifer-broadleaved communities has given rise to anomalous contemporary patterns with virtually no regeneration in some areas (driven by absence of conifer seed sources) vs. massive regeneration in others (Carswell et al., 2007).

The pollen record seems to only detect the very largest of disturbances because of its typically large spatial and temporal scales. Once these are factored in, there appears to be little overall trend in conifer-broadleaved forest toward angiosperm dominance. There is little signal in the deglacial and Holocene pollen record from extant conifer-broadleaved tracts that conifers have ever been reduced to low levels (Figures 4, 5–9). During the first few thousand years of conifer spread during the deglacial period, conifer pollen input appears to have been higher than subsequently: most sites show this period of great conifer abundance did not last. However, in those areas that have remained under conifer-broadleaved forests throughout the Holocene, the conifers appear to have always been abundant. There is one exception. During the late deglacial-early Holocene period, coastal southern South Island and Stewart Island appear to have had a broadleaved-tree fern community with *Weinmannia racemosa* and *Metrosideros umbellata* prominent members, and conifers all but excluded for an extended period (Pickrill et al., 1992; McGlone and Wilson, 1996). Conifer dominance was not established until well into the mid Holocene (Figure 9). This island has extremely oceanic climate by global standards (Meurk, 1984) which the low insolation, warm winter-cool summer regime of the early Holocene intensified. The conifer strategy, which relies, in the absence of landscape-level disturbance, on environmental conditions unfavorable to angiosperms to regenerate well, was negated. A recent parallel at a more local level may be found in some fertile, dark, moist gullies where tree ferns, palms and broadleaves appear to permanently exclude conifer regeneration.

Conifers and Drylands

New Zealand conifers extend into semi-arid areas (rainfall < 500 mm a⁻¹) and were dominant across a wider “dryland” (Penman deficit ≥ 270 mm a⁻¹) region (Figure 10) mainly to the east of the axial ranges that made up some 19% of the land area of New Zealand prior to human settlement in the thirteenth century (Rogers et al., 2005). Because dryland conifer forest was largely destroyed by Polynesian fires (Perry et al., 2012b) little is known about its ecology. Figure 11 shows how human clearances have reduced the representation of current forests to vestigial levels in areas with less than about 900 mm a⁻¹ rainfall, and how conifers dominated the pre-deforestation pollen rain in this dryland zone. The pre-deforestation extension of taxa, such as



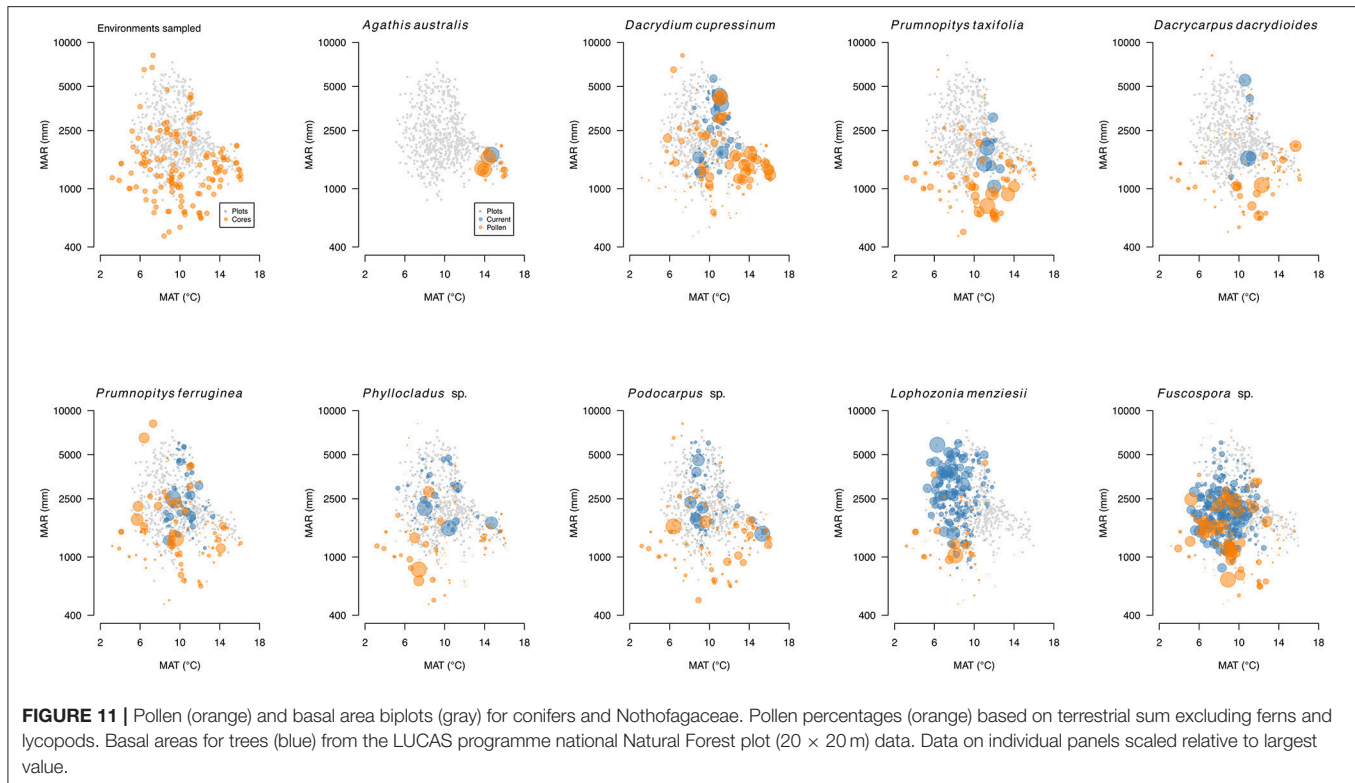
Dacrycarpus dacrydioides, *Halocarpus*, *Podocarpus*, *Phyllocladus*, and *Prumnopitys taxifolia* into the dryland zone is particularly clear and thus palynological investigations have focused much more on this zone than have ecological ones.

Conifer forests were more widespread during the early deglacial and *Prumnopitys taxifolia* and *Podocarpus* spp. dominated the transition from shrubland-grassland to closed forests (McGlone and Bathgate, 1983; McGlone and Topping, 1983; Newnham et al., 1989; Vandergoes et al., 1997; Sandiford et al., 2003; Augustinus et al., 2012; Jara et al., 2015). These early *Prumnopitys* and *Podocarpus* forests were not accompanied by an abundance of tree ferns, nor significant amounts of tall angiosperm trees, as the later *Dacrydium* dominated forests were and still are, and thus it seems that the early deglacial was drier than now. Dryland pollen sequences show that the forests existing just before deforestation strongly resembled the first forests to establish after the early deglacial *Myrsine-Muehlenbeckia* shrubland/grasslands, and then changed little during the Holocene (McGlone et al., 2003). In the driest areas of the southeastern South Island, conifer-broadleaved forest co-existed with patches of grassland and shrubland (McGlone, 2001b; Walker et al., 2004a; Rogers et al., 2005). It was only on the wet, western flanks of the Southern Alps (where

Dacrydium cupressinum was abundant; Newnham et al., 2007) and Northland (where *Fuscospora* was abundant) that this classic tall dryland conifer forest failed to establish.

A generalized dryland pattern that prevailed just before the Polynesian deforestation can be reconstructed from macrofossil and pollen data (Molloy, 1968; McGlone et al., 2003). The pre-deforestation pollen rain of the drylands was largely dominated by conifers (Figure 11), and the drylands may have supported denser conifer stands than elsewhere (Hall and McGlone, 2006). Tall *Prumnopitys taxifolia*- and *Podocarpus totara*-dominated associations on the lowland, deeper, more fertile soils extended up into inland valleys in higher rainfall areas, with *Dacrycarpus dacrydioides* prominent on swamp or lagoon soils. Stonier, shallower soils throughout were dominated by *Podocarpus laetus*, especially on the midslopes of the inland valleys. Areas with cold winters and dry, droughty summers would have favored *Phyllocladus alpinus* dominance, with the most leached or acid soils carrying a cover of *Halocarpus bidwillii* shrubland. *Prumnopitys taxifolia* dominated the dryland pollen rain in most places, but there are only a few macrofossil or charcoal remains to corroborate this dominance. *Podocarpus laetus* (like the other *Podocarpus* species) is not well represented in the pollen rain, but occurs as a continuous component alongside *Prumnopitys taxifolia*. Preserved wood of *Podocarpus laetus* is widespread on tussock-clad hill slopes throughout eastern districts and is often accompanied by *Phyllocladus alpinus* charcoal (Molloy et al., 1963; Ogden et al., 1998; Wardle, 2001b). Pollen and charcoal show that the driest regions of the central southeastern South Island, and intermontane valley bottoms of the eastern central Southern Alps had *Phyllocladus alpinus* and *Halocarpus bidwillii* low forest to scrub cover.

A wide range of angiosperm shrubs and trees co-existed with the dryland conifers but only a handful of these were tall or capable of dominating forest tracts. The few remaining fragments of dryland forest suggest that they would have been heavily stocked with conifers over a low and subordinate canopy of small angiosperm trees, such as *Melicactus ramiflorus*, *Griselinia littoralis*, *Elaeocarpus hookerianus*, and *Hoheria angustifolia*. Most of these species are in the 10–15 m height range, with only *Sophora microphylla*, *Kunzea* spp., and *Plagianthus regius* taller (15–20 m), but even they rarely match the 20–50 m heights of the podocarps. The *Kunzea* species complex of Myrtaceae small leaved (leptophyll), wind-dispersed shrubs to tall trees formed extensive forest tracts: the taller *Kunzea* (*K. serotina*, *K. robusta*, and *K. ericoides*) range throughout the mainland islands and occupied the very driest sites but generally they do not form an integral part of mature conifer forest; rather they occur as ecotonal or early successional dominants (de Lange, 2014). Interestingly, their small, linear needle-like leaves, erect multi-branched form, ectomycorrhizal status, ability to occupy bare ground, relatively fast growth and resistance to stresses, and rapid recovery after disturbance, including fire, is strongly reminiscent of Northern Hemisphere *Pinus*. It is unlikely that the dryland conifers were as dependent for regeneration on large-scale disturbance as they are in denser, moist forests, as these dryland forests lacked a dense understory, ferns being particularly sparse.



Conifers and the Nothofagaceae

A striking feature of many pollen profiles from the New Zealand mainland south of the Northland Peninsula, and in particular along the axial ranges, is the rise to dominance over the postglacial period of the Nothofagaceae (Figures 4, 5–9). On the basis of their Southland pollen diagrams, Cranwell and von Post (1936) divided the New Zealand postglacial into three periods: (I) Grassland; (II) Podocarp forest; (III) Nothofagaceae forest and grassland mosaic period. Period I was regarded as the final stages of the glaciation, with cool, severe climates with little regional differentiation; Period II, wet with probably maximum warmth; and Period III, climatic deterioration (Cranwell, 1938). That cooling climates had driven the spread of Nothofagaceae was readily accepted at first because *Fuscospora cliffortioides* and *Lophozonia menziesii* favor cooler regions and climatic explanations for anomalous Nothofagaceae distributions became popular for a time (Holloway, 1954; Nicholls, 1956). However, it had also been long known that the Nothofagaceae have a number of broad gaps in their distribution (the Taranaki volcanoes, the central and highest section of the Southern Alps, central Southland and Stewart Island; Cockayne, 1928). Willett (1950) suggested that the forest cover is in a state of disequilibrium because of the lasting effects of exclusion of Nothofagaceae trees at the height of the LGM by ice or severe climates and thus attributed the long-term forest dynamics of glacial affected areas to the slow, but inexorable encroachment of Nothofagaceae trees into conifer-broadleaf dominated associations. The Nothofagaceae have winged, but

poorly dispersed seeds and a requirement for ectomycorrhizal infection (Wardle, 1984) and thus dispersal limitation became the favored explanation for Nothofagaceae gaps at all scales (Molloy et al., 1963; Burrows, 1965; Moar, 1971). Palynological evidence suggests that neither of these explanations—glacial exclusion or deteriorating climates—is sufficient alone. To see why, we have to look at how the environmental niche of Nothofagaceae and conifers differ.

New Zealand Nothofagaceae, in general, occupy sites with cooler mean annual temperatures than the tall tree conifers (Leathwick, 1995) and dominate most current tree lines (Case and Duncan, 2014). While overlapping to a large extent with conifers in their environmental tolerances (Figure 11), and thus co-existing over wide areas, Nothofagaceae are mostly absent from the warmest locations—mainly the north of the North Island and southern North Island lowlands. Like conifers, they are vulnerable to having their regeneration suppressed by fast-growing broadleaves under warm, moist climates but lack the slow-growing emergent strategy that permits conifers to persist in dense broadleaved forests (Lusk et al., 2013). They are also largely absent from the drier, more drought-prone, frostier regions where several tall conifer trees (most notably *Podocarpus laetus* and *Prumnopitys taxifolia*) are abundant. However, ecosystem models predict that Nothofagaceae should dominate over most of its range gaps (Hall and McGlone, 2001, 2006; Leathwick, 2001).

The absence of Nothofagaceae from the seasonally dry and frosty areas, such as the south-eastern South Island, even though model results project its presence, seems unproblematic once

the limitations of the regeneration niche (which is not explicitly included in the models) is understood. The models project Nothofagaceae dominance because it is quite frost resistant but also fast-growing, and excellent at colonizing slips and clearings (Wardle, 1984; Richardson et al., 2011). However, they are poor at regenerating in grassland—where their sensitivity to late season dryness appears to be a factor—and are subject to local dispersal and mycorrhizal limitations. As Wardle (1984, pp. 381–382) comments, “Beech seedlings are poor competitors and have difficulty in establishing where the forest understory is dense, especially where turf or fern covers the ground. Young seedlings are prone to unseasonal frosts and both winter and summer desiccation. Even saplings over 2 m high can be killed by winter desiccation. Establishment success is therefore usually poor in the open, particularly where the climate tends to be cold and dry.”

If difficulties with establishment are overcome, Nothofagaceae have on average more rapid height growth and biomass accumulation than do competing conifers (Wardle, 1991). This advantage is particularly marked at tree line in relation to the competing conifers *Podocarpus laetus*, *Phyllocladus alpinus*, and *Halocarpus biformis*. In upland Nothofagaceae forest, *Phyllocladus alpinus* and *Halocarpus* spp. are often confined to the more stressed sites, such as frost-prone terraces and valley heads (Wardle, 1985) or on poorly drained soils. In broad terms, the Nothofagaceae have higher photosynthetic rates and therefore are well equipped to take advantage of high insolation days and short summers (Richardson et al., 2005a; Whitehead et al., 2011). The Nothofagaceae are also ectomycorrhizal and this brings with it the ability to directly use nutrients locked into organic complexes and also to lower the nutrient content of organic soils to such an extent that they are largely unsuitable for trees with arbuscular mycorrhizal infection (Dickie et al., 2014). However, these advantages over conifers are lessened under cloudy, low insolation summers (growth rate premium reduced) and long, mild winters (breakdown of soil organic matter and release of nutrients enhanced). When this is the climatic regime, other angiosperm broadleaved species prevail, dense fern groundcover forms restricting regeneration of the Nothofagaceae seedlings. We thus have the early Holocene conifer-dominant treeline associations of *Phyllocladus alpinus*, *Halocarpus bidwillii* and *H. biformis*, *Podocarpus laetus* and *P. nivalis*, and *Libocedrus bidwillii* (McGlone et al., 2011; McGlone and Basher, 2012) remnants of which persist throughout the axial ranges but most commonly in the central Southern Alps. There is a strong association of these conifer-dominant treelines with low insolation situations, such as in the southern Ruahine and northern Tararua Ranges (Rogers and McGlone, 1994), but limited Nothofagaceae spread across alpine-montane valley systems most likely contributed to this pattern (Wardle and Lee, 1990; McGlone et al., 1996; Hall and McGlone, 2006).

Mixed Nothofagaceae-conifer tall lowland forest is common in some regions, but most prevalent in the north-western South Island. Trade-offs in growth-rate and regeneration strategy can facilitate their long-term co-occurrence (Lusk and Smith, 1998). However, the propensity of Nothofagaceae to form monospecific stands means they are either segregated by site

from conifers—with Nothofagaceae along river courses or ridges—or the tall conifers (mainly *Dacrydium cupressinum*, *Prumnopitys ferruginea*, *P. taxifolia*, and *Podocarpus laetus*) form a discontinuous, sparse overstratum (Wardle, 1984, 1991). Only rarely are isolated Nothofagaceae trees scattered in conifer-broadleaved forest (Wardle, 1984). Holocene pollen sequences from the wide Nothofagaceae gap in central western South Island show that these boundaries have been largely static over the mid to late Holocene both at the *Fuscospora* dominated northern edge (Pocknall, 1980) and in the *Lophozonia menziesii* dominated southern margin of the gap (Li et al., 2008). Ecosystem models also predict mixed conifer-Nothofagaceae associations in both regions (Hall and McGlone, 2006).

NEW ZEALAND CONIFERS FROM A GLOBAL BIOGEOGRAPHIC PERSPECTIVE

New Zealand Conifers: Relictual?

Extant New Zealand conifers are clearly not relict. They are ubiquitous within the New Zealand mainland, and their close relatives thrive in similar oceanic forest environments elsewhere (McGlone et al., 2016). Their ecological success should not be measured by their species richness, but by their dominance of the forest biomass (Bond, 1989) and on this measure they are the most successful plant group in New Zealand. The lineages from which they come mostly evolved during the Palaeogene-early Neogene (Pittermann et al., 2012; Yang et al., 2012; Lu et al., 2014). Some are quite recent: the alpine-upper montane shrub and small tree group of *P. lawrencei* (SE Australia), *P. gnidioides* (New Caledonia) and *P. nivalis* (New Zealand) is indicated by molecular clock methods to have originated <5 ma ago (Condamine et al., 2017) and this is consistent with the timing of the uplift of the Southern Alps of New Zealand (Heenan and McGlone, 2013). *Prumnopitys taxifolia* (New Zealand) and *P. andina* (southern South America) are a closely related two-species clade, and may have diverged only 10 ma ago. The New Zealand conifers are therefore not holdovers from pre-angiosperm or even pre Gondwana-separation times but represent continuing adaptation to changing environments and competitors. However, that said, rainforest conifers have had to compensate for the structural and physiological limitations imposed by their hydraulics based on narrow tracheids, narrow, simple veined leaves, sluggish stomatal responses and, overall, low photosynthetic and growth rates (Brodribb et al., 2012). They do this by leveraging the inbuilt stress tolerance these attributes bring with them, and the longevity that accompanies their slow growth rate [hence Bond's (1989) “tortoise” analogy].

Given conifer dominance in many different New Zealand forest types we suggest that, rather than having severe disadvantages, they have been extraordinarily successful in a range of niches characteristic of an oceanic temperate environment. The biology and biogeographic history of the New Zealand conifers therefore can only be understood against the constraints and opportunities presented by the uncommon climate and unusual geographic position of the New Zealand archipelago.

Adaptation and Historical Contingency

Despite sharing its highly oceanic, moist climate regime with restricted temperate coastal regions elsewhere on the margins of the major continents New Zealand is, from a biogeographical viewpoint, unique. The archipelago has the only large temperate islands that are remote from a continental mainland and therefore never connected during the course of a glacial-interglacial cycle. Small, oceanic landmasses experience muted climatic extremes—both seasonally and at glacial-interglacial scales. However, during the extreme cold and dry of a glacial maximum, the archipelago has to fall back on its own floristic resources as it has no access to permanent cold boreal, arctic or dry steppe zones. Even New Zealand treelines cannot fill the gap, as they have exceptionally mild climates (Cieraad et al., 2012; Cieraad and McGlone, 2014). The trees of New Zealand, therefore, are evolutionarily adjusted to a limited climatic range. The brief intervals of a few thousand years during which the southern third of the archipelago experiences glacial cold, dry climates merely punctuate an otherwise highly oceanic environment.

Given the double filter of oceanicity and isolation, do New Zealand conifers represent unique adaptations to the oceanic climate regime? And has historical contingency played a role in that some niches have not been filled? Globally, oceanic temperate forests are extraordinarily diverse in terms of their structural and taxonomic makeup (DellaSala, 2011). They include single canopy deciduous angiosperm forests of the western fringe of Europe, dense, conifer-dominated forests of north-western North America, tall evergreen *Eucalyptus* forests of eastern Australia, but also structurally and taxonomically similar southern conifer-evergreen angiosperm forest of the southern Atlantic coast of Brazil, southern Chile and the highlands of New Guinea. Near-identical oceanic climate regimes have therefore generated very different structural and plant functional trait solutions. We argue that the southern conifers have, by virtue of their continuous presence in oceanic environments, arrived at an evolutionary solution that takes advantage of their stress resistant physiology and morphology and minimizes the consequences of the accompanying slow growth. In an oceanic temperate, evergreen forest, supra-canopy space is potentially available, but only to trees with foliage that can endure winter conditions and survive episodic drying, wind, and high insolation in summer. The hydraulic physiology and leaf morphology of the conifers is clearly superior in this zone to that of all but a few angiosperms. The trade-off is the sacrifice of fast-seedling and sapling growth, which they partially offset with specialized juvenile growth forms. Once established, their longevity is the key to their long-term success as they can wait for the rare occasions which favor large-scale regeneration. Disturbance of a size that permits them to regenerate must be (at an evolutionary timescale) as certain as the alternation of seasons, and this is recognized in the conceptual models developed to explain their regeneration strategy (Ogden, 1985; Ogden and Stewart, 1995; Enright et al., 1999).

It is only under certain climatic conditions that the conifers fail to persist. The first is under hyperoceanic situations—such as that of Stewart Island during the early Holocene. Here, we

suggest, a fern-rich ground layer, dense broadleaf shrub and canopy with abundant tree ferns can successfully resist conifer invasion. At a small scale, these conditions also prevail in shady gullies on rich soils where only sporadic conifer regeneration is possible (Coomes et al., 2005). The second situation in which the New Zealand conifers are at a disadvantage is in the presence of Nothofagaceae. *Libocedrus bidwillii*, *Phyllocladus alpinus* and *Halocarpus* dominated the subalpine and upper montane zone in the earlier part of the postglacial, but in nearly all locations have since lost this dominance during the Holocene. While the relatively slow spread rates of Nothofagaceae account for some of the early prevalence of conifer-dominated associations in alpine/montane environments, the underlying driver is almost certainly a climatic switch beginning around 9,000 years ago, from long, low insolation summers and mild winters—which favored slow-growing conifers—to short, high insolation summer and colder, longer winters—which favored the fast-growing mycorrhizal Nothofagaceae (Wilmshurst et al., 2002).

Vacant Tree Niches?

It is possible that there is a vacant tree niche in New Zealand currently represented by the winter cold dryland environments of the rain-shadow of the Southern Alps and a vacant conifer niche at tree line. During the full glacial, a very large area of New Zealand had only sparse, scattered forest, and the open, dry eastern lowlands something approaching open herb field with prostrate shrubs. In Northern Hemisphere temperate regions the LGM was characterized by open conifer dominated parklands unless the desert-steppe climates prevailed (McGlone et al., 2012). The current rapid spread of exotic fast-growing mycorrhizal wilding pines (in particular *Pinus contorta* and *P. nigra*) into lowland to montane fire-induced grassland/shrublands (Ledgard, 2001) indicates a vacant “conifer” niche in the drylands that is only partly filled by the Myrtaceous *Kunzea*. Evolution of such a tree type presumably requires a permanent, highly seasonal, winter-cold environment that is absent in the Southern Hemisphere from all but Antarctica. At some tree lines in the drier eastern side of the axial mountain ranges, exotic pines are spreading above the Nothofagaceae tree line and this likewise suggests a tree line “pine/fir/spruce” niche remains unfilled for similar reasons (Cieraad et al., 2014; Tomiolo et al., 2016).

ARE PALYNOLOGY AND ECOLOGY MUTUALLY SUPPORTIVE?

In New Zealand, history cannot be ignored. Besides the alternation of glacial-interglacial cycles, frequent, massive disruption caused by earthquakes, volcanic eruptions, cyclonic storms and the recent imposition of historically unprecedented human-lit fires have left major historical legacies. Therefore, in New Zealand, palaeoecological and neocological researchers frequently collaborate as our exploration of conifer history shows. Not only that, neocologists have often taken the lead in study of the past, as exemplified by Peter Wardle with his Quaternary investigations of soil charcoal (Wardle, 2001a), Colin Burrows

and the palaeoecology of the South Island mountains (Burrows et al., 1993), Susan Walker, Bill Lee and Geoff Rogers on the history of the drylands of the southern South Island (Walker et al., 2004b), and the ground-breaking neo-palaeoresearch by ecologist John Ogden and colleagues on many aspects of northern plant successions and Quaternary history (for example: Ogden et al., 1992, 1997).

The answer then to the question posed by Bill Harris many years ago is that the unbroken legacy of Lennart von Post and Lucy Cranwell continues in New Zealand, palaeoecology and ecology combining in a productive relationship to document the past, understand the present, and anticipate the future.

AUTHOR CONTRIBUTIONS

MM co-led the paleoecological section of the review and wrote the first draft; SR and OB undertook analyses of pollen

and ecological data, and prepared the figures; SR and GP led the neoecological component of the review; JW organized underpinning pollen databases and co-led the paleoecological component. All authors contributed to draft revisions of the ms.

ACKNOWLEDGMENTS

This research was supported by SSIF funding for Crown Research Institutes from the New Zealand Ministry of Business, Innovation and Employment's Science and Innovation Group. We thank Rewi Newnham and Marcus Vandergoes for permission to republish their Okarito pollen data and Susan Walker for access to the data **Figure 10** and Jamie Wood for drafting **Figure 2**. We acknowledge the use of data drawn from the Natural Forest plot data collected between January 2002 and March 2007 by the LUCAS programme for the Ministry for the Environment.

REFERENCES

- Alloway, B. V., Stewart, R. B., Neall, V. E., and Vucetich, C. G. (1992). Climate of the Last Glaciation in New Zealand, based on aerosolic quartz influx in an andesitic terrain. *Quaternary Res.* 38, 170–179. doi: 10.1016/0033-5894(92)90054-M
- Augustinus, P., Cochran, U., Kattel, G., D'costa, D., and Shane, P. (2012). Late quaternary paleolimnology of onepoto maar, Auckland, New Zealand: implications for the drivers of regional paleoclimate. *Q. Int.* 253, 18–31. doi: 10.1016/j.quaint.2011.02.028
- Augustinus, P., D'costa, D., Deng, Y. B., Hagg, J., and Shane, P. (2011). A multiproxy record of changing environments from ca. 30 000 to 9000 cal. a BP: onepoto maar palaeolake, Auckland, New Zealand. *J. Quat. Sci.* 26, 389–401. doi: 10.1002/jqs.1463
- Bannister, P. (2007). A touch of frost? Cold hardiness of plants in the Southern Hemisphere. *N. Z. J. Botany* 45, 1–33. doi: 10.1080/00288250709509700
- Battersby, P. F., Wilmschurst, J. M., Curran, T. J., McGlone, M. S., and Perry, G. L. W. (2017). Exploring fire adaptation in a land with little fire: serotiny in *Leptospermum scoparium* (Myrtaceae). *J. Biogeogr.* 44, 1306–1318. doi: 10.1111/jbi.12950
- Bond, W. (1989). The tortoise and the hare: ecology of angiosperm dominance and gymnosperm persistence. *Biol. J. Linnean Soc.* 36, 227–249. doi: 10.1111/j.1095-8312.1989.tb00492.x
- Bray, J. R. (1989). The use of historical vegetation dynamics in interpreting prehistorical vegetation change. *J. R. Soc. N. Z.* 19, 151–160. doi: 10.1080/03036758.1989.10426444
- Brodribb, T. J., and Cochard, H. (2009). Hydraulic failure defines the recovery and point of death in water-stressed conifers. *Plant Physiol.* 149, 575–584. doi: 10.1104/pp.108.129783
- Brodribb, T. J., Pittermann, J., and Coomes, D. A. (2012). Elegance versus speed: examining the competition between conifer and angiosperm trees. *Int. J. Plant Sci.* 173, 673–694. doi: 10.1086/666005
- Burns, B. R., and Leathwick, J. R. (1996). Vegetation-environment relationships at Waipoua Forest, Northland, New Zealand. *N. Z. J. Bot.* 34, 79–92. doi: 10.1080/0028825X.1996.10412695
- Burrows, C. (1965). Some discontinuous distributions of plants within New Zealand and their ecological significance. 11: disjunctions between Otago-Southland and Nelson-Marlborough and related distribution patterns. *Tuatara* 13, 9–29.
- Burrows, C. J. (1996). Germination behaviour of seeds of the New Zealand woody species *Ascarina lucida*, *Coprosma grandifolia*, *Melicactus lanceolatus*, and *Solanum laciniatum*. *N. Z. J. Bot.* 34, 509–515. doi: 10.1080/0028825X.1996.10410131
- Burrows, C. J., Randall, P., Moar, N. T., and Butterfield, B. G. (1993). Aranuian vegetation history of the Arrowsmith Range, Canterbury, New Zealand. 3. Vegetation changes in the Cameron, upper south Ashburton and Paddle Hill Creek catchments. *N. Z. J. Bot.* 31, 147–174. doi: 10.1080/0028825X.1993.10419491
- Cameron, E. K. (2000). Lucy May Cranwell, M. A., DSc, DSc(Hon), FLS(Lond.), FRSNZ, 1907–2000-Obituary. *N. Z. J. Bot.* 38, 527–535. doi: 10.1080/0028825X.2000.9512702
- Cameron, R. (1954). Mosaic or cyclical regeneration in North Island podocarp forests. *N. Z. J. For.* 7, 55–64.
- Carswell, F. E., Richardson, S. J., Doherty, J. E., Allen, R. B., and Wiser, S. K. (2007). Where do conifers regenerate after selective harvest? A case study from a New Zealand conifer-angio sperm forest. *For. Ecol. Manage.* 253, 138–147. doi: 10.1016/j.foreco.2007.07.011
- Case, B. S., and Duncan, R. P. (2014). A novel framework for disentangling the scale-dependent influences of abiotic factors on alpine treeline position. *Ecography* 37, 838–851. doi: 10.1111/ecog.00280
- Cieraad, E., and McGlone, M. S. (2014). Thermal environment of New Zealand's gradual and abrupt treeline ecotones. *N. Z. J. Ecol.* 38, 12–25.
- Cieraad, E., McGlone, M. S., and Huntley, B. (2014). Southern Hemisphere temperate tree lines are not climatically depressed. *J. Biogeogr.* 41, 1456–1466. doi: 10.1111/jbi.12308
- Cieraad, E., McGlone, M., Barbour, M. M., and Huntley, B. (2012). Seasonal Frost Tolerance of Trees in the New Zealand Treeline Ecotone. *Arct. Antarct. Alp. Res.* 44, 332–342. doi: 10.1657/1938-4246-44.3.332
- Cockayne, L. (1928). *The Vegetation of New Zealand*. Leipzig: Engelmann.
- Condamine, F. L., Leslie, A. B., and Antonelli, A. (2017). Ancient islands acted as refugia and pumps for conifer diversity. *Cladistics* 33, 69–92. doi: 10.1111/cla.12155
- Coomes, D. A., Allen, R. B., Bentley, W. A., Burrows, L. E., Canham, C. D., Fagan, L., et al. (2005). The hare, the tortoise and the crocodile: the ecology of angiosperm dominance, conifer persistence and fern filtering. *J. Ecol.* 93, 918–935. doi: 10.1111/j.1365-2745.2005.01012.x
- Coomes, D. A., and Bellingham, P. J. (2011). "Temperate and tropical podocarps: how ecologically alike are they?" in *Smithsonian Contributions to Botany: Ecology of the Podocarpaceae in Tropical Forests*, eds B. L. Turner and L. A. Cernusak (Washington, DC: Smithsonian Institution Scholarly Press), 119–140.
- Cranwell, L. M. (1938). Fossil pollens: the key to the vegetation of the past. *N. Z. J. Sci. Technol.* 19, 628–645.
- Cranwell, L. M., and von Post, L. (1936). Post-Pleistocene pollen diagrams from the southern hemisphere. I New Zealand. *Geografiska Annaler*. 18, 308–347.

- Darvill, C. M., Bentley, M. J., Stokes, C. R., and Shulmeister, J. (2016). The timing and cause of glacial advances in the southern mid-latitudes during the last glacial cycle based on a synthesis of exposure ages from Patagonia and New Zealand. *Quat. Sci. Rev.* 149, 200–214. doi: 10.1016/j.quascirev.2016.07.024
- D'Costa, D., Boswijk, G., and Ogden, J. (2009). Holocene vegetation and environmental reconstructions from swamp deposits in the Dargaville region of the North Island, New Zealand: implications for the history of kauri (*Agathis australis*). *Holocene* 19, 559–574. doi: 10.1177/0959683609104026
- de Jonge, V. N., Pinto, R., and Turner, R. K. (2012). Integrating ecological, economic and social aspects to generate useful management information under the EU Directives' 'ecosystem approach'. *Ocean Coast. Manag.* 68, 169–188. doi: 10.1016/j.ocecoaman.2012.05.017
- de Lange, P. J. (2014). A revision of the New Zealand *Kunzea ericoides* (Myrtaceae) complex. *PhytoKeys* 40, 1–185. doi: 10.3897/phytokeys.40.7973
- DellaSala, D. A. (2011). *Temperate and Boreal Rainforests of the World: Ecology and Conservation*. Washington, DC: Island Press.
- Dickie, I. A., Koele, N., Blum, J. D., Gleason, J. D., and McGlone, M. S. (2014). Mycorrhizas in changing ecosystems. *Botany* 92, 149–160. doi: 10.1139/cjb-2013-0091
- Dorken, V. M., and Parsons, R. F. (2016). Morpho-anatomical studies on the change in the foliage of two imbricate-leaved New Zealand podocarps: *Dacrycarpus dacrydioides* and *Dacrydium cupressinum*. *Plant Syst. Evol.* 302, 41–54. doi: 10.1007/s00606-015-1239-5
- Ebbett, R., and Ogden, J. (1998). Comparative seedling growth of five endemic New Zealand podocarp species under different light regimes. *N. Z. J. Bot.* 36, 189–201. doi: 10.1080/0028825X.1998.9638781
- Elliot, M. B. (1998). Late Quaternary pollen records of vegetation and climate change from Kaitaia Bog, far northern New Zealand. *Rev. Palaeobot. Palynol.* 99, 189–202. doi: 10.1016/S0034-6667(97)00048-1
- Elliot, M., Neall, V., and Wallace, C. (2005). A Late Quaternary pollen record from Lake Tangonge, far northern New Zealand. *Rev. Palaeobot. Palynol.* 136, 143–158. doi: 10.1016/j.revpalbo.2005.05.003
- Enright, N. J., Ogden, J., and Rigg, L. S. (1999). Dynamics of forests with Araucariaceae in the western Pacific. *J. Veget. Sci.* 10, 793–804. doi: 10.2307/3237304
- Haenfling, C., Newnham, R., Rees, A., Jara, I., Homes, A., and Clarkson, B. (2017). Holocene history of a raised bog, northern New Zealand, based on plant cuticles. *Holocene* 27, 309–314. doi: 10.1177/0959683616658524
- Hall, G. M. J., and McGlone, M. S. (2001). Forest reconstruction and past climatic estimates for a deforested region of south-eastern New Zealand. *Landsc. Ecol.* 16, 501–521. doi: 10.1023/A:1013199209388
- Hall, G. M. J., and McGlone, M. S. (2006). Potential forest cover of New Zealand as determined by an ecosystem process model. *N. Z. J. Bot.* 44, 211–232. doi: 10.1080/0028825X.2006.9513019
- Harris, W. (1963). Evidence for ecologically significant changes in climate during the post-glacial period in New Zealand: paleo-ecological evidence from pollen and spores. *Proc. N. Z. Ecol. Soc.* 10, 38–44.
- Hawkins, B. J., and Sweet, G. B. (1989). Evolutionary interpretation of a high temperature growth response in 5 New Zealand forest tree species. *N. Z. J. Bot.* 27, 101–107. doi: 10.1080/0028825X.1989.10410148
- Heenan, P. B., and McGlone, M. S. (2013). Evolution of New Zealand alpine and open-habitat plant species during the late Cenozoic. *N. Z. J. Ecol.* 37, 105–113.
- Holloway, J. T. (1954). Forests and climate in the South Island of New Zealand. *Trans. R. Soc. N. Z.* 82, 329–410.
- Horrocks, M., and Ogden, J. (1998). The Effects of the Taupo Tephra Eruption of c. 1718 BP on the Vegetation of Mt Hauhungatahi, Central North Island, New Zealand. *J. Biogeogr.* 25, 649–660. doi: 10.1046/j.1365-2699.1998.2540649.x
- Horrocks, M., Deng, Y., Ogden, J., Alloway, B. V., Nichol, S. L., and Sutton, D. G. (2001). High spatial resolution of pollen and charcoal in relation to the c600-year-BP Kaharoa Tephra: implications for Polynesian settlement of Great Barrier Island, Northern New Zealand. *J. Archaeol. Sci.* 28, 153–168. doi: 10.1006/jasc.2000.0568
- Jara, I. A., Newnham, R. M., Vandergoes, M. J., Foster, C. R., Lowe, D. J., Wilmshurst, J. M., et al. (2015). Pollen-climate reconstruction from northern South Island, New Zealand (41 degrees S), reveals varying high- and low-latitude teleconnections over the last 16,000 years. *J. Quaternary Sci.* 30, 817–829. doi: 10.1002/jqs.2818
- Kirkpatrick, J. B., and DellaSala, D. A. (2011). "Temperate rainforests of Australasia," in *Temperate and Boreal Rainforests of the World: Ecology and Conservation*, ed D. A. DellaSala (Washington, DC: Island Press), 195–212.
- Koch, G. W., Sillett, S. C., Jennings, G. M., and Davis, S. D. (2004). The limits to tree height. *Nature* 428, 851–854. doi: 10.1038/nature02417
- Kooyman, R. M., Wilf, P., Barreda, V. D., Carpenter, R. J., Jordan, G. J., Sniderman, J. M. K., et al. (2014). Paleo-Antarctic rainforest into the modern Old World tropics: the rich past and threatened future of the "southern wet forest survivors." *Am. J. Bot.* 101, 2121–2135. doi: 10.3732/ajb.1400340
- Kunert, N., Aparecido, L. M. T., Wolff, S., Higuchi, N., Dos Santos, J., De Araujo, A. C., et al. (2017). A revised hydrological model for the Central Amazon: the importance of emergent canopy trees in the forest water budget. *Agric. For. Meteorol.* 239, 47–57. doi: 10.1016/j.agrformet.2017.03.002
- Leathwick, J. R. (1995). Climatic relationships of some New Zealand forest tree species. *J. Vegetation Sci.* 6, 237–248. doi: 10.2307/3236219
- Leathwick, J. R. (2001). New Zealand's potential forest pattern as predicted from current species-environment relationships. *N. Z. J. Bot.* 39, 447–464. doi: 10.1080/0028825X.2001.9512748
- Leathwick, J. R., and Whitehead, D. (2001). Soil and atmospheric water deficits and the distribution of New Zealand's indigenous tree species. *Funct. Ecol.* 15, 233–242. doi: 10.1046/j.1365-2435.2001.00504.x
- Leathwick, J. R., Wilson, G., Rutledge, D., Wardle, P., Morgan, F., Johnston, K., et al. (2003). *Land Environments of New Zealand*. Auckland: David Bateman.
- Ledgard, N. (2001). The spread of lodgepole pine (*Pinus contorta*, Dougl.) in New Zealand. *For. Ecol. Manage.* 141, 43–57. doi: 10.1016/S0378-1127(00)00488-6
- Li, X., Rapson, G., and Flenley, J. R. (2008). Holocene vegetational and climatic history, Sponge Swamp, Haast, south-western New Zealand. *Quaternary Int.* 184, 129–138. doi: 10.1016/j.quaint.2007.09.011
- Lorrey, A. M., Vandergoes, M., Almond, P., Renwick, J., Stephens, T., Bostock, H., et al. (2012). Palaeocirculation across New Zealand during the last glacial maximum at similar to 21 ka. *Quat. Sci. Rev.* 36, 189–213. doi: 10.1016/j.quascirev.2011.09.025
- Lu, Y., Ran, J. H., Guo, D. M., Yang, Z. Y., and Wang, X. Q. (2014). Phylogeny and divergence times of gymnosperms inferred from single-copy nuclear genes. *PLoS ONE* 9:e107679. doi: 10.1371/journal.pone.0107679
- Lusk, C. H. (2002). Basal area in a New Zealand podocarp-broadleaved forest: are coniferous and angiosperm components independent? *N. Z. J. Bot.* 40, 143–147. doi: 10.1080/0028825X.2002.9512778
- Lusk, C. H., and Smith, B. (1998). Life history differences and tree species coexistence in an old-growth New Zealand rain forest. *Ecology* 79, 795–806. doi: 10.1890/0012-9658(1998)079[0795:LHDATS]2.0.CO;2
- Lusk, C. H., Duncan, R. P., and Bellingham, P. J. (2009). Light environments occupied by conifer and angiosperm seedlings in a New Zealand podocarp-broadleaved forest. *N. Z. J. Ecol.* 33, 83–89.
- Lusk, C. H., Jorgensen, M. A., and Bellingham, P. J. (2015). A conifer-angiosperm divergence in the growth vs. shade tolerance trade-off underlies the dynamics of a New Zealand warm-temperate rain forest. *J. Ecol.* 103, 479–488. doi: 10.1111/1365-2745.12368
- Lusk, C. H., Kaneko, T., Grierson, E., and Clearwater, M. (2013). Correlates of tree species sorting along a temperature gradient in New Zealand rain forests: seedling functional traits, growth and shade tolerance. *J. Ecol.* 101, 1531–1541. doi: 10.1111/1365-2745.12152
- Macinnis-Ng, C., Wyse, S., Veale, A., Schwendenmann, L., and Clearwater, M. (2016). Sap flow of the southern conifer, *Agathis australis* during wet and dry summers. *Trees-Struct. Funct.* 30, 19–33. doi: 10.1007/s00468-015-1164-9
- Macphail, M. K., and McQueen, D. R. (1983). The value of New Zealand pollen and spores as indicators of Cenozoic vegetation and climates. *Tuatara* 26, 37–56.
- Marra, M., and Leschen, R. A. B. (2004). Late Quaternary paleoecology from fossil beetle communities in the Awatere Valley, South Island, New Zealand. *J. Biogeogr.* 31, 571–586. doi: 10.1046/j.1365-2699.2003.00998.x
- Martin, T. J., and Ogden, J. (2005). Experimental studies on the drought, waterlogging, and frost tolerance of *Ascarina lucida* Hook. f (*Chloranthaceae*) seedlings. *N. Z. J. Ecol.* 29, 53–59.
- McGlone, M. S. (2001a). A late Quaternary pollen record from marine core P69, southeastern North Island, New Zealand. *N. Z. J. Geol. Geophys.* 44, 69–77. doi: 10.1080/00288306.2001.9514923

- McGlone, M. S. (2001b). The origin of the indigenous grasslands of southeastern South Island in relation to pre-human woody ecosystems. *N. Z. J. Ecol.* 25, 1–15.
- McGlone, M. S. (2002). A Holocene and latest Pleistocene pollen record from Lake Poukawa, Hawke's Bay, New Zealand. *Glob. Planet. Change* 33, 283–299. doi: 10.1016/S0921-8181(02)00083-8
- McGlone, M. S. (2009). Postglacial history of New Zealand wetlands and implications for their conservation. *N. Z. J. Ecol.* 33, 1–23.
- McGlone, M. S., and Basher, L. (2012). "Holocene vegetation change at treeline, Cropp Valley, Southern Alps, New Zealand," in *Peopled Landscapes: Archaeological and Biogeographic Approaches to Landscape*, eds S. Haberle and B. David (Canberra, ACT: ANU E Press), 343–358.
- McGlone, M. S., and Bathgate, J. L. (1983). Vegetation and climate history of the Longwood Range, South Island, New Zealand, 12 000 B.P. to the present. *N. Z. J. Bot.* 21, 293–315. doi: 10.1080/0028825X.1983.10428560
- McGlone, M. S., and Moar, N. T. (1977). Ascarina decline and postglacial climatic change in New Zealand. *N. Z. J. Bot.* 15, 485–489. doi: 10.1080/0028825X.1977.10432554
- McGlone, M. S., and Moar, N. T. (1998). Dryland Holocene vegetation history, Central Otago and the Mackenzie Basin, South Island, New Zealand. *N. Z. J. Bot.* 36, 91–111. doi: 10.1080/0028825X.1998.9512549
- McGlone, M. S., and Neall, V. E. (1994). The late Pleistocene and Holocene vegetation history of Taranaki, North Island, New Zealand. *N. Z. J. Bot.* 32, 251–269. doi: 10.1080/0028825X.1994.10410470
- McGlone, M. S., and Topping, W. W. (1977). Aranuian (postglacial) pollen diagrams from Tongariro region, North Island, New Zealand. *N. Z. J. Bot.* 15, 749–760. doi: 10.1080/0028825X.1977.10429643
- McGlone, M. S., and Topping, W. W. (1983). Late Quaternary vegetation, Tongariro region, central North Island, New Zealand. *N. Z. J. Bot.* 21, 53–76. doi: 10.1080/0028825X.1983.10428525
- McGlone, M. S., and Wilson, H. D. (1996). Holocene vegetation and climate of Stewart Island, New Zealand. *N. Z. J. Bot.* 34, 369–388. doi: 10.1080/0028825X.1996.10410701
- McGlone, M. S., Buitenwerf, R., and Richardson, S. J. (2016). The formation of the oceanic temperate forests of New Zealand. *N. Z. J. Bot.* 54, 128–155. doi: 10.1080/0028825X.2016.1158196
- McGlone, M. S., Hall, G. M. J., and Wilmshurst, J. M. (2011). Seasonality in the early Holocene: extending fossil-based estimates with a forest ecosystem process model. *Holocene* 21, 517–526. doi: 10.1177/0959683610385717
- McGlone, M. S., Mark, A. F., and Bell, D. (1995). Late Peistocene and Holocene vegetation history, central Otago, South Island, New Zealand. *J. R. Soc. N. Z.* 25, 1–22. doi: 10.1080/03014223.1995.9517480
- McGlone, M. S., Mildenhall, D. C., and Pole, M. S. (1996). "History and palaeoecology of New Zealand Nothofagus forests," in *The Ecology and Biogeography of Nothofagus forest*, eds T. T. Veblen, R. S. Hill, and J. Read (New Haven, CT: Yale University Press), 83–130.
- McGlone, M. S., Moar, N. T., and Meurk, C. D. (1997). Growth and vegetation history of alpine mires on the Old Man Range, Central Otago, New Zealand. *Arc. Alp. Res.* 29, 32–44. doi: 10.2307/1551834
- McGlone, M. S., Newnham, R. M., and Moar, N. T. (2010). "The vegetation cover of New Zealand during the Last Glacial Maximum: do pollen records under-represent woody vegetation?," in *Altered Fire Ecologies: Fire, Climate and Human Influences on Terrestrial Landscapes*, eds S. Haberle, J. Stevenson, and M. Prebble (Canberra, ACT: ANU E Press), 49–68.
- McGlone, M. S., Turney, C. S. M., and Wilmshurst, J. M. (2004). Late-glacial and Holocene vegetation and climatic history of the Cass basin, central south island, New Zealand. *Quaternary Res.* 62, 267–279. doi: 10.1016/j.yqres.2004.09.003
- McGlone, M., Wardle, P., and Worthy, T. (2003). "Environmental change since the Last Glaciation," in *The Natural History of Southern New Zealand*, eds D. John, R. E. Fordyce, A. Mark, K. Probert and C. Townshend (Dunedin: Otago University Press), 105–128.
- McGlone, M., Wood, J., and Bartlein, P. J. (2012). "Environmental Change in the Temperate Forested Regions," in *The Sage Handbook of Environmental Change*, eds J. A. Matthews, P. J. Bartlein, K. R. Briffa, A. G. Dawson, A. De Vernal, T. Denham, S. C. Fritz and F. Oldfield (Los Angeles, CA: Sage), 188–214.
- McIntosh, P. D., Eden, D. N., and Burgham, S. J. (1990). Quaternary deposits and landscape evolution in northeast Southland, New Zealand. *Palaeogeogr. Palaeoclimatol. Palaeoecol.* 81, 95–113. doi: 10.1016/0031-0182(90)90042-6
- McWethy, D. B., Whitlock, C., Wilmshurst, J. M., McGlone, M. S., Fromont, M., Li, X., et al. (2010). Rapid landscape transformation in South Island, New Zealand, following initial Polynesian settlement. *Proc. Natl. Acad. Sci. U.S.A.* 107, 21343–21348. doi: 10.1073/pnas.1011801107
- Meurk, C. D. (1984). Bioclimatic zones for the antipodes-and beyond. *N. Z. J. Ecol.* 7, 175–181.
- Moar, N. (1973). Late Pleistocene vegetation and environment in southern New Zealand. *Palaeoecol. Afr. Surround. Isl. Antarct.* 8, 179–198.
- Moar, N. T. (1971). Contributions to the Quaternary history of the New Zealand flora. 6. Aranuian pollen diagrams from Canterbury, Nelson, and north Westland, South Island. *N. Z. J. Bot.* 9, 80–145. doi: 10.1080/0028825X.1971.10430172
- Moar, N. T. (1980). Late Otiran and early Aranuian grassland in central South Island. *N. Z. J. Ecol.* 3, 4–12.
- Molloy, B. P. J. (1968). "Recent history of the vegetation," in *The Natural History of Canterbury*, ed G. A. Knox (Wellington: A.H. & A.W. Reed), 340–360.
- Molloy, B. P., Burrows, C., Cox, J., Johnston, J., and Wardle, P. (1963). Distribution of subfossil forest remains, eastern South Island, New Zealand. *N. Z. J. Bot.* 1, 68–77. doi: 10.1080/0028825X.1963.10429322
- Moreno, P. I., Denton, G. H., Moreno, H., Lowell, T. V., Putnam, A. E., and Kaplan, M. R. (2015). Radiocarbon chronology of the last glacial maximum and its termination in northwestern Patagonia. *Quat. Sci. Rev.* 122, 233–249. doi: 10.1016/j.quascirev.2015.05.027
- Newnham, R. (1999). Environmental change in Northland, New Zealand during the last glacial and Holocene. *Quaternary Int.* 57–58, 61–70. doi: 10.1016/S1040-6182(98)00050-0
- Newnham, R. M. (1992). A 30,000 year pollen, vegetation and climate record from Otakairangi (Hikurangi), Northland, New Zealand. *J. Biogeogr.* 19, 541–554. doi: 10.2307/2845773
- Newnham, R. M., Alloway, B. V., Holt, K. A., Butler, K., Rees, A. B. H., Wilmshurst, J. M., et al. (2017). Last Glacial pollen-climate reconstructions from Northland, New Zealand. *J. Quaternary Sci.* 32, 685–703. doi: 10.1002/jqs.2955
- Newnham, R. M., and Lowe, D. J. (2000). Fine-resolution pollen record of late-glacial climate reversal from New Zealand. *Geology* 28, 759–762. doi: 10.1130/0091-7613(2000)28<759:FPROLC>2.0.CO;2
- Newnham, R. M., Lowe, D. J., and Green, J. D. (1989). Palynology, vegetation and climate of the Waikato lowlands, North Island, New Zealand, since c. 18,000 years ago. *J. R. Soc. N. Z.* 19, 127–150. doi: 10.1080/03036758.1989.10426443
- Newnham, R. M., Lowe, D. J., and Williams, P. W. (1999). Quaternary environmental change in New Zealand: a review. *Prog. Phys. Geogr.* 23, 567–610. doi: 10.1177/030913339902300406
- Newnham, R. M., Vandergoes, M. J., Hendy, C. H., Lowe, D. J., and Preusser, F. (2007). A terrestrial palynological record for the last two glacial cycles from southwestern New Zealand. *Quat. Sci. Rev.* 26, 517–535. doi: 10.1016/j.quascirev.2006.05.005
- Newnham, R., McGlone, M., Moar, N., Wilmshurst, J., and Vandergoes, M. (2013). The vegetation cover of New Zealand at the Last Glacial Maximum. *Quat. Sci. Rev.* 74, 202–214. doi: 10.1016/j.quascirev.2012.08.022
- Nicholls, J. (1956). The historical ecology of the indigenous forest of the Taranaki upland. *N. Z. J. For.* 7, 17–34.
- Ogden, J. (1985). An introduction to plant demography with special reference to New Zealand trees. *N. Z. J. Bot.* 23, 751–772. doi: 10.1080/0028825X.1985.10434241
- Ogden, J., and Stewart, G. H. (1995). "Community dynamics of the New Zealand conifers," in *Ecology of the Southern Conifers*, eds N. J. Enright and R. S. Hill (Melbourne, VIC: Melbourne University Press), 81–119.
- Ogden, J., Basher, L., and McGlone, M. (1998). Fire, forest regeneration and links with early human habitation: evidence from New Zealand. *Ann. Bot.* 81, 687–696. doi: 10.1006/anbo.1998.0637
- Ogden, J., Horrocks, M., Palmer, J. G., and Fordham, R. A. (1997). Structure and composition of the subalpine forest on Mount Hauhungatahi North Island, New Zealand, during the Holocene. *Holocene* 7, 13–23. doi: 10.1177/095968369700700102
- Ogden, J., Wilson, A., Hendy, C., Newnham, R. M., and Hogg, A. G. (1992). The late Quaternary history of kauri (*Agathis australis*) in New Zealand and its climatic significance. *J. Biogeogr.* 19, 611–622. doi: 10.2307/2845704
- Perry, G. L. W., Wilmshurst, J. M., and McGlone, M. S. (2014). Ecology and long-term history of fire in New Zealand. *N. Z. J. Ecol.* 38, 157–176.

- Perry, G. L. W., Wilmshurst, J. M., McGlone, M. S., Mcwethy, D. B., and Whitlock, C. (2012a). Explaining fire-driven landscape transformation during the initial burning period of New Zealand's prehistory. *Glob. Chang. Biol.* 18, 1609–1621. doi: 10.1111/j.1365-2486.2011.02631.x
- Perry, G. L. W., Wilmshurst, J. M., McGlone, M. S., and Napier, A. (2012b). Reconstructing spatial vulnerability to forest loss by fire in pre-historic New Zealand. *Glob. Ecol. Biogeogr.* 21, 1029–1041. doi: 10.1111/j.1466-8238.2011.00745.x
- Pickrill, R. A., Fenner, J. M., and McGlone, M. S. (1992). Late Quaternary evolution of a fjord environment in Preservation Inlet, New Zealand. *Quaternary Res.* 38, 331–346. doi: 10.1016/0033-5894(92)90042-H
- Pittermann, J., Stuart, S. A., Dawson, T. E., and Moreau, A. (2012). Cenozoic climate change shaped the evolutionary ecophysiology of the *Cupressaceae conifers*. *Proc. Natl. Acad. Sci. U.S.A.* 109, 9647–9652. doi: 10.1073/pnas.1114378109
- Pocknall, D. T. (1980). Modern pollen rain and Aranuian vegetation from Lady Lake, North Westland, New Zealand. *N. Z. J. Bot.* 18, 275–284. doi: 10.1080/0028825X.1980.10426925
- Pugh, J., and Shulmeister, J. (2010). "Holocene vegetation history of a high-elevation (1200 m) site in the Lake Heron Basin, inland Canterbury, New Zealand," in *Altered Ecologies: Fire, Climate and Human Influence on Terrestrial Landscapes*. *Terra Australis*, Vol. 32, eds S. Haberle, J. Stevenson, and M. Prebberle (Canberra, ACT: ANU E Press), 69–81.
- Reitalu, T., Kuneš, P., and Giesecke, T. (2014). Closing the gap between plant ecology and Quaternary palaeoecology. *J. Veget. Sci.* 25, 1188–1194. doi: 10.1111/jvs.12187
- Richardson, S. J., Allen, R. B., Whitehead, D., Carswell, F. E., Ruscoe, W. A., and Platt, K. H. (2005a). Climate and net carbon availability determine temporal patterns of seed production by *Nothofagus*. *Ecology* 86, 972–981. doi: 10.1890/04-0863
- Richardson, S. J., Hurst, J. M., Easdale, T. A., Wiser, S. K., Griffiths, A. D., and Allen, R. B. (2011). Diameter growth rates of beech (*Nothofagus*) trees around New Zealand. *N. Z. J. For.* 56, 3–11.
- Richardson, S. J., Peltzer, D. A., Allen, R. B., and McGlone, M. S. (2005b). Resorption proficiency along a chronosequence: responses among communities and within species. *Ecology* 86, 20–25. doi: 10.1890/04-0524
- Richardson, S. J., Smale, M. C., Hurst, J. M., Fitzgerald, N. B., Peltzer, D. A., Allen, R. B., et al. (2009). Large-tree growth and mortality rates in forests of the central North Island, New Zealand. *N. Z. J. Ecol.* 33, 208–215.
- Robbins, R. G. (1962). The podocarp-broadleaf forests of New Zealand. *Trans. R. Soc. N. Z. Bot.* 1, 33–75.
- Rogers, G. M., and McGlone, M. S. (1989). A postglacial vegetation history of the southern-central uplands of North Island, New Zealand. *J. R. Soc. N. Z.* 19, 229–248. doi: 10.1080/03036758.1989.10427179
- Rogers, G. M., and McGlone, M. S. (1994). A history of Kaiparoro clearing and the limits of *Nothofagus* in the northern Tararua Range, New Zealand. *N. Z. J. Bot.* 32, 463–482. doi: 10.1080/0028825X.1994.10412933
- Rogers, G. M., Walker, S., and Lee, W. G. (2005). *The Role of Disturbance in Dryland New Zealand: Past and Present*. Department of Conservation, Wellington.
- Rull, V. (2010). Ecology and palaeoecology: two approaches, one objective. *Open Ecol. J.* 3, 1–5. doi: 10.2174/1874213001003020001
- Sandiford, A., Horrocks, M., Newnham, R., Ogden, J., and Alloway, B. (2002). Environmental change during the last glacial maximum (c. 25 000–c. 16 500 years BP) at Mt Richmond, Auckland Isthmus, New Zealand. *J. R. Soc. N. Z.* 32, 155–167. doi: 10.1080/03014223.2002.9517688
- Sandiford, A., Newnham, R., Alloway, B., and Ogden, J. (2003). A 28 000–7600 cal yr BP pollen record of vegetation and climate change from Pukaki Crater, northern New Zealand. *Palaeogeogr. Palaeoclimatol. Palaeoecol.* 201, 235–247. doi: 10.1016/S0031-0182(03)00611-4
- Shulmeister, J., Goodwin, I., Renwick, J., Harle, K., Armand, L., McGlone, M. S., et al. (2004). The Southern hemisphere westerlies in the Australasian sector over the last glacial cycle: a synthesis. *Quaternary Int.* 118, 23–53. doi: 10.1016/S1040-6182(03)00129-0
- Smale, M. C., Coomes, D. A., Parfitt, R. L., Peltzer, D. A., Mason, N. W. H., and Fitzgerald, N. B. (2016). Post-volcanic forest succession on New Zealand's North Island: an appraisal from long-term plot data. *N. Z. J. Bot.* 54, 11–29. doi: 10.1080/0028825X.2015.1102747
- Sperry, J. S., Hacke, U. G., and Pittermann, J. (2006). Size and function in conifer tracheids and angiosperm vessels. *Am. J. Bot.* 93, 1490–1500. doi: 10.3732/ajb.93.10.1490
- Steward, G. A., and Beveridge, A. E. (2010). A review of New Zealand kauri (*Agathis australis* (D. Don) Lindl.): its ecology, history, growth and potential for management for timber. *N. Z. J. For. Sci.* 40, 33–59.
- Tomio, S., Harsch, M. A., Duncan, R. P., and Hulme, P. E. (2016). Influence of climate and regeneration microsites on *Pinus contorta* invasion into an alpine ecosystem in New Zealand. *Aims Environ. Sci.* 3, 525–540. doi: 10.3934/envirosci.2016.3.525
- Turney, C., Wilmshurst, J., Jones, R., Wood, J., Palmer, J., Hogg, A., et al. (2017). Reconstructing atmospheric circulation over southern New Zealand: establishment of modern westerly airflow 5,500 years ago and implications for Southern Hemisphere Holocene climate change. *Quat. Sci. Rev.* 159, 77–87. doi: 10.1016/j.quascirev.2016.12.017
- Vandergoes, M. J., Fitzsimons, S. J., and Newnham, R. M. (1997). Late glacial to Holocene vegetation and climate change in the eastern Takitimu Mountains, western Southland, New Zealand. *J. R. Soc. N. Z.* 27, 53–66. doi: 10.1080/03014223.1997.9517527
- Vandergoes, M. J., Newnham, R. M., Preusser, F., Hendy, C. H., Lowell, T. V., Fitzsimons, S. J., et al. (2005). Regional insolation forcing of late Quaternary climate change in the Southern Hemisphere. *Nature* 436, 242–245. doi: 10.1038/nature03826
- Veblen, T. T., and Stewart, G. H. (1982). On the conifer regeneration gap in New Zealand—the dynamics of *Libocedrus bidwillii* stands on South Island. *J. Ecol.* 70, 413–436.
- Walker, S., King, N., Monks, A., Williams, S., Burrows, L., Cieraad, E., et al. (2009). Secondary woody vegetation patterns in New Zealand's South Island dryland zone. *N. Z. J. Bot.* 47, 367–393. doi: 10.1080/0028825x.2009.9672713
- Walker, S., Lee, W. G., and Rogers, G. M. (2004a). Pre-settlement woody vegetation of Central Otago, New Zealand. *N. Z. J. Bot.* 42, 613–646. doi: 10.1080/0028825X.2004.9512915
- Walker, S., Lee, W. G., and Rogers, G. M. (2004b). The woody vegetation of Central Otago, New Zealand. *N. Z. J. Bot.* 42, 589–612. doi: 10.1080/0028825X.2004.9512914
- Wardle, J. A. (1984). *The New Zealand Beeches: Ecology, Utilization and Management*. Wellington: New Zealand Forest Service.
- Wardle, J. A. (2011). *Wardle's Native Trees of New Zealand and Their Story*. Wellington: New Zealand Farm Forestry Association.
- Wardle, P. (1963). The Regeneration gap of New Zealand gymnosperms. *N. Z. J. Bot.* 1, 301–315. doi: 10.1080/0028825X.1963.10429001
- Wardle, P. (1985). New Zealand timberlines. 2. A study of forest limits in the Crow Valley near Arthur's Pass, Canterbury. *N. Z. J. Bot.* 23, 235–261. doi: 10.1080/0028825X.1985.10425329
- Wardle, P. (1991). *Vegetation of New Zealand*. Cambridge: Cambridge University Press.
- Wardle, P. (2001a). Distribution of native forest in the upper Clutha district, Otago, New Zealand. *N. Z. J. Bot.* 39, 435–446. doi: 10.1080/0028825X.2001.9512747
- Wardle, P. (2001b). Holocene forest fires in the upper Clutha district, Otago, New Zealand. *N. Z. J. Bot.* 39, 523–542. doi: 10.1080/0028825X.2001.9512755
- Wardle, P., and Lee, W. G. (1990). Environmental and floristic gradients in Westland, New Zealand, and the discontinuous distribution of *Nothofagus*-comment. *N. Z. J. Bot.* 28, 479–481. doi: 10.1080/0028825X.1990.10412333
- Whitehead, D., Barbour, M. M., Griffin, K. L., Turnbull, M. H., and Tissue, D. T. (2011). Effects of leaf age and tree size on stomatal and mesophyll limitations to photosynthesis in mountain beech (*Nothofagus solandrii* var. *cliffortioides*). *Tree Physiol.* 31, 985–996. doi: 10.1093/treephys/tpq021
- Willett, R. (1950). The New Zealand Pleistocene snow line, climatic conditions, and suggested biological effects. *N. Z. J. Sci. Technol.* 32, 18–48.
- Wilmshurst, J. M., and McGlone, M. S. (1996). Forest disturbance in the central North Island, New Zealand, following the 1850 BP Taupo eruption. *Holocene* 6, 399–411. doi: 10.1177/095968369600600402
- Wilmshurst, J. M., McGlone, M. S., and Charman, D. J. (2002). Holocene vegetation and climate change in southern New Zealand: linkages between forest composition and quantitative surface moisture reconstructions from an ombrogenous bog. *J. Quaternary Sci.* 17, 653–666. doi: 10.1002/jqs.689

- Wilmshurst, J. M., Moar, N. T., Wood, J. R., Bellingham, P. J., Findlater, A. M., Robinson, J. J., et al. (2014). Use of Pollen and Ancient DNA as Conservation Baselines for Offshore Islands in New Zealand. *Conserv. Biol.* 28, 202–212. doi: 10.1111/cobi.12150
- Woodward, C., Shulmeister, J., Zawadzki, A., and Jacobsen, G. (2014). Major disturbance to aquatic ecosystems in the South Island, New Zealand, following human settlement in the Late Holocene. *Holocene* 24, 668–678. doi: 10.1177/0959683614526935
- Wright, I. C., McGlone, M. S., Nelson, C. S., and Pillans, B. J. (1995). An integrated latest Quaternary (Stage 3 to present) paleoclimatic and paleoceanographic record from offshore northern New Zealand. *Quaternary Res.* 44, 283–293. doi: 10.1006/qres.1995.1073
- Yang, Z. Y., Ran, J. H., and Wang, X. Q. (2012). Three genome-based phylogeny of Cupressaceae s.l.: further evidence for the evolution of gymnosperms and Southern Hemisphere biogeography. *Mol. Phylogenet. Evol.* 64, 452–470. doi: 10.1016/j.ympev.2012.05.004
- Conflict of Interest Statement:** The authors declare that the research was conducted in the absence of any commercial or financial relationships that could be construed as a potential conflict of interest.
- Copyright © 2017 McGlone, Richardson, Burge, Perry and Wilmshurst. This is an open-access article distributed under the terms of the Creative Commons Attribution License (CC BY). The use, distribution or reproduction in other forums is permitted, provided the original author(s) or licensor are credited and that the original publication in this journal is cited, in accordance with accepted academic practice. No use, distribution or reproduction is permitted which does not comply with these terms.



European Forest Cover During the Past 12,000 Years: A Palynological Reconstruction Based on Modern Analogs and Remote Sensing

Marco Zanon^{1,2*}, Basil A. S. Davis³, Laurent Marquer^{4,5,6}, Simon Brewer⁷ and Jed O. Kaplan^{8,9}

¹ Institute of Pre- and Protohistoric Archaeology, Christian-Albrechts-Universität zu Kiel, Kiel, Germany, ² Graduate School "Human Development in Landscapes", Christian-Albrechts-Universität zu Kiel, Kiel, Germany, ³ Institute of Earth Surface Dynamics, University of Lausanne, Lausanne, Switzerland, ⁴ Department of Physical Geography and Ecosystem Science, Lund University, Lund, Sweden, ⁵ GEODE, UMR-CNRS 5602, Université de Toulouse-Jean Jaurès, Toulouse, France, ⁶ Research Group for Terrestrial Palaeoclimates, Max Planck Institute for Chemistry, Mainz, Germany, ⁷ Department of Geography, University of Utah, Salt Lake City, UT, United States, ⁸ ARVE Research SARL, Pully, Switzerland, ⁹ Department of Archaeology, Max Planck Institute for the Science of Human History, Jena, Germany

OPEN ACCESS

Edited by:

Thomas Giesecke,
University of Göttingen, Germany

Reviewed by:

Martin Theuerkauf,
University of Greifswald, Germany
Pavel Tarasov,
Freie Universität Berlin, Germany

*Correspondence:

Marco Zanon
mzanon@gshdl.uni-kiel.de

Specialty section:

This article was submitted to
Agroecology and Land Use Systems,
a section of the journal
Frontiers in Plant Science

Received: 17 November 2017

Accepted: 12 February 2018

Published: 08 March 2018

Citation:

Zanon M, Davis BAS, Marquer L,
Brewer S and Kaplan JO (2018)
European Forest Cover During
the Past 12,000 Years:
A Palynological Reconstruction Based
on Modern Analogs and Remote
Sensing. *Front. Plant Sci.* 9:253.
doi: 10.3389/fpls.2018.00253

Characterization of land cover change in the past is fundamental to understand the evolution and present state of the Earth system, the amount of carbon and nutrient stocks in terrestrial ecosystems, and the role played by land-atmosphere interactions in influencing climate. The estimation of land cover changes using palynology is a mature field, as thousands of sites in Europe have been investigated over the last century. Nonetheless, a quantitative land cover reconstruction at a continental scale has been largely missing. Here, we present a series of maps detailing the evolution of European forest cover during last 12,000 years. Our reconstructions are based on the Modern Analog Technique (MAT): a calibration dataset is built by coupling modern pollen samples with the corresponding satellite-based forest-cover data. Fossil reconstructions are then performed by assigning to every fossil sample the average forest cover of its closest modern analogs. The occurrence of fossil pollen assemblages with no counterparts in modern vegetation represents a known limit of analog-based methods. To lessen the influence of no-analog situations, pollen taxa were converted into plant functional types prior to running the MAT algorithm. We then interpolate site-specific reconstructions for each timeslice using a four-dimensional gridding procedure to create continuous gridded maps at a continental scale. The performance of the MAT is compared against methodologically independent forest-cover reconstructions produced using the REVEALS method. MAT and REVEALS estimates are most of the time in good agreement at a trend level, yet MAT regularly underestimates the occurrence of densely forested situations, requiring the application of a bias correction procedure. The calibrated MAT-based maps draw a coherent picture of the establishment of forests in Europe in the Early Holocene with the greatest forest-cover fractions reconstructed between ~8,500 and 6,000 calibrated years BP. This forest maximum is followed by

a general decline in all parts of the continent, likely as a result of anthropogenic deforestation. The continuous spatial and temporal nature of our reconstruction, its continental coverage, and gridded format make it suitable for climate, hydrological, and biogeochemical modeling, among other uses.

Keywords: Modern Analog Technique, forest cover, pollen data, remote sensing, Europe, Younger Dryas, Holocene

INTRODUCTION

Determining the spatial structure of land cover and its variation through time is essential in order to understand the interplay between biosphere, atmosphere, and human societies. Knowledge of past vegetation dynamics is of great interest to a range of disciplines dealing with landscape, climate, human development, and their reciprocal interactions. For example, information concerning past forest cover influences the archeological narrative (e.g., Kreuz, 2007) and plays a tangible role in defining modern management strategies (Vera, 2000; Mitchell, 2005; Bradshaw et al., 2015); vegetation cover data are a central component of Earth system models dealing with carbon storage and release (e.g., Kaplan et al., 2002) and for investigating the feedbacks between land cover and climate (Gaillard et al., 2010); similarly, the simulation of past human–plants interactions is needed for the understanding of human imprint on ecosystems from early history up to the present day (Pongratz et al., 2008; Kaplan et al., 2009).

Recent landscape history makes use of different mapping technologies, ranging from historical and cartographic sources (e.g., Hohensinner et al., 2013) to satellite imagery (Bossard et al., 2000; DeFries et al., 2000; Hansen et al., 2013). Beyond the reach of these mapping means, our ability to infer past land cover depends on the interpretation of paleoenvironmental proxies. Past landscape information has been extracted from different archives, such as fossil pollen (e.g., Edwards et al., 2017), plant macrofossils (e.g., tree line studies; Nicolussi et al., 2005), mollusks (e.g., Preece et al., 1986), beetles (e.g., Whitehouse and Smith, 2004), biochemical tracers (e.g., McDuffee et al., 2004) and ancient DNA (Birks and Birks, 2016). Among the diverse sources available, each offering a different point of view on similar questions, the analysis of pollen grains remains unsurpassed in terms of spatial and temporal coverage. The simplest approach in palynology consists of using arboreal versus non-arboreal pollen percentages to estimate forest cover, and in using indicator species (e.g., Behre, 1981) to infer changes in land use. The growing availability of pollen archives at a continental scale has then made it possible to track species expansion/extinction based on isolines and threshold values (e.g., Huntley and Birks, 1983; Brewer et al., 2002, 2016; Ravazzi, 2002; Finsinger et al., 2006). These approaches can be qualified as purely qualitative, as the non-linear relationship between plant abundances and pollen percentages is acknowledged but not corrected for (Gaillard et al., 2008).

Semi-quantitative models have been developed by grouping individual taxa into plant functional types (PFTs) and biomes (Prentice et al., 1996; Peyron et al., 1998), thus providing a consistent methodology to distinguish major vegetation types.

The biomisation approach is able to recognize boundaries between plant communities (Williams et al., 2000), although difficulties have emerged at ecotones such as the forest–steppe boundary due to a bias in the method toward arboreal taxa. This bias arose from the original objective of the method to replicate potential natural vegetation (Peyron et al., 1998; Tarasov et al., 1998), and therefore to minimize the role of non-arboreal taxa symptomatic of anthropogenically deforested landscapes. A further problem has been the categorical nature of the biome assignment, leading to difficulties in recognizing gradual ecotonal transitions and producing spatially continuous reconstructions. Often the results have been mapped as point estimates (e.g., Prentice et al., 2000). Continuous spatial fields have been attempted using different techniques, such as in Peng et al. (1995), Collins et al. (2012), and Fyfe et al. (2015). While biomes are distinguished into forest and non-forest types, Collins et al. (2012) also used forest and non-forest PFTs derived from the same biomisation formulae as a more continuous measure of forest cover.

A first attempt to achieve a real quantification was pioneered by Prentice and Parsons (1983), Prentice (1985), and Sugita (1993, 1994), gradually evolving into the Landscape Reconstruction Algorithm (LRA). The LRA models – these are REVEALS for regional plant abundance and LOVE for local plant abundance (Sugita, 2007a,b) – make use of a comprehensive set of parameters (region-specific pollen productivity estimates, fall speed of pollen, basin size) and assumptions (e.g., wind speed and direction, atmospheric conditions) to simulate pollen dispersal/deposition mechanisms and decrease biases deriving from the non-linear relationships between plant abundances and pollen data.

Pollen-based vegetation reconstructions produced with the LRA are currently available for most of Europe outside of the Mediterranean (e.g., Nielsen and Odgaard, 2010; Sugita et al., 2010; Nielsen et al., 2012; Cui et al., 2013, 2014; Fyfe et al., 2013; Overballe-Petersen et al., 2013; Marquer et al., 2014, 2017; Mazier et al., 2015; Trondman et al., 2015). A wider application of the method to the Mediterranean depends on the collection of reliable pollen productivity estimates for the region, which are not currently available. A different quantitative approach, not requiring pollen productivity estimates demanded by the LRA method, was developed and applied in North America by Williams (2002) and Williams and Jackson (2003). This approach uses instead the Modern Analog Technique (MAT), based on the basic assumption that pollen samples sharing a similar composition are the by-product of comparable vegetation assemblages. Therefore, given two pollen samples – a modern and a fossil one – composed by a similar mixture of taxa, the environmental parameters of the first (e.g., forest cover,

climate variables) can be directly transferred to the latter. The relationship between pollen assemblages and forest cover in the Williams method is established using a calibration dataset of modern pollen samples where the forest cover around the pollen site is estimated using satellite remote sensing from the Advanced Very High-Resolution Radiometer (AVHRR). Past forest cover is then reconstructed by assigning to each fossil sample the average forest cover of its closest modern analogs from amongst the modern samples in the calibration dataset. This approach was applied to Northern Eurasia (Tarasov et al., 2007; Kleinen et al., 2011) and to the whole forest-tundra ecotone of the Northern Hemisphere (Williams et al., 2011). Its application in Europe has been so far limited to point reconstructions for a few selected time windows (Williams et al., 2011).

In the present study, we test the capabilities of the MAT for continuous forest-cover reconstructions at a continental scale and from the Pleistocene/Holocene transition to the present day. We follow the methods used by Tarasov et al. (2007) and Williams et al. (2011) but with improved modern calibration and fossil datasets and spatially continuous mapping. The size of modern and fossil pollen data sets have been increased by 80 and 50%, respectively, compared to the European data used by Williams et al. (2011), while the quality of the metadata and chronological controls for the fossil data have also been greatly improved (Fyfe et al., 2009; Davis et al., 2013; Giesecke et al., 2013). The AVHRR-based forest-cover data (1 km resolution) used in all previous MAT applications has been upgraded with a 30-m resolution dataset (Hansen et al., 2013) based on LANDSAT.

Our results are presented here as both maps for the whole of Europe at 1,000-year intervals, and as regional area-average time-series. The full set of 49 maps, each one covering an ~250-year interval, is available as Supplementary Material. Each map displays interpolated forest-cover data with continental coverage at a resolution of five arc-minutes. The predictive ability of our model was assessed through standard statistical indicators based on analysis of the modern training set [r^2 and Root Mean Square Error of Prediction (RMSEP) from cross-validation exercises]. In addition, down core evaluation was also undertaken through a comparison between the MAT and the REVEALS-based forest-cover reconstructions for specific sites, thus testing the performance of our method against methodologically independent forest-cover reconstructions.

MATERIALS AND METHODS

Fossil and Modern Pollen Data

The fossil pollen dataset used in our analysis is the same as presented in Mauri et al. (2015) and based largely on the European Pollen Database (EPD) with some additional data coming from the PANGAEA data archive¹ and Collins et al. (2012) (Supplementary Figure S1). All age-depth models for all sites used calibrated ¹⁴C chronologies, with those for EPD sites based on the latest available chronologies from Giesecke et al. (2013).

¹www.pangaea.de

The European Modern Pollen Database (EMPD; Davis et al., 2013) was selected as the source for modern palynological data (Supplementary Figure S2). The EMPD includes nearly 5,000 samples covering Eurasia and the circum-Mediterranean, which were filtered based on quality-control criteria (see section “Quality Filtering”).

Pollen spectra in both the modern and fossil datasets were converted into PFTs following the approach developed by Prentice et al. (1996) and refined by Peyron et al. (1998). Pollen taxa are grouped into PFTs following combinations of plant habit (e.g., woody, herbaceous), phenology (e.g., evergreen, deciduous), leaf form (e.g., broad-leaved, needle-leaved), and climatic range (Prentice, 1985). Differential pollen productivity and dispersal are not accounted for during PFT assignment. The main steps within the taxa-to-PFTs algorithm are presented in Supplementary Tables S1–S3. The full procedure is described in Peyron et al. (1998). The capabilities of PFTs in pollen-based climatic and ecological reconstructions have been tested in European contexts through the Holocene (Collins et al., 2012; Davis et al., 2015; Mauri et al., 2015), and were found preferable to taxa approaches in MAT-based climate reconstructions (Davis et al., 2003).

Remote Sensing Data

Modern forest-cover values were extracted from the Global Forest Change dataset (Hansen et al., 2013), which includes estimates of forest-cover fraction for the year 2000. The forest-cover dataset produced by Hansen et al. (2013) was preferred over the AVHRR-based maps from DeFries et al. (2000) used in previous studies (Tarasov et al., 2007; Williams et al., 2011). While DeFries et al. (2000) offer a wider range of maps covering different vegetation categories, the dataset from Hansen et al. (2013) offers a much higher resolution and a wider range of values. DeFries et al. (2000) provide separate quantitative data on broadleaf, deciduous, evergreen, needle leaf, and total forest cover at a resolution of 1-km. Pixel values are continuous in the range 10–80% of forest cover (woody fraction), with specific codes to mark non-vegetated areas and areas with forest cover lower than 10%. In contrast, Hansen et al. (2013) offer a resolution of 1 arcsecond, equivalent to around 30-m at the equator, and a full range of pixel values from 0 to 100% canopy closure.

The average forest-cover values for the modern pollen data set were extracted by placing a search window around the location of each sample. We applied a general search radius of 50 km to approach a more consistent comparison between MAT and REVEALS estimates, because the REVEALS method suggests that its reconstructions are representative of a 50-km radius around the sites in question (see section “Comparison between MAT and REVEALS Estimates of Past forest cover”). A circular search window was preferred over a square one (used, e.g., in Williams et al., 2011), thus assuming a pollen source area with equal contributions from vegetation from all directions. The forest-cover value of every grid cell falling within the search radius was then distance-weighted using a two-dimensional Gaussian function centered on the pollen sample and subsequently averaged. A Gaussian curve was preferred primarily due to ease of implementation. Future model versions

might include more “fat-tailed” distributions (e.g., Dawson et al., 2016). Given the predominance of moss polsters and soil samples in the EMPD, a value of $\sigma = 500$ m was used in order to assign a prevalent weight to the circular region immediately closer to the sample site (Supplementary Figure S3). A smaller σ value (100 m) was applied only to samples collected in densely forested areas (forest cover > 40% and EMPD sampling context described as “dense forest” or “forest undefined”). In these cases, the 100 m value was preferred over the 500 m one only when it yielded higher forest-cover values, suggesting the presence of denser forests right at the sampling location. A higher distance–weight parameter ($\sigma = 10$ km) was applied to samples collected from lakes in order to simulate a wider pollen source area. This σ -value is drawn from the optimal search window half-widths tested in previous studies (Williams and Jackson, 2003; Tarasov et al., 2007; Williams et al., 2011). Similarly to the procedure applied to moss and soil samples, a smaller σ -value (500 m) was applied to small water bodies (surface < 20 ha) surrounded by forested landscapes in order to emphasize the contribution of perilacustrine arboreal vegetation (Matthias and Giesecke, 2014). Since pixels occupied by water bodies were not included in the averaging procedure, weight is automatically added to the outer regions of the search window as both lake size and the number of pixels containing water around the core site increase. Bog sites therefore have the maximum weighting close to the core site. With lakes, the weight given to more distant pixels naturally increases as lake size increases and more pixels containing just water are excluded.

It should be stressed that pollen dispersal mechanisms vary largely from site to site depending on multiple factors (e.g., vegetation density, wind speed, pollen grains size and density, topography). Computational constraints, the wide diversity of the EMPD samples and, above all, the current availability of metadata prevent the calculation of sample-specific search windows and weight factors within this study. The application of narrow distance-weighting parameters (100 m and 500 m) was prompted by empirical and simulation studies on pollen deposition dynamics (e.g., Wright, 1952; Tinsley and Smith, 1974; Lavigne et al., 1996). Local foliage – as an example – might disrupt pollen dispersal, either by acting as a simple physical obstacle (Prentice, 1985) or via electrostatic capture (Bowker and Crenshaw, 2007), causing large amounts of pollen to reach the ground within few meters of the source. Sugita (1994) and Calcote (1995) estimate that between 20 and 60% of the pollen load in forest hollows comes from within a radius of < 100 m. Genetic analysis on plant communities appear to reach similar conclusions despite radically different methodological approaches. DNA paternity tests on *Pinus sylvestris* populations show that as much as ~50% of the pollen reaching female cones may come from individuals located within a 10 m radius, and that more than 90% of the pollen-carried genetic material may come from within a radius of ~200 m (Robledo-Arnuncio and Gil, 2005). When small *Quercus* sp. stands are considered (ca. ≤ 6 ha, equivalent – for comparative purposes – to a circular region with $r = \sim 140$ m), between ~30 and >80% of successful pollinations were ascribed to pollen coming from within the stand (Streiff et al., 1999; Gerber et al., 2014; Moracho et al., 2016). Surface pollen samples might therefore primarily record

a signal from local/extra-local pollen sources (e.g., few dozens to several hundred meters, *sensu* Jacobson and Bradshaw, 1981). In the context of our study, a σ -value = 500 m is meant to stress the importance of nearby pollen sources, while a 100-m value points to a dominant contribution from local dense arboreal cover. Arguably, the LRA could be used to estimate the pollen contribution from vegetation at any given distance from a sample. This effort would at the very least require pollen productivity estimates for all taxa and regions involved in the present study, which are currently not available. As a consequence, the use of only three σ values (100 m, 500 m, and 10 km) represents a necessary simplification.

Definition of Forest Cover

Study-specific definitions of forest cover should be kept in mind when interpreting and comparing the results from different quantitative approaches. REVEALS-based estimates of forest cover correspond to the overall regional tree abundance expressed in relative percentage cover. Age and size of trees are not assumed to be critical factors influencing the results, although they can have an influence on pollen productivity estimates and pollen dispersal and deposition (Jackson, 1994; Matthias et al., 2012; Baker et al., 2016). Analog-based approaches draw their definition of forest from their respective land cover data sets. Hansen et al. (2013) use a definition comparable to DeFries et al. (2000), describing forest-cover values per pixel as canopy closure percentages for all vegetation taller than 5 m. Significantly, DeFries et al. (2000) point out that a satellite-based mapping approach might identify shrubs as herbaceous vegetation if they are low to the ground, and as woody vegetation if they are taller. In an attempt to address this potential issue, we combined global vegetation height data (Simard et al., 2011) with the CORINE data set (Büttner et al., 2014) in order to detect areas occupied by forests but with a dominant tree height lower than 5 m. Modern samples with a median tree height = 0 m within the area covered by 1σ of the distance–weight function (i.e., the area surrounding the samples that contributes the most to tree cover quantification) were excluded from the analog pool. This filter was applied only to areas covered by the CORINE data set and only to lacustrine samples. The rationale behind the latter discrimination lies in our decision to prioritize the exclusion of easily discernible low-quality samples while at the same time limiting the occurrence of false positives. In this specific case, the relatively coarse resolution of the tree-height data set (1 km), prompted us to apply a tree-height filter only to samples with $\sigma = 10$ km.

Quality Filtering

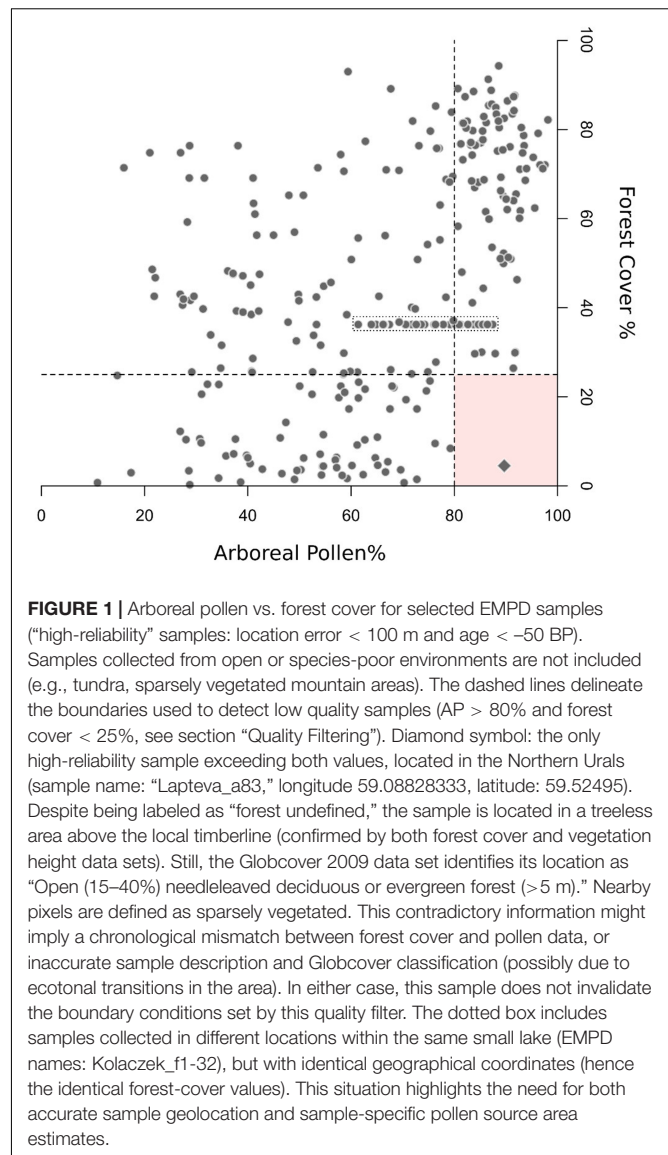
The available EMPD metadata were used extensively in conjunction with additional land cover data sets in order to identify pairing inaccuracies between pollen samples and the related vegetation data (e.g., due to location or chronology errors, see section “Sources of Uncertainty”) through multiple lines of evidence. After duplicate removal, samples with estimated geolocation errors higher than 100 m were excluded from further elaborations. An additional reliability check was performed by comparing the elevation of each sample as recorded in the EMPD with the elevation for the same latitude and longitude

extracted from a high-resolution Digital Elevation Model. Control elevation values were obtained from Mapzen's Elevation Service², accessed through the R package "elevatr" (Hollister and Shah, 2017). Any difference greater than 200 m resulted in the exclusion of the sample. Samples from riverine or estuarine contexts were excluded too due to the likely presence of pollen floated over long distances. Samples were also filtered to remove those with low pollen counts, retaining only samples with a total sum of terrestrial taxa greater than 100 pollen grains. The Globcover 2009 data set (Arino et al., 2008) was used in addition to the already-mentioned tree height and forest-cover data sets. Samples collected in open landscapes (e.g., sampling context identified as "treeless vegetation," "pasture") but falling in forested Globcover classes and having simultaneously more than 15% forest cover (Globcover lower limit for open forests) and median tree height > 0 were excluded from the analog pool. Similarly, samples collected in forested environments (e.g., "open forest," "closed forest") but falling within open Globcover classes and having at the same time forest cover < 15% and median tree height = 0 were excluded from the training set too. The high-reliability samples (estimated geolocation error < 100 m and estimated age < -50 BP; **Figure 1**) in the filtered EMPD were then used to find potential inaccuracies in surface samples with insufficient metadata. Any sample with arboreal pollen > 80% associated to forest-cover values < 25% was considered as potentially carrying low-quality information and excluded from the model. Beside geolocation and chronological inaccuracies, this filter addresses also samples collected under isolated trees, or in small thickets not detectable by the forest-cover data set. These threshold values are drawn from **Figure 1** and find support in the available literature. As an example, in open or semi-open contexts such as alpine meadows or arid shrublands, AP values are in the range of 40–50% (e.g., Davies and Fall, 2001; Court-Picon et al., 2006). Even above the tree line, in contexts affected by long-distance pollen transport, rare is the case where AP percentages reach values above 80% (e.g., Cañellas-Boltà et al., 2009). Nonetheless, given the common occurrence of long-distance airborne AP in species-poor environments (e.g., Pardoe, 2014), samples collected in extensive treeless contexts (e.g., tundra, alpine grasslands, deserts) are not included in **Figure 1** and are not affected by this filter. A comparable filter was not applied to situations with low AP and high forest cover values due to difficulties in identifying equally distinctive boundaries. See the discussion for additional considerations on data selection.

The filtering process led to the removal of ~52% of the EMPD content, resulting in 2,526 usable samples (Supplementary Figure S2). Of these, 211 samples were distance-weighted using a σ -value = 100 m, 1,894 samples using a σ -value = 500 m, and 421 samples using a σ -value = 10 km.

Past Forest-Cover Reconstruction

Forest-cover reconstructions are based on the MAT (Overpeck et al., 1985; Guiot, 1990; Jackson and Williams, 2004). The basic assumption behind the MAT is that pollen samples sharing similar combinations of taxa originate from comparable plant



assemblages. The vegetation parameters of a modern pollen sample can therefore be transferred to any fossil sample sharing a similar palynological composition. In order to define how different two samples are, the floristic assemblages of both the fossil and the training sample are reduced to a single coefficient of dissimilarity. Squared-chord distance was selected as the dissimilarity index of choice because of its ability to differentiate between vegetation types (Overpeck et al., 1985; Gavin et al., 2003). Analog computations were performed using the R package 'rioja' (Juggins, 2016). The optimal maximum number of analogs, $k = 8$, was determined via leave-one-out (LOO) cross-validation. Reconstructed forest-cover percentages were then recalculated as the weighted average of the forest-cover values of the best analogs whose chord distance did not exceed a threshold T . The value of T is not straightforward to define since it is data dependent (Davis et al., 2015). We opted for a value of $T = 0.3$, as it has proved sufficient to

²www.mapzen.com

discriminate between major vegetation assemblages in Europe (Huntley, 1990).

The fossil dataset was divided into 49 timeslices ranging from 12,000 to 0 calibrated years BP (years before AD 1950; hereafter BP). Each timeslice covers a 250-year window with the exception of the most recent one, which is asymmetric as it cannot project into the future, and therefore covers an interval of 185 years centered on 0 BP.

Mapping Procedure

The reconstructed forest covers from each pollen record (i.e., point estimates) within each timeslice have been interpolated onto a uniform spatial and temporal grid using a four-dimensional (longitude, latitude, elevation, and time) Thin Plate Spline algorithm (TPS) fitted to a Digital Elevation Model (five arc-minutes resolution) using the R package ‘fields’ (Furrer et al., 2013). A three-dimensional TPS (latitude, longitude, elevation) was applied to the 0 BP timeslice in order to limit skewed results due to its unbalanced sample distribution around the 0 BP mark. This follows the same procedure used in mapping Holocene climate and vegetation used by Davis et al. (2003), Collins et al. (2012), and Mauri et al. (2015).

The maps of forest cover also include changes in European coastlines and ice sheets throughout the Holocene following Mauri et al. (2015). Small inland bodies of water are ignored in the reconstructed maps. Areas with low site/sample density over several time-windows have been excluded from our reconstruction, a process that was also used to define the borders of the study region. The results for some marginal areas (i.e., western North Africa and the eastern portion of the study area) are included but are not addressed in the paper, which focuses on the data-rich area of Europe north of the Mediterranean and west of 44°E.

To provide a comparison with traditional approaches based on the interpretation of arboreal pollen (AP) percentages, we also applied the same interpolation procedure to AP values (sum of woody taxa percentages, excluding dwarf shrubs and vines) for every fossil timeslice. The complete series of 49 forest-cover maps and 49 AP maps is included in the Supplementary Materials (Supplementary Figures S4, S5). All maps were produced using GMT 4.5.15 (Wessel et al., 2013).

Forest-cover error estimates were calculated for each timeslice by interpolating the standard error of the analog-based reconstruction for every fossil sample. The standard error itself was calculated as the standard deviation of the n best analogs (after applying the chord threshold) divided by the square root of n . This first interpolated error estimate was then added to the standard error generated by the interpolation process itself (Furrer et al., 2013; Mauri et al., 2015). For computational reasons, error estimates are provided in gridded form at a resolution of 1° (Supplementary Figure S6). Additional errors deriving from non-quantifiable uncertainties within data sources (see section “Sources of Uncertainty”) or from methodological limits (e.g., use of PFTs, lack of distinction between species-specific pollen productivity/dispersal; see section “No-Analog Situations and the PFT Approach”) can’t be quantified with the available data or technical knowledge. Therefore, these

error sources are not accounted for in the calculation of error estimates.

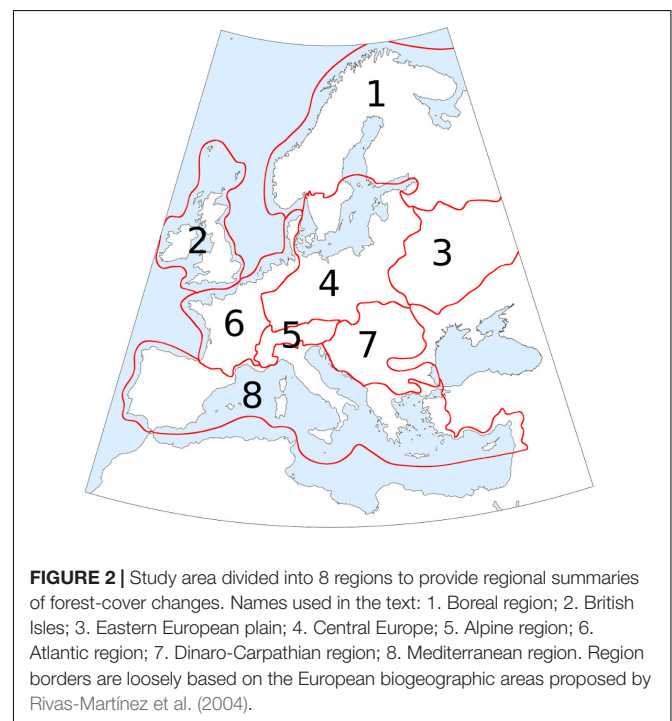
In order to provide regional summaries of forest cover and AP changes, the study area was divided into eight regions (Figure 2) and area-average estimates of forest cover were calculated for each region based on the gridded maps. The region borders are loosely based on the European biogeographic areas proposed by Rivas-Martínez et al. (2004). The area-average estimates of forest cover and AP percentages were then summarized in the form of time-series graphs covering the whole set of 49 time-slices.

Evaluation of the Reconstruction Method

Performance of the Transfer Function and Interpolation Using Modern Data

The ability of MAT to reconstruct forest cover for the present time was first assessed using a two-fold cross-validation exercise. The modern pollen dataset was randomly split into two separate sets of equal size, subsequently using one as a training dataset to reconstruct the forest cover of the other and *vice-versa*. The whole process was repeated 999 times. The resulting r^2 , RMSEP, plus a simple reading of the residuals, were used to assess the basic performance of the method. The RMSEP has the same unit as the environmental variable, and is therefore expressed as percentages of forest cover.

An h-block cross-validation test (Telford and Birks, 2009) was not performed. With the h-block test, all samples within a distance h of a test sample are omitted from analog selection. This test is generally applied to climate reconstructions, in order to exclude or mitigate the effects of spatial autocorrelation in the training set. The European land cover is much less uniform than the European climate, being instead characterized by high



fragmentation and spatial diversity even over short distances (Palmieri et al., 2011; Kallimanis and Koutsias, 2013). Due to the high spatial variability of pollen spectra/parent vegetation pairings, the h-block test might not represent an optimal solution for land cover reconstructions.

Additionally, we tested the joint ability of MAT and interpolation algorithms to reproduce the modern forest-cover patterns visible in Hansen et al. (2013). For this purpose, modern forest-cover values were reconstructed under less restrictive conditions via simple LOO cross validation. LOO-derived modern forest-cover values were then interpolated using the procedure described in Section “Mapping Procedure.” The same procedure was applied to AP percentages derived from the EMPD.

Reconstruction of Holocene Forest Cover in the Alps

The Alpine region provides an excellent context to test the performance of the 4-D interpolation due to its high topographic variability, the abundance of fossil pollen archives, and the numerous studies concerning local tree line and timberline dynamics. Therefore, as an additional test, we compared the MAT-based forest-cover values reconstructed at different elevations in the Alpine region with the data from Hansen et al. (2013) for the present and with independent macrofossil-based timberline/treeline reconstructions for the Holocene. To achieve this result, we grouped all the pixels (grid cells) falling within the Alpine region (n. 5 in **Figure 2**) into 200-vertical-meter elevation bands, except for those below 400 m which were grouped into a single band. This process was repeated for each of the 49 paleo-timeslices, as well as for the present day using both the LOO-based reconstruction and the map from Hansen et al. (2013).

As with the maps, areas with low site/sample density were excluded from the analysis. A lack of pollen sites at the very highest altitudes meant that for this test the analysis was limited to below 2,800 m throughout the Holocene, with a slightly lower limit of 2,400 m before 11,000 BP and 2,600 m from 10,000 to 11,000 BP when there were fewer sites above those altitudes.

A basic definition of “forest” in alpine contexts includes a minimum canopy cover above 40% (e.g., Burga and Perret, 2001) or 50–60% (Szerencsits, 2012). We adopt an intermediate threshold, following the upper altitudinal boundary of forest cover values >50% in our reconstruction. We interpret this minimum value as an indicator of widespread forested environments across the whole region, and use it as a simplistic threshold to track forest behavior in our reconstructions around the timberline ecotone (maximum vertical extent of alpine forests).

Comparison Between MAT and REVEALS Estimates of Past Forest Cover

Forest-cover reconstructions based on MAT have been evaluated against methodologically independent REVEALS reconstructions for selected fossil pollen records (five large lakes, >50 ha surface) in central and northern Europe. The REVEALS model (Sugita, 2007a) provides pollen-based estimates of regional plant abundances for 25 taxa (trees,

shrubs, and herbs) in percentage cover and associated standard errors. Note that REVEALS estimates inferred from large lakes give the most reliable reconstructions of regional plant abundance (Trondman et al., 2015; Marquer et al., 2017).

We used five REVEALS target sites published in Marquer et al. (2014) for the method-independent evaluation of the MAT-based forest-cover reconstructions. These five pollen records were selected because the data was publicly available from EPD, and because the sites are all located in central and northern Europe, where pollen-productivity estimates are available to run REVEALS for the major pollen taxa (Broström et al., 2008; Mazier et al., 2012). For further details about the pollen records, see Marquer et al. (2014).

Several tests have been done to decrease the 500-year time intervals of the reconstructions in Marquer et al. (2014) to the lowest reliable time intervals: 400-, 300-, 200-, and 100-year time intervals were used for reconstructions and the results show that 200-year time intervals provide a good compromise between the size and number of the time intervals available and good REVEALS standard errors. The REVEALS model was therefore run for 200-year time windows covering the last 11,700 years: the number of time windows is dependent on the length of the record at each target site. The protocol for running REVEALS follows Marquer et al. (2014, 2017) and Trondman et al. (2015). For this test, the time resolution of the MAT estimates matches the REVEALS parameters.

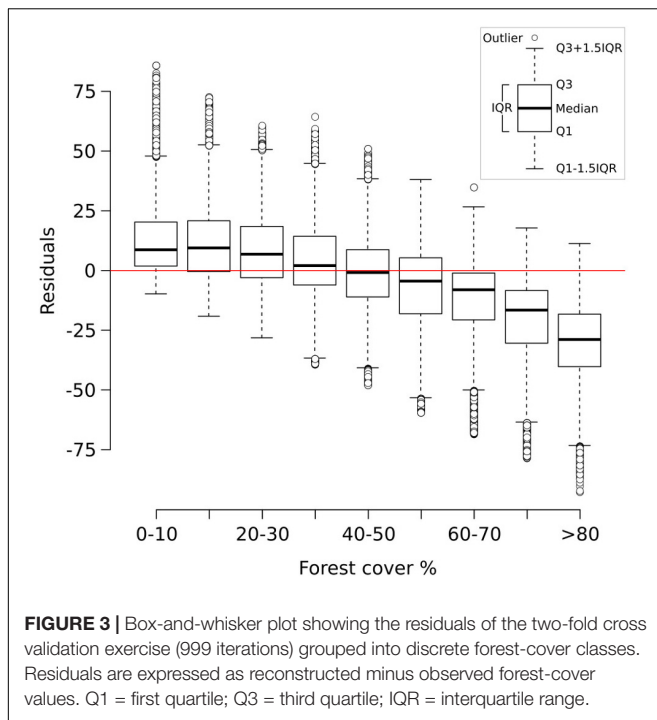
The REVEALS estimates for the 25 taxa were grouped into open-land and forest categories, and the associated standard errors were calculated again. The REVEALS forest covers include covers of *Abies*, *Alnus*, *Betula*, *Carpinus*, *Corylus*, *Fagus*, *Fraxinus*, *Juniperus*, *Picea*, *Pinus*, *Quercus*, *Salix*, *Tilia*, and *Ulmus*, and represent the regional cover within 50 km around each target site.

RESULTS

Model Validation

Performance of the Cross-Validation Exercise

The two-fold cross-validation exercise shows that the MAT-based forest-cover model is able to account for close to 50% of the variance ($r^2 = 0.49$) and that the RMSEP (20.7%) is lower than the standard deviation of the data set (29%). These values reflect the wide array of uncertainties affecting the model (see sections “Sources of Uncertainty”, “No-analog Situations and the PFT Approach”, “forest-cover Underestimation”), yet they suggest that it can identify and reproduce a relationship between remote sensing data and pollen percentages. An analysis of the residuals of the two-fold cross-validation (**Figure 3**) highlights negligible bias in the 0–70% forest-cover range, with the median error lying well in the range of $\pm 10\%$ points. A larger discrepancy between observations and the reconstruction is especially visible at sites with very high forest cover (>80%), where the median reconstructed values tend to be more than 25% points lower than the observed forest cover. These differences might depend on a combination of factors. For instance, high-forest-cover samples (>80%) are the least represented in the



calibration dataset, likely making them more prone to be affected by poor analogs. The lowest residuals are concentrated in southern Europe (Supplementary Figure S7) probably reflecting the limited representation in the modern dataset of large units of Mediterranean forest. These issues are revisited in the discussion section.

MAT-REVEALS Comparison

The comparison between MAT and REVEALS estimates (Figure 4) shows generally similar trends (overall correlation coefficient: $r = 0.75$; Figure 5A). This level of agreement is notable, considering the quite different approaches of the two methodologies toward landscape reconstruction. Disagreements in absolute values constitute the main difference between the two models. The MAT assigns lower forest covers to early pioneering pine and birch woodlands (~12,000–10,000 BP); during this phase, most of the closest modern analogs are chosen within the tundra biome or in proximity of the forest-tundra ecotone (Supplementary Figure S8). Differences between the models might then depend on a combination of factors, including potential forest-cover overestimation by REVEALS in Early Holocene contexts, and tree-height detection limits for MAT estimates. Major differences in terms of absolute values persist across all pairs after 10,000 BP, with the full development of mixed deciduous woodlands. The REVEALS curves rise to values higher than 85–90% before acquiring an overall stable neutral trend. After a comparable initial positive trend, the MAT curves stabilize at around 60–70%. Differences of ~18–25 percentage points persist across the whole Mid-Holocene (Supplementary Table S4). This consistent behavior reinforces the results of the cross-validation exercise (Figure 3), pointing to a limited performance of the MAT in densely forested contexts. As

noted in section “Performance of the Cross-validation Exercises,” the reasons behind this behavior might depend on a lack of suitable analogs in the training data set, in turn resulting from the low residual forest cover across present-day Europe. Different approaches toward forest-cover quantification might play a notable role too, i.e., sum of all forest-forming taxa, regardless of their habitus (REVEALS) vs. tree-height detection limits of the underlying forest cover map (MAT). Undetectable trees lower than 5 m might then account for at least part of the difference between the MAT and REVEALS curves.

Consistently, the only two no-analog situations (gaps in the MAT curves of Krageholmssjön and Raigstavere) are recorded at around 8,000 BP, testifying further to limits in the training data set concerning the reconstruction of early Mid-Holocene forests. The occurrence of no-analog situations in our reconstructions is addressed in section “Quantification of No-analog Occurrences.”

The agreement between MAT and REVEALS curves improves in the Late Holocene, when forest-cover decline brings the REVEALS values below 80%. The average difference in absolute values between the two reconstructions is reduced to ~10–17 percentage points in the last 4,000 years of the sequences (Supplementary Table S4).

Quantification of No-Analog Occurrences

The MAT-REVEALS comparison shows few gaps in the MAT-based curves (sites of Krageholmssjön and Raigstavere, Figure 4), highlighting the occurrence of missing analogs and prompting us to explore the extent of this issue. For an appropriate comparison, we ran the MAT algorithm for the whole fossil and modern data sets using selected pollen taxa (i.e., without any transformation into PFT scores) and PFT scores (as described in section “Fossil and Modern Pollen Data”) separately. The full list of taxa used in this simulation is presented in Supplementary Table S5. The occurrence of no-analog samples for every timeslice is presented in Figure 6. Consistently with the parameters of our model, a no-analog situation is detected when the closest analog to a fossil sample has a squared chord distance higher than 0.3 (Huntley, 1990).

The taxa-based approach results in large portions of the fossil data sets presenting no-analog situations (Figure 6A). The period between ~9,000 and 6,000 BP shows the highest values, with over 30% of the samples in each timeslice having no close analogs in the training set. The effect of the PFT approach is visible in Figure 6B: the highest no-analog percentages are still concentrated between ~9,000 and 6,000 BP, but with values rarely exceeding 2%. A more detailed region-by-region subdivision is presented in Supplementary Figure S9.

Bias Correction

The results of the two-fold cross-validation exercise highlight a mild overestimation of forest cover at values $\lesssim 30\%$ and, above all, a growing bias for values $\gtrsim 50\%$. This systematic underrepresentation of high forest-cover values is clearly visible in the MAT-REVEALS downcore comparison, possibly suggesting a comparable bias spread across all

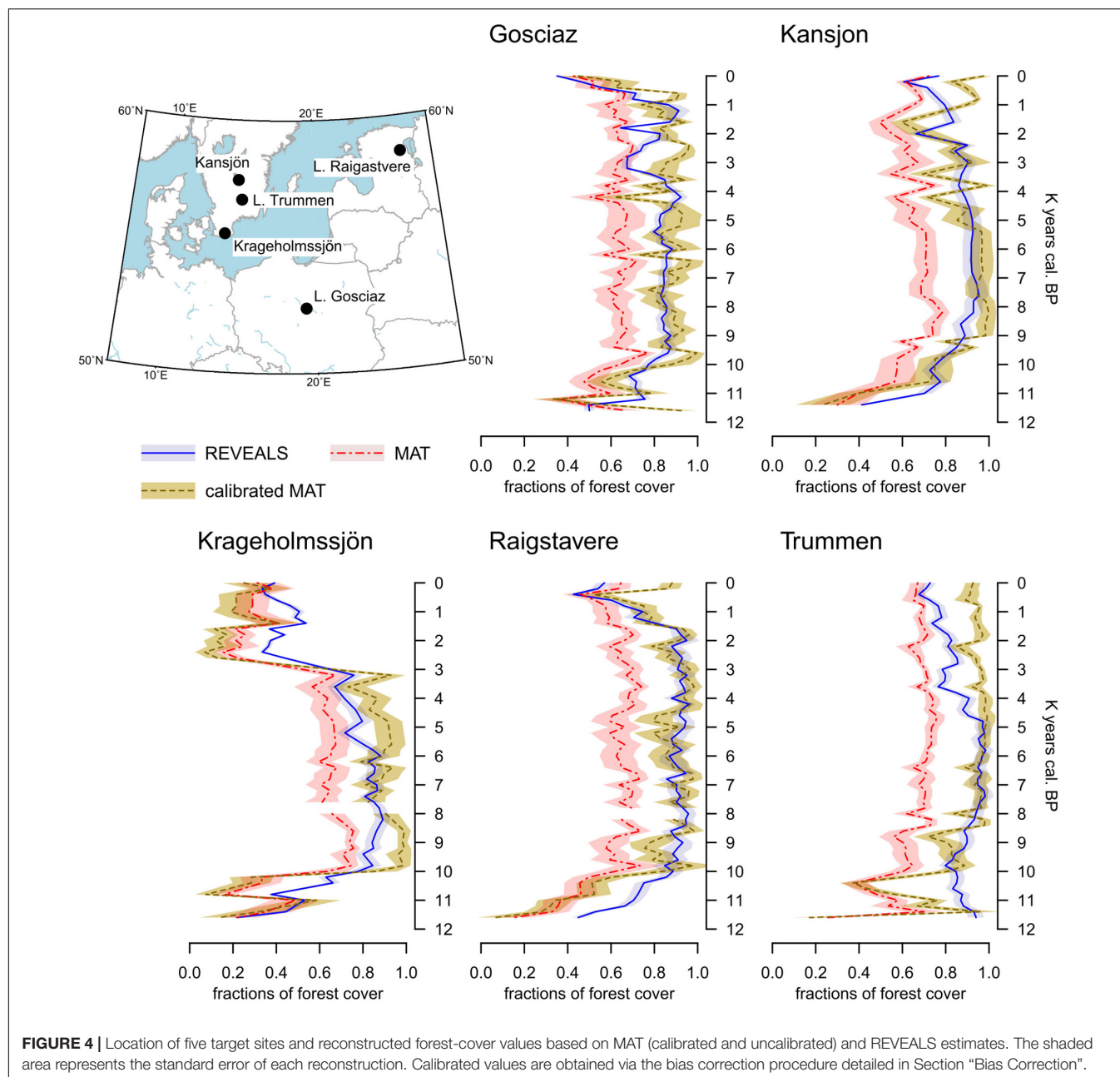
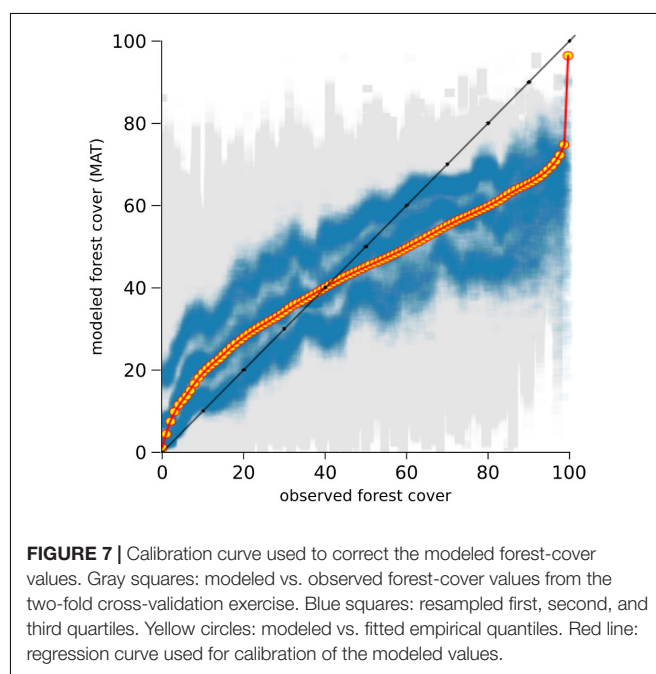
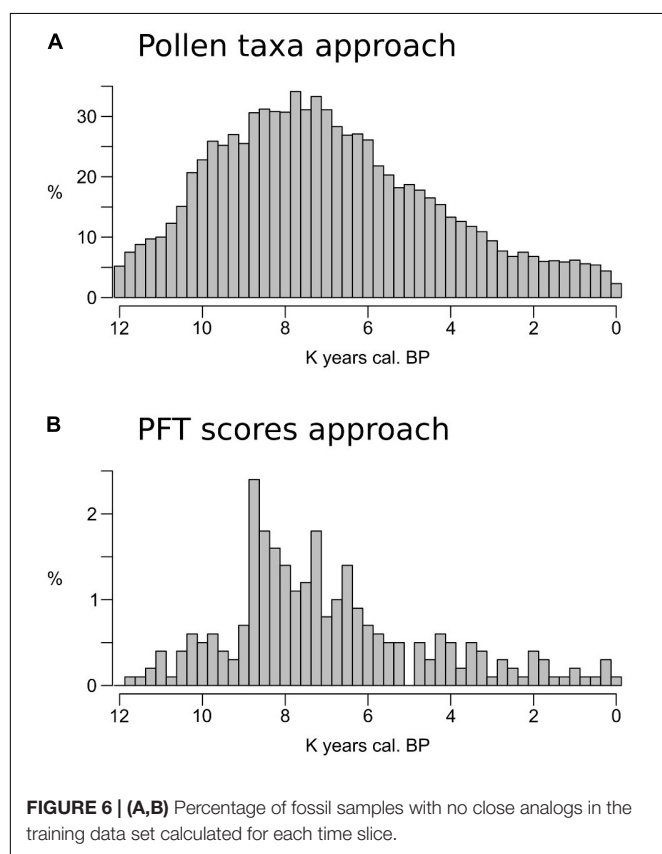
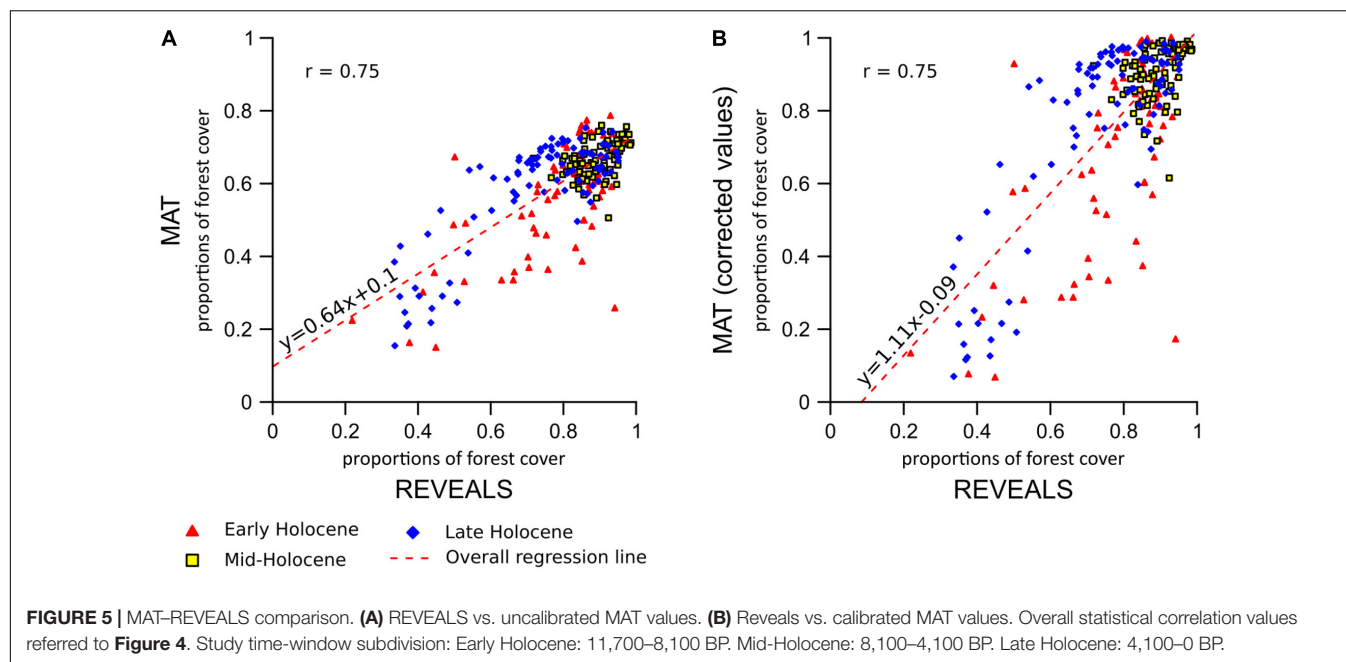


FIGURE 4 | Location of five target sites and reconstructed forest-cover values based on MAT (calibrated and uncalibrated) and REVEALS estimates. The shaded area represents the standard error of each reconstruction. Calibrated values are obtained via the bias correction procedure detailed in Section “Bias Correction”.

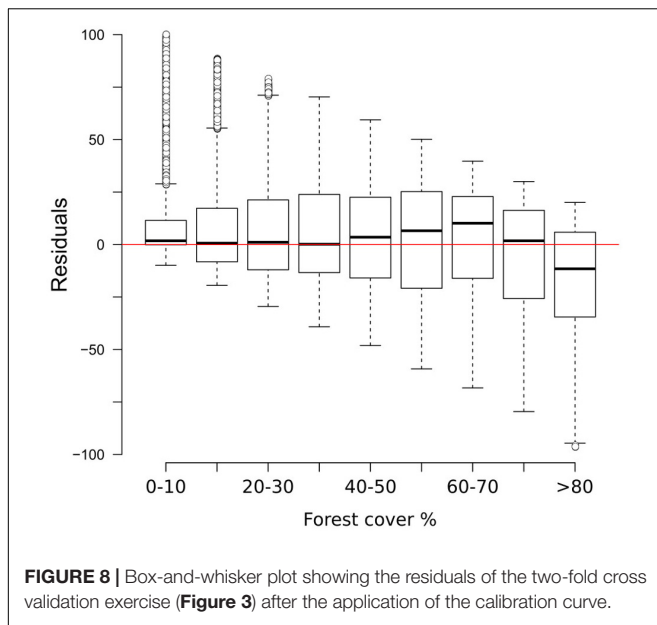
Holocene reconstructions. Considering the seemingly systematic occurrence of this modeling error, we employ an empirical distribution correction approach (Lafon et al., 2013) to rectify the forest-cover reconstructions in our model. The results of the two-fold cross-validation exercise (999 iterations) were resampled using randomly distributed 5%-wide windows (10 randomly placed windows for every iteration) in order to address the predominance of low forest-cover samples in the training set. The first, second, and third quartile were extracted within each window. Robust empirical quantiles for modeled vs. observed forest cover were estimated via Quantile Mapping (R package ‘qmap,’ Gudmundsson, 2016), based on every second percentile between 1 and 100. A smooth spline

regression curve was fitted to the resulting quantile–quantile plot (Figure 7) and used as a calibration curve for the modeled forest-cover values. The resampling strategy and regression parameters were tested via trial-and-error, opting for a solution that minimizes the bias for high forest-cover classes. The application of the bias correction curve to the two-fold cross-validation iterations is visible in Figure 8, where it shows a largely corrected median bias across all forest-cover classes. The correction of MAT values in the MAT–REVEALS comparison (Figure 4) shows how the calibration curve succeeds in closing the gaps between the two models during the Mid-Holocene (Supplementary Table S4), while at the same time preserving the relative trend between timeslices. It should still be noted



that the bias-correction procedure is applied mechanically to all samples regardless of their age, composition or location. As a consequence, this simple calibration approach might result in an over- or under-correction of forest-cover values. Any

decrease in agreement between MAT and REVEALS might be ascribed to these effects. Examples include the exacerbation of low forest-cover values in the Late Holocene section of Kragholmssjön, or marked shifts from 60–70% (uncalibrated) to >90% (calibrated) forest-cover values within the most recent timeslices of Kansjön and Raigstavere. Similarly, the monotonic behavior that characterizes most of the MAT-based Trummen curve results in a growing discrepancy between MAT and REVEALS from ~5,000 BP onward. These differences are nonetheless counterbalanced by a general and notable

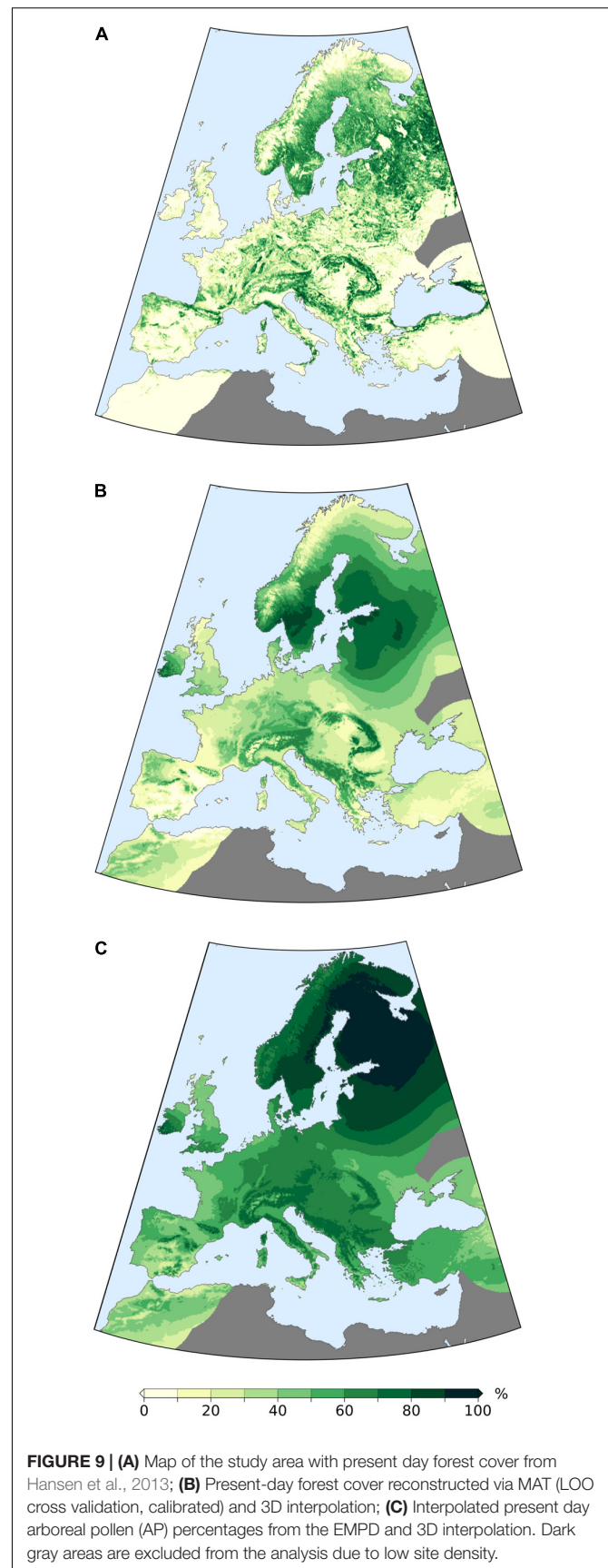


improvement in the correlation between MAT and REVEALS (overall regression line with slope = 1.11 and intercept = -0.09 ; Figure 5B).

The forest-cover reconstructions presented in the following sections are based on the application of this bias correction procedure.

Evaluation of the Interpolation Procedure

A visual comparison between actual modern cover from Hansen et al. (2013) (Figure 9A) and the MAT-based, interpolated modern forest-cover map (obtained via LOO method, Figure 9B) is used to evaluate the ability of the interpolation procedure to reproduce the main patterns in forest cover at the European scale. Higher forest densities are correctly reconstructed in mountain areas, notably at mid-low elevations in the Alps and along the Apennines, in the Balkan Peninsula and in the Carpathians, and partly in northern Iberia. In northern Europe, extensive forested areas are reconstructed around the Gulf of Bothnia and in western Russia. By comparison, the interpolated AP map displays similar distributions in central and southeastern Europe, but differs substantially in the remaining areas. Particularly visible is the pattern in northern Europe, where high AP values are present well beyond the northernmost limit of densely forested areas and show a generally limited spatial variability. A region-by-region comparison is presented in Figure 10, together with the full extent of the fossil-database reconstructions. The synthesis in Figure 10 highlights how a combination of MAT and interpolation succeeds in producing forest-cover values that are within the range derived from Hansen et al. (2013), while AP values regularly exceed it. Non-overlapping values are produced only for the British Isles, presumably due to the relatively poor spatial distribution of modern samples available for this specific region (Supplementary Figure S2).



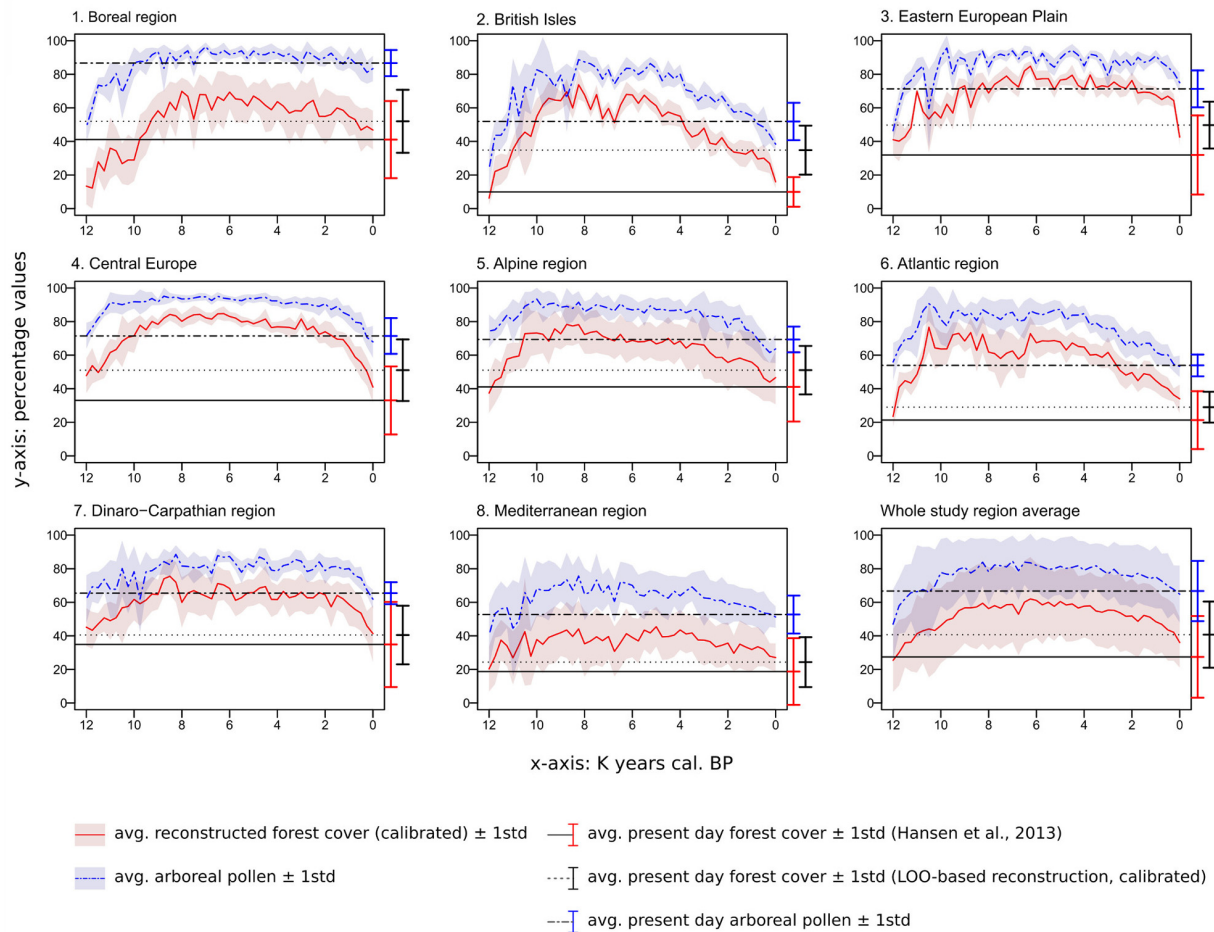


FIGURE 10 | Time series for the whole study area and the eight regions (time vs. percentages of reconstructed forest cover and percentage of arboreal pollen). Areas covered by water or ice are not included in the calculation of average forest-cover/AP values and their relative standard deviation. The deviation from the mean does not represent the error of the reconstruction but is simply a measure of inter-regional variability. The horizontal lines provide a comparison with present-day values for each region, i.e., modern forest cover from Hansen et al. (2013) (**Figure 9A**), interpolated LOO-based modern forest cover (**Figure 9B**) and interpolated percentage of arboreal pollen (**Figure 9C**).

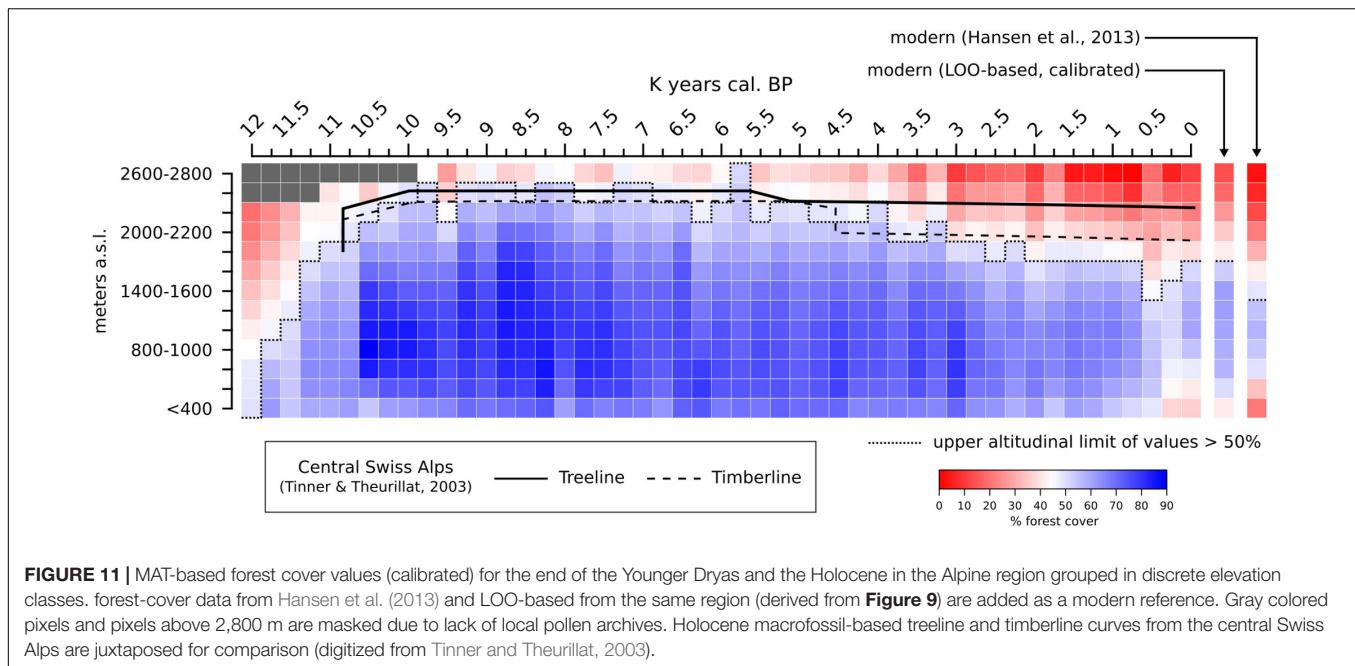
Forest-Cover Elevation in the Alpine Environment

A summary of the average MAT-derived forest cover in the Alps at different altitudes during the Holocene is presented in **Figure 11**. The overall lowest forest-cover values are reconstructed at the end of the Younger Dryas period, before 11,700 BP, when values > 50% are not recorded in the regional synthesis. A sharp increase in forest-cover percentages is immediately visible after 11,500 BP, rapidly leading to the maximum altitudinal development of dense Alpine forests in our reconstruction (~10,000–7,000 BP). A gradual negative trend is then recorded between ~7,000 and 2,250 BP, lowering the 50% threshold from ~2,600 m to ~1,800 m. Eventually, after ~500 BP, values below 800 m decrease noticeably too, bringing the overall forest-cover situation close to the modern one across all elevation bands. In **Figure 11**, the 50% boundary in both the 0 BP timeslice and LOO-based modern timeslice is located at 1,800 m. By comparison, the satellite-based modern forest cover is placed 400 m lower, at 1,400 m. It should be noted

that the satellite-based 1,400–1,600-m elevation class has a forest cover value only slightly lower than the threshold value (48.9%), causing a seemingly abrupt difference in elevation between the satellite-based and MAT-based forest covers. Comparing the 0 BP timeslice with the satellite-based and the LOO-based forest covers returns a correlation coefficient $r = 0.98$ in both cases. Similarly, comparing the satellite-based and LOO data results in $r = 0.97$.

Forest-Cover Reconstructions Late Pleistocene and Holocene Onset (Figures 10, 12A,B)

During the last stage of the Pleistocene, the average forest-cover ranges from ~6% (British Isles) to ~48% (Central Europe), with an overall study area average of ~25%. The highest percentages are reconstructed along a diagonal belt spanning from the circum-alpine area to central-eastern Europe (**Figure 12A**). The beginning of the Holocene is marked by a general increase in forest cover, with particularly steep trajectories in the British Isles,



in the Atlantic region and, resulting in an isolated peak, in Eastern Europe.

First Half of the Holocene (Figures 10, 12C–G)

Maximum forest development is reached between ~8,500 and 6,000 BP, with intensity and timing varying from area to area. Only the Atlantic region displays an early and isolated maximum around 10,500 BP. Wide standard deviations are visible across most regions within the same time slice. Positive forest-cover trends last until 6,250 BP in the Eastern European plain. The highest average values are recorded in Central Europe, with percentages often above 80%. The least forested region is the Mediterranean, where forest cover rarely exceeds 40%.

A phase of decline and stagnation lasting from ~8,250 to 6,500 BP is visible in the British Isles, in the Atlantic and Dinaro-Carpathian regions, and in the Mediterranean. With the end of this phase, forest cover values recover and return approximately to pre-decline levels. A similar decline begins in the Alps after 8,250 BP, but is not followed by forest recovery.

Second Half of the Holocene (Figures 10, 12H–L)

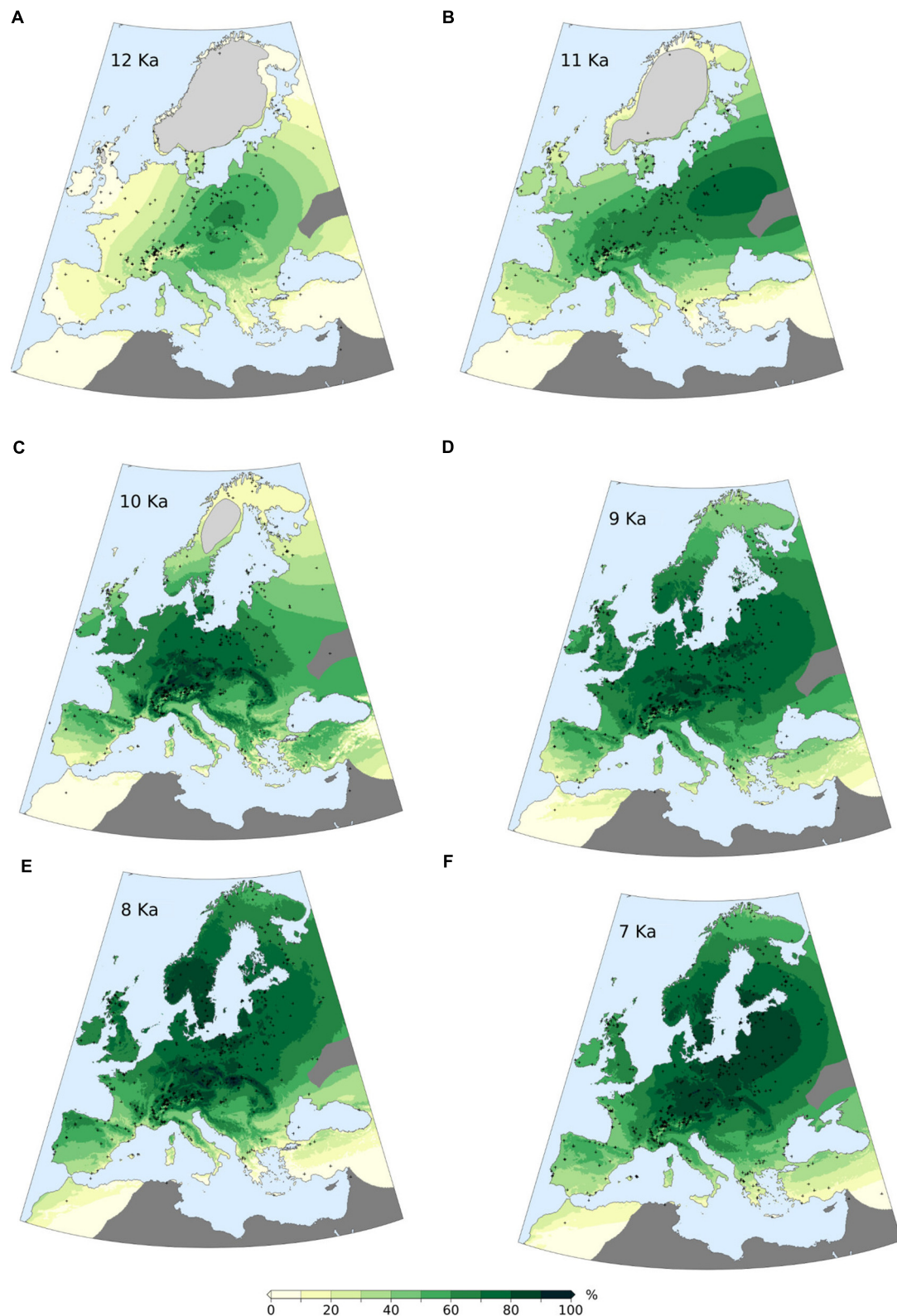
The negative trend observed in the Alps since 8,250 BP continues during the second half of the Holocene. A comparable stable decline is visible across most regions generally from 6,000 BP. The contraction of forested areas varies across Europe in terms of intensity and timing, but invariably leads from Early/Mid-Holocene maxima to present-day values without any interposed major recovery phase. Only the Dinaro-Carpathian region shows a predominant neutral trend until ~1,500 BP, then followed by a rather steep decline to present-day values. A notable increase in steepness occurs in Central Europe after 1,500 BP too, while in the British Isles, in the Eastern European Plain and in the Alps occurs after ~750 BP.

DISCUSSION

We reconstruct for the first time spatially continuous fields of forest cover over the entire European continent for the last 12,000 years based on quantitative criteria. The large spatial and long temporal scale of the study and the hundreds of individual sites on which it is based preclude a detailed analysis of individual local areas, so we restrict our discussion here to the main strengths and weaknesses of the model. It should be remembered that the reconstruction is based on aggregate results from several sites, and it is to be expected that individual site reconstructions may show different trends when viewed in isolation.

Sources of Uncertainty

Williams and Jackson (2003), Jackson and Williams (2004), and Mauri et al. (2015) present an extensive summary of potential error sources affecting models based on pollen and modern analogs. These include the quantity and quality of the fossil and modern pollen data, chronological uncertainties, and the completeness and accuracy of attendant metadata. Whilst it is possible to apply rigorous quality control criteria, there is a direct trade-off in terms of the number of samples, and consequently the spatial, temporal, and ecological coverage. This can be particularly important for instance for the size of the modern pollen training set, and therefore the number of analogs that are available to the MAT. For instance, a sample count of 400–600 pollen grains belonging to terrestrial species is generally considered a safe minimum threshold to minimize statistical fluctuations of taxa percentages within a sample (Birks and Birks, 1980), with lower pollen counts being occasionally imposed by the sample nature itself (e.g., bad preservation, low volume). Applying a minimum pollen count (terrestrial taxa only) of 600 grains would lead to a >60% sample

**FIGURE 12 |** Continued

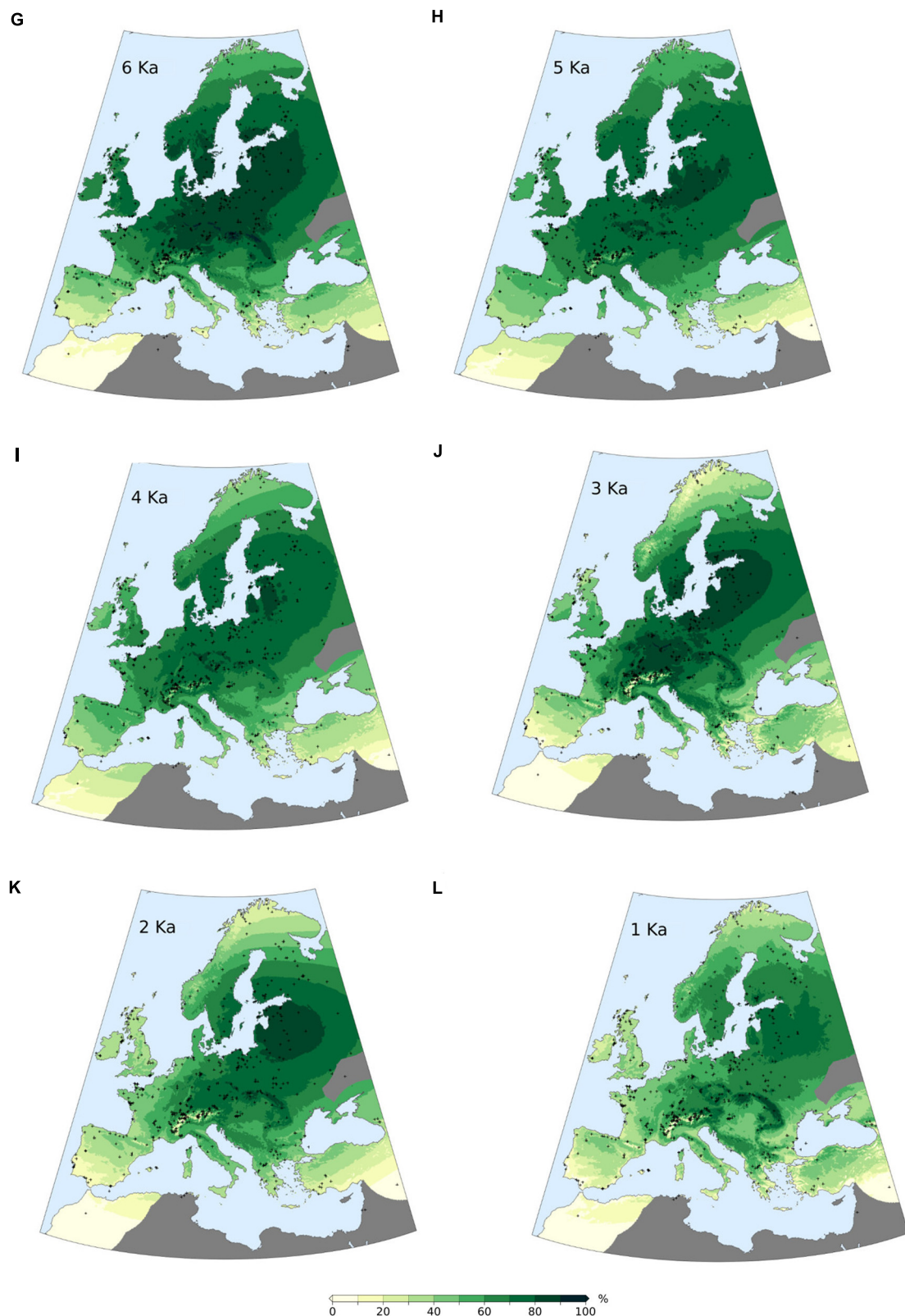


FIGURE 12 | MAT-based forest-cover values (calibrated) for selected time slices during the past 12,000 years (**A–L**). Gray crosses represent pollen sites locations. Light gray areas over northern Europe and Scotland represent Early Holocene ice cover. Dark gray areas are excluded from the analysis due to low site density.

loss in both the training and the fossil databases, affecting the spatial coverage and the general variability of both data sets. In our reconstruction we used a smaller sub-set of taxa selected from the total terrestrial count, and therefore we chose a smaller threshold of 100 terrestrial pollen grains as the minimum count.

The size of the count influences the taxonomic diversity of the sample, as does the skill of the analyst. Furthermore, additional vegetation parameters, such as habitus-related aspects are not always inferable from pollen data. Even when two species exhibit clearly different growth habits, their pollen grains might prove difficult to differentiate, as exemplified by the *Betula* genus. Dwarf birch (*Betula nana*), an arctic/cool temperate low shrub, is not distinguishable from arboreal birches through grain size alone, requiring instead to calculate the ratio of equatorial diameter to pore height (Birks, 1968). It is not possible to ascertain to which extent this distinction constitutes a common practice among analysts (e.g., it is admittedly avoided in Solovieva et al., 2015). This specific issue is at least partly mitigated by the PFT approach: *B. nana* pollen grains are assigned to the arctic-alpine PFT, while undifferentiated *Betula* pollen may be categorized as either boreal summer-green or arctic-alpine depending on the remaining floristic assemblage of a given sample (Peyron et al., 1998 and Supplementary Tables S1–S3). Woody vegetation growth habit and size might be variously affected by environmental properties too, such as water availability and soil composition. These variables are not accounted for in the analog selection process, and can lead to associate fossil pollen spectra to incorrect modern vegetation parameters.

An additional source of uncertainty stems from the definition of forest in the Hansen et al. (2013) forest-cover dataset, which specifies that “forest” has a minimum height of 5 m. However, the LANDSAT sensors used to create the dataset do not detect tree height. Therefore, “forest” cover mapped in this dataset is subject to uncertainty and areas mapped as forest could in reality be something else, which would lead to irreconcilable differences between pollen spectra and tree cover. For example, forest could be mapped in the dataset when the vegetation cover is in fact rather a dense, tall shrubland, e.g., in the arctic. While indistinguishable to a satellite-based sensor, an arctic shrubland might have a very different floristic composition than, e.g., boreal forest, and this difference would be obvious in a pollen spectrum. This mismatch between observations from satellites and modern pollen samples would result in calibration uncertainty, where areas with similar forest cover have different pollen spectra, and vice versa.

Sample misplacement is another source for incorrect matches between pollen and satellite data. The high grid resolution of the remote sensing data and the small σ -value of the pixel-weighting equation result in a high sensitivity of the search window to shifts in its position. The EMPD provides reliability estimates for sample geolocation, which – combined with randomized location checks – have been used in the present work to exclude samples with known large uncertainties. This information is not available for the whole dataset, especially for older samples, due to gaps in the documentation or specific limitations (e.g., lack of GPS logging devices during fieldwork operations). Surface

samples with unknown location reliability amount to >50% of the total. Despite this lack of metadata, they were included in the elaboration in order not to depopulate the analog pool.

An additional issue revolves around the availability of remote-sensing data. While satellite-based forest-cover data are available only for selected time periods, i.e., the year 2000 for Hansen et al. (2013) and years 1992–1993 in the case of DeFries et al. (2000), during the past decades European forest cover experienced a general increase, with localized areas of forest loss (Lambrechts et al., 2009; Potapov et al., 2015). For comparison, the EMPD samples with known age were collected mostly between the years 1978 and 2010. As a consequence, pollen spectra might be paired with non-contemporary vegetation patterns. The relevance of this issue can be proportional to the age difference between the two data sets, as a wider gap would simply leave more time for landscape transformations to take place. Nonetheless, chronology-based filters were explicitly avoided, since wide chronological differences do not necessarily imply significant vegetation changes.

All of these examples are meant to highlight how surface-pollen datasets would benefit from both enhanced sample density and metadata quality, ideally not only covering a wider range of vegetation assemblages, but also containing redundancy that would allow for stricter and task-oriented selection of samples. Furthermore, improvements in remotely sensed land-cover data would be desirable, e.g., using new sensors that directly integrate the spectral and physical characteristics of the vegetation into a single dataset. It is important to remember that good transfer function performance may equally be dependent on having a reliable calibration dataset as on having good pollen data.

No-Analog Situations and the PFT Approach

The ability of MAT to find a proper set of analogs is challenged by the many factors influencing plant biology and distribution through time (Jackson and Williams, 2004). Pollen production and dispersal can be influenced by the age of the plant, with younger specimens producing less pollen than older ones (Jackson, 1994; Matthias et al., 2012). Similarly, varying concentrations of atmospheric CO₂ have a direct effect on the production of flowering shoots, leading to an increase in pollen production with growing CO₂ values (Ziska and Caulfield, 2000; Ladeau and Clark, 2006). Growth-speed limitations and interspecies competition might result in a lagged expansion within a potential bioclimatic space (e.g., Gardner and Willis, 1999). Furthermore, a growing human influence on the landscape in the second half of the Holocene played a role in the expansion of disturbance-dependent taxa outside of their niches (e.g., Perego et al., 2011), and possibly also contributed to early extinction events (Wick and Möhl, 2006). A combination of these and other factors led to the rise and decline of plant communities that potentially have no close parallels in contemporary vegetation.

Changes in pollen productivity within the same species represent an issue that is difficult to address and common to all

pollen-based models. On the other hand, the sensitivity of the MAT to migration lags, extinction events, and gaps in the training data set can be lessened by avoiding a taxa-based approach. The use of PFT scores, as used in the present study, groups pollen taxa in broader classes defined by physical, phenological and climatic factors. The absence of specific taxa from an area does not hinder the performance of a PFT-based reconstruction as long as their potential bioclimatic space is occupied by species with comparable traits. The low occurrence of no-analog situations in our reconstructions (**Figure 6B**) proves the effectiveness of the PFT approach, and suggests that no-analogs do not affect the performance of the model. Yet a concentration of no-analogs between ~9,000 and 6,000 BP remains notable. It occurs during the phase of maximum European forest development and highlights from a different perspective the noted model weakness with dense forest covers.

Still, the use of PFTs should not be regarded as a complete solution to the no-analog issue, but more as a viable and more robust alternative to taxa-based approaches. In fact, notable differences between taxa remain unaccounted for within the PFT method and contribute to the overall uncertainty of the model. As an example, beech (*Fagus*), lime (*Tilia*), and elm (*Ulmus*) share the same PFT (Cool-temperate summer-green; Peyron et al., 1998) despite having widely different pollen productivity estimates (beech: 0.76–6.7; lime: 1.3; elm: 0.8. Values are relative to the pollen productivity of Poaceae; Broström et al., 2008). Two samples with the same proportion of cool-temperate summer-green taxa (e.g., one composed primarily of beech and one of lime/elm) might then still be the product of different vegetation patterns. Beech spread gradually across Europe during the Holocene and is well represented in modern pollen diagrams (e.g., Magri, 2008). On the other hand, lime and elm are minor components of the present-day pollen landscape, having reached their palynological peak during the Early/Mid-Holocene (e.g., Huntley and Birks, 1983). Modern samples with beech might then be selected as best analogs for fossil samples lacking this taxon but containing lime and elm. The occurrence of such pairings – considering the potentially much higher pollen productivity of beech – could contribute too to the underestimation of Early/Mid-Holocene forest cover.

Forest-Cover Underestimation

The results of the two-fold cross-validation exercise and the MAT-REVEALS comparison (see sections “Performance of the Cross-validation Exercise and MAT-REVEALS Comparison”) highlight a distinct issue with the reconstruction of high forest covers. A visible contribution to this issue is given by the limited availability of EMPD samples from highly forested contexts, but additional factors could play important roles too. Notably, the modern European landscape is largely deforested. As a consequence, any sample misplacement or incorrect distance-weighting could more likely lead to pair pollen samples with low forest-cover values. The use of PFTs could impact the model performance too, as noted in section “No-Analog Situations and the PFT Approach.” Most importantly, the MAT does not have any intrinsic ability to differentiate between local pollen sources and long-distance transport, an issue exacerbated by the

generally poor pollen dispersal capabilities of open-landscape species (i.e., –simplifying –most herbaceous taxa). The under-representation of non-arboreal species results in samples with comparably high AP values but widely different forest-cover percentages (e.g., Broström et al., 1998 and **Figure 1** in the present paper), likely hindering a fine distinction between moderately and highly forested contexts.

These issues could be addressed by driving the analog selection process through a series of constraints. An example might involve calculating the average pollen productivity estimates of all PFTs, and reducing the analog pool to samples with comparable traits. Similarly, pollen accumulation rates could be used to detect predominant long-distance transport. Testing these solutions is currently prevented by a lack of necessary information, as pollen productivity estimates for the whole study area and for all taxa involved are currently not available. Similarly, the EMPD does not contain information concerning pollen accumulation rates. These limits led us to tackle the forest underestimation issue through a single correction equation applied to all sampling contexts and vegetation assemblages (see section “Bias Correction”).

Comparison With Current Land-Cover Change Narratives

Unraveling the fine reasons behind the regionally diverse forest cover trends remains beyond the scope of this paper. We will mostly constrain our analysis to a comparison between our data and the land cover dynamics emerging from qualitative interpretations and quantitative models. The interpolated results of our reconstruction draw a coherent picture of forest advancement and retreat spanning the last 12 millennia. While the limits of the method constitute an undeniable source of approximation, it is important to note that the reconstructions are often consistent with existing narratives of vegetation development from a regional to a continental scale, although these have virtually all been based on a qualitative interpretation of pollen data.

Late Pleistocene

The average forest cover across most of Europe just before the onset of Holocene warming points to a landscape dominated by non-arboreal vegetation. In agreement with this reconstruction, the traditional interpretation of pollen data describes a steppe-like environment with prevalent shrub and xerophytic vegetation covering most of the deglaciated areas of Western and Southern Europe (Walker and Lowe, 1990; Bakels, 1995; Guiter et al., 2005). Similarly, the presence of a steppic landscape matches several interpretations of Central Mediterranean (e.g., Bordon et al., 2009; Tinner et al., 2009; Combourieu-Nebout et al., 2013) and Eastern Mediterranean archives (e.g., Rossignol-Strick, 1995; Roberts et al., 2001; Langgut et al., 2011). In contrast, Lawson et al. (2004) point to a limited woodland contraction phase inserted in a context of gradual postglacial forest recovery. The expansion of an unforested environment during the Younger Dryas period is a phenomenon acknowledged in the Iberian Peninsula as well (Carrión et al., 2010). Here, the treeless conditions reconstructed in **Figure 12A** appear to be fitting

for high-elevation sites and areas affected by a decrease in precipitation (Carrión and Van Geel, 1999; Carrión, 2002; Muñoz Sobrino et al., 2004), but might underestimate the presence of pine and oak woodlands growing in more favorable locations (Rubiales et al., 2010).

The higher forest-cover percentages emerging in central Europe probably reflect the presence of surviving Allerød pine/birch woodlands stretching from the Alpine piedmont (Wick, 2000) to Central Europe (Andres et al., 2001; Bos, 2001; Sobkowiak-Tabaka et al., 2017). Moving northward to the Baltic coast, the conditions inferred from pollen diagrams describe increasingly open birch and pine forests (Jahns, 2007; Nelle and Dörfler, 2008) gradually giving way to tundra-like conditions (Kihno et al., 2011). The relatively high forest cover values reconstructed around the Baltic Ice Lake may appear excessive considering the local importance of heliophilous taxa and the low pollen accumulation rates of forest species (Veski et al., 2012). Reworked pollen grains of thermophilous trees (e.g., Jahns, 2007) might arguably inflate model estimates. Nonetheless, macrofossil remains and pollen threshold values point to persistent populations of birch, pine, and spruce even at high latitudes and close to the ice margin (Kullman, 2002; Heikkilä et al., 2009).

Post-glacial Forest Recovery

The beginning of the Holocene is marked by warmer temperatures and greater moisture availability that promoted a rapid, wholesale transformation of land cover. The rise of forest-cover values over most of Europe is in line with the vegetation changes inferred from pollen diagrams. Existing woodlands densified and patchy tree stands replaced tundra parkland vegetation (e.g., Nelle and Dörfler, 2008; Robin et al., 2011). Growing forest density across Southern and Central Europe reflects the rapid expansion of thermophilous trees in pollen diagrams (Brewer et al., 2002; Giesecke et al., 2011). The 10,500 BP timeslice is characterized by an unusually high land-cover variability (high standard deviations in **Figure 10**), occurring together with visibly higher error estimates (Supplementary Figure S6). Significantly, this time window envelops the abrupt rise of hazel in central and southern European pollen diagrams (~10,600 BP, Giesecke et al., 2011). This synchronous and fast paced event possibly resulted in widespread forest-cover differences at both intra-site (sudden palynological change between adjacent samples) and inter-site level (neighboring sites having different forest covers due to chronological factors – i.e., limits of their respective age–depth models), ultimately producing inflated error estimates propagating through site-poor areas. Peak levels of forest development are generally reconstructed between ~8,500 and 6,000 BP, following the maximum extent reached by mixed deciduous forests (Brewer et al., 2002). Rising forest-cover values in Scandinavia reflect the colonizing wave of pioneering birch woodlands over the newly deglaciated landscapes (Bjune et al., 2004). Values higher than 50% are reconstructed in Northern Scandinavia after 8,000 BP, reflecting the widespread occurrence of birch and pine-birch forests at high latitudes (Seppa, 1998; Barnekow, 2000; Bjune et al., 2004).

Compared to other regions, there is only a modest increase in forest cover density in the Mediterranean between Late Pleistocene and Early and Mid-Holocene. These low values possibly reflect a combination of denser forests spreading inland and at upland sites, (Carrión et al., 2010; Sadori et al., 2011), and the contemporary development of coastal matorral/maquis shrublands (Carrión and Dupré, 1996; Pantaléon-Cano et al., 2003; Tinner et al., 2009; Calò et al., 2012).

Middle/Late Holocene Forest Cover Decline

During the second half of the Holocene, forest-cover percentages are characterized by negative trends that bring the curves to present-day values. Increasing human pressure is regarded as the primary driver behind such behavior (Kaplan et al., 2009; Davis et al., 2015; Fyfe et al., 2015), although the role of climate should not be dismissed (Marquer et al., 2017). Forest cover over Northern Europe will have been influenced by the Early Holocene rise in temperatures and later Holocene cooling after the Mid-Holocene thermal optimum, whilst forests in Southern Europe were more influenced by similar trends in moisture (Davis et al., 2003). The estimated increase in carrying capacity of early agricultural societies implies an expansion of productive surfaces (croplands, pastures) at the expense of woodlands and wetlands. A growing exploitation of forest resources, primarily timber and fuel, must be accounted for as well, contributing to the general widespread and growing forest-cover reduction. The average picture described by our model is spatially and chronologically comparable to the synthesis presented by Fyfe et al. (2015), based on the categorization (Pseudobiomization, PBM) of Europe's land surface into aggregated land-cover classes (e.g., forest, semi-open vegetation, open vegetation). At a pan-European scale, both models reproduce a period of maximum forest extent between ~8,500 and 6,000 BP. Notably, this phase of relative stability is followed in both models by a very gradual forest decline. This negative trend then accelerates after 1,400 BP in Fyfe et al. (2015) and after 1,500 BP in our model (study area average, **Figure 10**). Additional similarities between the PBM and MAT can be found at a smaller scale too. Fyfe et al. (2015) describe a clear distinction between Western and Eastern Europe, with the first displaying consistently lower forest values. This East-West distinction is also visible in REVEALS estimates by Nielsen et al. (2012) and Trondman et al. (2015), and in the multi-model comparison by Pirzamanbein et al. (2014), confirming it as a robust feature of European land-cover history. The same pattern is clearly visible in our reconstruction since the Early Holocene, placing its origin before the expansion of Neolithic agriculture (Fyfe et al., 2015), and possibly reflecting – at least in part – an interplay of continentality and soil texture gradients (Nielsen et al., 2012).

The differences between Eastern and Western Europe are not limited to absolute land-cover values: the two regions show different forest-loss dynamics too. Fyfe et al. (2015) show a visible negative trend across their Western region (Western France) from ~4,500 BP. On the other hand, Eastern Europe (Czech/Slovakia) presents only a very mild decline between ~6,000 and 1,500 BP, then followed by a sudden and much

sharper forest collapse. The Western France trajectory shares clear similarities with our Atlantic region curve, including a forest decline and recovery episode between ~8,000 and 6,000 BP. The Czech/Slovakia situation matches forest-decline patterns in both Central Europe and in the Dinaro-Carpathian region (sudden decline after ~1,500 BP) in the MAT-based model.

It is worth noting that quantitative landscape reconstructions by Nielsen et al. (2012), Pirzamanbein et al. (2014), and Trondman et al. (2015) agree on producing widespread Open Landscape values between ~0 and 30% at 6,000 BP for central and northern Europe (i.e., ~70–100% forest cover). These values are matched by the MAT-based reconstruction for the same area and time slice (range 60–90%), confirming further the validity of the MAT calibration algorithm.

In the British Isles, Woodbridge et al. (2014) set the onset of Neolithic land use in Britain at ~6,000 BP; this is also when our MAT-based forest cover begins its negative trend. A notable difference consists in a re-afforestation event detected by Woodbridge et al. (2014) between 5,400 and 4,200 BP which temporarily interrupts the overall negative Late Holocene decline. This event is not visible in the MAT-based curve, possibly due to a non-perfect comparability between the PBM land cover classes and the continuous MAT reconstruction.

The Mediterranean region shows an overall weak and gradual increase in open areas when compared with other more dramatic regional dynamics. The largely open landscape reconstructed during the Early/Middle Holocene is likely to play a primary role in lessening any evidence of radical human impact, yet other factors might contribute to this modest change in land cover too. As an example, even severe disturbance events (e.g., Cremaschi et al., 2006) might simply not be visible due to the spatial and temporal coverage of the underlying fossil database.

Vertical Performance of the Interpolation Procedure in the Alpine Region

It has been widely argued that pollen percentages alone are not sufficient to infer the local presence of tree populations in extreme environments at the limits of tree growth (e.g., Ponel et al., 1992; Tinner et al., 1996; Ali et al., 2003). Under these conditions, flowering season is negatively affected and trees tend to propagate via vegetative multiplication and not through sexual reproduction (Black and Bliss, 1980; Kullman, 1992; Charalampopoulos et al., 2013), likely altering their palynological signature. The combined interpretation of pollen percentages and influx may help in identifying clearer vegetation thresholds (Hicks, 1994), potentially countering the effect of upslope and long distance pollen transport. Still, the presence of macrofossils is considered the most solid piece of evidence to reconstruct vegetation history across the timberline (e.g., Birks and Birks, 2000). Considering the limits of pollen data in high-elevation contexts, in the present section we evaluate the capabilities of our model to detect much broader forest dynamics. Importantly, it again should be remembered that we reconstruct the area-average forest cover of the entire Alpine region, and that this might variously differ from individual site records and smaller regional studies.

By end of the Younger Dryas period (11,700 BP), alpine forests became rather open even in the lowlands (Ammann et al., 2007; Vescovi et al., 2007). This situation appears to be broadly compatible with our model, which does not produce values >50% before 11,750 BP. The following abrupt positive shift of the 50% threshold matches well the upward movement of forests at the transition into the Holocene (Tinner and Kaltenrieder, 2005). In their simulation of alpine biomass, Heiri et al. (2006) detect a short-lived dieback event around 10,500 BP. Notably, the MAT-based model records a mild stagnation episode of the 50% threshold approximately around the same period, between ~11,250 and 10,500 BP (**Figure 11**). Differences in the scale of the reconstructions, chronological uncertainties and temporal interpolation might explain the slight offset between the two events. Speculatively, the forest-cover stagnation seen in our model could be ascribed to the combined effects of the cool Preboreal oscillation (11,363/11,100 BP; Schwander et al., 2000) on alpine forests (Gobet et al., 2005), and to the dieback identified by Heiri et al. (2006). Major dieback events are described by Heiri et al. (2006) also between ~9,500–9,300 BP and ~6,500–6,000 BP, both matching mild – but not necessarily significant – elevation drops of the 50% threshold in our reconstruction. The prominent dieback described by Heiri et al. (2006) at 8,000 BP does not appear to be resolved in **Figure 11**, probably because of the temporal resolution of samples in the underlying pollen dataset. An overall regional change is anyway visible in **Figure 10**, where alpine forest-cover values drop noticeably after ~8,250 BP. Between 9,750 and ~7,000 BP the 50% threshold fluctuates mostly between 2,400 and 2,600 m. The lower value is in good agreement with the timberline elevation proposed by Tinner and Theurillat (2003) for the Swiss Central Alps, based on macrofossil analysis (**Figure 11**). Notably, estimates for maximum forest limits range from 2,500 m (Tessier et al., 1993) to 2,800 m (Talon, 2010) in the French Alps. After ~7,000 BP, the upper limit of the 50% threshold begins to drop quite steadily, likely reflecting the contribution of different local forest dynamics to our regional average. Treeline decline is visible as early as 6,350 BP in the Austrian Alps (Nicolussi et al., 2005), while it is recorded after ~5,750 in the Central Swiss Alps (**Figure 11** and Tinner and Theurillat, 2003). The abrupt timberline drop reconstructed by Tinner and Theurillat (2003) between 4,750 and 4,250 BP appears to be diluted in time in our reconstruction (**Figure 11**). The 50% threshold never exceeds 2,400 m after 5,750 BP, possibly reflecting the origin of anthropogenic pastures above 2,300 m during the Copper Age (~5,600 BP, Pini et al., 2017) and a subsequent continuous and growing exploitation of the high alpine landscape.

Ultimately, a comparison between our model and independent palaeo-ecological studies suggests that a combination of MAT and interpolation can reproduce broad vertical vegetation patterns (i.e., fluctuations of the upper limit of region-wide dense forests) at a resolution sufficient for large-scale vegetation models. The reconstruction of sharper forest-vs.-no-forest cutoffs remains beyond the capability of the interpolation procedure. Finer results could be achieved through the incorporation of complementary proxy data (i.e.,

plant macro remains, charcoal), although with the caveat that such data remain much less widely available than pollen records.

CONCLUSION

In this study we applied the MAT to generate a continuous, continental-scale reconstruction of European forest-cover spanning the last 12,000 years. Our reconstruction follows the general methodology published by Tarasov et al. (2007) and Williams et al. (2011). When compared with these studies, our work presents a series of improvements that extend the reliability and spatial/temporal coverage of the reconstruction. An increased number of samples in the modern database allows for stricter quality control and provides a better representation of different vegetation types. A larger fossil database allows for higher spatial density and better dating control. The satellite-based forest-cover data set used in previous studies (DeFries et al., 2000) was replaced with a higher resolution map (Hansen et al., 2013), leading to more reliable pairings between vegetation and modern pollen data. Furthermore, pollen taxa were aggregated into PFTs in order to reduce the occurrence of no-analog situations. The main improvement in mapping our results is the use of four-dimensional spatial interpolation (Mauri et al., 2015). This procedure extrapolates reconstructed vegetation data between a grid of fossil sites in both space and time, producing a set of forest-cover maps with continuous coverage and regular time-step at a continental scale. These characteristics represent a rather unique feature within the category of pollen-based quantitative vegetation reconstructions, and make these maps suitable for comparison with vegetation models and anthropogenic land-cover change scenarios.

The reliability of our reconstructions is supported by a comparison with methodologically independent data sets. forest-cover reconstructions based on the MAT (this study) and on the LRA were compared for selected sites (Marquer et al., 2014) in the circum-Baltic area. Both methodologies present widely comparable trends. Notable divergences are visible especially during the Mid-Holocene, with REVEALS consistently producing higher values. The limits of the MAT concerning the reconstruction of high forest covers can be ascribed to limitations within both the available training data set and the method itself. A visible role is played by the scarce representation of densely forested areas in the EMPD, an issue further exacerbated by the averaging nature of the MAT. Furthermore, the MAT does not have any intrinsic capability to correct for differential pollen productivity, or identify samples largely affected by long-distance pollen transport. These problems could be addressed through targeted sampling campaigns, aimed at improving the coverage of specific vegetation patterns in the EMPD, and possibly by introducing constraints based on pollen productivity and accumulation rates. Given the systematic occurrence of biased MAT results and the current inapplicability of constraint-based procedures, we opted to tackle this issue through a statistical approach to bias correction. We used Quantile Mapping to extract a calibration curve from the output of the cross-validation exercise. The effectiveness of this calibration approach is testified

by a visible reduction of the overall bias in both the cross-validation test and the comparison with REVEALS data.

The resulting continental-scale maps draw a coherent picture of vegetation development across Europe since the end of the Younger Dryas period. forest cover trends fit well in accepted narratives based on qualitative and quantitative interpretations of palaeovegetation data.

As a further test, we evaluated the vertical performance of the interpolation procedure against macrofossil-based tree line/timberline studies in the Alps. Detecting ecotones in alpine environments via pollen percentages is a task affected by wide margins of error. Consequently, we focused our comparison on broader vegetation patterns (i.e., variations in the upper limit of region-wide dense forests). A combination of MAT and spatio-temporal interpolation proved able to track major tree cover fluctuations in proximity of the timberline, thus reinforcing the broad reliability of the interpolation algorithm across a highly dynamic landscape.

AUTHOR CONTRIBUTIONS

MZ and BD designed the research. MZ performed the data analysis and presentation. LM contributed the independent (REVEALS) forest-cover reconstructions to aid method validation. MZ, BD, LM, SB, and JK were involved with substantial contributions in refining the methodology, writing, and reviewing the manuscript.

FUNDING

This research has been supported by grants from the Italian Ministry of Research and Education (FIRB RBID08LNFJ), the Swiss National Science Foundation (PP0022_119049), the European Research Council (COEVOLVE 313797), the Graduate School “Human Development in Landscapes” at Kiel University (GSC 208/2), and by the DFG Collaborative Research Centre SFB 1266.

ACKNOWLEDGMENTS

This study depends on the resources provided by the European Pollen Database and the PANGAEA data archive. The work of the data contributors and the EPD and PANGAEA communities is gratefully acknowledged.

SUPPLEMENTARY MATERIAL

The Supplementary Material for this article can be found online at: <https://www.frontiersin.org/articles/10.3389/fpls.2018.00253/full#supplementary-material>

The grid files of reconstructed forest cover, associated error estimates, and arboreal pollen percentages are available for download from <https://doi.pangaea.de/10.1594/PANGAEA.886656>

REFERENCES

- Ali, A. A., Carcaillet, C., Guendon, J.-L., Quinif, Y., Roiron, P., and Terral, J.-F. (2003). The early Holocene treeline in the southern French alps: new evidence from travertine formations. *Glob. Ecol. Biogeogr.* 12, 411–419. doi: 10.1046/j.1466-822X.2003.00055.x
- Ammann, B., Birks, H., Walanus, A., and Wasylikowa, K. (2007). “Late glacial multidisciplinary studies,” in *Encyclopedia of Quaternary Science*, ed. S. A. Elias (Amsterdam: Elsevier), 2475–2486. doi: 10.7892/boris.30415
- Andres, W., Bos, J. A., Houben, P., Kalis, A. J., Nolte, S., Rittweger, H., et al. (2001). Environmental change and fluvial activity during the Younger Dryas in central Germany. *Quat. Int.* 79, 89–100. doi: 10.1016/S1040-6182(00)00125-7
- Arino, O., Bicheron, P., Achard, F., Latham, J., Witt, R., and Weber, J.-L. (2008). *GlobCover. The Most Detailed Portrait of Earth. ESA*. Available at: http://www.esa.int/esapub/bulletin/bulletin136/bul136d_arino.pdf [accessed October 29, 2017].
- Bakels, C. C. (1995). Late glacial and Holocene pollen records from the Aisne and Vesle valleys, Northern France: the pollen diagrams Maizy-Cuiry and Bazoches. *Meded. Rijks Geol. Dienst* 52, 223–234.
- Baker, A. G., Zimny, M., Keczynski, A., Bhagwat, S. A., Willis, K. J., and Latalowa, M. (2016). Pollen productivity estimates from old-growth forest strongly differ from those obtained in cultural landscapes: evidence from the Białowieża National Park, Poland. *Holocene* 26, 80–92. doi: 10.1177/0959683615596822
- Barnekow, L. (2000). Holocene regional and local vegetation history and lake-level changes in the Torneträsk area, northern Sweden. *J. Paleolimnol.* 23, 399–420. doi: 10.1023/A:1008171418429
- Behre, K.-E. (1981). The interpretation of anthropogenic indicators in pollen diagrams. *Pollen Spores* 23, 225–245.
- Birks, H. H., and Birks, H. J. B. (2000). Future uses of pollen analysis must include plant macrofossils. *J. Biogeogr.* 27, 31–35. doi: 10.1046/j.1365-2699.2000.00375.x
- Birks, H. J. B. (1968). The Identification of *Betula nana* pollen. *New Phytol.* 67, 309–314. doi: 10.1111/j.1469-8137.1968.tb06386.x
- Birks, H. J. B., and Birks, H. H. (1980). *Quaternary Palaeoecology*. London: Edward Arnold.
- Birks, H. J. B., and Birks, H. H. (2016). How have studies of ancient DNA from sediments contributed to the reconstruction of Quaternary floras? *New Phytol.* 209, 499–506. doi: 10.1111/nph.13657
- Bjune, A., Birks, H. J. B., and Seppä, H. (2004). Holocene vegetation and climate history on a continental-oceanic transect in northern Fennoscandia based on pollen and plant macrofossils. *Boreas* 33, 211–223. doi: 10.1080/03009480410001244
- Black, R. A., and Bliss, L. C. (1980). Reproductive ecology of *Picea mariana* (Mill.) BSP., at tree line near Inuvik, Northwest Territories, Canada. *Ecol. Monogr.* 50, 331–354. doi: 10.2307/2937255
- Bordon, A., Peyron, O., Lézine, A.-M., Brewer, S., and Fouache, E. (2009). Pollen-inferred late-glacial and Holocene climate in southern Balkans (Lake Maliq). *Quat. Int.* 200, 19–30. doi: 10.1016/j.quaint.2008.05.014
- Bos, J. A. (2001). Lateglacial and early Holocene vegetation history of the northern Wetterau and the Amöneburger Basin (Hessen), central-west Germany. *Rev. Palaeobot. Palynol.* 115, 177–204. doi: 10.1016/S0034-6667(01)00069-0
- Bossard, M., Feranec, J., and Otahel, J. (2000). *CORINE Land Cover Technical Guide: Addendum 2000*. Technical Report No. 40. Copenhagen: European Environment Agency.
- Bowker, G. E., and Crenshaw, H. C. (2007). Electrostatic forces in wind-pollination—Part 2: simulations of pollen capture. *Atmos. Environ.* 41, 1596–1603. doi: 10.1016/j.atmosenv.2006.10.048
- Bradshaw, R. H., Jones, C. S., Edwards, S. J., and Hannon, G. E. (2015). Forest continuity and conservation value in Western Europe. *Holocene* 25, 194–202. doi: 10.1177/0959683614556378
- Brewer, S., Cheddadi, R., De Beaulieu, J. L., and Reille, M. (2002). The spread of deciduous *Quercus* throughout Europe since the last glacial period. *For. Ecol. Manag.* 156, 27–48. doi: 10.1016/S0378-1127(01)00646-6
- Brewer, S., Giesecke, T., Davis, B. A. S., Finsinger, W., Wolters, S., Binney, H., et al. (2016). Late-glacial and Holocene European pollen data. *J. Maps* 13, 921–928. doi: 10.1080/17445647.2016.1197613
- Broström, A., Gaillard, M.-J., Ihse, M., and Odgaard, B. (1998). Pollen-landscape relationships in modern analogues of ancient cultural landscapes in southern Sweden — a first step towards quantification of vegetation openness in the past. *Veg. Hist. Archaeobot.* 7, 189–201. doi: 10.1007/BF01146193
- Broström, A., Nielsen, A. B., Gaillard, M.-J., Hjelte, K., Mazier, F., Binney, H., et al. (2008). Pollen productivity estimates of key European plant taxa for quantitative reconstruction of past vegetation: a review. *Veg. Hist. Archaeobot.* 17, 461–478. doi: 10.1007/s00334-008-0148-8
- Burga, C. A., and Perret, R. (2001). “Monitoring of eastern and southern swiss alpine timberline ecotones,” in *Biomonitoring: General and Applied Aspects on Regional and Global Scales Tasks for Vegetation Science*, eds C. A. Burga and A. Kratochwil (Dordrecht: Springer), 179–194. doi: 10.1007/978-94-015-9686-2_11
- Büttner, G., Soukup, T., and Kosztra, B. (2014). *CLC2012 Addendum to CLC2006 Technical Guidelines. Final Draft*. Copenhagen: EEA.
- Calcote, R. (1995). Pollen source area and pollen productivity: evidence from forest hollows. *J. Ecol.* 83, 591–602. doi: 10.2307/2261627
- Calò, C., Henne, P. D., Curry, B., Magny, M., Vescovi, E., La Mantia, T., et al. (2012). Spatio-temporal patterns of Holocene environmental change in southern Sicily. *Palaeogeogr. Palaeoclimatol. Palaeoecol.* 32, 110–122. doi: 10.1016/j.palaeo.2012.01.038
- Cañellas-Boltà, N., Rull, V., Vigo, J., and Mercadé, A. (2009). Modern pollen—vegetation relationships along an altitudinal transect in the central Pyrenees (southwestern Europe). *Holocene* 19, 1185–1200. doi: 10.1177/0959683609345082
- Carrión, J. S. (2002). Patterns and processes of Late Quaternary environmental change in a montane region of southwestern Europe. *Quat. Sci. Rev.* 21, 2047–2066. doi: 10.1016/S0277-3791(02)00010-0
- Carrión, J. S., and Dupré, M. (1996). Late Quaternary vegetational history at Navarrés, Eastern Spain. A two core approach. *New Phytol.* 134, 177–191. doi: 10.1111/j.1469-8137.1996.tb01157.x
- Carrión, J. S., Fernández, S., González-Sampériz, P., Gil-Romera, G., Badal, E., Carrión-Marco, Y., et al. (2010). Expected trends and surprises in the Lateglacial and Holocene vegetation history of the Iberian Peninsula and Balearic Islands. *Rev. Palaeobot. Palynol.* 162, 458–475. doi: 10.1016/j.revpalbo.2009.12.007
- Carrión, J. S., and Van Geel, B. (1999). Fine-resolution Upper Weichselian and Holocene palynological record from Navarrés (Valencia, Spain) and a discussion about factors of Mediterranean forest succession. *Rev. Palaeobot. Palynol.* 106, 209–236. doi: 10.1016/S0034-6667(99)00009-3
- Charalampopoulos, A., Damialis, A., Tsiripidis, I., Mavrommatis, T., Halley, J. M., and Vokou, D. (2013). Pollen production and circulation patterns along an elevation gradient in Mt Olympus (Greece) National Park. *Aerobiologia* 29, 455–472. doi: 10.1007/s10453-013-9296-0
- Collins, P. M., Davis, B. A. S., and Kaplan, J. O. (2012). The mid-Holocene vegetation of the Mediterranean region and southern Europe, and comparison with the present day: Mid-Holocene Mediterranean vegetation. *J. Biogeogr.* 39, 1848–1861. doi: 10.1111/j.1365-2699.2012.02738.x
- Combourieu-Nebout, N., Peyron, O., Bout-Roumazeilles, V., Goring, S., Dormoy, I., Joannin, S., et al. (2013). Holocene vegetation and climate changes in the central Mediterranean inferred from a high-resolution marine pollen record (Adriatic Sea). *Clim. Past* 9, 2023–2042. doi: 10.5194/cp-9-2023-2013
- Court-Picon, M., Buttler, A., and de Beaulieu, J.-L. (2006). Modern pollen/vegetation/land-use relationships in mountain environments: an example from the Champsaur valley (French Alps). *Veg. Hist. Archaeobot.* 15:151. doi: 10.1007/s00334-005-0008-8
- Cremaschi, M., Pizzi, C., and Valsecchi, V. (2006). Water management and land use in the terramare and a possible climatic co-factor in their abandonment: the case study of the terramare of Poviglio Santa Rosa (northern Italy). *Quat. Int.* 151, 87–98. doi: 10.1016/j.quaint.2006.01.020
- Cui, Q.-Y., Gaillard, M.-J., Lemdahl, G., Stenberg, L., Sugita, S., and Zernova, G. (2014). Historical land-use and landscape change in southern Sweden and implications for present and future biodiversity. *Ecol. Evol.* 4, 3555–3570. doi: 10.1002/ece3.1198
- Cui, Q.-Y., Gaillard, M.-J., Lemdahl, G., Sugita, S., Greisman, A., Jacobson, G. L., et al. (2013). The role of tree composition in Holocene fire history of the hemiboreal and southern boreal zones of southern Sweden, as revealed by the application of the Landscape Reconstruction Algorithm: implications for

- biodiversity and climate-change issues. *Holocene* 23, 1747–1763. doi: 10.1177/0959683613505339
- Davies, C. P., and Fall, P. L. (2001). Modern pollen precipitation from an elevational transect in central Jordan and its relationship to vegetation: modern vegetation and pollen in Jordan. *J. Biogeogr.* 28, 1195–1210. doi: 10.1046/j.1365-2699.2001.00630.x
- Davis, B. A. S., Brewer, S., Stevenson, A. C., and Guiot, J. (2003). The temperature of Europe during the Holocene reconstructed from pollen data. *Quat. Sci. Rev.* 22, 1701–1716. doi: 10.1016/S0277-3791(03)00173-2
- Davis, B. A. S., Collins, P. M., and Kaplan, J. O. (2015). The age and post-glacial development of the modern European vegetation: a plant functional approach based on pollen data. *Veg. Hist. Archaeobot.* 24, 303–317. doi: 10.1007/s00334-014-0476-9
- Davis, B. A. S., Zanon, M., Collins, P., Mauri, A., Bakker, J., Barboni, D., et al. (2013). The European modern pollen database (EMPD) project. *Veg. Hist. Archaeobot.* 22, 521–530. doi: 10.1007/s00334-012-0388-5
- Dawson, A., Paciorek, C. J., McLachlan, J. S., Goring, S., Williams, J. W., and Jackson, S. T. (2016). Quantifying pollen-vegetation relationships to reconstruct ancient forests using 19th-century forest composition and pollen data. *Quat. Sci. Rev.* 137, 156–175. doi: 10.1016/j.quascirev.2016.01.012
- DeFries, R. S., Hansen, M. C., Townshend, J. R. G., Janetos, A. C., and Loveland, T. R. (2000). A new global 1-km dataset of percentage tree cover derived from remote sensing. *Glob. Change Biol.* 6, 247–254. doi: 10.1046/j.1365-2486.2000.00296.x
- Edwards, K. J., Fyfe, R. M., and Jackson, S. T. (2017). The first 100 years of pollen analysis. *Nat. Plants* 3:17001. doi: 10.1038/nplants.2017.1
- Finsinger, W., Tinner, W., Vanderknaap, W., and Ammann, B. (2006). The expansion of hazel (*Corylus avellana* L.) in the Southern Alps: a key for understanding its early Holocene history in Europe? *Quat. Sci. Rev.* 25, 612–631. doi: 10.1016/j.quascirev.2005.05.006
- Furrer, R., Nychka, D., and Sain, S. (2013). *fields: Tools for Spatial Data*. Available at: <http://www.image.ucar.edu/fields>
- Fyfe, R. M., de Beaulieu, J.-L., Binney, H., Bradshaw, R. H. W., Brewer, S., Le Flao, A., et al. (2009). The European pollen database: past efforts and current activities. *Veg. Hist. Archaeobot.* 18, 417–424. doi: 10.1007/s00334-009-0215-9
- Fyfe, R. M., Twiddle, C., Sugita, S., Gaillard, M.-J., Barratt, P., Caseldine, C. J., et al. (2013). The Holocene vegetation cover of Britain and Ireland: overcoming problems of scale and discerning patterns of openness. *Quat. Sci. Rev.* 73, 132–148. doi: 10.1016/j.quascirev.2013.05.014
- Fyfe, R. M., Woodbridge, J., and Roberts, N. (2015). From forest to farmland: pollen-inferred land cover change across Europe using the pseudobiomization approach. *Glob. Change Biol.* 21, 1197–1212. doi: 10.1111/gcb.12776
- Gaillard, M.-J., Sugita, S., Bunting, J., Dearing, J., and Bittmann, F. (2008). Human impact on terrestrial ecosystems, pollen calibration and quantitative reconstruction of past land-cover. *Veg. Hist. Archaeobot.* 17, 415–418. doi: 10.1007/s00334-008-0170-x
- Gaillard, M.-J., Sugita, S., Mazier, F., Trondman, A.-K., Broström, A., Hickler, T., et al. (2010). Holocene land-cover reconstructions for studies on land cover-climate feedbacks. *Clim. Past* 6, 483–499. doi: 10.5194/cp-6-483-2010
- Gardner, A. R., and Willis, K. J. (1999). Prehistoric farming and the postglacial expansion of beech and hombeam: a comment on Küster. *Holocene* 9, 119–121. doi: 10.1191/09596839968254353
- Gavin, D. G., Oswald, W. W., Wahl, E. R., and Williams, J. W. (2003). A statistical approach to evaluating distance metrics and analog assignments for pollen records. *Quat. Res.* 60, 356–367. doi: 10.1016/S0033-5894(03)00088-7
- Gerber, S., Chadšuf, J., Gugerli, F., Lascoux, M., Buiteveld, J., Cottrell, J., et al. (2014). High rates of gene flow by pollen and seed in oak populations across Europe. *PLoS One* 9:e85130. doi: 10.1371/journal.pone.0085130
- Giesecke, T., Bennett, K. D., Birks, H. J. B., Björne, A. E., Bozlova, E., Feurdean, A., et al. (2011). The pace of Holocene vegetation change – testing for synchronous developments. *Quat. Sci. Rev.* 30, 2805–2814. doi: 10.1016/j.quascirev.2011.06.014
- Giesecke, T., Davis, B., Brewer, S., Finsinger, W., Wolters, S., Blaauw, M., et al. (2013). Towards mapping the late Quaternary vegetation change of Europe. *Veg. Hist. Archaeobot.* 23, 75–86. doi: 10.1007/s00334-012-0390-y
- Gobet, E., Tinner, W., Bigler, C., Hochuli, P. A., and Ammann, B. (2005). Early-Holocene afforestation processes in the lower subalpine belt of the Central Swiss Alps as inferred from macrofossil and pollen records. *Holocene* 15, 672–686. doi: 10.1191/0959683605hl843rp
- Gudmundsson, L. (2016). *qmap: Statistical Transformations for Post-Processing Climate Model Output*. Available at: <https://cran.r-project.org/web/packages/qmap/index.html>
- Guiot, J. (1990). Methodology of the last climatic cycle reconstruction in France from pollen data. *Palaeogeogr. Palaeoclimatol. Palaeoecol.* 80, 49–69. doi: 10.1016/0031-0182(90)90033-4
- Guitier, F., Andrieu-Ponel, V., Digerfeldt, G., Reille, M., de Beaulieu, J.-L., and Ponel, P. (2005). Vegetation history and lake-level changes from the Younger Dryas to the present in Eastern Pyrenees (France): pollen, plant macrofossils and lithostratigraphy from Lake Racou (2000 m a.s.l.). *Veg. Hist. Archaeobot.* 14, 99–118. doi: 10.1007/s00334-005-0065-z
- Hansen, M. C., Potapov, P. V., Moore, R., Hancher, M., Turubanova, S. A., Tyukavina, A., et al. (2013). High-resolution global maps of 21st-century forest cover change. *Science* 342, 850–853. doi: 10.1126/science.1244693
- Heikkilä, M., Fontana, S. L., and Seppä, H. (2009). Rapid Lateglacial tree population dynamics and ecosystem changes in the eastern Baltic region. *J. Quat. Sci.* 24, 802–815. doi: 10.1002/jqs.1254
- Heiri, C., Bugmann, H., Tinner, W., Heiri, O., and Lischke, H. (2006). A model-based reconstruction of Holocene treeline dynamics in the Central Swiss Alps. *J. Ecol.* 94, 206–216. doi: 10.1111/j.1365-2745.2005.01072.x
- Hicks, S. (1994). Present and past pollen records of Lapland forests. *Rev. Palaeobot. Palynol.* 82, 17–35. doi: 10.1016/0034-6667(94)90017-5
- Hohensinner, S., Sonnlechner, C., Schmid, M., and Winiwarter, V. (2013). Two steps back, one step forward: reconstructing the dynamic Danube riverscape under human influence in Vienna. *Water Hist.* 5, 121–143. doi: 10.1007/s12685-013-0076-0
- Hollister, J., and Shah, T. (2017). *elevatr: Access Elevation Data from Various APIs*. Available at: <https://cran.r-project.org/web/packages/elevatr/index.html>
- Huntley, B. (1990). Dissimilarity mapping between fossil and contemporary pollen spectra in Europe for the past 13,000 years. *Quat. Res.* 33, 360–376. doi: 10.1016/0033-5894(90)90062-P
- Huntley, B., and Birks, H. J. B. (1983). *An Atlas of Past and Present Pollen Maps for Europe, 0-13,000 Years Ago*. Cambridge: Cambridge University Press. doi: 10.1016/0034-6667(86)90044-8
- Jackson, S. T. (1994). “Pollen and spores in Quaternary lake sediments as sensors of vegetation composition: theoretical models and empirical evidence,” in *Sedimentation of Organic Particles*, ed. A. Traverse (Cambridge: Cambridge University Press), 253–286. doi: 10.1017/CBO9780511524875.015
- Jackson, S. T., and Williams, J. W. (2004). Modern analogs in quaternary paleoecology: here today, gone yesterday, gone tomorrow? *Annu. Rev. Earth Planet. Sci.* 32, 495–537. doi: 10.1146/annurev.earth.32.101802.120435
- Jacobson, G. L., and Bradshaw, R. H. (1981). The selection of sites for paleovegetational studies. *Quat. Res.* 16, 80–96. doi: 10.1016/0033-5894(81)90129-0
- Jahns, S. (2007). Palynological investigations into the Late Pleistocene and Holocene history of vegetation and settlement at the Löddigsee, Mecklenburg, Germany. *Veg. Hist. Archaeobot.* 16, 157–169. doi: 10.1007/s00334-006-0074-6
- Juggins, S. (2016). *rioja: Analysis of Quaternary Science Data*. Available at: <https://cran.r-project.org/web/packages/rioja/index.html> [accessed August 24, 2016].
- Kallimanis, A. S., and Koutsias, N. (2013). Geographical patterns of Corine land cover diversity across Europe: the effect of grain size and thematic resolution. *Prog. Phys. Geogr.* 37, 161–177. doi: 10.1177/0309133312465303
- Kaplan, J. O., Krumhardt, K. M., and Zimmermann, N. (2009). The prehistoric and preindustrial deforestation of Europe. *Quat. Sci. Rev.* 28, 3016–3034. doi: 10.1016/j.quascirev.2009.09.028
- Kaplan, J. O., Prentice, I. C., Knorr, W., and Valdes, P. J. (2002). Modeling the dynamics of terrestrial carbon storage since the Last Glacial Maximum. *Geophys. Res. Lett.* 29:d2074. doi: 10.1029/2002GL015230
- Kihno, K., Saarse, L., and Amon, L. (2011). Late Glacial vegetation, sedimentation and ice recession chronology in the surroundings of Lake Prossa, central Estonia. *Est. J. Earth Sci.* 60, 147–158. doi: 10.3176/earth.2011.3.03
- Kleinen, T., Tarasov, P., Brovkin, V., Andreev, A., and Stebich, M. (2011). Comparison of modeled and reconstructed changes in forest cover through the past 8000 years: Eurasian perspective. *Holocene* 21, 723–734. doi: 10.1177/0959683610386980

- Kreuz, A. (2007). Closed forest or open woodland as natural vegetation in the surroundings of Linearbandkeramik settlements? *Veg. Hist. Archaeobot.* 17, 51–64. doi: 10.1007/s00334-007-0110-1
- Kullman, L. (1992). The ecological status of grey alder (*Alnus incana* (L.) Moench) in the upper subalpine birch forest of the central Scandes. *New Phytol.* 120, 445–451. doi: 10.1111/j.1469-8137.1992.tb01085.x
- Kullman, L. (2002). Boreal tree taxa in the central Scandes during the Late-Glacial: implications for Late-Quaternary forest history. *J. Biogeogr.* 29, 1117–1124. doi: 10.1046/j.1365-2699.2002.00743.x
- Ladeau, S. L., and Clark, J. S. (2006). Pollen production by *Pinus taeda* growing in elevated atmospheric CO₂. *Funct. Ecol.* 20, 541–547. doi: 10.1111/j.1365-2435.2006.01133.x
- Lafon, T., Dadson, S., Buys, G., and Prudhomme, C. (2013). Bias correction of daily precipitation simulated by a regional climate model: a comparison of methods. *Int. J. Climatol.* 33, 1367–1381. doi: 10.1002/joc.3518
- Lambrechts, C., Wilkie, M., Rucevska, I., Sen, M., Conrad, K. M., Joshi, M., et al. (eds). (2009). *Vital Forest Graphics. UNEP/GRID-Arendal*. Nairobi: United Nations Environment Programme.
- Langgut, D., Almogi-Labin, A., Bar-Matthews, M., and Weinstein-Evron, M. (2011). Vegetation and climate changes in the South Eastern Mediterranean during the Last Glacial-Interglacial cycle (86 ka): new marine pollen record. *Quat. Sci. Rev.* 30, 3960–3972. doi: 10.1016/j.quascirev.2011.10.016
- Lavigne, C., Godelle, B., Reboud, X., and Gouyon, P. H. (1996). A method to determine the mean pollen dispersal of individual plants growing within a large pollen source. *Theor. Appl. Genet.* 93, 1319–1326. doi: 10.1007/BF00223465
- Lawson, I., Frogley, M., Bryant, C., Preece, R., and Tzedakis, P. (2004). The Lateglacial and Holocene environmental history of the Ioannina basin, north-west Greece. *Quat. Sci. Rev.* 23, 1599–1625. doi: 10.1016/j.quascirev.2004.02.003
- Magri, D. (2008). Patterns of post-glacial spread and the extent of glacial refugia of European beech (*Fagus sylvatica*). *J. Biogeogr.* 35, 450–463. doi: 10.1111/j.1365-2699.2007.01803.x
- Marquer, L., Gaillard, M.-J., Sugita, S., Poska, A., Trondman, A.-K., Mazier, F., et al. (2017). Quantifying the effects of land use and climate on Holocene vegetation in Europe. *Quat. Sci. Rev.* 171, 20–37. doi: 10.1016/j.quascirev.2017.07.001
- Marquer, L., Gaillard, M.-J., Sugita, S., Trondman, A.-K., Mazier, F., Nielsen, A. B., et al. (2014). Holocene changes in vegetation composition in northern Europe: why quantitative pollen-based vegetation reconstructions matter. *Quat. Sci. Rev.* 90, 199–216. doi: 10.1016/j.quascirev.2014.02.013
- Matthias, I., and Giesecke, T. (2014). Insights into pollen source area, transport and deposition from modern pollen accumulation rates in lake sediments. *Quat. Sci. Rev.* 87, 12–23. doi: 10.1016/j.quascirev.2013.12.015
- Matthias, I., Nielsen, A. B., and Giesecke, T. (2012). Evaluating the effect of flowering age and forest structure on pollen productivity estimates. *Veg. Hist. Archaeobot.* 21, 471–484. doi: 10.1007/s00334-012-0373-z
- Mauri, A., Davis, B. A. S., Collins, P. M., and Kaplan, J. O. (2015). The climate of Europe during the Holocene: a gridded pollen-based reconstruction and its multi-proxy evaluation. *Quat. Sci. Rev.* 112, 109–127. doi: 10.1016/j.quascirev.2015.01.013
- Mazier, F., Broström, A., Bragée, P., Fredh, D., Stenberg, L., Thiere, G., et al. (2015). Two hundred years of land-use change in the South Swedish Uplands: comparison of historical map-based estimates with a pollen-based reconstruction using the landscape reconstruction algorithm. *Veg. Hist. Archaeobot.* 24, 555–570. doi: 10.1007/s00334-015-0516-0
- Mazier, F., Gaillard, M.-J., Kuneš, P., Sugita, S., Trondman, A.-K., and Broström, A. (2012). Testing the effect of site selection and parameter setting on REVEALS-model estimates of plant abundance using the Czech Quaternary Palynological Database. *Rev. Palaeobot. Palynol.* 187, 38–49. doi: 10.1016/j.revpalbo.2012.07.017
- McDuffee, K. E., Eglinton, T. I., Sessions, A. L., Sylva, S., Wagner, T., and Hayes, J. M. (2004). Rapid analysis of 13 C in plant-wax *n*-alkanes for reconstruction of terrestrial vegetation signals from aquatic sediments: ANALYSIS OF 13 C IN PLANT-WAX *N*-ALKANES. *Geochim. Geophys. Geosyst.* 5:Q10004. doi: 10.1029/2004GC000772
- Mitchell, F. J. G. (2005). How open were European primeval forests? Hypothesis testing using palaeoecological data. *J. Ecol.* 93, 168–177. doi: 10.1111/j.1365-2745.2004.00964.x
- Moracho, E., Moreno, G., Jordano, P., and Hampe, A. (2016). Unusually limited pollen dispersal and connectivity of Pedunculate oak (*Quercus robur*) refugial populations at the species' southern range margin. *Mol. Ecol.* 25, 3319–3331. doi: 10.1111/mec.13692
- Muñoz Sobrino, C., Ramil-Rego, P., and Gómez-Orellana, L. (2004). Vegetation of the Lago de Sanabria area (NW Iberia) since the end of the Pleistocene: a palaeoecological reconstruction on the basis of two new pollen sequences. *Veg. Hist. Archaeobot.* 13, 1–22. doi: 10.1007/s00334-003-0028-1
- Nelle, O., and Dörfler, W. (2008). A summary of the late- and post-glacial vegetation history of Schleswig-Holstein. *Mitt. Arbeitsgemeinschaft Geobot. Schlesw. Holst. Hambg.* 65, 45–68.
- Nicolussi, K., Kaufmann, M., Patzelt, G., van der Plicht, J., and Thurner, A. (2005). Holocene tree-line variability in the Kauner Valley, Central Eastern Alps, indicated by dendrochronological analysis of living trees and subfossil logs. *Veg. Hist. Archaeobot.* 14, 221–234. doi: 10.1007/s00334-005-0013-y
- Nielsen, A. B., Giesecke, T., Theuerkauf, M., Feeser, I., Behre, K.-E., Beug, H.-J., et al. (2012). Quantitative reconstructions of changes in regional openness in north-central Europe reveal new insights into old questions. *Quat. Sci. Rev.* 47, 131–149. doi: 10.1016/j.quascirev.2012.05.011
- Nielsen, A. B., and Odgaard, B. V. (2010). Quantitative landscape dynamics in Denmark through the last three millennia based on the Landscape Reconstruction Algorithm approach. *Veg. Hist. Archaeobot.* 19, 375–387. doi: 10.1007/s00334-010-0249-z
- Overballe-Petersen, M. V., Nielsen, A. B., and Bradshaw, R. H. W. (2013). Quantitative vegetation reconstruction from pollen analysis and historical inventory data around a Danish small forest hollow. *J. Veg. Sci.* 24, 755–771. doi: 10.1111/jvs.12007
- Overpeck, J. T., Webb, T., and Prentice, I. C. (1985). Quantitative interpretation of fossil pollen spectra: dissimilarity coefficients and the method of modern analogs. *Quat. Res.* 23, 87–108. doi: 10.1016/0033-5894(85)90074-2
- Palmieri, A., Dominici, P., Kasanko, M., and Martino, L. (2011). *Diversified Landscape Structure in the EU Member States. Eurostat Stat. Focus* 21. Available at: <http://edz.bib.uni-mannheim.de/edz/pdf/statinf/11/KS-SF-11-021-EN.PDF> [accessed September 26, 2017].
- Pantaléon-Cano, J., Yll, E.-I., Pérez-Obiol, R., and Roure, J. M. (2003). Palynological evidence for vegetational history in semi-arid areas of the western Mediterranean (Almería, Spain). *Holocene* 13, 109–119. doi: 10.1191/0959683603hl598rp
- Pardoe, H. S. (2014). Surface pollen deposition on glacier forelands in southern Norway II: spatial patterns across the Jotunheimen–Jostedalbreen region. *Holocene* 24, 1675–1685. doi: 10.1177/0959683614551213
- Peng, C. H., Guiot, J., Campo, E. V., and Cheddadi, R. (1995). “Temporal and spatial variations of terrestrial biomes and carbon storage since 13 000 yr BP in Europe: reconstruction from pollen data and statistical models,” in *Boreal Forests and Global Change*, ed. M. J. Apps (Dordrecht: Springer), 375–390. doi: 10.1007/978-94-017-0942-2_36
- Perego, R., Badino, F., Deaddis, M., Ravazzi, C., Vallè, F., and Zanon, M. (2011). L'origine del paesaggio agricolo pastorale in nord Italia: espansione di *Orlaya grandiflora* (L.) Hoffm. nella civiltà palafitticola. *Not. Archeol. Bergomensi* 19, 161–173.
- Peyron, O., Guiot, J., Cheddadi, R., Tarasov, P., Reille, M., de Beaulieu, J.-L., et al. (1998). Climatic reconstruction in Europe for 18,000 YR B.P. from pollen data. *Quat. Res.* 49, 183–196. doi: 10.1006/qres.1997.1961
- Pini, R., Ravazzi, C., Raiteri, L., Guerreschi, A., Castellano, L., and Comolli, R. (2017). From pristine forests to high-altitude pastures: an ecological approach to prehistoric human impact on vegetation and landscapes in the western Italian Alps. *J. Ecol.* 105, 1580–1597. doi: 10.1111/1365-2745.12767
- Pirzamanbein, B., Lindström, J., Poska, A., Sugita, S., Trondman, A.-K., Fyfe, R., et al. (2014). Creating spatially continuous maps of past land cover from point estimates: a new statistical approach applied to pollen data. *Ecol. Complex.* 20, 127–141. doi: 10.1016/j.ecocom.2014.09.005
- Ponel, P., de Beaulieu, J. L., and Tobolski, K. (1992). Holocene paleoenvironment at the timberline in the Taillefer Massif: pollen analysis, study of plant and insect macrofossils. *Holocene* 2, 117–130. doi: 10.1177/095968369200200203
- Pongratz, J., Reick, C., Raddatz, T., and Claussen, M. (2008). A reconstruction of global agricultural areas and land cover for the last millennium. *Glob. Biogeochem. Cycles* 22:GB3018. doi: 10.1029/2007GB003153
- Potapov, P. V., Turubanova, S. A., Tyukavina, A., Krylov, A. M., McCarty, J. L., Radeloff, V. C., et al. (2015). Eastern Europe's forest cover dynamics from 1985

- to 2012 quantified from the full Landsat archive. *Remote Sens. Environ.* 159, 28–43. doi: 10.1016/j.rse.2014.11.027
- Preece, R. C., Coxon, P., and Robinson, J. E. (1986). New biostratigraphic evidence of the post-glacial colonization of Ireland and for Mesolithic forest disturbance. *J. Biogeogr.* 13, 487–509. doi: 10.2307/2844814
- Prentice, C., Guiot, J., Huntley, B., Jolly, D., and Cheddadi, R. (1996). Reconstructing biomes from palaeoecological data: a general method and its application to European pollen data at 0 and 6 ka. *Clim. Dyn.* 12, 185–194. doi: 10.1007/BF00211617
- Prentice, I. C. (1985). Pollen representation, source area, and basin size: toward a unified theory of pollen analysis. *Quat. Res.* 23, 76–86. doi: 10.1016/0033-5894(85)90073-0
- Prentice, I. C., Jolly, D., and Biome 6000 participants (2000). Mid-Holocene and glacial-maximum vegetation geography of the northern continents and Africa. *J. Biogeogr.* 27, 507–519. doi: 10.1046/j.1365-2699.2000.00425.x
- Prentice, I. C., and Parsons, R. W. (1983). Maximum likelihood linear calibration of pollen spectra in terms of forest composition. *Biometrics* 39, 1051–1057. doi: 10.2307/2531338
- Ravazzi, C. (2002). Late Quaternary history of spruce in southern Europe. *Rev. Palaeobot. Palynol.* 120, 131–177. doi: 10.1016/S0034-6667(01)00149-X
- Rivas-Martínez, S., Penas, A., and Díaz, T. E. (2004). *Biogeographic and Bioclimatic Maps of Europe*. León: Universidade León.
- Roberts, N., Reed, J. M., Leng, M. J., Kuzucuoğlu, C., Fontugne, M., Bertaux, J., et al. (2001). The tempo of Holocene climatic change in the eastern Mediterranean region: new high-resolution crater-lake sediment data from central Turkey. *Holocene* 11, 721–736. doi: 10.1191/09596830195744
- Robin, V., Rickert, B.-H., Nadeau, M.-J., and Nelle, O. (2011). Assessing Holocene vegetation and fire history by a multiproxy approach: the case of Stadthagen Forest (northern Germany). *Holocene* 22, 337–346. doi: 10.1177/0959683611423687
- Robledo-Arnuncio, J. J., and Gil, L. (2005). Patterns of pollen dispersal in a small population of *Pinus sylvestris* L. revealed by total-exclusion paternity analysis. *Heredity* 94, 13–22. doi: 10.1038/sj.hdy.6800542
- Rossignol-Strick, M. (1995). Sea-land correlation of pollen records in the eastern Mediterranean for the glacial-interglacial transition: biostratigraphy versus radiometric time-scale. *Quat. Sci. Rev.* 14, 893–915. doi: 10.1016/0277-3791(95)00070-4
- Rubiales, J. M., García-Amorena, I., Hernández, L., Génova, M., Martínez, F., Manzanque, F. G., et al. (2010). Late Quaternary dynamics of pinewoods in the Iberian Mountains. *Rev. Palaeobot. Palynol.* 162, 476–491. doi: 10.1016/j.revpalbo.2009.11.008
- Sadori, L., Jahns, S., and Peyron, O. (2011). Mid-Holocene vegetation history of the central Mediterranean. *Holocene* 21, 117–129. doi: 10.1177/0959683610377530
- Schwander, J., Eicher, U., and Ammann, B. (2000). Oxygen isotopes of lake marl at Gerzensee and Leysin (Switzerland), covering the Younger Dryas and two minor oscillations, and their correlation to the GRIP ice core. *Palaeogeogr. Palaeoclimatol. Palaeoecol.* 159, 203–214. doi: 10.1016/S0031-0182(00)00085-7
- Seppä, H. (1998). Postglacial trends in palynological richness in the northern Fennoscandian tree-line area and their ecological interpretation. *Holocene* 8, 43–53. doi: 10.1191/095968398674096317
- Simard, M., Pinto, N., Fisher, J. B., and Baccini, A. (2011). Mapping forest canopy height globally with spaceborne lidar. *J. Geophys. Res. Biogeosci.* 116:G04021. doi: 10.1029/2011JG001708
- Sobkowiak-Tabaka, I., Kubiak-Martens, L., Okuniewska-Nowaczyk, I., Ratajczak-Szczerba, M., Kurawska, A., and Kufel-Diakowska, B. (2017). Reconstruction of the Late Glacial and Early Holocene landscape and human presence in Lubrza, Western Poland, on the basis of multidisciplinary analyses. *Environ. Archaeol.* 1–14. doi: 10.1080/14614103.2016.1268993
- Solovieva, N., Klimaschewski, A., Self, A. E., Jones, V. J., Andrén, E., Andreev, A. A., et al. (2015). The Holocene environmental history of a small coastal lake on the north-eastern Kamchatka Peninsula. *Glob. Planet. Change* 134, 55–66. doi: 10.1016/j.gloplacha.2015.06.010
- Streiff, R., Ducouso, A., Lexer, C., Steinkellner, H., Gloessl, J., and Kremer, A. (1999). Pollen dispersal inferred from paternity analysis in a mixed oak stand of *Quercus robur* L. and *Q. petraea* (Matt.) Liebl. *Mol. Ecol.* 8, 831–841. doi: 10.1046/j.1365-294X.1999.00637.x
- Sugita, S. (1993). A model of pollen source area for an entire lake surface. *Quat. Res.* 39, 239–244. doi: 10.1006/qres.1993.1027
- Sugita, S. (1994). Pollen representation of vegetation in quaternary sediments: theory and method in patchy vegetation. *J. Ecol.* 82, 881–897. doi: 10.2307/2261452
- Sugita, S. (2007a). Theory of quantitative reconstruction of vegetation I: pollen from large sites REVEALS regional vegetation composition. *Holocene* 17, 229–241. doi: 10.1177/0959683607075837
- Sugita, S. (2007b). Theory of quantitative reconstruction of vegetation II: all you need is LOVE. *Holocene* 17, 243–257. doi: 10.1177/0959683607075838
- Sugita, S., Parshall, T., Calcote, R., and Walker, K. (2010). Testing the landscape reconstruction algorithm for spatially explicit reconstruction of vegetation in northern Michigan and Wisconsin. *Quat. Res.* 74, 289–300. doi: 10.1016/j.yqres.2010.07.008
- Szerencsits, E. (2012). Swiss tree lines - a GIS-based approximation. *Landsc. Online* 28, 1–18. doi: 10.3097/LO.201228
- Talon, B. (2010). Reconstruction of Holocene high-altitude vegetation cover in the French Southern Alps: evidence from soil charcoal. *Holocene* 20, 35–44. doi: 10.1177/0959683609348842
- Tarasov, P., Williams, J. W., Andreev, A., Nakagawa, T., Bezrukova, E., Herzschuh, U., et al. (2007). Satellite- and pollen-based quantitative woody cover reconstructions for northern Asia: verification and application to late-Quaternary pollen data. *Earth Planet. Sci. Lett.* 264, 284–298. doi: 10.1016/j.epsl.2007.10.007
- Tarasov, P. E., Cheddadi, R., Guiot, J., Bottema, S., Peyron, O., Belmonte, J., et al. (1998). A method to determine warm and cool steppe biomes from pollen data; application to the Mediterranean and Kazakhstan regions. *J. Quat. Sci.* 13, 335–344. doi: 10.1002/(SICI)1099-1417(199807/08)13:4<335::AID-JQS375>3.0.CO;2-A
- Telford, R. J., and Birks, H. J. B. (2009). Evaluation of transfer functions in spatially structured environments. *Quat. Sci. Rev.* 28, 1309–1316. doi: 10.1016/j.quascirev.2008.12.020
- Tessier, L., Beaulieu, J.-L. D., Couteaux, M., Edouard, J.-L., Ponel, P., Rolando, C., et al. (1993). Holocene palaeoenvironments at the timberline in the French Alps—a multidisciplinary approach. *Boreas* 22, 244–254. doi: 10.1111/j.1502-3885.1993.tb00184.x
- Tinner, W., Ammann, B., and Germann, P. (1996). Treeline fluctuations recorded for 12,500 years by soil profiles, pollen, and plant macrofossils in the Central Swiss Alps. *Arct. Alp. Res.* 28, 131–147. doi: 10.2307/1551753
- Tinner, W., and Kaltenrieder, P. (2005). Rapid responses of high-mountain vegetation to early Holocene environmental changes in the Swiss Alps. *J. Ecol.* 93, 936–947. doi: 10.1111/j.1365-2745.2005.01023.x
- Tinner, W., and Theurillat, J.-P. (2003). Uppermost limit, extent, and fluctuations of the timberline and treeline ecocline in the Swiss central Alps during the past 11,500 years. *Arct. Antarct. Alp. Res.* 35, 158–169. doi: 10.1657/1523-0430(2003)035[0158:ULEAFO]2.0.CO;2
- Tinner, W., van Leeuwen, J. F. N., Colombaroli, D., Vescovi, E., van der Knaap, W. O., Henne, P. D., et al. (2009). Holocene environmental and climatic changes at Gorgo Basso, a coastal lake in southern Sicily, Italy. *Quat. Sci. Rev.* 28, 1498–1510. doi: 10.1016/j.quascirev.2009.02.001
- Tinsley, H. M., and Smith, R. T. (1974). Surface pollen studies across a woodland/heath transition and their application to the interpretation of pollen diagrams. *New Phytol.* 73, 547–565. doi: 10.1111/j.1469-8137.1974.tb02132.x
- Trondman, A.-K., Gaillard, M.-J., Mazier, F., Sugita, S., Fyfe, R., Nielsen, A. B., et al. (2015). Pollen-based quantitative reconstructions of Holocene regional vegetation cover (plant-functional types and land-cover types) in Europe suitable for climate modelling. *Glob. Change Biol.* 21, 676–697. doi: 10.1111/gcb.12737
- Vera, F. W. M. (2000). *Grazing Ecology and Forest History*. Wallingford: CABI Publishing. doi: 10.1079/9780851994420.0000
- Vescovi, E., Ravazzi, C., Arpent, E., Finsinger, W., Pini, R., Valsecchi, V., et al. (2007). Interactions between climate and vegetation during the Lateglacial period as recorded by lake and mire sediment archives in Northern Italy and Southern Switzerland. *Quat. Sci. Rev.* 26, 1650–1669. doi: 10.1016/j.quascirev.2007.03.005
- Veski, S., Amon, L., Heinsalu, A., Reitalu, T., Saarse, L., Stivrins, N., et al. (2012). Lateglacial vegetation dynamics in the eastern Baltic region between 14,500 and 11,400 calyrBP: a complete record since the Bölling (GI-1e) to the Holocene. *Quat. Sci. Rev.* 40, 39–53. doi: 10.1016/j.quascirev.2012.02.013

- Walker, M. J., and Lowe, J. J. (1990). Reconstructing the environmental history of the last glacial-interglacial transition: evidence from the Isle of Skye, Inner Hebrides, Scotland. *Quat. Sci. Rev.* 9, 15–49. doi: 10.1016/0277-3791(90)90003-S
- Wessel, P., Smith, W. H. F., Scharroo, R., Luis, J., and Wobbe, F. (2013). Generic mapping tools: improved version released. *EOS Trans. Am. Geophys. Union* 94, 409–410. doi: 10.1002/2013EO450001
- Whitehouse, N. J., and Smith, D. N. (2004). “Islands” in Holocene forests: implications for forest openness, landscape clearance and ‘culture-steppe’ species. *Environ. Archaeol.* 9, 199–208. doi: 10.1179/env.2004.9.2.199
- Wick, L. (2000). Vegetational response to climatic changes recorded in Swiss Late Glacial lake sediments. *Palaeogeogr. Palaeoclimatol. Palaeoecol.* 159, 231–250. doi: 10.1016/S0031-0182(00)00087-0
- Wick, L., and Möhl, A. (2006). The mid-Holocene extinction of silver fir (*Abies alba*) in the Southern Alps: a consequence of forest fires? Palaeobotanical records and forest simulations. *Veg. Hist. Archaeobot.* 15, 435–444. doi: 10.1007/s00334-006-0051-0
- Williams, J. W. (2002). Variations in tree cover in North America since the last glacial maximum. *Glob. Planet. Change* 35, 1–23. doi: 10.1016/S0921-8181(02)00088-7
- Williams, J. W., and Jackson, S. T. (2003). Palynological and AVHRR observations of modern vegetational gradients in eastern North America. *Holocene* 13, 485–497. doi: 10.1191/0959683603hl613rp
- Williams, J. W., Tarasov, P., Brewer, S., and Notaro, M. (2011). Late Quaternary variations in tree cover at the northern forest-tundra ecotone. *J. Geophys. Res.* 116:G01017. doi: 10.1029/2010JG001458
- Williams, J. W., Webb, T., Richard, P. H., and Newby, P. (2000). Late Quaternary biomes of Canada and the eastern United States. *J. Biogeogr.* 27, 585–607. doi: 10.1046/j.1365-2699.2000.00428.x
- Woodbridge, J., Fyfe, R. M., Roberts, N., Downey, S., Edinborough, K., and Shennan, S. (2014). The impact of the Neolithic agricultural transition in Britain: a comparison of pollen-based land-cover and archaeological 14C date-inferred population change. *J. Archaeol. Sci.* 51, 216–224. doi: 10.1016/j.jas.2012.10.025
- Wright, J. W. (1952). *Pollen Dispersion of Some Forest Trees*. Northeastern Forest Experiment Station Paper No. 46. Washington, DC: U.S. Department of Agriculture.
- Ziska, L. H., and Caulfield, F. A. (2000). Rising CO₂ and pollen production of common ragweed (*Ambrosia artemisiifolia* L.), a known allergy-inducing species: implications for public health. *Funct. Plant Biol.* 27, 893–898. doi: 10.1071/PP00032

Conflict of Interest Statement: The authors declare that the research was conducted in the absence of any commercial or financial relationships that could be construed as a potential conflict of interest.

Copyright © 2018 Zanon, Davis, Marquer, Brewer and Kaplan. This is an open-access article distributed under the terms of the Creative Commons Attribution License (CC BY). The use, distribution or reproduction in other forums is permitted, provided the original author(s) and the copyright owner are credited and that the original publication in this journal is cited, in accordance with accepted academic practice. No use, distribution or reproduction is permitted which does not comply with these terms.



Pollen from the Deep-Sea: A Breakthrough in the Mystery of the Ice Ages

**María F. Sánchez Goñi^{1,2*}, Stéphanie Desprat^{1,2}, William J. Fletcher³,
César Morales-Molino^{1,2}, Filipa Naughton^{4,5}, Dulce Oliveira^{1,2,4}, Dunia H. Urrego⁶ and
Coralie Zorzi⁷**

¹ École Pratique des Hautes Études, EPHE PSL University, Paris, France, ² Environnements et Paléoenvironnements Océaniques et Continentaux, UMR 5805, Université de Bordeaux, Pessac, France, ³ Quaternary Environments and Geoarchaeology, Department of Geography, School of Environment, Education and Development, The University of Manchester, Manchester, United Kingdom, ⁴ Instituto Português do Mar e da Atmosfera, Portuguese Institute of Sea and Atmosphere, Lisbon, Portugal, ⁵ Center of Marine Sciences, Algarve University, Faro, Portugal, ⁶ College of Life and Environmental Sciences, University of Exeter, Exeter, United Kingdom, ⁷ GEOTOP, Université du Québec à Montréal, Montreal, QC, Canada

OPEN ACCESS

Edited by:

Valenti Rull,
Instituto de Ciencias de la Tierra
Jaume Almera (CSIC), Spain

Reviewed by:

Francesc Burjachs,
Institut Català de Recerca i
Estudis Avançats (ICREA), Spain
Jean-Pierre Suc,
UMR 7193, Institut des Sciences
de la Terre Paris (ISTEP), France

*Correspondence:

María F. Sánchez Goñi
maria.sanchez-goni@u-bordeaux.fr

Specialty section:

This article was submitted to
Agroecology and Land Use Systems,
a section of the journal
Frontiers in Plant Science

Received: 12 July 2017

Accepted: 09 January 2018

Published: 26 January 2018

Citation:

Sánchez Goñi MF, Desprat S,
Fletcher WJ, Morales-Molino C,
Naughton F, Oliveira D, Urrego DH
and Zorzi C (2018) Pollen from
the Deep-Sea: A Breakthrough
in the Mystery of the Ice Ages.
Front. Plant Sci. 9:38.
doi: 10.3389/fpls.2018.00038

Pollen from deep-sea sedimentary sequences provides an integrated regional reconstruction of vegetation and climate (temperature, precipitation, and seasonality) on the adjacent continent. More importantly, the direct correlation of pollen, marine and ice indicators allows comparison of the atmospheric climatic changes that have affected the continent with the response of the Earth's other reservoirs, i.e., the oceans and cryosphere, without any chronological uncertainty. The study of long continuous pollen records from the European margin has revealed a changing and complex interplay between European climate, North Atlantic sea surface temperatures (SSTs), ice growth and decay, and high- and low-latitude forcing at orbital and millennial timescales. These records have shown that the amplitude of the last five terrestrial interglacials was similar above 40°N, while below 40°N their magnitude differed due to precession-modulated changes in seasonality and, particularly, winter precipitation. These records also showed that vegetation response was in dynamic equilibrium with rapid climate changes such as the Dangaard-Oeschger (D-O) cycles and Heinrich events, similar in magnitude and velocity to the ongoing global warming. However, the magnitude of the millennial-scale warming events of the last glacial period was regionally-specific. Precession seems to have imprinted regions below 40°N while obliquity, which controls average annual temperature, probably mediated the impact of D-O warming events above 40°N. A decoupling between high- and low-latitude climate was also observed within last glacial warm (Greenland interstadials) and cold phases (Greenland stadials). The synchronous response of western European vegetation/climate and eastern North Atlantic SSTs to D-O cycles was not a pervasive feature throughout the Quaternary. During periods of ice growth such as MIS 5a/4, MIS 11c/b and MIS 19c/b, repeated millennial-scale cold-air/warm-sea decoupling events occurred on the European margin superimposed to a long-term air-sea decoupling trend. Strong air-sea thermal contrasts promoted the production of water vapor that was then transported northward by the

westerlies and fed ice sheets. This interaction between long-term and shorter time-scale climatic variability may have amplified insolation decreases and thus explain the Ice Ages. This hypothesis should be tested by the integration of stochastic processes in Earth models of intermediate complexity.

Keywords: vegetation, millennial-scale climate variability, Dansgaard-Oeschger cycles, Heinrich events, glaciations, interglacials, Europe, Quaternary

INTRODUCTION

“To look in the oceans for direct evidence of past continental climates seems paradoxical. However, marine sediments contain far better terrestrial paleoclimate records than most continental deposits (Heusser, 1986/1987).” This visionary statement, based on previous seminal works published in the 1960s in a special issue of *Marine Geology on Marine Palynology* (e.g., Groot and Groot, 1966; Traverse and Ginsburg, 1966; Zagwijn and Veenstra, 1966), anticipated the major contribution that pollen analysis from marine cores would make to Paleoclimatology in subsequent decades. It is now well-established that long and continuous deep-sea sedimentary sequences collected near the continents provide high-quality and chronologically well-constrained pollen records documenting past changes in the vegetation and climate of the adjacent landmasses. Since the pioneering work of Heusser, Hooghiemstra, Rossignol-Strick, Van Campo, and Turon in the 1970 and 1980s in the North Pacific and the Atlantic Oceans and the Mediterranean and Arabian Seas (for references see **Supplementary Table S1**), an increasing number of deep-sea pollen records has been published from the Iberian and South African margins, the Mediterranean Sea, and the South Pacific and Indian Oceans. They mainly span all or a part of the last 1 million years. These records, which compare without chronological ambiguity marine and terrestrial stratigraphies, are pivotal for documenting potential leads and lags between regional atmospherically-driven vegetation, oceanic conditions and ice dynamics. The relevance of this approach was shown in two seminal papers where the authors demonstrated that the Eemian interglacial, ca. 128,000 years ago (128 ka), was not exactly the terrestrial equivalent of the marine interglacial Marine Isotope Stage (MIS) 5e, and that warmth and forest persisted in south-western Europe during periods of Northern Hemisphere ice growth (Sánchez Goñi et al., 1999; Shackleton et al., 2003). Therefore, pollen-rich marine records are of prime importance for understanding the interactions between the ocean and the atmosphere leading to the orbitally-paced deglaciations and glacial inception. More recently, coupled analysis of pollen and marine climatic tracers at a finer resolution has revealed a unique suitability to investigate the timing and amplitude of rapid millennial-scale climate changes in different regions of the world as well (e.g., Sánchez Goñi et al., 2008). This direct sea-land comparison approach also allows testing whether vegetation response to short periods of forcing is in dynamic equilibrium with climate (Webb, 1986) or if there is a lag between climate change and vegetation response (disequilibrium hypothesis, Birks, 1981; Bennett and Willis, 1995), due to species competition or different migration rates.

In the first part of the paper, we focus on the suitability of pollen analysis in deep-sea sediments to trace vegetation and atmospheric conditions through time, highlighting its key role in understanding the mechanisms underlying climate change via the direct comparison with ocean and ice dynamics. We also present a global compilation of pollen records obtained from Quaternary deep-sea cores, and identify the regions where few marine pollen records exist despite their relevance for the study of climate variability. The second part is devoted to the responses of the European vegetation and climate to long-term and, particularly, millennial-scale climate changes. We focus on western Europe because this region is directly affected by North Atlantic millennial-scale iceberg discharges, atmospheric Greenland warming and cooling events (Shackleton et al., 2000), and the close influence of the Northern Hemisphere ice growth and decay, as well as being strongly implicated in the feedback processes bringing the Earth's system to glaciations (Ruddiman and McIntyre, 1984). The third part of the paper aims to show that the interactions between short-term and long-term climate variability may be the potential missing piece of the Ice Age puzzle (Hodell, 2016), given that the Milankovitch astronomical theory of climate, i.e., changes in the seasonal distribution of the solar energy, alone cannot explain the ice age cycles (Milankovitch, 1941).

UNDERSTANDING PAST CLIMATE CHANGES

Climate is the sum of meteorological phenomena that characterizes the mean state of the atmosphere (i.e., temperature, precipitation, greenhouse gases – GHG) over 30 years that depends, in turn, on the dynamics of various components of the climate system (Claussen, 2007). Insolation is the external astronomical (orbital) forcing that determines Earth's regional climates and is defined as the amount of energy per surface unit that the Earth receives from the Sun. Insolation is controlled by the distance between the Earth and the Sun that depends on eccentricity (the shape of the Earth's orbit), obliquity (the tilt of the Earth's axis) and precession (the orientation of the Earth's axis); the latter determines the amplitude of the seasons. These orbital parameters vary over time and trigger major climate changes with cyclicities of 100,000, 40,000, and 21,000 years (e.g., Berger and Loutre, 2004). A change in insolation affects the Earth's five main climatic reservoirs-atmosphere, ocean, land surfaces, cryosphere, and vegetation- and each of them affects, in turn, the Earth's other reservoirs through feedback mechanisms that amplify or reduce the original climate change

(Ruddiman, 2001). Thus the frequency, duration and magnitude of a given climate change is the result of the interactions between orbital external forcing and internal feedback loops involving, for example, ocean currents, particularly the Atlantic Meridional Overturning Circulation (AMOC), ice-sheet and sea-ice dynamics, vegetation, volcanic eruptions, GHG concentrations, and albedo (Ruddiman, 2001).

Marine and terrestrial palaeoclimatic records and ice archives allow the reconstruction of past climate changes in the Earth's different reservoirs. However, understanding the mechanisms controlling the frequency, duration and amplitude of climate changes requires the comparison of these different records on a common timescale, a challenging task due to the fragmentary nature of certain sequences and the uncertainties inherent in different dating methods and age models used. The age models of marine and terrestrial cores are mostly based on radiometric dates (^{14}C , U/Th...) and isotopic stratigraphy/orbital tuning, while the ice archives are dated by mean of layer counting or physical models of ice accumulation. The three types of records have uncertainties ranging from a few decades to several centuries and even millennia (e.g., Bazin et al., 2013). Continuous pollen-rich deep-sea sedimentary sequences trace the regional vegetation history and, consequently, the climate of the landmasses nearby and represent a unique way to circumvent the aforementioned issues when comparing different records (vegetation/atmosphere, marine, and ice). Marine climatic indicators from these sequences allow the quantitative reconstruction of sea surface temperature (SST) and salinity (e.g., planktonic foraminifera, dinoflagellate cysts, calcareous nannofossil and diatom assemblages, alkenones), deep ocean conditions (e.g., Mg/Ca, benthic foraminifer assemblages, carbon isotopic ratio $-\delta^{13}\text{C}-$ of benthic foraminifera, Pa/Th), iceberg dynamics (Ice Rafted Debris or IRD, the coarse sediments transported by icebergs) and the ice volume stored in the ice caps [oxygen isotopic ratio $-\delta^{18}\text{O}-$ of benthic foraminifera; although a bias exists between this isotopic ratio and global ice volume (Skinner and Shackleton, 2006)] (Figure 1). This approach is usually named "direct land-sea correlation or comparison," although the insights extend not only to terrestrial and marine conditions but also to the cryosphere. Other indicators found in marine sediments give complementary information on terrestrial climate such as charcoal particles providing relevant information about climatically-driven fire regime prior the beginning of human impact on the environment (Daniau et al., 2007, 2013), dust concentrations (e.g., deMenocal, 2004; Jullien et al., 2007) and terrestrial organic compounds or biomarkers (δD , GDGT, $\delta^{13}\text{C}$ from leaf waxes) that give useful information on precipitation and, in some cases, on temperatures (e.g., Weijers et al., 2007).

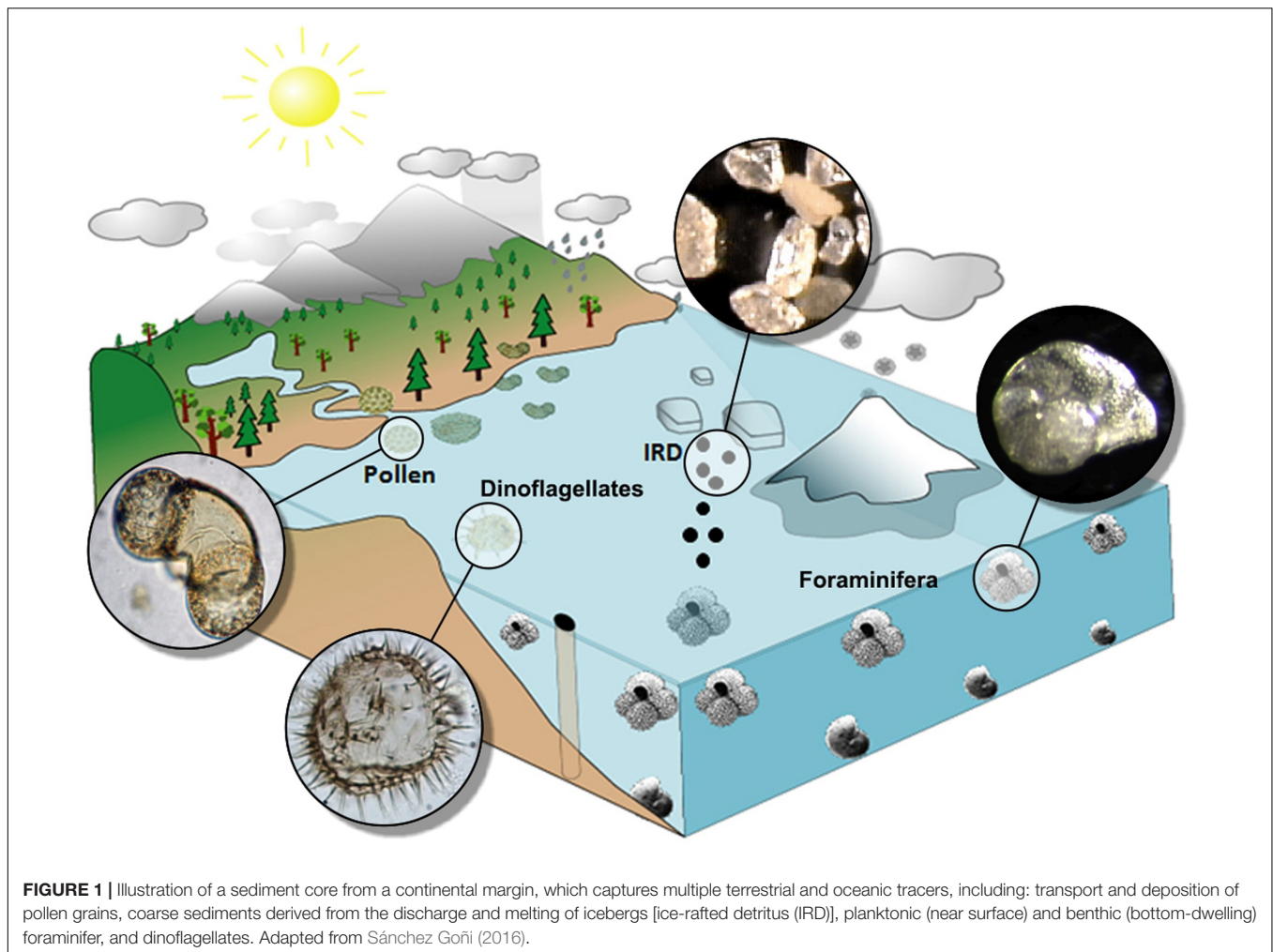
This direct correlation allows the identification of possible synchronicity or time-lags between the response of these reservoirs to a given climate change and, therefore, provides insights into the feedback processes underlying this climate change. Finally, the comparison between directly correlated palaeoclimatic data and model simulations allows the assessment of the reliability of the mechanisms implicated in the different models to reproduce the observed climate change (e.g., Sánchez

Goñi et al., 2012). However, before identifying regional land-sea linkages associated with past climate changes, it is crucial to understand the present-day regional pollen signals.

Pollen in Deep-Sea Sediments

A substantial quantity of pollen grains produced, released and dispersed from terrestrial higher plants (as well as spores of lower plants) reaches the ocean mainly by fluvial and atmospheric transport processes, with oceanic currents playing a negligible role (Koreneva, 1966; Stanley, 1966). The relative contribution of one or other transport vector is regionally-dependent (Dupont, 2011). In the Arctic, for instance, pollen is also transported by sea ice scouring and sediment transport in addition to northeasterly winds (Mudie and McCarthy, 2006). Marine sediments located further than 300 km offshore are weakly influenced by rivers and the dominant pollen transport is aeolian (e.g., Hooghiemstra et al., 1988). In contrast, the pollen preserved in marine sediments located under the influence of river plumes (nepheloid layers) is mainly of fluvial origin (e.g., Heusser and Balsam, 1977; Cambon et al., 1997; Mudie and McCarthy, 2006). Once it arrives in ocean surface waters, pollen is ingested by planktonic organisms and later integrated into their fecal pellets or agglomerated with clays (Mudie and McCarthy, 2006; Beaudouin et al., 2007). Due to these processes, pollen buoyancy decreases and is little influenced by ocean currents. It thus becomes an integral part of marine snow and crosses the water column with a relatively high speed (estimated at ~ 100 m/day in the Atlantic water column) before being deposited at the bottom of the oceans (Hooghiemstra et al., 1992). Furthermore, sediments under the influence of upwelling are particularly rich in pollen for two reasons: the intensification of the downward particle transport through the water column (Ratmeyer et al., 1999) and the better preservation in almost anoxic sediments (Dupont, 2011).

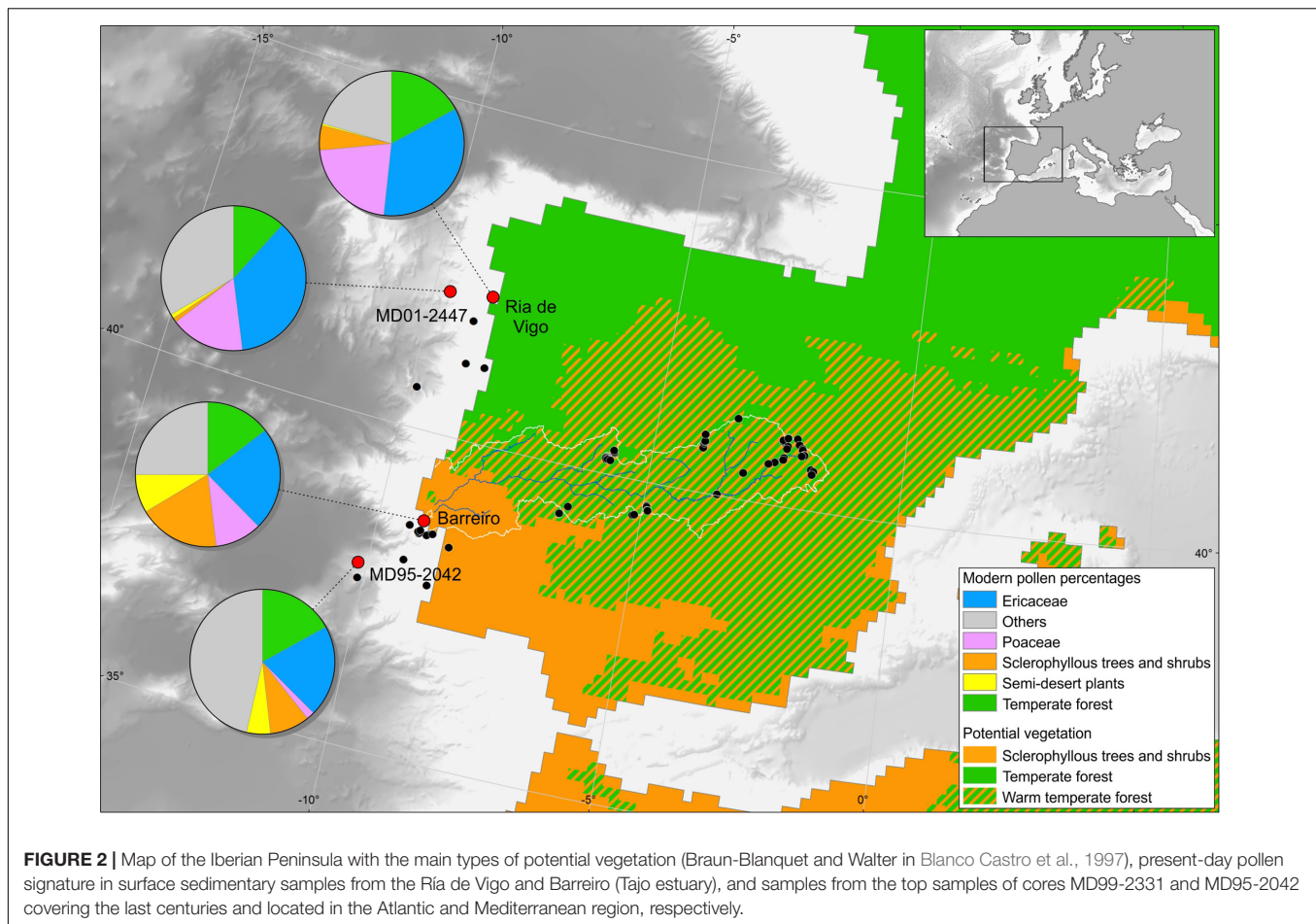
Pollen studies on modern deep ocean surface sediments from the Iberian margin (Turon, 1984a; Naughton et al., 2007), the Bay of Biscay (Turon, 1984b), the Mediterranean (Koreneva, 1971; Beaudouin et al., 2007), the African margin (Hooghiemstra et al., 1986; Dupont and Wyputta, 2003), and the western and eastern margins of North America and the Gulf of Mexico (Heusser and Balsam, 1977; Heusser, 1985; Heusser and Van de Geer, 1994) showed that pollen assemblages from the sediment surface of the ocean floor reflect an integrated image of the regional vegetation of the adjacent continent and, consequently, the climatic parameters under which this vegetation has developed. Palynological richness, i.e., the number of pollen types per sample standardized to a constant pollen sum, is similar in fossil samples from deep-sea cores, modern terrestrial and deep-sea surface samples, and fossil assemblages from lakes and estuaries, oscillating between 15 and 25 morphotypes with respect to a pollen sum of at least 100 terrestrial pollen grains (e.g., Sánchez Goñi and Hannon, 1999; Naughton et al., 2007). An ongoing study on the pollen representation of modern vegetation in moss-pollsters along the Tajo basin shows that palynological richness ranges from 13 to 41 with respect to a pollen sum of 500 terrestrial pollen grains. In particular, Naughton et al. (2007) demonstrated by comparison of modern pollen spectra from the deep ocean, estuaries and continent that the pollen signal of the



Iberian margin is similar to that found in estuarine sediments from western Iberia that reliably represents the broad regional vegetation of the related hydrographic basins (**Figure 2**). On the one hand, pollen assemblages from the northern part of the margin reflect the composition of temperate forest that develops in northwestern Iberia dominated by deciduous oaks. On the other hand, pollen samples from the southern part of the margin capture the composition of Mediterranean forest, i.e., warm-temperate forest dominated by sclerophyllous trees and shrubs that characterizes southern Iberia (**Figure 2**). In this region, pollen is mainly transported by the rivers because the dominant winds come from the north-west and the hydrographic Iberian basins are large and thus favor the transport of sediment load, including pollen (Dupont and Wyputta, 2003; Naughton et al., 2007). From a botanist's point of view, this type of study has therefore a limitation for reconstruction of ancient local plant communities (Groot and Groot, 1966). However, the similarity of western European terrestrial pollen sequences and eastern North Atlantic deep-sea pollen records (e.g., Naughton et al., 2007 for the last 18,000 years in north-west Iberia; Fletcher and Sánchez Goñi, 2008 for the last 50,000 years in south-east Iberia; Sánchez Goñi et al., 2012 for the Last Interglacial in western

France) demonstrate once more that marine pollen records provide a reliable image of the vegetation history of the adjacent landmasses (Groot and Groot, 1966). Moreover, the regional vegetation is directly linked to climate conditions as the present-day distribution of the major biomes is governed by climatic parameters (Bailey, 1998). For western Europe Gouveia et al. (2008) have recently shown the rapidity with which vegetation in this region responds to North Atlantic atmospheric processes, i.e., the westerlies.

The comparison between terrestrial and marine modern pollen samples to better interpret marine pollen records has been further improved and applied to south-western Africa (Urrego et al., 2015). In particular, modern pollen spectra were used to assess the distribution of Poaceae pollen abundance and other pollen taxa with potential indicator value for large biomes in southern Africa, and therefore climatic zones in this region. For instance, pollen percentages of Poaceae up to 70% reflect the Nama-karoo and its transition with the fined-leaved savanna. These results can substantially change the interpretation of the marine pollen fossil record collected off northwestern South Africa. Contrary to the studies that interpret the increase of Poaceae pollen percentages as the result of



humidity-driven savanna expansions in southwestern Africa, the new pollen calibration study offers an alternative interpretation indicating that fine-leaved savanna developed in this region due to the aridity increase during the warm and humid Northern Hemisphere periods of the last interglacial (Urrego et al., 2015). This approach should be applied to other regions to improve the interpretation of marine pollen assemblages in terms of vegetation cover and composition. However, the quantification of the vegetation abundance from marine pollen assemblages to infer, among others, changes in albedo and their influence on climate change, remains a challenge. The REVEALS model was conceived to obtain quantitative reconstructions of regional vegetation cover around large lakes from pollen data, which resembles the spatial scale of marine pollen samples (Sugita, 2007). Nevertheless, this model only considers atmospheric pollen dispersal and deposition, thus disregarding the importance of pollen input from inlet streams and surface run-off, which are often the main vectors delivering pollen to the marine environment (Sugita, 2007).

The concentration (usually between 1,000 and 50,000 grains cm^{-3}) and taxonomical diversity of marine pollen assemblages are in general high enough to allow the quantitative estimation of annual and, more importantly, seasonal temperatures and precipitation (e.g., Sánchez Goñi et al., 2002, 2005, 2016a;

Desprat et al., 2007; Combourieu Nebout et al., 2009) (Figure 3). Knowledge about past climate seasonality is crucial to understand natural climate variability (Carré and Cheddadi, 2017) and the sensitivity of vegetation to changes in this parameter makes pollen data particularly well-suited to track shifts in seasonality through time. Quantitative pollen-based climatic estimates are based on different techniques. The most frequently used is the Modern Analog Technique (MAT) based on a comparison of past assemblages to modern pollen assemblages through the calculation of the shortest weighted distance (Guiot, 1990). This method requires high-quality, taxonomically consistent modern pollen and climate datasets. The modern database includes different continental pollen spectra (moss polsters, soil surface samples, and lacustrine sediments) from Eurasia and northern Africa (Peyron et al., 1998; Bordon et al., 2009). This continental pollen database is, however, slightly modified to estimate climatic parameters from marine pollen samples. Since *Pinus* pollen is overrepresented in marine sediments (Heusser and Balsam, 1977; Hooghiemstra et al., 1988), this pollen type is excluded from the calculation of pollen percentages for marine pollen spectra as well as from the continental pollen database. As potential errors would be similar for adjacent samples of the same record, we consider that this approach is still valid for the quantification of climate

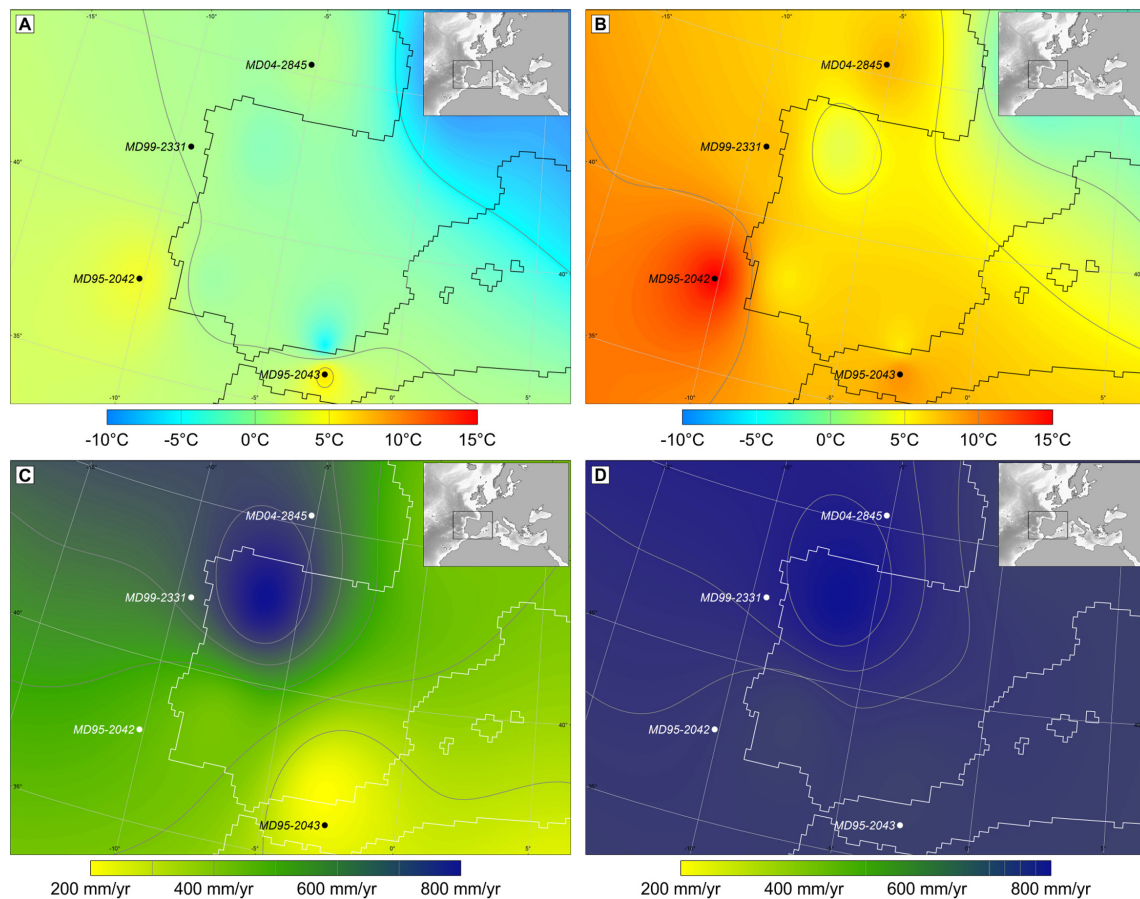


FIGURE 3 | Maps of western Europe with pollen-based quantitative climate estimates, winter temperature and annual precipitation, and sea surface temperature (SST) on its margin during Heinrich stadial (HS) 4 and Greenland interstadial (GI) 8. **(A)** Air and sea surface winter temperatures during HS 4, **(B)** air and sea surface winter temperature during GI 8, **(C)** annual precipitation during HS 4, and **(D)** annual precipitation during GI 8. These maps interpolate the temperatures and precipitation estimated from four cores strategically located in the Atlantic and Mediterranean regions (Sánchez Goñi et al., 2002 and unpublished data). Black circles indicate the location of cores MD95-2043, MD95-2042, MD99-2331, and MD04-2845 (Naughton et al., 2007; Fletcher and Sánchez Goñi, 2008; Sánchez Goñi et al., 2008).

change anomalies. The application of the MAT to estimate quantitatively climatic parameters for marine pollen records should be further improved by integrating marine modern pollen assemblages in the database, and by application of other reconstruction approaches that rely less strongly on the availability of suitable modern analogs, such as indicator approaches (Kühl et al., 2002) and biomisation (Prentice et al., 1996).

A Global Compilation of Deep-Sea Pollen Records

During the last 60 years, several oceanographic cruises organized in the framework of the international programs IMAGES (International Marine Global change Study) and ODP/IODP (International Ocean Drilling Program) have retrieved a large number of pollen-rich marine cores along different oceanic margins. Most of these cores come from oceanic rises and abyssal plains that are the most favorable areas for marine palynological work as terrigenous sediments are predominant

(Groot and Groot, 1966). We have performed a literature survey to compile pollen records from deep-sea cores spanning the last 1 million years, finding 129 sites all over the world (**Supplementary Table S1** and **Figure 4**). This compilation shows that there are 74 high-resolution pollen sequences (better than 1000 years between adjacent samples) and highlights the paucity of pollen records from the Indian (e.g., Rossignol-Strick, 1983) and the South Pacific (e.g., Montade et al., 2013; Seillès et al., 2016) Oceans. Likewise, almost half of the records ($n = 57$) do not cover periods older than the Last Glacial Maximum, and few sequences ($n = 19$) record several orbital climatic cycles. Therefore, the regional expression of long-term and rapid, millennial-scale, global climate changes is far from being well-documented, particularly in the Indian Ocean where only two out of the six available records cover the last climatic cycle (last 150,000 years) with a coarse time resolution (worse than 1000 years between consecutive samples). To fill this gap, IODP expedition 353 “Indian Monsoon Rainfall” collected a sedimentary sequence

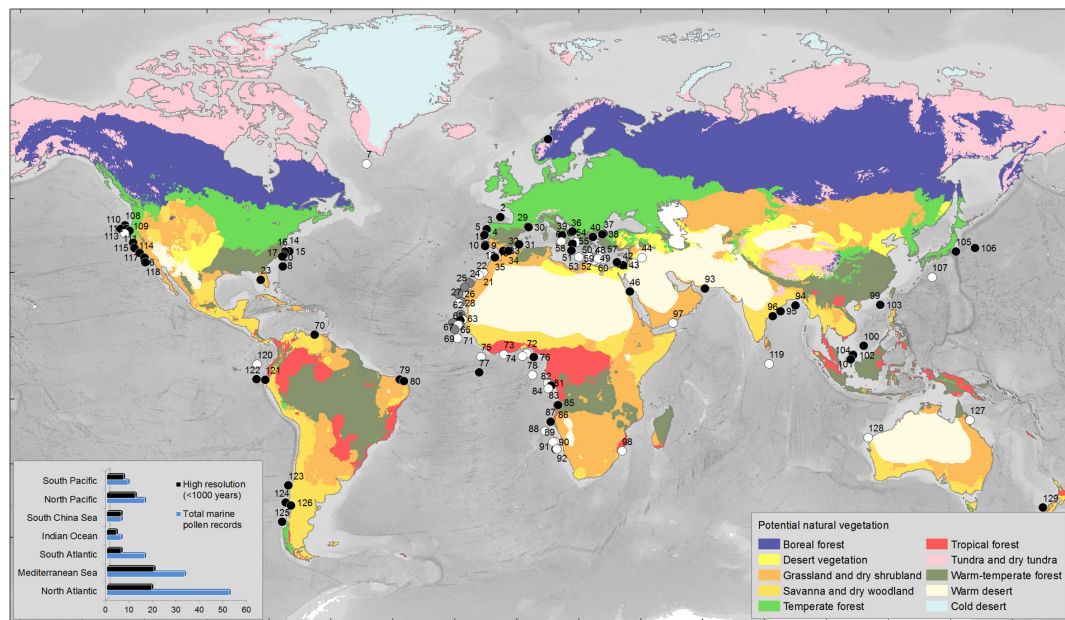


FIGURE 4 | Global map with the main types of potential vegetation (Levavasseur et al., 2012) and the marine pollen records covering different intervals of the last 2.58 Myrs. We have restricted the selection to pollen records from sections cored in the present-day marine realm. Black circles indicate the pollen records with a temporal resolution better than 1000 years (<1000 years) between adjacent samples. White circles indicate the pollen records with a temporal resolution worse than 1000 years (> 1000 years) between adjacent samples. Gray circles indicate records where no information about the resolution is given. Left bottom corner: histogram indicating the number of marine pollen records by region and the number of high resolution records among the 129 records compiled in this work (see **Supplementary Table S1** for details and references). Warm-temperate forest biome includes the Mediterranean forest; Temperate forest biome includes the Atlantic forest; Grassland and dry shrubland include the Mediterranean plants, i.e., sclerophyllous trees and shrubs such as *Quercus ilex* type (holm oak, kermes oak), *Q. suber* type (cork oak), *Olea* (olive tree), *Phillyrea*, *Pistacia*, and *Cistus* (rockroses); Desert and Tundra-dry tundra are the present-day closest vegetation biomes to the past semi-desert and steppe environments inferred from the pollen analysis of last glacial sedimentary sequences, respectively.

in 2015 on the eastern Indian margin, site U1446, which will enable to trace for the first time past vegetation and Indian summer monsoon variability over the last 1 million years.

EUROPEAN VEGETATION AND CLIMATE RESPONSE TO LONG-TERM AND RAPID CLIMATE VARIABILITY

General Setting

Since 1995, the Marion Dufresne and Joides Resolution oceanographic ships have retrieved several high-resolution pollen-rich deep-sea sedimentary sequences from the eastern North Atlantic and the Mediterranean Sea within the framework of the IMAGES and IODP programs. These sequences are strategically located in the present-day Mediterranean and Atlantic regions, characterized by a markedly seasonal climate, with warm and dry summers and wet and mild winters, and a year-round humid climate with warm summers and cool winters, respectively. In winter, both regions are under the influence of the westerlies, but in summer the Azores high affects southern Iberia inducing a pronounced summer drought while the westerlies still play a prominent role from northern Iberia northward. Additionally, the region located below 40°N is affected by

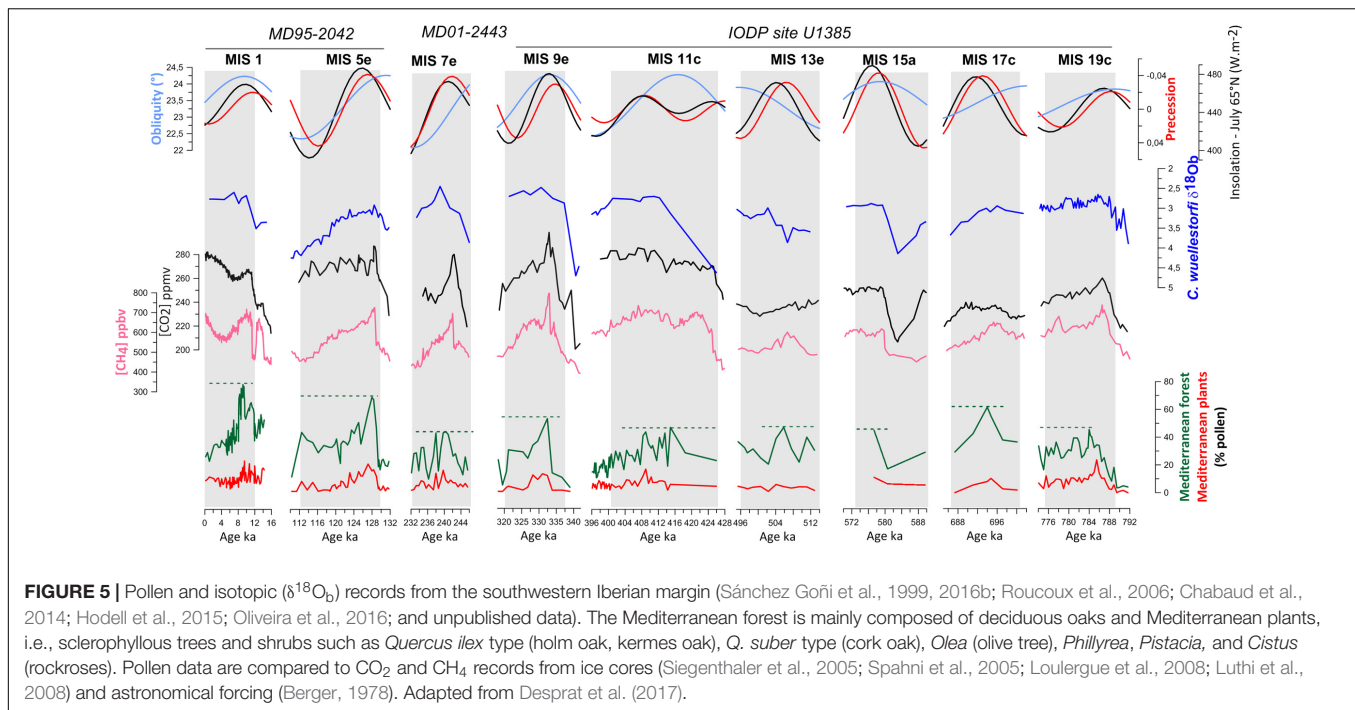
precession, and the subtropical ocean water currents (Ruddiman and McIntyre, 1984).

At present, the seasonal distribution of precipitation, with a relatively abundant amount of rainfall from autumn to spring and a pronounced summer drought, determines the dominance of Mediterranean forest (Polunin and Walters, 1985; Gouveia et al., 2008). This forest comprises evergreen sclerophyllous woodland (evergreen *Quercus*, *Olea*, *Pistacia*, *Phillyrea*, *Cistus*) at low altitudes, and deciduous forest (mostly deciduous *Quercus*) at higher elevation. On the contrary, the occurrence of Atlantic forest, dominated by deciduous *Quercus* (oak), is today controlled by winter length and harshness, given that annual rainfall is high and summer drought absent or negligible (Polunin and Walters, 1985). Therefore, deciduous *Quercus* is included in both the 'Atlantic forest' and the 'Mediterranean forest' assemblages.

Pollen analysis of these European margin sequences has allowed the reconstruction of the responses of western European vegetation and climate to long- and short-term global climate changes of the Ice Ages.

European Vegetation and Climate Response to Past Global Long-term Climate Changes

Geological archives show that the Earth's climate has experienced large changes during the last 2.58 million years (Shackleton



and Opdyke, 1973; Hays et al., 1976), with alternating warm (interglacial) and cold (glacial) periods. During the glacial periods ice occupied large regions of the Northern Hemisphere resulting in low sea level stands while during interglacials the ice sheets only covered Greenland and sea level was similar or higher than at present. These changes in ice volume are identified in marine sedimentary sequences by measuring the oxygen isotope composition ($\delta^{18}\text{O}$) of benthic foraminifer carbonate shells, providing the basis of the marine isotopic stratigraphy. Depleted values define the interglacial periods *sensu lato* (s.l.) or odd numbered MIS, while heavy values mark the glacial periods corresponding to even-numbered MIS. Within interglacial periods, an alternation of ice retreats, called “e,” “c” and “a,” and ice advances, “d” and “b,” is observed, also resulting from orbital forcing. The interglacial period *sensu stricto* (s.s.) corresponds to the substage with minimal ice volume, often located just after deglaciation (Railsback et al., 2015).

Two long and continuous pollen-rich sedimentary sequences are available from the southwestern and northwestern Iberian margin covering the last 1.5 million years and 425,000 years, respectively. These Iberian margin sequences are each composed of three cores: the southern sequence is a composite of cores MD95-2042, MD01-2443, and IODP U1385 located at around 37°N (Figure 5; Sánchez Goñi et al., 1999, 2016b; Roucoux et al., 2006; Chabaud et al., 2014; Oliveira et al., 2016), and the northern one is a composite of cores MD99-2331, MD01-2447, and MD03-2697 collected at 42°N (Desprat et al., 2005, 2006, 2007, 2009; Sánchez Goñi et al., 2005, 2008; Naughton et al., 2007, 2009, 2016). The pollen analysis of the 425,000-year northern sequence is completed (Desprat et al., 2017) while that of the southern site is in progress (Figure 5). Further north,

the sequence MD04-2845 collected on the European margin, off western France, spans the last 140,000 years (Sánchez Goñi et al., 2008, 2012).

Both Iberian margin pollen sequences show an alternation of glacial periods dominated by Mediterranean steppe in southern Iberia (that we call semi-desert although it rarely included true semi-desert taxa such as *Lygeum*) and steppe/heathlands to the north, and interglacial periods when Mediterranean and Atlantic forests expanded over southern and northern Iberia, respectively. Tree pollen percentages are a good estimate for the magnitude of the interglacial in both Iberian regions. The magnitude of past Mediterranean forest expansions is interpreted as an indicator of the amount of winter precipitation in southern Iberia, given that relatively warm temperatures and summer drought occurred. The magnitude of the Atlantic forest expansion during different interglacials will mainly reflect the amplitude of the warming above 40°N, as forest development in the Atlantic domain requires a climate with a growth period of 4–6 months, and a mild winter period of 3–4 months (Polunin and Walters, 1985). Two or even three major phases of forest expansion occurred during all these interglacials, related with ice volume minima during sub-stages “a,” “c,” and “e” within each MIS (Figure 5). However, forest development in general reached its maximum during the earliest phase of each stage, concomitant with the highest sea level, indicating that warmest and wettest conditions occurred then, and subsequently identifying this phase with the terrestrial interglacial *sensu stricto*.

Pollen records from the Iberian margin show that the magnitude of forest development substantially differed from one interglacial to another in the south (MIS 19 to MIS 1, Mediterranean forest pollen = 40 to 80%, Figure 5), while in

the north the magnitude of the forest expansion was similar (Atlantic forest pollen = 80%; Desprat et al., 2017). These data suggest that temperatures were similarly warm during the last five interglacials in northwestern Iberia, whereas the amount of winter precipitation in the south was quite variable. The Holocene (MIS 1, ~10 ka), the last interglacial (MIS 5e, ~128 ka) and MIS 17c (~690 ka) would have been the wettest followed by MIS 9e (~335 ka), MIS 11c (~415 ka) and MIS 19c (~784 ka), and MIS 7e (~240 ka) being the driest. Excluding the Lake Orhid pollen record (Sadori et al., 2016), these results coincide with what is observed in the European sequences of Tenaghi Philippon and Praclaux located above 40°N (Reille et al., 2000; de Beaulieu et al., 2001; Tzedakis et al., 2006), which show similar expansions of the temperate forest during the interglacials of the last 400,000 years. So far no long terrestrial pollen sequence exists below 40°N for comparison with the southwestern Iberian margin pollen record.

The comparison of the Iberian observations with those at higher latitudes illustrates the regional variability of the magnitude and impacts of climate change. Due to the combined forcing of insolation and GHG, climatic models indicate that MIS 5e, MIS 9e, and MIS 11c were the warmest at the highest latitudes, associated with the strongest melting of ice sheets (Yin and Berger, 2012, 2015). This scenario is in marked contrast with data from southwestern Europe showing that these interglacials were not particularly warm. Our pollen data suggest that substantial differences in precipitation occurred across the different interglacials. Nevertheless, it is difficult to propose a relationship between warming at high latitudes due to GHG increase and dryness in the Mediterranean region, contrary to what climate models project for the end of this century (Hoerling et al., 2012). Identifying forcing factors responsible for the interglacial diversity in terms of precipitation in the Mediterranean region is a subject of debate. A good candidate is the orbital parameter of precession that influences regions below 40°N (Ruddiman and McIntyre, 1984). Precession controls the amplitude of the seasonality and, therefore, the amount of winter precipitation in subtropical regions as recently suggested by models (Yin and Berger, 2012) and observations (e.g., Sánchez Goñi et al., 2008; Oliveira et al., 2016, 2017).

Rapid Climate Changes: A Focus on the Last Glacial Period

More recently, geological archives have also shown that millennial-scale changes punctuated this long-term climatic variability at the global scale as these changes are registered in North Atlantic SSTs (Voelker and Workshop Participant, 2002; Martrat et al., 2007) as well as in air temperatures over Greenland (North Greenland Ice-Core Project Members [NGRIP], 2004; Barker et al., 2011) and Antarctica (Augustin et al., 2004). These changes occur independently of the boundary climate state, i.e., in glacial and interglacial periods, and are generally associated with changes in ice volume (Siddall et al., 2003), GHG concentration (Knutti et al., 2004; Spahni et al., 2005; Louergue et al., 2008), and AMOC

(Oppo et al., 2006; Lynch-Stieglitz, 2017). The magnitude and frequency of these short-term climatic oscillations were larger when ice caps reached a critical mass (McManus et al., 1999) even if they were not the trigger (Barker et al., 2015).

So far, the best studied millennial-scale climate variability is that observed during the last glacial period (MIS 4, MIS 3 and MIS 2, i.e., ~73–14.7 ka) characterized by a series of warming and cooling events called Dansgaard-Oeschger (D-O) cycles that were first identified in the atmosphere of Greenland and usually lasted 500–2,000 years (Dansgaard et al., 1984). These cycles recorded in the $\delta^{18}\text{O}$ of the ice cores were characterized by a large (7 to 16°C) and rapid (within a few decades) warming event followed by a progressive decrease in temperature and a final abrupt cooling (Wolff et al., 2010). The warming and progressive cooling phase is termed Greenland Interstadial (GI), and the final cooling leading to the cold phase termed Greenland Stadial (GS). The GI phases lasted between 100 and 2,600 years (Wolff et al., 2010). Also during the last glacial period, repeated iceberg discharges cooled the surface of the North Atlantic (Heinrich, 1988; Bond et al., 1993). On the one hand, massive iceberg discharges from the Laurentide ice sheet, the so-called Heinrich events (HE), occurred with a cyclicity of 7,000–10,000 years while, on the other hand, weaker discharges coincided with iceberg fragmentation from the British-Icelandic-Scandinavian (BIS) ice cap (Elliot et al., 2001). We define a HE as the time period synchronous with the deposition of the coarse sediment Heinrich layer in a given region following the iceberg discharge while the Heinrich Stadial (HS) is the cold interval associated with the HE (Sánchez Goñi and Harrison, 2010). Some GSs encompass the HSs while the others are associated with the BIS minor iceberg discharges. These cold intervals are related to decreases in the AMOC (McManus et al., 2004; Lynch-Stieglitz, 2017) but the cause of the ice sheet collapse remains a subject of debate (e.g., Alvarez-Solas and Ramstein, 2011; Barker et al., 2015). The duration of the iceberg discharge has been simulated to be between 50 and 200 years (Roche et al., 2004) and data show that the HSs lasted longer, up to 3000 years (Sánchez Goñi and Harrison, 2010). HE and HS time intervals coincide in the Ruddiman belt, the preferential zone of IRD deposition that extends roughly between 45 and 50°N, while this is not the case outside (Naughton et al., 2009). Since the discovery of these millennial-scale climate changes, D-O cycles and HEs, the paleoclimatic community has dedicated major efforts to investigate the regional expression of this variability, the oceanic and atmospheric mechanisms involved in its transmission, and the interaction with long-term climate forcing such as the orbital parameters and ice volume. The following subsection summarizes the great contribution that palynological research conducted on marine sediments has done so far to increase current understanding of these processes in western Europe.

D-O Cycles

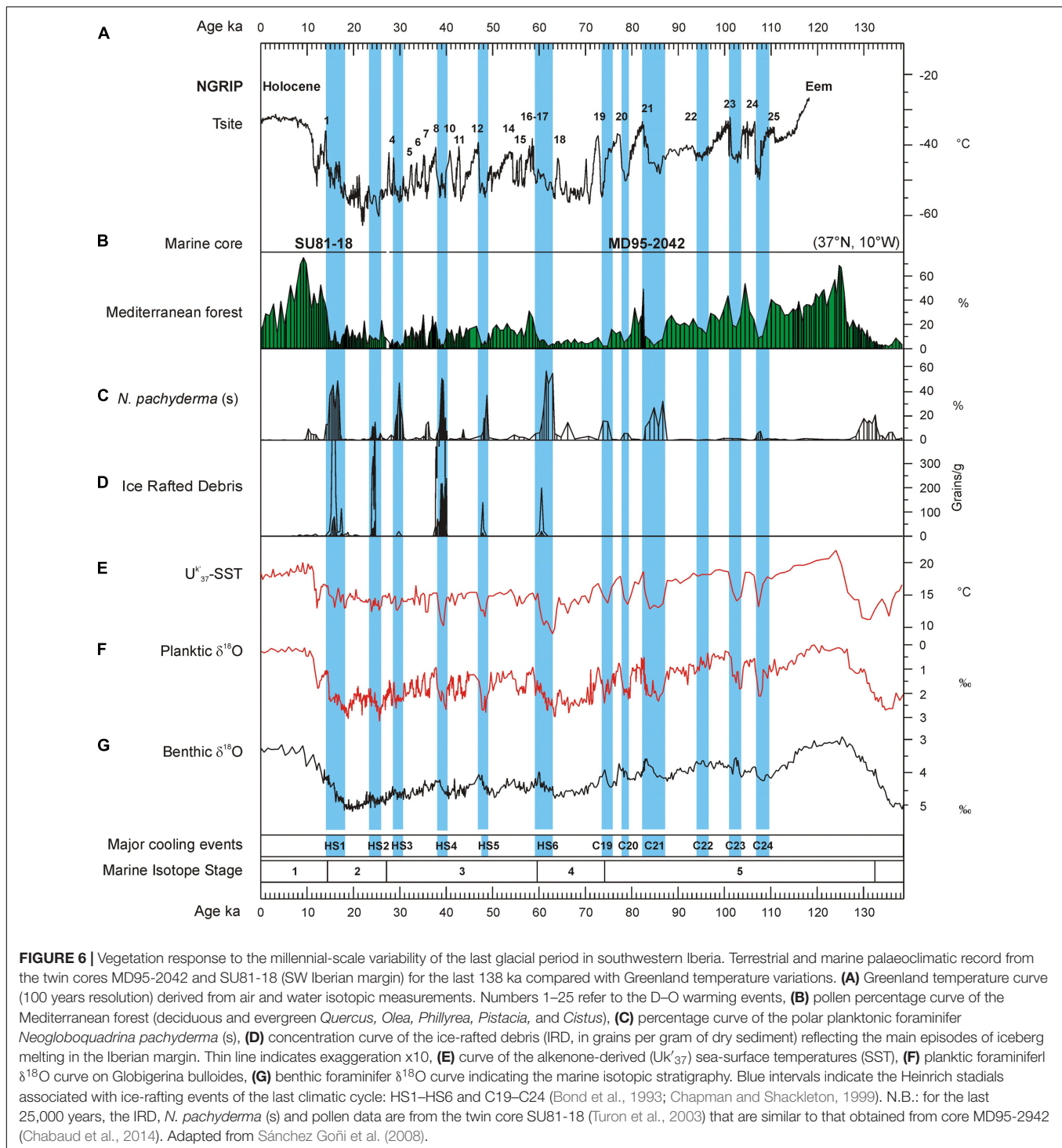
Until the end of the 1990s, investigations into European pollen records reported no changes in the dominant steppe

vegetation through the last glacial period (e.g., Follieri et al., 1988; Pons and Reille, 1988; Reille and de Beaulieu, 1990). Allen et al. (1999) published a pollen record from southern Italy showing for the first time millennial-scale changes between forest expansion and contraction that corresponded to the rapid climate variability detected in Greenland and the North Atlantic Ocean. However, the chronological uncertainties between ice, terrestrial and marine sequences precluded the demonstration of whether forest expansions corresponded to North Atlantic and Greenland warming or, inversely, to cooling events. Marine pollen records have unequivocally shown that cooling events in the North Atlantic and high latitudes corresponded in western Europe with herbaceous community expansion and warming events with enhanced forest development (Roucoux, 2000; Sánchez Goñi et al., 2000, 2002, 2008). The aforementioned marine pollen records from the European margin and an additional record, MD95-2043, from the Alboran Sea (western Mediterranean, **Figure 4**) (Sánchez Goñi et al., 2002; Fletcher and Sánchez Goñi, 2008) also show that vegetation quickly, within 100 years, responded to the D-O cycles and HEs, and that there was a dynamical equilibrium between vegetation response and climate change for short periods of forcing. Cold episodes in North Atlantic surface temperatures related to GS, not only those associated with HEs, were synchronous with forest reductions in Iberia and western France, while forest expansions correlated with increases in SST (**Figure 6**) (Sánchez Goñi et al., 2008).

Notably, below 40°N, Mediterranean forest reached its maximum development at the onset of the Eemian (MIS 5), the D-O 24, D-O 21, D-O 17-16, D-O 8-7, and D-O 1 warming events, and the beginning of the Holocene (MIS 1), indicating the occurrence of enhanced hot/dry summers and wet/cool winters (**Figure 7**). The Atlantic sites, above 40°N, showed a contrasting pattern: during GI 12 and GI 14 the Atlantic forest experienced a strong development while the impact of D-O 17-16 and D-O 8-7 warming was rather limited. The comparison of the Mediterranean and Atlantic palaeoclimatic records reveal that there was a spatial variability in the amplitude of the forest expansions for any given D-O warming of the last glacial period (Sánchez Goñi et al., 2008) (**Figure 7**). The comparison of these changes in vegetation with the evolution of orbital parameters shows that the maxima in the Mediterranean forest were always synchronous with low precession values. This observation suggests that precession minima strengthened Mediterranean climate through promoting marked seasonality. The floristic composition of the Mediterranean forest corroborates that Mediterranean climate reached its best expression during precession minima (Sánchez Goñi et al., 2008). For example, pollen data from the Alboran Sea core show that Mediterranean sclerophylls such as evergreen *Quercus*, *Olea*, *Cistus*, *Phillyrea*, *Coriaria myrtifolia*, and *Pistacia* were particularly abundant during GI 8, under enhanced seasonality associated to a minimum in precession (Fletcher and Sánchez Goñi, 2008). On the contrary, the same sequence records that the abundance of the less drought-tolerant Ericaceae (heather) was higher during GI 12,

when precession reached a maximum and seasonality was reduced (Fletcher and Sánchez Goñi, 2008). In contrast, the maximum expansion of the Atlantic forest coincides with maxima in obliquity. For northern latitudes above 40°N obliquity seems to play a major role in modulating the increase of annual temperatures (**Figure 7**). The amplitude of temperature changes in Greenland was strong at D-O 17-16, D-O 12 and D-O 8, and weak at D-O 14 (Sánchez Goñi et al., 2008), thus also differing from the climatic patterns at lower latitudes. This means that the strongest warming events in Greenland were not necessarily particularly warm in other regions of the world. The Iberian Peninsula and wider Mediterranean region are particularly interesting from a palaeoclimatic point of view because they appear to straddle the transition zone from obliquity- to precession-influence on the climatic signal of millennial-scale warming events. Preliminary comparison between European margin and terrestrial pollen records across Europe roughly confirms the contrasting latitudinal response over Europe to the D-O warming events despite the independent and sometimes uncertain chronologies of individual records (Fletcher et al., 2010). A more in-depth comparison of these pollen records is in progress based on the harmonized chronology recently developed in the framework of the INQUA International Focus Group (IFG) ACER project (Sánchez Goñi et al., 2017).

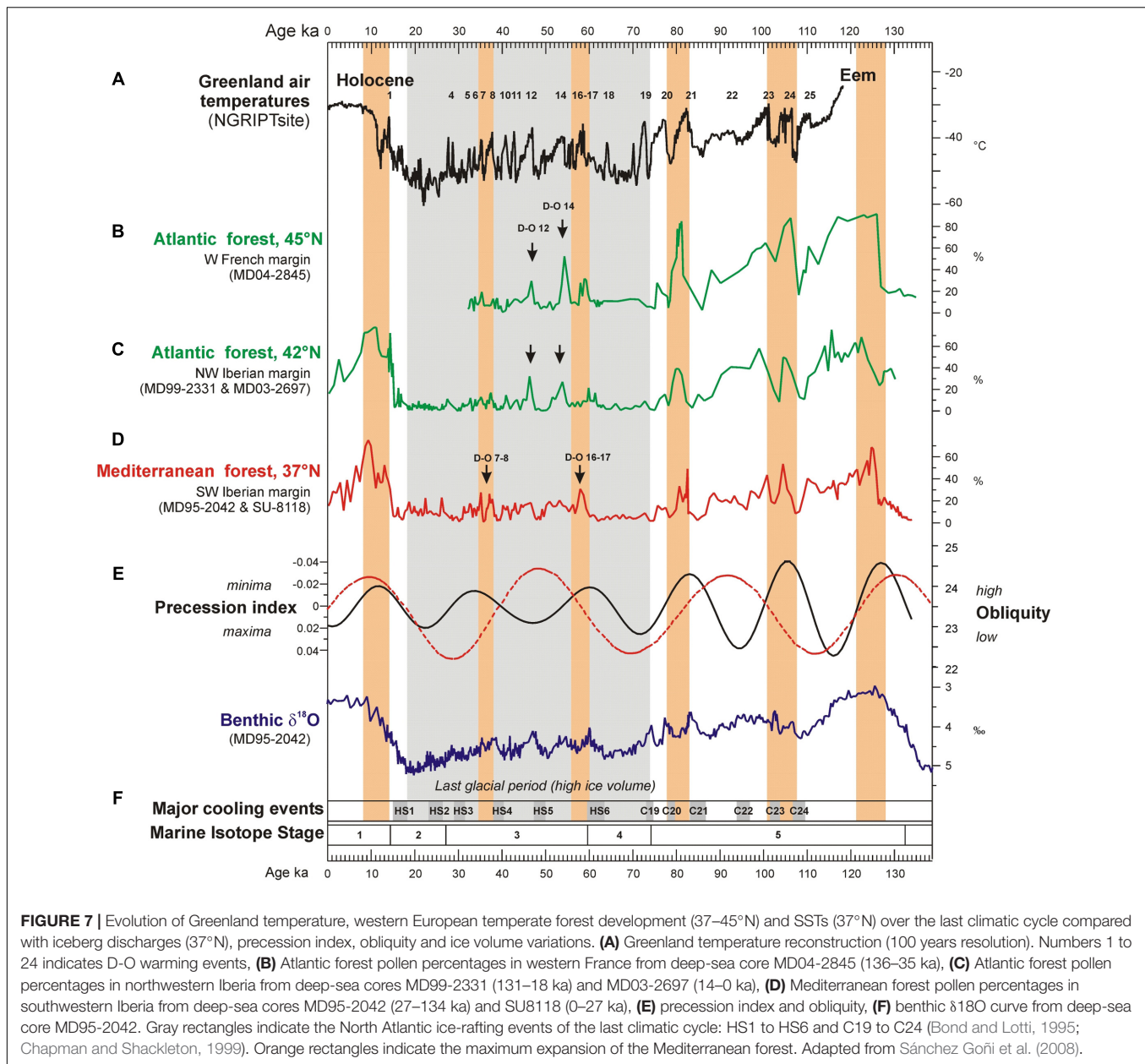
A zoom into D-O 7 and D-O 8 cycles, 41,000–34,000 ka, shows that semi-desert plants (mainly *Artemisia*, Chenopodiaceae and *Ephedra*) characterized the vegetation of southern Iberia during GSs, with open Mediterranean woodland establishing during GIs (Sánchez Goñi et al., 2008; **Figure 8**). Simultaneously, Ericaceae and Poaceae dominated the vegetation of north-western Iberia during GSs (**Figure 8**), being partially replaced by Atlantic woodlands with *Pinus* and deciduous *Quercus* during warmer periods (GIs). The composition of the pinewoods of south-western/central Iberia during the last glacial also varied in response to abrupt climate changes according to the quantitative study of *Pinus* pollen grains by Desprat et al. (2015). Thus, although *P. nigra* was the dominant pine species throughout the last glacial period, *P. sylvestris* was more abundant during the colder GSs and HSs and Mediterranean pines (*P. pinaster*, *P. pinea*, *P. halepensis*) during the warmer GIs and early- to mid-Holocene. Further north, *Artemisia*, Cyperaceae and *Calluna* dominated in western France during the cold periods, whereas *Betula*, deciduous *Quercus* and conifers (*Pinus*, *Abies*, *Picea*) expanded slightly in the landscape during warming episodes (Sánchez Goñi et al., 2008; **Figure 8**). These sequences illustrate the spatial floristic diversity of western Europe in response to the D-O cycles. Interestingly, the latitudinal boundary between the Atlantic and the Mediterranean vegetation during the last glacial period seems to have been similar to that at present-day, i.e., below 40°N. Finally, it is worth highlighting that temperate forest expanded when summer SST in the North Atlantic crossed the threshold of 12°C (Sánchez Goñi et al., 2008) (**Figure 8**), which is the same threshold value that explains the distribution of the temperate forest in both sides of the North Atlantic Ocean at present (Van Campo, 1984).



A Close-up on HS and GI Phases

Marine pollen records unequivocally show that HSs were associated with the expansion of herbaceous vegetation reflecting cold and dry conditions in western Europe. However, a closer observation of HS 4 (40.2–38.3 ka), HS 2 (26.5–24.3 ka), and HS 1 (18–15.6 ka) in core MD99-2331 retrieved off northwestern Iberia suggests that two major phases occurred

within these stadials (**Figure 9**) (Naughton et al., 2009). The first phase was characterized by almost no IRD in the north-western Iberian margin but SSTs were low and large reductions of *Pinus* and Atlantic forest pollen indicate very cold atmospheric conditions as well. The first episode was the wettest one according to the maximum percentages of *Calluna*, typical at present of central European mires



(Polunin and Walters, 1985), and high pollen concentration (not shown). The second phase of these stadials was drier and warmer as shown by the increase of semi-desert plants, and *Pinus* and temperate forest pollen percentages, respectively.

A synthesis of all available North Atlantic sites recording the last four HS shows complex climatic and IRD deposition patterns that are summarized in **Figure 10** (Naughton et al., 2009). In the first phase, the wettest and coldest conditions in the Iberian Peninsula were coetaneous with low IRD deposition and low SST in the Iberian margin. A contrasting pattern is detected in the Ruddiman belt (45–50°N) with high IRD deposition and cold SST while in Florida a dry climate was associated with cool SST off this peninsula. During the second phase, dryness in Iberia

and high IRD deposition in its margin are observed at the same time as wetness in Florida and moderate IRD deposition in the Ruddiman belt. A simple oceanographic mechanism related to changes in the strength of the AMOC alone cannot explain this complex scenario but rather an atmospheric mechanism must be involved. During the first phase, strong SST cooling of the North Atlantic as far as the southern Azores and the Gulf of Cádiz was associated with relatively high precipitation in south-western Europe. At the same time, $\delta^{13}\text{C}$ measurements on benthic foraminifer and Pa/Th ratios indicate a gradual decrease of deep sea ventilation and a slowdown of the AMOC, respectively (Naughton et al., 2009). The southward displacement of the thermal front produced a strong mid-latitude meridional temperature gradient that led to the southward displacement

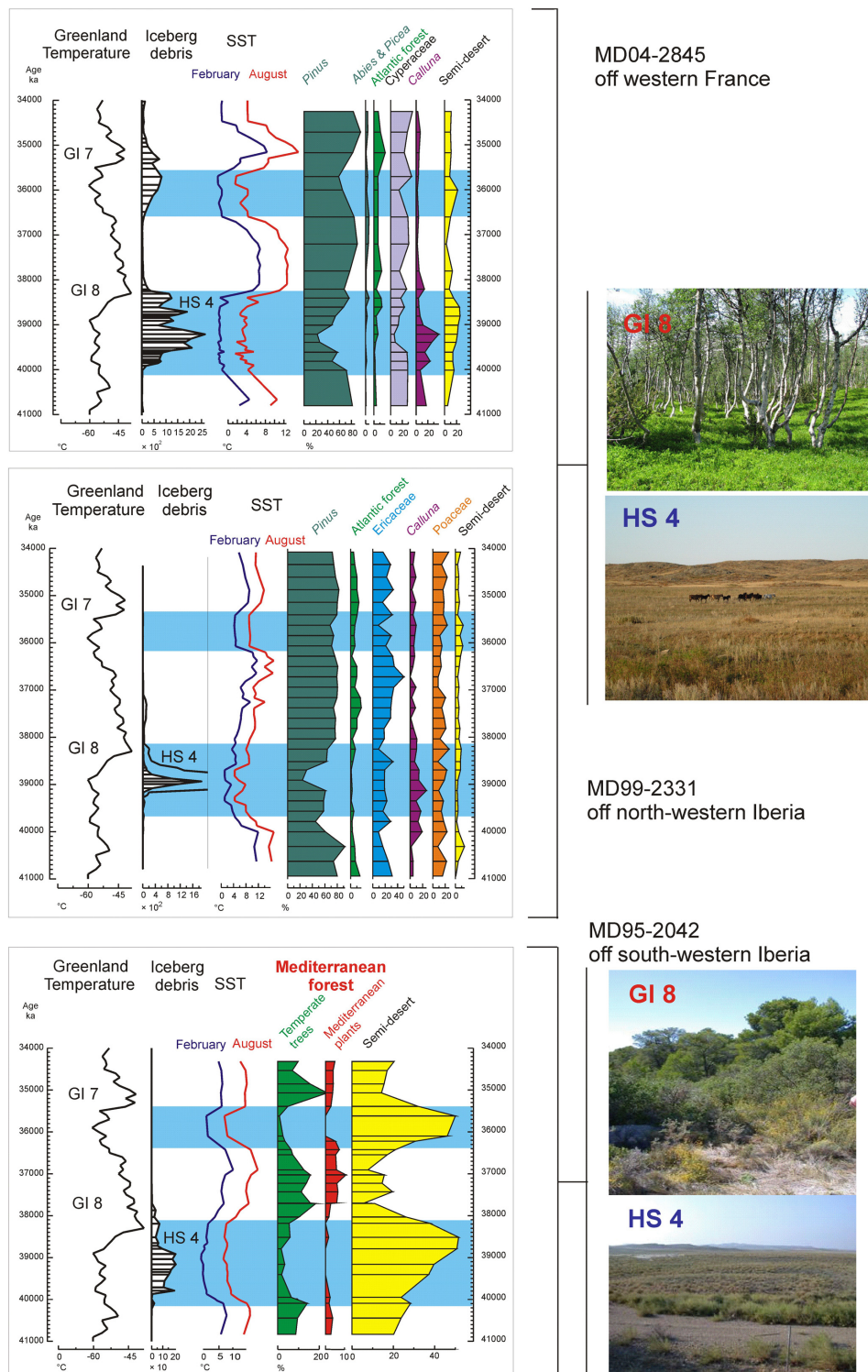


FIGURE 8 | A “zoom” on the interval 41–34 ka, from the three western European margin cores. The location of these cores is shown in **Figure 3**. GI (Greenland Interstadial), HS (Heinrich Stadial), GS (Greenland Stadial). In contrast with the Atlantic region, *Pinus* pollen percentages in core MD95-2042 (not shown) are similar through all the considered interval, during GI and GS, and oscillate between 60 and 90%. The pictures named HS 4 and GI 8 suggest analog present-day landscapes: semi-desert (*Ephedra distachya*-type, *E. fragilis*-type, Chenopodiaceae that now is included in the Amaranthaceae pollen morphotype, *Artemisia*) and open forest in the Mediterranean region and steppe (Poaceae, Cyperaceae, Asteraceae, Ericaceae and semi-desert plants) and *Pinus*–*Betula* forest in central Europe, respectively. SST: sea surface temperatures estimate from planktonic foraminifer assemblages using the Modern Analog Technique (MAT) (Guiot and De Vernal, 2007). Blue rectangles indicate the cold intervals, HS 4 and GS 8. Adapted from Sánchez Goñi (2014).

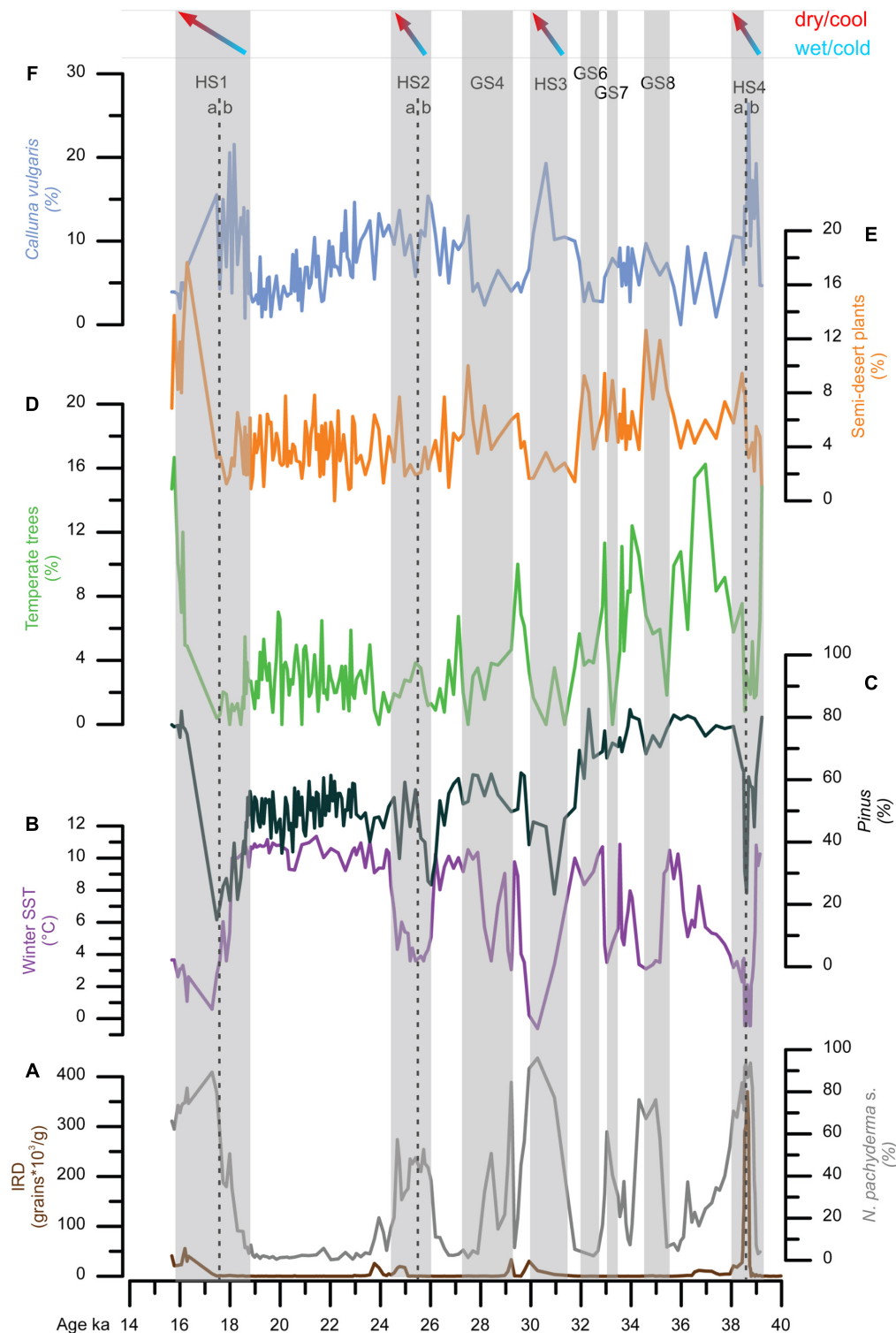


FIGURE 9 | Direct land-sea correlation of MD99-2331 record. From bottom to top: **(A)** ice-rafted debris (IRD) concentrations (brown line), percentages of polar planktonic foraminifer [*N. pachyderma* s.] (gray line), **(B)** winter SST estimates based on planktonic foraminifer associations, **(C)** pollen percentages of temperate trees (*Acer*, *Alnus*, *Betula*, *Corylus*, *Juniperus-Cupressus*-type, deciduous and evergreen *Quercus*, *Fraxinus excelsior*-type, *Salix*, *Tilia*, and *Ulmus*), and *Pinus*, **(D)** pollen percentages of **(E)** semi-desert plants and **(F)** *Calluna vulgaris*. Gray bars represent the HS 4, HS 3 (~GS 5), HS 2 (~GS 3) and HS 1 and GS 8, GS 7, GS 6, GS 4. HS 4, HS 3 and HS 1 are divided in two phases, a and b. HS 4 (a: ~39.5–38.6 ka; b: ~38.6–38 ka); HS 2 (a: ~26–25.5 ka; b: ~25.5–24 ka); HS 1 (a: ~18.8–17.5 ka; b: ~17.5–15.8 ka). Adapted from Naughton et al. (2009).

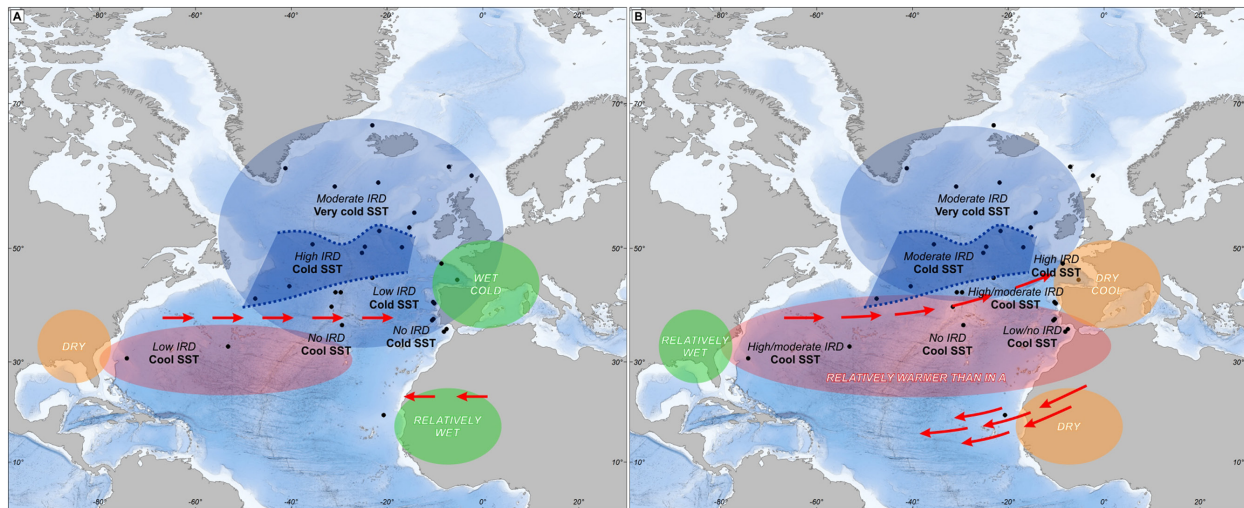


FIGURE 10 | Mapping oceanic and atmospheric patterns of Heinrich events in the North Atlantic region within: **(A)** the first phase and **(B)** the second phase of HS 4, HS 2 and HS 1. The gray zone in the middle of the North Atlantic represents the Ruddiman belt. Adapted from Naughton et al. (2009).

of the westerlies and increased precipitation in southwestern Europe. The scenario highlighted by our synthesis suggests that a mechanism similar to that of the present-day NAO in negative mode could have played a role (Naughton et al., 2009).

During the second phase of HS4, HS2 and HS1, climatic proxies indicate a northward migration of the thermal front associated with the northward shift of the westerlies and dryness in western Europe. This is accompanied in simulations by the southward displacement of the Inter Tropical Convergence Zone (ITCZ) (Kageyama et al., 2009) as detected from the increased of trade winds offshore Senegal (Jullien et al., 2007). As a whole, this configuration is similar to that currently produced by the positive mode of the NAO (Naughton et al., 2009). A marine pollen record from the Bay of Bengal indicates that HS 2 was associated with extremely weak summer and winter Indian monsoons, thus adding support for the southward migration of the ITCZ (Zorzi et al., 2015) during this period as also shown by South American and Asian speleothem records (e.g., Wang et al., 2004, 2008) and other marine sequences off western Africa (e.g., Weldeab et al., 2007).

The multi-phase structure of HS 4, HS 2 and HS 1 is supported by changes in ^{17}O -excess, increase in CO_2 and methane mixing ratio and heavier $\delta\text{D-CH}_4$ and $\delta^{18}\text{O}_{\text{atm}}$ observed in Greenland ice cores (Guillevic et al., 2014). In particular, in the second part of GS 9 (39.9–38.1 ka) the HS 4 imprint in Greenland would be characterized by a lower-latitude signal (without no changes in high-latitude temperature) associated with the southward migration of the ITCZ and a cold Europe (Guillevic et al., 2014). These data evidence a decoupling during GS 9 between stable cold Greenland temperature and low-latitude climate variability.

A decoupling between high and lower latitudes is also observed during GI 12 (46.8–44.3 ka) and GI 8 (38.2–36.6 ka)

(Sánchez Goñi et al., 2009). After the northern hemispheric rapid warming at the GS-GI transition, the trend during the first part of the GI is a Greenland cooling and an Iberian warming. This increase of the North Atlantic climatic gradient led to moisture transportation to Greenland from mid latitudes (lightest d-excess) and to a drying episode in Iberia. The subsequent temperature decrease in Greenland and Iberia associated with the precipitation increase in the latter region occurred when the major source of Greenland precipitation shifted to lower latitudes (d-excess increase). These examples of decoupling during GS and GI provide new targets for benchmarking climate model simulations and testing mechanisms associated with millennial variability (Guillevic et al., 2014).

INTERACTIONS BETWEEN MILLENNIAL AND ORBITAL CLIMATE VARIABILITY: THE MISSING PIECE OF THE ICE AGE PUZZLE?

Changes in insolation roughly explain the timing of deglaciation and glacial inception (Milankovitch, 1941; Shackleton and Opdyke, 1973; Hays et al., 1976). However, internal feedback processes are needed to explain the ice age cycles, and previous research has mostly focused on those loops related to atmospheric and oceanic circulation (e.g., Risebrobakken et al., 2007; Bar-Or et al., 2008), GHG concentrations (e.g., Ganopolski et al., 2016), and vegetation-albedo feedback (Crucifix and Loutre, 2002; Desprat et al., 2005; Sánchez Goñi et al., 2005). So far little attention has been paid to the interactions between shorter (millennial-scale) and longer (10,000 to 100,000 years) term climate variability that may amplify the original orbital forcing (Hodell, 2016). Another important missing piece of the Ice Age puzzle involves the still debated origin of the

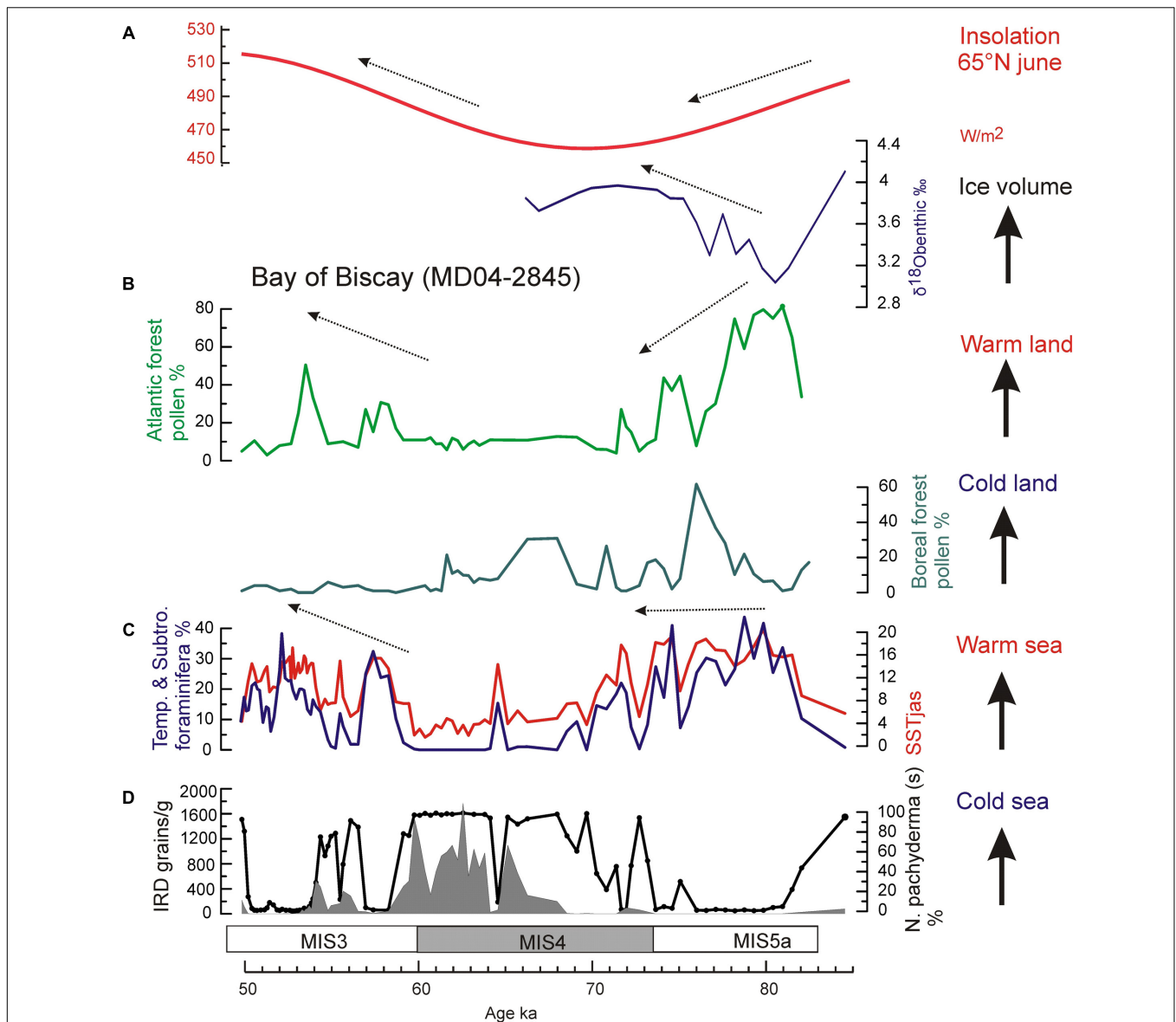


FIGURE 11 | Insolation changes versus marine and terrestrial palaeoclimatic records from core MD04-2845 for the interval 85–50 ka (Sánchez Goñi et al., 2013): **(A)** insolation curve at 65°N in June (Berger, 1978), and $\delta^{18}\text{O}$ benthic foraminifer isotopic record (*Cibicides wuellerstorfi* > 150 μm), **(B)** pollen records of Atlantic and Boreal forests in western France, **(C)** foraminifer-based summer SST (red line) in the Bay of Biscay, and percentages of temperate and subtropical foraminifer assemblages (blue line), and **(D)** IRD concentration and *N. pachyderma* (s) percentage (black solid line) records.

short-term climatic variability at high versus low latitudes, which has implications for the start of glaciations (Berger et al., 2006).

Internal Mechanisms Linking Changes in Earth's Orbit to Ice Ages

In this section, we firstly focus on the specific mechanisms linking changes in Earth's orbit to Ice Ages taking as a test bed the onset of the last glaciation (i.e., MIS 5a/4 transition: ~80–70 ka), when one of the largest ice accumulations of the last 250,000 years occurred.

Ruddiman and McIntyre (1979) showed unequivocally that the ice growth in the northern hemisphere was contemporaneous with persistent warmth and high salinity in the subpolar North Atlantic (44–54° N) when boreal summer insolation was decreasing. This apparent paradox was interpreted as the development of a strong thermal gradient between a warm subpolar North Atlantic and a cold nearby land leading to an increase of moisture. This moisture was transported toward the north by storm tracks and fell as snow following the decrease in insolation. However, this theoretical model involving a warm ocean-cold land thermal contrast was not confirmed at that time due to the lack of data. Also, the interglacial/glacial

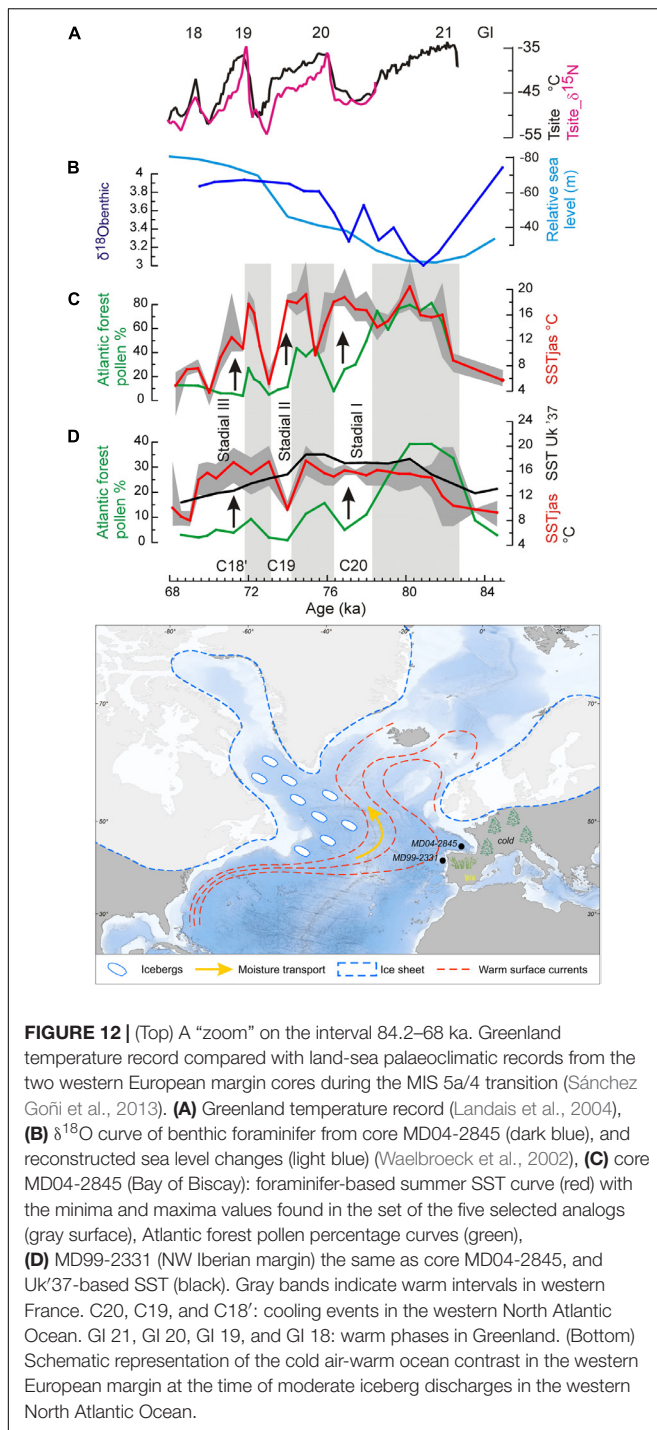


FIGURE 12 | (Top) A “zoom” on the interval 84.2–68 ka. Greenland temperature record compared with land-sea palaeoclimatic records from the two western European margin cores during the MIS 5a/4 transition (Sánchez Goñi et al., 2013). **(A)** Greenland temperature record (Landais et al., 2004), **(B)** $\delta^{18}O$ curve of benthic foraminifer from core MD04-2845 (dark blue), and reconstructed sea level changes (light blue) (Vaelbroeck et al., 2002), **(C)** core MD04-2845 (Bay of Biscay): foraminifer-based summer SST curve (red) with the minima and maxima values found in the set of the five selected analogs (gray surface), Atlantic forest pollen percentage curves (green), **(D)** MD99-2331 (NW Iberian margin) the same as core MD04-2845, and UK '37-based SST (black). Gray bands indicate warm intervals in western France. C20, C19, and C18': cooling events in the western North Atlantic Ocean. GI 21, GI 20, and GI 19, and GI 18: warm phases in Greenland. (Bottom) Schematic representation of the cold air-warm ocean contrast in the western European margin at the time of moderate iceberg discharges in the western North Atlantic Ocean.

transitions were then thought to be gradual but we know now that they were punctuated by millennial-scale events. Thus, one may wonder whether sub-orbital climatic variability, i.e., D-O cycles and HEs, affected this orbitally-controlled ice growth.

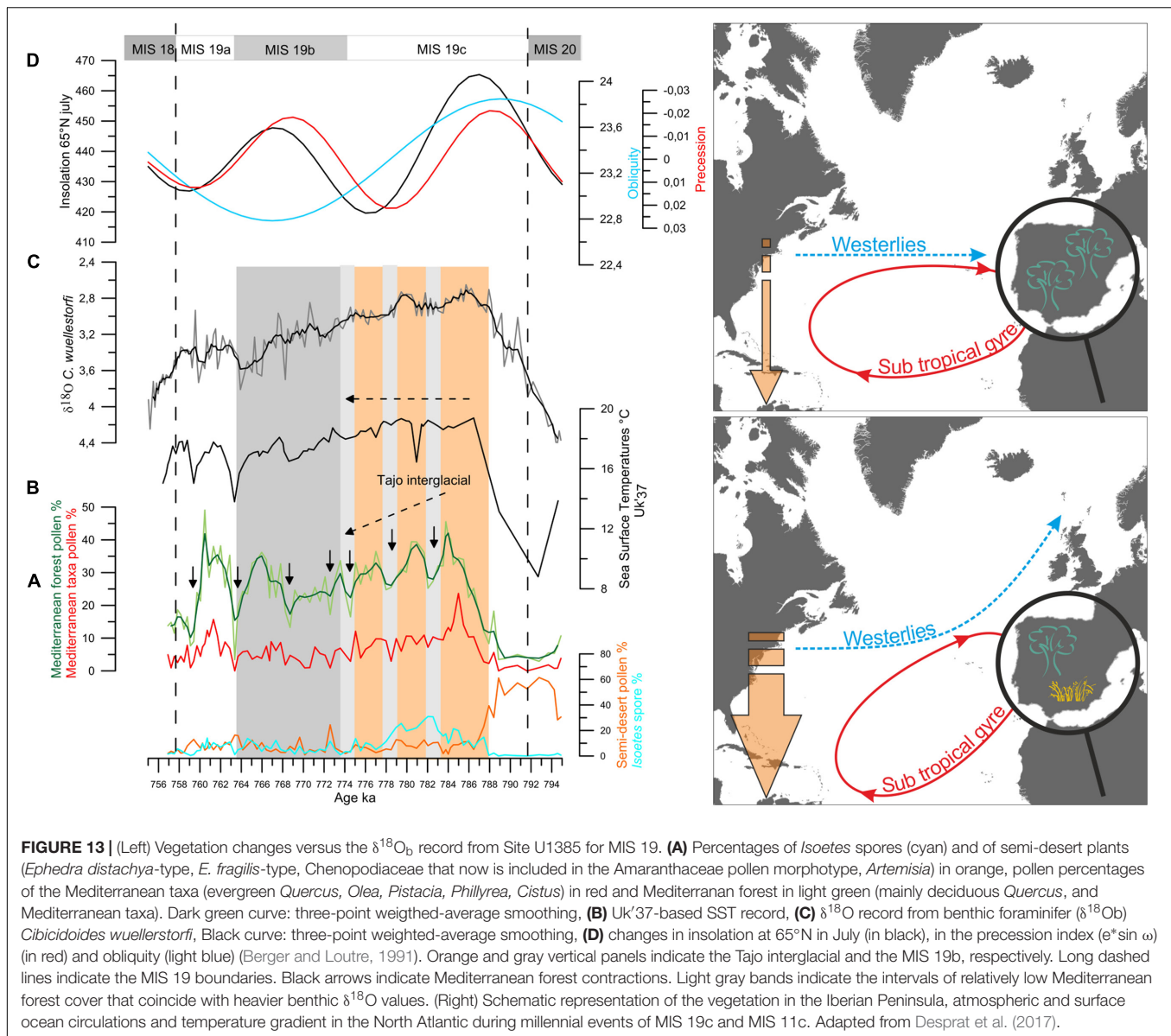
During the MIS 5a/4 transition, the direct land-sea correlation of the core MD04-2845, located at 45°N in the northern subtropical Atlantic, shows that the increase in ice volume

at orbital scale was contemporaneous with a progressive cooling in western Europe, as indicated by the replacement of temperate forest by boreal forest (mainly *Abies* and *Picea*). The simultaneous stabilization of warm SST in the Bay of Biscay demonstrates for the first time a long-term increase of the thermal warm sea-cold land gradient toward the MIS 4 glacial (Sánchez Goñi et al., 2013) (Figure 11). At sub-orbital scale, a decoupling with cooling on land synchronous with warming in SST is furthermore observed (Figure 12). Three successive episodes of strong land-sea thermal gradient and another three with weak gradients occurred during the MIS 5a/4 transition, superimposed on the long-term increasing trend in the thermal gradient (Sánchez Goñi et al., 2013).

The strong land-sea thermal gradients coincided with the North Atlantic cold events C20, C19, and C18' marked by moderate iceberg discharges in the western side of the North Atlantic (McManus et al., 1994) and related to Greenland cold episodes GS 21, GS 20, and GS 19 (Rasmussen et al., 2014) while the weak gradients coincided with the warm episodes in the North Atlantic and Greenland, GI 20, GI 19, and GI 18. Whereas the events C20, C19, and C18' were cold in the subpolar gyre and cold conditions installed in western Europe, the northern subtropical gyre remained warm. Increased snowfall in northern Europe and subsequent ice growth resulted from the high rates of moisture production resulting from the abovementioned strong land-sea thermal gradient and its transport by northward tracking storms. Southward displacement of tundra by 10° in latitude during cold phases C20, C19 and C18', as suggested by boreal forest colonization of western Europe, probably amplified ice growth owing to the increase in surface albedo (Crucifix and Loutre, 2002). Weak gradients slowed down the process but still allowed ice accumulation. The marine and pollen palaeoclimatic records from core MD99-2331, off north-western Iberia, show the same orbital and sub-orbital increases in the land-sea thermal gradient, excluding during C19 (Figure 12). In contrast, further south, in the south-western Iberian margin, the thermal gradient remained weak throughout the MIS 5a/4 transition. In summary, the direct comparison between marine and terrestrial records from the European margin demonstrates for the first time a long-term increase in the thermal gradient between the cold air and warmer sea, and three short intervals of even more pronounced thermal gradients during the last entering in glaciation. This synergy between orbital and millennial-scale variability provided a substantial source of moisture that was transported, through northward-tracking storms, to feed ice sheets in colder Greenland, northern Europe, and the Arctic.

The Origin of the Millennial-Scale Variability and the Implication for the Ice Ages

The origin of the short-lived climate changes is still a subject of debate. On the one hand, some authors propose that high-latitude processes such as iceberg discharges and changes



in the AMOC would have forced the rapid climate changes observed in the mid and low latitudes of the North Atlantic Ocean throughout the Pleistocene (Ganopolski and Rahmstorf, 2001). On the other hand, other authors put forward a low-latitude forcing mechanism via the harmonics of precession. Actually, the tropical latitudes receive over the course of the year a daily irradiance characterized by a double maximum that originates in the equatorial insolation cyclicities at 5,500 and 11,000 years (Berger et al., 2006). A direct consequence of this process would be a larger latitudinal thermal gradient and the enhanced transport of warmth and moisture by either atmospheric (westerlies) or oceanic circulation (subtropical gyre) from equatorial to high latitudes in the North Atlantic (Berger et al., 2006).

This low latitude forcing has also been suggested during periods of low eccentricity, when precession changes are

mutated, such as the last 45,000 years and MIS 19, centered at 800,000 years ago, based only on paleoceanographic evidence (e.g., McIntyre and Molino, 1996; Ferretti et al., 2015). Our recent land-sea direct correlation studies at the IODP Site U1385 (south-western Iberian margin) have provided firm evidence on the transport of energy from equatorial regions to the high latitudes by means of the westerlies during the MIS 19 and MIS 11, the astronomically closest analogs to the present interglacial. During MIS 19 and MIS 11, Mediterranean forest pollen percentages indicate two and three long-term major Mediterranean forest expansions, respectively, following maxima in insolation (Figure 13 for MIS 19 as an example). These major forest episodes point to the occurrence of a well-established Mediterranean climate, with higher winter precipitations and warmer and drier summers. Forest expansion in south-western Iberia therefore indicates that the prevailing

zonal configuration of the westerlies during these interglacials brought precipitation to this region (Oliveira et al., 2016; Sánchez Goñi et al., 2016b). During MIS 19c and MIS 11c, a long-term decrease in the Mediterranean forest cover indicating a progressive cooling and drying trend contrasts with the SST record showing quite stable and warm conditions (around 18°C) in the subtropical gyre. During these intervals, freshwater input is not detected on this margin and the progressive increase in the local benthic foraminifer $\delta^{13}\text{C}$ indicates good deep water ventilation (Oliveira et al., 2016; Sánchez Goñi et al., 2016b). These long-term trends were punctuated by major contractions of the Mediterranean forest coeval with increases in Mediterranean semi-desert plants, which may indicate intervals when the westerlies were slightly deflected toward the north with a subsequently reduced influence in south-western Iberia. Repeated meridional shifts in the westerlies during MIS 19c and MIS 11c would have implied successive large masses of warm and moist air reaching the high latitudes of the North Atlantic via the western boundary current of the North Atlantic subtropical gyre. At sub-orbital time scales a decoupling also occurred during MIS 19c and MIS 11c with several drying and cooling events on land concomitant with stable warm SST.

The direct comparison of marine and pollen proxies shows therefore a clear air-sea decoupling during MIS 19c and MIS 11c at orbital and millennial time-scales. In contrast, the other cool and dry events during MIS 19b-19a and MIS 11b-11a were contemporaneous with SST cooling in the subtropical gyre and IRD deposition at in the subpolar gyre (IODP Site U1314 and ODP Site 980), which evidences the input of large amounts of icebergs in the subpolar North Atlantic (Oppo et al., 1998; Alonso-Garcia et al., 2011). Interestingly, the atmospheric cool and dry events during MIS 19c and MIS 11c were not associated with freshwater pulses in either the subtropical or subpolar gyres indicating that the cause of these events was not primarily related to high latitude ice-sheet dynamics. Fourier spectral analysis applied to the pollen and marine records, excluding the benthic foraminifer $\delta^{18}\text{O}$ record, show dominant 5,000- and 10,000-year cyclicities for MIS 19 and MIS 11, likely related with the fourth and second harmonics of precession, respectively (Oliveira et al., 2016; Sánchez Goñi et al., 2016b; Oliveira, 2017). For MIS 19c, the comparison of the Mediterranean forest pollen record and its 5-kyr bandpass filter output curve with the variations in the largest amplitude of the seasonal cycle reconstructed at the equator shows good correspondence between the two records although the magnitude of changes was larger during MIS 19b-19a than during MIS 19c (Sánchez Goñi et al., 2016b). This good correspondence gives support to the low latitude origin of the observed repeated shift of the westerlies in southwestern Iberia at 37°N likely related to the harmonics of precession.

The stronger forest contractions during MIS 19b-19a and MIS 11b-11a would be explained by the regional SST cooling linked to the freshwater fluxes arriving at the subpolar gyre and reducing the AMOC. These data show once more that cold and dry episodes occurred independently of the amount

of ice volume (Oppo et al., 1998; Desprat et al., 2009). In contrast, their intensity and duration are modulated by positive feedback mechanisms on the AMOC associated with ice dynamics and, particularly, with freshwater pulses from iceberg discharges and melting (Barker et al., 2015; Oliveira et al., 2016).

During the MIS 19c/19b transition the three cold land-warm sea decoupling events coincide with three increases in the benthic $\delta^{18}\text{O}$ values concomitant with decreases in sea level. This observation suggests that for a period of low amplitude changes in insolation a tropically-driven strong warm sea-cold land contrast at millennial-timescale in the western European margin likely contributed to the increase of moisture. Similarly to that described previously for the MIS 5a/4 transition, these repeated millennial-scale episodes of moisture increase fed the ice caps through northward storm tracks and triggered the onset of the successive glacial period, at around 774,000 years ago.

CONCLUSION

Pollen analysis from deep-sea sedimentary sequences constitutes a powerful tool for reconstructing regional vegetation and climate changes that, in turn, influenced the global climate. One of the main advantages of pollen records from marine sediment sequences is that they allow direct correlations of climate change over land, in the ocean and in the ice domain, with minimum chronological uncertainty. This is because marine proxies (e.g., $\delta^{18}\text{O}$ from foraminifer, dinoflagellate cysts, IRD) and terrestrial tracers (e.g., pollen) can be analyzed from the same sediment sample so ocean-ice-atmosphere paleoreadings can be obtained for the same time slice. A second crucial advantage is that besides pollen records, very few other palaeoclimate markers exist that are sensitive to the seasonality of temperature and precipitation. The pollen richness of marine sediments allows the quantitative estimation of temperatures, precipitation and, more importantly, their seasonality, one of the key parameters for understanding climate change. However, further research is necessary for improving the quantification of key climatic parameters, particularly seasonality in subtropical and tropical regions, and of vegetation cover and composition to better estimate albedo changes and their impact on global climate.

This overview has shown that European vegetation and climate responded to long-term and shorter-term climate changes. There was a dynamic equilibrium between vegetation and climate for short periods of forcing such as the D-O cycles and HEs that were similar in magnitude and velocity to the present-day global warming. However, the magnitude of the millennial-scale changes of the last glacial period was regionally-specific. Regions below 40°N appear to have been imprinted by precession, through changes in the amplitude of seasonal contrasts and particularly winter precipitation, while the amplitude of warming in northern regions seems to have been modulated by obliquity that determines the annual temperatures. Within GS and GI, particularly during HS 4, GI 12 and GI 8, a

decoupling between high and lower latitudes is observed, a decoupling that has also been identified for the amplitude of the European interglacials. In the mid-latitude regions above 40°N the forest expansion maxima, i.e., the warmest peaks, of the last five terrestrial interglacials is similar while below 40°N their magnitude differed. In this latter region, the main factor for forest expansion is winter precipitation, and this climatic parameter depends on precession.

The overview presented here also suggests that millennial scale climatic variability likely played an important role in glacial inception whatever the boundary climatic conditions were. During one of the largest and fastest ice growth phases at the MIS 5a/4 transition, the millennial variability associated with moderate iceberg discharges in the western North Atlantic Ocean pushed the warm and saline Gulf Stream toward the European margin and created optimal conditions to develop repeated and pronounced air-sea thermal contrasts in this region. The synergy between low and high frequency climate changes amplified moisture production and snow fall in the high latitudes of the Northern Hemisphere. Within interglacials MIS 11 and MIS 19, the cyclicity of the harmonics of precession, repeatedly warming the low latitudes and increasing the latitudinal thermal gradient, created similar pronounced increases of the air-sea thermal gradient in the European margin that favored moisture production and the onset of ice growth. The theoretical model proposed here, and therefore the physical mechanisms involving rapid changes in the westerlies, in the direction of the subtropical gyre and in the air-sea thermal contrast superimposed to the long-term change, needs to be evaluated by model experiments. In particular, some authors (e.g., Crucifix et al., 2016) propose the integration of stochastic models in the Earth Model of Intermediate Complexity with the aim to analyze the effect of the rapid, millennial scale, variability on the long-term glacial-interglacial climate changes.

REFERENCES

- Allen, J. R. M., Brandt, U., Brauer, A., Hubberten, H.-W., Huntley, B., Keller, J., et al. (1999). Rapid environmental changes in southern Europe during the last glacial period. *Nature* 400, 740–743. doi: 10.1038/23432
- Alonso-García, M., Sierro, F. J., Kucera, M., Flores, J. A., Cacho, I., and Andersen, N. (2011). Ocean circulation, ice sheet growth and interhemispheric coupling of millennial climate variability during the mid-Pleistocene (ca 800–400 ka). *Quat. Sci. Rev.* 30, 3234–3247. doi: 10.1016/j.quascirev.2011.08.005
- Alvarez-Solas, J., and Ramstein, G. (2011). On the triggering mechanism of Heinrich events. *Proc. Natl. Acad. Sci. U.S.A.* 108, E1359–E1360. doi: 10.1073/pnas.1116575108
- Augustin, L., Barbante, C., Barnes, P. R., Barnola, J. M., Bigler, M., and Castellano, E. (2004). Eight glacial cycles from an Antarctic ice core. *Nature* 429, 623–628. doi: 10.1038/nature02599
- Bailey, R. G. (1998). *Ecoregions: The Ecosystem Geography of the Oceans and Continents*. New York, NY: Springer.
- Barker, S., Chen, J., Gong, X., Jonkers, L., Knorr, G., and Thornalley, D. (2015). Icebergs not the trigger for North Atlantic cold events. *Nature* 520, 333–336. doi: 10.1038/nature14330
- Barker, S., Knorr, G., Edwards, R. L., Parrenin, F., Putnam, A. E., Skinner, L. C., et al. (2011). 800,000 years of abrupt climate variability. *Science* 334, 347–351. doi: 10.1126/science.1203580

AUTHOR CONTRIBUTIONS

MFSG designed the synthesis and wrote the manuscript. All the co-authors contributed to the writing of the manuscript.

FUNDING

Financial support was provided by WarmClim, a LEFE-INSU, IMAGO project. CM-M was supported by an IdEx Bordeaux post-doctoral fellowship, FN by Climhol (PTDC/AAC-CLI/100157/2008) and Ultimatum (IF/01489/2015), DO by the Portuguese Foundation for Science and Technology (FCT) through the doctoral grant (SFRH/BD/9079/2012).

ACKNOWLEDGMENTS

A substantial part of this review is based on marine sedimentary cores that were collected during the IMAGES I, GEOSCIENCES, and ALIENOR oceanographic cruises, and IODP Expedition 339. The authors are grateful to the coring and logistic teams inboard of the R/V Marion Dufresne II and Joides Resolution. They are grateful to Vincent Hanquiez for helping with the drawing of the figures.

SUPPLEMENTARY MATERIAL

The Supplementary Material for this article can be found online at: <https://www.frontiersin.org/articles/10.3389/fpls.2018.00038/full#supplementary-material>

TABLE S1 | List of the 129 deep-sea pollen records distributed over the world.

- Bar-Or, R., Erlick, C., and Gildor, H. (2008). The role of dust in glacial-interglacial cycles. *Quat. Sci. Rev.* 27, 201–208. doi: 10.1016/j.quascirev.2007.10.015
- Bazin, L., Landais, A., Lemieux-Dudon, B., Toyé Mahamadou Kele, H., Veres, D., Parrenin, F., et al. (2013). An optimized multi-proxy, multi-site Antarctic ice and gas orbital chronology (AICC2012): 120–800 ka. *Clim. Past* 9, 1715–1731. doi: 10.5194/cp-9-1715-2013
- Beaudouin, C., Suc, J.-P., Escarguel, G., Arnaud, M., and Charmasson, S. (2007). The significance of pollen signal in present-day marine terrigenous sediments: the example of the Gulf of Lions (Western Mediterranean Sea). *Geobios* 40, 159–172. doi: 10.1016/j.geobios.2006.04.003
- Bennett, K. D., and Willis, K. J. (1995). The role of ecological factors in controlling vegetation dynamics on long temporal scales. *G. Bot. Ital.* 129, 243–254. doi: 10.1080/11263509509436132
- Berger, A. (1978). Long-term variations of daily insolation and Quaternary climatic changes. *J. Atmos. Sci.* 35, 2362–2367. doi: 10.1175/1520-0469(1978)035<2362:LTVODI>2.0.CO;2
- Berger, A., and Loutre, M. F. (1991). Insolation values for the climate of the last 10 million years. *Quat. Sci. Rev.* 10, 297–317. doi: 10.1016/0277-3791(91)90033-Q
- Berger, A., and Loutre, M. F. (2004). Astronomical theory of climate change. *J. Phys. IV France* 121, 1–35. doi: 10.1051/jp4:2004121001
- Berger, A., Loutre, M. F., and Mélice, J. L. (2006). Equatorial insolation: from precession harmonics to eccentricity frequencies. *Clim. Past* 2, 131–136. doi: 10.5194/cp-2-131-2006

- Birks, H. J. B. (1981). "The use of pollen analysis in the reconstruction of past climates: a review," in *Climate and History*, eds T. M. L. Wigley, M. J. Ingram, and G. Farmer (Cambridge: Cambridge University Press), 111–138.
- Blanco Castro, E., Casado González, M. A., Costa Tenorio, M., Escribano Bombín, R., García Antón, M., Génova Fuster, M., et al. (1997). *Los Bosques Ibéricos*. Barcelona: Planeta, 572.
- Bond, G., Broecker, W., Johnsen, S., McManus, J., Labeyrie, L., Jouzel, J., et al. (1993). Correlations between climate records from North Atlantic sediments and Greenland ice. *Nature* 365, 143–147. doi: 10.1038/365143a0
- Bond, G., and Lotti, R. (1995). Iceberg discharges into the North Atlantic on millennial time scales during the Last Glaciation. *Science* 267, 1005–1009. doi: 10.1126/science.267.5200.1005
- Bordon, A., Peyron, O., Lézine, A.-M., Brewer, S., and Fouache, E. (2009). Pollen-inferred Late-Glacial and Holocene climate in southern Balkans (Lake Maliq). *Quat. Int.* 200, 19–30. doi: 10.1016/j.quaint.2008.05.014
- Cambon, G., Suc, J.-P., Aloisi, J.-C., Giresse, P., Monaco, A., Touzani, A., et al. (1997). Modern pollen deposition in the Rhone delta area (Lagoonal and marine sediments), France. *Grana* 36, 105–113. doi: 10.1080/00173139709362596
- Carré, M., and Cheddadi, R. (2017). Seasonality in long-term climate change. *Quaternaire* 28, 173–177. doi: 10.4000/quaternaire.8018
- Chabaud, L., Sánchez Goñi, M. F., Desprat, S., and Rossignol, L. (2014). Land-sea climatic variability in the eastern North Atlantic subtropical region over the last 14,200 years: atmospheric and oceanic processes at different timescales. *Holocene* 24, 787–797. doi: 10.1177/0959683614530439
- Chapman, M. R., and Shackleton, N. J. (1999). Global ice-volume fluctuations, North Atlantic ice-rafter events, and deep-ocean circulation changes between 130 and 70 ka. *Geology* 27, 795–798. doi: 10.1130/0091-7613(1999)027<0795:GIVFNA>2.3.CO;2
- Claussen, M. (2007). "Introduction to climate forcing and climate feedbacks," in *The Climate of Past Interglacials: Developments in Quaternary Science*, Vol. 7, eds F. Sirocko, M. Claussen, M. F. Sánchez Goñi, and T. Litt (Amsterdam: Elsevier), 3–11. doi: 10.1016/S1571-0866(07)80026-1
- Combouret, N., Peyron, O., Dormoy, I., Desprat, S., Beaudoin, C., Kotthoff, U., et al. (2009). Rapid climatic variability in the west Mediterranean during the last 25 000 years from high resolution pollen data. *Clim. Past* 5, 503–521. doi: 10.5194/cp-5-503-2009
- Crucifix, M., and Loutre, M. F. (2002). Transient simulations over the last interglacial period (126–115 kyr BP): feedback and forcing analysis. *Clim. Dyn.* 19, 417–433. doi: 10.1007/s00382-002-0234-z
- Crucifix, M., Mitsui, T., and Lenoir, G. (2016). "Challenges for ice age dynamics: a dynamical systems perspective," in *Nonlinear and Stochastic Climate Dynamics*, eds C. Franzke and T. J. O'Kane (Cambridge: Cambridge University Press), 1–32.
- Daniau, A. L., Sánchez Goñi, M.-F., Beaufort, L., Laggoun-Défarge, F., Loutre, M.-F., and Duprat, J. (2007). Dansgaard-Oeschger climatic variability revealed by fire emissions in southwestern Iberia. *Quat. Sci. Rev.* 26, 1369–1383. doi: 10.1016/j.quascirev.2007.02.005
- Daniau, A.-L., Sánchez Goñi, M. F., Martínez, P., Urrego, D. H., Bout-Roumazeilles, V., Desprat, S., et al. (2013). Orbital-scale climate forcing of grassland burning in southern Africa. *Proc. Natl. Acad. Sci. U.S.A.* 110, 5069–5073. doi: 10.1073/pnas.1214292110
- Dansgaard, W., Johnsen, S., Clausen, H. B., Dahl-Jensen, D., Gundestrup, N., Hammer, C. U., et al. (1984). "North Atlantic climatic oscillations revealed by deep Greenland ice cores," in *Climate Processes and Climate Sensitivity*, eds J. E. Hansen and T. Takahashi (Washington, DC: American Geophysical Union), 288–298.
- de Beaulieu, J.-L., Andrieu-Ponel, V., Reille, M., Gröger, E., Tzedakis, C., and Svoboda, H. (2001). An attempt at correlation between the Velay pollen sequence and the Middle Pleistocene stratigraphy from central Europe. *Quat. Sci. Rev.* 20, 1593–1602. doi: 10.1016/S0277-3791(01)00027-0
- deMenocal, B. (2004). African climate change and faunal evolution during the Plio-Pleistocene. *Earth Planet. Sci. Lett.* 204, 3–24. doi: 10.1016/S0012-821X(04)00003-2
- Desprat, S., Diaz Fernandez, M., Coulon, T., Ezzat, L., Pessaro-Langlois, J., Gil, L., et al. (2015). Pinus nigra (European black pine) as the dominant species of the last glacial pinewoods in south-western to central Iberia: a morphological study of modern and fossil pollen. *J. Biogeogr.* 42, 1998–2009. doi: 10.1111/jbi.12566
- Desprat, S., Oliveira, O., Naughton, F., and Sánchez Goñi, M. F. (2017). L'étude du pollen des séquences sédimentaires marines pour la compréhension du climat: l'exemple des périodes chaudes passées. *Quaternaire* 28, 259–269. doi: 10.4000/quaternaire.8102
- Desprat, S., Sánchez Goñi, M. F., McManus, J. F., Duprat, J., and Cortijo, E. (2009). Millennial-scale climatic variability between 340 000 and 270 000 years ago in SW Europe: evidence from a NW Iberian margin pollen sequence. *Clim. Past* 5, 53–72. doi: 10.5194/cp-5-53-2009
- Desprat, S., Sánchez Goñi, M. F., Naughton, F., Turon, J. L., Duprat, J., Malaizé, B., et al. (2007). "Climate variability of the last five isotopic interglacials from direct land-sea-ice correlation," in *The Climate of Past Interglacials*, eds F. Sirocko, M. Claussen, M. F. Sánchez Goñi, and T. Litt (Amsterdam: Elsevier), 375–386.
- Desprat, S., Sánchez Goñi, M. F., Turon, J.-L., Duprat, J., Malaizé, B., and Peyrouquet, J.-P. (2006). Climatic variability of Marine Isotope Stage 7: direct land-sea-ice correlation from a multiproxy analysis of a north-western Iberian margin deep-sea core. *Quat. Sci. Rev.* 25, 1010–1026. doi: 10.1016/j.quascirev.2006.01.001
- Desprat, S., Sánchez Goñi, M. F., Turon, J.-L., McManus, J. F., Loutre, M. F., Duprat, J., et al. (2005). Is vegetation responsible for glacial inception during periods of muted insolation changes? *Quat. Sci. Rev.* 24, 1361–1374. doi: 10.1016/j.quascirev.2005.01.005
- Dupont, L. (2011). Orbital scale vegetation change in Africa. *Quat. Sci. Rev.* 30, 3589–3602. doi: 10.1016/j.quascirev.2011.09.019
- Dupont, L. M., and Wypytta, U. (2003). Reconstructing pathways of aeolian pollen transport to the marine sediments along the coastline of SW Africa. *Quat. Sci. Rev.* 22, 157–174. doi: 10.1016/S0277-3791(02)00032-X
- Elliot, M., Labeyrie, L., Dokken, T., and Manthé, S. (2001). Coherent patterns of ice-rafter debris deposits in the Nordic regions during the last glacial (10–60 ka). *Earth Planet. Sci. Lett.* 194, 151–163. doi: 10.1016/S0012-821X(01)00561-1
- Ferretti, P., Crowhurst, S. J., Naafs, B. D. A., and Barbante, C. (2015). The marine isotope stage 19 in the mid-latitude North Atlantic Ocean: astronomical signature and intra-interglacial variability. *Quat. Sci. Rev.* 108, 95–110. doi: 10.1016/j.quascirev.2014.10.024
- Fletcher, W. J., and Sánchez Goñi, M. F. (2008). Orbital- and sub-orbital-scale climate impacts on vegetation of the western Mediterranean basin over the last 48,000 yr. *Quat. Res.* 70, 451–464. doi: 10.1016/j.yqres.2008.07.002
- Fletcher, W. J., Sánchez Goñi, M. F., Allen, J. R. M., Cheddadi, R., Combouret-Nebout, N., Huntley, B., et al. (2010). Millennial-scale variability during the last glacial in vegetation records from Europe. *Quat. Sci. Rev.* 29, 2839–2864. doi: 10.1016/j.quascirev.2009.11.015
- Follieri, M., Magri, D., and Sadori, L. (1988). 250,000-year pollen record from valle di Castiglione (Roma). *Pollen Spores* 30, 329–356.
- Ganopolski, A., and Rahmstorf, S. (2001). Rapid changes of glacial climate simulated in a coupled climate model. *Nature* 409, 153–158. doi: 10.1038/35051500
- Ganopolski, A., Winkelmann, R., and Schellnhuber, H. J. (2016). Critical insolation–CO₂ relation for diagnosing past and future glacial inception. *Nature* 529, 200–203. doi: 10.1038/nature16494
- Gouveia, C., Trigo, R. M., DaCamara, C. C., Libonati, R., and Pereira, J. M. C. (2008). The North Atlantic Oscillation and European vegetation dynamics. *Int. J. Climatol.* 28, 1835–1847. doi: 10.1002/joc.1682
- Groot, J. J., and Groot, C. R. (1966). Marine palynology: possibilities, limitations, problems. *Mar. Geol.* 4, 387–395. doi: 10.1016/0025-3227(66)90007-7
- Guilleux, M., Bazin, L., Landais, A., Stowasser, C., Masson-Delmotte, V., Blunier, T., et al. (2014). Evidence for a three-phase sequence during Heinrich Stadial 4 using a multiproxy approach based on Greenland ice core records. *Clim. Past* 10, 2115–2133. doi: 10.5194/cp-10-2115-2014
- Guiot, J. (1990). Methodology of the last climatic cycle reconstruction from pollen data. *Palaeogeogr. Palaeoclimatol. Palaeoecol.* 80, 49–69. doi: 10.1016/0031-0182(90)90033-4
- Guiot, J., and De Vernal, A. (2007). "Transfer functions: methods for quantitative paleoclimatology based on microfossils," in *Developments in Marine Geology*, Vol. 1, eds C. Hillaire-Marcel and A. de Vernal (Amsterdam: Elsevier), 523–563.
- Hays, J. D., Imbrie, J., and Shackleton, N. J. (1976). Variations in the Earth's orbit pacemaker of the ice ages. *Science* 194, 1121–1132. doi: 10.1126/science.194.4270.1121

- Heinrich, H. (1988). Origin and consequences of cyclic ice rafting in the northeast Atlantic Ocean during the past 130,000 years. *Quat. Res.* 29, 142–152. doi: 10.1016/0033-5894(88)90057-9
- Heusser, L. E., and Balsam, W. L. (1977). Pollen distribution in the N.E. Pacific Ocean. *Quat. Res.* 7, 45–62. doi: 10.1016/0033-5894(77)90013-8
- Heusser, L. E., and Van de Geer, G. (1994). Direct correlation of terrestrial and marine paleoclimatic records from four glacial-interglacial cycles-DSDP site 594 Southwest Pacific. *Quat. Sci. Rev.* 13, 273–282. doi: 10.1016/0277-3791(94)90030-2
- Heusser, L. E., and Vm, Bryant Jr. (1985). “Quaternary palynology of marine sediments in the northeast Pacific, northwest Atlantic, and Gulf of Mexico,” in *Pollen Records of Late-Quaternary North American Sediments*, ed. R. G. Holloway (Dallas, TX: AASP Foundation), 385–403.
- Heusser, L. E. (1986/1987). Pollen in marine cores: evidence of past climates. *Oceanus* 29, 64–70.
- Hodell, D. A. (2016). The smoking gun of the ice ages. *Science* 354, 1235–1236. doi: 10.1126/science.aal4111
- Hodell, D. A., Lourens, L., Crowhurst, S., Konijnendijk, T., Tjallingii, R., Jiménez-Espejo, F., et al. (2015). A reference time scale for site U1385 (Shackleton Site) on the SW Iberian Margin. *Glob. Planet. Change* 133, 49–64. doi: 10.1016/j.gloplacha.2015.07.002
- Hoerling, M., Eischeid, J., Perlwitz, J., Quan, X. W., Zhang, T., and Pegion, P. (2012). On the increased frequency of Mediterranean drought. *J. Clim.* 25, 2146–2161. doi: 10.1175/JCLI-D-11-00296.1
- Hooghiemstra, H., Lézine, A.-M., Leroy, S. A. G., Dupont, L., and Marret, F. (1988). Late Quaternary palynology in marine sediments: a synthesis of the understanding of pollen distribution patterns in the NW African setting. *Quat. Int.* 148, 29–44. doi: 10.1016/j.quaint.2005.11.005
- Hooghiemstra, H., Stalling, H., Agwu, C. O. C., and Dupont, L. M. (1992). Vegetational and climatic changes at the northern fringe of the Sahara 250,000–5000 years BP: evidence from 4 marine pollen records located between Portugal and the Canary Islands. *Rev. Palaeobot. Palynol.* 74, 1–53. doi: 10.1016/0034-6667(92)90137-6
- Hooghiemstra, H., Agwu, C. O. C., and Beug, H.-J. (1986). Pollen and spore distribution in recent marine sediments: a record of NW-African seasonal wind patterns and vegetation belts. *Meteor. Forsch. C* 40, 87–135.
- Jullien, E., Grousset, F. E., Malaizé, B., Duprat, J., Sánchez Goni, M. F., Eynaud, F., et al. (2007). Tropical “dusty Heinrich-like events” vs. high-latitude “icy Heinrich events”. *Quat. Res.* 68, 379–386. doi: 10.1016/j.yqres.2007.07.007
- Kageyama, M., Mignot, J., Swingedouw, D., Marzin, C., Alkama, R., and Marti, O. (2009). Glacial climate sensitivity to different states of the Atlantic Meridional Overturning Circulation: results from the IPSL model. *Clim. Past* 5, 551–570. doi: 10.5194/cp-5-551-2009
- Knutti, R., Flückiger, J., Stocker, T. F., and Timmermann, A. (2004). Strong hemispheric coupling of glacial climate through freshwater discharge and ocean circulation. *Nature* 430, 851–856. doi: 10.1038/nature02786
- Koreneva, E. V. (1966). Marine palynological researches in the U.S.S.R. *Mar. Geol.* 4, 565–574. doi: 10.1016/0025-3227(66)90016-8
- Koreneva, E. V. (1971). “Spores and pollen in Mediterranean bottom sediments,” in *The Micropaleontology of Oceans*, eds B. M. Funnel and W. R. Riedel (Cambridge: Cambridge University Press), 361–371.
- Kühl, N., Gebhardt, C., Litt, T., and Hense, A. (2002). Probability density functions as botanical-climatological transfer functions for climate reconstruction. *Quat. Res.* 58, 381–392. doi: 10.1006/qres.2002.2380
- Landais, A., Barnola, J. M., Masson-Delmotte, V., Jouzel, J., Chappellaz, J., Caillon, N., et al. (2004). A continuous record of temperature evolution over a whole sequence of Dansgaard-Oeschger during Marine Isotopic Stage 4 (76 to 62 kyr BP). *Geophys. Res. Lett.* 31, 101–113. doi: 10.1029/2004GL021193
- Levasseur, G., Vrac, M., Roche, D. M., and Paillard, D. (2012). Statistical modelling of a new global potential vegetation distribution. *Environ. Res. Lett.* 7:044019. doi: 10.1088/1748-9326/7/4/044019
- Louergue, L., Schilt, A., Spahni, R., Masson-Delmotte, V., Blunier, T., Lemieux, B., et al. (2008). Orbital and millennial-scale features of atmospheric CH₄ over the past 800,000 years. *Nature* 453, 383–386. doi: 10.1038/nature06950
- Luthi, D., Le Floch, M., Bereiter, B., Blunier, T., Barnola, J.-M., Siegenthaler, U., et al. (2008). High-resolution carbon dioxide concentration record 650,000–800,000 years before present. *Nature* 453, 379–382. doi: 10.1038/nature06949
- Lynch-Stieglitz, J. (2017). The Atlantic Meridional Overturning Circulation and abrupt climate change. *Annu. Rev. Mar. Sci.* 9, 83–104. doi: 10.1146/annurev-marine-010816-060415
- Martrat, B., Grimalt, J. O., Shackleton, N. J., De Abreu, L., Hutterli, M. A., and Stocker, T. F. (2007). Four cycles of recurring deep and surface water destabilizations on the Iberian margin. *Science* 317, 502–507. doi: 10.1126/science.1139994
- McIntyre, A., and Molino, B. (1996). Forcing of Atlantic Equatorial and subpolar millennial cycles by precession. *Science* 274, 1867–1870. doi: 10.1126/science.274.5294.1867
- McManus, J. F., Bond, G. C., Broecker, W. S., Johnsen, S., Labeyrie, L., and Higgins, S. (1994). High-resolution climate records from the North Atlantic during the last interglacial. *Nature* 371, 326–329. doi: 10.1038/371326a0
- McManus, J. F., Francois, R., Gherardi, J.-M., Keigwin, L. D., and Brown-Leger, S. (2004). Collapse and rapid resumption of Atlantic meridional circulation linked to deglacial climate changes. *Nature* 428, 834–837. doi: 10.1038/nature02494
- McManus, J. F., Oppo, D. W., and Cullen, J. L. (1999). A 0.5-million-year record of millennial-scale climate variability in the North Atlantic. *Science* 283, 971–975. doi: 10.1126/science.283.5404.971
- Milankovitch, M. M. (1941). *Kanon der Erdbestrahlung*. Beograd: Königlich Serbische Akademie.
- Montade, V., Combouret-Nebout, N., Kissel, C., Haberle, S. H., Siani, G., and Michel, E. (2013). Vegetation and climate changes during the last 22,000 yr from a marine core near Taitao Peninsula, southern Chile. *Palaeogeogr. Palaeoclimatol. Palaeoecol.* 369, 335–348. doi: 10.1016/j.palaeo.2012.11.001
- Mudie, J., and McCarthy, F. M. G. (2006). Marine palynology: potentials for onshore-offshore correlation of Pleistocene-Holocene records. *Trans. R. Soc. S. Afr.* 61, 139–157. doi: 10.1080/00359190609519964
- Naughton, F., Sánchez Goñi, M. F., Desprat, S., Turon, J.-L., Duprat, J., Malaizé, B., et al. (2007). Present-day and past (last 25,000 years) marine pollen signal off western Iberia. *Mar. Micropaleontol.* 62, 91–114. doi: 10.1016/j.marmicro.2006.07.006
- Naughton, F., Sánchez Goñi, M. F., Kageyama, M., Bard, E., Duprat, J., Cortijo, E., et al. (2009). Wet to dry climatic trend in north western Iberia within Heinrich events. *Earth Planet. Sci. Lett.* 284, 329–342. doi: 10.1016/j.epsl.2009.05.001
- Naughton, F., Sánchez Goñi, M. F., Rodrigues, T., Salgueiro, E., Costas, S., Desprat, S., et al. (2016). Climate variability across the last deglaciation in NW Iberia and its margin. *Quat. Int.* 414, 9–22. doi: 10.1016/j.quaint.2015.08.073
- North Greenland Ice-Core Project Members [NGRIP] (2004). High resolution climate record of the northern hemisphere reaching into the last glacial interglacial period. *Nature* 431, 147–151.
- Oliveira, D. (2017). *Comprendre les Périodes Chaudes Pendant et Après la Transition du Pléistocène Moyen (MIS 31 et MIS 11) Dans la Péninsule Ibérique*. Bordeaux: Université de Bordeaux.
- Oliveira, D., Desprat, S., Rodrigues, T., Naughton, F., Hodell, D., Trigo, R., et al. (2016). The complexity of millennial-scale variability in southwestern Europe during MIS 11. *Quat. Res.* 86, 373–387. doi: 10.1016/j.yqres.2016.09.002
- Oliveira, D., Desprat, S., Yin, Q., Naughton, F., Trigo, R., Rodrigues, T., et al. (2017). Unraveling the forcings controlling the vegetation and climate of the best orbital analogues for the present interglacial in SW Europe. *Clim. Dyn.* 1, 1–20. doi: 10.1007/s00382-017-3948-7
- Oppo, D. W., McManus, J. F., and Cullen, J. L. (1998). Abrupt climate events 500,000 to 340,000 Years Ago: evidence from subpolar North Atlantic sediments. *Science* 279, 1335–1338. doi: 10.1126/science.279.5355.1335
- Oppo, D. W., McManus, J. F., and Cullen, J. L. (2006). Evolution and demise of the Last Interglacial warmth in the subpolar North Atlantic. *Quat. Sci. Rev.* 25, 3268–3277. doi: 10.1016/j.quascirev.2006.07.006
- Peyron, O., Guiot, J., Cheddadi, R., Tarasov, P., Reille, M., de Beaulieu, J.-L., et al. (1998). Climatic reconstruction in Europe for 18,000 yr B.P. from Pollen Data. *Quat. Res.* 49, 183–196. doi: 10.1006/qres.1997.1961
- Polunin, O., and Walters, M. (1985). *A Guide to the Vegetation of Britain and Europe*. New York, NY: Oxford University Press, 238.
- Pons, A., and Reille, M. (1988). The Holocene and Upper Pleistocene pollen record from Padul (Granada, Spain): a new study. *Palaeogeogr. Palaeoclimatol. Palaeoecol.* 66, 243–263. doi: 10.1016/0031-0182(88)90202-7
- Prentice, I. C., Guiot, J., Huntley, B., Jolly, D., and Cheddadi, R. (1996). Reconstructing biomes from palaeoecological data: a general method and its

- application to European pollen data at 0 and 6 ka. *Clim. Dyn.* 12, 185–194. doi: 10.1007/BF00211617
- Railsback, L. B., Gibbard, L., Head, M. J., Voarintsoa, N. R. G., and Toucanne, S. (2015). An optimized scheme of lettered marine isotope substages for the last 1.0 million years, and the climatostratigraphic nature of isotope stages and substages. *Quat. Sci. Rev.* 111, 94–106. doi: 10.1016/j.quascirev.2015.01.012
- Rasmussen, S. O., Bigler, M., Blockley, S. P., Blunier, T., Buchardt, S. L., Clausen, H. B., et al. (2014). A stratigraphic framework for abrupt climatic changes during the Last Glacial period based on three synchronized Greenland ice-core records: refining and extending the INTIMATE event stratigraphy. *Quat. Sci. Rev.* 106, 14–28. doi: 10.1016/j.quascirev.2014.09.007
- Ratmeyer, V., Balzer, W., Begametti, G., Chiappello, I., Fischer, G., and Wyputta, U. (1999). Seasonal impact of mineral dust on deep-ocean particle flux in the eastern subtropical Atlantic Ocean. *Mar. Geol.* 159, 241–252. doi: 10.1016/S0025-3227(98)00197-2
- Reille, M., and de Beaulieu, J.-L. (1990). Pollen analysis of a long upper Pleistocene continental sequence in a Velay maar (Massif Central, France). *Palaeogeogr. Palaeoclimatol. Palaeoecol.* 80, 35–48. doi: 10.1016/0031-0182(90)90032-3
- Reille, M., de Beaulieu, J.-L., Svobodova, V., Andrieu-Ponel, V., and Goeury, C. (2000). Pollen analytical biostratigraphy of the last five climatic cycles from a long continental sequence from the Velay region (Massif Central, France). *J. Quat. Sci.* 15, 665–685. doi: 10.1002/1099-1417(200010)15:7<665::AID-JQS560>3.0.CO;2-G
- Risebrobakken, B., Dokken, T., Ottera, O. H., Jansen, E., Gao, Y., and Drange, H. (2007). Inception of the Northern European ice sheet due to contrasting ocean and insolation forcing. *Quat. Res.* 67, 128–135. doi: 10.1016/j.yqres.2006.07.007
- Roche, D., Paillard, D., and Cortijo, E. (2004). Constraints on the duration and freshwater release of Heinrich event 4 through isotope modelling. *Nature* 432, 379–382. doi: 10.1038/nature03059
- Rossignol-Strick, M. (1983). African monsoons, an immediate climate response to orbital insolation. *Nature* 304, 46–49. doi: 10.1038/304046a0
- Roucoux, K. H. (2000). *Millennial Scale Vegetation and Climate Variability in North-West Iberia during the Last Glacial Stage*. Cambridge: University of Cambridge.
- Roucoux, K. H., Tzedakis, C., de Abreu, L., and Shackleton, N. J. (2006). Climate and vegetation changes 180,000 to 345,000 years ago recorded in a deep-sea core off Portugal. *Earth Planet. Sci. Lett.* 249, 307–325. doi: 10.1016/j.epsl.2006.07.005
- Ruddiman, W. F. (2001). *Earth's Climate: Past and Future*. New York, NY: W.H. Freeman & Sons.
- Ruddiman, W. F., and McIntyre, A. (1979). Warmth of the subpolar North Atlantic Ocean during northern hemisphere ice-sheet growth. *Science* 204, 173–175. doi: 10.1126/science.204.4389.173
- Ruddiman, W. F., and McIntyre, A. (1984). Ice-age thermal response and climatic role of the surface Atlantic Ocean, 40°N to 63°N. *Geol. Soc. Am. Bull.* 95, 381–396. doi: 10.1130/0016-7606(1984)95<381:ITRACR>2.0.CO;2
- Sadori, L., Koutsodendris, A., Panagiotopoulos, K., Masi, A., Bertini, A., Combourieu-Nebout, N., et al. (2016). Pollen-based paleoenvironmental and paleoclimatic change at Lake Ohrid (south-eastern Europe) during the past 500ka. *Biogeosciences* 13, 1423–1437. doi: 10.5194/bg-13-1423-2016
- Sánchez Goñi, M. F. (2014). “Rapid climatic variability in Europe over the last glacial,” in *Transitions, Ruptures et Continuité en Préhistoire*, ed. J. Jaubert (Paris: Bulletin de la Société Préhistorique de France), 185–193.
- Sánchez Goñi, M. F. (2016). Le climat au temps des peintres de Lascaux. *Dossiers Archéol.* 376, 42–47.
- Sánchez Goñi, M. F., Bakker, P., Desprat, S., Carlson, A., Van Meerbeeck, C. J., Peyron, O., et al. (2012). European climatic optimum and enhanced Greenland ice sheet melting during the last interglacial. *Geology* 40, 627–630. doi: 10.1130/G32908.1
- Sánchez Goñi, M. F., Bard, E., Landais, A., Rossignol, L., and d'Errico, F. (2013). Air-sea temperature decoupling in Western Europe during the last interglacial-glacial transition. *Nat. Geosci.* 6, 837–841. doi: 10.1038/ngeo1924
- Sánchez Goñi, M. F., Cacho, I., Turon, J.-L., Guiot, J., Sierro, F. J., Peypouquet, J.-P., et al. (2002). Synchronicity between marine and terrestrial responses to millennial scale climatic variability during the last glacial period in the Mediterranean region. *Clim. Dyn.* 19, 95–105. doi: 10.1007/s00382-001-0212-x
- Sánchez Goñi, M. F., Desprat, S., Daniau, A.-L., Bassinot, F. C., Polanco-Martínez, J. M., and Harrison, S. P. (2017). The ACER pollen and charcoal database: a global resource to document vegetation and fire response to abrupt climate changes during the last glacial period. *Earth Syst. Sci. Data* 9, 679–695. doi: 10.5194/essd-9-679-2017
- Sánchez Goñi, M. F., Eynaud, F., Turon, J.-L., and Shackleton, N. J. (1999). High resolution palynological record off the Iberian margin: direct land-sea correlation for the Last Interglacial complex. *Earth Planet. Sci. Lett.* 171, 123–137. doi: 10.1016/S0012-821X(99)00141-7
- Sánchez Goñi, M. F., and Hannon, G. (1999). High altitude vegetational patterns on the Iberian Mountain chain (north-central Spain) during the Holocene. *Holocene* 9, 39–57. doi: 10.1191/095968399671230625
- Sánchez Goñi, M. F., and Harrison, S. (2010). Millennial-scale climate variability and vegetation changes during the Last Glacial: concepts and terminology. *Quat. Sci. Rev.* 29, 2823–2827. doi: 10.1111/j.1365-2486.2012.02766.x
- Sánchez Goñi, M. F., Landais, A., Cacho, I., Duprat, J., and Rossignol, L. (2009). Contrasting intrainterstadial climatic evolution between high and middle latitudes: a close-up of Greenland Interstadials 8 and 12. *Geochem. Geophys. Geosyst.* 10:Q04U04.
- Sánchez Goñi, M. F., Landais, A., Fletcher, W. J., Naughton, F., Desprat, S., and Duprat, J. (2008). Contrasting impacts of Dansgaard-Oeschger events over a western European latitudinal transect modulated by orbital parameters. *Quat. Sci. Rev.* 27, 1136–1151. doi: 10.1016/j.quascirev.2008.03.003
- Sánchez Goñi, M. F., Loutre, M. F., Peyron, O., Santos, L., Duprat, J., Malaizé, B., et al. (2005). Increasing vegetation and climate gradient in Western Europe over the Last Glacial Inception (122–110 ka): data-model comparison. *Earth Planet. Sci. Lett.* 231, 111–130. doi: 10.1016/j.epsl.2004.12.010
- Sánchez Goñi, M. F., Ortu, E., Banks, W. E., Giraudeau, J., Leroyer, C., and Hanquiez, V. (2016a). The expansion of Central and Northern European Neolithic populations was associated with a multi-century warm winter and wetter climate. *Holocene* 26, 1188–1199. doi: 10.1177/0959683616638435
- Sánchez Goñi, M. F., Rodrigues, T., Hodell, D. A., Polanco-Martínez, J. M., Alonso-García, M., Hernández-Almeida, I., et al. (2016b). Tropically-driven climate shifts in southwestern Europe during MIS 19, a low eccentricity interglacial. *Earth Planet. Sci. Lett.* 448, 81–93. doi: 10.1016/j.epsl.2016.05.018
- Sánchez Goñi, M. F., Turon, J.-L., Eynaud, F., and Gendreau, S. (2000). European climatic response to millennial-scale climatic changes in the atmosphere-ocean system during the Last Glacial period. *Quat. Res.* 54, 394–403. doi: 10.1006/qres.2000.2176
- Seillès, B., Sánchez Goñi, M. F., Ledru, M.-P., Urrego, D. H., Martínez, P., Hanquiez, V., et al. (2016). Holocene land-sea climatic links on the equatorial Pacific coast (Bay of Guayaquil, Ecuador). *Holocene* 26, 567–577. doi: 10.1177/0959683615612566
- Shackleton, N. J., Hall, M. A., and Vincent, E. (2000). Phase relationships between millennial-scale events 64,000–24,000 years ago. *Paleoceanography* 15, 565–569. doi: 10.1029/2000PA000513
- Shackleton, N. J., and Opdyke, N. D. (1973). Oxygen isotope and palaeomagnetic stratigraphy of Equatorial Pacific core V28-238: oxygen isotope temperatures and ice volumes on a 10⁵ year and 10⁶ year scale. *Quat. Res.* 3, 39–55. doi: 10.1016/0033-5894(73)90052-5
- Shackleton, N. J., Sánchez Goñi, M. F., Paillet, D., and Lancelot, Y. (2003). Marine isotope substage 5e and the eemian interglacial. *Glob. Planet. Change* 757, 151–155. doi: 10.1016/S0921-8181(02)00181-9
- Siddall, M., Rohling, E. J., Almogi-Labin, A., Hemleben, C., Meischner, D., Schmelzer, I., et al. (2003). Sea-level fluctuations during the last glacial cycle. *Nature* 423, 853–858. doi: 10.1038/nature01690
- Siegenthaler, U., Stocker, T. F., Monnin, E., Lüthi, D., Schwander, J., Stauffer, B., et al. (2005). Stable carbon cycle-climate relationship during the late pleistocene. *Science* 310, 1313–1317. doi: 10.1126/science.1120130
- Skinner, L. C., and Shackleton, N. J. (2006). Deconstructing Terminations I and II: revisiting the glacioeustatic paradigm based on deep-water temperature estimates. *Quat. Sci. Rev.* 25, 3312–3321. doi: 10.1016/j.quascirev.2006.07.005
- Spahni, R., Chappellaz, J., Stocker, T. F., Loulergue, L., Hausamann, G., Kawamura, K., et al. (2005). Atmospheric methane and nitrous oxide of the Late Pleistocene from Antarctic ice cores. *Science* 310, 1317–1321. doi: 10.1126/science.1120132
- Stanley, E. (1966). The application of palynology to oceanology with reference to the northwestern Atlantic. *Deep Sea Res. II* 13, 921–939. doi: 10.1016/0011-7471(76)90911-6

- Sugita, S. (2007). Theory of quantitative reconstruction of vegetation I: pollen from large sites REVEALS regional vegetation composition. *Holocene* 17, 229–241. doi: 10.1177/0959683607075837
- Traverse, A., and Ginsburg, R. N. (1966). Palynology of the surface sediments of Great Bahama Bank, as related to water movement and sedimentation. *Mar. Geol.* 4, 417–459. doi: 10.1016/0025-3227(66)90010-7
- Turon, J.-L. (1984a). Direct land/sea correlations in the last interglacial complex. *Nature* 309, 673–676. doi: 10.1038/309673a0
- Turon, J.-L. (1984b). *Le Palynoplancton dans l'Environnement Actuel de l'Atlantique Nord-oriental: Evolution Climatique et Hydrologique Depuis le Dernier Maximum Glaciaire*. Bordeaux: Université de Bordeaux I, 313.
- Turon, J.-L., Lézine, A.-M., and Denèfle, M. (2003). Land-sea correlations for the last glaciation inferred from a pollen and dinocyst record from the Portuguese margin. *Quat. Res.* 59, 88–96. doi: 10.1016/S0033-5894(02)00018-2
- Tzedakis, C., Hooghiemstra, H., and Pälike, H. (2006). The last 1.35 million years at Tenaghi Philippon: revised chronostratigraphy and long-term vegetation trends. *Quat. Sci. Rev.* 25, 3416–3430. doi: 10.1016/j.quascirev.2006.09.002
- Urrego, D. H., Sánchez Goñi, M. F., Daniau, A. L., Lechevrel, S., and Hanquiez, V. (2015). Increased aridity in southwestern Africa during the warmest periods of the last interglacial. *Clim. Past* 11, 1417–1431. doi: 10.5194/cp-11-1417-2015
- Van Campo, M. M. (1984). Relations entre la végétation de l'Europe et les températures de surface océaniques après le dernier maximum glaciaire. *Pollen Spores* XXVI, 497–518.
- Voelker, A. H. L., and Workshop Participant (2002). Global distribution of centennial-scale records for Marine Isotope Stage (MIS) 3: a database. *Quat. Sci. Rev.* 21, 1185–1212. doi: 10.1016/S0277-3791(01)00139-1
- Waelbroeck, C., Labeyrie, L., Michel, E., Duplessy, J. C., McManus, J. F., Lambeck, K., et al. (2002). Sea-level and deep water temperature changes derived from benthic foraminifer isotopic records. *Quat. Sci. Rev.* 21, 295–305. doi: 10.1016/S0277-3791(01)00101-9
- Wang, X., Auler, A. S., Edwards, R. L., Cheng, H., Cristalli, S., Smart, L., et al. (2004). Wet periods in northeastern Brazil over the past 210 kyr linked to distant climate anomalies. *Nature* 432, 740–743. doi: 10.1038/nature03067
- Wang, Y. J., Cheng, H., Edwards, R. L., Kong, X., Shao, X., Chen, S., et al. (2008). Millennial- and orbital-scale changes in the East Asian Monsoon over the past 224,000 years. *Nature* 451, 1090–1093. doi: 10.1038/nature06692
- Webb, T. III (1986). Is vegetation in equilibrium with climate? How to interpret late-Quaternary pollen data. *Vegetatio* 67, 75–91. doi: 10.1007/BF00037359
- Weijers, J. W. H., Schefuß, E., Schouten, S., and Damsté, J. S. S. (2007). Coupled thermal and hydrological evolution of tropical Africa over the last deglaciation. *Science* 315, 1701–1704. doi: 10.1126/science.1138131
- Weldeab, S., Lea, D. W., Schneider, R. R., and Andersen, N. (2007). 155,000 years of West African monsoon and ocean thermal evolution. *Science* 316, 1303–1307. doi: 10.1126/science.1140461
- Wolff, E. W., Chappellaz, J., Blunier, T., Rasmussen, S. O., and Svensson, A. C. (2010). Millennial-scale variability during the last glacial: the ice core record. *Quat. Sci. Rev.* 29, 2828–2838. doi: 10.1016/j.quascirev.2009.10.013
- Yin, Q., and Berger, A. (2015). Interglacial analogues of the Holocene and its natural near future. *Quat. Sci. Rev.* 120, 28–46. doi: 10.1016/j.quascirev.2015.04.008
- Yin, Q. Z., and Berger, A. (2012). Individual contribution of insolation and CO₂ to the interglacial climates of the past 800,000 years. *Clim. Dyn.* 38, 709–734. doi: 10.1007/s00382-011-1013-5
- Zagwijn, W. H., and Veenstra, H. J. (1966). A pollen-analytical study of cores from the Outer Silver Pit, North Sea. *Mar. Geol.* 4, 539–551. doi: 10.1016/0025-3227(66)90014-4
- Zorzi, C., Sánchez Goñi, M. F., Anupama, K., Prasad, S., Hanquiez, V., Johnson, J., et al. (2015). Indian monsoon variations during three contrasting climatic periods: the Holocene, Heinrich Stadial 2 and the last interglacial-glacial transition. *Quat. Sci. Rev.* 125, 50–60. doi: 10.1016/j.quascirev.2015.06.009

Conflict of Interest Statement: The authors declare that the research was conducted in the absence of any commercial or financial relationships that could be construed as a potential conflict of interest.

Copyright © 2018 Sánchez Goñi, Desprat, Fletcher, Morales-Molino, Naughton, Oliveira, Urrego and Zorzi. This is an open-access article distributed under the terms of the Creative Commons Attribution License (CC BY). The use, distribution or reproduction in other forums is permitted, provided the original author(s) and the copyright owner are credited and that the original publication in this journal is cited, in accordance with accepted academic practice. No use, distribution or reproduction is permitted which does not comply with these terms.

Advantages of publishing in Frontiers



OPEN ACCESS

Articles are free to read
for greatest visibility
and readership



FAST PUBLICATION

Around 90 days
from submission
to decision



HIGH QUALITY PEER-REVIEW

Rigorous, collaborative,
and constructive
peer-review



TRANSPARENT PEER-REVIEW

Editors and reviewers
acknowledged by name
on published articles

Frontiers

Avenue du Tribunal-Fédéral 34
1005 Lausanne | Switzerland

Visit us: www.frontiersin.org

Contact us: info@frontiersin.org | +41 21 510 17 00



REPRODUCIBILITY OF RESEARCH

Support open data
and methods to enhance
research reproducibility



DIGITAL PUBLISHING

Articles designed
for optimal readership
across devices



FOLLOW US

[@frontiersin](https://twitter.com/frontiersin)



IMPACT METRICS

Advanced article metrics
track visibility across
digital media



EXTENSIVE PROMOTION

Marketing
and promotion
of impactful research



LOOP RESEARCH NETWORK

Our network
increases your
article's readership